1983 - 1

REEFS AND BANKS OF THE NORTHWESTERN GULF OF MEXICO: THEIR GEOLOGICAL, BIOLOGICAL, AND PHYSICAL DYNAMICS

FINAL REPORT

Northern Gulf of Mexico Topographic Features Synthesis
Contract No. AA851-CT1-55

COAR COPY

Submitted to the
U.S. Department of the Interior
Minerals Management Service
Outer Continental Shelf Office
New Orleans, Louisiana

Technical Report No. 83-1-T

Research Conducted Through
the Texas A&M Research Foundation

1983

TEXAS A&M UNIVERSITY COLLEGE OF GEOSCIENCES

REEFS AND BANKS OF THE NORTHWESTERN GULF OF MEXICO:

THEIR GEOLOGICAL, BIOLOGICAL, AND PHYSICAL DYNAMICS

FINAL REPORT

Northern Gulf of Mexico Topographic Features Monitoring and Data Synthesis
Contract No. AA851-CT1-55

Submitted to the
U.S. Department of the Interior
Minerals Management Service
Outer Continental Shelf Office
New Orleans, Louisiana

Department of Oceanography
Texas A&M University
College Station, Texas

Technical Report No. 83-1-T

Research Conducted Through
the Texas A&M Research Foundation

1983

This volume has been reviewed by the Minerals Management Service and approved for publication. Approval does not signify that the contents necessarily reflect the views and policies of the Service, nor does mention of trade names or commercial products constitute endorsement or recommendation for use.

CONTRIBUTORS

Program Manager
William J. Merrell, Jr.

Assistant Program Manager
Sylvia C. Herrig

Principal Investigators
Texas A&M University
Department of Oceanography

Richard Rezak
Geological

Research Staff

Patricia Brown
Jeffrey L. Payne
David Risch
Kyung-Sik Woo

Thomas J. Bright
Biological

Research Staff

Scott L. Baggett
Christopher L. Combs
Allison Craig
George Dennis
Steve Gittings
George Kraemer
Gregory Minnery
Richard H. Titgen

David W. McGrail
Sedimentological & Physical

Research Staff

Michael R. Carnes
Thomas M. Cecil
Lawrence Goldberg
Fern B. Halper
Jeffrey W. Hawkins
Doyle Horne

Editor

Rose Norman

FOREWORD

In this report oceanographers Richard Rezak, Thomas J. Bright, and David W. McGrail, aided by the exceptional editorial skills of technical writer Rose Norman, have attempted to describe the complex natural environment of the Texas-Louisiana shelf in terms readily understandable by decision-makers in government and industry and by interested citizens. Such writing represents a formidable challenge to scientists. Yet it is of considerable importance to them as well as to the reader because it forces them to examine and clarify scientific arguments to the point where they can be explained in simple, straightforward terms.

I believe that the benefits and occasional frustrations of such writing are described best by Thomas Huxley in the preface to his "Discourses: Biological and Geological" published in 1894. Huxley wrote:

> I found that the task of putting the truths learned in the field, the laboratory and the museum, into language which, without bating a jot of scientific accuracy shall be generally intelligible, taxed such scientific and literary faculty as I possessed to the uttermost; indeed; my experience has furnished me with no better corrective of the tendency to scholastic pedantry which besets all those who are absorbed in pursuits remote from the common ways of men, and become habituated to think and speak in the technical dialect of their own little world, as if there were no other.

I hope that you will agree with me that the authors of this report have lived up to Huxley's high standards by producing a document that is both scientifically accurate and easily readable.

William J. Merrell
College Station, Texas
July 1983

ACKNOWLEDGEMENTS

This report reflects the work of dedicated support staff and the valuable services of Texas A&M University personnel and others. The authors wish to extend their thanks to the following people:

1. For final drafting of maps and other art work, Kathy Roemer and Christopher Mueller-Wille, Cartographic Services Unit, Texas A&M University, Department of Geography.

2. For original drafting of structure and roughness maps, Jeff Payne, Gregory Minnery, Patricia Brown, Kyung-Sik Woo, and David Risch, Department of Oceanography, Texas A&M University.

3. For laboratory analyses, Milton P. Looney, Dale Harber, John Stafford, and Gregory Minnery.

4. For assembly of current meter arrays, data collection, and data analysis, Lauren Sahl, Fern Halper, Thomas Cecil, Jeffrey Hawkins, and Lawrence Goldberg.

5. For computer programming, data analysis, and numerical modeling, Michael Carnes, Assistant Research Scientist, Department of Oceanography, Texas A&M University.

6. For computer programming and analysis of boundary layer data, designing current meter arrays, and writing software for the PHISH system, Doyle Horne, Research Associate, Department of Oceanography, Texas A&M University.

7. For design and construction of the PHISH SYSTEM hardware, for calibrating instrumentation, and for maintaining all electronics equipment, James Stasney.

8. For their excellent support of our field work, the Marine and Electronics Technicians and personnel of the Marine Operations facility of Texas A&M University.

9. For exceptionally professional seamanship in support of our field work, the Captain and Crew of the R/V GYRE.

10. For program management, William J. Merrell, Jr., Program Manager, and Sylvia C. Herrig, Assistant Program Manager, MMS Project, Texas A&M University.

11. For editorial management, Rose Norman, Research Associate, Department of Oceanography, Texas A&M University.

12. For proofreading and numerous copy preparation duties, Cathy Crotzer, Marketing Department, Diane Fletcher, English Department, and Roxanne Bogucki, Wildlife and Fisheries Department, Texas A&M University.

13. For word processing, Lori Lingbeck.

TABLE OF CONTENTS

Page

CONTRIBUTORS..... iii

FOREWORD..... v

ACKNOWLEDGEMENTS..... vi

LIST OF FIGURES..... ix

LIST OF TABLES..... xxv

INTRODUCTION..... 1

Chapter

1. REGIONAL GEOLOGIC SETTING

PHYSIOGRAPHY OF THE GULF OF MEXICO..... 5
TEXAS-LOUISIANA CONTINENTAL SHELF..... 9
SUMMARY..... 29

2. CIRCULATION, HYDROGRAPHY, AND DISTRIBUTION OF SUSPENDED SEDIMENT ON THE CONTINENTAL SHELVES IN THE GULF OF MEXICO

FORCING MECHANISMS..... 31
WIND-DRIVEN SURFACE FLOW AND THE LOOP CURRENT IN THE DEEP BASIN..... 38
LONG-TERM, LARGE SCALE OBSERVATIONS..... 45
SEDIMENT DYNAMICS AND THE NEPHELOID LAYER..... 76
CONCLUSIONS..... 93

3. A SUMMARY OF HARD-BOTTOM BIOTIC COMMUNITIES IN THE GULF OF MEXICO

REGIONAL REEFS AND HARD BANKS..... 95
BIOGEOGRAPHIC RELATIONSHIPS..... 103
SUMMARY..... 108

4. GEOLOGY OF THE FLOWER GARDEN BANKS

GENERAL DESCRIPTION..... 111
PHYSIOGRAPHY AND STRUCTURE..... 114
SEDIMENTARY FACIES..... 132
SUMMARY..... 139

TABLE OF CONTENTS (Continued)

Page

5. FLOW, BOUNDARY LAYERS, AND SUSPENDED SEDIMENT AT THE FLOWER GARDEN BANKS

GENERAL SETTING..... 141
METHODS..... 142
TEMPERATURE AND SALINITY..... 147
FLOW FIELD AROUND THE BANKS..... 155
BOUNDARY LAYERS AND SUSPENDED SEDIMENT..... 204
TURBID BOTTOM LAYERS AND SUSPENDED SEDIMENT..... 219
CONCLUSIONS..... 230

6. ZONATION, ABUNDANCE, AND GROWTH OF REEF-BUILDERS AT THE FLOWER GARDEN BANKS

HABITAT DESCRIPTION AND ZONATION..... 231
POPULATION STUDIES ON HIGH DIVERSITY REEFS..... 256
CORAL GROWTH AND MORTALITY..... 263
DISCUSSION..... 270
CONCLUSIONS..... 276

7. THE EAST FLOWER GARDEN BRINE SEEP, A UNIQUE ECOSYSTEM

DESCRIPTION, DYNAMICS AND ORIGIN OF SEEP..... 277
BIOTA..... 288
BRINE SEEP ECOSYSTEM FUNCTION..... 302
CONCLUSIONS..... 310

8. CLASSIFICATION AND CHARACTERIZATION OF BANKS

SYSTEM OF CLASSIFICATION..... 311
SOUTH TEXAS RELICT CARBONATE SHELF REEFS..... 316
NORTH TEXAS-LOUISIANA REEFS AND BANKS ON DIAPIRIC STRUCTURES..... 326
ENVIRONMENTAL CONTROLS..... 392

9. ECOSYSTEM DYNAMICS

DEVELOPMENT OF FUNCTIONAL MODELS OF THE EAST FLOWER GARDEN CORAL REEF SYSTEM..... 401
PARTIAL EVALUATION OF MODEL FROM EXISTING DATA..... 437
DATA NEEDS FOR FULL MODEL EVALUATION..... 466

SELECTED REFERENCES..... 469

APPENDIX: GEOLOGIC TIME SCALE

LIST OF FIGURES

Figure Page

CHAPTER 1

1.1 Bathymetry of Gulf of Mexico region showing physiographic provinces and major topographic features..... 6

1.2 Sediment distribution, Gulf of Mexico Outer Continental Shelf..... 7

1.3 Sketch map showing paleoshelf edges in Gulf Coast basin and distribution of major Tertiary depocenters..... 10

1.4 Generalized cross-section of northern Gulf of Mexico margin..... 11

1.5 Coastal environments and shelf sediments, Texas-Louisiana continental shelf..... 12

1.6 Sparker profile showing channeling in Holocene sediments off Matagorda Bay..... 16

1.7 Sparker profile showing Baker Bank, a typical South Texas Outer Continental Shelf bank..... 17

1.8 Post-glacial sea level curves..... 22

1.9 Paleogeography of the northwest Gulf of Mexico at about 19,000 years B.P., when sea level is believed to have been at about -65 fathoms..... 24

1.10 Regional fracture pattern of southern United States..... 26

1.11 Distribution of pre-Middle Jurassic (Callovian) rocks in northern and eastern Gulf of Mexico regions..... 27

1.12 Tectonic map of northern Gulf of Mexico region..... 28

CHAPTER 2

2.1 Distribution of data upon which this analysis of circulation, hydrography and sediment dynamics on the continental shelves of the Gulf of Mexico was based..... 30

2.2 Tide curves at various places in the Gulf of Mexico, 23-30 June 1948..... 33

2.3 Ellipses for the K_1 diurnal tidal currents..... 34

2.4 Ellipses for the M_2 semidiurnal tidal currents..... 35

LIST OF FIGURES (Continued)

CHAPTER 2

Figure Page

2.5 Mean monthly wind stress vectors for the Gulf of Mexico.. 37

2.6 Idealized surface drift based on surface drifter data from Parker et al., 1979..... 40

2.7 Mean monthly velocity vectors at 6 m depth for the Gulf of Mexico..... 42

2.8 Mean monthly velocity vectors at 100 m depth for the Gulf of Mexico (after Blumberg and Mellor, 1981)..... 43

2.9 Typical locations of the core of the Loop Current, and anticyclonic eddies where possible, over the course of a year..... 44

2.10 Parallel wind stress vectors striking an arcuate coastline..... 47

2.11 Mean geopotential anomaly (dyne/cm) of the sea surface relative to 70 db based on GUS III data for March, May, and July..... 50

2.12 Mean geopotential anomaly (dyne/cm) of the sea surface relative to 70 db based on GUS III data for September, November, and January..... 51

2.13 Shelf index map showing the locations of the CSA current meter mooring (near Baker Bank), NDBO buoys 42002 and 42008, and the TAMU current meter moorings along 95°W and near the Flower Garden Banks..... 52

2.14 Progressive vector diagrams constructed from velocity time-series records beginning on 22 April 1980 for a) the wind at NDBO buoy 42002 and the currents at the top, middle, and bottom meters on the CSA mooring near Baker Bank; b) the currents at all available meters on moorings 1,2, and 3 near the Flower Garden Banks; and c) records beginning on 14 Feb 1979 for the wind at NDBO buoy 42002 and the currents at the top, middle, and bottom meters on th CSA mooring near Baker bank..... 54

2.15 Progressive vector diagrams constructed from velocity time series records beginning on 14 February 1979 for the currents at the top, middle, and bottom meters on the CSA mooring near Baker Bank and from wind stress data at NDBO buoy 42002..... 55

LIST OF FIGURES (Continued)

CHAPTER 2 (Continued)

Figure Page

2.16 Monthly mean current vectors for a) all deployments and all moorings near the Flower Garden Banks over the period January 1979 to July 1981; and b) the CSA mooring near Baker Bank over the period March 1978 through March 1981..... 57

2.17 Sea-surface salinity from GUS III observations taken in February, May, August, and November 1964..... 59

2.18 Sea-surface salinity from observations taken in March 1982..... 60

2.19 Map of (a) mean surface temperature for Jan-Feb, and (b) mean bottom temperatures for Jan-Feb..... 62

2.20 Maps of (a) mean surface temperature for Jul-Aug, and (b) mean bottom temperatures for Jul-Aug..... 63

2.21 Sea-surface temperature based on satellite infrared imagery for 17 February 1982, South Texas shelf..... 64

2.22 Sea-surface temperature based on satellite infrared imagery for 23 February 1982, Texas-Louisiana shelf..... 65

2.23 Sea-surface temperature based on satellite infrared imagery for 6 April 1982, Texas-Louisiana shelf..... 66

2.24 Sea-surface temperature based on satellite infrared imagery for 6 April 1982, South Texas shelf..... 67

2.25 Map of mixed-layer depths for January-February..... 68

2.26 Seasonal progression of sigma-t versus depth near the Flower Garden Banks, constructed from: CTD data collected by TAMU in April 1979, September 1979, October 1979 October 1980, March 1981, and July 1981; monthly averages of temperature time-series data recorded on TAMU current meter moorings near the banks; and from GUS III station W-6 (27°55'N,94°36'W), cruises 13 to 24 of 1964..... 69

2.27 Sea-surface temperature based on satellite infrared imagery for 11 April 1982..... 71

LIST OF FIGURES (Continued)

CHAPTER 2 (Continued)

Figure Page

2.28 Progressive vector diagrams of wind from 1 March to 3 April 1982 at NDBO buoys 42008 and 42002..... 73

2.29 Progressive vector diagrams of currents measured at the 95°W array: (a) moorings 1 and 2 from 20 March to 30 April 1982, and (b) mooring 3 from 20 March to 1 May 1982..... 74

2.30 Time-series records of the wind from NDBO buoy 42002, and the water temperature, transmissivity, and current velocity from mooring 2 of the 95°W array between 20 March and 4 May 1982..... 75

2.31 Sample current record from the bottom current meter (4 m from bottom in 73 m of water) of the CSA mooring near Baker Bank..... 80

2.32 Map showing location of stations taken during March 1981 and March 1982 cruises over the Texas-Louisiana shelf and slope..... 84

2.33 Map showing location of stations on the cross-shelf transect along 95°W over the Texas-Louisiana shelf and slope in May 1982..... 85

2.34 Cross-shelf vertical section of temperature, salinity, and sigma-t along section A, occupied in March 1982 (see Figure 2.32 for station location)..... 87

2.35 Along-shore vertical sections of temperature and salinity along transect E occupied in March 1982..... 88

2.36 Cross-shelf vertical sections of temperature, salinity, and sigma-t along 95°W, occupied in May 1982..... 89

2.37 Cross-shelf vertical sections of temperature along 95°W across the Texas-Louisiana shelf, as in Figure 2.36 but showing locations and depths of current meters on moorings 1, 2, and 3..... 90

2.38 Temperature at the Florida Middle Ground versus time during 1978 and 1979..... 92

LIST OF FIGURES (Continued)

CHAPTER 2 (Continued)

Figure Page

2.39 Map of Gulf of Mexico summarizing the primary near-surface circulation patterns which may be responsible for carrying biotic communities into the Gulf and from there either anticyclonically around the western Gulf or to the Florida shelf via the Loop Current and spin-off eddies..... 94

CHAPTER 3

3.1 Zones and locations of major biogeographic significance in the Gulf of Mexico..... 96

CHAPTER 4

4.1 Location map of Flower Garden Banks, northwestern Gulf of Mexico..... 110

4.2 East Flower Garden Bank bathymetry, showing location of sub-bottom profiles in Figures 4.5, 4.6, an 4.8..... 112

4.3 West Flower Garden Bank bathymetry, showing location of sub-bottom profiles and side-scan sonar records in Figures 4.10 to 4.16..... 113

4.4 Structure map of East Flower Garden Bank region..... 115

4.5 CDP Sparker profile across the central graben at the East Flower Garden Bank, also shown in Figure 4.6..... 116

4.6 A 3.5 kHz sub-bottom profile showing the central graben at the East Flower Garden Bank..... 117

4.7 Diagrammatic representation of step faulting at the East Flower Garden Bank..... 118

4.8 CDP Sparker profile showing step faulting at the East Flower Garden Bank..... 119

4.9 East Flower Garden Brine Complex: 1 - brine seeps; 2 - brine lake; 3 - overflow; 4 - canyon with mixing stream..... 121

4.10 Structure/Isopach map of West Flower Garden Bank..... 124

4.11 A 3.5 kHz north-south sub-bottom profile across the western part of the West Flower Garden Bank..... 125

LIST OF FIGURES (Continued)

CHAPTER 4 (Continued)

Figure Page

4.12 A 3.5 kHz north-south sub-bottom profile across the central part of the West Flower Garden Bank..... 126

4.13 A 3.5 kHz north-south sub-bottom profile across the central part of the West Flower Garden Bank, including the living high diversity coral reef..... 127

4.14 Side-Scan sonar record showing surface features in a central portion of the West Flower Garden Bank, near the living high diversity coral reef..... 128

4.15 Side-Scan sonar record showing surface features in a central part of the West Flower Garden Bank (just south of the record shown in Figure 4.13)..... 129

4.16 Side-Scan sonar record showing fault scarp with reef overgrowth in the northern part of the West Flower Garden Bank..... 130

4.17 Side-Scan sonar record showing patch reefs in the *Amphistegina* Sand Facies at the West Flower Garden Bank..... 131

4.18 Sediment facies in the Flower Garden Banks area..... 133

4.19 Percent mud in bottom sediment in the Flower Garden Banks area..... 136

4.20 Sketch of the West Flower Garden Bank as it may have looked during the 121 to 134 m stillstand of the Gulf of Mexico..... 138

CHAPTER 5

5.1 Mooring positions for all six current meter array deployments from January 1979 to July 1981..... 140

5.2 Diagrammatic representation of dye emitter apparatus used in October 1980 boundary layer experiments at the Flower Garden Banks..... 145

LIST OF FIGURES (Continued)

CHAPTER 5 (Continued)

Figure Page

5.3 Diagrammatic representation of tautline mooring on which vanes and dye emitters were assembled for 1979 and 1980 boundary layer experiments at the Flower Garden Banks..... 146

5.4 Seasonal progression of sigma-t versus depth near the Flower Garden Banks, as in Figure 2.26..... 148

5.5 Composite plots of temperature and salinity profiles taken near the East and West Flower Garden Banks on three cruises..... 149

5.6 Hydrographic station location map for the BALTIC SEAL cruise, October 10-20, 1980..... 150

5.7 Hydrographic station location map for the GYRE cruise, March 3-8, 1981..... 151

5.8 Hydrographic station location map for the NORTH SEAL cruise, July 13-17, 1981..... 152

5.9 Hydrographic stations at the East Flower Garden Bank for the NORTH SEAL Cruise, July 13-17, 1981..... 153

5.10 Temperature on the East Flower Garden reef at 27 m, representing the transition from deep winter conditions to those of spring..... 154

5.11 Plot of salinity, temperature, transmissivity, and sigma-t from the East Flower Garden..... 156

5.12 One-month averages of speed and direction for current meters in three depth ranges..... 157

5.13 Monthly mean current vectors for all deployments and all moorings..... 158

5.14 Progressive vector diagram, winds at NDBO Buoy 42002, 25 Oct 80 - 9 Feb 81..... 160

5.15 Progressive vector diagrams, currents at the Flower Garden Banks, October 80 - February 81..... 161

5.16 Spectral representations of the mid-depth currents at mooring 1 illustrating summer conditions..... 165

LIST OF FIGURES (Continued)

CHAPTER 5 (Continued)

Figure Page

5.17 Spectral representations of the near-bottom currents at mooring 1 illustrating summer conditions..... 166

5.18 Spectral representations of the mid-depth currents at mooring 3 illustrating spring/summer conditions..... 167

5.19 Spectral representations of the near-bottom currents at mooring 3 illustrating spring/summer conditions..... 168

5.20 Spectral representations of the very near-bottom currents at mooring 3 illustrating spring/summer conditions..... 169

5.21 Spectral representations of the mid-depth currents at mooring 3 illustrating winter conditions..... 170

5.22 Spectral representations of the near-bottom currents at mooring 3 illustrating winter conditions..... 171

5.23 Spectral representations of the very near-bottom currents at mooring 3 illustrating winter conditions..... 172

5.24 Spectral representations of the mid-depth currents at mooring 2 illustrating winter conditions..... 173

5.25 Time series of horizontal currents at the upper and lower meters of moorings 1, 2, and 3..... 177

5.26 Wave-like perturbations in the sea surface isotherms at the shelf edge outlined with a heavy line..... 179

5.27 Wind and current meter records during the passage of Tropical Storm Claudette..... 181

5.28 Bottom velocity vectors from all July 1979 stations plotted with directional sense only..... 189

5.29 Horizontal velocity vectors at a depth of 70 m determined from PHISH stations taken on the October 1980 BALTIC SEAL cruises..... 190

5.30 Horizontal velocity vectors at 1 m from bottom determined from PHISH stations taken on the October 1980 BALTIC SEAL..... 191

LIST OF FIGURES (Continued)

CHAPTER 5 (Continued)

Figure Page

5.31 Vertical section of temperature from northwest to southeast across the East Flower Garden Bank..... 192

5.32 Horizontal velocity vectors at 1 m from bottom determined from PHISH stations taken on the March 1981 GYRE cruise..... 193

5.33 Horizontal velocity vectors at a depth of 5 m determined from PHISH stations taken on the March 1981 GYRE cruise..... 194

5.34 Ratio of the variance along the major axis to the variance along the minor axis, plotted in the direction of the major axis for (a) all meters on mooring 2 deployed before March 1981, and (b) all meters on mooring 2 for the March to July 1981 deployment..... 198

5.35 Ratio of the variance along the major axis to the variance along the minor axis, plotted in the direction of the major axis for (a) all meters on mooring 1; (b) all meters on mooring 3; and (c) all meters on mooring 4..... 199

5.36 Shaded region in each circle shows the range of directions of the major axis of velocity variances for most one-month velocity segments at each mooring..... 200

5.37 Large scale bedforms on the West Flower Garden Bank as determined from a digital side-scan sonar mosaic..... 201

5.38 Large scale bedforms on the East Flower Garden Bank as determined from side-scan sonar records..... 202

5.39 Time series of temperature and horizontal velocity from meter 2 of mooring 2, located near the southwest edge of the East Flower Garden Bank at 5 m from the bottom.... 203

5.40 Location of October 1980 submersible dive stations where dye emission experiments were made..... 211

5.41 Profiles of transmissivity, temperature, salinity, density, and horizontal velocity at stations a) 10S and b) C2..... 214

LIST OF FIGURES (Continued)

CHAPTER 5 (Continued)

Figure Page

5.42 Profiles of transmissivity, temperature, salinity, density, and horizontal velocity at stations a) 10 and b) 11..... 215

5.43 Temperature and transmissivity, July 1981, on a southwest transect at the East Flower Garden Bank..... 216

5.44 Profiles of transmissivity, temperature, salinity, density, and horizontal velocity at stations a) 19S and b) 5W..... 217

5.45 Profiles of transmissivity, temperature, salinity, density, and horizontal velocity at station 8E..... 218

5.46 Raw velocity and transmissivity time series records for April to June 1980 from a) mooring 1 meter 2, and b) mooring 3 meter 2..... 222

5.47 Mud contours in 20% intervals..... 223

5.48 Time series of temperature, transmissivity, and horizontal velocity lowpassed with a 28-hour filter near the bottom on a) mooring 1 at 95 m depth and b) mooring 3 at 100 m depth near the Flower Garden Banks..... 224

5.49 Band-Passed time series of temperature, transmissivity, and horizontal velocity, both stick plots and individual orthogonal components near the bottom on mooring 3, northeast of the West Flower Garden Bank..... 225

5.50 Band-Passed time series of temperature, transmissivity, and horizontal velocity, both stick plots and individual orthogonal components near the bottom on mooring 1, northeast of the East Flower Garden Bank..... 226

5.51 Comparison of the mid-depth north-south component of velocity at mooring 1 to that at mooring 3..... 227

5.52 Comparison of the near-bottom north-south component of velocity at mooring 1 to that at mooring 3..... 228

5.53 Comparison of near-bottom transmissivity measured at mooring 1 to that at mooring 3..... 229

LIST OF FIGURES (Continued)

CHAPTER 6

Figure Page

6.1 Conspicuous biota and biotic zones on the southeastern part of East Flower Garden Bank..... 234

6.2 Biotic zonation, East Flower Garden Bank..... 235

6.3 Biotic zonation, West Flower Garden Bank..... 236

6.4 Bray-Curtis cluster for 5 m depth intervals at the East and West Flower Garden Banks together. Attributes are relative square roots of abundance for invertebrates and algae..... 237

6.5 Depth zone relationships derived from interpretation of Bray-Curtis clusters for East and West Flower Garden invertebrates and algae..... 238

6.6 Typical Flower Gardens coral reef top (21 m depth)..... 239

6.7 Brain corals (Colpophyllia and Diploria), coarse carbonate sand, and reef fishes at 20 m depth on Flower Gardens at base of coral head..... 239

6.8 Madracis mirabilis, dominant coral of Madracis zone (28 m depth, East Flower Garden)..... 239

6.9 Leafy algae zone (28 m depth, East Flower Garden)..... 239

6.10 Relative abundance of benthic algae, stony corals, alcyonarians, and antipatharians below 30 m depth (high diversity coral reefs excluded)..... 246

6.11 Depth ranges of recognizable biotic zones and sedimentary facies (other than hard bottoms)..... 249

6.12 Aggregation of white urchins, Pseudoboletia maculata, at 59 m depth on bottom covered with very small nodules..... 251

6.13 Patch of living Halimeda sp. at about 55 m depth, East Flower Garden..... 251

6.14 Crusts of coralline algae on hard substratum of "partly drowned reef" at the East Flower Garden (60 m depth)..... 251

6.15 Hard sponges attached to carbonate rock coated with veneer of sediment..... 251

LIST OF FIGURES (Continued)

CHAPTER 6 (Continued)

Figures Page

6.16 Typical photographic mosaic of 10 m long transect at 24 m depth on the West Flower Garden Bank..... 257

6.17 X-Radiographs of cores taken from Montastrea annularis and Diploria strigosa at the East and West Flower Garden Banks, showing annual bands..... 264

6.18 Accretionary growth rates for Montastrea annularis, Diploria strigosa, and Stephanocoenia michelinii..... 266

6.19 Seasonal averages of Montastrea annularis encrusting growth and retreat measurements made between September 1978 and September 1980..... 269

CHAPTER 7

7.1 Brine seep, eastern edge of East Flower Garden Bank..... 278

7.2 Sand waves in brine lake..... 281

7.3 Overflow from Gollum's Lake (lower left) into the mixing stream (white stream bed curves to left and disappears behind cliff) in Gollum's Canyon..... 281

7.4 Sulfur bacteria--diatom "mat" covering substratum in stream..... 281

7.5 Cottonwick (Haemulon melanurum) hovering just above and in the mixing stream near Cottonwick Rock..... 281

7.6 Profiles of sulfide and salinity both in the brine lake and along a vertical transect at the Cottonwick Rock..... 283

7.7 The East Flower Garden brine seep area with location of soft-bottom stations sampled and current profiles of the brine stream at three stations, measured by a Savonius rotor placed on the manipulator arm of the submersible..... 286

7.8 Numbers of annelids, tanaids, and gastrotrichs along a transect from Gollum's Lake down Gollum's Canyon and out onto the sandy bottom adjacent to the canyon mouth..... 292

7.9 Numbers of copepods, ostracods, and gnathostomulids along a transect from Gollum's Lake down Gollum's Canyon to the Anchor and out onto the sandy bottom adjacent to the canyon mouth..... 293

LIST OF FIGURES (Continued)

CHAPTER 7 (Continued)

Figure Page

7.10 Numbers of turbellarians, nematodes, amphipods, and total biota along a transect from Gollum's Lake down Gollum's Canyon to the Anchor and out onto the sandy bottom adjacent to the canyon mouth..... 294

7.11 Locations of the hard-bottom stations sampled in the East Flower Garden brine seep area..... 297

7.12 Abundances of important taxa and total fauna on the Gollum's Lake transect..... 299

7.13 Total numbers of selected taxa from the Cottonwick Rock stations..... 300

7.14 The East Flower Garden brine seep system: driving forces and biological processes..... 307

CHAPTER 8

8.1 Location map of banks discussed in text..... 314

8.2 (a) USGS Del Norte model 561 sparker profile across Baker Bank; b) bathymetric map of Baker Bank showing location of sparker profile..... 317

8.3 Bathymetry of Southern Bank showing locations of cores and cross section in Figure 8.4..... 319

8.4 Cross-Section through Southern Bank with locations of four cores showing sediment types around the bank..... 321

8.5 Diagrammatic representation of biota at Southern Bank..... 323

8.6 Bathymetry at Sonnier Banks, showing location of the sub-bottom profile and side-scan record shown in Figure 8.7..... 327

8.7 Structure/Isopach map of Sonnier Banks..... 328

8.8 A 7 kHz sub-bottom profile and side-scan sonar record across the east side of the Sonnier Banks area..... 329

8.9 Bathymetry of Fishnet Bank, indexing location of profiles shown in Figures 8.11 and 8.12, and side-scan sonar records shown in Figures 8.13 and 8.14..... 331

LIST OF FIGURES (Continued)

CHAPTER 8 (Continued)

Figure Page

8.10 Structure/Isopach map of Fishnet Bank..... 332

8.11 Boomer profile across Fishnet Bank..... 333

8.12 A 3.5 kHz sub-bottom profile across the eastern edge of Fishnet Bank (see Figure 8.9)..... 334

8.13 Side-Scan sonar record showing the pattern of outcrops at Fishnet Bank..... 335

8.14 Side-Scan sonar records showing outcrop patterns on Fishnet Bank..... 336

8.15 Diagrammatic representation of biota at Sonnier Banks.... 338

8.16 Bathymetry of Geyer Bank, showing location of boomer profiles and side-scan sonar records shown in Figures 8.17, 8.18, and 8.20..... 343

8.17 North-South boomer profile across Geyer Bank..... 345

8.18 East-West boomer profile across Geyer Bank..... 346

8.19 Structure/Isopach map of Geyer Bank..... 347

8.20 Side-Scan sonar record showing sand waves and reef..... 348

8.21 Bathymetry at Diaphus Bank, indexing location of boomer profile and side-scan sonar record shown in Figures 8.22 and 8.24..... 351

8.22 North-South boomer profile across Diaphus Bank..... 352

8.23 Structure/Isopach map of Diaphus Bank..... 353

8.24 Side-Scan sonar record across Diaphus Bank..... 354

8.25 Bathymetry of Alderdice Bank, indexing boomer and seismic reflection profiles shown in Figures 8.26 and 8.27, and side-scan sonar records shown in Figures 8.29 and 8.30..... 357

8.26 North-South boomer profile across the main peak at Alderdice Bank..... 358

8.27 North-South profile across the east side of Alderdice Bank showing renewed uplift of salt..... 359

LIST OF FIGURES (Continued)

CHAPTER 8 (Continued)

Figure Page

8.28 Structure/Isopach map of Alderdice Bank..... 360

8.29 Side-Scan sonar record across outcrops and reefs at Alderdice Bank..... 361

8.30 Side-Scan sonar record across basalt outcrop at Alderdice Bank..... 362

8.31 Bathymetry of Sackett Bank, indexing location of boomer profiles and side-scan sonar records shown in Figures 8.32 to 8.33..... 364

8.32 Boomer seismic profile across Sackett Bank..... 365

8.33 A 7 kHz profile and side-scan sonar record across Sackett Bank..... 366

8.34 Structure map of Sackett Bank..... 367

8.35 Bathymetry at Rezak-Sidner Bank, indexing location of boomer profiles shown in Figures 8.35 and 8.36..... 369

8.36 North-South boomer profile across Rezak-Sidner Bank..... 370

8.37 East-West boomer profile across Rezak-Sidner Bank..... 371

8.38 Structure/Isopach map of Rezak-Sidner Bank..... 373

8.39 Diagrammatic representation of biota at Geyer Bank..... 377

8.40 Diagrammatic representation of biota at Sackett Bank..... 383

8.41 Diagrammatic representation of biota at Diaphus Bank..... 389

8.42 Diagrammatic representation of biota at Alderdice Bank..... 390

8.43 Comparison of biotic zones to temperature, salinity, turbidity, and light differences at selected banks..... 394

8.44 Chart of coralline algae relative abundance by depth on shelf-edge carbonate banks..... 397

LIST OF FIGURES (Continued)

CHAPTER 9

Figure Page

9.1 East Flower Garden reef - conceptual model..... 410

9.2 East Flower Garden reef - graphical model of producers and coral polyps..... 414

9.3 East Flower Garden coral reef - conceptual and graphical model of consumer species..... 418

9.4 Solar radiation reaching the sea surface and various depths at the East Flower Garden Bank..... 439

9.5 Monthly water temperatures at selected depths in the vicinity of the East Flower Garden Bank, based on two-year averages..... 441

LIST OF TABLES

Table Page

CHAPTER 2

2.1 Deployment Periods of Current Meters in the Gulf of Mexico, 1973-1983 30

2.2 Amplitude and Phase of the Barotropic Tidal Currents Near the Flower Garden Banks for the M_2 and K_1 Constituents 77

CHAPTER 4

4.1 Relationship Between Sediment Facies and Biological Zones at the East Flower Garden Bank 134

CHAPTER 5

5.1 Current Meter Associated Time Series Data Inventory, East and West Flower Garden Banks, All Deployments from January 1979 to July 1981 143

5.2 Theoretical Frequency and Period of Major Tidal Constituents and of Inertial Currents 174

5.3 Tidal Current Amplitudes at Mooring 3 for 6 March to 4 April 1981 175

5.4 Results of Airy Wave Theory Calculations 183

5.5 Average Direction of Major Axis of Variance 199

5.6 Boundary Measurements at West Flower Garden Bank 210

5.7 Measured Angular Shearing in the Bottom Boundary Layer 210

CHAPTER 6

6.1 Flower Garden Reef Builders 241

6.2 Dominance of Major Hermatypic Corals on the Hard Substratum within the *Diploria*-*Montastrea*-*Porites* Zone 260

6.3 Shannon-Weaver Indices of Coral Diversity and Evenness 262

6.4 Accretionary Growth Rates of Corals from the East and West Flower Gardens 267

LIST OF TABLES (Continued)

CHAPTER 6 (Continued)

Table Page

6.5 Rates of Encrusting Growth and Retreat of Colony Borders Across Underlying Reef Rock at the East and West Flower Gardens..... 268

6.6 Occurrence of Hermatypic Corals in the Western Atlantic..... 271

6.7 Comparison of Coral Abundances and Shannon-Weaver Diversity Values..... 275

CHAPTER 7

7.1 Chemical Characteristics of Brine, Brine-Seawater Mixture, and Seawater Near the East Flower Garden Brine Lake..... 280

7.2 Estimations of Residence Time, Volumes of Brine Produced, and Total Salt and Sulfide Production..... 284

CHAPTER 8

8.1 Depth Ranges of Biotic Zones on Outer Continental Shelf Hard Banks in the Northwestern Gulf of Mexico..... 315

CHAPTER 9

9.1 Definition and Composition of Categories in the Conceptual Model of the East Flower Garden Coral Reef Ecosystem..... 404

9.2 Input-Output Characteristics of Reservoirs of the East Flower Garden Coral Reef Conceptual Model..... 406

9.3 General Form of Equations Used to Describe Pathways Affecting Primary Production in the Models of the East Flower Garden Coral Reef Ecosystem..... 423

9.4 General Form of Equations Used to Describe Pathways Affecting Secondary Production in the Models of the East Flower Garden Coral Reef Ecosystem..... 446

9.5 General Form of Equations Used to Describe Pathways Relating to Storage Compartments of the East Flower Garden Coral Reef Ecosystem..... 433

9.6 Calculation of Monthly Progression of Solar Radiation at the Sea Surface and at Various Water Depths..... 438

LIST OF TABLES (Continued)

CHAPTER 9 (Continued)

Table Page

9.7 Water Column Characteristics..... 443

9.8 Derived Data for the East Flower Garden Reef Surface..... 445

9.9 Biomass Calculations for Zooxanthellae and Coral Tissue.. 447

9.10 Soft Algae Biomass Calculations..... 448

9.11 Coralline and Endolithic Algae Calculations..... 450

9.12 Biomass Estimates for Some of the Major Plankton Feeder Groups of the Coral Reef Zone for Which Data are Available..... 451

9.13 Biomass Estimates for Major Herbivore Groups of the Coral Reef Zone for which Data are Available..... 452

9.14 Biomass Estimates for Major Omnivore Groups of the Coral Reef Zone for which Data are Available..... 453

9.15 Biomass Estimates for Major Transient and Resident Predator Groups of the Coral Reef Zone for which Data are Available..... 454

9.16 Biomass Summary and Caloric Conversions for the Live Coral Zone..... 456

9.17 Biomass Summary and Caloric Conversions for the Algal-Sponge Zone..... 460

9.18 Gross Primary Production Calculations for the Live Coral Zone..... 462

9.19 Gross Primary Production Calculations for the Algal-Sponge Zone..... 463

9.20 Standing Crop and Production Estimates for the Live Coral Zone..... 464

9.21 Standing Crop and Production Estimates for the Algal-Sponge Zone..... 465

9.22 Estimated Mean Annual Accretion Rates of *Montastrea annularis* for Representative Water Depths of the Live Coral Zone..... 466

INTRODUCTION

The purpose of this report is to provide a synthesis of scientific information regarding the geology, biology, and physical oceanography of the Texas-Louisiana Outer Continental Shelf, especially scientific knowledge and data related to the topographic features extending above the seafloor. A considerable portion of the data collected on the shelf is the result of a series of studies funded by the Bureau of Land Management (BLM; now Minerals Management Service, MMS) and conducted principally by investigators at Texas A&M University. This report relies primarily on data generated during these investigations, which started in 1974. However, it also incorporates the scientific literature generated by other studies before and during these BLM-sponsored investigations. This chapter documents the early work which described topographic features of the Texas-Louisiana Shelf, describes the structure of this report, and summarizes the chief conclusions.

BACKGROUND

Initial interest in the banks on the Outer Continental Shelf was expressed over 50 years ago in a paper on the Mississippi Delta (Trowbridge, 1930). In that paper, Trowbridge recorded the presence of a bathymetric prominence having a relief of 33 m and a covering of coarse sediments. Six years later the U.S. Coast and Geodetic Survey carried out a detailed survey of the Gulf of Mexico west of the Mississippi River. Analysis of these data led Shepard (1937) to suggest that the numerous pinnacles were due to the intrusion of salt into the sediments. Later, Carsey (1950) reported 164 "topographic features" which occur along the shelf off the coast of Texas and Louisiana.

Pulley (1963) was the first to report that the Flower Garden Banks were indeed flourishing coral reefs. In 1961, with the assistance of scuba divers, he photographed and collected live corals from both banks. At about the same Richard Rezak, while employed by the Shell Development Company, Houston, Texas, was invited to participate in a short cruise to the Flower Garden Banks. Bathymetric profiles and Van Veen grabs confirmed Stetson's description of living coral and coralline algae (1953). Levert and Ferguson (1969) further substantiated Stetson's and Pulley's findings.

The Department of Oceanography at Texas A&M University conducted several cruises to the Flower Garden Banks during the period from 1968 to 1974. Their work began as separate geological and biological investigations but very early on became a joint effort funded by Texas A&M University and the Flower Garden Ocean Research Center at the University of Texas Marine Biomedical

Institute. The goal of the geological effort was to develop a conceptual model of a coral reef growing on a terrigenous shelf for hydrocarbon exploration. Biological efforts sought to document the fauna and flora of the reef and bank environments.

Edwards (1971), in his Ph.D. dissertation, presented a most comprehensive report on the West Flower Garden Bank. He used 3.5 kHz and air gun seismic profiles for the first time to illustrate the salt diapir sub-bottom structure of that bank. Edwards also described very accurately the sediment distribution and the biota associated with each sediment facies.

The initial Texas A&M investigation for BLM (now Minerals Management Service) began in late 1974 (Bright and Rezak, 1976). This study provided baseline biological and geological information to facilitate judgements as to the need for and the nature of protective regulations to be imposed on drilling operations near these banks. Seventeen banks were mapped using precision navigation, precision depth recorder, and side-scan sonar. Three of the areas mapped showed no topographic relief and were not studied further. Six of the seventeen banks were examined and sampled using the Texas A&M submersible DRV DIAPHUS. All seafloor observations were documented using 35 mm color still photography and black and white video tape recordings. Surface samples of sediments (grabs and cores) were taken at five of the banks. An important discovery made in 1975 was the existence of a layer of turbid water that blankets the continental shelf and surrounds and/or covers all of the banks examined on the South Texas Outer Continental Shelf. The layer of turbid water is associated with increased sedimentation and limited light penetration, both of which have a profound influence on the biota of the banks and the sediments on and around them. This turbid layer is known as the nepheloid layer.

A second investigation, initiated in 1976 (Bright and Rezak, 1978a), extended the mapping program to three more banks and included additional submersible work on four banks. At four of the seven banks investigated, studies included post drilling environmental assessments, and at two banks the quantitative ecological relationship between the nepheloid layer and epibenthic community population dynamics was investigated. An important discovery during the course of this investigation was the presence of a high salinity brine lake at the East Flower Garden Bank. The brine lake has provided a unique opportunity for the study of the effects of natural brine discharges. The presence of the brine lake also provided information on the nature of salt tectonism at the East Flower Garden Banks and other banks near the shelf break.

Studies of the nepheloid layer at various banks and studies of the brine lake at the East Flower Garden Bank were continued in 1977 (Bright and Rezak, 1978b). Additional mapping studies in 1977 provided physiographic and sub-bottom data on eight more banks, seven of which were observed and sampled from the submersible. A

biological monitoring study was also initiated for the first time within the living coral facies of the East Flower Garden Bank. Biological monitoring of the East Flower Garden coral reef was continued in 1978 as were studies of the nepheloid layer at selected banks (Rezak and Bright, 1981). Both mapping and submersible observations were undertaken at nine banks not previously studied. Among these was the West Flower Garden Bank, where monitoring studies identical to those at the East Flower Garden Bank were initiated.

During the 1978-1980 study (Rezak and Bright, 1981), several technological changes were made. Provision for seismic and side-scan sonar equipment on mapping cruises made possible the preparation of a series of seafloor roughness maps and structure/isopach maps for several of the banks. Color video cassette recordings were made of the submersible observations, and the biological monitoring study at the Flower Garden Banks instituted several experimental techniques that permitted quantitative statistical analysis.

Significant advances were also made in the instrumentation used for hydrographic studies of the nepheloid layer. The deployment of current meter moorings and the development of a sophisticated new system for simultaneous hydrographic measurements have created a very large data base for measurements of turbidity, current velocities, temperature, and salinity in the region of the Flower Garden Banks.

Investigations from 1979 through 1981 focused on biological and hydrologic monitoring at the East and West Flower Garden Banks, as well as geological analysis and interpretation of sub-bottom, side-scan, and sedimentological data from these two banks (McGrail, Rezak, and Bright, 1982). Sub-bottom and side-scan data for seven selected banks were also analyzed and interpreted; with one exception, these data had been acquired in previous studies.

Geological studies at the Flower Garden Banks produced a sediment distribution map for the Flower Garden region and examined the relationship between sediment facies and biotic zones. Use of the EG&G Seafloor Mapping System made it possible to prepare a side-scan sonar mosaic for the West Flower Garden Bank. This mosaic is for all intents and purposes a photographic representation of the seafloor.

Biological investigations continued to be directed toward assessment of the health of biotic communities at the two banks. Biotic zonation maps were developed from direct observations and data gathered in the course of the continuing monitoring program. Identical coral ecology studies were carried out at the East and West Flower Garden coral reefs, and the results were compared.

Investigations of water and sediment dynamics at the Flower Garden Banks had three goals: 1) to study the hydrographic climate (salinity, temperature, turbidity, and currents) in which the banks exist; 2) to develop an understanding of the dynamics of the nepheloid layer, particularly as it impinges on the shelf-edge banks; and 3) to ascertain the nature of the shelf-edge flow, including the driving mechanisms.

The present study provides a synthesis of data from the five previous Texas A&M studies and the published record. The report is in three parts. The first part, Chapters 1 through 3, provides a regional setting for the geology, biology, and hydrography of the Texas-Louisiana Outer Continental Shelf. Chapters 4 through 7 describe the geology, biology, and hydrology of the Flower Garden Banks, which have been most intensively studied and are used as a model to which other banks on the Outer Continental Shelf are compared in the final part of the report. Chapter 8 is an attempt to categorize the many banks that we have examined and establish their relationship to the dynamic system that we have described at the Flower Garden Banks. Chapter 9 describes an ecosystems approach to the study of the reefs and banks of the Texas-Louisiana Outer Continental Shelf.

CONCLUSIONS

Water and sediment dynamics studies indicate that water flows around topographic prominences on the seafloor rather than flowing upslope and over the crest of the prominence. In terms of sediments or pollutants of any kind entrained in the nepheloid layer which exists around the bases of many high relief banks, it is physically impossible to transport sediment to the crest of the reef or bank. This conclusion is supported by both geological and biological evidence. No clay minerals have been found in sediments collected from depths shallower than 70 m at the Flower Garden Banks, and only traces have been found at depths of 80 to 85 m.

There is a very distinct biological boundary at a depth of about 88 m. Above that depth, the dominant organisms are clear water faunas. Below 88 m, the complexion of the fauna changes drastically and it is a turbid water fauna.

CHAPTER 1

REGIONAL GEOLOGIC SETTING

Richard Rezak

In order to establish an understanding of the processes active on the Outer Continental Shelf, this chapter will be devoted to a general description of the Gulf of Mexico with special emphasis on the physiography, sediments, and structure of the shelf in the northwestern Gulf of Mexico. The Gulf of Mexico is a small ocean basin which, together with the four basins of the Caribbean, constitutes the American Mediterranean (Harding and Nowlin, 1966). The Gulf covers an area of about 1.5 million square kilometres and has a maximum depth of about 3700 m. Figure 1.1 illustrates the bathymetry and major physiographic provinces of the Gulf.

PHYSIOGRAPHY OF THE GULF OF MEXICO

Continental Shelf

The continental shelf is the submerged portion of the continental platform that slopes gradually to depths between 100 and 200 m. It is widest off southern Florida (about 300 km) and narrowest off the modern Mississippi Delta (about 10 km). The West Florida and Yucatan shelves are characterized by carbonate sediments, whereas the East Mexico and Texas-Louisiana shelves are composed primarily of terrigenous sediments (Figure 1.2). Local areas of carbonate sediment production exist from Veracruz to the Mississippi Delta (Rezak and Edwards, 1972).

Continental Slope

The continental slope is quite variable in its degree of slope from place to place in the Gulf. In general, the upper slope shows a slight increase in declivity from the shelf. Throughout most of the Gulf, however, the lower part of the slope is an escarpment. The West Florida Escarpment is one of the steepest submarine slopes known, attaining a declivity of about 39° (810 m/km). The Campeche continental slope is somewhat less steep, while the slope of Texas and Louisiana is considerably less steep. The Campeche Escarpment forms the lower part of the Campeche continental slope, and the Sigsbee Scarp forms the base of the Texas-Louisiana continental slope. The very irregular topography of the Texas-Louisiana continental slope and the Gulf of Campeche (Figure 1.1) is due to

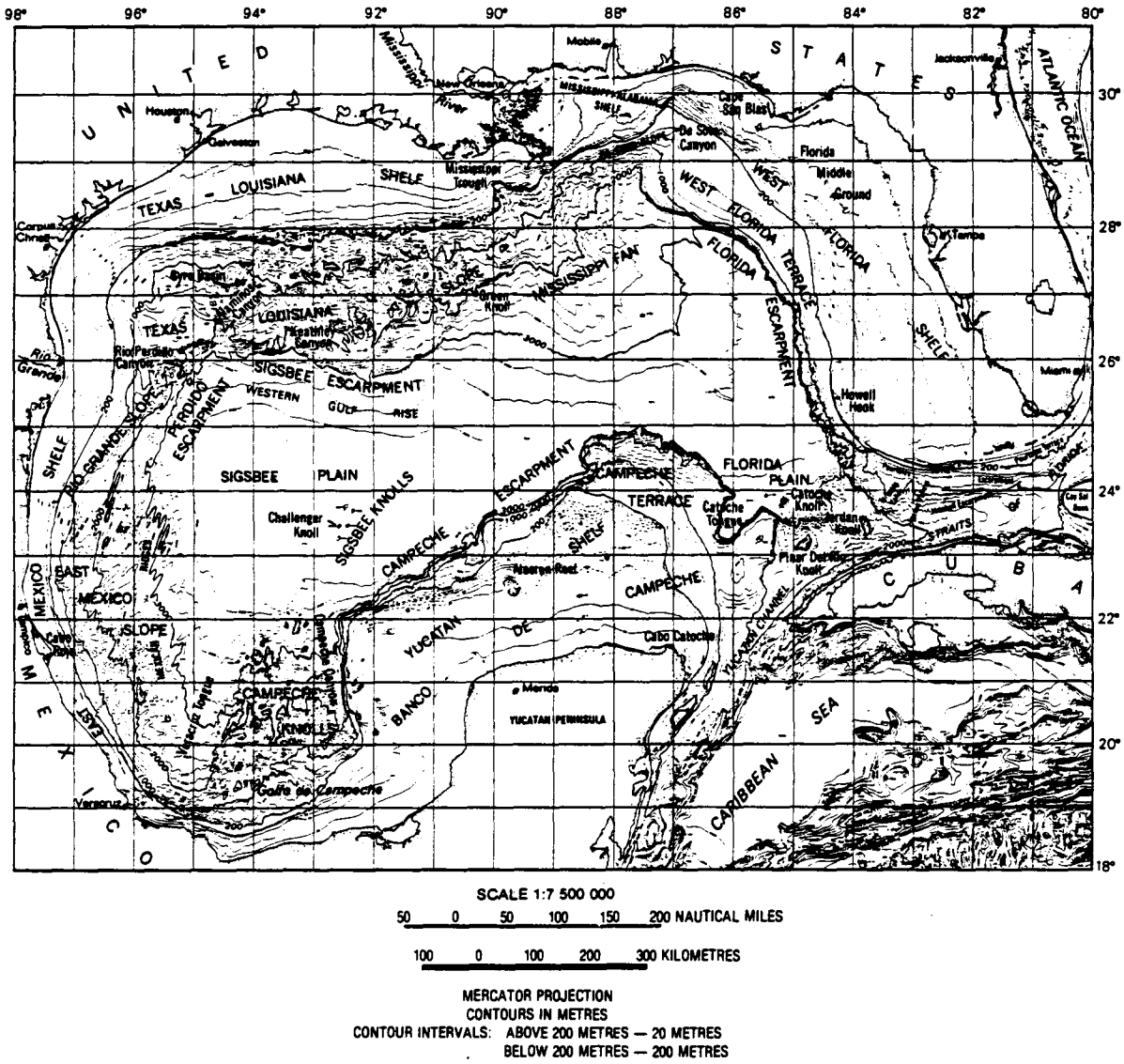

SCALE 1:7 500 000

50 0 50 100 150 200 NAUTICAL MILES

100 0 100 200 300 KILOMETRES

MERCATOR PROJECTION
CONTOURS IN METRES
CONTOUR INTERVALS: ABOVE 200 METRES — 20 METRES
BELOW 200 METRES — 200 METRES

Figure 1.1 Bathymetry of Gulf of Mexico region showing physiographic provinces and major topographic features. Contour intervals: 0 to 200 m in 20 m isobaths; > 200 m in 200 m isobaths. Reprinted with permission from Martin and Bouma (1978).

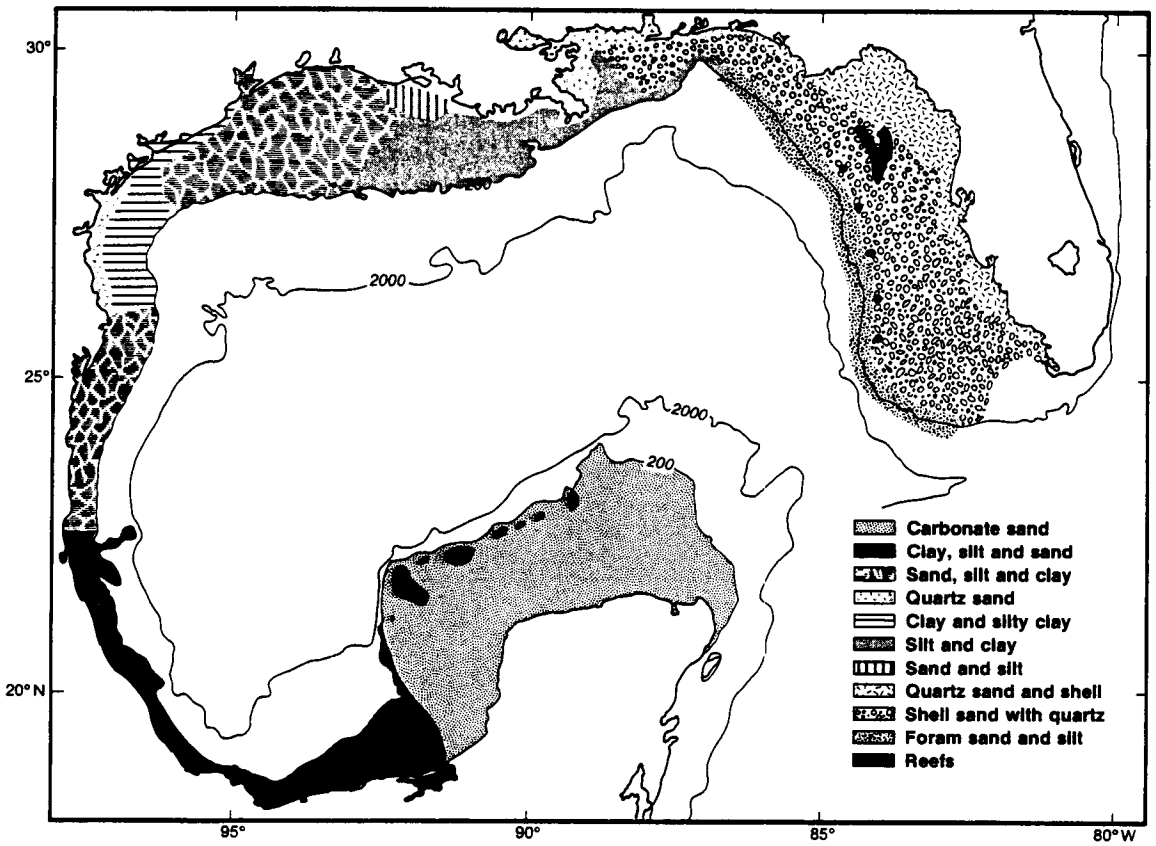

Figure 1.2 Sediment distribution, Gulf of Mexico Outer Continental Shelf.

salt diapirism, and the Sigsbee Escarpment is believed to be a wall of salt (Amery, 1978). The slope off the East Mexico shelf is characterized by a ridge system that is believed to be due to shale ridges at depth (Watkins et al., 1978).

Mississippi Fan

The Mississippi Fan is a very broad feature covering about 160,000 square kilometres in the bathyal and abyssal depth ranges. The fan has developed since Pleistocene time by the transport of sediment from the Mississippi River through the Mississippi Trough by slumping, debris flows, and turbidity flows.

Continental Rise and Sigsbee Abyssal Plain

The continental rise in the Western Gulf slopes gradually from the base of the continental slope and merges with the Sigsbee Abyssal Plain. The Sigsbee Plain is a very flat surface that has a maximum depth of 3700 m. It is underlain by turbidites and interbedded pelagic oozes.

GEOLOGIC HISTORY OF THE GULF OF MEXICO

Mesozoic Era

The basic structure and stratigraphic framework of the Gulf of Mexico was formed by events that took place during the Late Triassic and Jurassic periods (Salvador, 1980; see appendix for geologic time scale). Late Triassic and Early Jurassic time saw continental conditions in the area now occupied by the Gulf of Mexico. As the North American Plate began to move away from the African and South American Plates, tensional grabens began to form in the area. These were filled with red beds and volcanics. Due to continued subsidence of the area, Pacific waters began to encroach by way of Central Mexico in the latter part of the Middle Jurassic. Throughout the latter part of the Middle Jurassic and the early part of the Late Jurassic, the area was intermittently covered by shallow seawater that evaporated and produced the extensive salt deposits that are known today as the Louann Salt. Connection with the Atlantic Ocean was finally estabished late in the Kimmeridgian (Late Jurassic). At this time, evaporite conditions ceased and shallow marine limestones began to be deposited. Deposition of shallow marine limestones continued into the Middle Cretaceous (Aptian to Cenomanian) and culminated in an extensive shelf-edge reef complex composed mainly of rudistids, corals, algae, and foraminifers. The

reef complex occurs in the subsurface of south Texas, trends northeastward into southern Louisiana, and then trends southeastward to the West Florida Escarpment, where it has been sampled by rock dredging (Antoine et al., 1967; Bryant et al., 1969).

During Late Cretaceous time there was a marked rise in sea level, and the sediments of the northern Gulf became mainly sandstones, shale, marl, and chalk.

Cenozoic Era

The most significant feature of post-Mesozoic history of the Gulf has been the tremendous seaward growth of the Texas-Louisiana Continental Shelf. Early in Cenozoic Time the Gulf began to receive the detritus from the Laramide orogeny to the west and northwest. The major transporters of this sediment have been the Mississippi and Rio Grande Rivers. The supply of sediment has been so great that the rate of subsidence could not accommodate the great volume of material. As a consequence, the shelf edge prograded by as much as 400 km from the edge of the Cretaceous shelf to the present shelf break (Figure 1.3). This great wedge of sediment is illustrated in Figure 1.4. Note that the thickness of the sediments near the present coastline is approximately 15 km.

TEXAS-LOUISIANA CONTINENTAL SHELF

Physiography

The northwestern Gulf of Mexico shelf is dominated by one major (Mississippi) and two minor (Brazos-Colorado and Rio Grande) deltas. Other streams in the area are building deltas in bays and estuaries behind barrier islands (Figure 1.5). The sediments on the continental shelf reflect the environments of their adjacent coasts. This is to be expected as sea level has risen approximately 130 m during the past 16,000 to 18,000 years, and these same environments have migrated across the shelf to their present positions. Consequently, we have adopted the areas delineated by Curray (1960) to subdivide the sediments of the shelf and their adjacent coastal areas (Figure 1.5).

Central Louisiana Area

Of the four areas Curray (1960) defines, the Central Louisiana Area is most affected by the Mississippi River outflow (Figure 1.5).

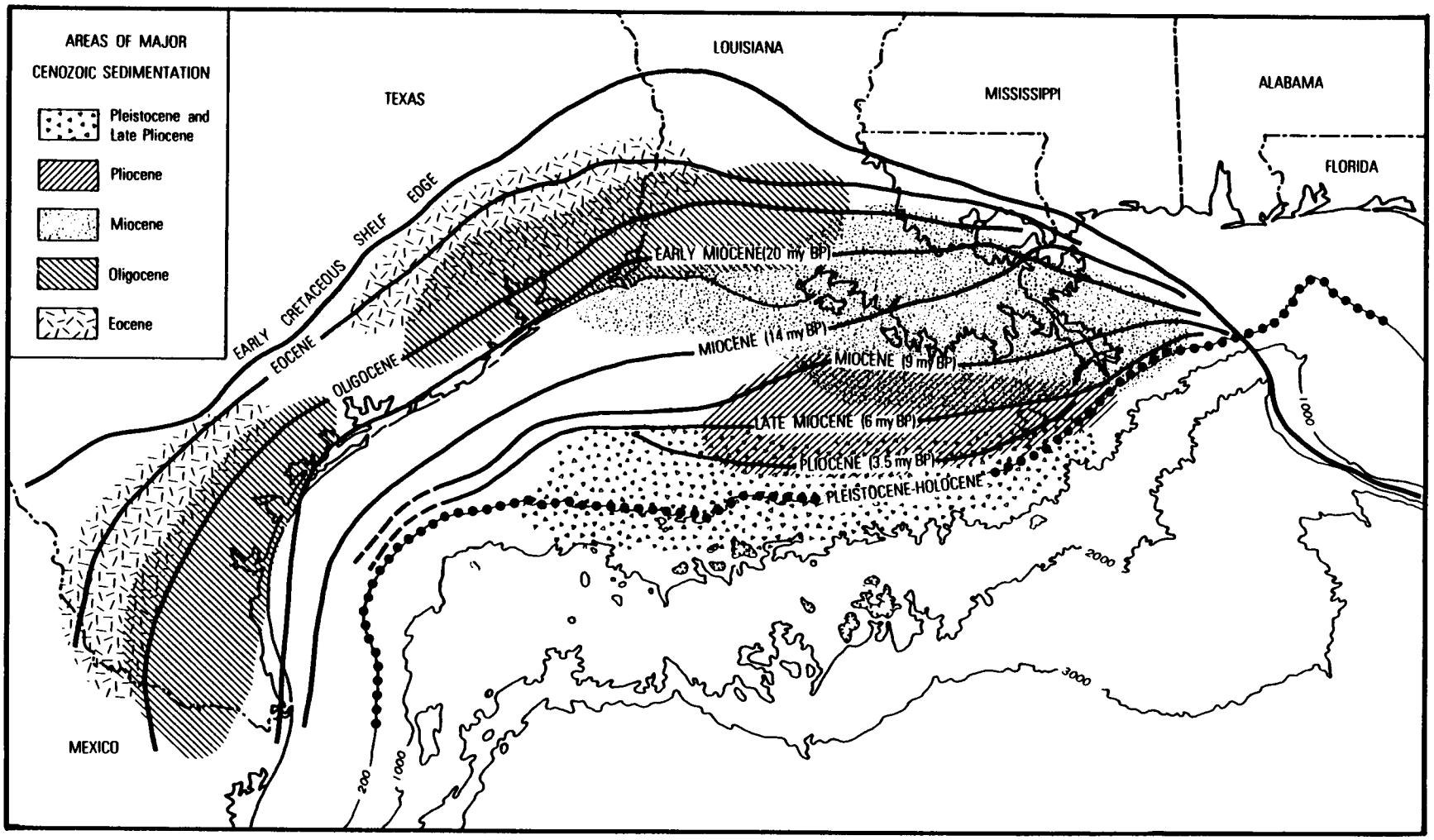

Figure 1.3 Sketch map showing paleoshelf edges in Gulf Coast basin and distribution of major Tertiary depocenters. Reprinted with permission from Martin (1978).

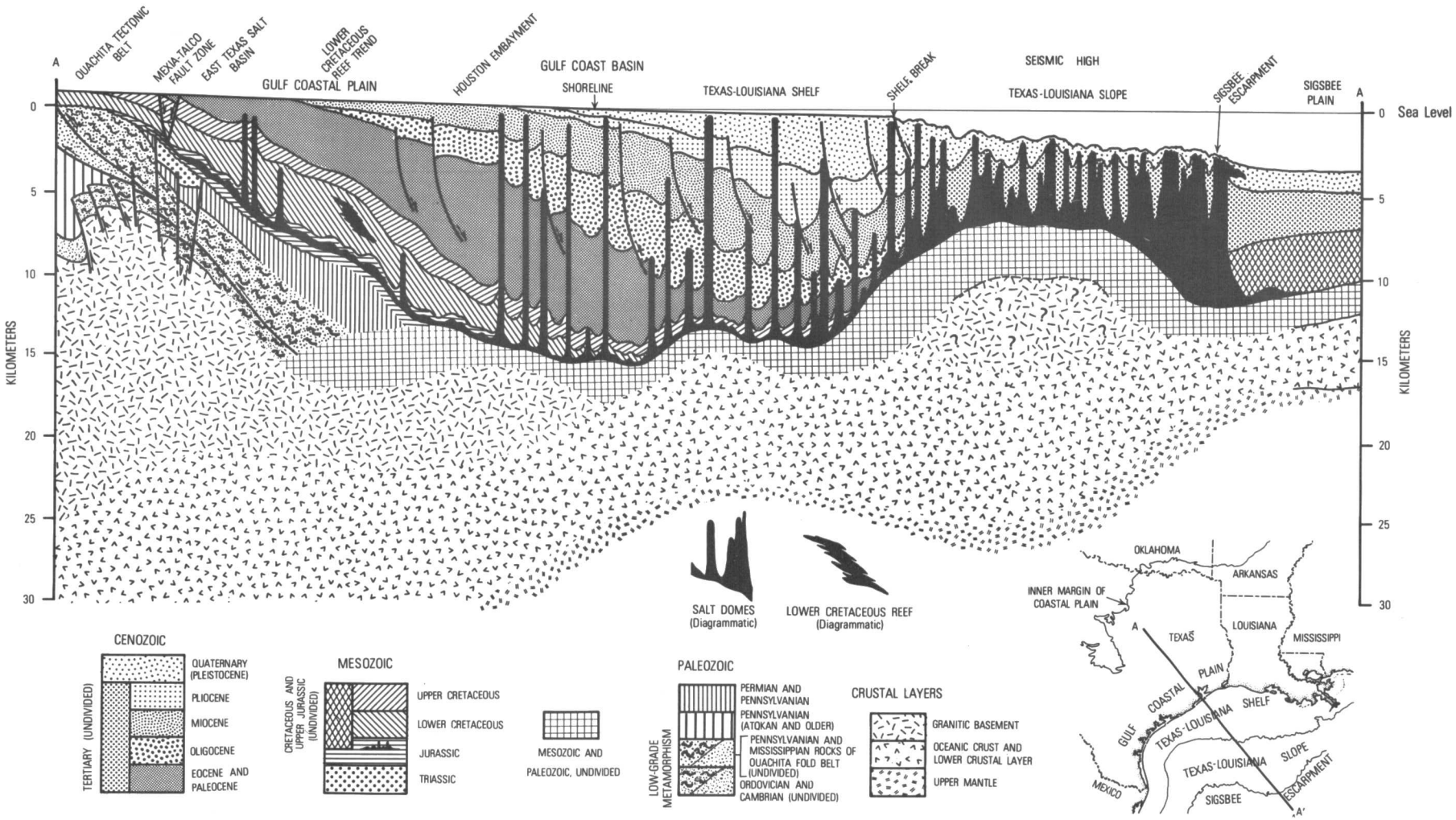

Figure 1.4 Generalized cross-section of northern Gulf of Mexico margin. Reprinted with permission from Martin (1978).

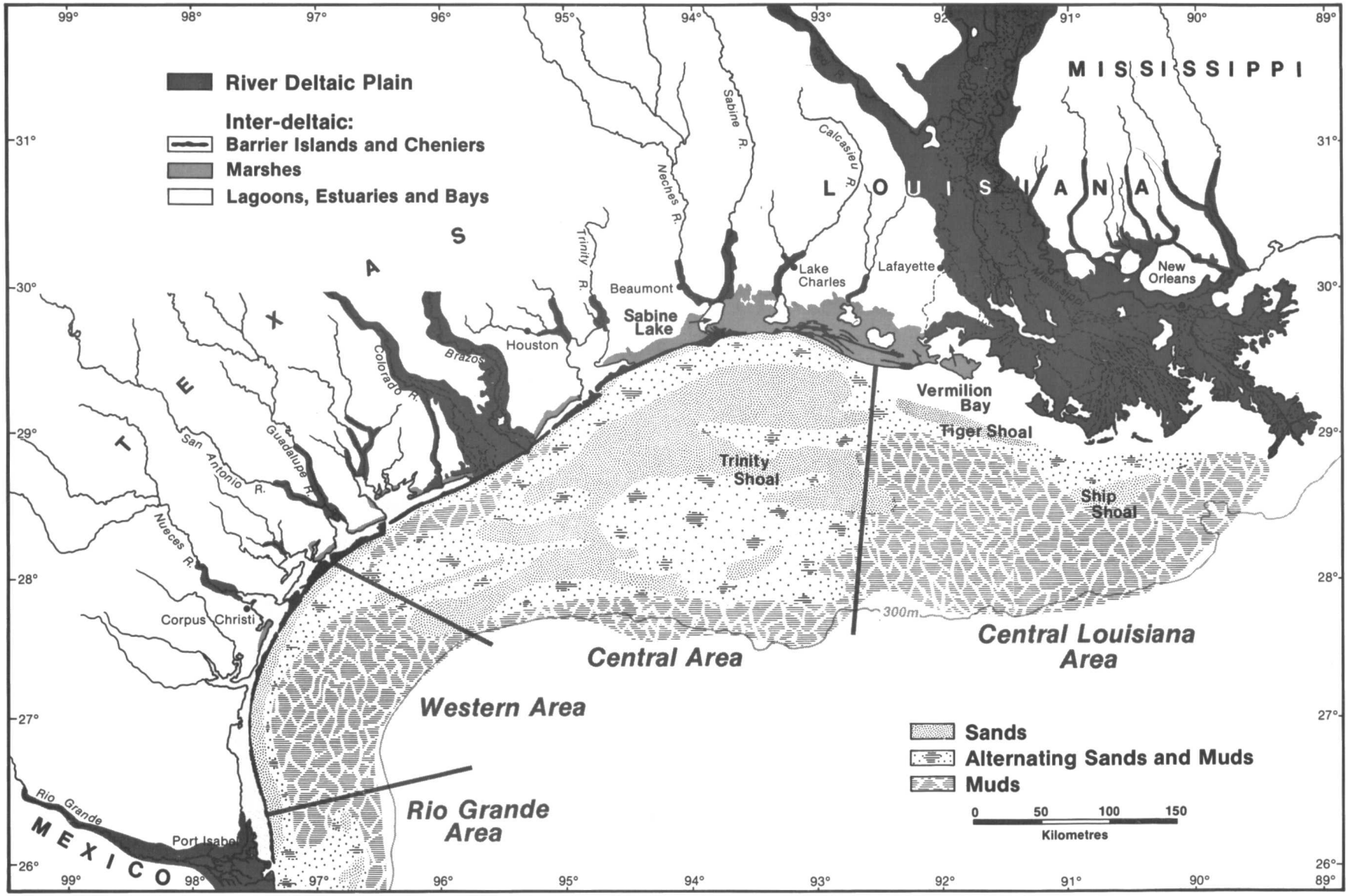

Figure 1.5 Coastal environments and shelf sediments, Texas-Louisiana continental shelf. Sediment distribution, after Curray (1960).

The western edge of this area is White Lake, just west of Vermilion Bay. The outflow of the Mississippi has migrated back and forth along this portion of the Gulf coast since Early Tertiary time. During, the Miocene, the outflow was close to Sabine Lake; since that time it has migrated eastward to Mississippi Sound and then back toward the west and its present position. Sub-bottom profiles in these areas show an abundance of sand-filled distributary channels with interdistributary swamp and lake deposits between them. Close to the shelf break, particularly near the head of the Mississippi Trough, large slumps and debris flows are common. Shoal areas, such as Tiger and Trinity off Vermilion Bay and Ship Shoal farther to the east, are probably remnants of the Late Pleistocene deltas.

Central Area

To the west of the present delta, from just west of Vermilion Bay westward to Sabine Lake, lies the area known as the Chenier Plain (Figure 1.5). This plain consists of low ridges of sand separated by marshy swales underlain by sandy muds. The sand ridges (cheniers) are beach deposits that have been formed in a rather unusual manner. LeBlanc (1972) presented a conceptual development model for these beach ridges. Shoreline accretion in this area is mainly by massive influxes of mud and sand from the Mississippi River Delta, eroded and transported westward into the Chenier Plain area where they are deposited as muddy tidal flats. Repeated minor fluctuations in sea level over long periods of time eroded the margin of the mud flats and winnowed the fine sediment particles, leaving a lag of fine sand and silt, with coarser shell debris along the shoreline. Later, renewed influx of muds moves the shoreline further seaward, and the cycle is repeated. The very rapid rate of sedimentation in this area has effectively sealed streams such as the Calcasieu and Mermentau Rivers, creating vast coastal marshes and lakes.

The coast between Sabine Pass and Port Isabel is characterized by barrier islands that separate lagoons and embayments from the main body of the Gulf of Mexico. Most of the streams that flow into the Gulf along this stretch of coastline do not drain very large areas, and climate varies from subhumid in the Galveston area to semi-arid south of Corpus Christi.

The Central Area extends to the southwestern tip of the Matagorda Peninsula. The Brazos-Colorado deltaic plain has filled in the lagoon behind the barrier island from the east end of Matagorda Bay to the west end of Galveston Bay. This process may occur very rapidly. For example, the Colorado River built its delta across the eastern area of Matagorda Bay to the Matagorda peninsula in a period of 25 to 30 years, between approximately 1930 and 1956. Since 1956 it has been building a delta outside of the

barrier bar. However, strong longshore currents carry a large amount of this sediment southwestward along the coast.

Western Area

The Western Area extends from the southern tip of Matagorda Island to a point about 10 miles north of Port Isabel. The area is characterized by an almost continuous barrier island and the absence of any major streams. The semi-arid nature of the climate in this area precludes any significant transport of sediment to the shelf along this stretch of coastline. This area could be designated as the South Texas interdeltaic plain lying between the deltas of the Brazos-Colorado complex and the Rio Grande River. Shideler (1977) shows the shelf sediments in this area to range from silty sands to muds. In the central part of the area, off Corpus Christi and Baffin Bay, the sediments are primarily clayey silts. The coarser sediments are close to the northern and southern limits of Shideler's study area, near the deltas. Sub-bottom profiles also show distinctive features of the interdeltaic plain. Pyle (1977) illustrates the sub-bottom structure in this area using minisparker records. Figure 1.6 (Pyle's Figure 16), a line across part of the ancestral Brazos-Colorado Delta, indicates abundant channeling in the youngest seismic unit. His Figures 15 and 19 show lines within the interdeltaic plain that indicate no channeling in the youngest seismic unit. Figure 1.7 is a reproduction of Pyle's (1977) Figure 29 showing a minisparker profile across Baker Bank. This line reveals the absence of channels and the very regular reflectors typical of this area.

Rio Grande Delta Area

The Rio Grande Delta was actively built during Pleistocene and Holocene time. Until recent times, the Rio Grande River supplied a significant amount of sediment to the continental shelf. However, with the construction of the numerous dams on the river, the amount of sediment transported by the Rio Grande has decreased significantly. Berryhill (1981) illustrates a major stream valley (possibly the Nueces River) that flowed southward along the inner shelf during the latest Wisconsin low sea level stand. This stream joined with the Rio Grande and contributed sediment to the ancestral Rio Grande Delta.

Hard Banks

Hard banks are distributed over the entire shelf from the Mississippi Delta to Port Isabel, Texas. Several hundred hard banks

are known to exist on the continental shelf and upper continental slope. Most of the banks are associated with salt diapirs, but many are not. Some are bare Tertiary and Cretaceous bedrock, while others are heavily encrusted by organisms associated with coralgal reefs (reefs built from both coral and coralline algae; Bathurst, 1975).

The coralgal reefs may be living, as they are at the Flower Garden Banks, or they may be drowned, as they are on the South Texas Shelf due to the presence of turbid bottom water. A line drawn from Port O'Conner (near Matagorda Bay) towards the shelf break, in a southeasterly direction, separates two major areas of hard banks. To the south lies an area of numerous midshelf banks that are not associated with salt domes; to the north and east is an area of mid and outer shelf banks that are mostly involved with salt tectonics, although some may be growing on shale diapirs.

Several classifications of banks have been proposed. These have been based upon various combinations of three factors: 1) position on shelf (nearshore, midshelf, and outer shelf); 2) total relief on the bank; and 3) water depths adjacent to the bank. Aside from the fact that there are no high relief features in nearshore, shallow water and that some of the banks in deeper water have high relief, there is little relationship between any of these factors. However, location on the shelf is a key factor: 1) it determines the maximum amount of relief on the bank; 2) it strongly affects maximum and minimum water temperature; and 3) relief and temperature control the distribution of the biotic assemblages on the banks. Position on the shelf also reflects the maturity of the underlying salt diaper (see Chapter 8).

Recent Sediments

The normal sediments on the Texas-Lousiana Continental Shelf are land derived sandy muds with varying amounts of biologically produced skeletal material. The sources of the land derived sediment are the major streams that flow into the northwestern Gulf of Mexico. The Mississippi River is the major sediment contributor, with an annual sediment discharge of 497 billion kilograms, of which 45% is clay, 36% silt, and 19% is very fine to fine sand (Everett, 1971). The other rivers of the region contribute minor amounts of sediment to the Gulf because their deltas are mostly in estuaries behind the barrier islands and beaches that are more or less continuous from the Calcasieu River to the Rio Grande. Curray (1960), in describing the distribution of sediments on the northwest Gulf of Mexico continental shelf, divided the shelf into four areas: 1) the Rio Grande area, 2) the Western area, 3) the Central area, and 4) the Central Louisiana area (Figure 1.5). The Rio Grande area and the Central area are characterized by sandy sediments. The Central Louisiana and the Western areas are underlain primarily by

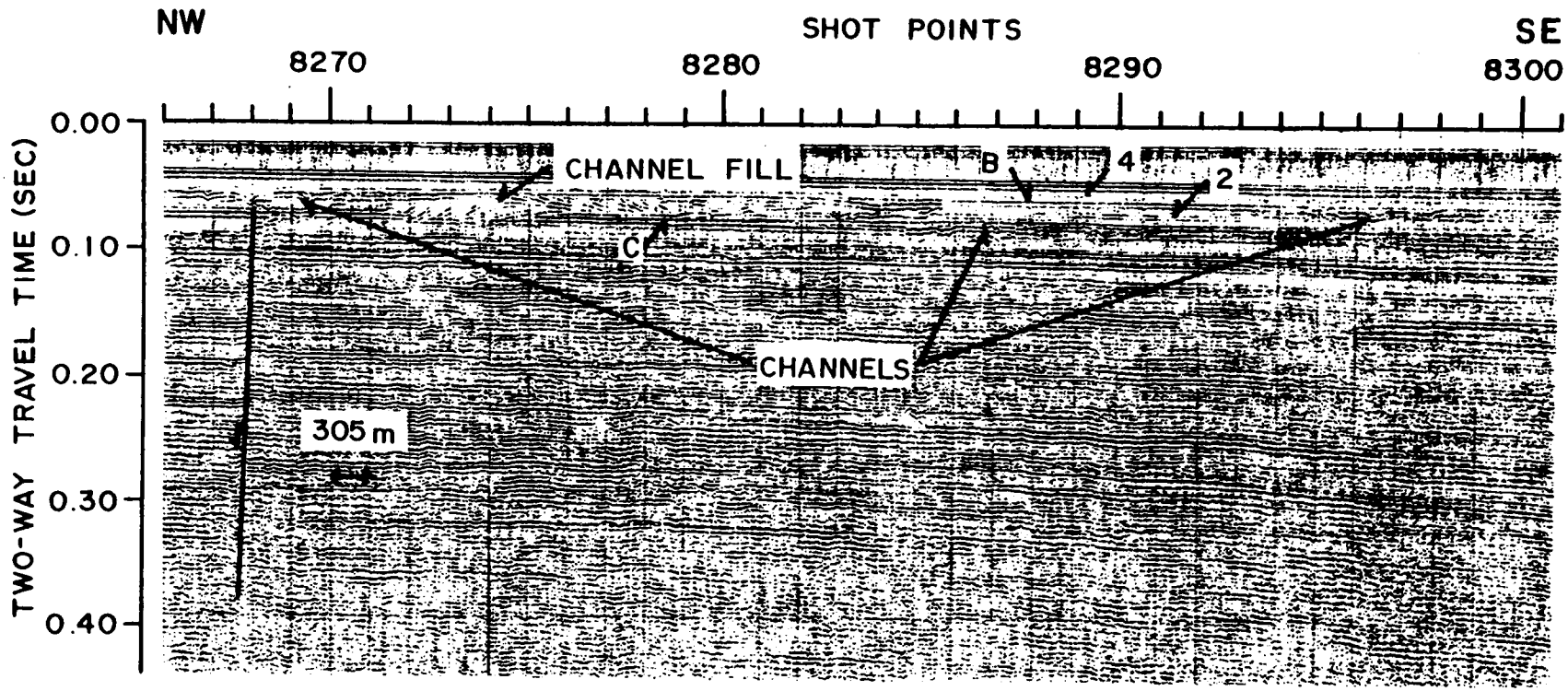

Figure 1.6 Sparker profile showing channeling in Holocene sediments off Matagorda Bay (Pyle, 1977). Vertical Exaggeration 12.5x.

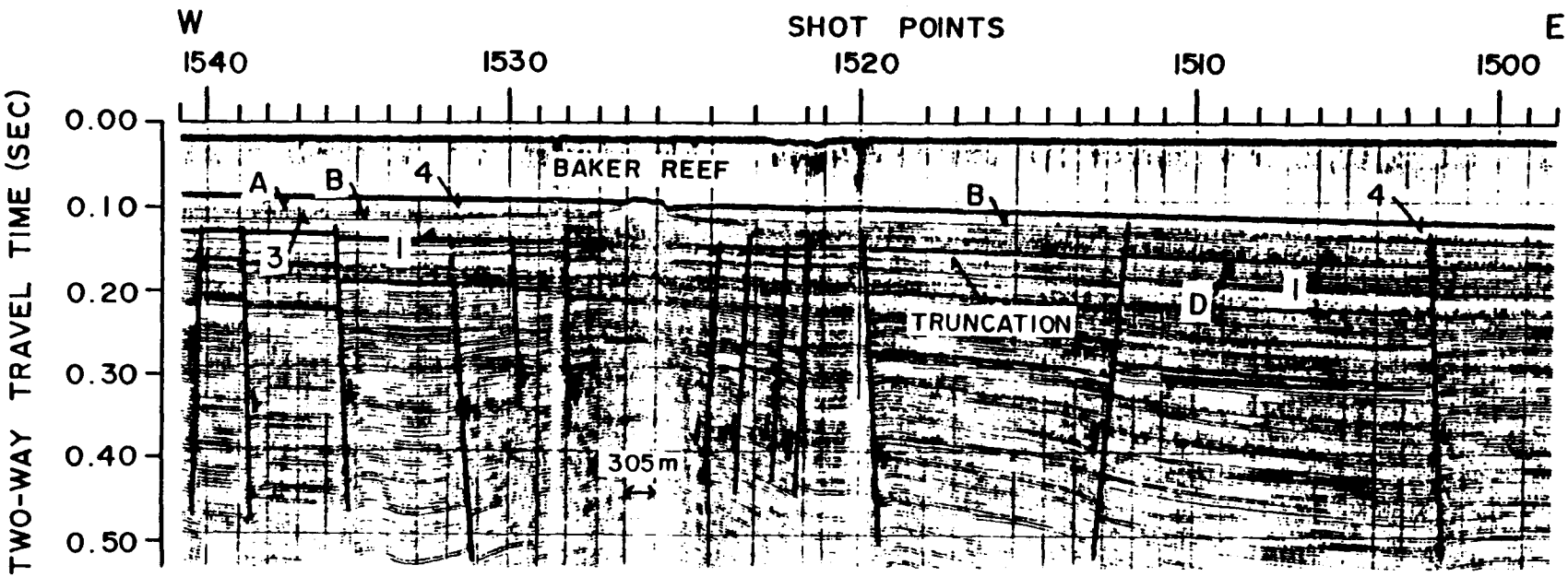

Figure 1.7 Sparker profile showing Baker Bank, a typical South Texas OCS bank (Pyle, 1977). Note continuous reflectors beneath bank. Vertical Exaggeration 11x.

muds. One of the significant conclusions resulting from API Project 51 (Curray, 1960) is that most of the transport of sand is only to areas close to the shoreline and that sand is not being transported from the rivers to any part of the middle or outer shelf between the Mississippi and Rio Grande Deltas. Silt and clay, on the other hand, are distributed independently of the sand. Sands on the middle and outer shelf are relict Pleistocene and Holocene sediments.

Much has been written concerning the sources of sediments on the Texas-Louisiana shelf (Van Andel, 1960; Van Andel and Poole, 1960; Davies and Moore, 1970; Shideler, 1978; Berryhill, 1975), and the consensus is that most of the sediment is derived from the Mississippi and Rio Grande Rivers, with some contribution from the Brazos-Colorado Delta (Berryhill et al., 1976; Davies and Moore, 1970). Heavy mineral studies cannot unambiguously determine the extent to which a certain source has contributed to a sediment or if indeed it has at all (Hawkins, 1983). In his study of the sediments in the Central area, Hawkins (1983) used quartz grain shape analysis to differentiate among the sources contributing to sediments on the shelf. The objective of his study was to compare the results of heavy mineral counts and quartz grain shape analysis (Ehrlich and Weinberg, 1970) to determine sources of fine sand in the area. Hawkins concluded that much of the sand in the Central area is a mixture of Colorado River, Brazos River, Trinity River, and Red River sands with very little influence in the sand fraction from the Mississippi River. Hawkins' conclusion that the sediments in this area are the result of the Pleistocene progradation of deltas across the shelf agrees with Winker (1982) and Curray (1960).

There has been much speculation concerning the rates of sedimentation on the Texas-Louisiana Continental Shelf. Van Andel and Curray (1960) suggested that rates will vary with time, depending upon the state of equilibrium between the rate and type of sediment supplied by the river and the rate of winnowing and redistribution by marine agents. Of the deltas formed by streams flowing onto the Texas-Louisiana Shelf, the Mississippi River Delta area has the highest rate of sedimentation and progradation because of the dominance of fluviatile over marine processes. The Rio Grande and Brazos-Colorado Rivers, on the other hand, do not transport the volume of sediment that the Mississippi does, and consequently marine processes dominate. Most of the sediment is removed from the area, leaving a narrow zone of littoral deposits along a non-prograding delta front. Other streams, such as the Nueces, San Antonio, Guadalupe, Trinity, Neches, and Sabine Rivers, flow into bays that are separated from the Gulf of Mexico by bay-mouth bars and barrier islands. These streams have little or no influence upon continental shelf sedimentation. As a consequence, the large area designated as the Central Area (Figure 1.5) by Curray (1960) has very low sedimentation rates, and in some parts of the shelf there are no sediments being deposited at the present time.

Curray's Central Area is underlain by relict Pleistocene and Early Holocene deltaic deposits as described earlier in this chapter.

Recent geochemical studies of sediments on the Texas Continental Shelf between Mexico and Matagorda Bay have used the ^{210}Pb method to determine sedimentation rates (Berryhill and Trippet, 1980, 1981a, 1981b; Holmes, 1982). Unfortunately, the Berryhill and Trippet papers do not include any text, and the Holmes paper is rather cryptic in that Holmes' maps are inconsistent with each other and with his text. Holmes (1982) states that of the 36 cores analyzed, 16 showed constant decrease in the log activity of ^{210}Pb versus depth, indicating a constant rate of sedimentation. Fifteen cores had no excess ^{210}Pb, indicating that there has been no sediment accumulation in the area of the 15 cores for at least the past 150 years. Yet Holmes' midshelf minimum sedimentation rate (his Figure 5) occurs in the same area as his high surface ^{210}Pb activity (his Figure 6). Holmes states that the ^{210}Pb activity in the sediments of the continental shelf ranged from 25 to 1.0 dpm/g (decays per minute per gram). However, Holmes' Figure 6 shows isopleths ranging only from 6 to 20 dpm/g.

A very disturbing feature of the maps in the Berryhill and Trippett publications and the paper by Holmes is the lack of conformity of the sedimentation rate isopleths to bathymetric contours. One would expect such high rates of sedimentation to be reflected in the bathymetry, but for some unexplained reason they are not (see Berryhill and Trippet, 1980, 1981a, 1981b; Holmes, 1982, Figure 5).

Classification of Sediments

At this point we need to discuss the principles of classification and how these apply to the sediments of the Texas-Louisiana shelf. These sediments range in composition from terrigenous through mixtures of terrigenous and carbonate skeletal sediments to pure carbonate sediments. Each of these three kinds of sediment has its own classification problems.

Sediments may be classified according to texture, mineralogy, or genesis. A textural classification is used to describe terrigenous sediments because they have been subject to transport from the continent by moving fluids. Determining the particle size distribution in such sediments allows interpretation of the process of transportation and the velocities required to transport the sediments. A greater flow velocity is required to transport a sand grain than is needed to transport a grain of silt.

The classification of terrigenous sediments in general use by sedimentologists today is that of Folk (1974). In his classification scheme, Folk used the grade scale devised by Wentworth (1922).

According to this grade scale, the diameters of the sediment particles are as follows:

Gravel	> 2.0 mm	
Sand	0.0625 - 2.0 mm	
Silt	0.0020 - 0.0625 mm	Mud
Clay	< 0.0020 mm	

Folk places major emphasis on the presence of even minute quantities of gravel because he regards the proportion of gravel as a function of the highest current velocity at the time of deposition. Consequently, even a trace of gravel (0.01%) is enough to term the sediments "slightly gravelly." This emphasis on the importance of gravel creates a problem when dealing with sediments that are mixtures of land-derived detritus and locally produced skeletal matter. For example, if an echinoid living on the bottom dies and its skeleton is buried by mud, sampling at that site will yield a sediment consisting of mud and the dissociated plates of the echinoid skeleton. In the analysis, these plates could conceivably amount to 5 or 6% of the sediment, requiring that it be classified a gravelly mud. Yet the presence of 6% gravel is in no way related to the current velocities at the time the sediment was deposited. Present studies indicate that the amount of gravel in the sediment on the OCS is not a function of the highest current velocities at that site but rather proximity to a reef, either living or drowned. This concept has not been understood by those who cite the presence of large amounts of gravel at depths of 60 to 100 m as an indication of strong bottom currents. The consequences of this erroneous reasoning have great bearing upon the theorized fate of pollutants introduced into the bottom boundary layer by shunting of cuttings and mud from drilling platforms.

In carbonate sediments, which are produced by biological activity and accumulate more or less in situ, textural analysis is of little value in the interpretation of the origin of the sediment. Carbonate particles, either whole or fragmented skeletons, give carbonate sediments a clastic texture that may be described in terms of the terrigenous sediment classification. However, the interpretation based upon that classification may be completely erroneous as it is not possible to distinguish between mechanically deposited carbonates (calcarenites) and sediments that accumulate by in situ deposition and fragmentation of skeletons (bioclastics) (Logan, 1969). The only textural parameter useful for in situ accumulations of carbonate sediment is the ratio between the amount of sediment finer than and coarser than 0.0625 mm. This will give an indication of the current regime at the depositional site, a clean skeletal sand indicating currents strong enough to remove silt- and clay-sized particles from the site, and a muddy sand indicating currents too weak to remove silt- and clay-sized particles. A

knowledge of the nature of the constituent particles is basic to the understanding of the origin of carbonate sediments. The sediment is intimately related to the fauna and flora from which it was derived, and the name of the carbonate sediment facies is derived from the dominant skeletal component in that facies.

Late Quaternary Sea Level Fluctuations

Poag (1973) reviewed the published record of Late Quaternary sea levels and compiled a list of 26 still stands and their ages in the Gulf of Mexico. Poag concluded that "it is fully expectable that the 'post glacial' sea level rose in cyclical pulses." However, eustatic changes in sea level due to the growth and withdrawal of the polar ice caps are complicated by isostatic and tectonic movements of the seafloor. Isostatic adjustments are caused by two mechanisms. Differential loading of the shelf by seawater during high stands of sea level causes depression of the outer shelf. Lowering of sea level removes the differential load, and the outer shelf begins to rebound. A more permanent isostatic adjustment is caused by sediment loading. The Mississippi River has been disgorging its sediment load onto the Louisiana shelf and slope since long before the beginning of the Pleistocene. Over 3048 m (10,000 ft) of shelf sediments have accumulated since the beginning of the Pleistocene in the vicinity of the Mississippi Canyon. The tremendous mass of the sediment has caused a major amount of subsidence in the area. McFarlan (1961) devised a graphic method for determining the amount of subsidence due to sediment loading. He estimated that the maximum structural subsidence following deposition of approximately 270 m of "post-glacial" sediment was 41 m in the vicinity of the head of Mississippi Canyon. Structural movement decreased to zero shoreward (approximately 30°N latitude) and laterally away from the axis of Mississippi Canyon (approximately 200 km east and west of the axis).

Tectonic movements are caused by salt diapirism. Tectonism may cause local shoaling (upthrusting of salt) or local deepening (dissolution of salt at crest of diapir and subsequent collapse of overlying sediments). Tectonism is probably the most important factor in creating errors in sea-level curves. Broecker (1961) casts serious doubt on the validity of McFarlan's (1961) sea-level curve. At best, sea-level curves based upon ^{14}C age dating alone are tenuous. Much more detailed information is needed on the regional nature and ages of unconformities in addition to the diagenetic history of the involved sediments.

The sea-level curves of Ballard and Uchupi (1970) and Curray (1960) seem to be fairly close except for the time between about 14,000 to 20,000 years BP. Ballard and Uchupi (1970) propose a low stand of sea level of -150 m at 15,000 years BP, while Curray's curve bottoms out at slightly less than -120 m at 20,000 years BP

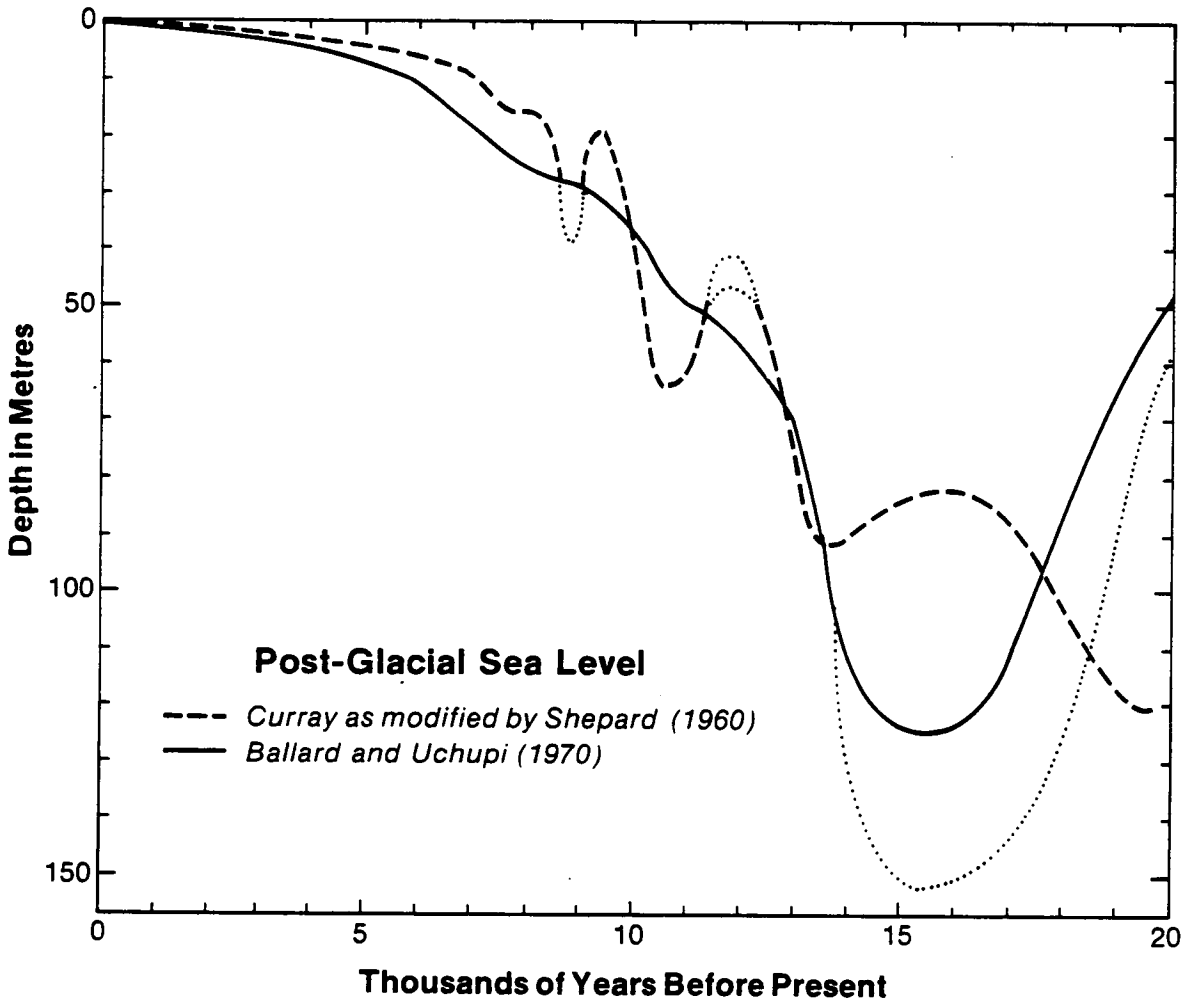

Figure 1.8 Post-glacial sea level curves. The dotted portions of the two curves are the original authors' indecision as to where the curve should be drawn.

(Figure 1.8). We have observed drowned reefs at about -150 m at the West Flower Garden Bank, which lends credence to that part of Ballard and Uchupi's curve. Changes in paleogeography as interpreted by Curray (1960) are shown in Figure 1.9.

Regional Structure

The major structural features on the Outer Continental Shelf are gravity faults and salt diapirs penetrating a thick monoclinal accumulation of Mesozoic and Cenozoic sediments (Figure 1.4). Gravity faults may be locally controlled by salt diapirs, or they may be regional in extent such as some growth faults that parallel the shelf break (Figure 1.10). Faulting associated with salt diapirs develops patterns that are controlled by regional stresses (Withjack and Scheiner, 1982). Martin (1978) proposed five significant causative factors as explanations of Gulf Coast growth faults: 1) crustal loading and basement tectonics; 2) slumping along shelf-edges and flexures as a result of rapid sediment accumulation; 3) salt and shale flow into local structures and systems of regional extent; 4) gravitational creep and sliding; and 5) differential compaction due to abrupt changes in sediment thickness and facies. Examination of bathymetric charts such as National Oceanographic Survey charts NH 15-11 (Bouma Bank), NH 15-12 (Ewing Bank), NG 15-2 (Garden Banks), and NG 15-13 (Green Canyon) reveals reentrants at the shelf break that more or less coincide with alignment of salt structures on the shelf and upper slope. The reentrants are real; they have been mapped by several different investigators. The orientation of these lineaments approximates the orientation of fractures in the Mississippi Embayment (Figure 1.10) and the Triassic and Jurassic grabens in northern and northwestern Florida (Figure 1.11). The 200 m and 500 m isobaths on Figure 1.11 between 90 and 94°W longitude show the orientation of the reentrants.

The similarity between these patterns and those of the pre-Middle Jurassic fault basins is striking. The modern fault systems are most likely inherited from the Early Jurassic structures in areas between the Middle Jurassic salt basins, where little or no salt was deposited. See Figure 1.12 for locations of salt basins in East Texas, Louisiana, and Mississippi. The same patchy distribution of salt could occur beneath the continental shelf. There are areas of higher and lower concentrations of salt diapirs on the continental shelf and slope off Louisiana and Texas (Figure 1.12). Lateral movement of the salt was caused by the overburden of the thick wedge of Tertiary sediments. The salt flowed into the faulted areas underlying the Late Cretaceous sediments and rose along faults, which were readily available avenues, to form the salt diapirs and ridges that we now see on the continental shelf and slope.

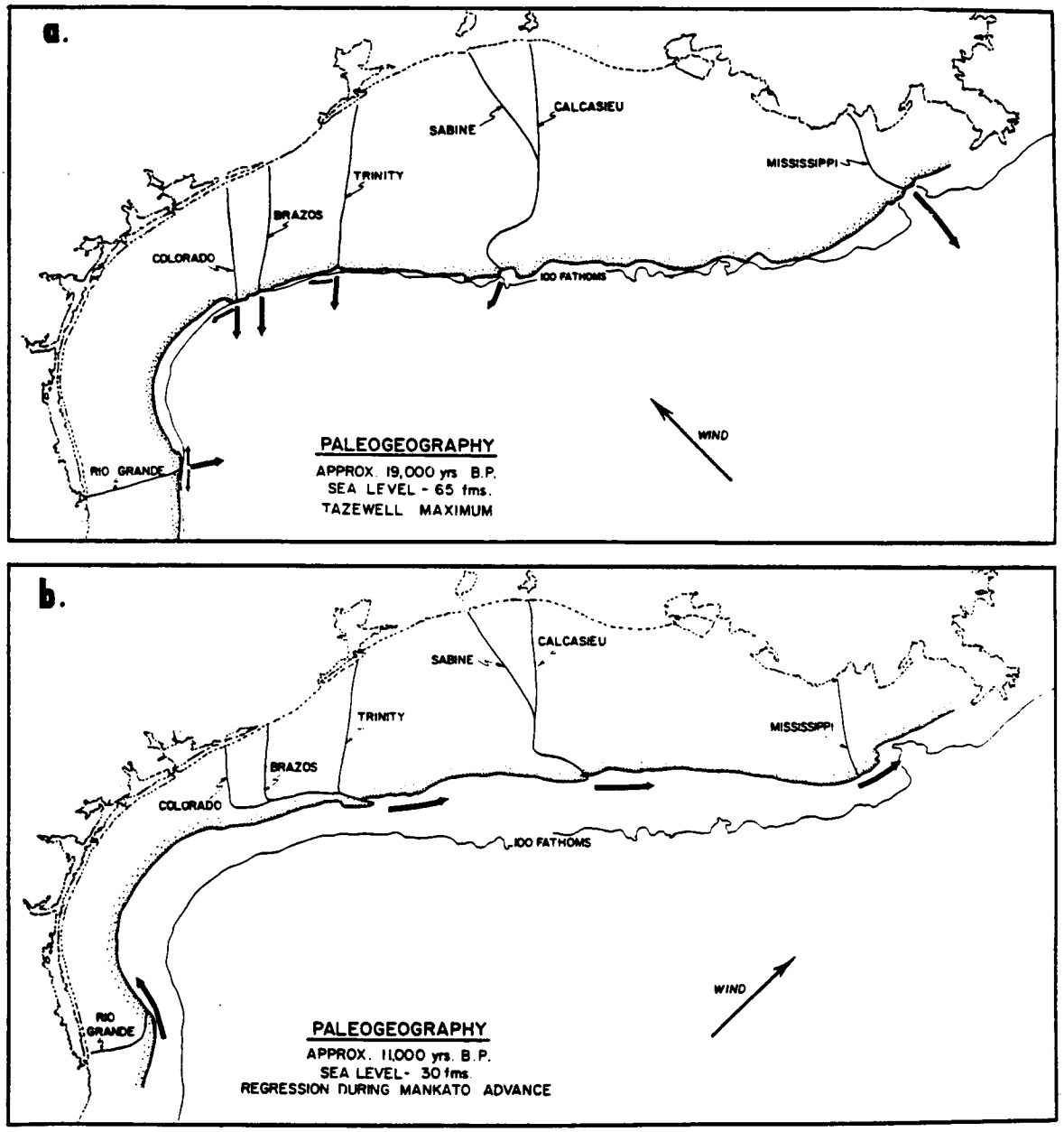

Figure 1.9 a) Paleogeography of the northwest Gulf of Mexico approximately 19,000 years B.P., when sea level is believed to have been at about -65 fathoms. This correlates with the maximum of the Tazewell glaciation. b) Paleogeography of the northwest Gulf of Mexico at about 11,000 years B.P., when sea level is believed to have been approximately -30 fathoms. This stage was during the regression from -22 fathoms to -35 fathoms during the advance of the Mankato glaciers of North America, following the Two Creeks interval. Wind was from the southwest during this period.

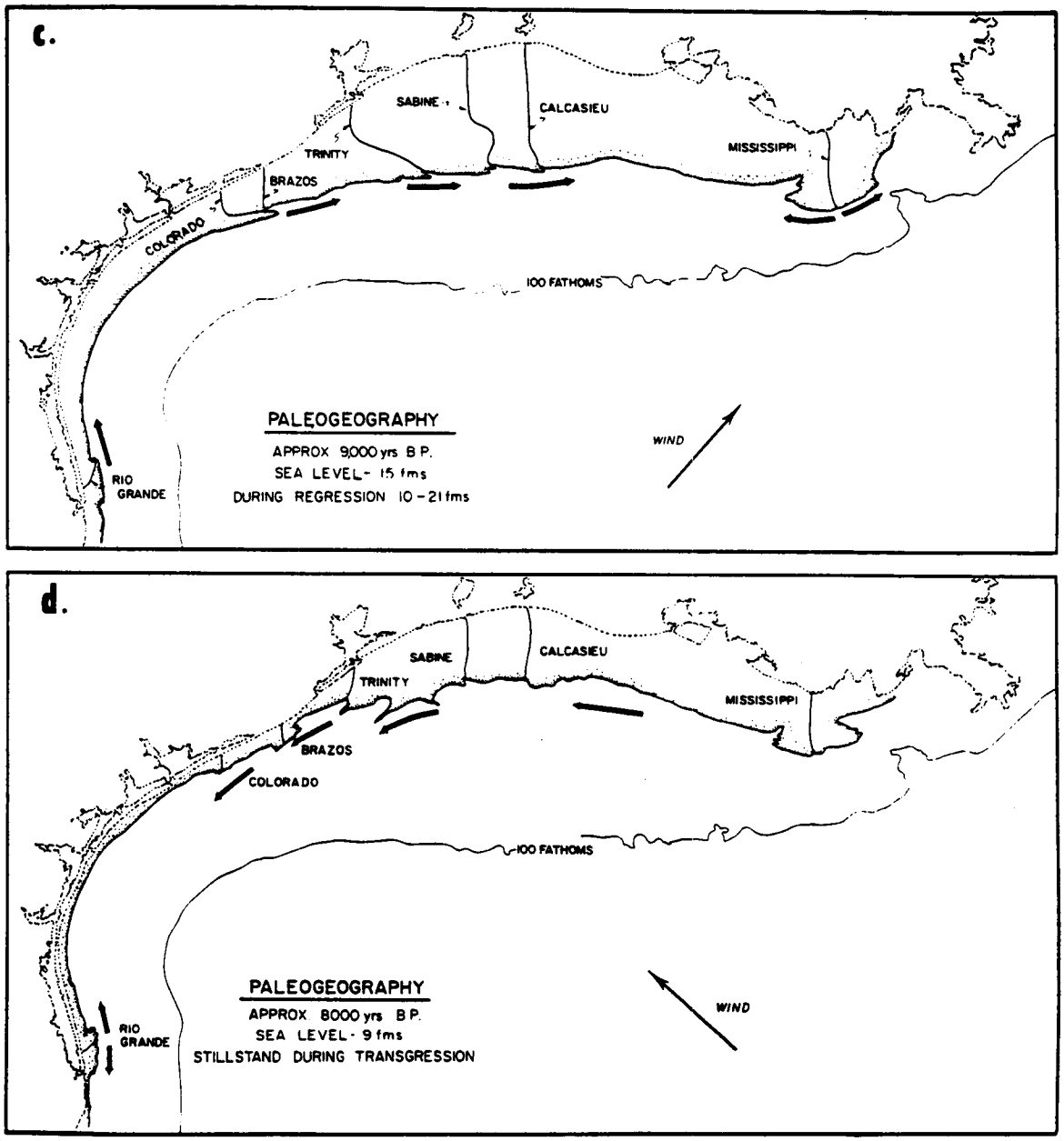

Figure 1.9 (Continued)
c) Paleogeography of the northwest Gulf of Mexico approximately 9000 years B.P., when sea level was at about -15 fathoms. This stage was during the temporary regression from approximately -10 fathoms to -21 fathoms. Wind was from the southwest during this period. d) Paleogeography of the northwest Gulf of Mexico approximately 8000 years B.P., when sea level was at about -9 fathoms. This was a period of stillstand of sea level before the final stage of transgression to the present level. Reprinted with permission from Curray (1960).

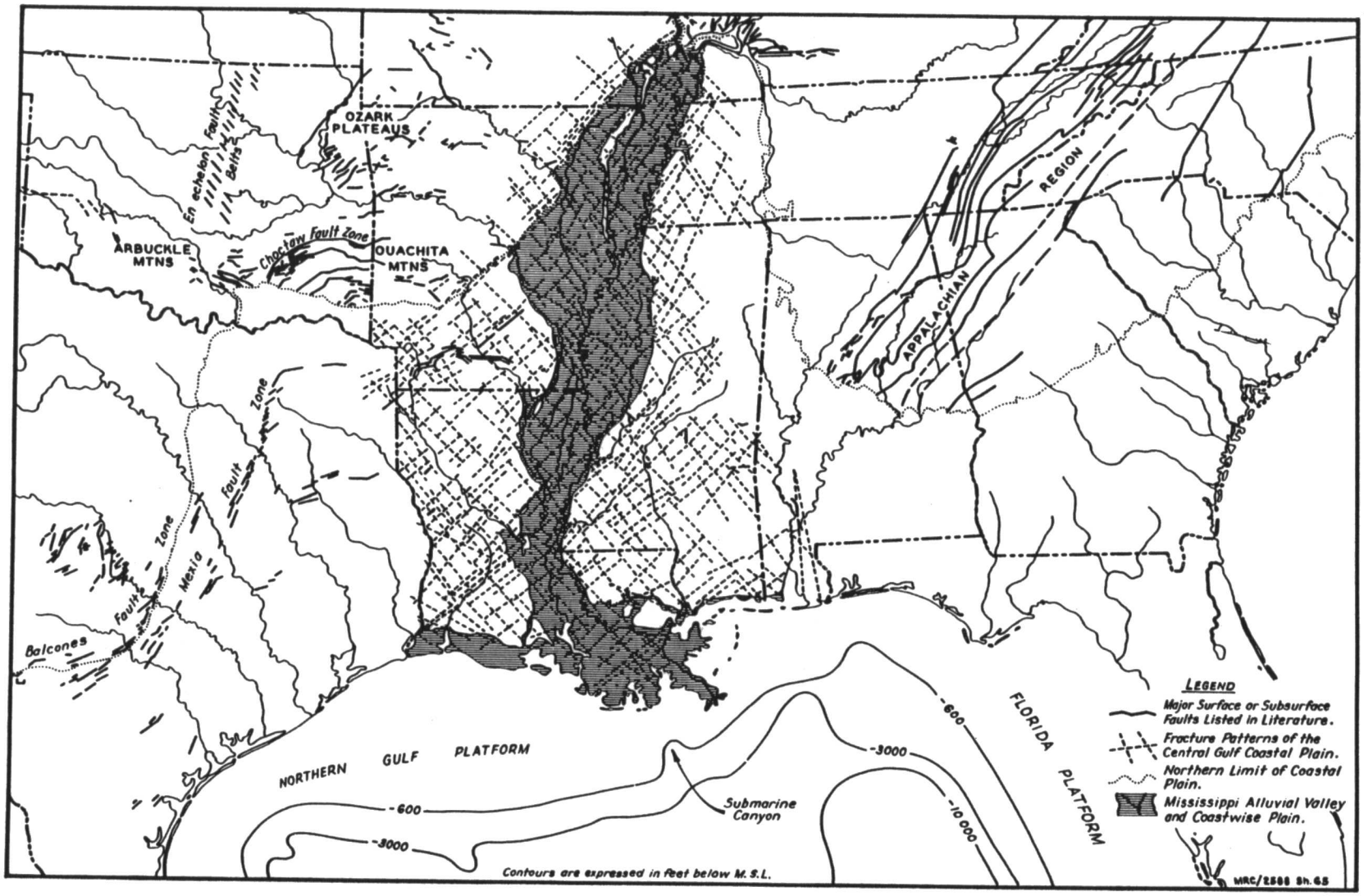

Figure 1.10 Regional fracture pattern of southern United States. Reprinted with permission from Murray (1961).

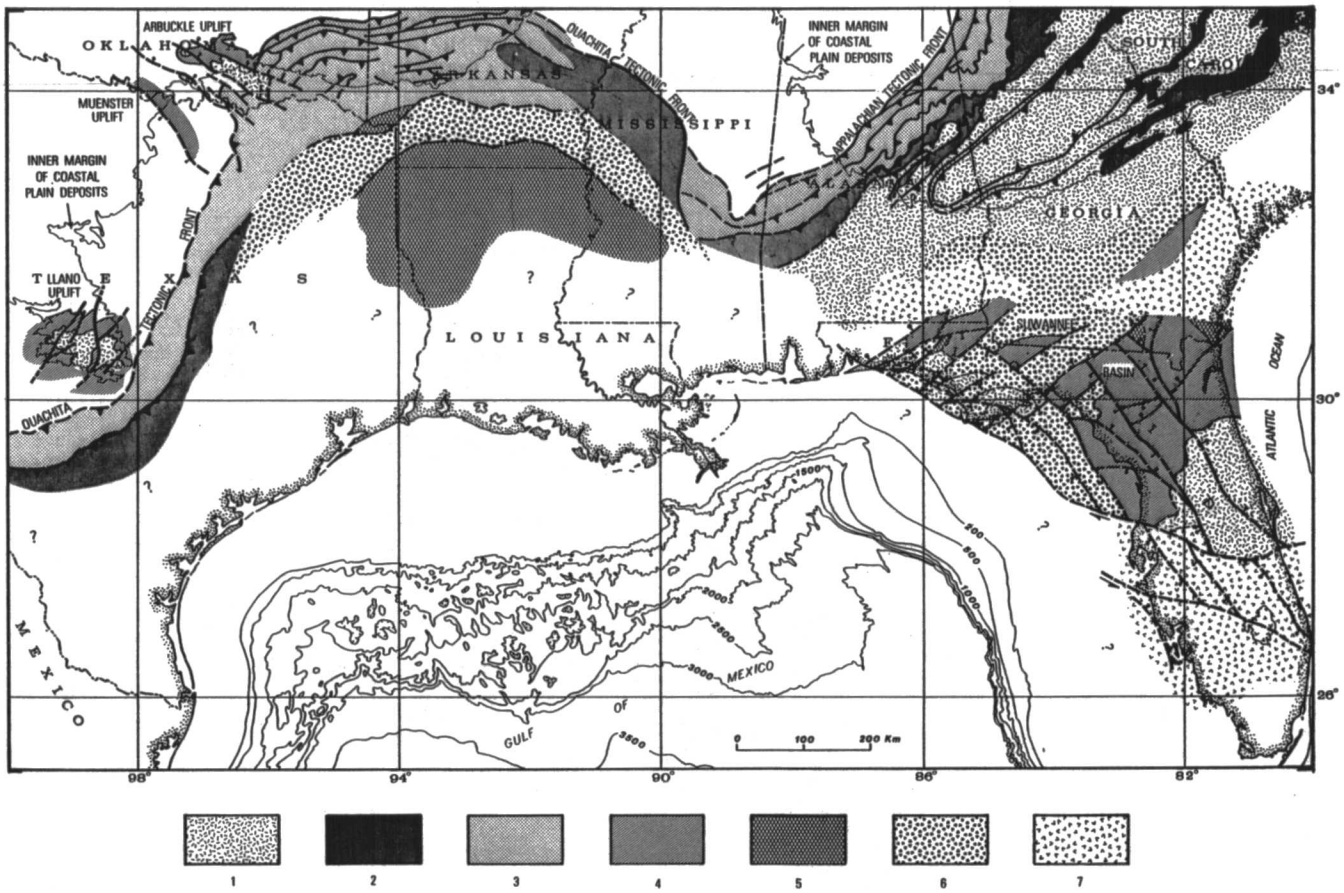

Figure 1.11 Distribution of pre-Middle Jurassic (Callovian) rocks in northern and eastern Gulf of Mexico regions. Explanation of patterns and symbols: (1) Precambrian and Paleozoic metamorphic and plutonic basement rocks; (2) Precambrian and Paleozoic metasedimentary rocks: slate, quartzite, marble, and schist; (3) Paleozoic sedimentary rocks deformed by Paleozoic orogenies; (4) Lower Paleozoic platform deposits, undeformed; (5) Upper Paleozoic platform deposits--undeformed; (6) Triassic and Jurassic graben deposits (red beds and diabase), Eagle Mills Formation, Newark Group, and equivalent; (7) Triassic and Lower Jurassic volcanic and plutonic complex, mainly volcanic rocks of Early Jurassic age. Bar and ball on downthrown side of normal fault; sawteeth on overthrust plate of reverse fault. Reprinted with permission from Martin (1978).

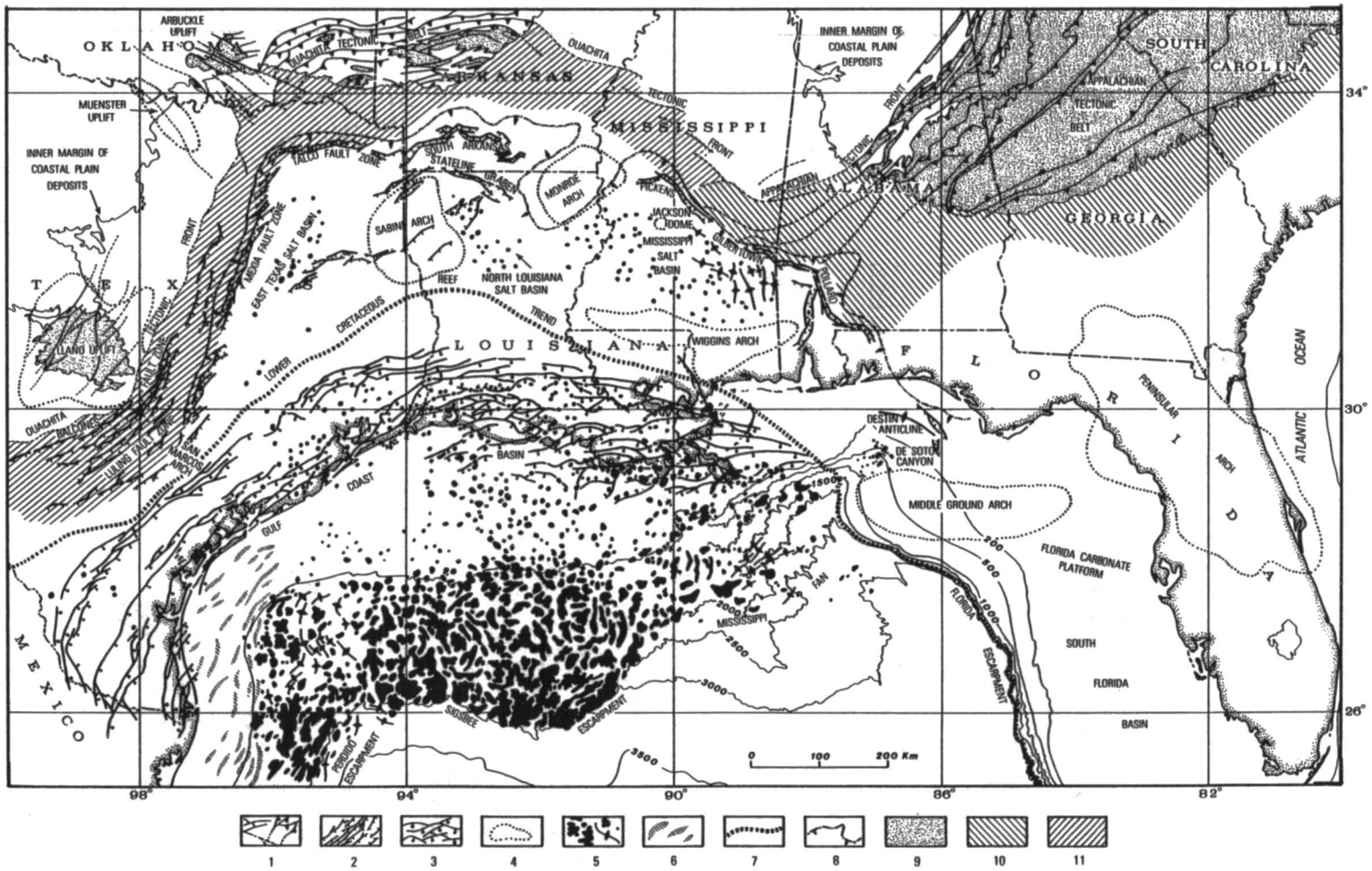

Figure 1.12 Tectonic map of northern Gulf of Mexico region. Explanation of patterns and symbols: (1) reverse fault, sawteeth on overthrust plate; (2) normal fault, hachures on downthrown side; (3) fault of undetermined movement; (4) broad anticline, or arch, of regional extent; (5) salt diapirs and massifs indicating relative size and shape; (6) shale anticlines and swells (non-diapiric), showing general trend; (7) Lower Cretaceous reef trend; (8) updip limits of Louann Salt; (9) uplifts of exposed Paleozoic strata and crystalline basement rocks; (10) buried Ouachita tectonic belt; (11) Blue Ridge and piedmont. Scale: 1° latitude equals 110 km. Reprinted with permission from Martin (1978).

SUMMARY

The Gulf of Mexico is a small ocean basin that originated approximately 160 million years ago (late Jurassic time) due to the rifting of the North American, African, and South American plates. The shallow, primordial Gulf has gradually evolved into its present configuration, being enlarged due to continued spreading, deepened due to subsidence, and being slowly filled by sedimentation. The spreading phase ended during the Cretaceous Period (approximately 80 to 100 million years ago). Sedimentation and subsidence will continue as long as streams flow into the Gulf from the continent and lime-secreting organisms continue to thrive in areas of low stream outflow.

The Western Gulf, from the Mississippi Delta to the Campeche Canyon on the west side of the Yucatan Shelf, illustrates very clearly the influence of deltaic sedimentation on the continental shelf of the Gulf. The Mississippi River, because of its great drainage area, has been the major contributor of deltaic sediments throughout Cenozoic time, and as a consequence has built an extremely large coastal plain - continental shelf complex in the northwestern Gulf of Mexico. The narrowing of the coastal plain - continental shelf complex southward into Mexico is due to the limited drainage areas of the streams flowing into that part of the Gulf.

The West Florida Shelf and the Yucatan Shelf are broad, shallow areas that are composed primarily of carbonate sediments produced by lime-secreting organisms. These areas of little or no continental sediment influx are underlain by thousands of metres of shallow-water carbonate sediments, indicating that accumulation of carbonate skeletons on the seafloor in these areas has kept pace with subsidence for many tens of millions of years.

The final structural complication in the northwestern Gulf is the formation of salt diapirs on the Outer Continental Shelf and continental slope. It is on these structures that most of the banks and reefs discussed in this report occur.

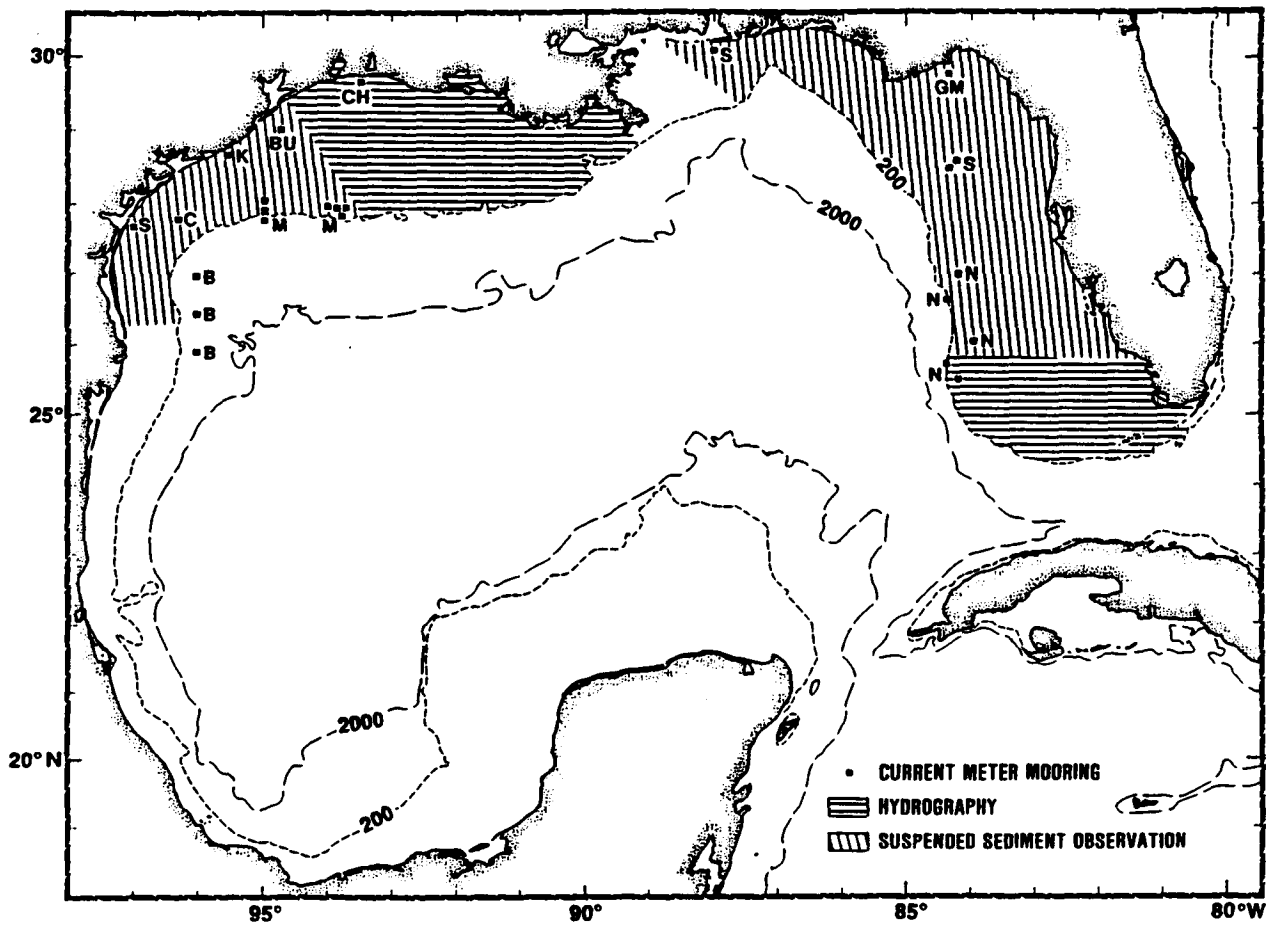

Figure 2.1 Distribution of data upon which this analysis of circulation, hydrography and sediment dynamics on the continental shelves of the Gulf of Mexico was based. The diagonal pattern indicates areas for which there is both hydrographic and suspended sediment data. The horizontal line pattern indicates areas for which only hydrographic data were available. The deployment periods for the current meters and the sources of these current meter data appear in Table 2.1.

Table 2.1 Deployment Periods of Current Meters in Gulf of Mexico, 1973-1983, Keyed to Notation in Figure 2.1

	Deployment Period	Sources
B =	July 1980 to February 1981	Brooks and Eble (1982)
BU =	September 3 to 4, 1973	Forristal et al. (1977)
C =	March 1978 - March 1981	Continental Shelf Associates (1982)
CH =	January 1979 to August 1979	Crout and Hamiter (1981)
GM =	August 1978 to September 1978	Marmorino (1982)
K =	1977 to 1982	Cochrane and Kelly (1982)
M =	March 1982 to May 1982, 95°W transect	This Report
M =	January 1979 to July 1981, Flower Gardens region	McGrail and Carnes (1983)
N =	August 1973 to April 1974	Niller (1976)
S =	October 1978 to December 1979, Florida Middle Ground and Anderson Reef	Hopkins and Schroeder (1981)
S =	43-day deployment, 1977, South Texas Shelf	Smith (1980)

CHAPTER 2

CIRCULATION, HYDROGRAPHY, AND DISTRIBUTION OF SUSPENDED SEDIMENT ON THE CONTINENTAL SHELVES IN THE GULF OF MEXICO

A firm knowledge of the behavior of the flow field over the continental shelves in the Gulf of Mexico is critical to understanding both modern sedimentary processes and the zoogeography on those shelves. Unfortunately, the quantity of high quality direct measurements of current velocities on these shelves is woefully small. The locations of current meter moorings from which either data or interpretation of data are available are shown in Figure 2.1. There is a substantially greater amount of hydrographic data available, but it is clustered geographically (see Figure 2.1), and the station spacings are rather coarse for resolving anything but large scale, long-term differences. As shown in Figure 2.1, observations of suspended sediment are exceedingly sparse, and are reported in such a variety of units that they are comparable only in a relative sense.

With that necessary caveat, it is also appropriate to state that it is possible to deduce a great deal of useful information from the data set available, in spite of its shortcomings.

FORCING MECHANISMS

A very limited number of mechanisms drive flow phenomena on continental shelves. However, they all vary with respect to the amplitude of their input, in both time and space, and they all operate at the same time. Those mechanisms are

- astronomical forcing (tides)
- atmospheric forcing (primarily wind)
- differential heating
- river runoff
- interaction with shallow flow of the deep basin.

Tides

Tides are a good place to start a discussion of forcing and flow responses because they are nearly alone in being truly periodic. Therefore, one can predict tide heights, phase, and currents for any station merely by observing the tides for a sufficiently long time without recourse to determining how the tide propagates or what its amplitude is in deep water.

Tides are, of course, caused by the gravitational attraction of the moon and sun. Out of this duo we are able to derive six major tidal constituents: the principal diurnal lunar tide (O_1); the principal diurnal solar tide (P_1); the diurnal luni-solar tide (K_1); the principal semidiurnal lunar tide (M_2); the principal semidiurnal solar tide (S_2); and the larger lunar elliptic (N_2). Of these six components, the most important (largest amplitudes) are the O_1, K_1, M_2, and S_2. In addition, there are fortnightly variations (Mf) in the amplitudes of these constituents as the moon goes through its phases relative to the sun. Maximum amplitudes occur when the sun and moon are aligned (in phase), and minimum amplitudes occur when the moon and sun are 90° apart (in quadrature). These changes are known as spring (maximum) and neap (minimum) tides.

In any given basin the tide may be directly forced by the variation in gravity, or it may be driven indirectly by entry of the tidal wave through a port or entrance. The latter is known by the term co-oscillating tide. It is also possible, of course, for the tide to be a combination of the two.

The Gulf of Mexico is essentially a small (1.555×10^6 km^2) ocean basin with two ports, one port located at the Florida Straits and the other at the Straits of Yucatan. The tides of the Gulf vary from diurnal (one high and one low tide per day) to mixed. The mixed tide is semidiurnal (two high and two low tides per day) but with a large inequality between the heights of the succeeding highs and/or lows. Representative tide records are shown in Figure 2.2. Note the contrast between the tides of the Gulf and those of Miami, which lies on the Atlantic seaboard where semidiurnal tides are the rule. The records also show that the Gulf of Mexico has a microtidal environment with a maximum range of less than 1 m.

Reid and Whitaker (1981) have shown, rather persuasively, that the diurnal portion of the tide is primarily a co-oscillating tide driven by that in the Caribbean Sea and Atlantic Ocean. They show that the contribution due to direct forcing is only on the order of 15%. For the M_2 and S_2 components, direct forcing accounts for 65% of the signal. From the results of their model, Reid and Whitaker (in press) suggest that the semidiurnal tide rotates counterclockwise about an amphidromic point at the tip of the Yucatan Peninsula. The tidal ellipses (major and minor axes) for the K_1 and M_2 tides from the Reid and Whitaker (in press) model are shown in Figures 2.3 and 2.4.

Atmospheric Forcing

The wind blowing over the sea surface produces three types of response in the sea, two of them direct and one indirect. First,

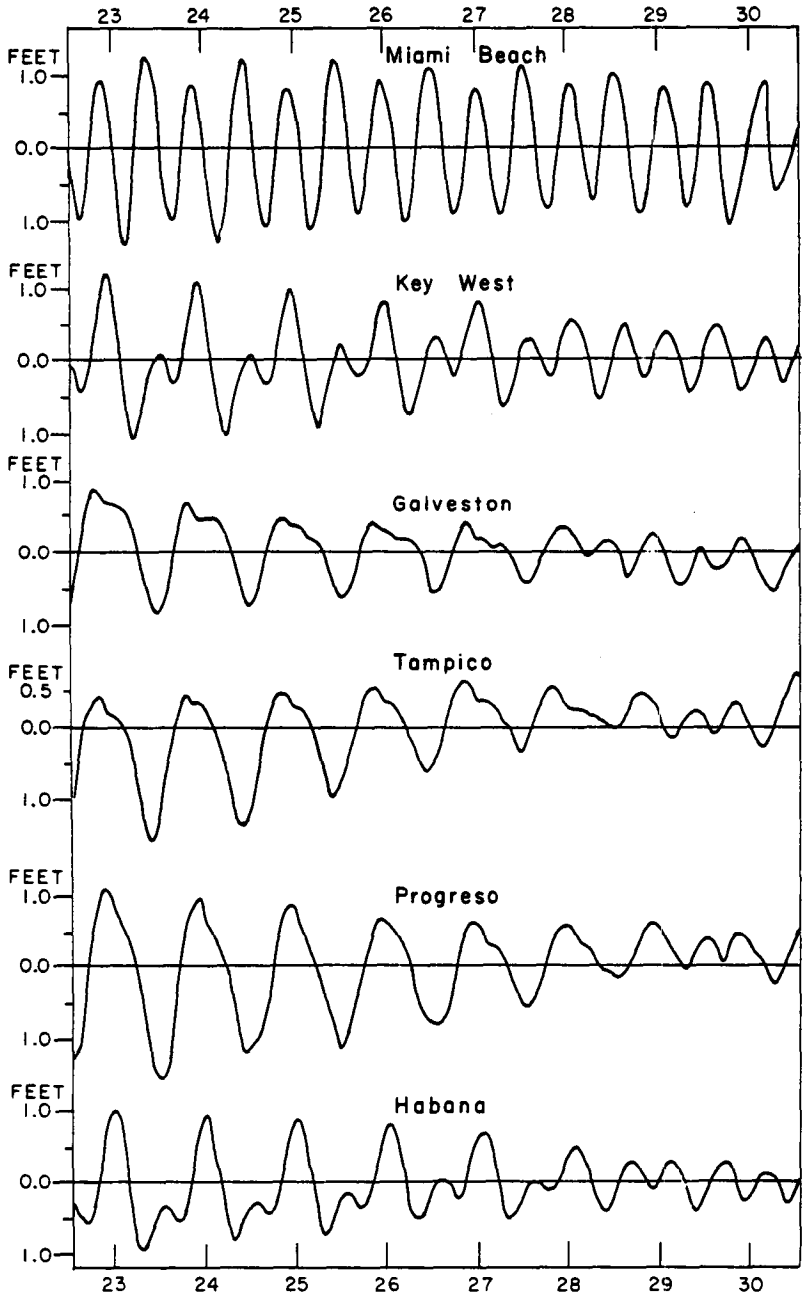

Figure 2.2 Tide curves at various places in the Gulf of Mexico, 23-30 June 1948 (Marmer, 1954).

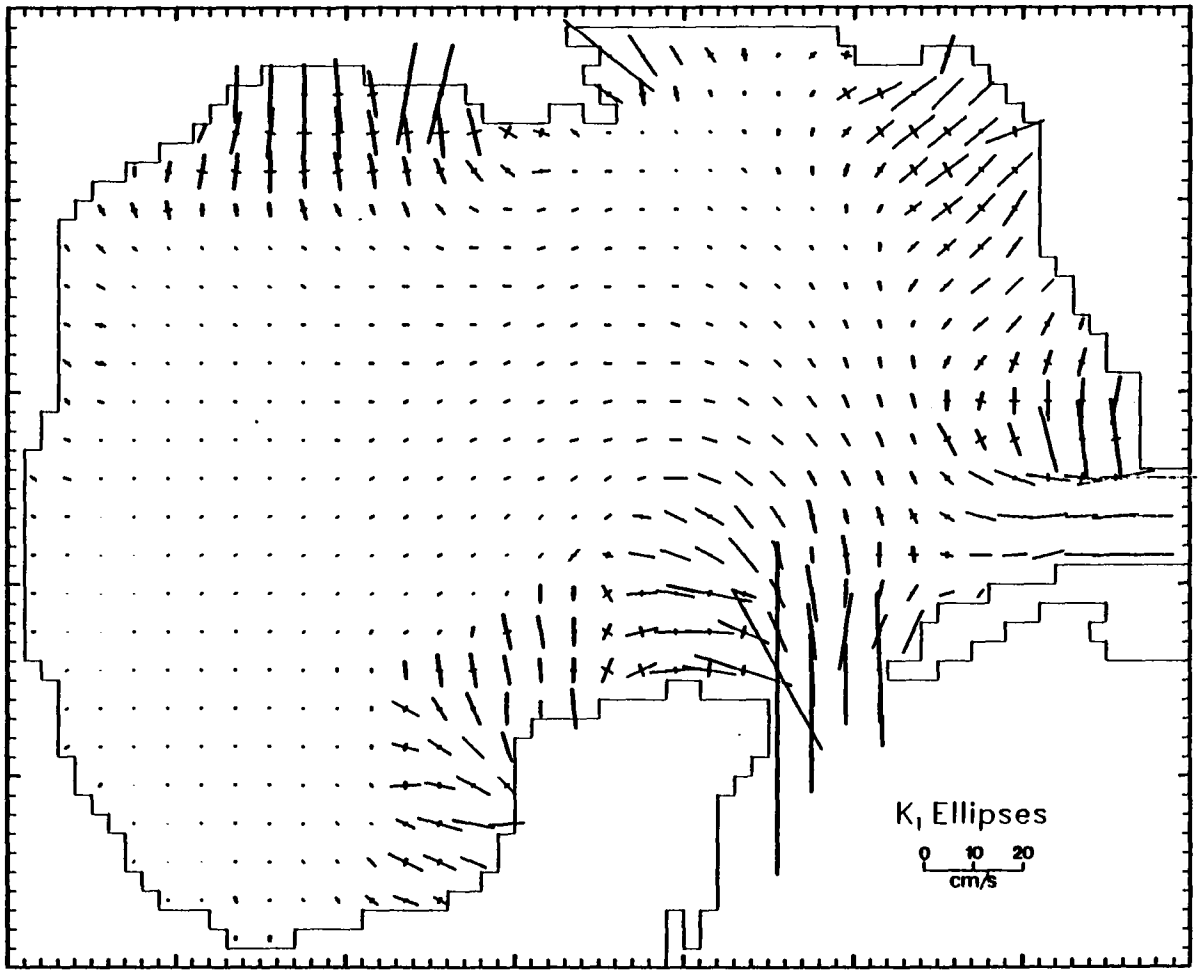

Figure 2.3 Ellipses for the K_1 diurnal tidal currents. The lines are the major and minor axes of the current ellipses in their proper orientation. The length of the axes are proportional to the speed in cm/s. Plots are courtesy of R.O. Reid and R. Whitaker, Texas A&M University (unpublished), based on a model described by Reid and Whitaker (in press).

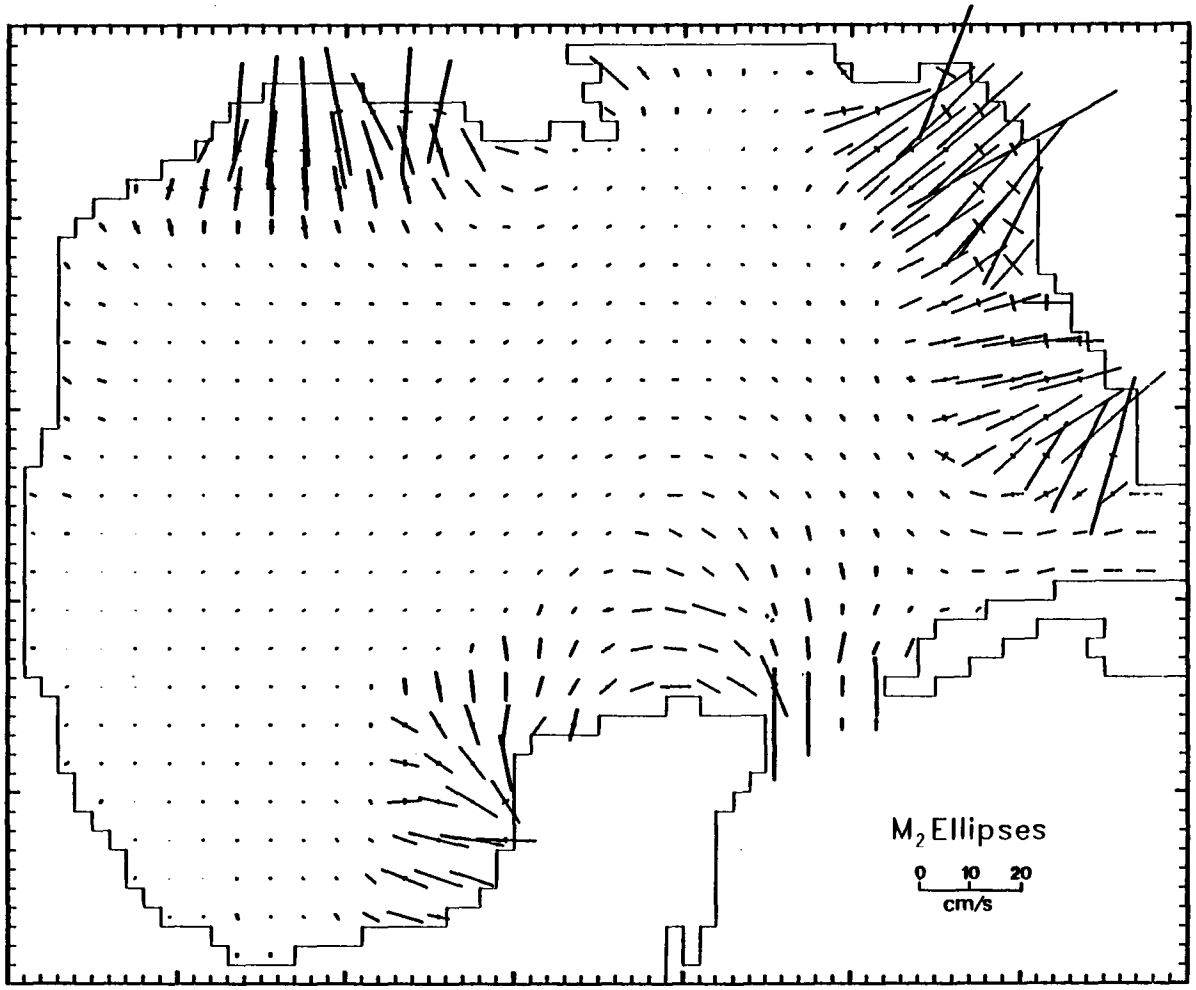

Figure 2.4 Ellipses for the M_2 semidiurnal tidal currents. The lines are the major and minor axes of the current ellipses in their proper orientation. The length of the axes are proportional to the speed in cm/s. Plots are courtesy of R.O. Reid and R. Whitaker, Texas A&M University (unpublished), based on a model described by Reid and Whitaker (in press).

the wind deforms the sea surface into that bane of mal de mers, surface gravity waves. It also induces surface currents by direct frictional drag (stress) on the sea surface. The frictionally driven currents redistribute water, producing horizontal pressure gradients between areas where the water is blown out and those where it is blown in. The resulting pressure gradients, in turn, drive flow which is only indirectly coupled to the wind.

Blumberg and Mellor (1981) computed wind stress over the Gulf of Mexico on a monthly basis at a 1° grid spacing from over a million reports of wind velocity from ship observations. They did this as input for a numerical model of the wind driven circulation in the Gulf of Mexico. The average wind stress vectors for January, March, June, and September from Blumberg and Mellor (1981) are shown in Figure 2.5. In January the regional wind stress over the Gulf is, in general, from northeast to southwest. By March the stress vectors have swung more westerly so that they are, in general, oriented east to west. In the summer months, represented by June, the Gulf has come under the influence of the Bermuda High Pressure system so that the stress vectors point primarily to the northwest. Where Blumberg and Mellor wind stress vectors can be compared with those calculated by Cochrane and Kelly (1982) from shore stations along the northwestern Gulf, they agree rather well, at least in orientation.

These monthly mean stress fields are perturbed in the winter by the intrusion of polar air masses into the Gulf. This intrusion takes the form of a frontal passage. Along the south side of the front there is usually a low pressure trough. Strong southerly winds flow into the trough heralding the approach of the cold front. As the front passes, strong north winds bring the polar air out over the Gulf.

In the summer and fall, tropical cyclones may migrate into the Gulf producing large anticlockwise wind systems that significantly alter the local flow field.

Differential Heating

Inequalities in insolation due to latitudinal variations across the Gulf produce horizontal variances in the water density. This produces variances in the pressure field and that, in turn, causes circulation. One might think of it as convection on a very large scale.

On the shelf, winter cold air outbreaks can extract very large amounts of heat from the shelf waters, thereby altering their

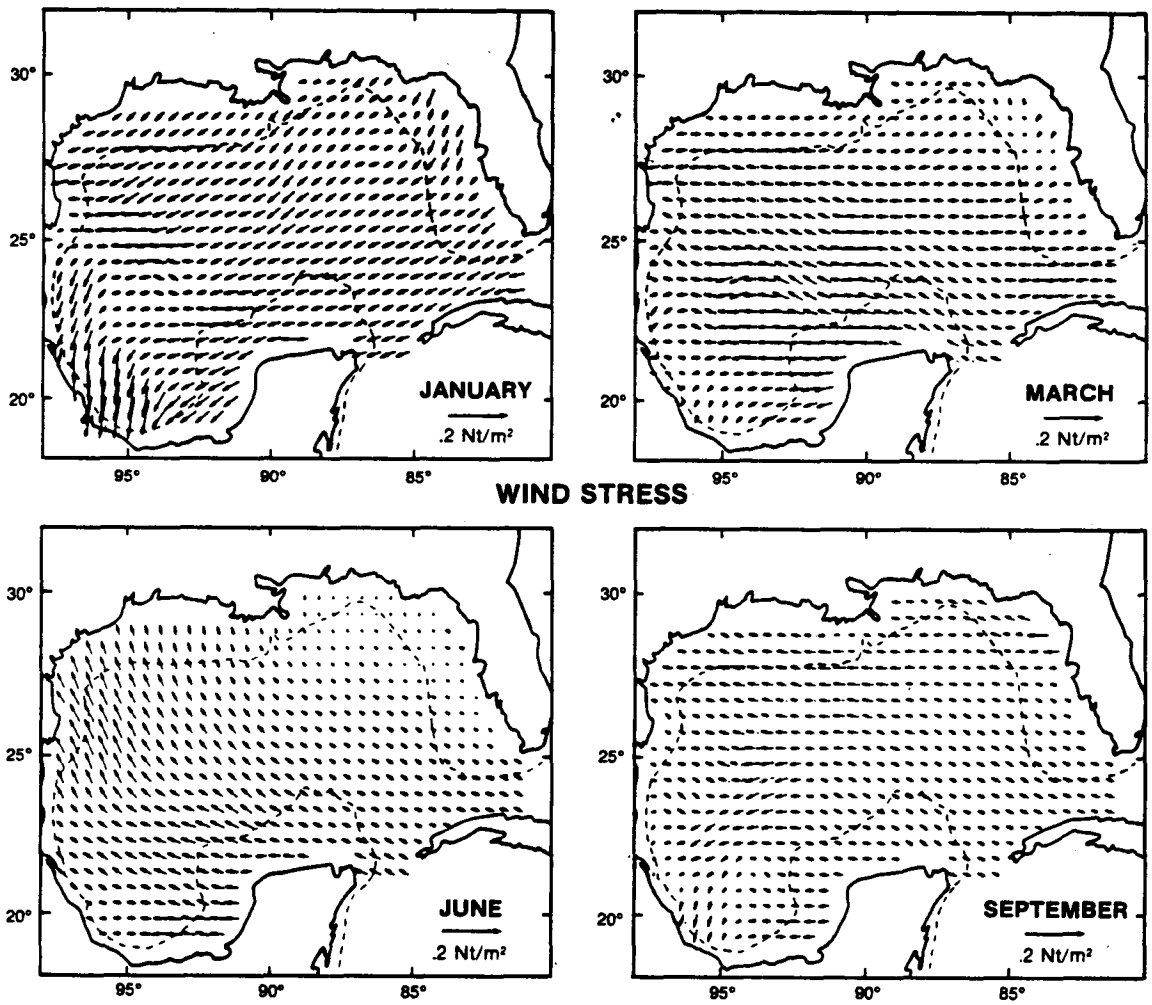

Figure 2.5 Mean monthly wind stress vectors for the Gulf of Mexico (after Blumberg and Mellor, 1981).

density structure. These changes can happen over very short time scales.

Runoff

The Louisiana continental shelf receives the outflow of one of the world's largest rivers, the Mississippi. At peak discharges in April it can deliver more than 10^4 m^3/s to the Gulf. This volume of water poured on the surface of the Gulf produces strong local pressure gradients that induce currents which would not otherwise exist. The outflow also produces the classic estuarine responses, with surface flow out away from the river mouth and bottom flow toward the river mouth.

Cochrane and Kelly (1982) show that the outflow hugs the Texas-Louisiana coast throughout much of the year and is augmented by the outflow from rivers to the west of the Mississippi. They suggest that this stand of brackish water along the coast sets up a pressure gradient that adds to the wind-driven, west-to-southwest mean flow along the Texas coast.

Interaction with Shallow Flow of the Deep Gulf

In addition to locally produced circulation, the Gulf is intruded by a jet of swift flowing water, the Loop Current. This current enters through the Yucatan Straits and exits through the Florida Straits after "looping" up toward Alabama. The northward extension of the Loop Current in the Gulf varies considerably. Its descending limb courses along the steep Florida continental slope. This flow fluctuates, causing cross-shelf variances in the horizontal pressure and, one would suspect, a flow field. It also should entrain some of the shelf-edge water and drag it toward the south. As the Loop Current enters the Gulf, it often becomes unstable and develops meanders. These may pinch off and form rings that propagate into the western Gulf (see Elliott, 1982, and Merrell and Morrison, 1981). These rings may also influence flow on the outer shelf and slope off Texas as they spin down.

WIND-DRIVEN SURFACE FLOW AND THE LOOP CURRENT IN THE DEEP BASIN

One of the simplest methods of studying surface flow is the use of drifters. Unfortunately, surface drifters provide only two data points (drop position and time, and location and time of retrieval), so the path from start to end cannot be traced. Some conclusions can, however, be drawn about wind-driven surface flow.

The Office of Naval Research supported a project by researchers at Texas A&M University to deploy a large number of woodhead drifters from research vessels and ships of opportunity passing through the Caribbean Sea and Gulf of Mexico. The project ran from 1975 through 1978.

Woodhead drifters are yellow plastic disks 18 cm in diameter with red plastic stems 52 cm in length. A serial number, offer of reward for information regarding the date and location of the drifter's recovery, and address of the researcher are imprinted on the disk. In the period from October 1975 through December 1978, 15,684 of these drifters were released. The statistics of the releases and recoveries were reported by Parker et al. (1979). Of the 15,684 drifters launched, reports on 2127, or 14%, were returned to Texas A&M University.

A rather remarkable observation arising from the study is that drifters released anywhere in the Gulf of Mexico west of a line from the Mississippi Delta to the middle of the Yucatan Strait washed ashore, almost exclusively, on the Texas shore. The greatest number of drifters were found between the southern tip of Padre Island and Galveston Bay. Drifters released to the east of the above mentioned line were found, almost exclusively, on the east coast of Florida in the area between Miami and Cape Canaveral. This includes drifters released on the West Florida Shelf.

This distribution fits well with expectations based on the wind stress fields of Blumberg and Mellor (1981) (Figure 2.5) and a knowledge of the Loop Current. In general, the wind stress should produce a significant westward drift in the surface waters of the Gulf of Mexico. It is no particular suprise then that surface drifters accumulate at the western end of the basin. The convergence on Padre Island, as will be demonstrated, is a function of the shape of the coastline in the western Gulf. Similarly, the absence of drifter returns from the west Florida coast is consistent with the expectation that surface waters should be blown offshore by the westward wind stress.

The Loop Current shows up in this data set as the only obvious agent that could entrain drifters in the eastern Gulf of Mexico and move them out through the Straits of Florida. It then carries them up the east coast of the peninsula where the westward wind stresses there drive the surface waters, and drifters, onshore. It is the entrainment of most drifters in the eastern Gulf by the Loop Current that accounts for the paucity of drifters from that area that find their way to the Texas shelf.

One problem with drifters is that one knows only where they were released and where they were found, not the path they took between those two points. However, the general pattern they reveal is useful as a control on possibilities offered by theoretical models (Figure 2.6).

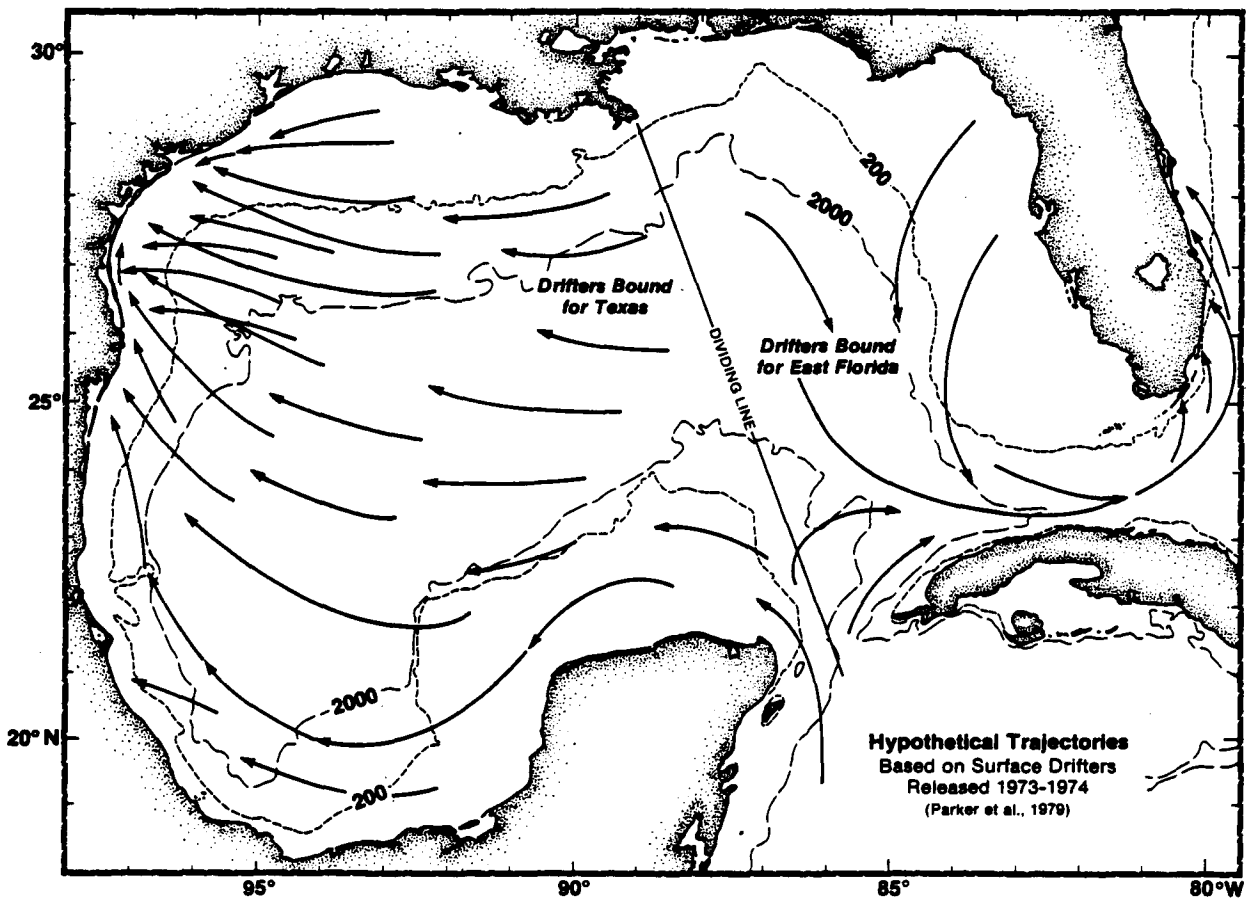

Figure 2.6 Idealized surface drift based on surface drifter data from Parker et al., 1979. The dividing line is the demarcation between release points for which nearly all drifters went west and those for which the drifters exited the Gulf through the straits of Florida.

Blumberg and Mellor's (1981) model of circulation in the Gulf of Mexico is of interest because it provides suggestions of how the flow field behaves over the whole Gulf. It is possible, therefore, to compare its predictions for areas where observations exist to test its validity and to gain some insight into circulation patterns where data are sparse. Their model is rather comprehensive in that it treats both barotropic and baroclinic modes, contains provisions for eddy (turbulent) viscosity, uses realistic bathymetry, and uses input through the boundaries to drive the model.

The horizontal velocity vectors for the level 6 m below the sea surface generated by the model at 90-day increments are shown in Figure 2.7. Similar vector plots for the 100 m level appear as Figure 2.8. The flow patterns on the shelves are consistent with the drifter data of Parker et al. (1979), but the flow patterns for the deep basin are not. The model does develop a Loop Current which would remove drifters from the eastern Gulf. The flow field the model portrays in the western Gulf would, however, carry the drifters to the north and northeast and not toward the western boundary of the basin. This may be related to a more disturbing failure of the model, which is that it does not shed eddies from the Loop Current. These eddies and their importance to the western Gulf of Mexico are well documented (see for example Nowlin and McLellan, 1967; Behringer et al., 1977; Elliott, 1982; and Merrell and Morrison, 1981).

The models of Hurlbert and Thompson (1982) do generate variations in the intrusion of the Loop Current which lead to meanders that pinch off, forming anticyclonic (clockwise rotating) rings. These drift westward toward the western boundary of the basin. Variations in the Loop Current intrusion and a pinched off ring were shown in the data of Ichiye et al. (1973) (Figure 2.9). Nowlin and McLellan (1967) suggested that a large anticyclonic gyre occupied a major portion of the western Gulf. This study was based on a rather coarse grid of hydrographic stations taken on two cruises. Blaha and Sturges (1981) put forth the hypothesis that the anticyclonic flow is generated by the curl of the wind stress. However, Elliott (1979) showed that when the wind stress curl was calculated on a finer scale than that used by Blaha and Sturges, it yielded a cyclonic circulation in the Gulf of Campeche, with anticyclonic circulation to the north.

Elliott (1982) showed that eddies were shed from the Loop Current at a rate of slightly more than one per year, that they drifted to the west at about 2 km/day, and that they contributed significantly to the salt and heat transport into the western Gulf of Mexico. Merrell and Morrison (1981) drew upon Nowlin and McLellan (1967), Elliott (1979), Blaha and Sturges (1981) and new hydrographic data from the western Gulf of Mexico to present a rather complicated picture of circulation at the western margin of the basin. They hypothesized that the wind stress produces a cyclonic circulation in the Gulf of Campeche, that an anticyclonic

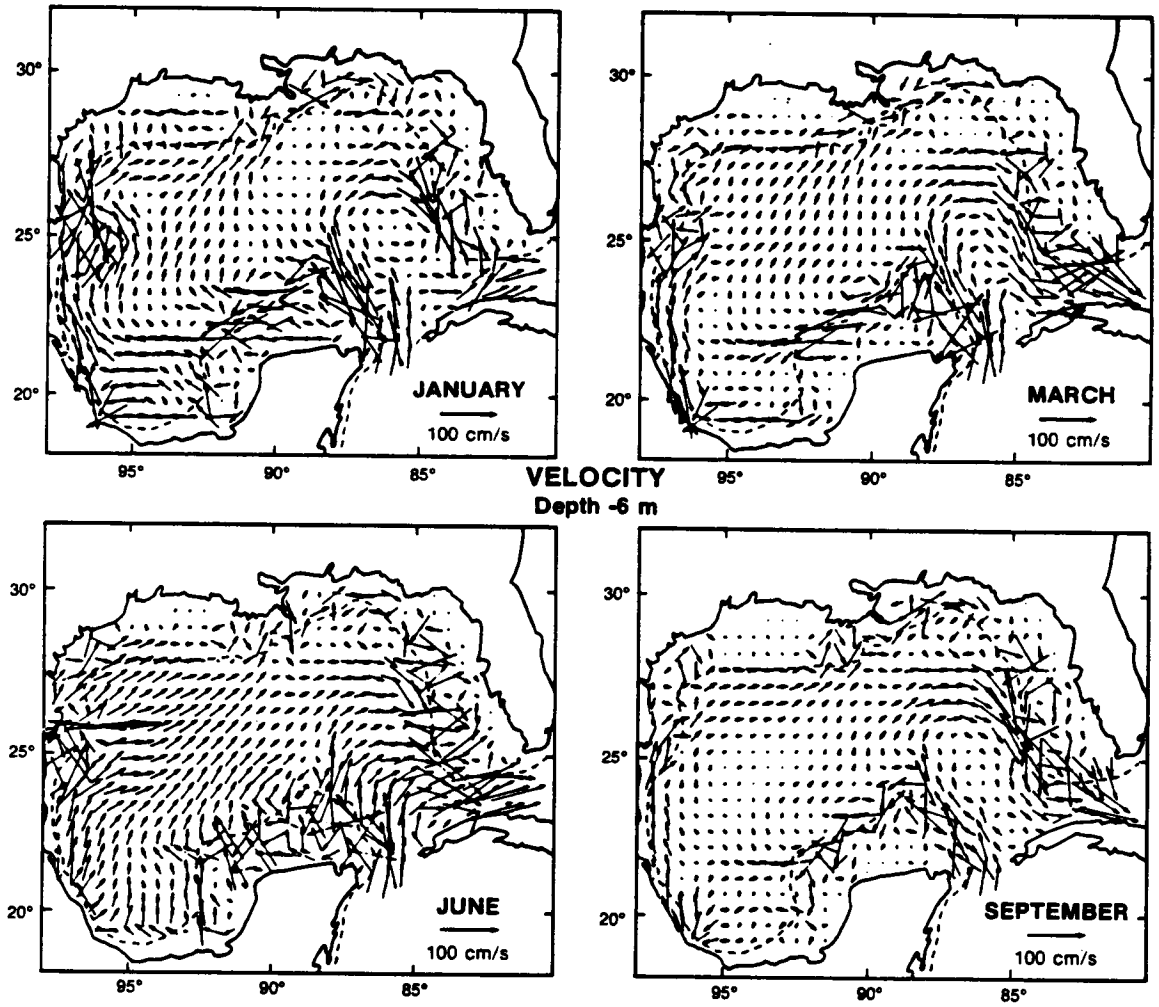

Figure 2.7 Mean monthly velocity vectors at 6 m depth for the Gulf of Mexico (after Blumberg and Mellor, 1981).

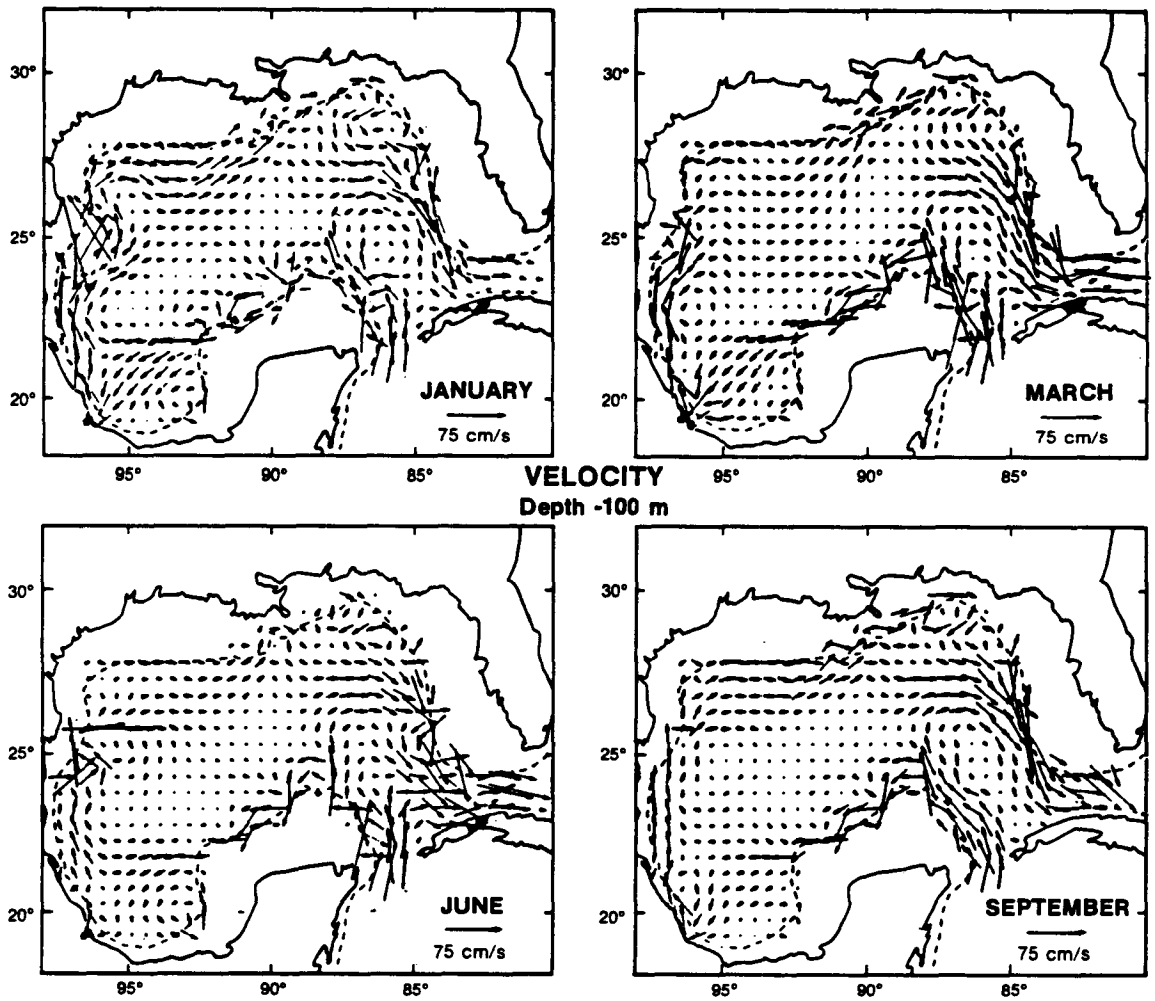

Figure 2.8 Mean monthly velocity vectors at 100 m depth for the Gulf of Mexico (after Blumberg and Mellor, 1981).

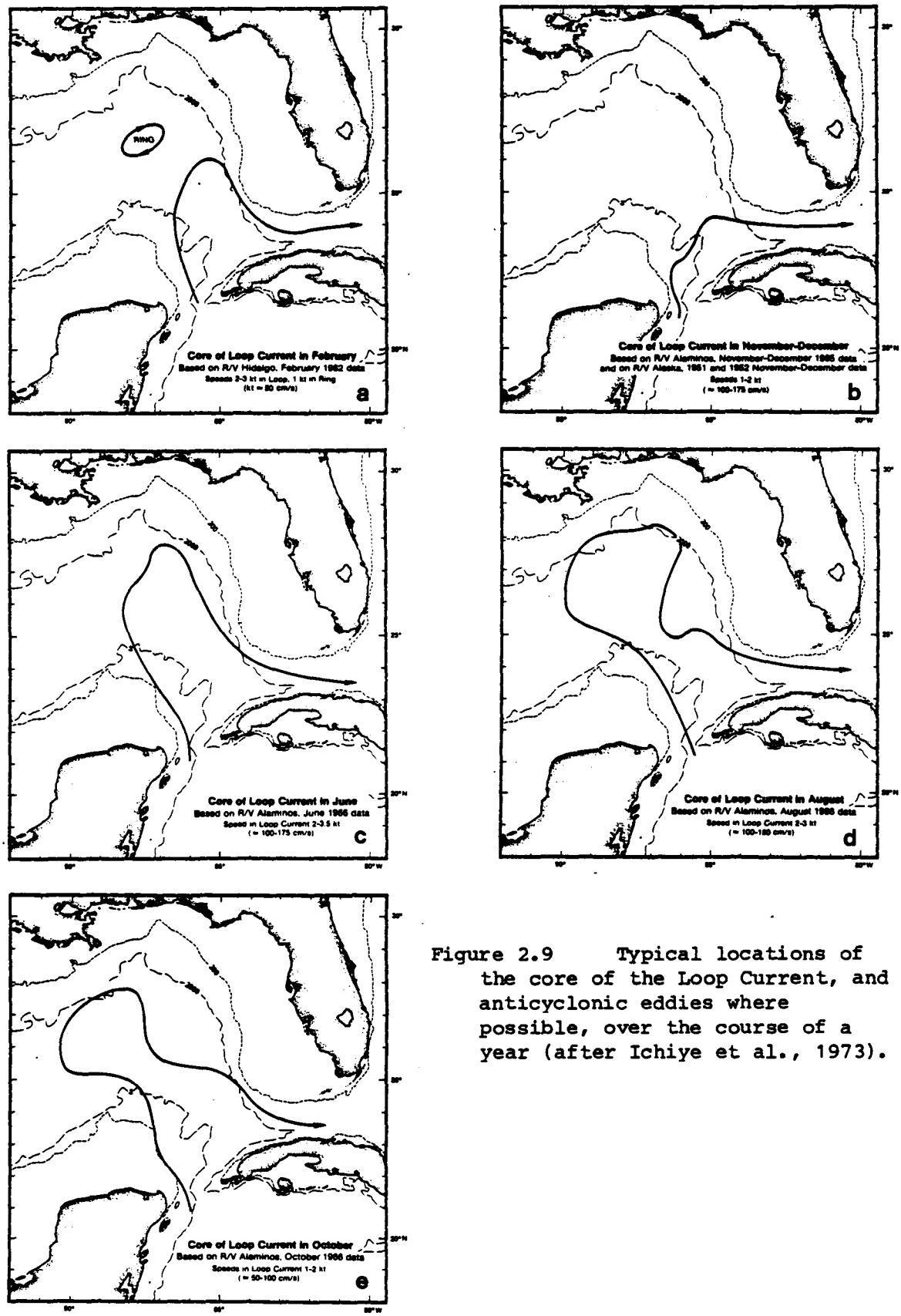

Figure 2.9 Typical locations of the core of the Loop Current, and anticyclonic eddies where possible, over the course of a year (after Ichiye et al., 1973).

gyre exists to the north of the Gulf of Campeche as a result of westward drifting anticyclonic rings shed by the Loop Current, and that a second cyclonic eddy may exist even farther north (above 24°30'N latitude). Merrell and Morrison (1981) postulate that the northern cyclone is also generated by the Loop Current. These can only form when the Loop Current is at its full northern extension. At that time a low pressure trough forms to the west of the northward-flowing limb of the Loop Current. A cyclonic eddy could then form if a meander enfolded the trough. They suggest, therefore, that the northern cyclone may not always be present because the Loop Current does not reach full extension every year.

In summary, then, circulation in the deep basin of the eastern Gulf of Mexico is dominated by the Loop Current, which is generated outside the Gulf. Judging from the drifter data of Parker et al. (1979), this current entrains the surface waters of the eastern Gulf and sweeps them out though the straits of Florida. Though the Loop Current varies considerably in the extent of its northern penetration into the Gulf, it is clear that the current maintains a persistent anticyclonic circulation in the waters of the basin east of a line from the Mississippi Delta to the Straits of Yucatan.

Circulation in the deep basin west of the Mississippi Delta-Yucatan Straits line is much more complicated that that in the east. The western basin appears to be dominated by large (200 km) anticyclonic and, perhaps, cyclonic eddies spun off by the Loop Current; these drift to the western boundary. There, the eddies interact with the local wind-driven circulation in some complex and, as yet, incomprehensible fashion. Whatever the nature of the interaction, the circulation of the deep western Gulf should exhibit significant year-to-year variation because of the annual variance in the number of rings or eddies spawned. Also, the Parker et al. (1979) drifter data show, unequivocally, that the surface waters of the western Gulf converge on the Texas coast whatever their circuitous path to that location might be.

LONG-TERM, LARGE SCALE OBSERVATIONS

The distribution of observations on the continental margins around the Gulf of Mexico is very uneven (see Figure 2.1). The shelf off Mexico, for example, is virtually devoid of reported observations. The only information available upon which to base speculations is the drifter data of Parker et al. (1979) and mathematical models. Similarly, there is very little information about the segment of shelf from DeSoto Canyon west to the Mississippi Delta. Only the Texas-Louisiana and West Florida shelves have had any large-scale hydrographic surveys or long-term current meter moorings from which data are available.

Mexican Shelf

The drifter returns from releases on the Mexican shelf in October and November 1976 imply a rather complex circulation pattern. Drifters released on the Yucatan banks and throughout the Gulf of Campeche were found on Padre Island, Texas. On the other hand, a very few drifters from the western Gulf of Campeche went southeastward and landed at Veracruz. This matches up fairly well with the 6 m depth velocity vectors from Blumberg and Mellor's (1981) model (Figure 2.7). Their velocity field on the Mexican shelf shows an anticyclonic drift with a convergence at Veracruz for all periods except midsummer.

From these data it appears that water which enters through the Straits of Yucatan along the shelf sweeps westward across the broad carbonate platform of the Yucatan Peninsula, swings southwest along the outer shelf in the Bay of Campeche, then heads north to the Texas shelf. This must be viewed as a long-term, general flow that would have many perturbations superimposed on it. It is not possible to make any estimate of the effect of the cyclonic and anticyclonic gyres of the deep basin on the shelf circulation. However, the surface waters of these gyres do become entrained in the shelf flow somehow because the drifters released in them come to rest on the Texas coast (Figure 2.6).

Texas-Louisiana Shelf

Seasonal Circulation Patterns

The monthly averaged wind stress field over the Texas-Louisiana shelf is relatively uniform in magnitude and direction (Figure 2.5). However, the orientation of the coastline varies from essentially north-south along the western boundary of the Gulf to essentially east-west between Galveston, Texas and the Mississippi Delta. Both Smith (1980) and Cochrane and Kelly (1982) have observed that the coastal currents are best correlated with the alongshore component of the wind stress. Smith (1980) further suggests that convergence in the alongshore flow ought to occur where the wind stress is normal on an arcuate coast. That should be the case because at that point the alongshore wind stress would be zero. Consider Figure 2.10. In that figure the wind stress is perpendicular to the coast at location 1, so there is no component of stress parallel to the coast. At position 2, however, the wind stress is not perpendicular to the coast, so it possesses a component of stress in the down coast (SW) direction. At position 3, the alongshore wind stress component is directed up coast (NE). In very shallow water the flow goes in the direction of the alongshore windstress, so it converges at location 1.

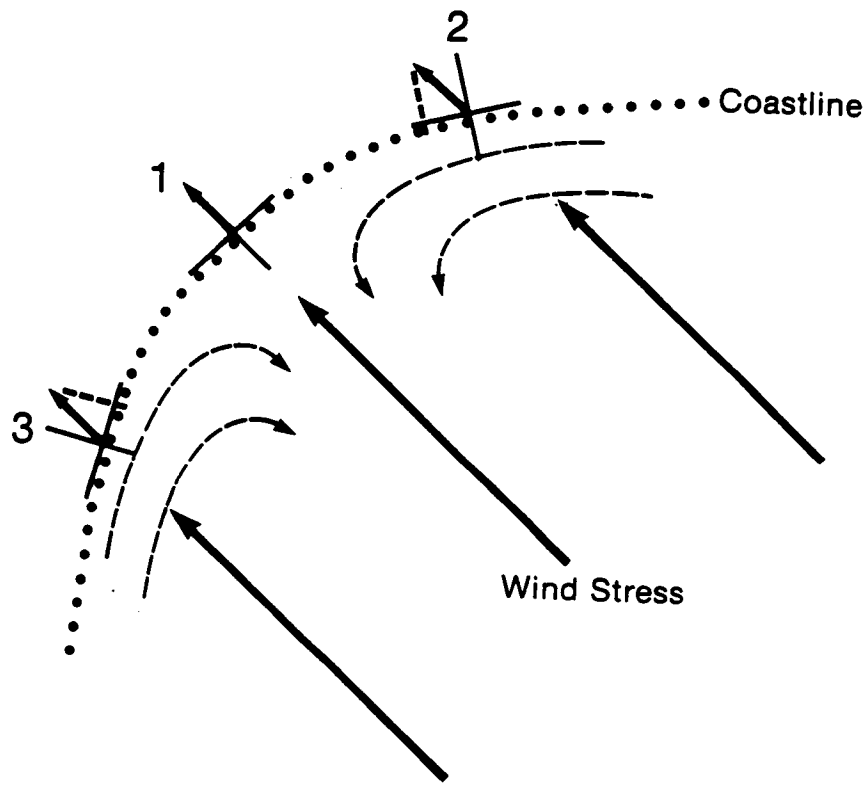

Figure 2.10 Parallel wind stress vectors striking an arcuate coastline. At point 1, the stress vector is perpendicular to the coast, so no alongshore current is generated. At point 2 the stress vector crosses the coast at an angle, so the alongshore component of the stress vector is downcoast. At point 3 just the opposite is true: there is convergence of the alongshore flow at point 1.

Using a combination of historical data (meteorological and oceanographic), long-term current meter records (see Figure 2.1 for locations), processed satellite imagery, and monthly hydrographic transects of the inner shelf, Cochrane and Kelly (1982) have developed an interesting model of the mean monthly flow on the Texas-Louisiana shelf. The essence of their model appears in Figures 2.11 and 2.12. These charts show the mean geopotential anomaly at the sea surface (relative to the 70 decibar surface) with streamlines. With the exception of July, the coastal flow on the east-west segment of the shelf is down coast, or westerly. In the spring, a northerly flow develops on the north-south shelf segment. The convergence zone between these two flows migrates northeasterly very rapidly in the midsummer, so that in July the coastal currents are all up coast, with considerable cross-shelf exchange just west of the Mississippi Delta. Figure 2.5, the July wind stress of Blumberg and Mellor (1981), shows the mean wind stress to be normal to the shore at the Texas-Louisiana border.

Whereas the currents very near shore are driven directly by the alongshore component of the wind, the offshore flow tends to be directed to the right of the wind. This piles surface waters up against the coast along the east-west segment of the shelf during all periods when the wind stress is acting to the west. This sets up the coastal waters so that there is a pressure gradient normal to the shore. Under these conditions a geostrophic current should develop, with the Coriolis acceleration balancing the pressure gradient as shown in equation 1

$$u_f = \frac{-1}{\rho}\frac{\partial p}{\partial y} \qquad (1)$$

where u = x component of flow (positive to the east)
$f = 2\omega \sin\phi$ local angular velocity of the earth, in radians per second
ρ = density
p = pressure
y = north-south coordinate (positive to the north)

This means that pressure increasing to the north would drive a westerly flowing current.

During the periods of westerly flow at the coast, the discharge of the Mississippi River is tucked against the coast by the wind stress, and by its density contrast augments the westerly flow. Cochrane and Kelly (1982) were able to show that decreases in salinity at their study site (Figure 2.1) occurred about six weeks after periods of discharge maxima in the Mississippi River.

In the offshore region, the historical hydrography implies that the flow should be northward along the N-S shelf segment and

eastward along the E-W segment. This is in good agreement with Blumberg and Mellor's (1981) model and the observations of Nowlin and McLellan (1967).

Cochrane and Kelly (1982) suggest that during the winter preferential cooling of the rather saline mid-shelf waters would create a dynamic low on the shelf which would then set up a cyclonic circulation on the outer shelf. That is, it would set up a counterclockwise flow. This low appears on the shelf for all periods except July. It is, however, difficult to account for the re-establishment of the low after July if recourse must be made to a remnant of cooler water at mid-shelf left over from winter cooling.

Continental Shelf Associates, Inc. (CSA) maintained a current meter mooring 2 km to the SSE of Baker Bank from March 1978 through March of 1981 for Conoco, Inc. The mooring was set in 73 m of water with meters at depths of 12 m, 38 m, and 69 m. These data were released by Conoco, Inc. and provided by CSA to aid in the present study. The location of the mooring is shown in Figure 2.13, along with the location of the National Data Buoy Office (NDBO) buoy 42002 and the location of the moorings established by Texas A&M University researchers for the Minerals Management Service.

Progressive vector diagrams (PVD) for the currents at the CSA site and the East Flower Garden, as well as the surface winds recorded at NDBO 42002 were created from raw recorded data for the period from 23 April 1980 to 8 August 1980 (Figure 2.14). Before discussing these PVDs, it is essential that they be recognized for what they are. The current vector recorded at the beginning of each sample interval is multiplied by the time between samples. In the case of the CSA data, the interval is 30 minutes; it is one hour for the NDBO winds; and 20 minutes for the Flower Garden currents. The resulting vector gives a distance and direction, but it should not be viewed as a displacement. It is a representation of the time history of the flow through a point (the current meter). These vectors are plotted so that the origin for each new vector is the nose of the last vector, thus the name, progessive vector diagram.

In the first two and a half weeks of the record, the wind oscillated between flow from the southeast and flow from the northeast. Thereafter the wind was out of the southeast except for brief periods of flow from the east at the end of the third week, beginning of the seventh week, and middle of the tenth week.

The average flow for the period at the CSA site, near Baker Bank, was toward the northeast parallel to the local trend of the isobaths. During the first six weeks, the flow went through two counterclockwise rotations which are not clearly related to the wind. The first oscillations may be related to the passage of the last, weak cold fronts of the season seen in the wind record. However, the southerly flow at the upper meter (12 m) between weeks 4 and 6 is hard to reconcile with the steady southeasterly wind.

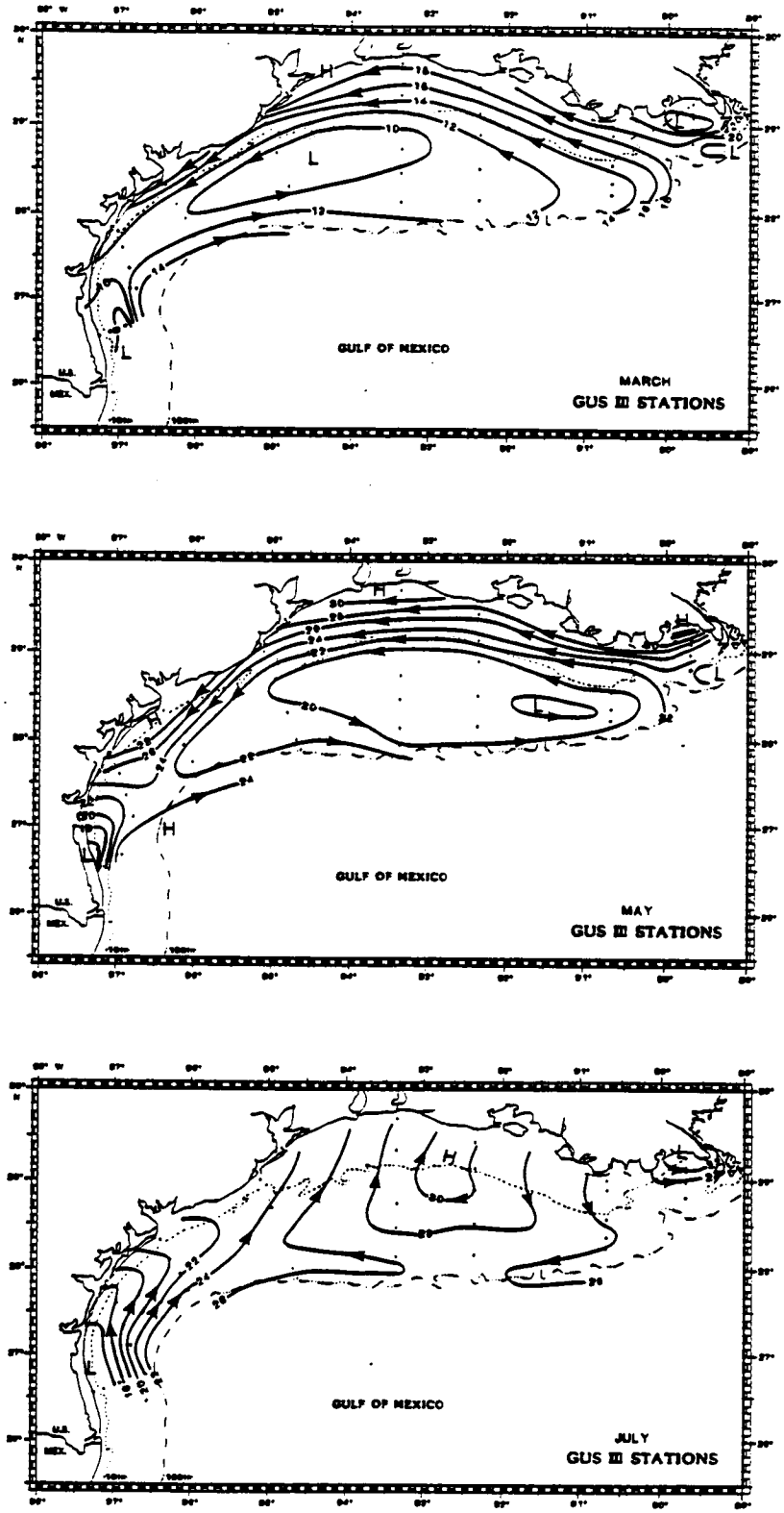

Figure 2.11 Mean geopotential anomaly (dyne/cm) of the sea surface relative to 70 db based on GUS III data for March, May, and July, 1962-1964 (from Cochrane and Kelly, 1982).

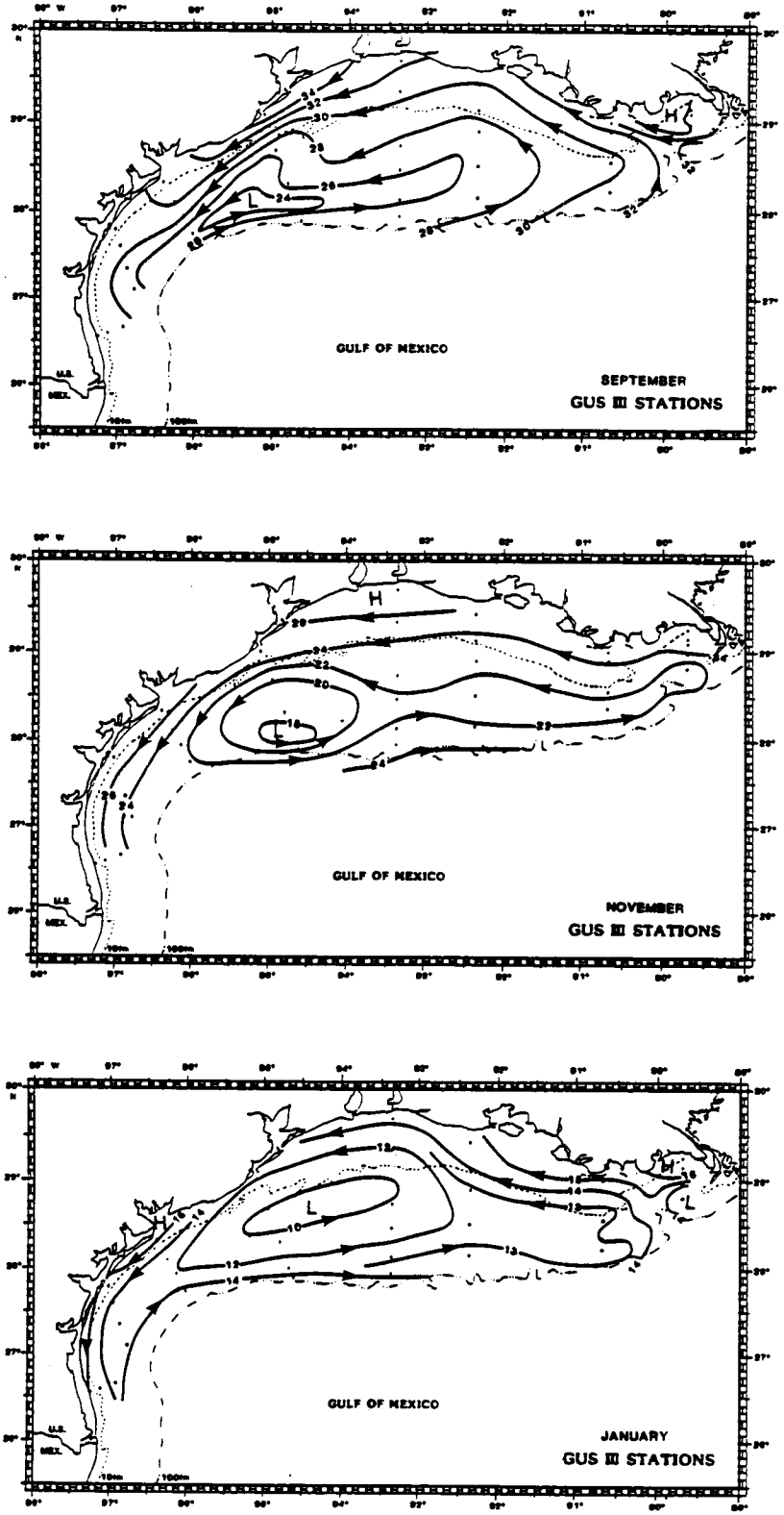

Figure 2.12 Mean geopotential anomaly (dyne/cm) of the sea surface relative to 70 db based on GUS III data for September, November, and January, 1962-1964 (Cochrane and Kelly, 1982).

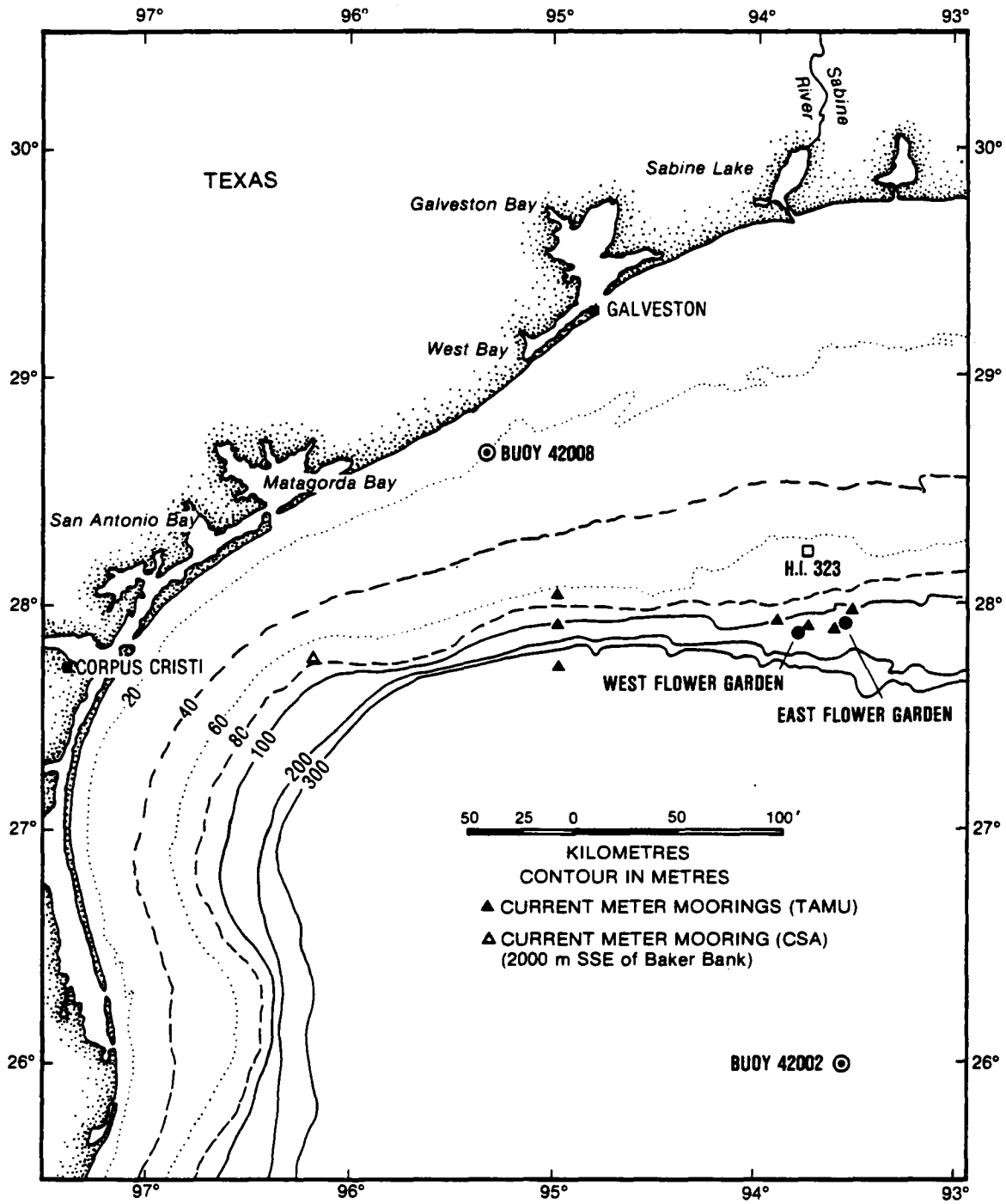

Figure 2.13 Shelf index map showing the locations of the CSA current meter mooring (near Baker Bank), NDBO buoys 42002 and 42008, and the TAMU current meter moorings along 95°W and near the Flower Garden Banks.

The record for the meter at 38 m depth possesses much tighter loops during the first six weeks, indicating slower flow than at the surface. There are also directional differences between the two, with more southerly flow at the surface. The near-bottom flow (69 m depth) exhibits reversals, rather than rotational events, during the first six weeks. It is also apparent that, were it not for the very large northerly flow between weeks 9 and 10, the net flow at the bottom would have been to the south.

Beginning about the middle of week 6, the flow at all depths turned to the north. The near-bottom flow reversed abruptly in the middle of week 7, then returned to northerly flow in the middle of week 8. This perturbation may be related to the wind shift during that period. The very strongest flow at all levels is between weeks 9 and 10. The wind was not appreciably stronger, but it did shift from southeasterly to southerly during this period.

The Flower Garden moorings were deployed in deeper water (about 100 m) than the mooring at the CSA site (73 m) (see Figure 2.13 for locations). Also mooring 2 was set at the base of the East Flower Garden Bank, so flow at that site is deformed by the bank.

The only current meter in the Flower Garden region as shallow as the top meter at the CSA site was the electromagnetic current meter (EMCM) on mooring 2. Unfortunately, the EMCM battery failed prematurely, leaving only a two-week record. This very short piece does suggest that the surface waters were responding to the reversals in the wind which occurred at that time (Figure 2.14). The mid-depth current (50 to 60 m) was, however, remarkably constant in its flow to the east. Ignoring the record from the bottom current meter on mooring 2 because of the strong topographic influence of the bank, one can see that the bottom flow in the Flower Gardens region was also to the east, much slower than the mid-depth flow, and oriented slightly more offshore.

Figure 2.15 is a PVD for the wind at the NDBO 42002 and the CSA site for 11 weeks starting on Valentine's Day 1979. During this period, flow at the level of the upper two meters responded much more directly to the wind. The bottom current also responded to variations in the wind, but it was flowing to the southwest with greater strength than mid-depth water was flowing to the northeast.

Monthly means for all moorings and all deployments (January 1979 to July 1981) were computed for the Flower Gardens site (Figure 2.16a). The records were divided into mid-depth (32 to 64 m), near bottom (11 to 18 m above bottom), and very near bottom (4 to 8 m above bottom). The mid-depth currents are dominated by a rather strong easterly flow except for two periods: mid-July 1979 to mid-August 1979 and December 1980. The cause of the anomalous flow in 1979 was the passage of Tropical Storm Claudette. This storm passed over the Flower Gardens travelling northward early on 25 July 1979. After passing over the region, the storm stalled over the

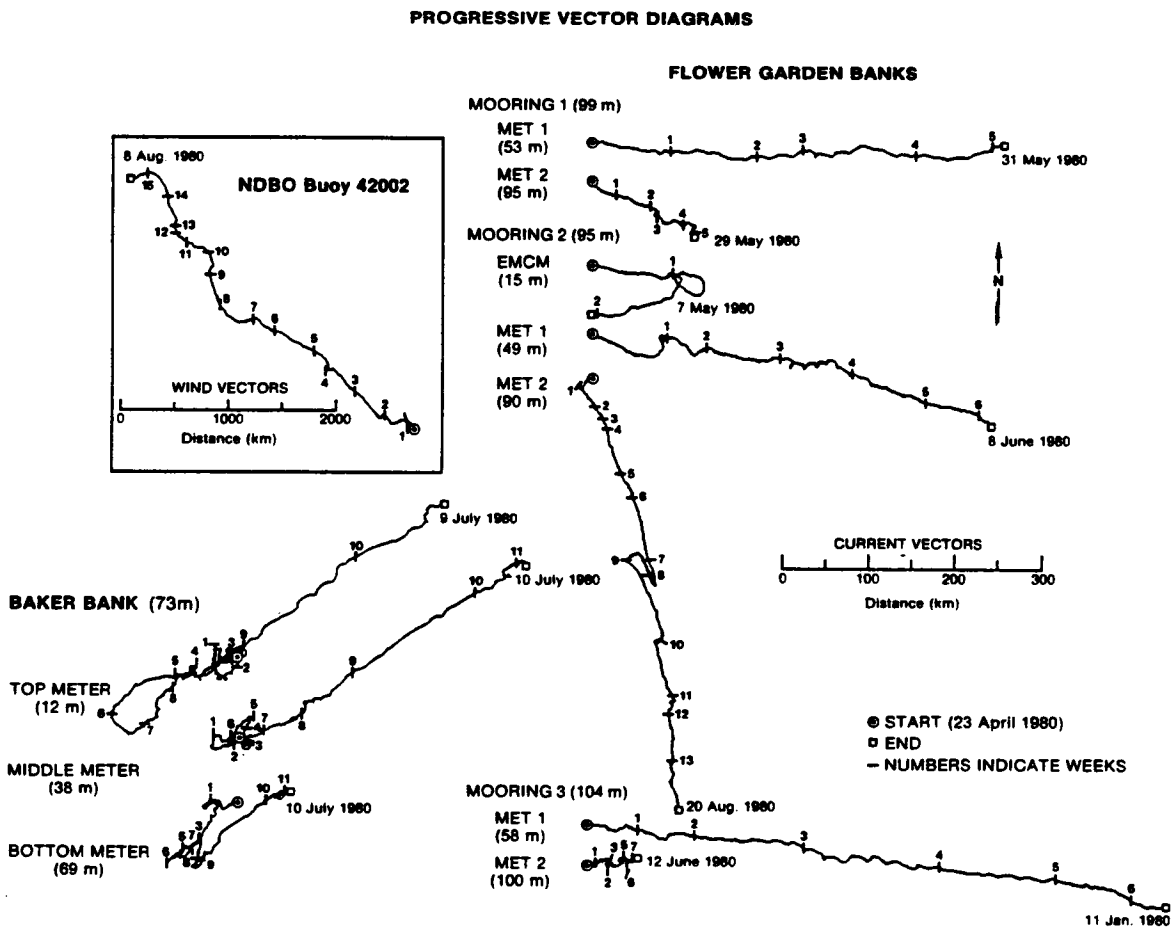

Figure 2.14 Progressive vector diagrams constructed from velocity time-series records beginning on 23 April 1980 for the wind at NDBO buoy 42002 and the currents at the top, middle, and bottom meters on the CSA mooring near Baker Bank; and the currents at all available meters on moorings 1, 2, and 3 near the Flower Garden Banks.

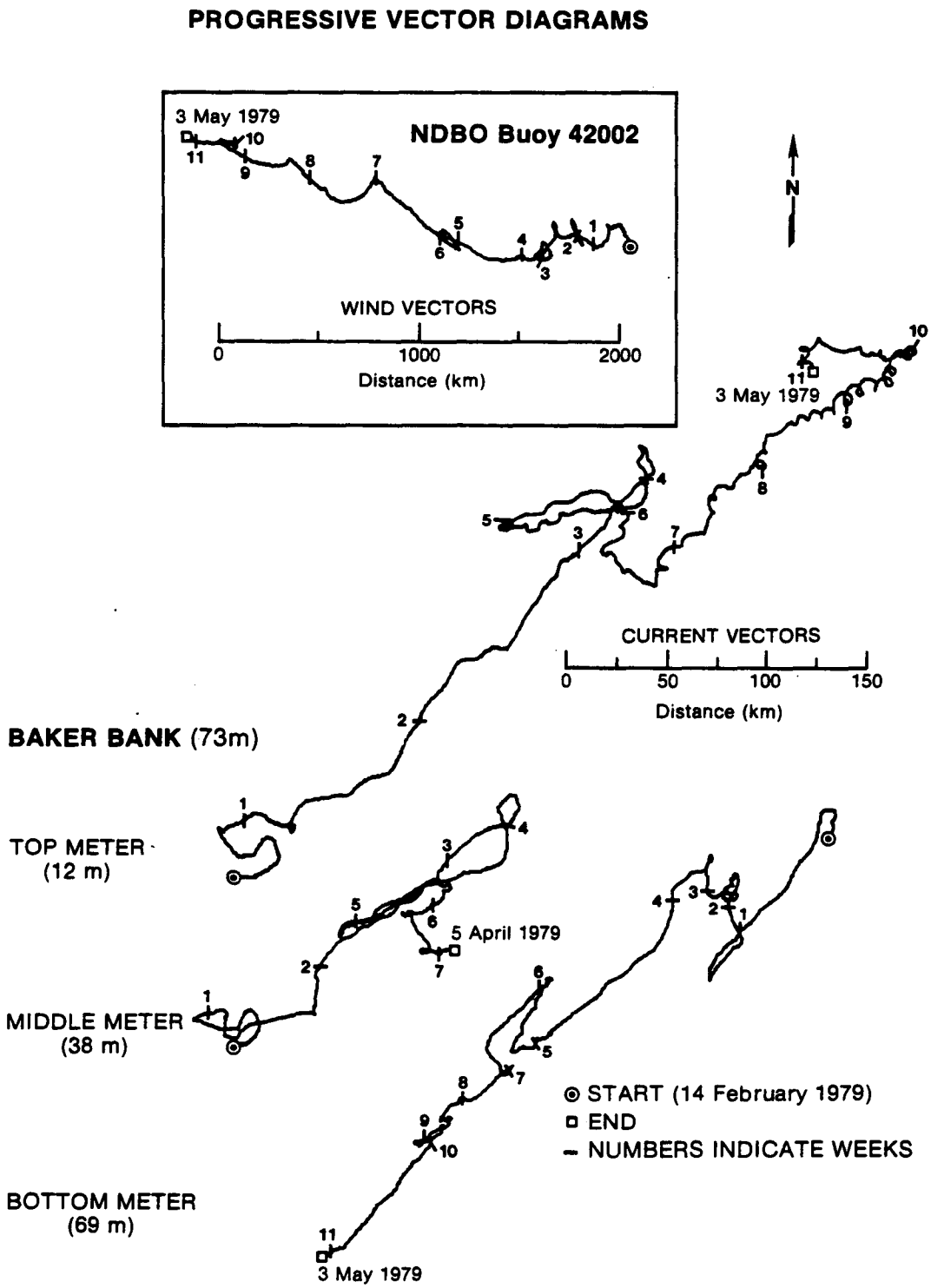

Figure 2.15 Progressive vector diagrams constructed from velocity time series records beginning on 14 February 1979 for the currents at the top, middle, and bottom meters on the CSA mooring near Baker Bank and from wind stress data at NDBO buoy 42002.

Texas coast resulting in several days of high winds over the northwestern Gulf. In the second period of westerly currents, several very strong cold frontal passages took place, resulting in a vector average wind out of the northeast.

The bottom currents were directed primarily toward the southeast. There was no apparent seasonal distribution to these vector means, but that may be due to the relatively small sample period.

For the monthly vector averages, the greatest variance was in the east-west, or u component, of flow. The cause of the variation was investigated by means of a multiple linear regression using the north-south τ_u component of wind stress and east-west or τ_u component of wind stress as the independent variables. The regression had the form

$$u = A + B\tau_u + C\tau_u$$

where A, B, and C were estimated from the data using the best fit according to the least-squares criterion. The values for these constants were found to be: A = 7.89 $\pm$ 3.28; B = 3.9 $\pm$ 8.9; and C = 23.3 $\pm$ 6.7. This model will account for approximately 70% of the variance in the u component of the mid-depth current. The low value of B, its large standard error, and the large value of C imply that the variance of the east-west component of flow is driven by the north-south component of the wind stress. The stronger the wind stress is to the north, the greater the magnitude of the eastward flowing current.

The same regression was run for the very near bottom meters, excluding those from mooring 2. The values for the constants on this run were: A = 8.25 $\pm$ 2.89; B = 16.1 $\pm$ 6.1; and C = -4.4 $\pm$ 4.4. For the bottom flow, it is obviously the east-west component of wind stress that is related to the variance. Again, approximately 70% of the variance of u could be accounted for by the model. This latter result may be related to the fact that very strong wind stress to the west over the shelf would produce onshore-directed Ekman flow at the surface and southwesterly-directed Ekman flow at the bottom. Convergence of the bottom flow from the inner shelf and the easterly bottom flow from the outer shelf would modulate the flow at the location of the Flower Garden Banks, as the model implies.

The set of monthly mean current vectors computed from all CSA mooring data are displayed in Figure 2.16b. The stronger currents (between 8 cm/s and 25 cm/s) at the top meter, 12 m from the surface, are directed primarily to the northeast, nearly parallel to the local shelf isobaths. However, for several cases with speeds less than 8 cm/s, the mean currents are directed nearly offshore or onshore. The few cases with a downcoast (southwest) component to

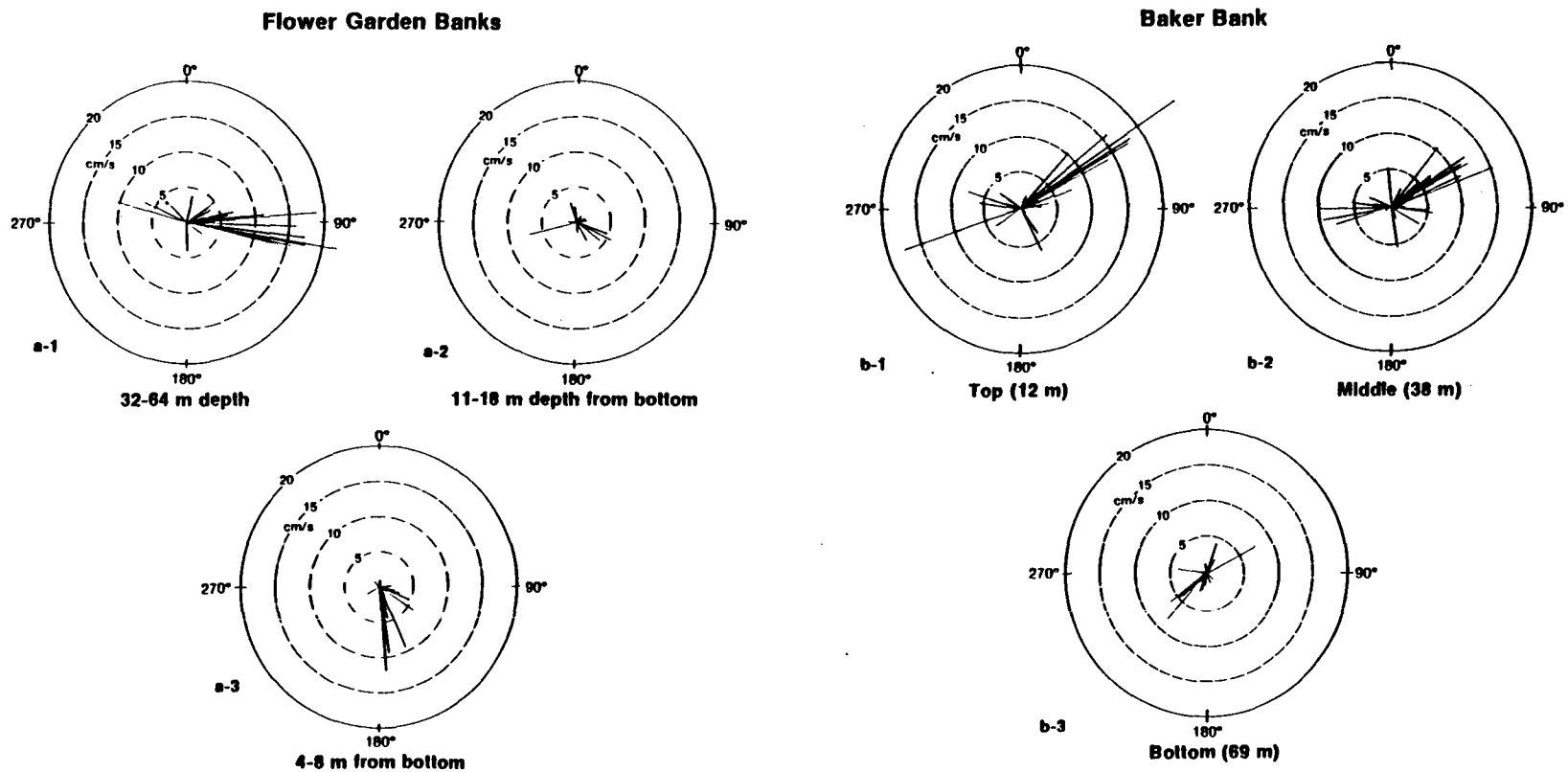

Figure 2.16 Monthly mean current vectors for a) all deployments and all moorings near the Flower Garden Banks over the period January 1979 to July 1981; and b) the CSA mooring near Baker Bank over the period March 1978 through March 1981.

the flow are found only in the late fall and early winter, and are perhaps related to the wind stress patterns found during this time of year. Over much of the year, the winds are from the southeast, but winds come from the northeast in late fall and early winter. The mid-depth currents (38 m depth) again show a predominance of northeast flow at higher speeds, but with a greater percentage of occurrences with lower speeds and nearly random directions. The bottom current averages in Figure 2.16b show a predominance of southwesterly flow, in the opposite direction to the surface currents and with less than half the speed. The few cases with upcoast flow at the bottom are found in the winter and spring.

Salinity Distribution

To belabor the obvious for a moment, the Mississippi River contributes an enormous volume of fresh water to the Texas-Louisiana shelf. Elliott (1982) provides an estimate that 371 km^3/yr are discharged to the western Gulf of Mexico by the Mississippi River. That is equivalent to approximately 5% of the water on the continental shelf between the Mississippi Delta and the 95°W meridian and on the order of 0.1% of the volume discharge of the Loop Current through the Yucatan Straits.

The discharge of the Mississippi River is not constant. In 1982 there were maxima in mid-February, early March, and late June, according to Cochrane and Kelly (1982). They further reported observations of corresponding decreases in the salinities measured at the site of their current meter moorings (Figure 2.1) in late March and late May but that the brackish water of the June maxima did not reach that site because the flow was up coast in late June and July.

The effects of the Mississippi effluent on the surface salinities of the Texas-Louisiana shelf are shown for alternate months of 1964 in Figure 2.17. In the winter, with discharge of the river at a minimum, oceanic waters with salinities of 36 ppt intrude to within a few kilometres of the coast. By May, the nearshore salinities have plunged to 20 ppt or less, and the 36 ppt isohaline has been pushed off the shelf. Also, notice that there is a suggestion in these May surface salinities that low salinity water is moving offshore and recurring to the east along the shelf break. A similar situation was found in March of 1982 (Sahl et al., 1982) when a thin veneer of water having a salinity of less than 36 ppt was found on the outer shelf between 95°30'W and 96°W (Figure 2.18). This is consistent with the model of Cochrane and Kelly (1982), which calls for cross-shelf flow near the region of Matagorda Bay and entrainment in the eastward flowing current on the outer shelf (Figures 2.11 and 2.12).

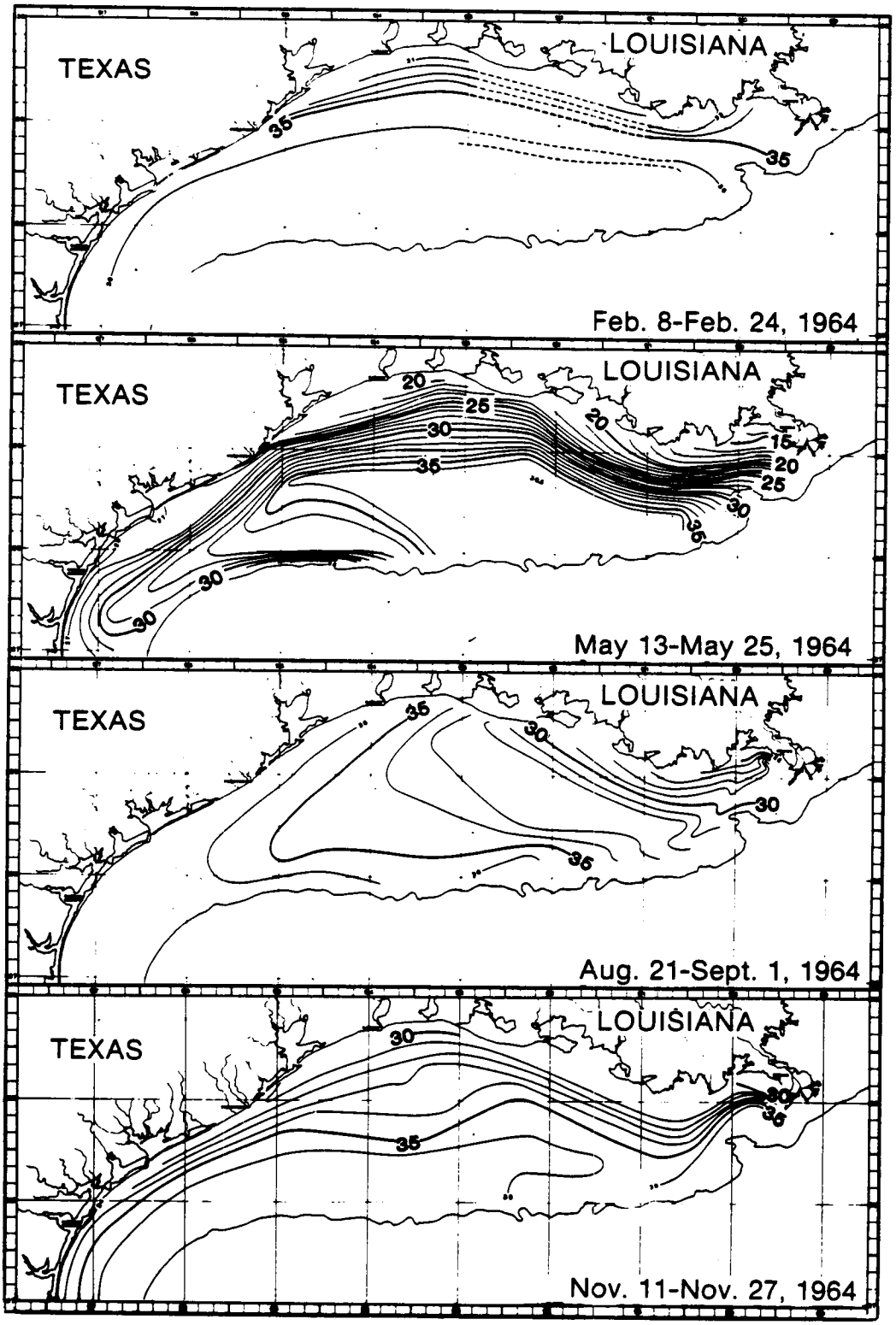

Figure 2.17 Sea-surface salinity from GUS III observations taken in February, May, August, and November 1964. (From Cochrane and Kelly, 1982.)

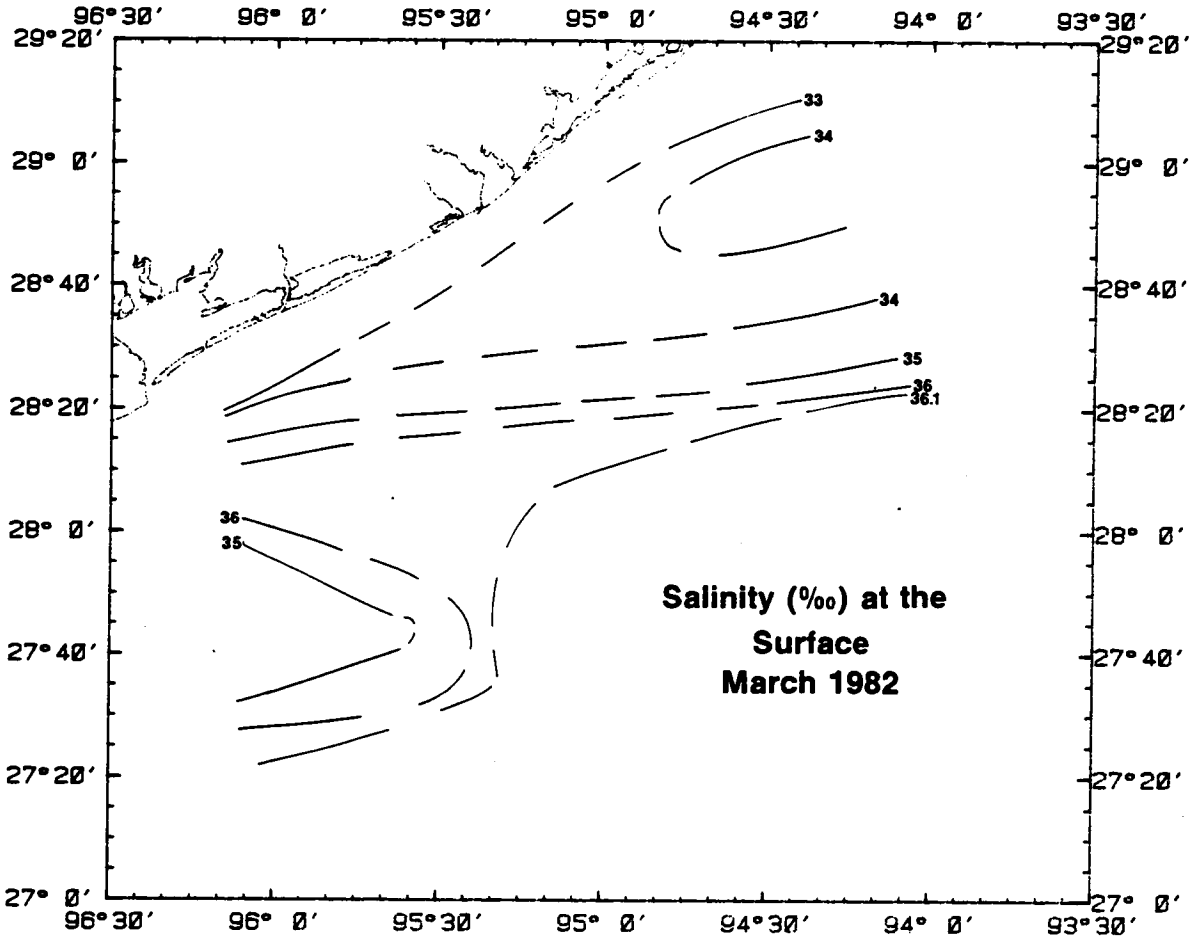

Figure 2.18 Sea-surface salinity from observations taken in March 1982 (Sahl et al., 1982).

The surface isohalines in August 1964 were not, as in other months, parallel to the coast (Figure 2.17). Rather, there was a tongue of relatively low salinity over the central shelf as far west as 94°W. This distribution may result from the blocking of the late June discharge of the Mississippi River by eastward flow over the entire shelf in July, and subsequent return to westward shelf flow in August, as suggested by Cochrane and Kelly (1982). By November 1964, the isohalines had become more parallel to the coast once again, with minimum nearshore salinities of 30 ppt or greater.

Temperature Distribution

Etter and Cochrane (1975) analyzed approximately 20 years of bathythermograph data collected on this segment of the shelf. They reported that surface and bottom temperatures were at a minimum in January and February (Figure 2.19) and at a maximum in July and August (Figure 2.20). The mean minimum surface temperatures show nearshore waters at approximately 14°C and offshore waters near 20°C. This can be compared to the sea surface temperature maps of 17 February 1982 (Figure 2.21) and 23 February 1982 (Figure 2.22) produced from the NOAA-7 satellite Advanced Very High Resolution Radiometer (AVHRR) digital data by Richard M. Barazotto of NOAA-National Environmental Satellite Service (NESS). In the satellite data, one can see the complex crenulations of the isotherms due to the large-scale, turbulent flow of the shelf. It is also apparent that there is a strong nearshore gradient from about 13.5 to 16°C and another region of rather pronounced gradient between 17 and 19°C. Overall, the mean monthly data of Etter and Cochrane (1975) are consistent with the snapshot of the sea surface temperature provided by the satellite data.

The bottom temperatures for late winter range from less than 13°C nearshore to a maximum of 18.5°C near the shelf break (Figure 2.20.

In late summer, the mean monthly data show little surface variance in temperature but a very strong cross-shelf thermal gradient at the bottom (Figure 2.20). The isotherms at the bottom are, in general, parallel to the local isobaths (Etter and Cochrane, 1975). The rapidity of the seasonal warming of the sea surface is shown in the satellite data from 6 April 1982 (Figures 2.23 to 2.24). Notice that the nearshore waters are 6 to 7°C warmer than that seen in mid-February.

Etter and Cochrane (1975) also plotted the mean depth of the surface mixed layer for the January to February period (Figure 2.25). This layer thickens offshore to a maximum of 75 m near the shelf edge. Data from our moorings at the Flower Garden Banks from 1979 to 1981 and that from our conductivity, temperature, and depth (CTD) surveys at the shelf edge (Figure 2.26) agree with those of

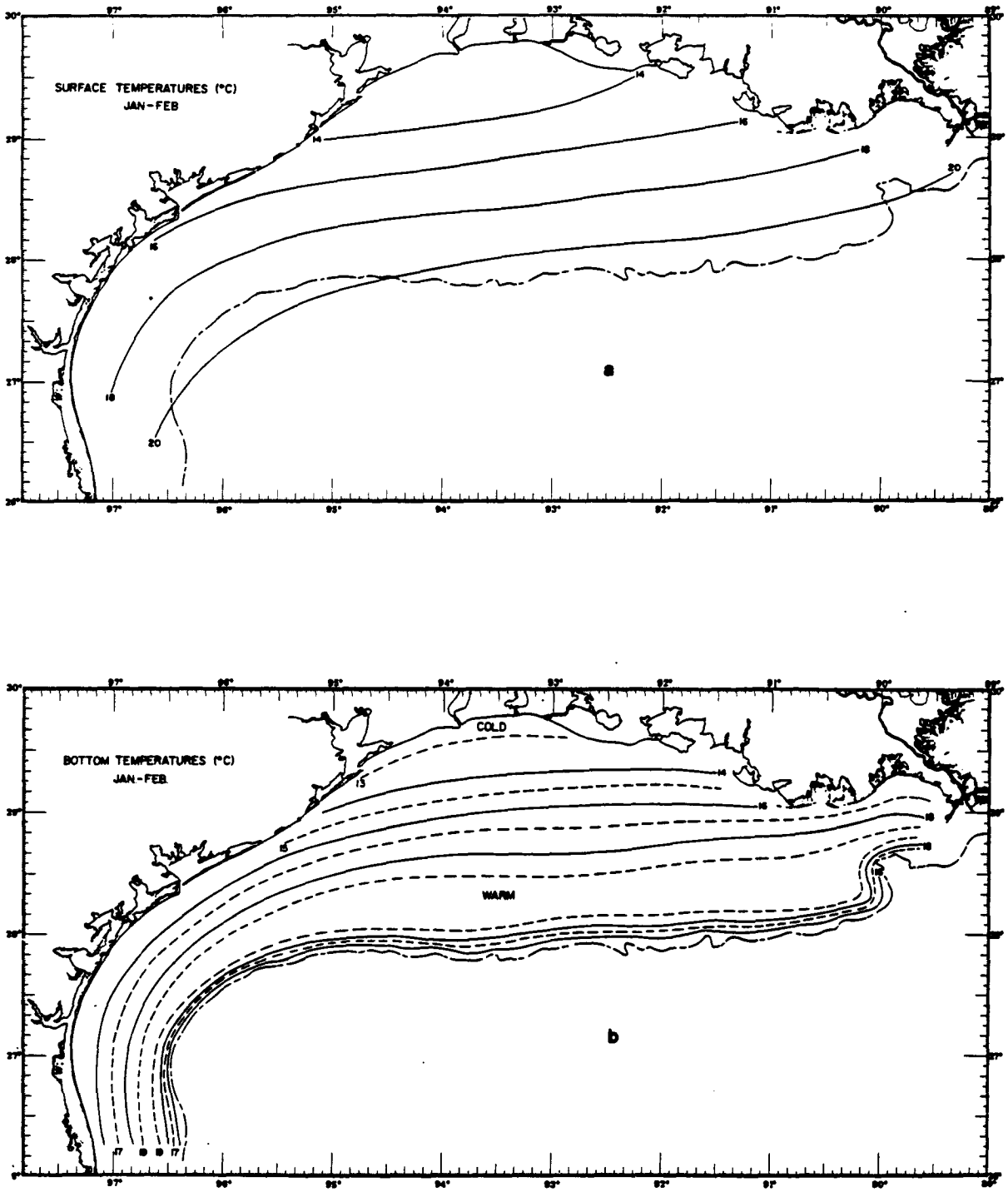

Figure 2.19 Map of (a) mean surface temperature (°C) for Jan-Feb, and (b) mean bottom temperatures for Jan-Feb. (From Etter and Cochrane, 1975.)

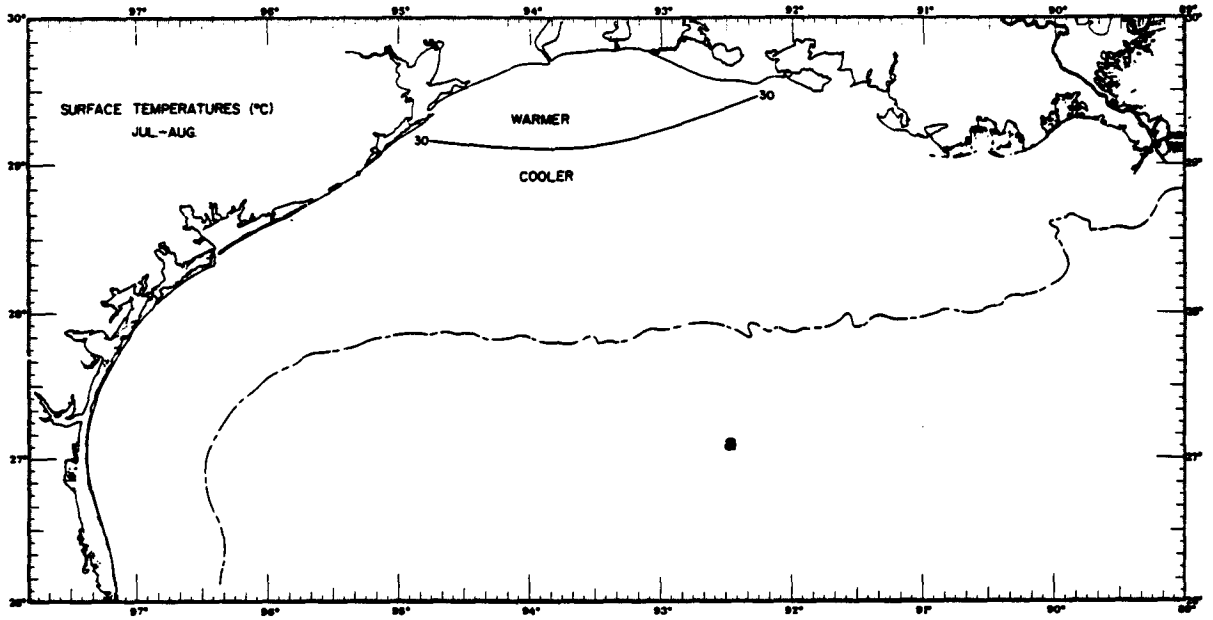

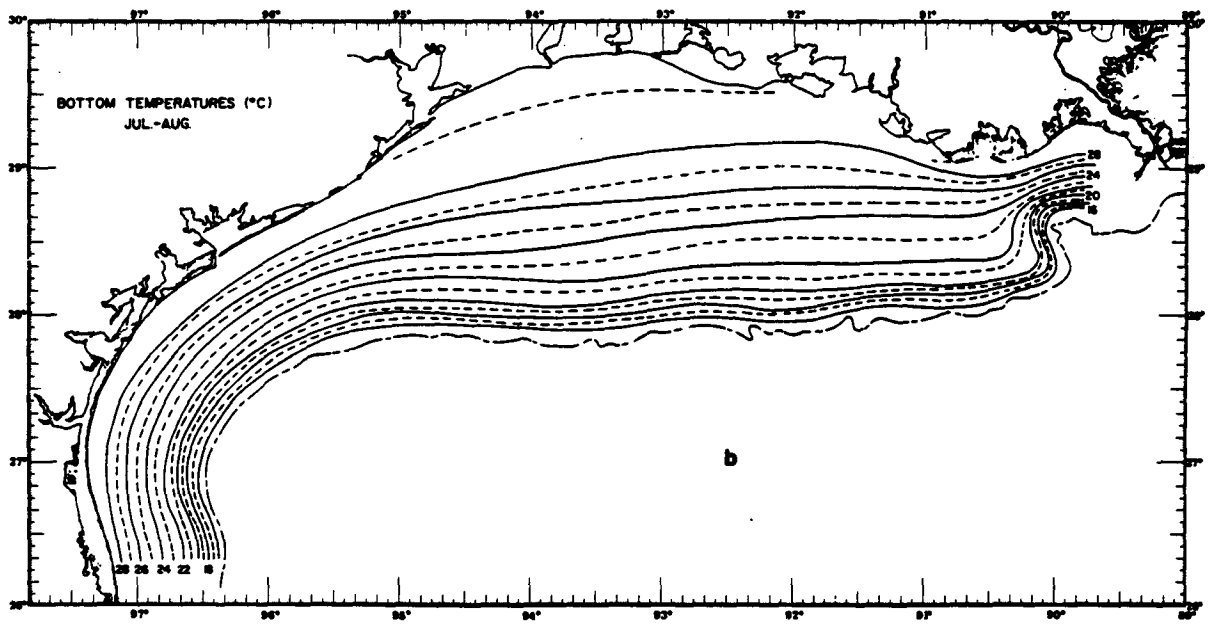

Figure 2.20 Maps of (a) mean surface temperature (°C) for Jul-Aug, and (b) mean bottom temperatures for Jul-Aug. (From Etter and Cochrane, 1975.)

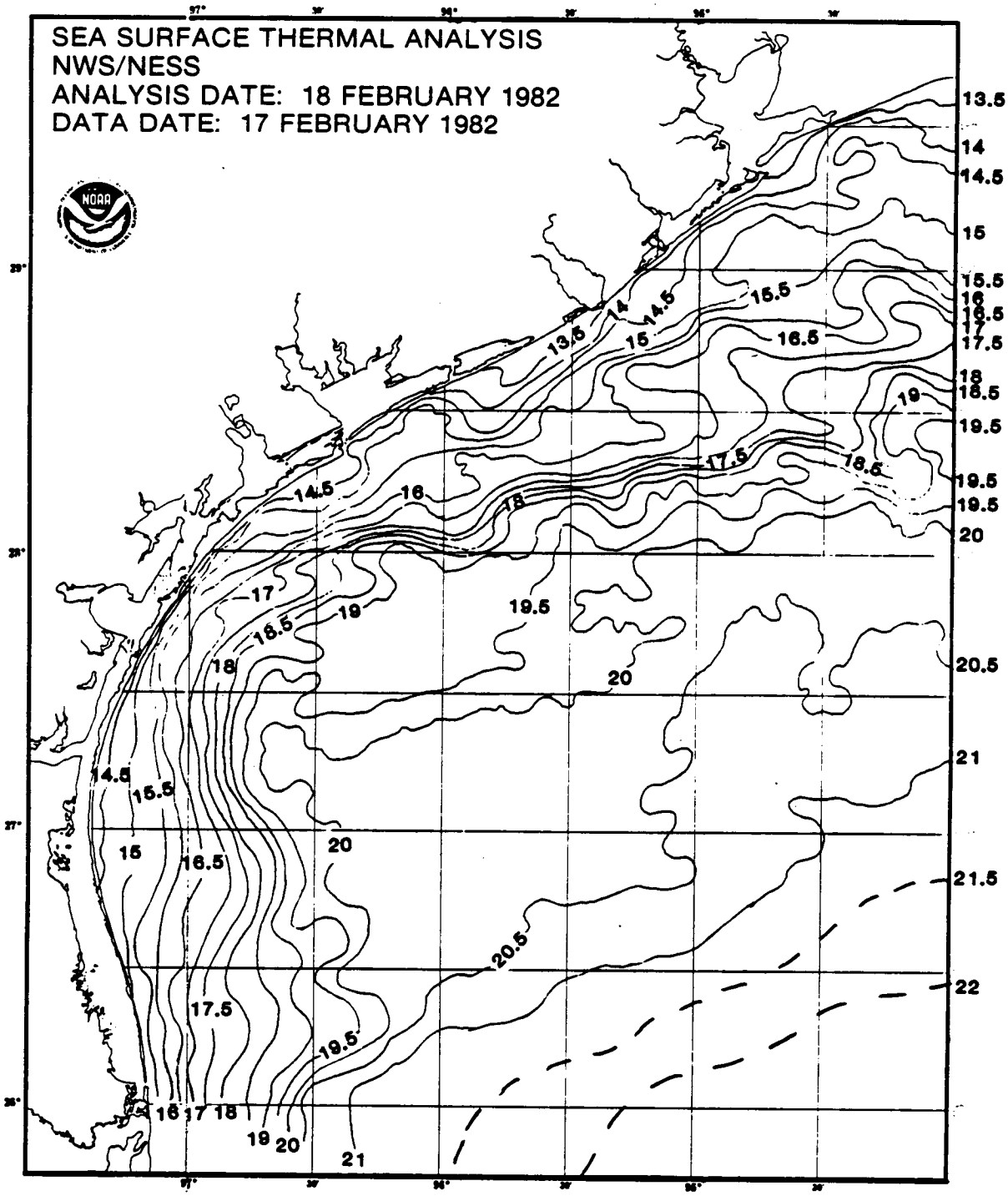

Figure 2.21 Sea-surface temperature based on satellite infrared imagery for 17 February 1982, South Texas shelf. (Courtesy of R. Barazotto, NWS/NESS, Slidell, LA.)

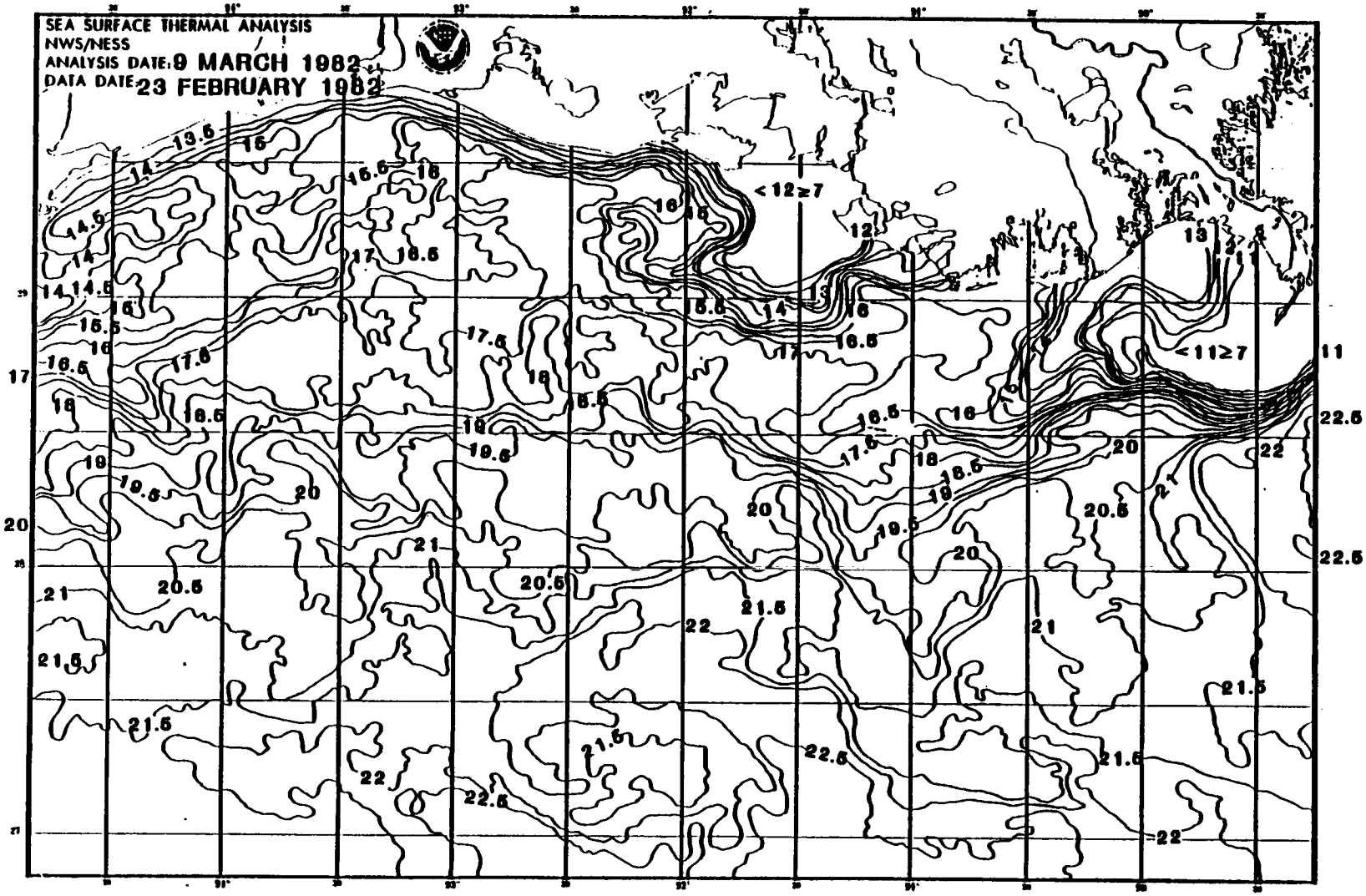

Figure 2.22 Sea-surface temperature based on satellite infrared imagery for 23 February 1982, Texas-Louisiana shelf. (Courtesy of R. Barazotto, NWS/NESS, Slidell, LA.)

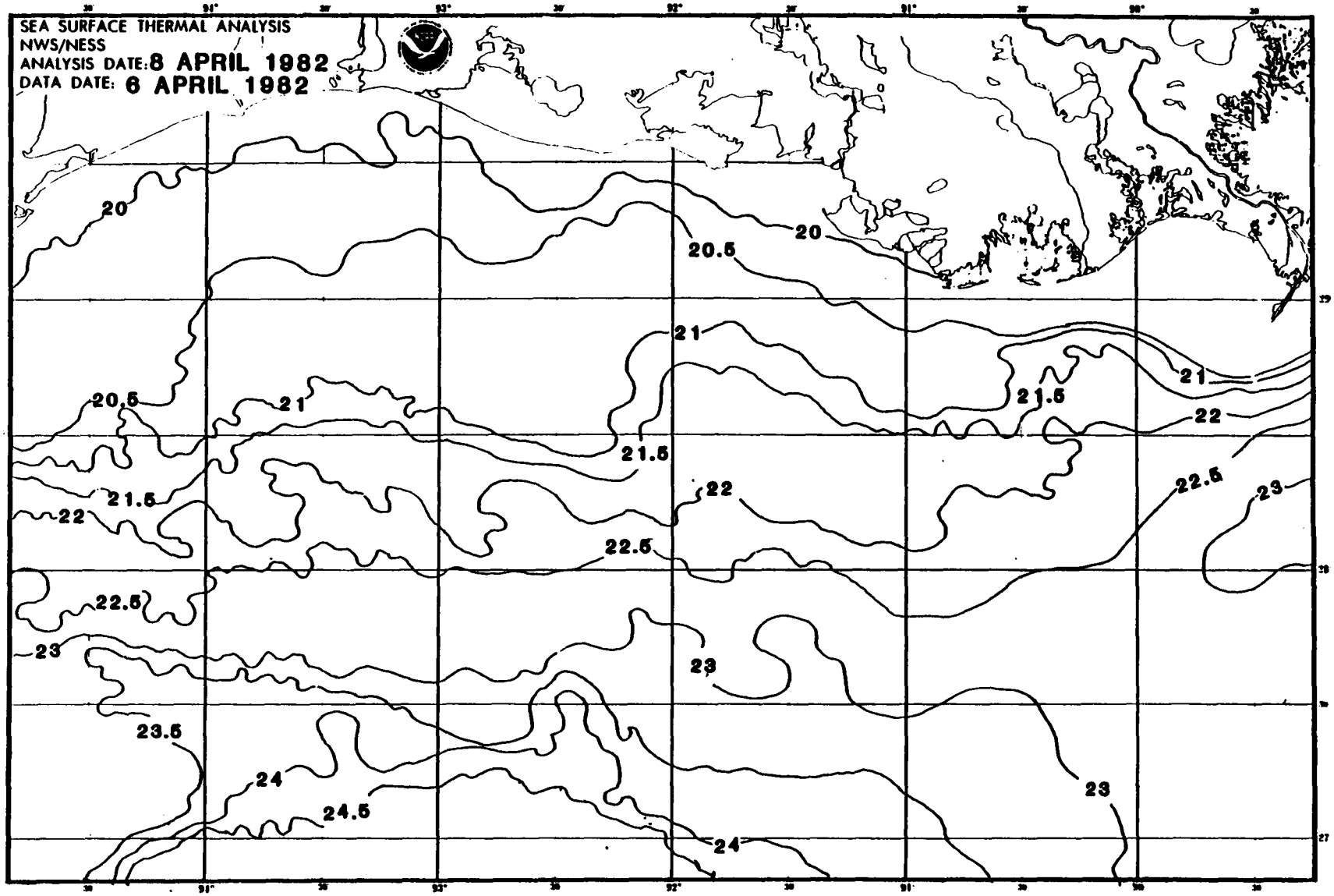

Figure 2.23 Sea-surface temperature based on satellite infrared imagery for 6 April 1982, Texas-Louisiana shelf. (Courtesy of R. Barazotto, NWS/NESS, Slidell, LA.)

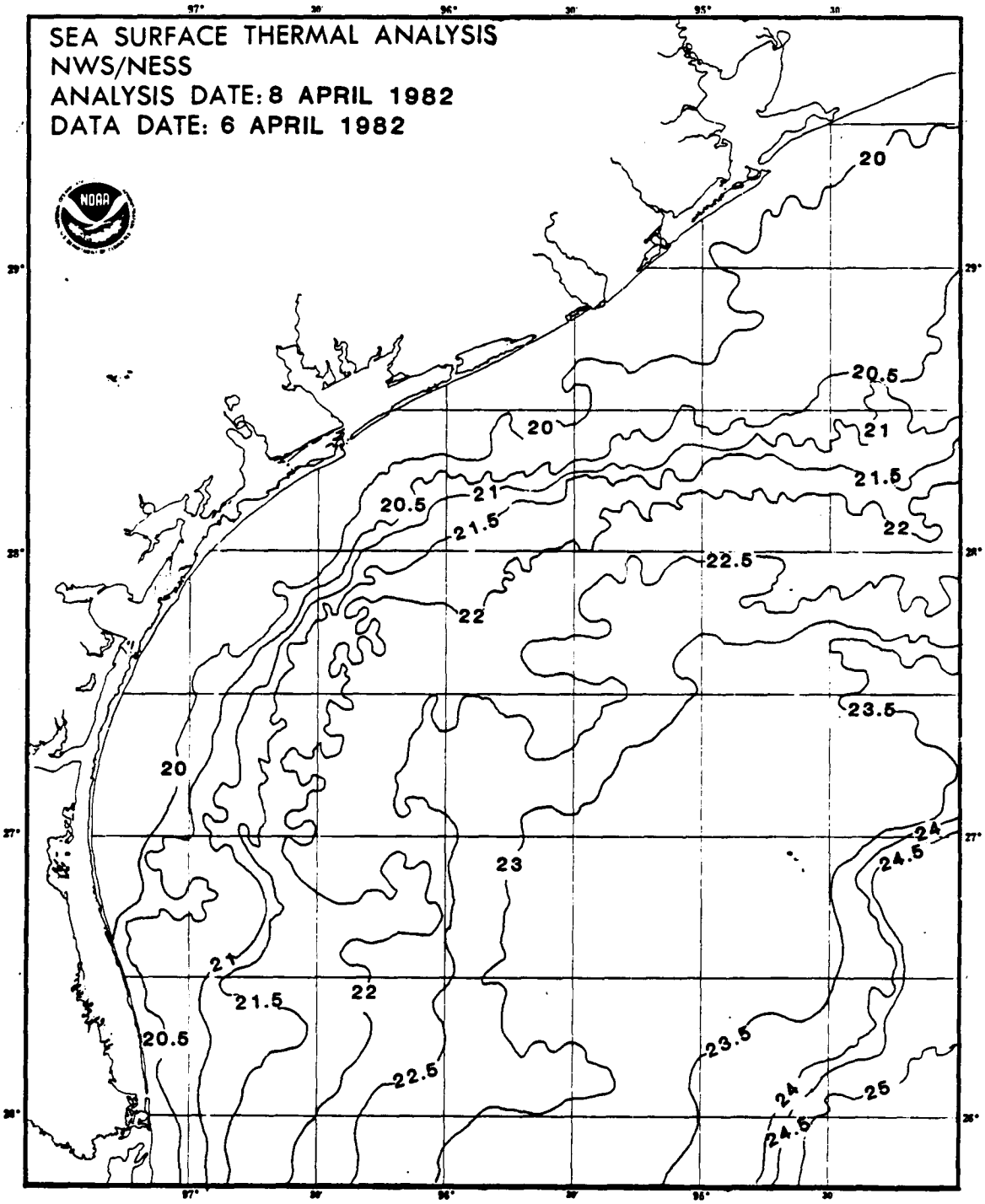

Figure 2.24 Sea-surface temperature based on satellite infrared imagery for 6 April 1982, South Texas shelf. (Courtesy of R. Barazotto, NWS/NESS.)

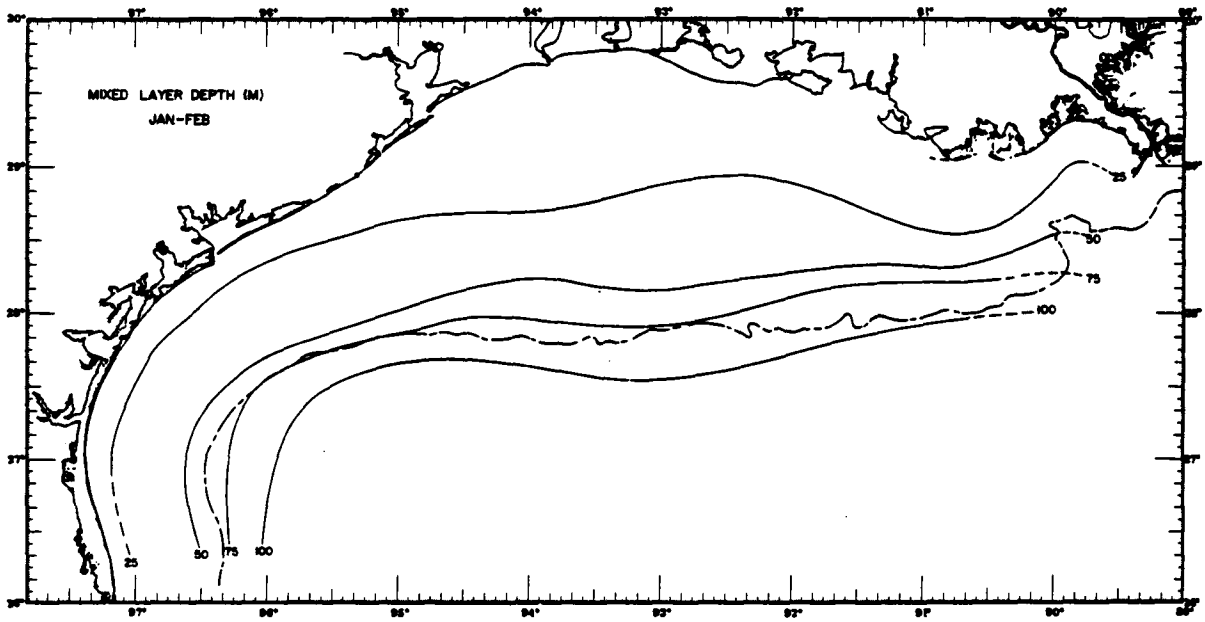

Figure 2.25 Map of mixed-layer depths (metres) for January-February. Dashed lines indicate lack of data, and curvature of such lines suggests most probable tendency. (From Etter and Cochrane, 1975.)

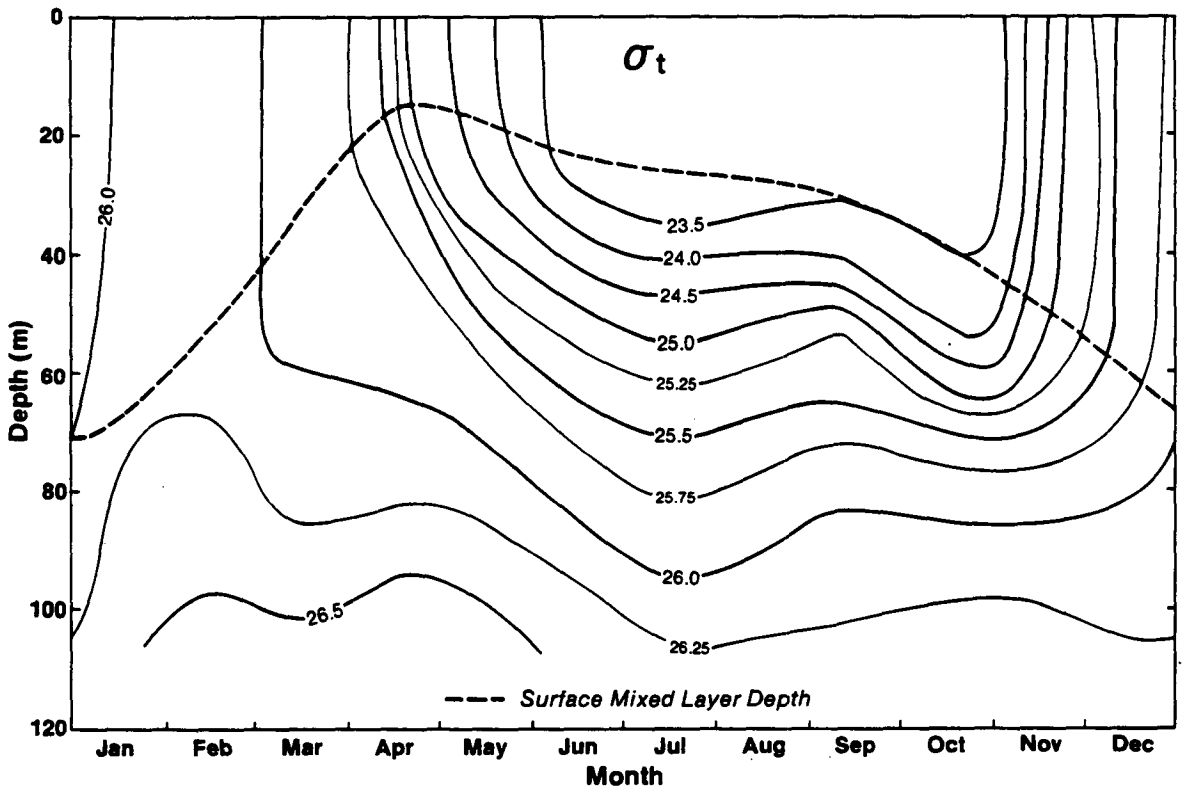

Figure 2.26 Seasonal progression of sigma-t versus depth near the Flower Garden Banks, constructed from: CTD data collected by TAMU in April 1979, September 1979, October 1979, October 1980, March 1981, and July 1981; monthly averages of temperature time-series data recorded on TAMU current meter moorings near the banks; and from GUS III station W-6 (27°55'N, 94°36'W), cruises 13 to 24 of 1964 (Angelovic, 1975). The approximate depth of the surface mixed layer is indicated by the dashed line.

Etter and Cochrane (1975). The mean temperature recorded by our current meters at depths of less than 60 m (in the mixed layer) for February was 18.57°C with a standard deviation of 0.6°C. The cycle of stratification for the shelf edge is also shown in Figure 2.26. Changes in density at the shelf edge are due, almost entirely, to changes in temperature.

Cochrane and Kelly (1982) proposed that the reason waters on the outer continental shelf stay so much warmer than nearshore waters is that the mixed layer on the outer shelf does not penetrate to the bottom. Nearshore, the winter storms do mix the water all the way to the bottom so that each passing cold front extracts heat from a relatively thin layer of water. Offshore, however, the heat capacity of the water is such that the cold frontal passages actually remove more heat from the shelf edge waters than from the nearshore, but the temperature of the relatively thick mixed layer remains relatively high.

Nowlin and Parker (1974) described the effect of cold air outbreaks on shelf waters in the Gulf of Mexico from data they gathered on two cruises in January of 1966. The first cruise was just prior to a cold frontal passage and the second, about 15 days later, was just after the frontal passage, while the region was still under the influence of the cold air. They found that just offshore, in water of 10 to 20 m depth, the temperature decreased by about 5°C, and salinities increased by approximately 1 ppt during the two-week period. At the shelf edge, 100 to 150 NM from shore, there was no change in the salinity, and the temperature decreased by only 1 to 2°C. Nowlin and Parker (1974) hypothesized that evaporation and heat loss to the cold, dry polar air and the nearshore waters greatly increased the density of that water, giving it the temperature and salinity characteristics of water found beneath the subtropical underwater of the deep Gulf. Data collected by researchers at Louisiana State University and Texas A&M University support this hypothesis (McGrail and Carnes, 1983; McGrail et al., 1982; Wiseman et al., 1982; Sahl et al., 1982).

Compare the sea surface temperature maps of 6 April 1982 (Figures 2.23 and 2.24) with the map made from data obtained on 11 April 1982 (Figure 2.27). As shown in Figure 2.28, the 6 April data were taken at the onset of northerly winds at the beginning of a cold frontal passage, and the 11 April map was obtained in the middle of a period of winds with a northerly component.

In the 11 April map, the very nearshore waters have lost nearly 1°C in temperature, but the offshore waters have actually gotten warmer in the area between 92°W and 94°W, causing a very sharp gradient near the coast. This gradient appears to be related to competing events. Both the southerly and northerly winds during the period between 6 April and 11 April had very strong alongshore components toward the east, creating rapid downcoast flow at the coast (Cochrane and Kelly, 1982). This rapid downcoast flow appears

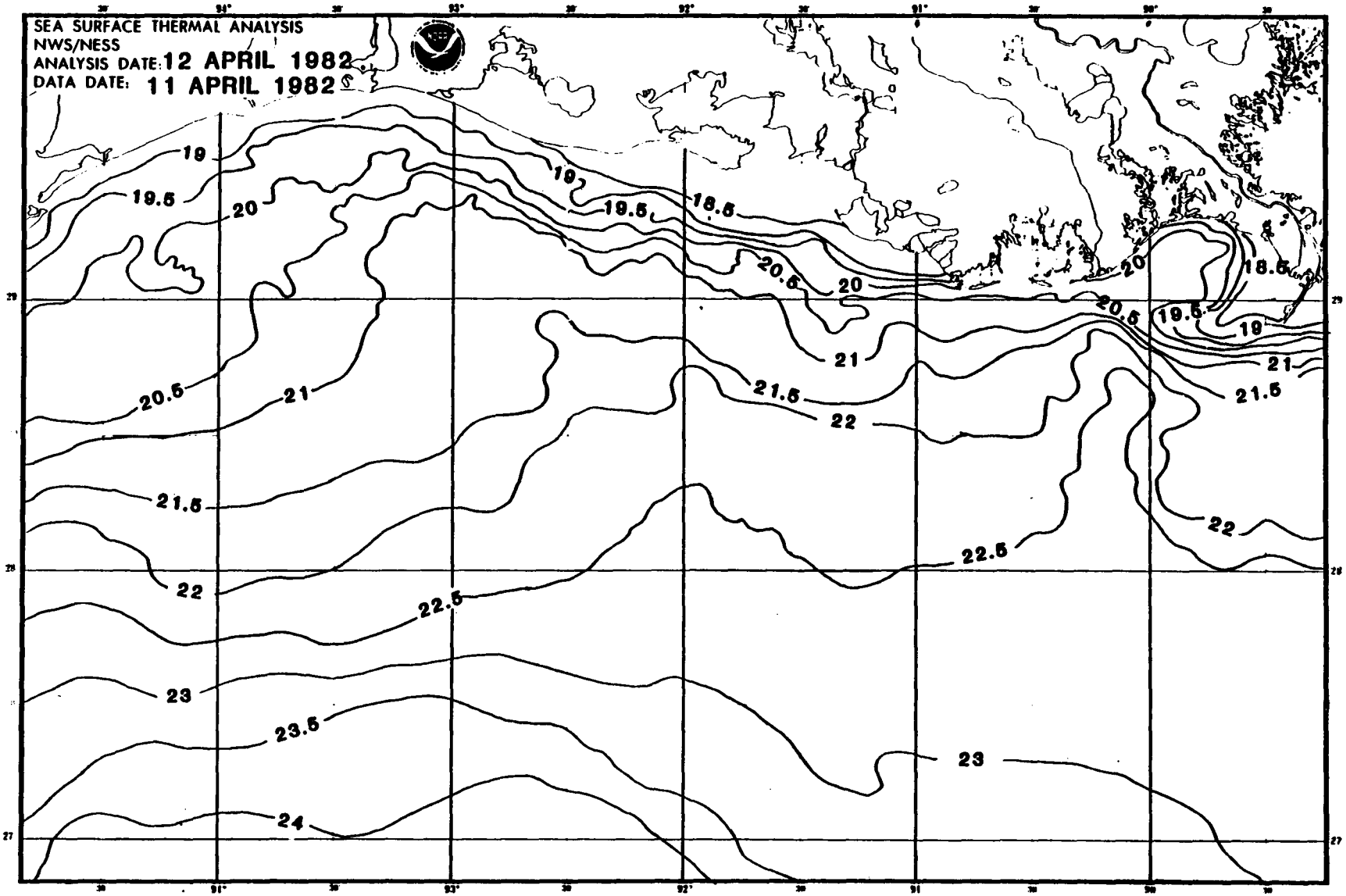

Figure 2.27 Sea-surface temperature based on satellite infrared imagery for 11 April 1982. (Courtesy of R. Barazotto, NWS/NESS, Slidell, LA.)

to have caused a suction just west of the delta through the Mississippi Canyon area that drew warmer water in from offshore and moved it to the west. Notice that the kink in the 21°C isotherm located near 92°W in the 6 April 1982 map appears to have propagated northwesterly to near 93°15'W by the time of the 11 April data.

In March of 1982 we deployed three current meter moorings across the shelf break along the 95°W meridian (see Figure 2.13). This deployment included the time during which the April satellite data were obtained. Records of the wind at NDBO 42002 and NDBO 42008 were also obtained for the duration of the deployment. The progressive vector diagrams (PVD) for the winds at the two buoys and their vector average are shown in Figure 2.28. It is obvious that the winds with a component from the north are much stronger at buoy 42008, which is close to shore, than at buoy 42002. It is likely that this effect is due to the weakening of the cold front as winds passed over the relatively warm water of the shelf. This difference in strength of the north winds leads to a difference in direction of the wind stress for the period. That near the coast is essentially to the west, while the wind stress at the site of buoy 42002 is directed toward the northwest. In both records there are, however, three major events during which the wind is out of the northeast. The first started on 22 March, the second started on 9 April, and the third started on 21 April (Figure 2.28).

The effect of these events on the currents may be seen in Figure 2.29. The strong wind event which started on 22 March reversed the surface flow (60 m) at mooring 2, turning it from easterly to westerly. At mooring 3 the flow from 43 m to 89 m changed from north-northwest to west. The near-bottom flow on both moorings 1 and 2 accelerated to the southwest, and the deeper flow at mooring 3 was veered from southeast to west.

The event on 9 April appears to have been too short-lived to have made any significant imprint on the flow. The mid-depth current (60 m) at mooring 2 returned to easterly flow during the period of south and southeast winds following the 9 April event, as did the bottom flow at both moorings 1 and 2. The current at the level of the two upper meters of mooring 3 was also swinging subtly to the northwest during this time. When the event of 22 April hit, the flow at all depths at the site of mooring 2 veered sharply to the southwest, as did the current near the bottom on mooring 1. At mooring 3 the flow at all depths turned sharply offshore.

These events are also shown in Figure 2.30. In this figure, the vector plot of the wind from NDBO 42002 and the recordings of instruments on mooring 2 are plotted on the same time scale. The temperature record of meter 1 shows little variance through this period except a distinct warming about the time of the frontal passage in late April. The temperature record at meter 3 also shows little variance except a general warming trend until the frontal passage (seen as a shift in the wind from out of the north) in late

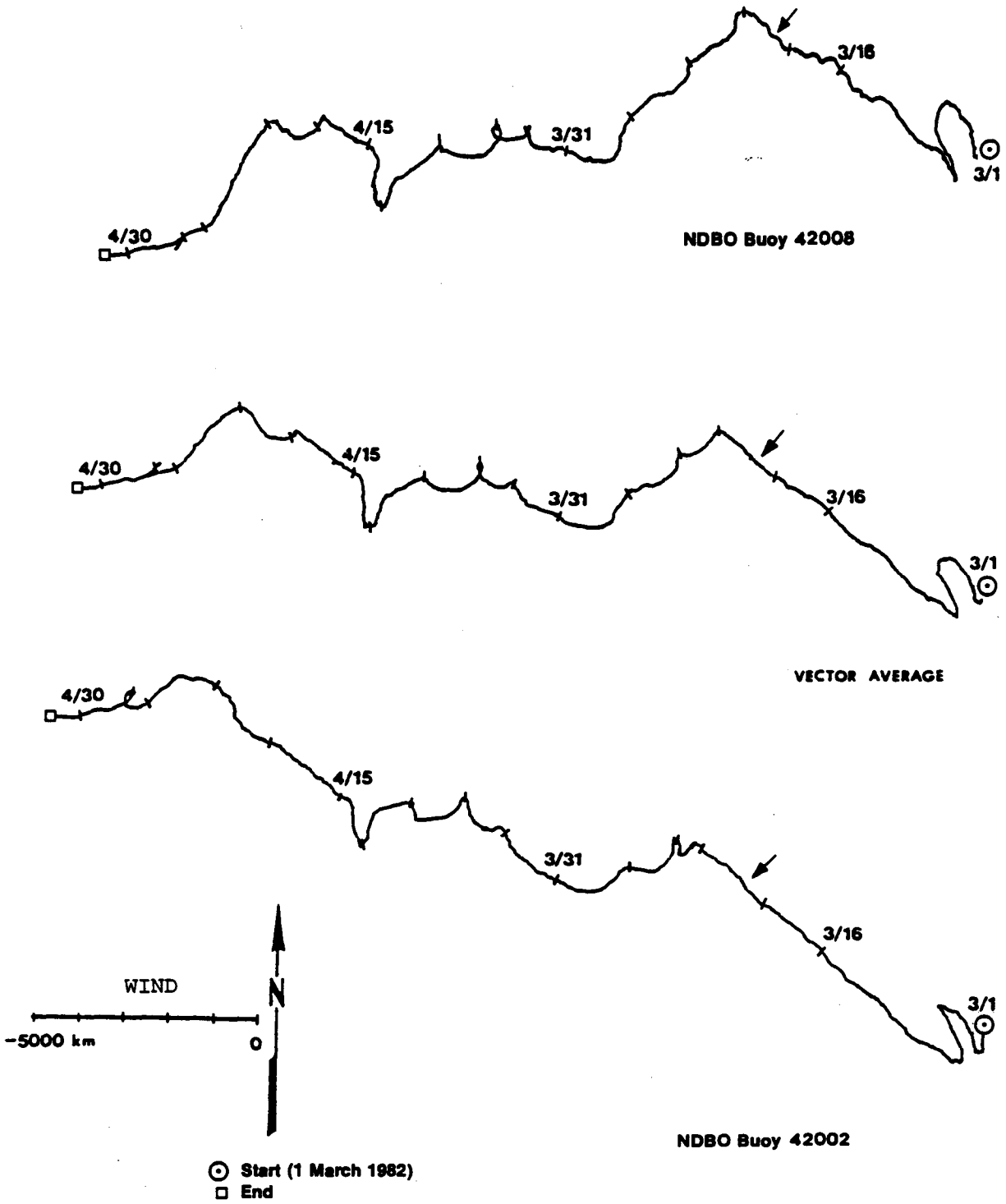

Figure 2.28 Progressive vector diagrams of wind from 1 March to 3 April 1982 at NDBO buoys 42008 and 42002 (locations shown on Figure 2.13). The middle diagram is the vector average of winds at 42008 and 42002. Arrows indicate the dates when current meters were deployed along the 95W transect.

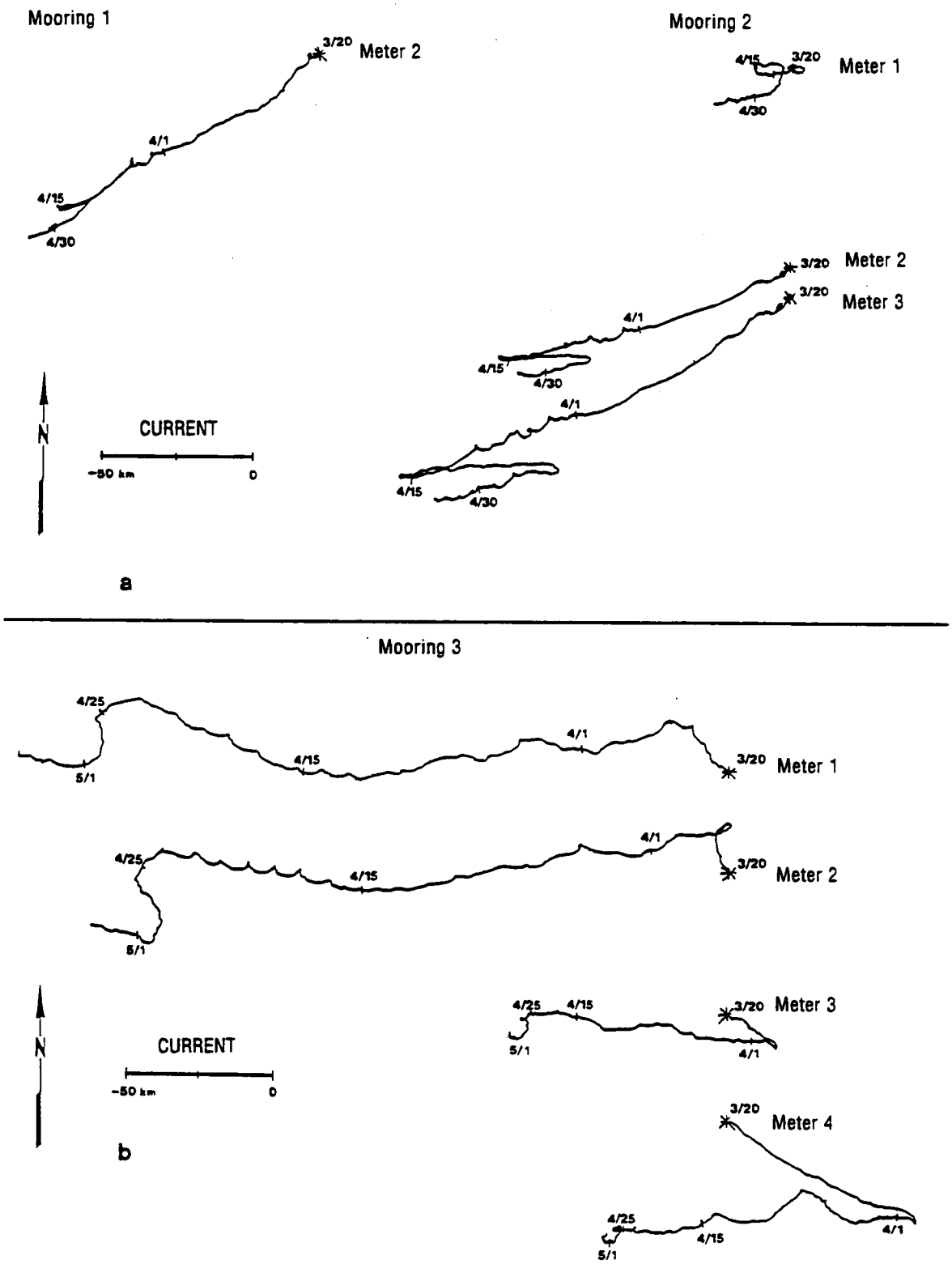

Figure 2.29 Progressive vector diagrams of currents measured at the 95°W array: a) moorings 1 and 2 from 20 March to 30 April 1982, and b) mooring 3 from 20 March to 1 May 1982. (See Figure 2.13 for location.)

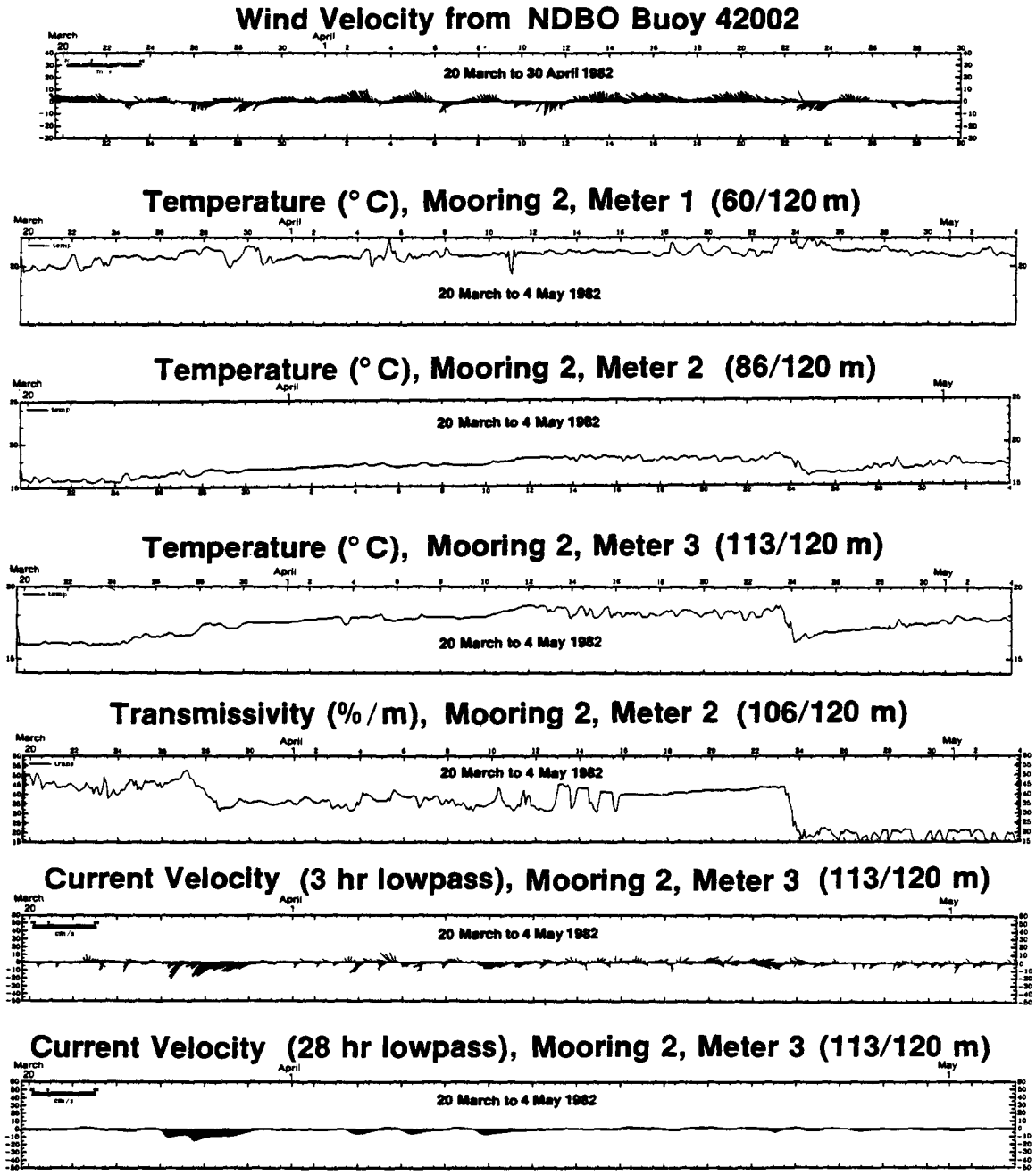

Figure 2.30 Time-series records of the wind from NDBO buoy 42002, and the water temperature, transmissivity, and current velocity from mooring 2 of the 95°W array between 20 March and 4 May 1982. Note the drop in both temperature and transmissivity during the cold front passage on 24 April 82.

April, when the temperature dropped nearly 3°C in six hours. Accompanying the drop in temperature, the current reversed, going from easterly and slightly onshore to westerly and offshore. Simultaneous with the temperature drop, the transmissivity on meter 2 (20 m above the bottom) dropped from about 50% to 18%. This means that the water went from rather clear to heavily laden with sediment.

Tide

The model of the tides in the Gulf of Mexico by Reid and Whitaker (1982) is in excellent agreement with the tidal currents we measured at the shelf edge near the Flower Garden Banks (Table 2.2). Our records do indicate phase and amplitude changes in the M_2 and K_1 tide, which implies that the baroclinic, or internal, mode is important for both constituents. Stronger K_1 internal tides are observed in the summer when stratification is at its maximum, but the M_2 internal tide does not show an appreciable seasonal variation. From Figures 2.3 and 2.4, it is apparent that the tidal currents on the east-west segment of the Texas shelf are highly elliptical and increase in strength toward the shore. The tidal currents on the north-south segment of the Texas shelf appear to be greatly attenuated for both the M_2 and K_1 constituents of the tide. In both areas, the major axis of the tidal current ellipses are nearly perpendicular to the coast.

SEDIMENT DYNAMICS AND THE NEPHELOID LAYER

The term "nepheloid" is derived from the Greek work "nephele," which means cloud. A nepheloid layer is, thus, a layer of water that is cloudy or turbid. For sedimentologists, it has come to mean sediment laden water usually, but not always, found near the bottom. There is no quantitative definition for nepheloidal, partly because there is a continuum from clear to opaque water as sediment is added, and partly because the amount of sediment required to cause any specific amount of light attenuation (cloudiness) varies with the sediment particles' size, shape, and index of refraction.

Measurements of suspended sediment concentrations are made in a variety of ways. The simplest is obtaining a volume of water, filtering it, and weighing the filtrate. This method provides a measure usually reported as milligrams per litre (mg/l). A similar method is to take an aliquot of water and run it though a particle counter such as the Coulter Counter. The sediment concentration may then be reported as the number of particles per cubic centimetre (cm^3). In order to reference a value reported per cm^3 to a value reported in the mg/l system, the size distribution and particle density must be known.

Table 2.2 Amplitude and Phase of the Barotropic Tidal Currents Near the Flower Garden Banks for the M_2 and K_1 Constituents. The Measured Values are Those Computed from Current Meters Moored at Mid-depth Near the Banks

Methods*	u (East-West) Amplitude (cm/s)	u (East-West) Phase (°)	v (north-south) Amplitude (cm/s)	v (north-south) Phase** (°)
		M_2 Tidal Constituent		
Measured by Vector Averaging	0.6	99	1.4	354
Model, WFG	0.3	116	1.3	357
Model, EFG	0.3	132	1.1	354
		K_1 Tidal Constituent		
Measured by Coherence Method	0.7	335	1.1	200
Model, WFG	0.7	344	1.2	213
Model, EFG	0.6	349	1.1	209

* Three techniques were used for obtaining values. The vector averaging method and the coherence method were used to eliminate the effects of internal tides. The model values were obtained for the East Flower Garden (EFG) and the West Flower Garden (WFG) region from a numerical model of the barotropic tides in the Gulf of Mexico developed by Reid and Whitaker (in press).

** The phase is relative to the local tidal potential.

The most common method for obtaining profiles of the sediment distribution is to use the attenuation of light over a given pathlength (relative transmittance) or the amount of light scattered (forward or back) over a given path. Instruments that use the first technique are called transmissometers; instruments using the second technique are commonly called nephelometers. Transmissometers yield values in percent transmittance per metre. The higher the value, the clearer the water. These values are referenced to mg/l by means of calibrations and by collecting water in a bottle at multiple points in the profile, filtering the samples from the bottles, and fitting the transmissivity values to the absolute mg/l values obtained by the filtration method.

Acoustic instruments have also been developed which use acoustic reflectance from the particles over a known pathlength to obtain profiles. These must be referenced in the same manner as the light instruments.

Unfortunately, the calibration techniques for the profiling instruments possess so much scatter that most reports of suspended sediment distributions are in relative rather than absolute terms of concentration.

Nepheloid layers only occur where the turbulence of the water is sufficiently high to offset the settling of the sedimentary particles under the influence of gravity. The larger the particles are the more intense the turbulence must be to maintain a suspension. Nepheloid layers are, therefore, usually composed of silt and clay particles because only the most energetic flows can maintain a sand suspension.

South Texas Shelf

The first comprehensive study of the nepheloid layer on the South Texas continental shelf was published by Shideler (1981). He used both a transmissometer and Coulter Counter to study the distribution of suspended sediment on the shelf. Shideler and his colleagues made six cruises in 18 months, occupying the same stations on each cruise in order to examine both spatial and temporal variances in the nepheloid layer. He found that the nepheloid layer thickened offshore to a maximum of 35 m near the shelf break and that the concentration of suspended sediment in the nepheloid layer decreased from a maximum near shore to a minimum at the shelf break. Shideler also found that the sediment in the nepheloid layer was dominated by inorganic detrital minerals. In addition to the offshore thickening of the nepheloid layer, Shideler found that it reached its maximum thickness in the central part of his study area, in the embayment between the drowned Rio Grande Delta and the drowned Brazos-Colorado Delta. Further, he found that the nepheloid layer was thinner and of smaller areal extent in the

fall than in the spring. He also shows a noticeable thickening of the nepheloid layer across the shelf toward the inlet at Matagorda Bay in his two March cruises (1976 and 1977) and his two May cruises (1976 and 1977) but not in his November cruises (1975 and 1976).

Shideler concluded that the nepheloid layer is generated and maintained by resuspension of muddy seafloor sediment as a result of bottom turbulence. He then offered a number of suggestions regarding the agents which might cause such resuspension. He showed that surface gravity waves in calm weather could only induce resuspension inshore of about 10 m, and even storm waves with 10-second periods are unlikely to be important in resuspension beyond 40 m depth. Beyond that, his conceptual model is flawed by a lack of oceanographic data. He proposed that the mid and outer shelf resuspension is generated by turbulence along the front that migrates back and forth under the influence of the tide, wind, and intrusions of the Loop Current. However, as can be seen in the data from the Reid and Whitaker (in press) model of the tides (Figures 2.3 and 2.4), tidal currents are on the order of 1.5 cm/s or less on that stretch of the shelf for both the M_2 and K_1 constituents. Also, the Loop Current has never been reported west of the Yucatan Peninsula.

The flow presented by Cochrane and Kelly (1982) in Figures 2.11 and 2.12 does offer a suggestion for the trend of the nepheloid layer toward Matagorda Bay in the spring. During this period, the coastal convergence zone is migrating upcoast, so that the turbid coastal waters carrying effluent from the Brazos and Colorado Rivers might be diverted offshore and to the south. In November, however, the flow appears to hug the coast.

The current meter records from the CSA site near Baker Bank show that near-bottom velocities at about the 75 m depth frequently exceed 20 cm/s (Figure 2.31), which is ample to keep silt and clay in suspension.

Holmes (1982) analysed the mineralogy of the suspended sediment in the nepheloid layer and that of the substrate on the South Texas continental shelf. He reports that the dominant clay minerals in the bottom sediment are members of the smectite group and that these minerals make up 34 to 75% of the clay fraction, with the mode being near 60%. In contrast, he found that the suspended sediment in the nepheloid layer is, in general, devoid of the smectite clays. He goes on to say that the near-bottom current velocity required to erode the mud on the mid to outer shelf is of the order of 10 to 30 cm/s. He then says that no currents of this magnitude have been measured on the seafloor, even during a storm passage. On the basis of these two points -- the absence of smectite in the nepheloid layer, and low supposed current velocities -- Holmes (1982) concluded that the nepheloid layer is unrelated to the bottom sediment. He suggests that a thin veneer of sediment is altered biogenically to illite (another clay mineral) and made available for

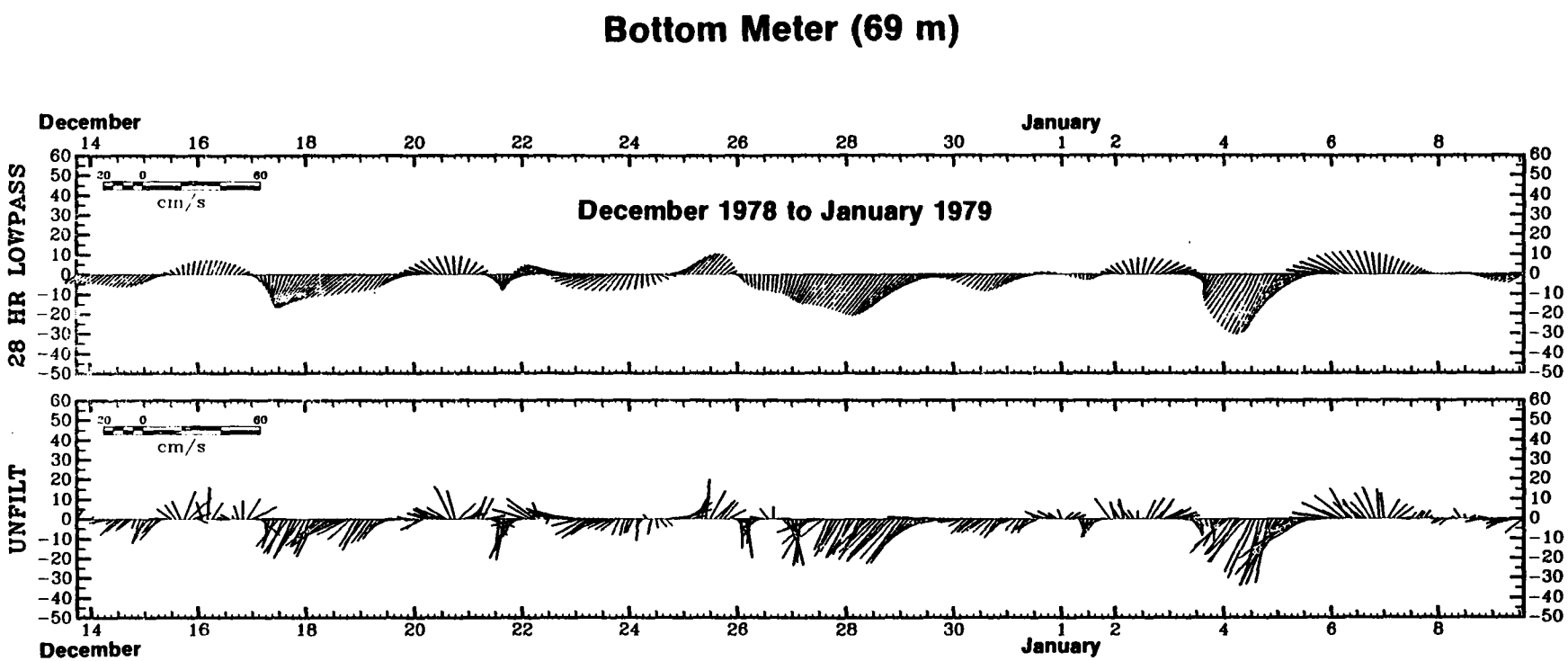

Figure 2.31 Sample current record from the bottom current meter (4 m from bottom in 73 m of water) of the CSA mooring near Baker Bank. The lower frame is the raw unfiltered data, while the upper frame shows the same record after filtering to remove currents with periods shorter than 28 hours. In this "stick plot" representation, the length of each stick is the magnitude and the orientation is the direction (in map coordinates) of the current at each point in time.

resuspension by annelid worms. Holmes, appears to be wrong on both points.

A sample of the bottom current meter (69 m in 73 m of water) record from the Baker Bank site is shown in Figure 2.31. Note that the speed of the current almost always exceeded 10 cm/s and reached maximums of over 35 cm/s. These peak velocities probably occurred during frontal passages. Also, in their report to Conoco, Inc., Continental Shelf Associates (1982) reported on the clay mineralogy of the bottom sediment, suspended sediment, and sediment retained in sediment traps from the vicinity of their current meter mooring. They reported the smectite group minerals under their alternate name, montmorillonite. Sediment from the traps averaged 43% montmorillonite; suspended sediment averaged 56.7% during one cruise and 53.2% during another; and the bottom sediment averaged 49.5% montmorillonite.

It is very likely that Holmes used too small a sample of suspended sediment for X-ray analysis or suffered some other procedural error. Even without Continental Shelf Associates' evidence that the mineralogy of the suspended sediment and substrate are identical, it presses the credulity to suppose worms could change the mineralogy of the clays, then supply the altered sediment to the water column and not the substrate.

In its essentials, the hypothesis of Curray (1960) regarding the source of mud on the South Texas continental shelf is probably correct. However, we find no evidence to suggest that hurricanes or tidal currents are important agents of sediment transport beyond midshelf depths. The general picture is that surface gravity waves and swift alongshore currents keep water inside the 10 m isobath turbid with resuspended sediment and preclude significant deposition of silt and clay. When the shelf flow is toward the north (summer), fine sediment from the Rio Grande is swept to the north along the coast and in the bottom boundary layer. This must have been a much more important source prior to the diversion of the Rio Grande waters for agricultural purposes. When the shelf flow is to the south (fall and winter), sediment from the Colorado, Brazos, and perhaps even the Mississippi Rivers are swept to the south in the bottom boundary layer. Deposition from these sources has produced the mud cover on the shelf between the two shelf-edge drowned deltas.

The nepheloid layer on the South Texas shelf appears to be derived from both local resuspension of the fine sediment and advection in the bottom boundary layer from coastal sources.

East Texas-Louisiana Shelf

Over the period from 1979 through 1982 we investigated sediment dynamics on the east-west segment of the Texas-Louisiana shelf. Two approaches were used: 1) surveys in which profiles of salinity, temperature, transmissivity, and horizontal current velocity components were taken on closely spaced stations; and 2) moored instruments which provided time series measurement of temperature, transmissivity, and current velocity. In addition, we used *in situ* flow visualization techniques to study the behavior of the bottom boundary layer. Results of these studies, up to 1981, were summarized in McGrail and Carnes (1983).

Cross-shelf transects were run in March 1981, March 1982, and May 1982 using station spacings of approximately 10 NM on the shelf and 5 NM on the shelf break and upper slope. On the March 1982 cruise, four shelf-perpendicular transects and one shore-parallel transect were run (Figure 2.32). Also, three current meter moorings were established at the shelf break along 95°W (Figure 2.13). The May 1982 transect was run from the shore to the current meter moorings along 95°W (Figure 2.33). The moorings were recovered at that time.

By combining and analyzing all of these data, we are able to offer the following picture of shelf sediment dynamics.

In the winter, cold air outbreaks and their attendant wind events homogenize the nearshore waters and produce surface gravity waves capable of considerable bottom agitation to depths of, perhaps, 40 m. The data of Cochrane and Kelly (1982) indicate that nearshore currents may exceed 75 cm/s during these frontal passages. The waves and currents combine to fill the nearshore waters with high sediment loads. From Nowlin and Parker (1974) and Wiseman et al. (1982) it is known that the frontal passages also create cold saline waters in this region. These waters sink and run offshore along the bottom because of their excess density. Also, the bottom boundary layer of westward-flowing current in a rotating system possesses southwesterly flow (see Weatherly, 1975, for a discourse on Ekman bottom boundary layers). Sediment entrained in this bottom flow is carried to the outer shelf. The bottom mixed layer and nepheloid layer thicken in the offshore direction as the bottom waters flow off the sloping shelf and out over water of equal density on the outer shelf. The mean flow on the outer shelf at the location of the Flower Garden Banks is toward the east even during the frontal passages. This sets up a northeastward flow in the bottom boundary layer offshore, causing convergence in the bottom waters. The convergence appears to migrate back and forth over the shelf break. This migration shows up in the bottom current meter records as oscillation between onshore and offshore flow, with attendant decreases and increases in temperature and fluctuations in transmissivity levels.

Occasionally, the flow on the outer shelf reverses and flows to the west, as it did in December 1980 at the Flower Garden site and during most of the six-week period that the moorings at the 95°W site were out. It is not entirely clear whether these reversals represent a displacement of the eastward-flowing shelf slope current seaward by unusually strong or persistent north winds, or an actual reversal of the shelf-edge flow field.

During the March 1981 cruise, the transect revealed a classic picture through the flow-field portrayed by Cochrane and Kelly (1982) (Figures 2.11 and 2.12). Inshore of the 70 m isobath, the isotherms sloped up in the offshore direction, and the flow was to the northwest at the surface, west at mid-depth, and southwest at the bottom. Seaward of the 70 m isobath, the isotherms were steeply inclined down in the offshore direction with very strong (75 to 100 cm/s) flow to the east. Near-bottom flow in most outer stations had a northerly component to it. A plume of turbid water extended from the nepheloid layer on the shelf out over the slope along the 17°C isotherm (McGrail and Carnes, 1983).

In March of 1982 the same transect revealed a somewhat different picture (Figure 2.34). The change in slope of isotherms occurred over the 40 m isobath, much closer to shore. The velocity profiles were rather chaotic, partly due to instrument malfunction, and partly because the shelf seemed to be undergoing a transition, with strong southerly components to the nearshore flow. As can be seen in the plot of sigma-t (density minus 1 multiplied by 10^3), it is obvious that there is a very strong nearshore front in the water column, with an inflection in the upper isopycnals at station 5. The slope of the isopycnals in the offshore region implies that flow was to the east. That is consistent with our profiling current meter records, as well as with records from a current meter moored at the West Flower Garden Bank by Continental Shelf Associates for Union Oil Company.

Note the extensive wedge of low salinity water extending nearly 90 km across the surface of the shelf waters. Also note that oceanic values of salinity extend to within 60 km of the coast. This wedge is undoubtedly the leading edge of the February discharge maximum from the Mississippi River reported by Cochrane and Kelly (1982). The influence of this brackish water can also be seen in the lens of relatively dirty water which extended 50 km seaward in a wedge of low salinity water.

Inshore of the 10 m isobath, the water was very turbid from top to bottom. The nepheloid layer at the base of the water column up to 50 km offshore was very heavily laden with suspended sediment. Transmissivity values as low as 5%/m for 660 nm light (red light emitting diode) were observed 3 m above the bottom in this region. This is, of course, the region where the haline front intersects the bottom. Farther offshore the minimum transmissivity values were on the order of 20 to 30%/m. These latter values correspond to

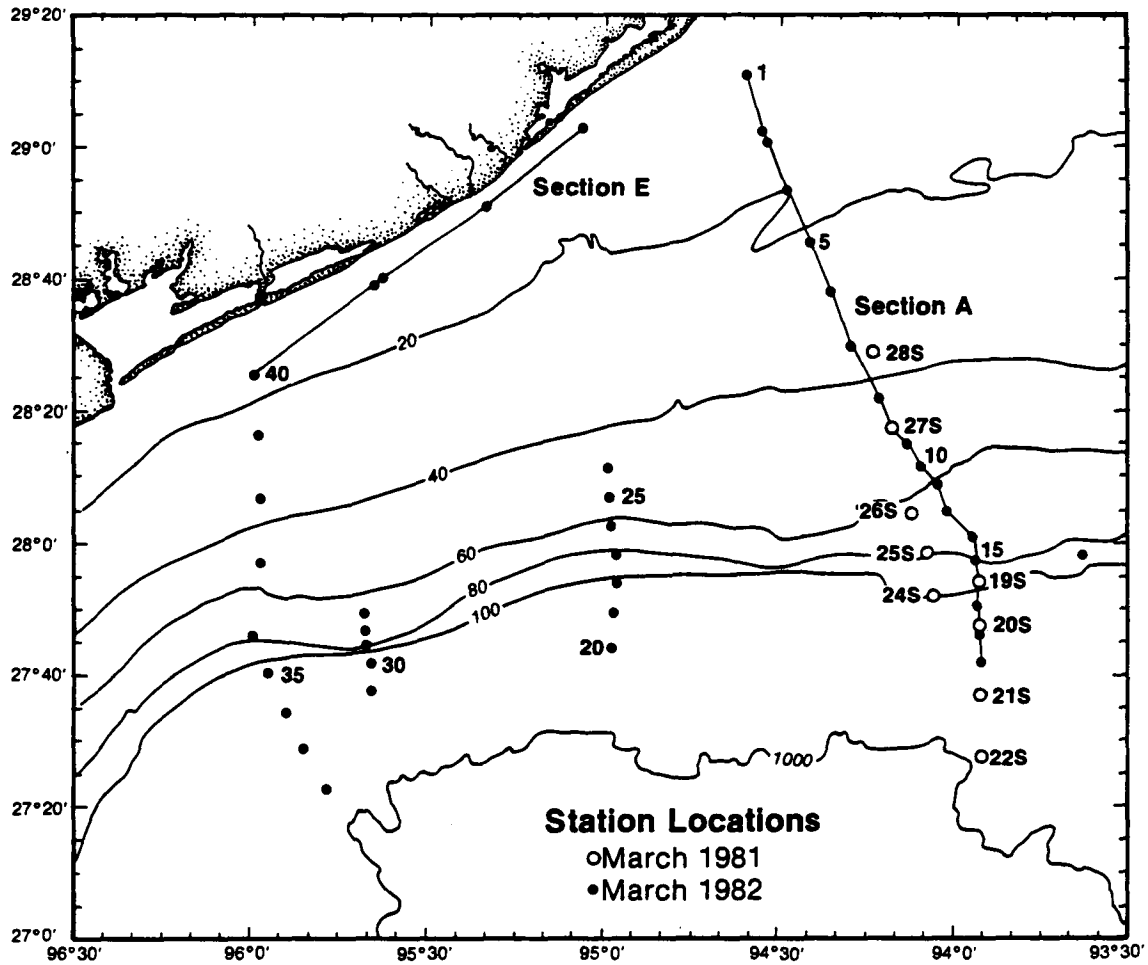

Figure 2.32 Map showing location of stations taken during March 1981 and March 1982 cruises over the Texas-Louisiana shelf and slope. Sections A (across shelf) and E (along shore) are indicated by the connected stations.

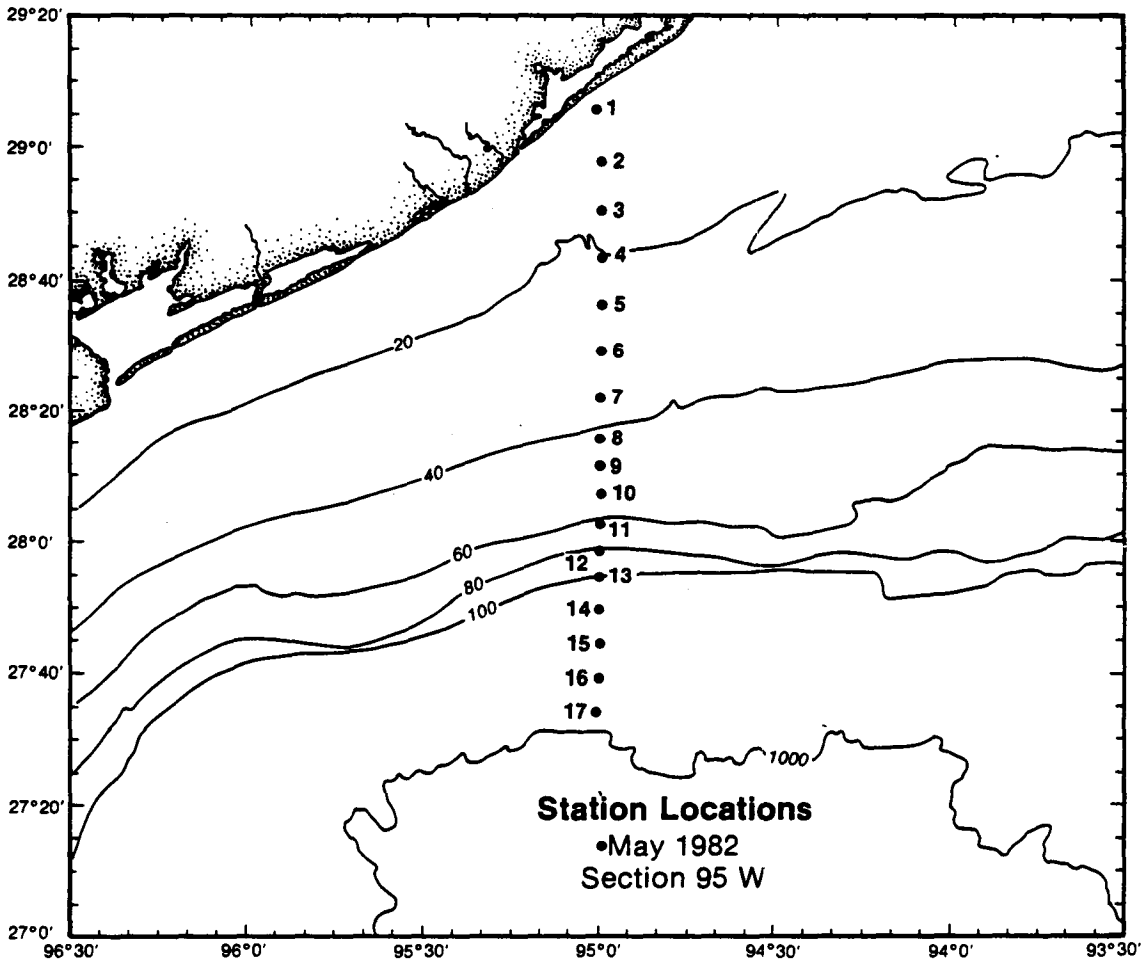

Figure 2.33 Map showing location of stations on the cross-shelf transect along 95°W over the Texas-Louisiana shelf and slope in May 1982.

somewhat more than 1 mg/l. The nepheloid layer extended across the shelf in a well mixed bottom layer of 10 to 15 m thickness and spilled over onto the slope.

Section E, run on the same cruise as section A in March of 1982, is a nearshore, coast-parallel section (Figure 2.35). It shows the alongshore variability in salinity, temperature, and suspended sediment concentrations. The transect cut across perturbations in the wedge of brackish, turbid water that serves to mix shelf and coastal waters. These eddies cause large-scale diffusion of sediment to the offshore waters and onshore diffusion of salt into the coastal water. Figure 2.36 shows the distribution of mass properties and suspended sediment in May of 1982 when the current meters were recovered. The location of those current meters relative to the 95°W transect is shown in Figure 2.37. From the salinity distribution, it is clear that effluent from the Mississippi River is dominating the coastal zone. This wedge of brackish water extends out almost 50 km at the surface and 40 km at the bottom, making the front much steeper than it was in March.

The isopycnals, with few exceptions, all slope down toward the coast, which implies westward flow, as the current meter confirmed. Again the nearshore water, inside of 15 m, was very turbid. The turbidity once again extended seaward in the brackish water at the surface out to approximately 50 km. A tongue of clear water penetrated to within about 35 km of the coast between about 8 m and 13 m depth.

The cross-shelf distribution of suspended sediment in the nepheloid layer is substantially more complex than it was in section A. Over the middle shelf the nepheloid layer varies in thickness from about 5 to 15 m, with minimum values of transmissivity essentially the same as on section A. At the shelf break, however, the nepheloid layer wells up to over 25 m in thickness, with minimum transmissivity values on the order of those in the coastal water. In addition, there was an isolated core of turbid water off the shelf break centered at about 60 m depth.

From the records of the moored instrument, one must conclude that either this very turbid water was delivered to the shelf break to the east of 95°W during the episode of strong offshore flow, or that it was being actively resuspended by strong local currents at the time of the transect. The current meter records (Figure 2.30) strongly suggest that the former is the more likely explanation.

It appears that the sediment is kept in suspension over much of the inner shelf by swift currents and turbulence. It is then advected to the shelf edge, where episodic deposition may take place. Some of the sediment is clearly swept over the shelf edge to the slope and deep basin. It may be that the increase in tidal currents shown by Reid and Whitaker (in press) (Figures 2.3 and 2.4) help to keep sediment from accumulating to any great extent in the

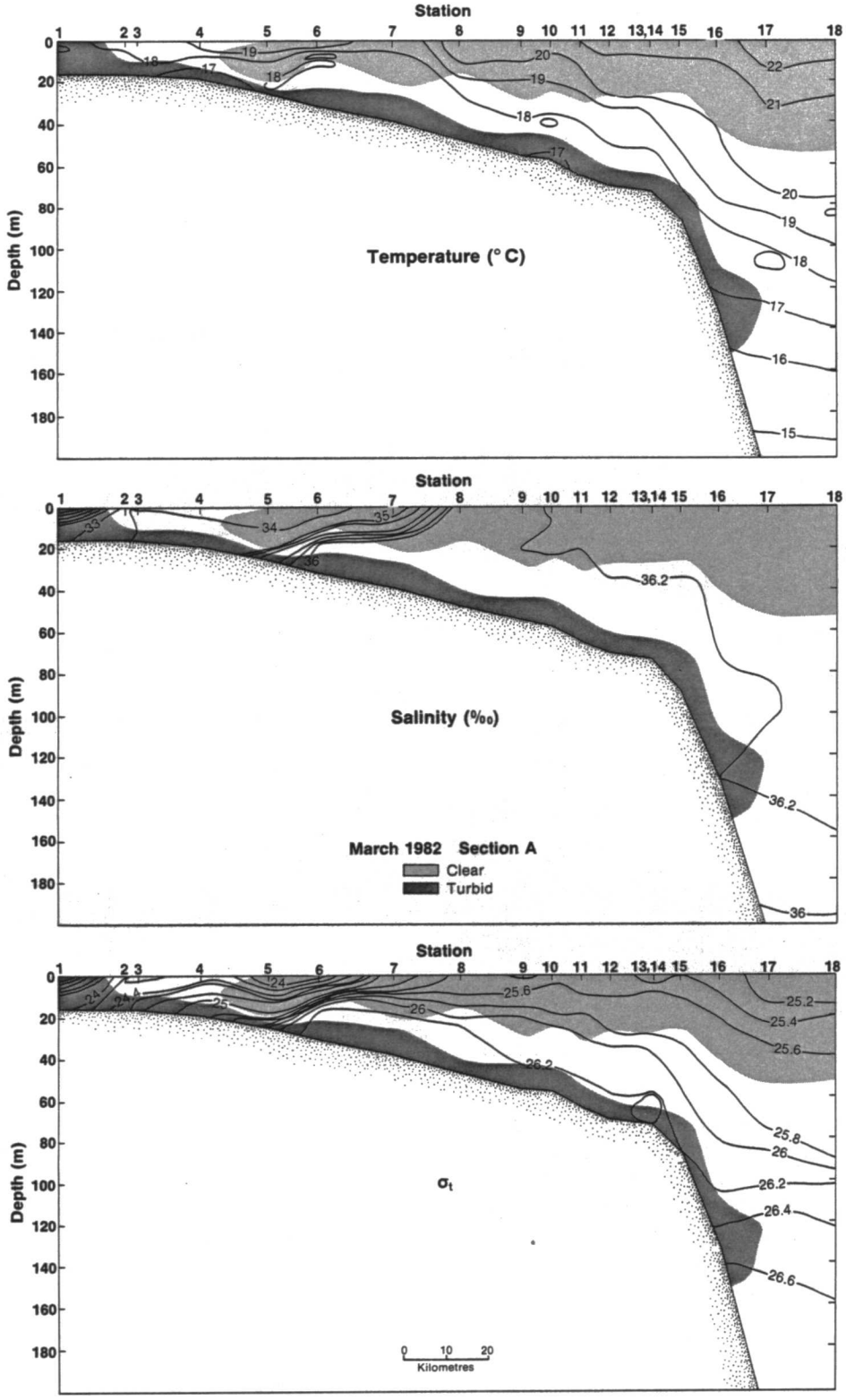

Figure 2.34 Cross-shelf vertical section of temperature, salinity, and sigma-t along section A, occupied in March 1982 (see Figure 2.32 for station location). Regions of turbid and clear water are indicated by darker and lighter shading, respectively, Undshaded regions are of intermediate water transparency. The contour interval for salinity is 0.2 ppt down to 35 ppt, and is 1 ppt for salinities less than 35 ppt.

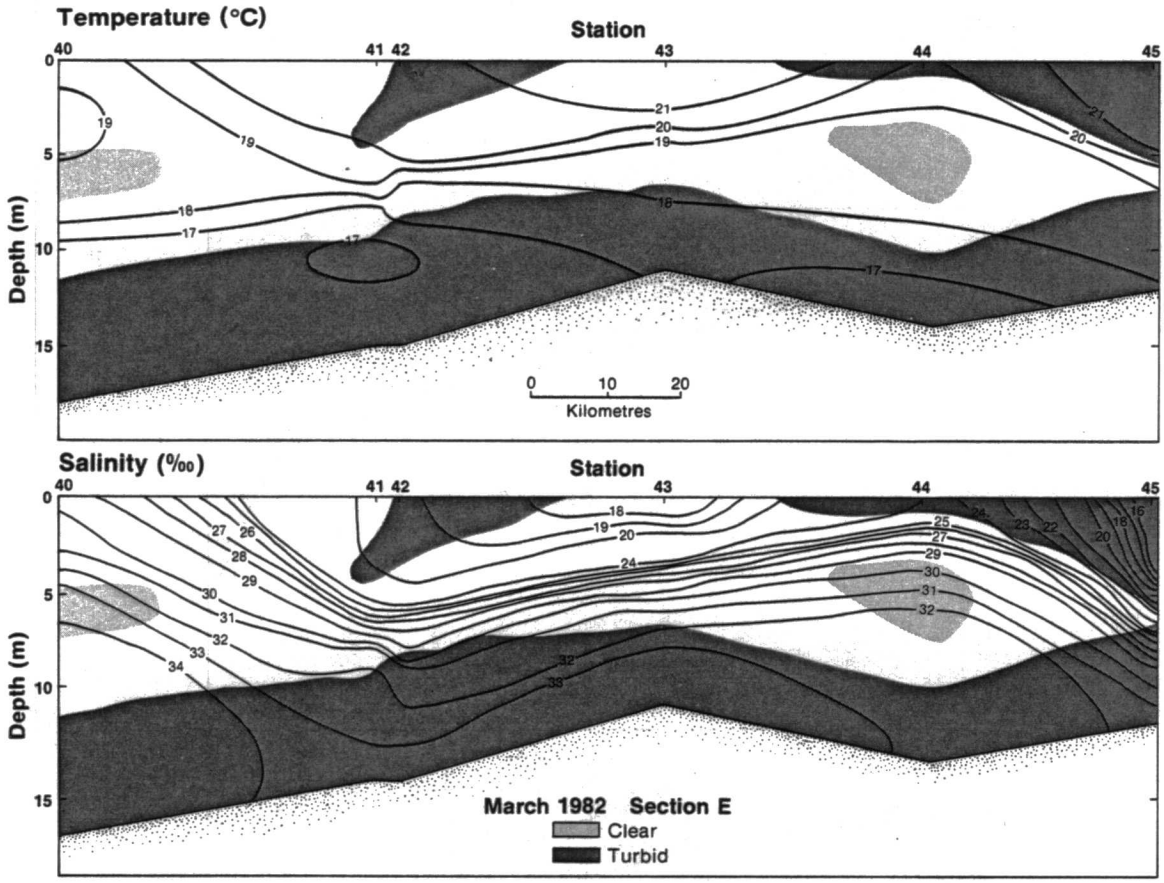

Figure 2.35 Along-shore vertical sections of temperature and salinity along transect E occupied in March 1982 (see Figure 2.32 for station locations). Regions of turbid and clear water are indicated by the darker and lighter shading, respectively. Undshaded regions are of intermediate water transparency. Regions marked clear in this figure are as turbid as regions marked turbid in transect A (Figure 2.34).

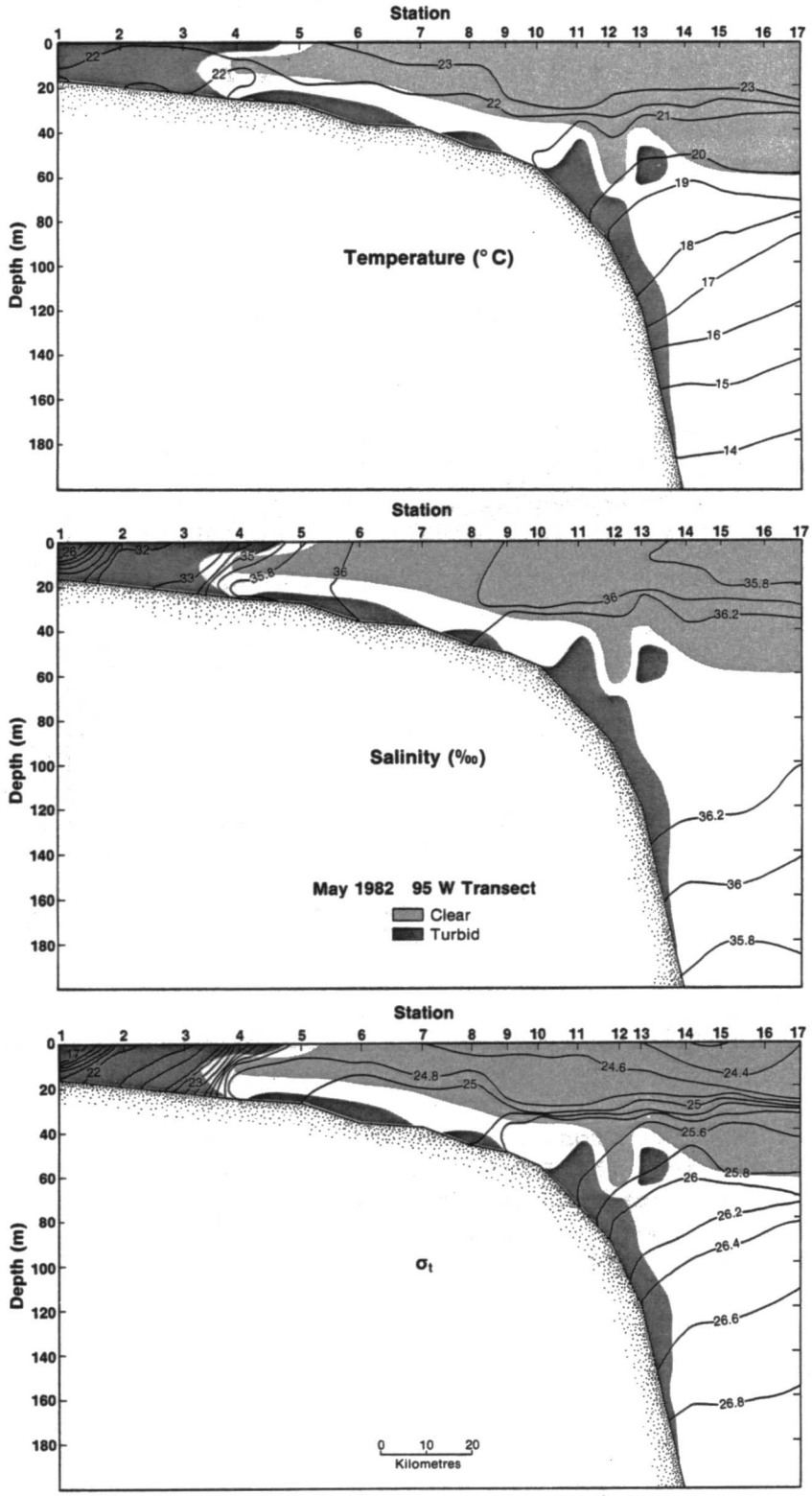

Figure 2.36 Cross-shelf vertical sections of temperature, salinity, and sigma-t along 95°W, occupied in May 1982. (See Figure 2.33 for station locations.) Regions of turbid and clear water are indicated by darker and lighter shading, respectively. Unshaded regions are of intermediate transparency. The contour interval for salinity is 0.2 ppt down to 35 ppt, and is 1 ppt for salinities less than 35 ppt.

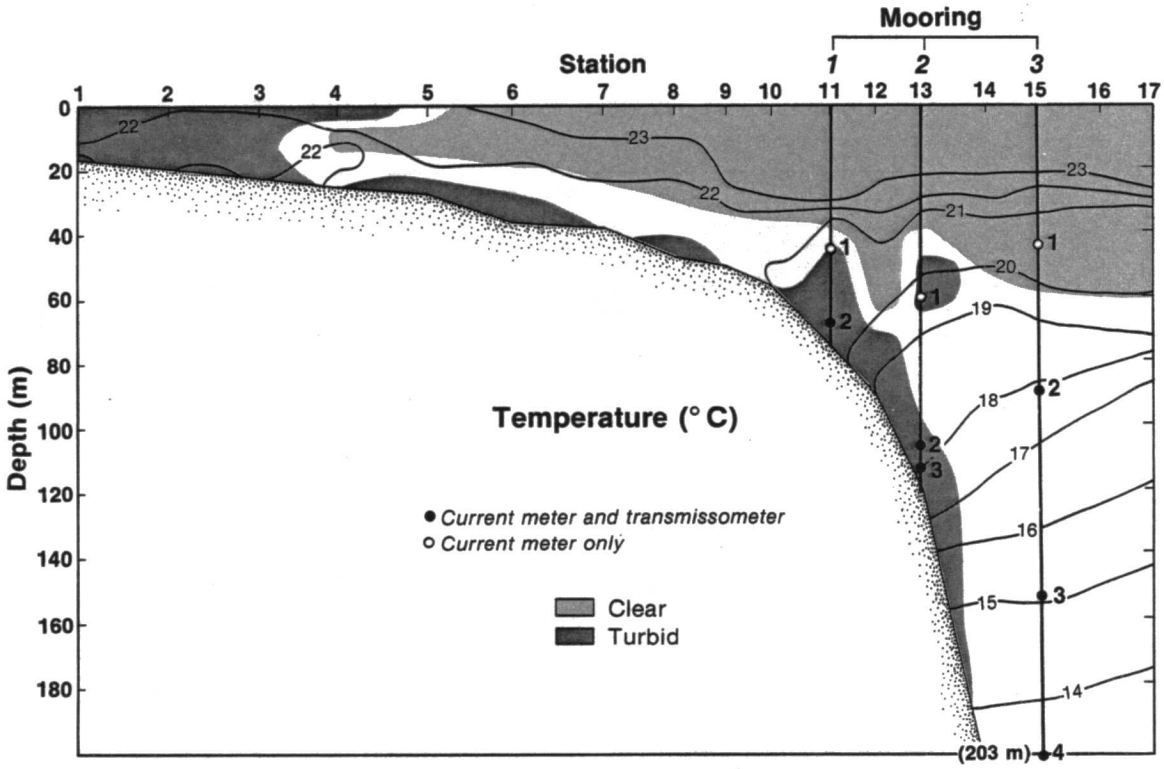

Figure 2.37 Cross-shelf vertical sections of temperature along 95°W across the Texas-Louisiana shelf, as in Figure 2.36 but showing locations and depths of current meters on moorings 1, 2, and 3. These moorings were deployed on 19 March 1982 and recovered on 4 May 1982.

central area of this shelf segment. The surface gravity waves and strong wind-driven coastal currents keep the deposition of mud to a minimum in the nearshore.

In the summer months the supply of sediment to the outer shelf is more restricted because of the lack of major wind events and the diminished supply of sediment at the coast. Otherwise, the bottom boundary layer on the inner shelf should carry fine sediment to the southwest when it becomes entrained in the southeast flow.

Our current meter records from the shelf edge suggest that hurricanes are not the important agent of sediment distribution that Curray (1960) hypothesized. The reason for this is that hurricanes occur when the shelf is still stratified so that they do not directly force the bottom flow on the outer shelf. In fact, they appear to produce effects on the outer shelf similar to those of a frontal passage. Obviously, a hurricane's influence in shallow water would be much more extreme. This is well illustrated by the current meter records of Schroeder (1981) from the Florida Middle Ground in 35 m of water during the passage of two major hurricanes, David and Frederic, in 1979. Still, the effects of the storm were very short-lived.

In summary, active deposition on this segment of the shelf appears to be limited to the coastal waters of Louisiana and the outer shelf and upper slope of the whole region. It also appears that fine sediment is advected over very long distances in the nepheloid layer before being deposited.

Circulation and Hydrography on the Florida Shelf

The Florida shelf seems to undergo much the same seasonal temperature cycles that the Texas shelf does. The annual temperature record for the Florida Middle Ground is given by Hopkins and Schroeder (1981) (Figure 2.38; see Figure 2.1 for location). Currents at this site are characterized by large variances and very low means (less than 2 cm/s). The West Florida shelf receives comparatively little fresh water runoff. Because of that and the fact that the adjacent mainland is a carbonate platform, the West Florida shelf receives no appreciable terrigenous sediment at all.

Niiler (1976) showed transects along the 26°N line of latitude from the coast to continental slope in June and February. The salinity at the coast was 36.0 ppt in June and slightly less than 35.8 ppt in February. These values reflect the lack of fresh water contribution to the shelf. Mixing over the West Florida shelf is reported by Niiler to penetrate to about 100 to 150 m in the winter. He stated that the temperature of the water inshore of about 100 m decreases through the winter because of its decreased heat capacity during cold air outbreaks. He also says that the shelf hydrography

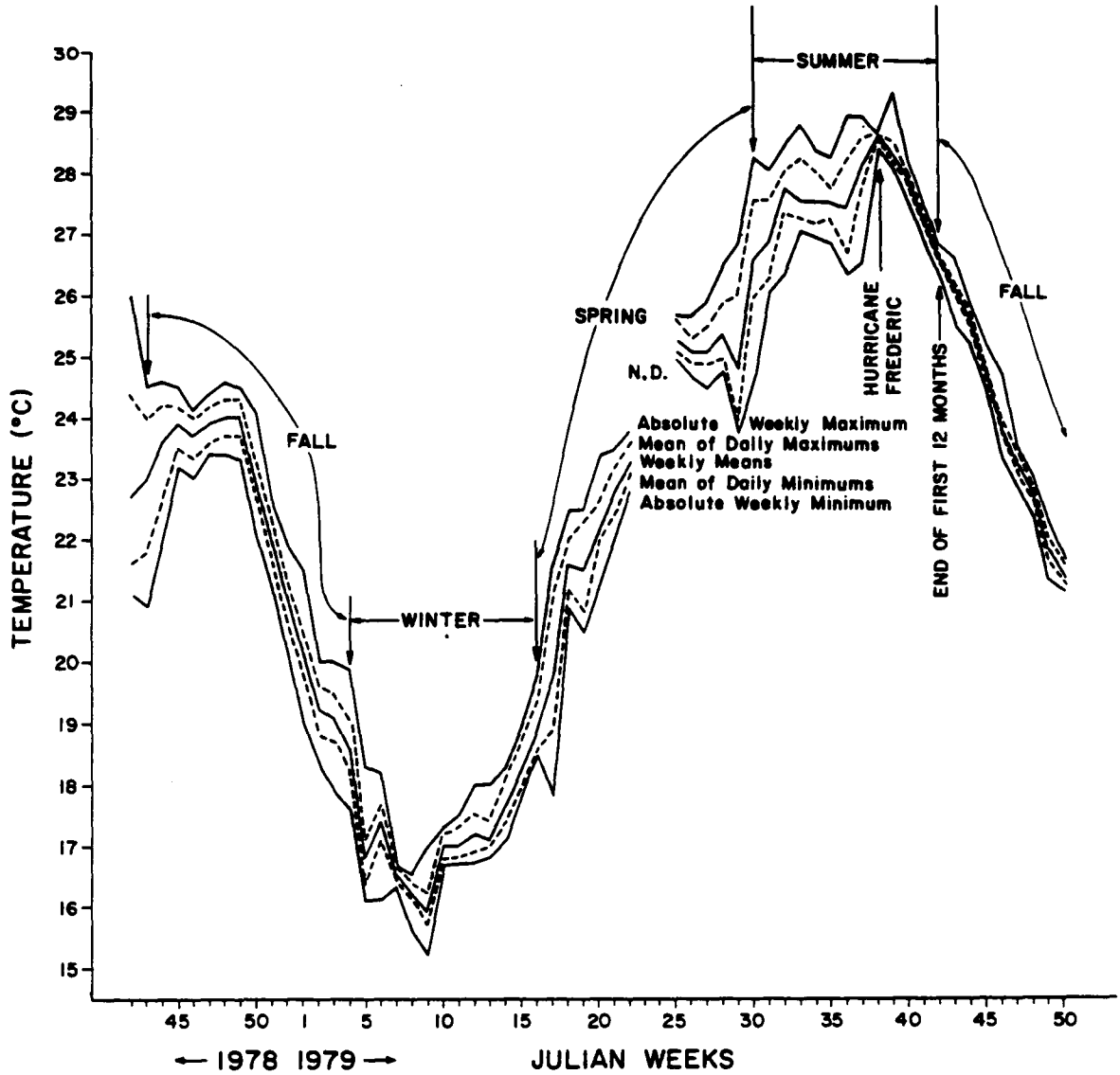

Figure 2.38 Temperature at the Florida Middle Ground versus time during 1978 and 1979 (Hopkins and Schroeder, 1981). The observation site is shown on Figure 2.1. Note that minimum temperatures in February and March range from above 15°C to about 16.5°C.

shows the presence of detached and semi-detached segments of water which have their origins in the Loop Current. He goes on to demonstrate that these are caused by shear between the fast-flow Loop Current and the shelf waters. The shear causes instabilities that develop into meanders that grow and become detached eddies. These appear to propagate to the north against the prevailing southward flow at the shelf edge.

The absence of silt and clay in the sediment provide much clearer water throughout the water column than exists on the Texas-Louisiana coast, as shown by Steward (1981). His transmissivity profiles and hydrography from the Alabama shelf, however, show it to be very similar to the Texas-Louisiana shelf, with a well developed nepheloid layer.

CONCLUSIONS

With respect to the biotic communities of the Gulf, it has been demonstrated that Caribbean populations can be carried north and east along the Outer Continental Shelf off Mexico, Texas, and Louisiana in an anticyclonic circulation pattern. Similar communities could be delivered to the Florida shelf by eddies that spin off the Loop Current and propagate to the north over the outer shelf.

The West Florida shelf and Yucatan platform are similar in that both are floored by carbonate sediment (Figure 1.2) and neither suffers appreciable salinity variations.

The shelves of Mexico, Texas, Louisiana, Mississippi, and Alabama are all floored with terrigenous sediment containing varying amounts of silt and clay (Figure 1.2). They also receive fresh water input that alters the nearshore salinity gradients. The presence of silt and clay, and other observations, suggest that nearshore waters are likely to be turbid top-to-bottom inside of the 10 m isobath and that the shelf will have a nepheloid layer that may reach 35 m or more in thickness.

In the winter, cold fronts create deep mixed layers. Shoreward of where these mixed layers intersect the bottom, the temperature of the water may become very low because of the limited heat capacity of the water. As each front comes through, it extracts more heat so that coastal waters off Texas may drop to 10 or 12°C. Offshore of the intersection of the mixed layer with the bottom, water temperatures remain relatively high because of the large heat reservoir of the thick lens of water. At the shelf edge of Texas, the water at a depth of about 50 m remains warmer than 17.5°C all year and above 18°C most of the year.

Figure 2.39 summarizes these characteristics of the shelf habitats.

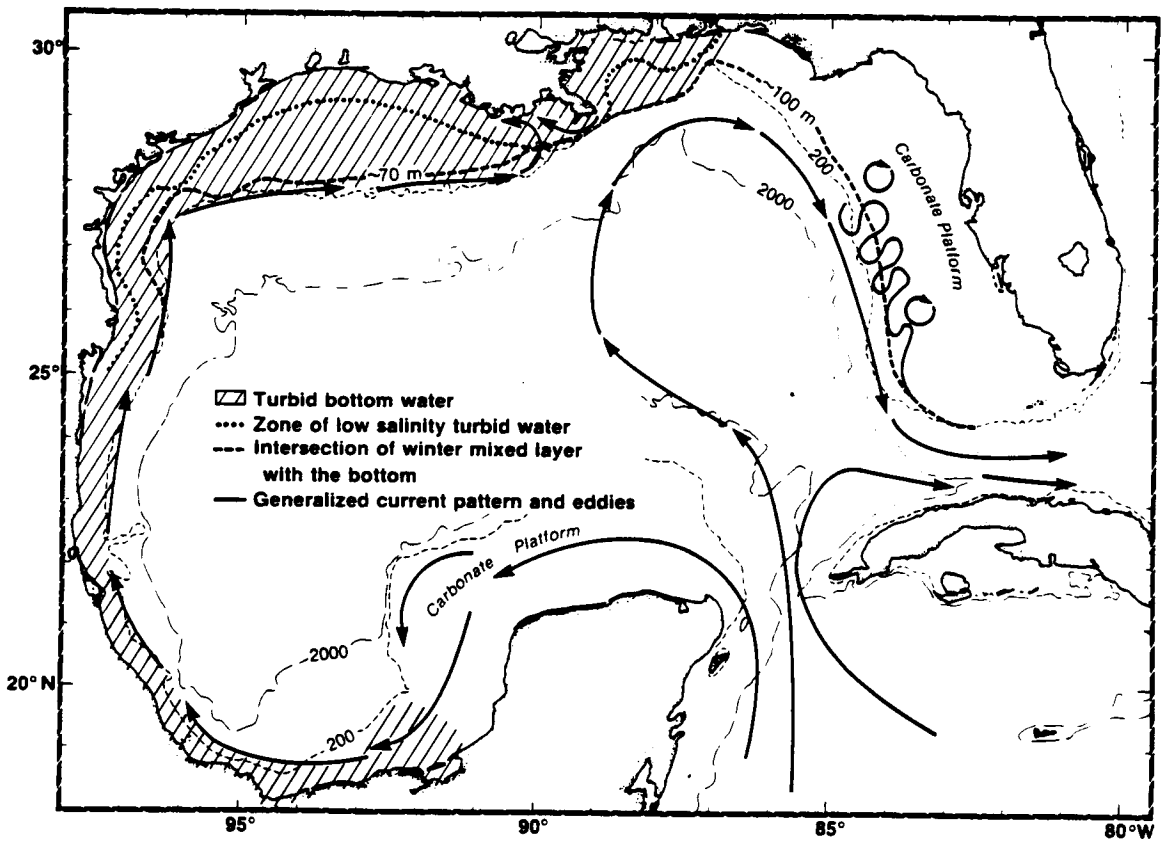

Figure 2.39 Map of Gulf of Mexico summarizing the primary near-surface circulation patterns which may be responsible for carrying biotic communities into the Gulf and from there either anticyclonically around the western Gulf or to the Florida shelf via the Loop Current and spin-off eddies. Diagonal pattern indicates regions of appreciable turbidity in the water column. Dotted line delineates seaward margin of near-shore, low-salinity turbid water. The dashed line near the Outer Continental Shelf indicates depths where the winter mixed layer intersects the bottom.

CHAPTER 3

A SUMMARY OF HARD-BOTTOM BIOTIC COMMUNITIES IN THE GULF OF MEXICO

Thomas J. Bright

The purpose of this chapter is to provide an overview of the biotic communities occupying hard bottoms in the Gulf of Mexico as background for more detailed accounts to follow of such communities on the Outer Continental Shelf off Texas and Louisiana. The inflow of warm tropical water from the Caribbean, carrying larvae from West Indian reef ecosystems, is of overwhelming importance in determining the nature of the Gulf of Mexico benthos. The resultant planktonic "ambience" of tropical forms provides a broad potential for adult community structure, which is selectively expressed at various locations on the continental shelf.

Primarily, community structure depends on structural and sedimentological characteristics of the substratum, river outflow, and seasonal and regional variations in water temperature, salinity, and turbidity (see Chapters 1 and 2). In the northern Gulf, which is in many ways a differentially stressed ecotone for tropical biota, the influence of coastal marine and climatic environments is particularly important in determining the degree of expression of tropical benthic communities. Thus, assessment of marine biogeographical relationships in the Gulf and adjacent regions requires that one have some view of the distribution of and general relationship between major hard-bottom communities from the shore to at least the continental shelf edge.

REGIONAL REEFS AND HARD BANKS

Rocky outcrops and hard banks are common on the continental shelf throughout the Gulf of Mexico, even on those parts covered primarily by soft terrigenous sediments. The biota associated with them vary from decidedly tropical coral reefs in the southern Gulf to less diverse assemblages more comparable to those of the coastal jetties in the north.

Emergent tropical coral reefs occur throughout the Caribbean, Bahamas, and offshore of the Florida Keys on the Atlantic side from the Dry Tortugas to Cape Florida (Miami). These reefs are most often dominated from low tide level to between 3 and 9 m, depending on conditions of wave energy and location, by the elkhorn coral *Acropora palmata*. Other important reef-building associates are the staghorn coral, *Acropora cervicornis*; fire coral, *Millepora complanata*; finger coral, *Porites porites*; brain corals, *Diploria* spp.; mountainous star coral, *Montastrea annularis*; and many more.

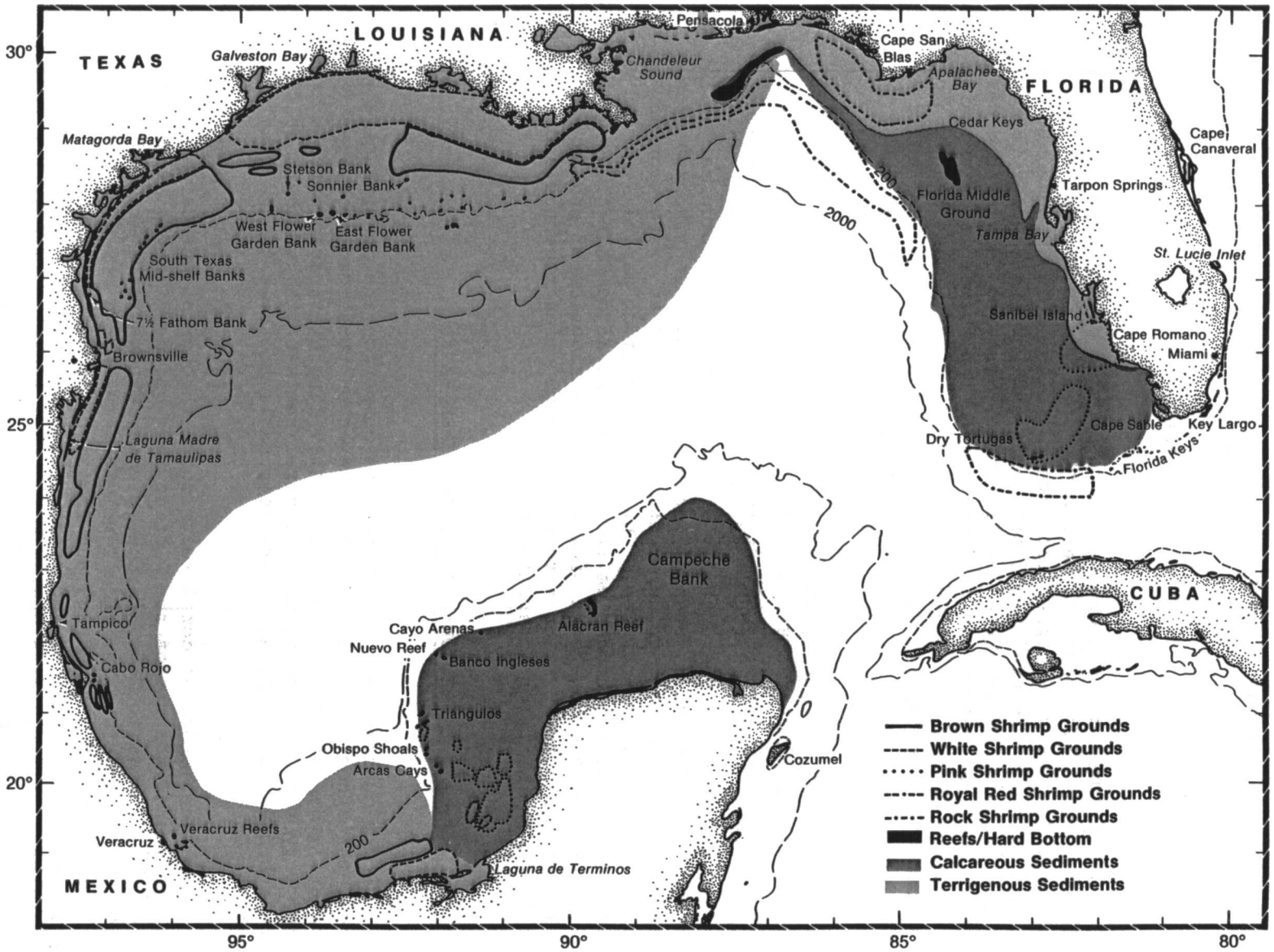

Figure 3.1 Zones and locations of major biogeographical significance in the Gulf of Mexico.

Shallow-water alcyonarians, including Gorgonia spp., Pseudopterogorgia, Plexaura, and Eunicea, are typically abundant. Submerged reef zones, down to 35 m or so in some areas of the Caribbean, are typically dominated by Montastrea annularis, Diploria spp., Colpophyllia spp., other faviid corals, and alcyonarians. The reefs support highly diverse communities of tropical algae, sessile and mobile reef invertebrates, and reef fishes.

Emergent coral reefs occur on the outer Yucatan shelf adjacent to islands and on the crests of submerged banks (Alacran reef, Cayo Arenas, Nuevo reef, Triangulos, and Arcas, Figure 3.1) (Logan, 1969). Similar emergent reefs are present nearshore off the city of Veracruz (Heilprin, 1890; Rannefeld, 1972) and off Cabo Rojo, near Tampico (Rigby and McIntyre, 1966). All have basically the same community structure and dominance patterns as emergent coral reefs in the Caribbean, the Florida Keys, and the Bahamas.

On the Atlantic coast of Florida, elements of the tropical coral reef biota decrease in importance in a south-to-north gradient from Cape Florida (Miami) to Palm Beach. The two corals most responsible for reef building (Acropora palmata and Montastrea annularis) are rare north of Miami, and substantial tropical reef structures do not occur. Only a few isolated colonies of Acropora palmata are found north of Ft. Lauderdale, and the area is characterized by alcyonarian dominated hardgrounds. Stony corals are present but do not build reefs (Jaap, pers. comm.).

From Palm Beach to Stuart (St. Lucie Inlet) heartier elements of the tropical reef biota occur, but there is a transition to low diversity Oculina (pretzel coral) bank communities which are the dominant coral communities northward to the Georgia border in 50 to 150 m depth (Avent et al., 1977; Reed, 1980). Fossil Oculina reefs occur on the continental shelf of the northwestern Gulf of Mexico buried deeply beneath recent sediment (for example, the author has samples from an oil well core which penetrated a 10 m thick Oculina reef 30 m below the seafloor).

Several varieties of ahermatypic corals (Astrangia, Phyllangia, and Oculina), "coral heads," and a few alcyonarians, including Leptogorgia virgulata and Leptogorgia setacea, occur at Gray's Reef (17 m depth) 17.5 NM off Sapelo Island, Georgia (NOAA, 1981). Patches of coral heads (Solenastrea hyades and Siderastrea siderea), ahermatypic corals (Oculina, Astrangia, Phyllangia, and Bollanophyllia), sea fans, algae, sponges and a fair number of tropical Atlantic reef fishes occur in Onslow Bay off the South Carolina coast (Huntsman and MacIntyre, 1971). Solenastrea and Siderastrea are also components of the South Florida reef ecosystem, but they are among the heartiest, occurring in Florida Bay, where temperature, turbidity, and salinity conditions vary considerably. The Carolina coral patches experience winter water temperatures at least as low as 10°C.

The most northerly true tropical coral reefs in the Atlantic occur in Bermuda due to the northward path of the warm Gulf Stream current. Though parts of these reefs are quite shallow, they differ from other emergent reefs in that they lack Acropora palmata and Acropora cervicornis and are dominated by head corals (Montastrea annularis, Diploria strigosa, Porites astreoides) and the typical Caribbean shallow-water alcyonarians.

Whereas numerous ledges and outcroppings on the west Florida shelf support associations of hearty corals and other tropical reef biota, shallow-water tropical coral reefs are non-existent north of the Tortugas. The Florida Middle Ground communities, dominated by the fire coral Millepora, and the scleractinians Madracis and Dichocoenia, exhibit moderate coral diversity and harbor an abundance of shallow-water alcyonarians, tropical invertebrates, and reef fishes. The Middle Ground is not, however, an active coral reef comparable to those found off the Florida Keys (Jaap, pers. comm.). The lack of true coral reefs on suitable substrata on the northwest Florida shelf is probably due to the occurrence of winter water temperatures (15 to 16°C) several degrees below that generally accepted as minimal for vigorous reef development (18°C).

Coral reefs do not occur nearshore in the western Gulf north of Cabo Rojo. Seven and One-Half Fathom Reef, a small sandstone prominence located 3.2 km offshore from central Padre Island, Texas, is largely covered by mats of tube-building polychaete worms, Phyllochaetopterus, sponges, ascidians, and hydroids. The bank, which crests at about 8.5 m depth from a surrounding bottom of 14 m, bears assemblages of mollusks and crustaceans of mixed warm temperate and tropical affinities and a substantial number of species in common with the south Texas jetties and other very nearshore banks farther north, such as Heald Bank off Galveston (Tunnell and Chaney, 1970; Tunnell, 1973; Felder and Chaney, 1979). Seven and One-Half Fathom Reef is commonly subject to winter temperatures ranging from 13 to 30°C, salinities 28 to 36 ppt, and highly turbid to fairly clear water conditions (Tunnell, 1973). Being in an area of converging currents, the reef is bathed by coastal waters from the more tropical southwestern Gulf in summer, and from the northern Gulf in winter. Therefore, Felder and Chaney considered at least the decapod fauna of the reef and of the jetties on the nearby south Texas coast, to be transitional between temperate and tropical.

The sediment laden rock outcrops forming Sebree Bank about 15 miles offshore from south Padre Island, harbor primarily the same types of coastal epifauna found on the other nearshore "live bottoms" in the northern Gulf and the southern Atlantic states (?Oculina, Phyllangia americana, bryozoans, sponges, hydroids etc.). Some tropical fishes and invertebrates frequent this bank, as well as nearshore oil platforms and jetties (e.g., Holacanthus ciliaris, H. bermudensis, Halichoeres, Chaetodon sedentarius, Pomacentrus, Hermodice carunculata, Stenorynchus seticornis, and others) (Greg

Boland, LGL Ecological Research Associates, pers. comm.). This however, is not unusual even as far north as the Carolinas, particularly in summer when water temperatures are high. These coastal banks exist in environmentally stressed and variable environments for hard bottom biota, with high turbidity and sedimentation, low winter temperatures and, in places, substantial decreases in salinity. None of the banks, including Seven and One-Half Fathom Reef, bear biotic communities which resemble those of tropical Atlantic coral reefs.

In fact, coral reefs are absent in the northwestern Gulf between the emergent reefs off Cabo Rojo and the submerged reefs atop the East and West Flower Garden Banks 100 NM southeast of Galveston, Texas. Here, coral reefs exist at the crests of the banks from 15 to 52 m depth. The shallowest of these (15 to 36 m) are dominated by the star coral Montastrea annularis, brain corals Diploria strigosa and Colpophyllia spp., and the mustard hill coral Porites astreoides. About one-third of the species of Caribbean reef-building corals occur on the banks, along with several hundred species of reef invertebrates and fishes. There are, however, no shallow water alcyonarians and no corals of the genus Acropora. Though they are the northernmost true tropical coral reefs on the continental shelf of North America, the Flower Garden reefs exist in oceanic water whose winter temperature does not typically drop below 18 to 19°C, barely above the accepted lower limit for reef development.

Siltstone-Claystone banks closer to shore off Texas (Stetson, Claypile, and Sonnier Banks), though cresting at suitable depths, are occupied by communities weakly dominated by sponges and crusts of the fire coral Millepora alcicornis. Much bare rock is in evidence. These bank communities, while composed largely of Caribbean biota, including a fair number of tropical reef fishes, are of much lower diversity than the Flower Gardens and are not comparable to tropical coral reefs. The substantial variability of temperature, salinity, and turbidity of inner and mid-shelf waters bathing these banks precludes active coral reef development.

Deep-water, reef-building communities dominated by coralline algae (as rhodoliths, pavements, and crusts) exist at greater depths (30 to 85 m or more) on the Flower Gardens, other shelf-edge banks between the Flower Gardens and the Mississippi, outer shelf banks on the Yucatan shelf, and on deeper "level" shelf bottoms off southwestern Florida seaward of the Key Largo reef tract and throughout the West Indies (Bright and Rezak 1977; Logan, 1969; Macdonald, 1982; MacIntyre, 1972). The coralline algae and sizeable attendant populations of stony corals Agaricia, Helioseris, and Madracis produce massive amounts of carbonate substratum in the northern Gulf, certainly much more than the few coral reefs are capable of. These deep reef communities are Caribbean in their affinities, and nearly as diverse biotically as the coral reefs. Tropical leafy algae are particularly conspicuous.

The same coastal-neritic hydrographic conditions which preclude coral reef development on the shallower mid-shelf banks off north Texas and Louisiana apparently prevent the expression of the deep-water reef-building communities on mid-shelf banks which crest between 55 and 70 m depth off South Texas (Southern, Baker, Hospital, and others). These carbonate structures, the remains of relict Pleistocene reefs, currently support only minor encrusting populations of coralline algae. The most conspicuous fauna are large white antipatharians Cirrhipathes (= Cirripathes), smaller branching antipatharians Antipathes, deep-water alcyonarians, sponges, occasional plates of the coral Agaricia, and an assemblage of fishes which is typical of deeper parts of offshore banks throughout the northwestern Gulf (Holanthias martinicensis, Chromis enchrysurus, Liopropoma eukrines, Serranus phoebe, Lutjanus campechanus, and Mycteroperca phenax, to name a few). Exposed reef rock with a veneer of fine sediment is common, and becomes the dominant condition below about 75 m depth, where epifaunal diversity is minimal.

Carbonate outcrops and surrounding sand and shell bottom at 50 to 60 m depth on the western rim of the DeSoto submarine canyon 25 km offshore near Pensacola, Florida bear low diversity communities of an apparently mixed tropical and temperate nature. Shipp and Hopkins (1978) described a "sand-shell-coralline algae slope" whereon they observed the Sea pansy Renilla, crabs Calappa, rock shrimp Sicyonia, starfishes Astropecten and Luidia, and the sand dollar Clypeaster, all fairly representative of Shrimp Ground fauna. Rather more tropical forms included the starfishes Narcissia, Linckia, and Goniaster and the slipper lobster Scyllarus.

The hard, block-like DeSoto Canyon substrate supports clusters of the stony coral, Oculina; alcyonarians, Lophogorgia; antipatharians; hydroids; crabs, Mithrax, Stenocionops, and Stenorynchus; a lobster, Scyllarides; hermit crabs, Dardanus and Petrochirus; gastropods, Fasciolaria and Scaphella; echinoids, Arbacia, Diadema, Eucidaris, and Lytechinus; the sea cucumber, Isostichopus; and large ophiuroids, including basket stars and Ophioderma. The fishes are basically Caribbean types. Many of the species are also found in the deeper zones of the shelf edge banks off north Texas and Louisiana and on the mid-shelf banks off south Texas.

The DeSoto Canyon hard-bottom community seems somewhat comparable to the more tropical south Texas mid-shelf carbonate banks and possibly other poorly known mid-shelf banks off Louisiana. All exist in neritic waters which may fluctuate seasonally between temperate and tropical temperatures, vary widely in turbidity, and be subject periodically to substantial decreases in salinity due to river outflow. None of these structures harbor effective reef-building populations at present and are probably best viewed as

stressed habitats occupied by some hearty representatives of the Caribbean biota.

Moore and Bullis (1960) reported a sizeable (1219 m long) deep water (230 to 280 m) coral reef on the Gulf of Mexico continental slope 40 miles east of the Mississippi River. The reef is composed of "one or two species of ramose, branching, colonial (ahermatypic) corals," primarily Lophelia prolifera. Lophelia apparently forms similar structures in deep water in the Caribbean, north of the Bahamas, and in the North Atlantic (Moore and Bullis, 1960).

Man has added significant amounts of hard substratum to the continental shelf of the northwestern Gulf of Mexico through the construction of offshore oil and gas platforms. These exist primarily off Louisiana (over 1100 structures), and Texas (about 120). Increasing numbers are expected off Texas and in Mexican waters as oil and gas production expands in the western Gulf. Fewer than five such platforms have been built east of the Mississippi.

Shinn (1974), George and Thomas (1979), and Gallaway and Lewbel (1982) described biotic zonation on Texas-Louisiana platforms. The platforms can be classified as coastal (surrounding bottom depth 0 to 30 m), offshore (30 to 60 m), or bluewater (over 60 m) on the basis of species composition, structure, and zonation of the biotic communities associated with them.

Coastal platform biofouling communities off Louisiana are dominated by acorn barnacles above about 12 m depth (usually either Balanus reticulatus or Balanus improvisus off Louisiana) with biomass decreasing with depth. George and Thomas (1979) indicated thick concentrations of the filamentous green alga Enteromorpha on the barnacle fouling mat just below the sea surface, with interspersed hydroids, Syncoryne; xanthid crabs, Neopanope texana; amphipods, Corophium; and pycnogonids. Below 2.4 to 6 m depth sea anemones, Aiptasia, replace the algae and hydroids on the barnacles, and cryptic blennies, Hypleurochilus, become common. Balanus improvisus was rare below 7.5 m, leaving Balanus reticulatus the dominant. They found no living barnacles below 12.2 m, below which hydroids dominated down to the bottom (18 m). Small corals (probably Astrangia) were present among the hydroids. Gallaway and Lewbel (1982) found that the large Mediterranean barnacle Megabalanus antillensis (= Balanus tintinnabulum) is dominant on the coastal platforms off Texas, rather than the smaller barnacles typical of the Louisiana platform.

Dominant fishes on coastal platforms are the Sheepshead, Archosargus probatocephalus; Atlantic spadefish, Chaetodipterus faber; Moonfish, Selene setipennis; Lookdown, Selene vomer; Gray trigger, Balistes capriscus; Bluefish, Pomatomus saltatrix; and Blue runner, Caranx crysos; often in large mixed schools. A few reef fishes are common, such as the Belted sand fish, Serranus subligarius; Rock hind, Epinephelus adscensionis; Flamefish, Apogon

maculatus; Sergeant major, Abudefduf saxatilis; Cocoa damselfish, Pomacentrus variabilis; Gray snapper, Lutjanus griseus; and groupers, Epinephelus and Mycteroperca.

Mid-shelf offshore platform assemblages differ from the coastal in that pelecypods rather than barnacles dominate the biofouling biomass, though barnacles are abundant. The tree oyster, Isognomon bicolor, oyster, Hyotissa, and the leafy jewel box, Chama macerophylla, are bivalves of particular importance. Significant populations of the sometimes dominant alcyonarian, Telesto, are considered indicative of offshore platforms (Gallaway and Lewbel, 1982). Red and green macroalgae are important in the upper 10 m.

Whereas Atlantic spadefishes dominate, and most of the coastal species are common, the offshore platform fish assemblage differs in having greater abundances of Gray and Red snappers, Lutjanus griseus and L. campechanus, and a richness of tropical species such as the Cocoa damselfish, Pomacentrus variabilis; Blue and French angelfishes, Holacanthus bermudensis and Pomacanthus paru; Sergeant major, Abudefduf saxatilis; Brown chromis, Chromis multilineatus; filefishes, Monacanthidae; surgeonfishes, Acanthuridae; Flamefish, Apogon maculatus; and Creole fish, Paranthias furcifer. Almacojack, Seriola rivoliana, and Amberjack Seriola dumerili; Barjacks, Caranx ruber; Rainbow runner, Elagates bipinnulata; Great barracuda, Sphyraena barracuda; Cobia, Rachycentron canadum; Crevalle jack, Caranx hippos; and hammerhead shark, Sphyrna, are present (Gallaway and Lewbel, 1982).

On outer shelf, bluewater platforms, stalked barnacles (Lepas), and algal mats predominate at the surface, and hydroids and pelecypods appear to dominate at greater depths. Invertebrates and leafy algae, characteristic of shelf-edge banks, are present (Spiny lobster, Panulirus argus; urchins, Diadema and Eucidaris; algae, Dictyota and Peyssonnellia; and others). The Mediterranean barnacle, so important on Texas coastal platforms, though present, is not a dominant on the bluewater platforms (Gallaway and Lewbel, 1982).

The most striking difference between bluewater platforms and those nearer to shore is in the fish populations. The large schools of Atlantic spadefish, Lookdowns, and Bluefish are absent from the bluewater platforms, seemingly replaced by numerous Creole fish, Almaco jacks, and Blue runners. The sheepshead is replaced by the Gray triggerfish and a number of tropical species. Tropicals are abundant, including schools of Creole wrasse, Clepticus parrae, and more solitary varieties such as the Spanish hogfish, Bodianus rufus; damselfishes; angelfishes; surgeonfishes; Rock beauty, Holacanthus tricolor; Red spotted hawkfish, Amblycirrhitus pinos; Great barracuda, and hammerhead sharks.

The outer to inner shelf transition from tropical reef assemblages to assemblages apparently of more temperate nature in the northwestern Gulf of Mexico is of considerable ecological

interest, particularly since it can be recognized on both natural hard bottoms and the man-made structures. A better knowledge of the biotic assemblages inhabiting the "ephemeral" offshore platforms (they must ultimately be removed by the oil companies), and the spatial and temporal variations in assemblages, would be of considerable use as an aid in determining the environmental factors controlling the nature, distribution, and biogeographic relationships of hard bottom benthos and reef fishes in the Gulf.

BIOGEOGRAPHIC RELATIONSHIPS

To place the hard-bottom assemblages in proper perspective, it is necessary to consider the general distribution patterns of all major benthic marine communities within the Gulf of Mexico, including those of the estuaries, coast, and offshore soft bottoms. Biogeographically pertinent aspects of the distribution of these communities may be summarized as follows:

1. Coastal

   a. Temperate salt marshes predominate in the northern Gulf from Tarpon Springs, Florida to at least Port Isabel, Texas (Humm, 1973).

   b. Stressed populations of tropical Black mangroves co-occur with the salt marshes as far north as the Mississippi sound (Humm, 1973; Hildebrand, 1957).

   c. Well-developed tropical mangrove forests dominated by Red and Black mangroves replace salt marshes southward from Tampa Bay and Laguna de Tamiahua in the Gulf and Jupiter Inlet on the East Florida coast. They are not significant in the northern Gulf or north of Cape Canaveral (Humm, 1973; Yanez-Arancibia et al., 1980; Ayala-Castanares, 1981).

   d. Temperate oyster reefs (*Crassostrea virginica*) are extensive in bays north of Cape Canaveral and in the northern Gulf from Cedar Keys, Florida to Port Aransas, Texas. Reduced reefs occur in Gulf estuaries as far south as Laguna de Terminos, Campeche (Bahr and Lanier, 1981; Taylor et al., 1973; Yanez-Arancibia et al., 1980; Fotheringham, 1980; Oppenheimer and Gordon, 1972).

   e. Tropical seagrass beds are abundant inshore throughout the Gulf except between Galveston and the Mississippi Delta, where they are limited by high turbidity and low salinities. Beds in the Mississippi Sound may be reproductively restrained by temperate conditions. Tropical seagrass beds are not important in the Atlantic, north of Cape Canaveral (Humm, 1973;

Hildebrand, 1957; Humm and Hildebrand, 1962; Yanez-Arancibia et al., 1980; Kim, 1964; Randall, 1965).

f. Jetties in the northern Gulf bear biota similar in many respects to those of jetties in the Carolinas. Tropical forms are more abundant on south Texas jetties (Port Aransas and Port Isabel). South Florida intertidal rocks support distinctly more tropical assemblages (Hedgpeth, 1954; Edwards, 1976; Fotheringham, 1980).

g. Leafy algae populations within the Gulf are basically tropical, with a diminishing number of tropical forms and an increasing admixture of temperate species on the coast proceeding north from south Florida (around Tampa) and South Texas (around Port Isabel). Many of the northern Gulf temperate species become inconspicuous inshore during the summer. Algae on the mid and outer shelves throughout the Gulf are distinctly tropical (Humm, 1973; Kim, 1964; Bright et al., 1981; Earle, 1969, 1972; Edwards, 1976; Humm and Hildebrand, 1962; Sorenson, 1979).

2. Offshore "Level Bottoms"

a. The White Shrimp Ground (inner shelf) and Brown Shrimp Ground (outer shelf) assemblages are present throughout the Gulf where terrigenous sediments predominate. White Shrimp Grounds are best developed adjacent to hyposaline estuarine environments (Pensacola to Texas and off Laguna de Terminos). Offshore Brown Shrimp Grounds (less estuarine dependent) are extensive from Pensacola to the Gulf of Campeche. Both are most extensive off Texas-Louisiana. Throughout their range, the shrimp ground communities are fairly uniform and the geographic ranges of the species extend substantially northward toward the Carolinas and southward into the Caribbean. Tropical and temperate characteristics are apparent at the southern and northern extremities of the Brown Shrimp Grounds within the Gulf, at least for the fish assemblages (Kutkuhn, 1962; Chittenden and McEachran, 1976; Hildebrand, 1954, 1955; Defenbaugh, 1976; Hedgpeth, 1953, 1954; Chittenden and Moore, 1977; Flint and Griffin, 1979; Thistle and Lewis, 1979).

b. Pink Shrimp Grounds (communities of more tropical affinities) are restricted to carbonate sand bottoms on the Yucatan and West Florida shelves, being best developed just north of the Tortugas and off southern Campeche (Hildebrand, 1955; Kutkuhn, 1962; Sanchez-Gil et al., 1981; Chittenden and McEachran, 1976).

c. Epibenthic communities of tropical origin occupy the carbonate substrata of continental shelves of Yucatan and West Florida, extending as far north as the mouth of the DeSoto Canyon off Pensacola. They are held offshore north of Cape Romano, Florida by coastal terrigenous sands and increasingly temperate coastal conditions. Rock outcrops on the West Florida shelf are occupied by epibenthos derived from tropical reef communities out to depths of at least 90 m. The diversity of tropical species apparently decreases in a northerly direction (Sanchez-Gil et al., 1981; Hoese and Moore, 1977; Cervignon, 1966).

d. Limited populations of heartier tropical epibenthos and fishes occur as far north as the Carolinas on the South Atlantic outer continental shelf (Hoese and Moore, 1977; Downey, 1973).

3. Reefs and Hard-Banks

a. Emergent tropical coral reefs occur southward from Miami, the Dry Tortugas and Cabo Rojo, Mexico. Tropical reef epibenthos diminish north of Miami and are replaced by more temperate submerged Oculina banks off St. Lucie Inlet. Certain hearty hermatypic corals occur as far north as the Carolinas. Tropical hard grounds (but not coral reefs) extend northward to the Florida Middle Ground, west Florida shelf. Submerged coral reefs and deep water tropical reef assemblages are present on shelf-edge banks off North Texas and Louisiana. Similar deep-water tropical reef assemblages occur on the outer southwest Florida shelf south of Charlotte Harbor and in the Atlantic off Key Largo.

b. Depauperate tropical epibenthic communities occupy mid-shelf banks in the northwestern Gulf of Mexico and hard bottoms on the north rim of the DeSoto Canyon where conditions tend to be seasonally variable, temperate, and neritic.

c. Environmentally stressed hard-bottoms nearshore in the northwestern Gulf bear basically temperate epifauna with admixed tropical forms (mainly some tropical fishes and mobile invertebrates).

d. Epibenthos on oil platforms off Texas are tropical near the shelf edge, mixed tropical and coastal on the mid shelf, and basically temperate with admixed tropical forms nearshore.

e. Throughout the northern Gulf, some tropical reef fishes move inshore during summer to occupy coastal platforms and hard grounds.

Correlating biotic distribution patterns with patterns of physical conditions within the Gulf, it is readily apparent that substratum type is the primary regional factor influencing the nature of marine benthic communities offshore. The terrigenous soft bottom (Figure 3.1) supports two distinct shrimp ground communities which have usually been considered warm temperate (Carolinian). However, these communities reach their greatest degrees of abundance and diversity on the mid and outer shelves of the northwestern and southern Gulf of Mexico where, if the substratum were carbonate and bottom turbidity low, one might expect decidedly tropical epibenthos to occur. Carbonate substrata within the Gulf generally support elements of the tropical (Caribbean) epibenthos, though offshore tropical diversity apparently decreases gradually toward the north.

A tropical biotic presence throughout the Gulf is the natural result of the fact that virtually all of the shallow marine water entering the area comes from the Caribbean, carrying a continual supply of tropical larvae. Substantial modification of this warm water mass occurs nearshore in the northern Gulf due to river inflow and cold winter air temperatures, and at the southern tip of Florida and the Gulf of Campeche due to river inflow (cold air also occasionally affects waters of Florida Bay and vicinity). Otherwise the immense epipelagic zone of the Gulf of Mexico is tropical, carrying tropical larvae prepared to occupy any appropriate substratum existing in suitable conditions of temperature, salinity, and turbidity.

Inshore along the northern Gulf coast, winter water temperatures may dip below 10°C in the bays and shallow nearshore waters. The effects of winter cold diminish toward the south, and perpetual tropical to subtropical epipelagic conditions (year round temperatures above 16 to 18°C) exist on the outer shelf.

Nearshore, low winter temperatures exclude most, but not all, of the tropical species, leading to a basically warm temperate coastal biota (marshes, oyster reefs, etc.) with a substantial tropical content (black mangroves, tropical grass beds, etc.) in the northern Gulf. Appearance of temperate species of algae in the winter (Earle, 1969) and tropical fishes during summer (Briggs, 1974) on coastal and nearshore hard bottoms and man-made structures is characteristic of the biologically transitional and environmentally variable northern Gulf coast. This condition extends down to at least Tarpon Springs in Florida and the Laguna Madre de Tamaulipas in Mexico. The transition to tropical is fairly complete by the Ten Thousand Islands, Florida and Cabo Rojo, Mexico (Figure 3.1) (Briggs, 1974; Hedgpeth, 1953; Pulley, 1952; Earle, 1969).

To make proper sense of the biogeographic relationships offshore, one must consider separately the biota of terrigenous soft bottoms versus those of calcareous substrata and hard banks. These two groups are neither very similar in species composition nor interdependent ecologically.

Latitudinally wide ranging fauna occupying terrigenous sands and muds tend not to vary greatly throughout the Gulf but show affinities to both the Carolinian warm temperate biota and the tropical Caribbean biota (somewhat more for the former). Briggs (1974) suggested that the White and Brown Shrimp Ground biota may have evolved in the northern Gulf of Mexico and spread to the south Atlantic coast during a period when the Florida peninsula was submerged (last submergence was during the Pliocene, over one million years ago). This might be carried further by speculating as follows:

1. the center of distribution and evolution for these assemblages is the northwestern Gulf of Mexico;

2. the evolutionary process is quite active;

3. the pelagic dispersal capabilities of the organisms (having evolved in, and living in, at least seasonally tropical conditions) are such that the warm waters of the southern Florida peninsula are no barrier;

4. the observed similarities between the Gulf and south Atlantic communities result from contemporary dispersal and recruitment processes; and

5. the reason these species are absent or rare as adults off southern Florida is that the carbonate substratum there is unsuitable habitat.

This line of reasoning makes it unnecessary to invoke a historical submergence of the Florida peninsula (with consequent continuous temperate marine conditions from the northern Gulf to the Carolinas), followed by its emergence as a barrier to dispersal, in order to explain the disjunct distribution of the supposed warm temperate Carolinian biota. In fact, the extremely high degree of affinity between the Gulf of Mexico north coastal and terrigenous offshore soft-bottom communities and those from Cape Hatteras to Cape Canaveral argues against such historical isolations spanning over a million years. Such similarities could not have been maintained that long without substantial transfer of genetic material in one direction or another. The patterns of currents in the Gulf, the Straits of Florida, and the Gulf Stream, rapidly moving great volumes out of the Gulf and up the Atlantic coast, strongly favor such transfer (through larval transport) from the Gulf to the south Atlantic. In addition, northern Gulf warm temperate biota are more diverse and have a substantially greater

degree of endemism (approximately 10%; Briggs, 1974) than do those on the southern Atlantic coast, indicating a center of distribution in the Gulf.

The clearly tropical offshore biota are much easier to interpret. They extend as far north as substratum and water quality will permit. In the eastern Gulf, this means at least to the mid-shelf Florida Middle Ground. There, temperatures may drop to slightly less than 16°C in winter and the fairly diverse tropical communities, though dominated by corals, do not form true coral reefs. In the western Gulf, the Flower Garden coral reefs at the shelf edge rarely experience temperatures as low as 18°C. The mid-shelf banks, upon which assemblages are biotically depauperate but which are primarily of tropical affinity, see winter temperatures somewhat less than 16°C. Thus, even with appropriate substratum, the mid-shelf bank tropical communities in the northern Gulf are inhibited due to marginal winter temperatures (below 18°C), low salinity in the western Gulf, and periodic or chronic high turbidity.

The tendency for elements of the tropical biota to extend farther north offshore than they do on the coast has been generally recognized not only for the Gulf (Briggs, 1974; Earle, 1969; Chittenden and McEachran, 1976) but also for the south Atlantic coast northward to the Carolinas (Earle 1969; Downey, 1973; Huntsman and MacIntyre, 1971). Indeed, on the outer shelves, tropical ecosystem components are, in places, virtually surrounded by supposed warm temperate habitats and biota, particularly in the northwestern Gulf of Mexico. In view of this, and the coastal mixture of temperate and tropical species in the northern Gulf, sharp boundaries between the warm temperate, Carolinian and tropical Caribbean biogeographic provinces are not appropriate. In fact, one may hypothesize that the entire Carolinian Province is largely a northerly expression of hearty species of southern affinity, with a substantial boreal (cold temperate) contingent.

SUMMARY

A universally valid latitudinal boundary between tropical and warm temperate biota in the region cannot be prescribed. The impact of temperate climatic conditions on community structure is certainly evident on the coast and inner shelf of the northern Gulf of Mexico. Even there, however, the basically temperate estuarine and nearshore assemblages are accompanied by tropical ecosystem components in significant abundance. Progressing offshore, the benthic biota become increasingly tropical in nature so that the general impression is of a more-or-less crescent shaped coastal and nearshore zone in the northern Gulf wherein there is an incomplete transition from tropical offshore to basically warm temperature coastal biota. North-south, tropical-temperate transitional

patterns offshore are more subtle and even less complete within the Gulf. Community types on the mid and outer shelves may be more dependent on substratum type and bathymetry than latitude.

Whatever the regional biogeographic relationships may be, it is certain that biotic communities occupying the outer continental shelf hard-banks in the northwestern Gulf of Mexico are of tropical origin. However, depending on their distance from shore, these communities are living either barely within acceptable ecological tolerance levels for thriving tropical reef assemblages (Flower Gardens and other shelf-edge banks) or below such limits (Sonnier, Stetson, and the South Texas fishing banks). The studies described in the following chapters add significantly to our knowledge of the benthic communities on these banks and certain ecological processes essential to regional reef construction and maintenance.

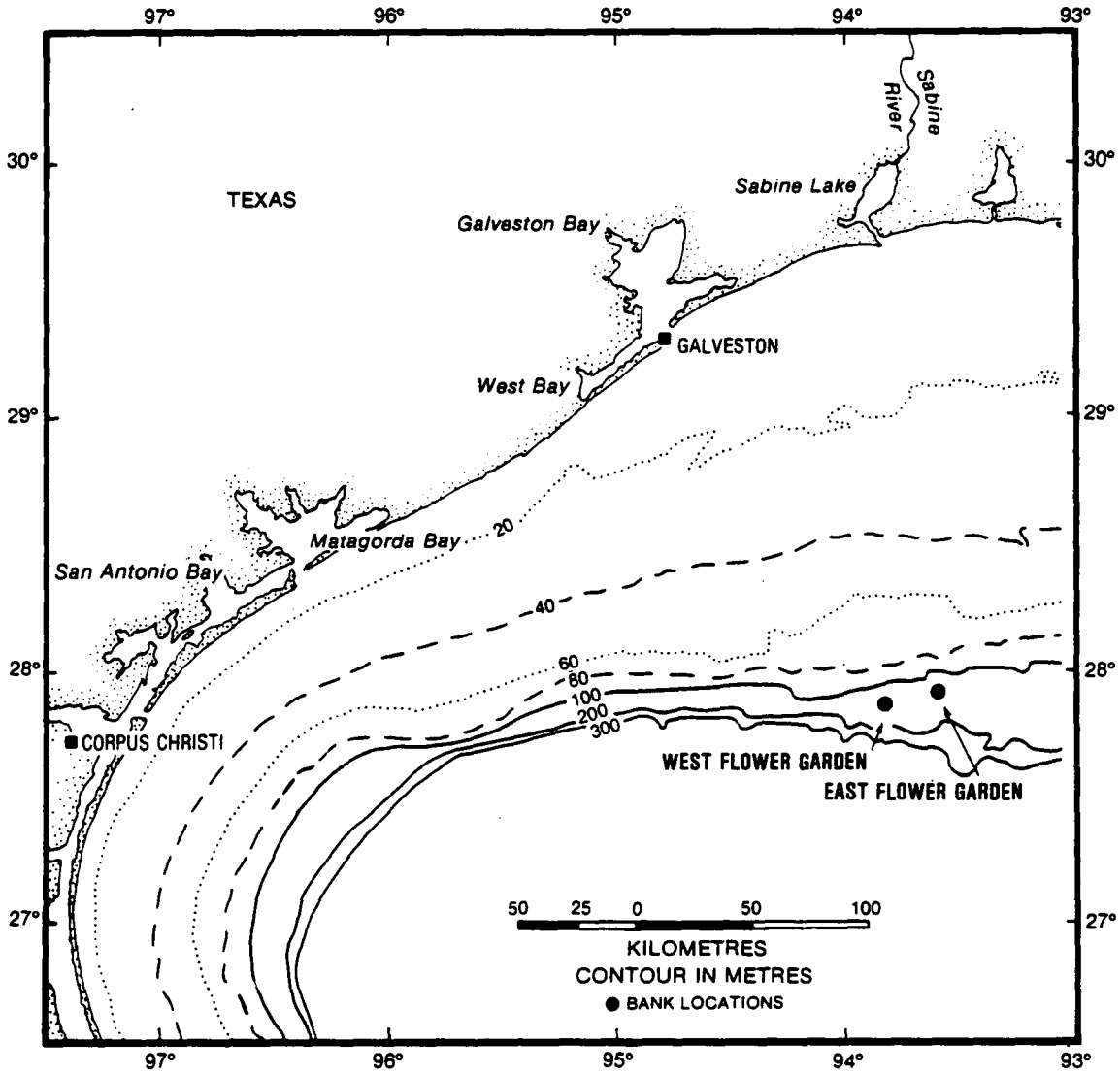

Figure 4.1 Location map of Flower Garden Banks, northwestern Gulf of Mexico.

CHAPTER 4

GEOLOGY OF THE FLOWER GARDEN BANKS

Richard Rezak

The Flower Garden Banks are similar in origin, general structure, and sediment distribution, but differ in the details of structure, physiography, and sedimentology. This chapter focuses on the specific differences in the geology of the two banks.

Our work on the geology of the Flower Garden Banks began in 1961. As a result of research cruises to the banks during 1961, 1968, 1969, and 1970, a Ph.D. dissertation was published as a Texas A&M Sea Grant Publication, describing the hydrology, biology, and geology of the West Flower Garden Bank (Edwards, 1971). Much of the descriptive material on the West Flower Garden Bank (WFG) presented here is based on the work conducted by Edwards, with details added from subsequent cruises to the bank. The geology of the East Flower Garden Bank (EFG) presented here is based upon work performed under BLM-TAMRF Contracts AA550-CT6-18 and AA851-CTO-25 (Bright and Rezak, 1978a; Rezak, 1982a).

GENERAL DESCRIPTION

The Flower Garden Banks are located near the shelf edge, approximately 107 NM due south of Sabine Pass (Figure 4.1). The East Flower Garden Bank is at 27°54'32"N latitude and 93°36'W longitude in Lease Blocks A-366, A-367, A-374, A-375, A-388, and A-389 of the High Island Area (Figure 4.2). The bank is pear-shaped and covers an area of about 67 km^2. Slopes are steep on the east and south sides of the bank, with gentle slopes on the west and north sides (Figure 4.2). The shallowest depth on the bank is about 20 m in the northeastern part of Lease Block A-388. The surrounding water depths are about 100 m to the west and north and about 120 m on the east and south sides. An elongate depression in the north-central part of Lease Block A-389 has a depth of 136 m. Total relief on the bank is about 116 m.

The West Flower Garden Bank is 12 km west of the East Flower Garden at latitude 27°52'27"N, longitude 93°48'47"W (Figure 4.1) in Lease Blocks A-383-385, A-397-399, and A-410 of the High Island Area, South Addition, and Lease Block GB-134 of the Garden Banks Area. It is a much larger bank, covering about 137 km^2. The bank is oval-shaped and oriented in a northeast-southwest direction (Figure 4.3). The crest of the bank lies at a depth of approximately 20 m. Surrounding depths vary from 100 m to the

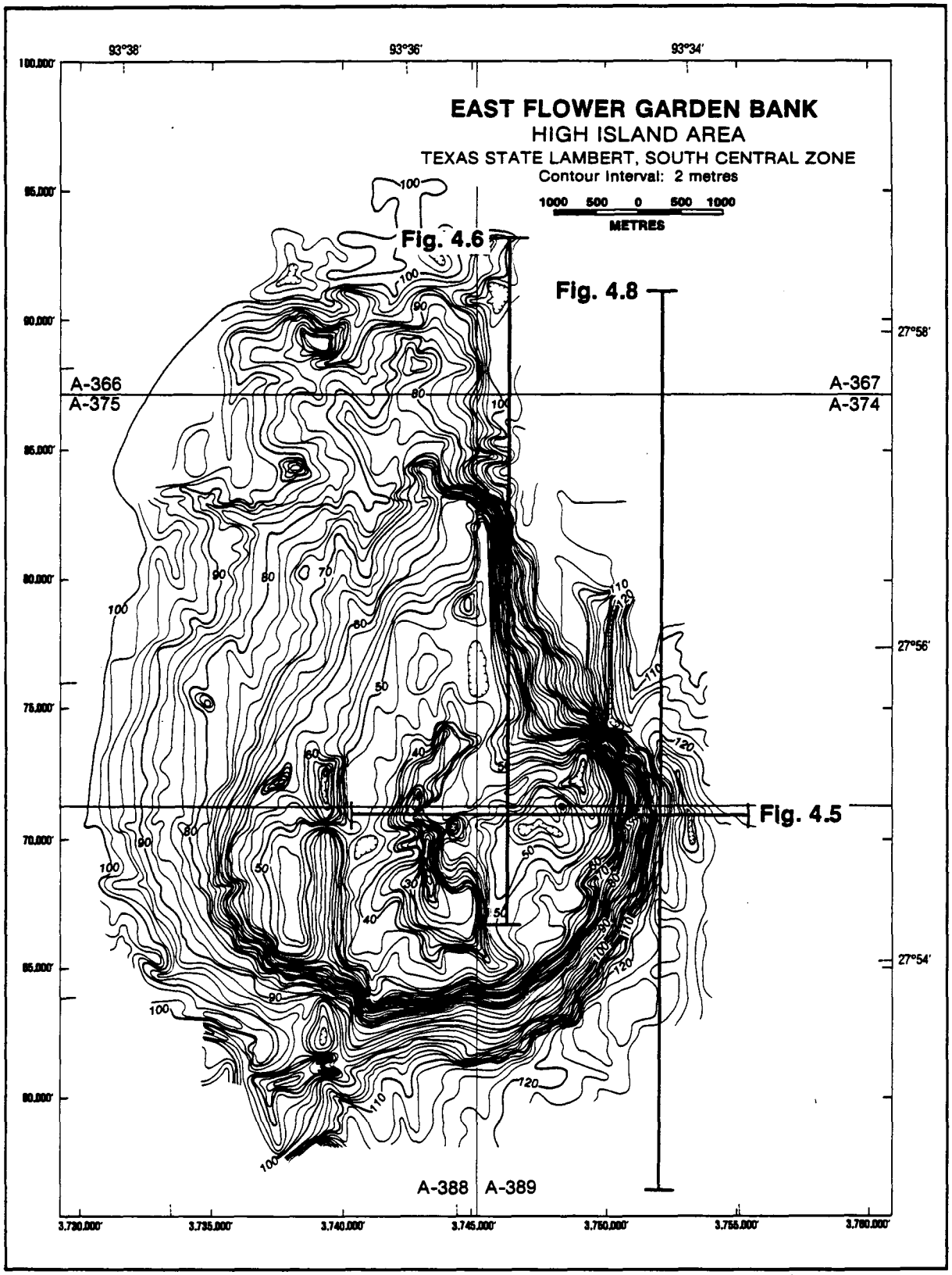

Figure 4.2 East Flower Garden Bank bathymetry, showing location of sub-bottom profiles in Figures 4.5, 4.6, and 4.8.

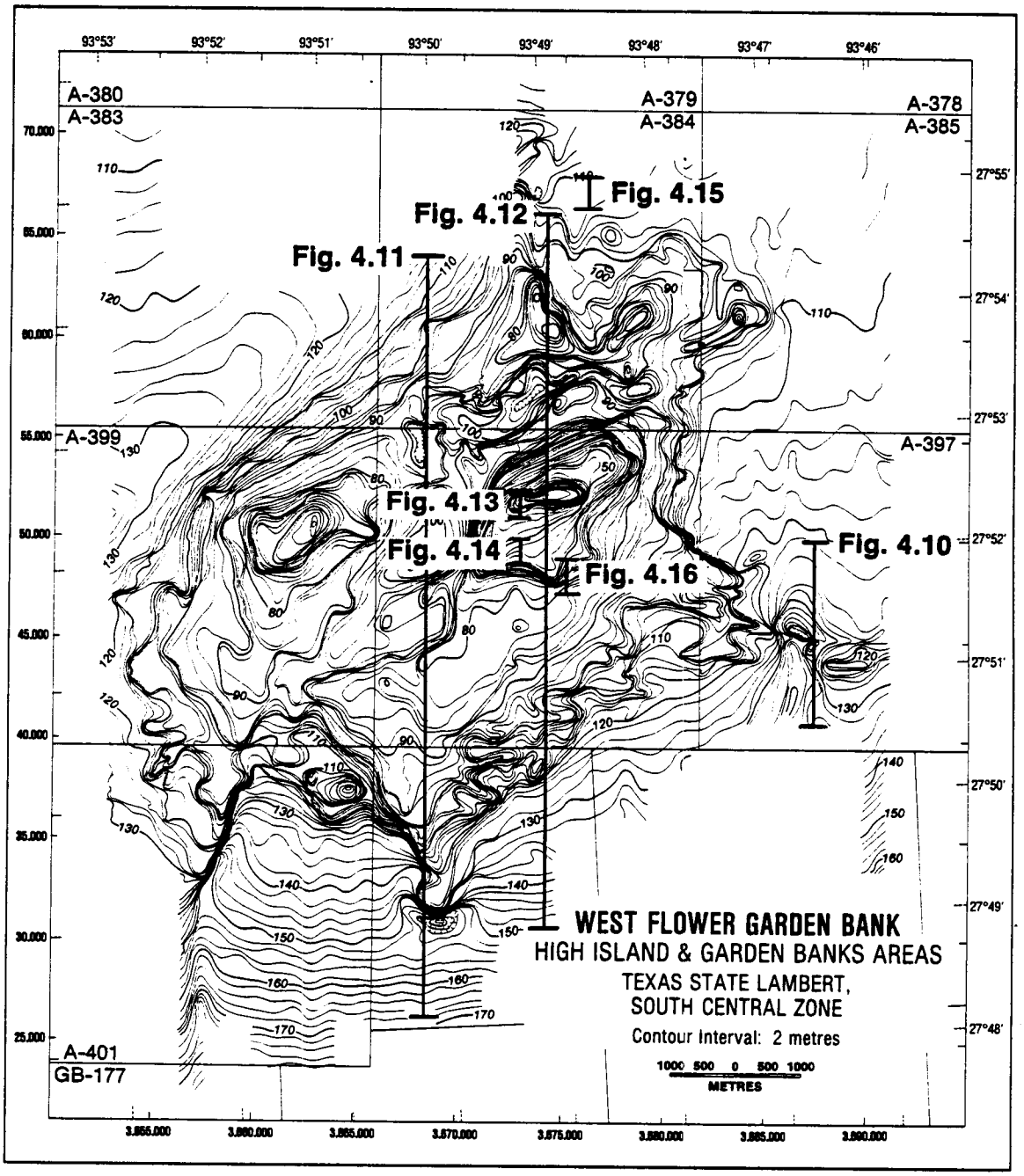

Figure 4.3 West Flower Garden Bank bathymetry, showing location of sub-bottom profiles and side-scan sonar records in Figures 4.10 to 4.16.

north, to 150 m to the south. Total relief on the bank is approximately 130 m.

PHYSIOGRAPHY AND STRUCTURE

Previous Research

In recent years it has been well documented that the East and West Flower Garden Banks are the surface expression of salt diapirs capped by living coral reefs at the crests (Nettleton, 1957; Edwards, 1971; Rezak, 1981, 1982a). Initial interest in the banks on the Outer Continental Shelf was expressed in a paper on the Mississippi Delta (Trowbridge, 1930), and as early as 1937 Shepard suggested that some of these banks were due to salt diapirism. Carsey (1950) speculated that these topographic features could easily be underlain by salt plugs but warned that they might be igneous plugs rather than salt domes. Stetson (1953) stated that the banks were either reefs that had kept pace with rising sea level or salt domes with a thin cap of calcareous organisms. Goedicke (1955) compared the banks to salt domes in the Persian Gulf region. In 1957, Nettleton published gravity data taken across the West Flower Garden Bank which clearly indicated a salt dome origin for that bank. Levert and Ferguson (1969) published a short paper reviewing previous studies and illustrating the living reef facies of both Flower Garden Banks. Edwards (1971) presented the most comprehensive report on the West Flower Bank. He used 3.5 kHz and air gun seismic profiles for the first time to illustrate the salt dome sub-bottom structure of that bank.

The most current discussion of the development and classification of salt diapirs is presented in Rezak and Bright (1981a). The East Flower Garden can now be classified as a young salt dome, and the West Flower Garden as a mature salt dome.

East Flower Garden Structure

Figure 4.4 is a structure map prepared from a CDP Sparker survey conducted by Aquatronics in 1974. Reflectors are present on the records over a major portion of the bank, and faults are much more easily delineated than on the 3.5 kHz profiles. The major fault trends are west-northwest to east-southeast, with minor trends towards the northeast and the southeast. North-South profiles show the faulting to be step-like, upslope, down-faulting typical of the tensional fractures produced during the domal uplift of sedimentary rocks over salt domes. The central graben (Figures 4.5, 4.6, 4.7, and 4.8) has developed partly due to tensional stresses developed

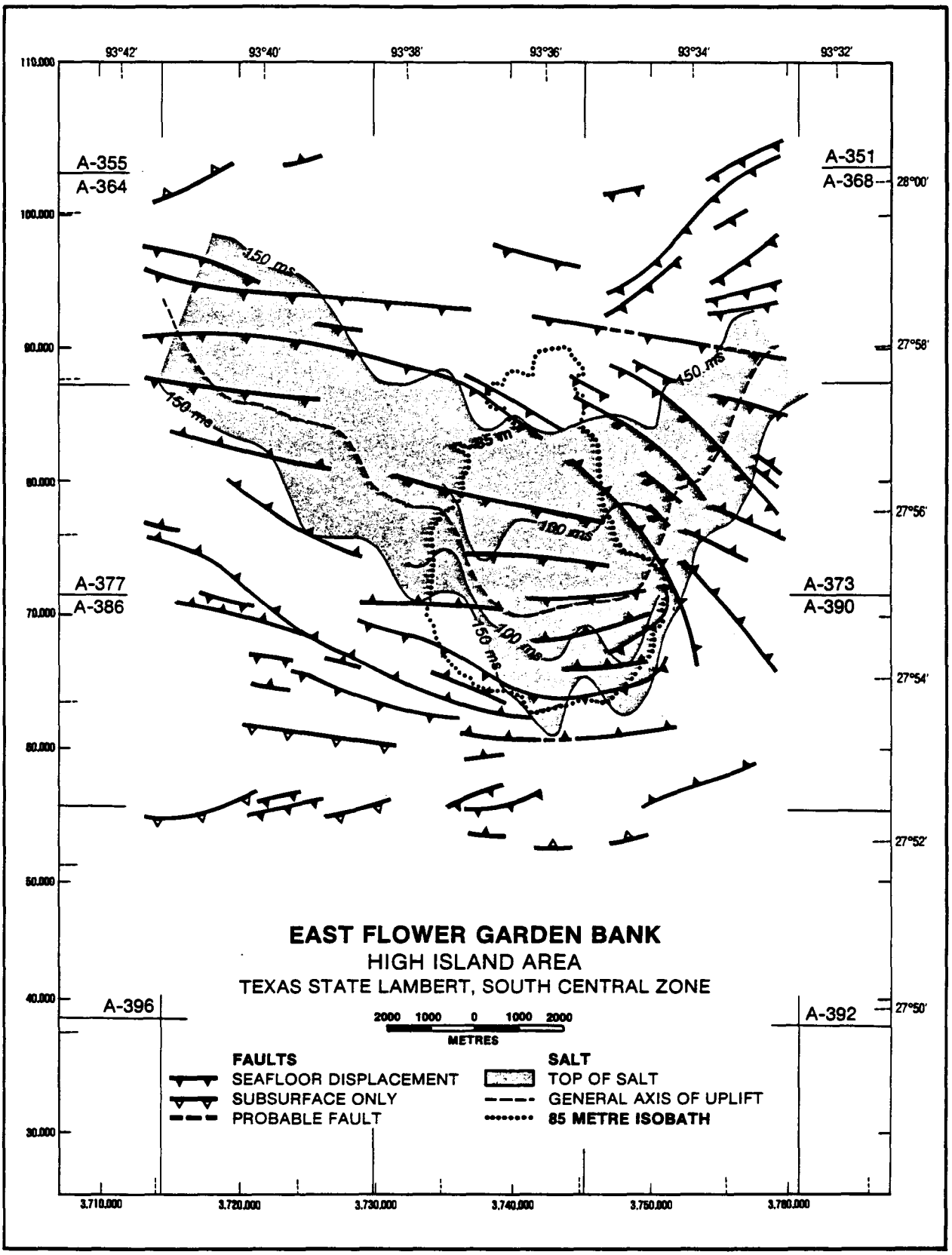

Figure 4.4 Structure map of East Flower Garden Bank region. The dotted line delineating the 85 m isobath is given to indicate the shape of the bank proper.

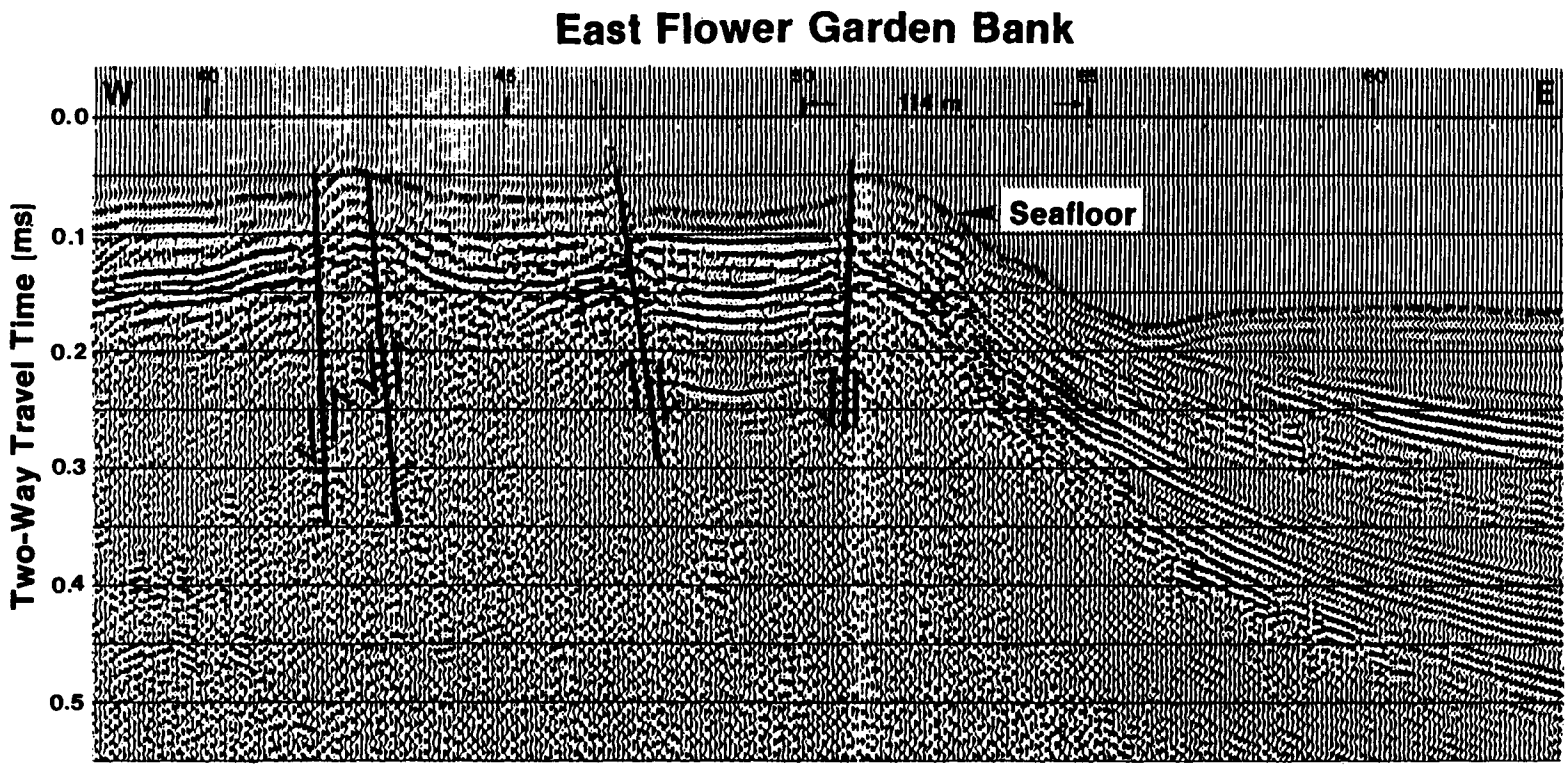

Figure 4.5 CDP Sparker profile across the central graben at the East Flower Garden Bank, also shown in Figure 4.6.

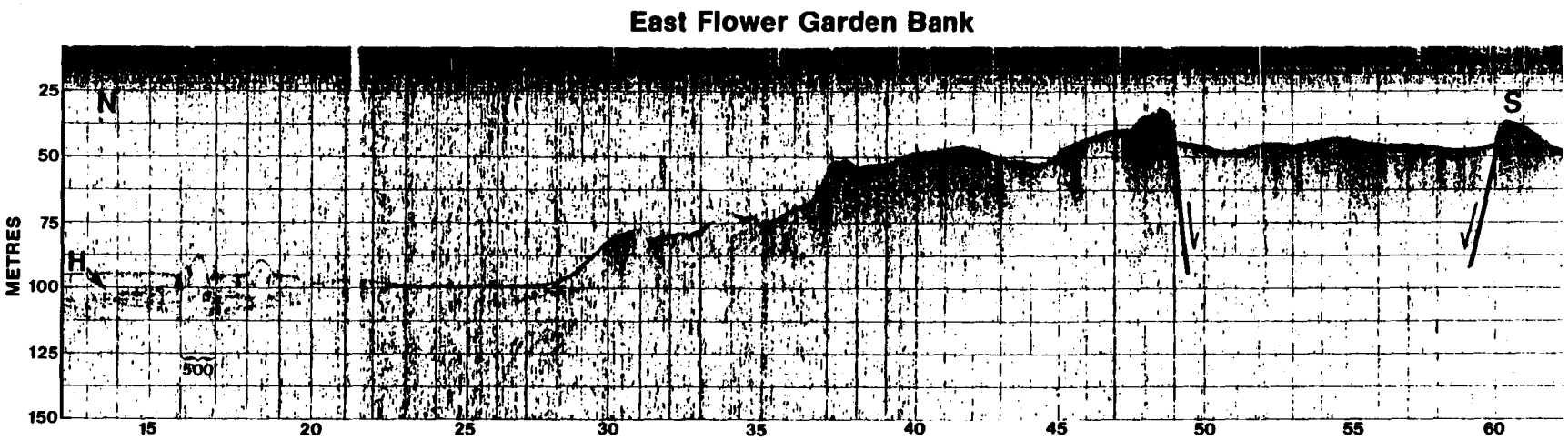

Figure 4.6 A 3.5 kHz sub-bottom profile showing the central graben (between shot points 49 and 60) at the East Flower Garden Bank. (See also Figure 4.5.)

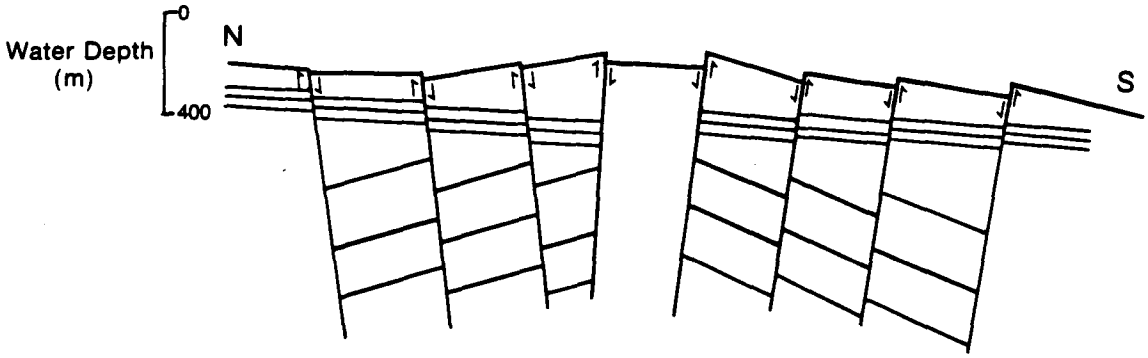

Figure 4.7 Diagrammatic representation of step faulting at the East Flower Garden Bank. (See also Figure 4.8.)

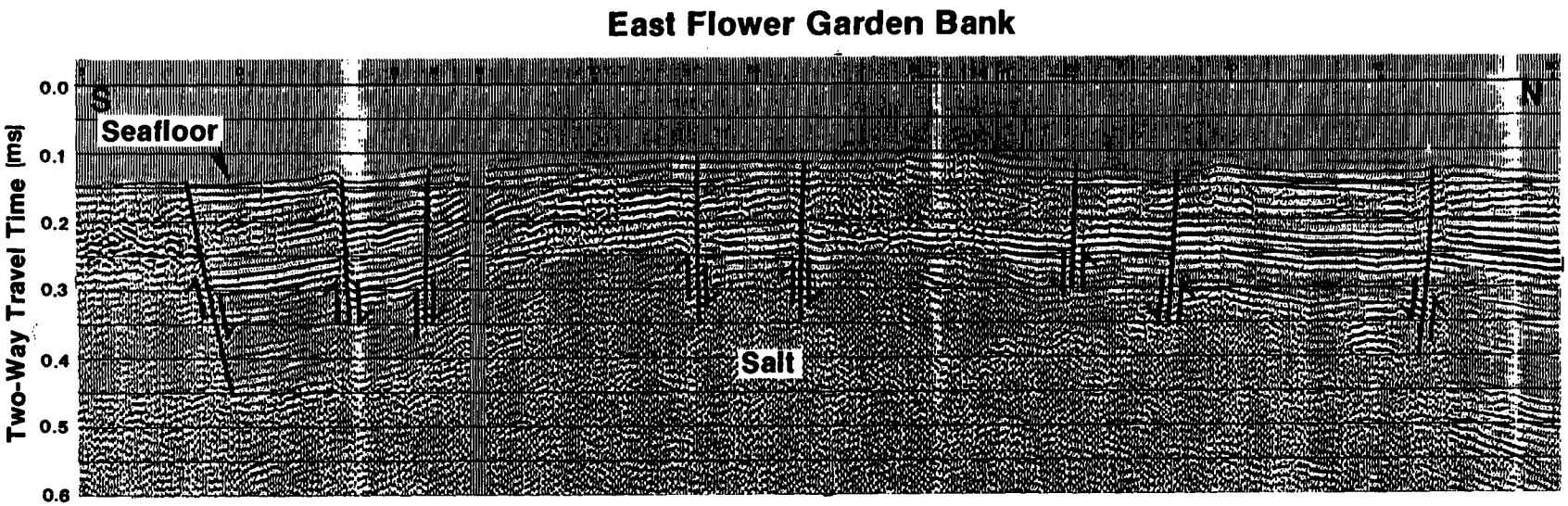

Figure 4.8 CDP Sparker profile showing step faulting at the East Flower Garden Bank.

during uplift and to removal of salt from the crest of the ridge by dissolution.

The shaded area on Figure 4.4 represents the trend and lateral extent of chaotic reflections, here interpreted to be salt. The reflections are mapped at 100 ms and 150 ms intervals (two-way travel time). Outside of the shaded area, bedded sediments occur down to the limit of seismic penetration. The dashed line indicates the axis of the uplift, which corresponds nicely with the central graben. Reflectors dip more steeply to the south of the axis than to the north. This is most probably due to the position of the bank on the shelf break. The axis of the salt ridge passes under the shallowest portion of the bank and through the northwest corner of Lease Block A-389. The brine seep complex described below and in Chapter 6 lies a short distance to the southeast.

East Flower Garden Brine Seep Complex

A brine seep complex at the East Flower Garden Bank has been described by Bright et al. (1980b) and Rezak and Bright (1981b). The primary brine system consists of interrelated components: numerous seeps (1), feeding a brine lake (2) that has an outflow into a canyon (3) that contains a mixing stream (4) that dilutes the brine to lower hypersaline concentrations (Figure 4.9).

The basin that contains the brine lake is 60 m from the edge of the bank, 4 m deep, oval-shaped, approximately 50 m across from west-northwest to east-southeast, and 30 m from north-northeast to south-southwest. The slope of the basin margin varies from 25° on the northwest side to almost vertical on the south-southeast side. A brine lake approximately 25 cm deep occupies part of the slightly lower eastern and central basin floor at 71 m depth. The lake is irregular in shape, with a cuspate "shoreline." Numerous brine seeps occur in the sandy bottom between the "shoreline" and reef rock wall of the basin. Dendritic rivulets of brine have been observed in the sands along the shoreline leading from the seeps to the lake.

Normally, the surface of the brine lake is perfectly flat. During submersible observation, small internal waves were created at the interface by movements of the research submersible. The waves were visible because of the presence of thin, white flakes (sulfuretum) floating at the interface. A canyon approximately 10 m wide at the bottom, 15 m wide at the top, and 60 m long extends from the east-southeast margin of the basin to the edge of the bank (79 m depth).

The residence time of brine in the basin is less than one day. The lake, 25 to 30 m long, 15 to 20 m wide, and generally less than 0.25 m deep, contains approximately 465 m^3 of brine. The overflow

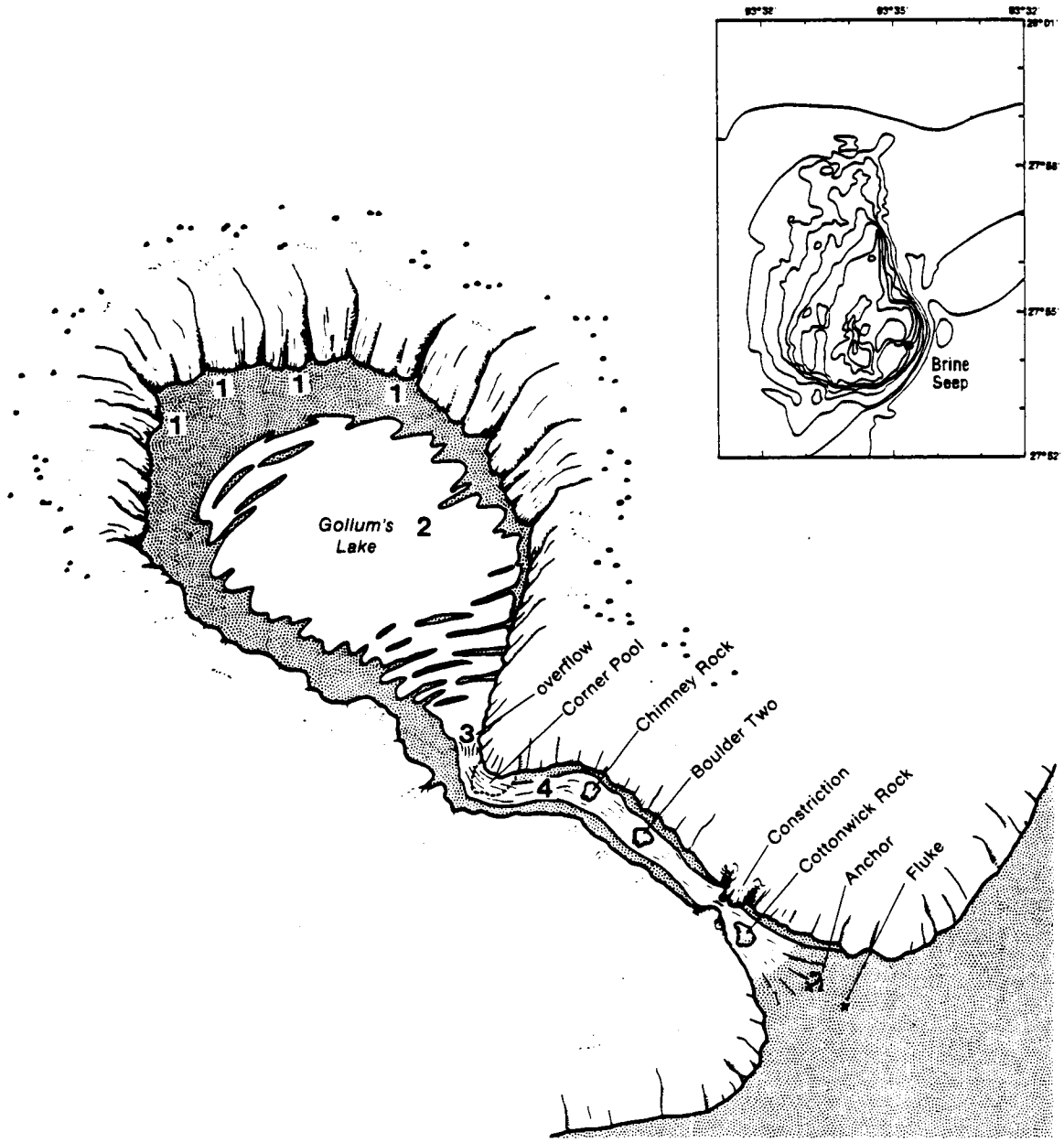

Figure 4.9 East Flower Garden Brine Complex: 1 - brine seeps; 2 - brine lake; 3 - overflow; 4 - canyon with mixing stream.

rate of brine from the lake into the canyon, calculated by current meter and direct measurement of outflow cross-section area, was determined to be 355 to 717 m^3/day. Residence time is therefore 0.65 to 1.3 days.

Both the depth of the brine lake and the overflow rate appeared unchanged during four years of observation (1976 to 1980). Seismic data indicate that the top of the salt may be within 30 m of the crest of the reef just to the northwest of the brine basin. The occurrence of another brine seep at 48 m on the bank suggests that the top of the salt may actually be slightly shallower than that. The brine results from dissolution of the salt by normal marine water that permeates the porous reef rock. Some of the numerous brine seeps that feed the lake are located several centimetres above the lake level around the "shoreline." Dendritic rivulets of brine have been observed in the sands along the "shoreline" leading from the seeps to the lake.

Based upon the measured outflow of the brine lake and the salinosity of the brine in the lake, calculations show that the amount of solid salt being removed from the crest of the salt diapir ranges from a minimum of 10,765 m^3/yr to 21,710 m^3/yr. As other seeps are known to exist at the East Flower Garden Bank, this is a minimum range for the removal of solid salt. The removal of such large volumes of solids from beneath the crest of the bank must create sizeable caverns beneath the cap rock and the overlying reef. Collapse of the crest of the reef into these caverns will depend upon the strength of the cap rock and overlying reef. If these structures are weak, the collapse may be gradual, keeping pace with the removal of salt. However, if either the cap rock or reef is strong, the caverns may attain a considerable size before failure occurs and the collapse becomes catastropic.

Chemical aspects of the East Flower Garden brine have been reported by Brooks et al. (1979) and by Bright et al. (1980b). The brine has a higher density than seawater, is anoxic, and contains exceptionally high levels of dissolved hydrocarbon gases (methane, ethane, and propane) and hydrogen sulfide. The density differential inhibits mixing of the lake brine with overlying seawater. Because of the lack of mixing, chemical characteristics of water above and below the interface differ drastically over a vertical distance of less than 2 cm (e.g., salinity: 36.7 ppt vs. 200 ppt).

Examination of the bathymetry at the East Flower Garden (Figure 4.2) reveals several shallow closed depressions in the southern part of the bank. One large depression close to the northeast corner of Lease Block A-389 is a part of the central graben shown in Figures 4.5, 4.6, and 4.8. Evidence for faulting at the crests of salt domes is shown on Figures 4.5 (East Flower Garden) and 4.11 (West Flower Garden). The shallow and discontinous nature of these closed depressions indicates that graben formation has been active for only a very short time. It is expected that fault movements will

continue as long as salt is being dissolved from the crest of the salt stock.

West Flower Garden Bank

Because the West Flower Garden is a much older salt dome, local relief on the bank proper is much greater than at the East Flower Garden. Although the structure of both banks is the result of normal faulting, there has been more movement along faults at the West Flower Garden. The chief source of these structural differences is the greater amount of salt removal at the West Flower Garden Bank.

The structure of the West Flower Garden Bank is typical of a mature salt diapir in which crestal faulting has occurred. The trough running from the southeast corner of Lease Block A-399 to the southeast corner of Lease Block A-384 (Figure 4.3) is a crestal graben, exhibiting far greater relief than the crestal graben at the East Flower Garden. Figure 4.10 is a structure/isopach map including faults delineated by Henry Berryhill (USGS; unpublished MS; on file at MMS, New Orleans) and those observed on our own 3.5 kHz records. Because of the poor reflectivity in the area of the graben on our records, it is difficult to display the borders of the crestal graben on this map. The large east-west fault on the southeastern margin of the bank (Lease Block A-397) is illustrated in Figure 4.11. This fault displaces the seafloor and appears to be the result of recent movement. Figures 4.12 and 4.13 illustrate the abundance of normal faults on this bank. Edwards (1971, his Figure 20) illustrates a one cubic inch air gun profile across the bank showing the crestal graben and numerous normal faults to the southeast of the bank. The numerous bathymetric prominences on the bank represent horsts that stand above the surrounding graben (Figure 4.3).

The living reef lies in the north-central portion of Lease Block A-398. It rises from depths of 40 to 50 m to a crest at about 20 m. Extending from near the base of the reef towards the northeast and the south is a broad terrace that extends to depths of about 60 to 70 m (Figure 4.3). The surface of this terrace is characterized by large waves of sediment consisting primarily of the Coral Debris Facies sand and gravels of the *Gypsina*-*Lithothamnium* Facies (Figures 4.14 and 4.15). The gravel waves are oriented normal to the isobaths. Below these depths are numerous lineations (faults and outcrops of Tertiary bedrock covered by drowned reefs, Figure 4.16) and patch reefs scattered to depths as great as 170 m (Figure 4.17). Most of the patch reefs above 90 m appear to have formed during the last rise of sea level.

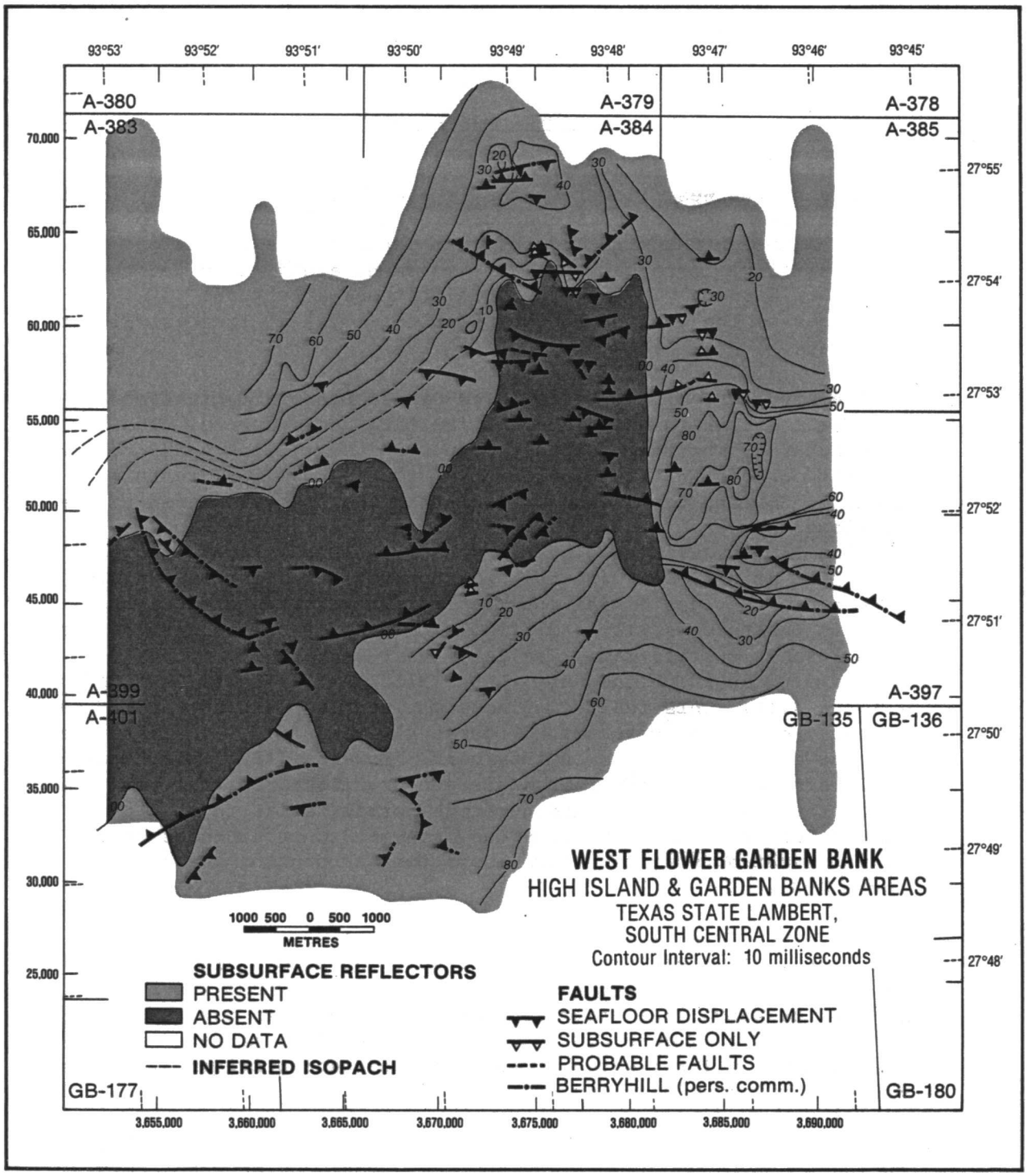

Figure 4.10 Structure/Isopach map of West Flower Garden Bank. Contours are isopachs (sediment thickness) from the seafloor to H shown in Figures 4.11 and 4.12.

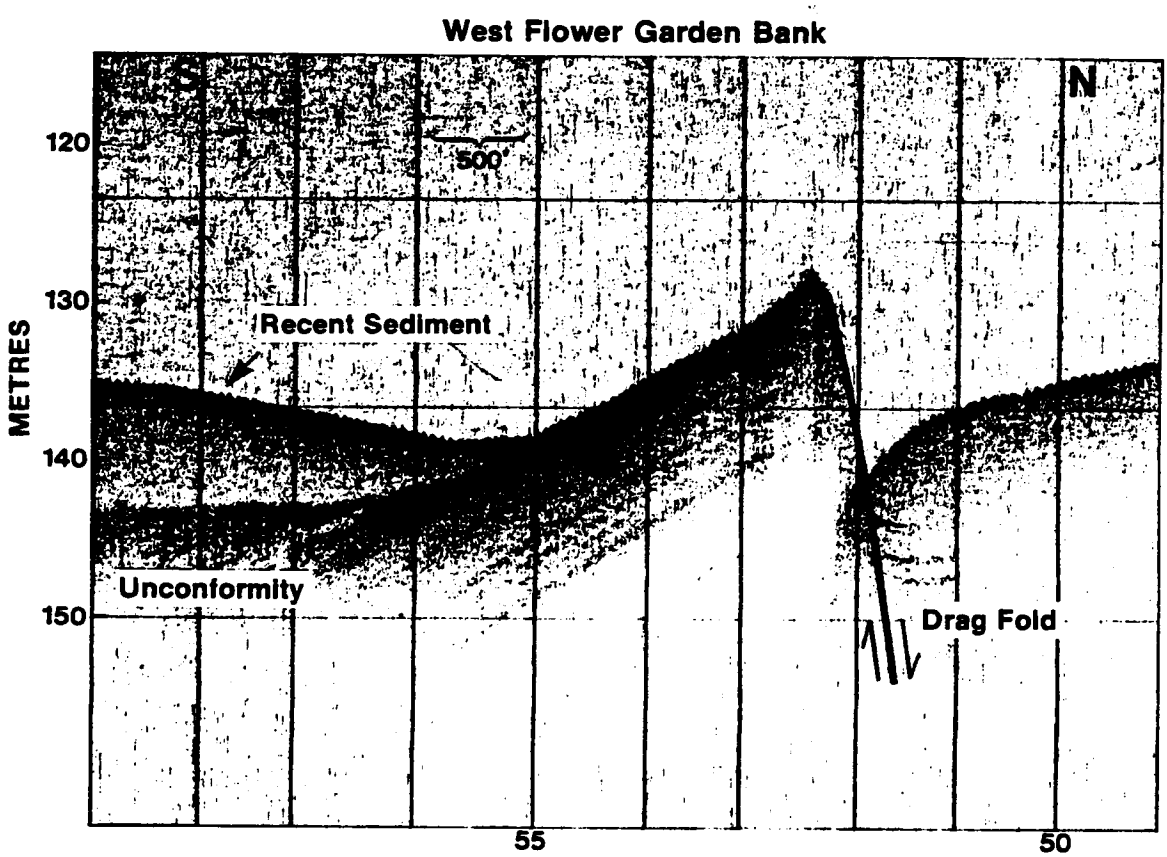

Figure 4.11 A 3.5 kHz north-south sub-bottom profile across the western part of the West Flower Garden Bank (Lease Block A-397; indexed on Figure 4.3).

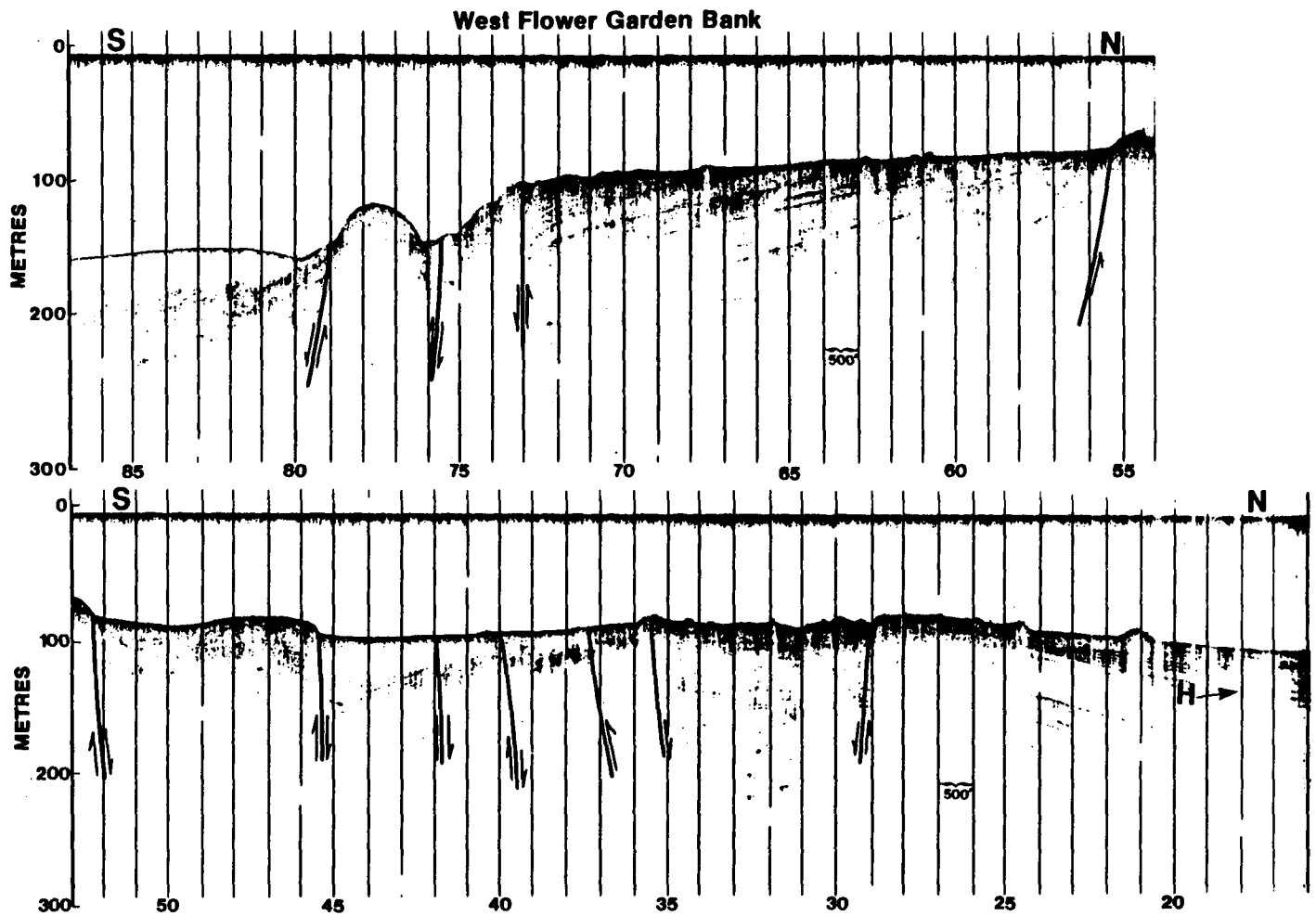

Figure 4.12 A 3.5 kHz north-south sub-bottom profile across the central part of the West Flower Garden Bank (location indexed in Figure 4.3). The right side of the upper profile joins with the left side of the lower profile. H = base of isopach interval.

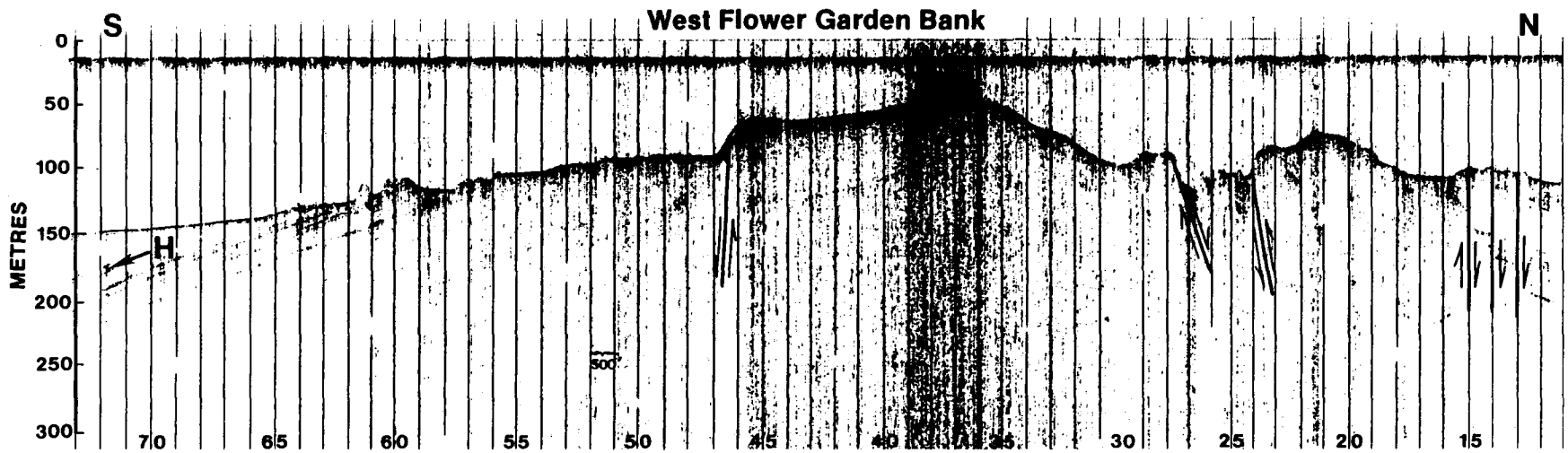

Figure 4.13 A 3.5 kHz north-south sub-bottom profile across the central part of the West Flower Garden Bank, including the living high diversity coral reef (location indexed in Figure 4.3). Note the lack of reflectors over most of the bank. H = base of isopach interval.

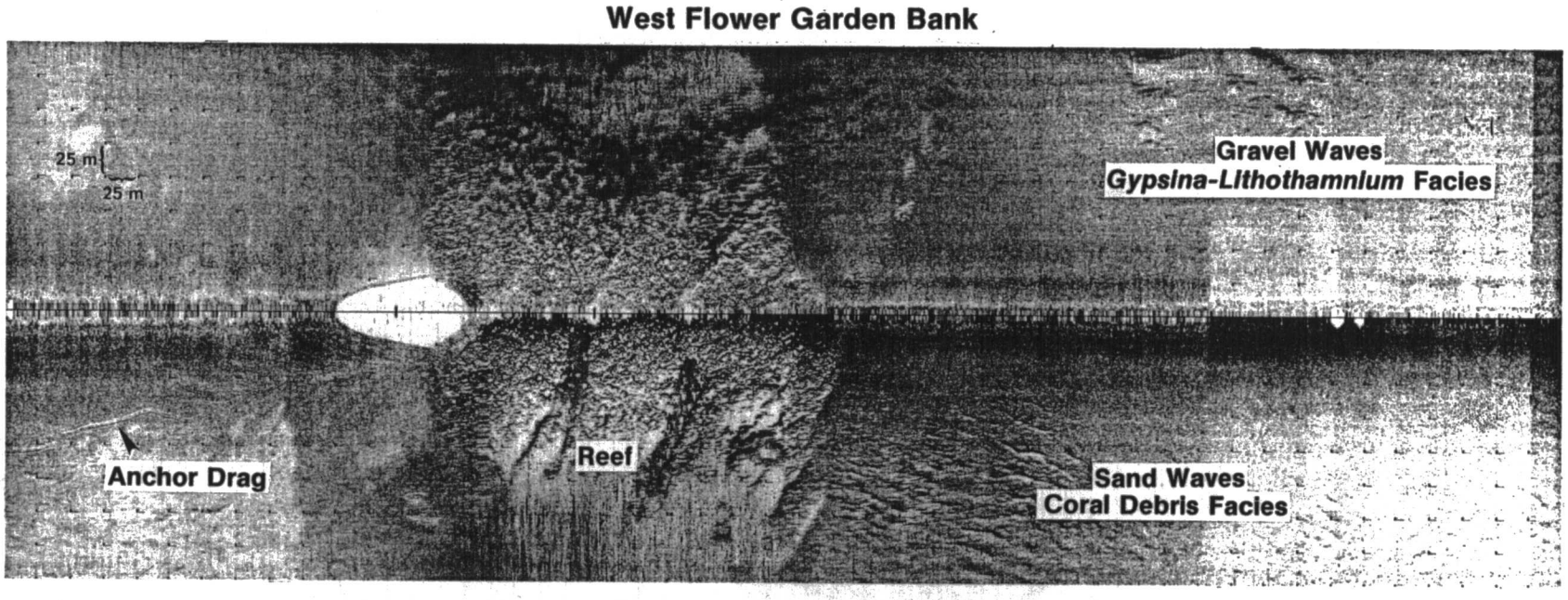

Figure 4.14 Side-Scan sonar record showing surface features in a central portion of the West Flower Garden Bank, near the living high diversity coral reef (Lease Block A-398; indexed in Figure 4.3). Water depth is 35 m on the reef, 40 m at sand waves, 45 m at gravel waves. Light areas on the reef are sand.

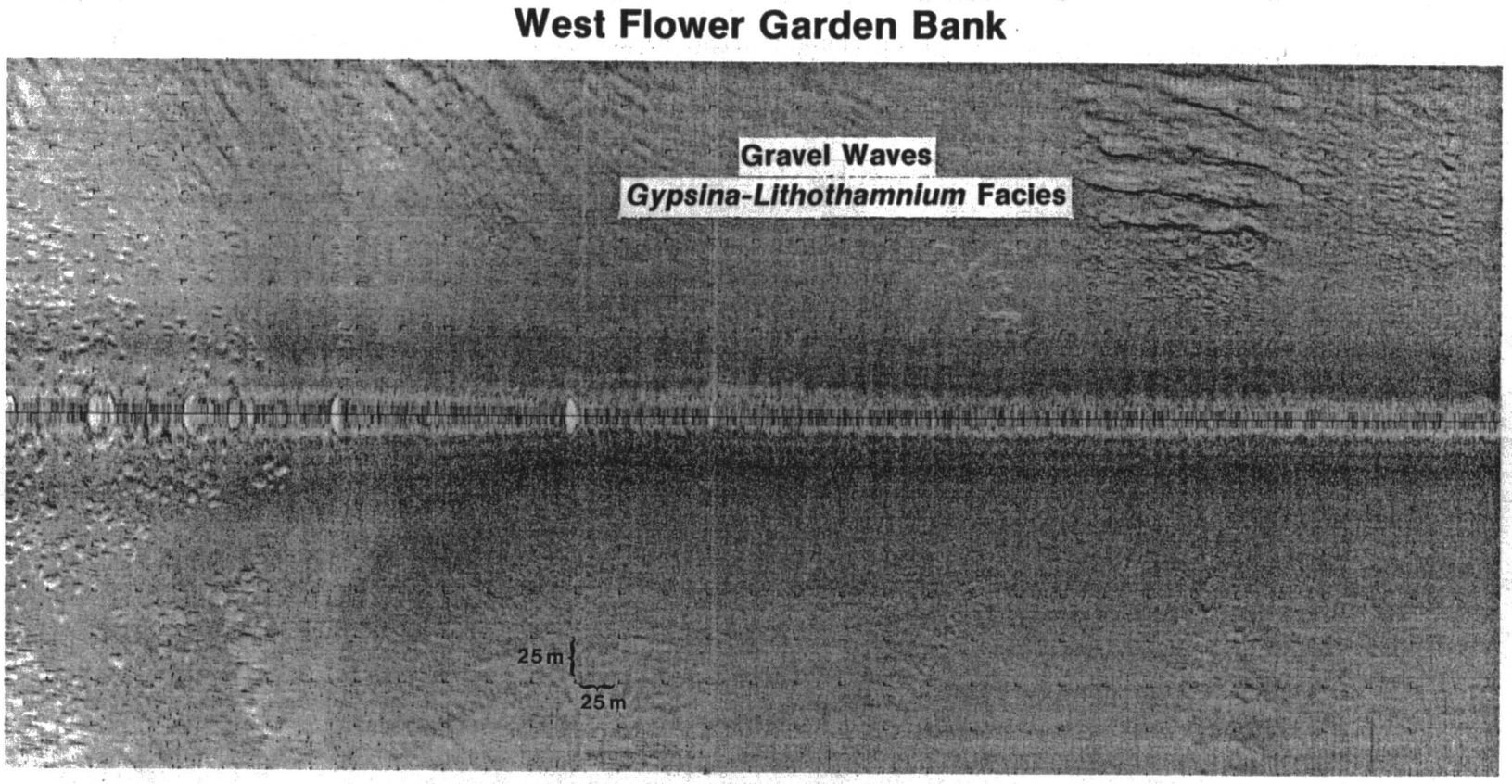

Figure 4.15 Side-Scan sonar record showing surface features in a central part of the West Flower Garden Bank (just south of the record shown in Figure 4.13; indexed in Figure 4.3). Water depth is 58 m.

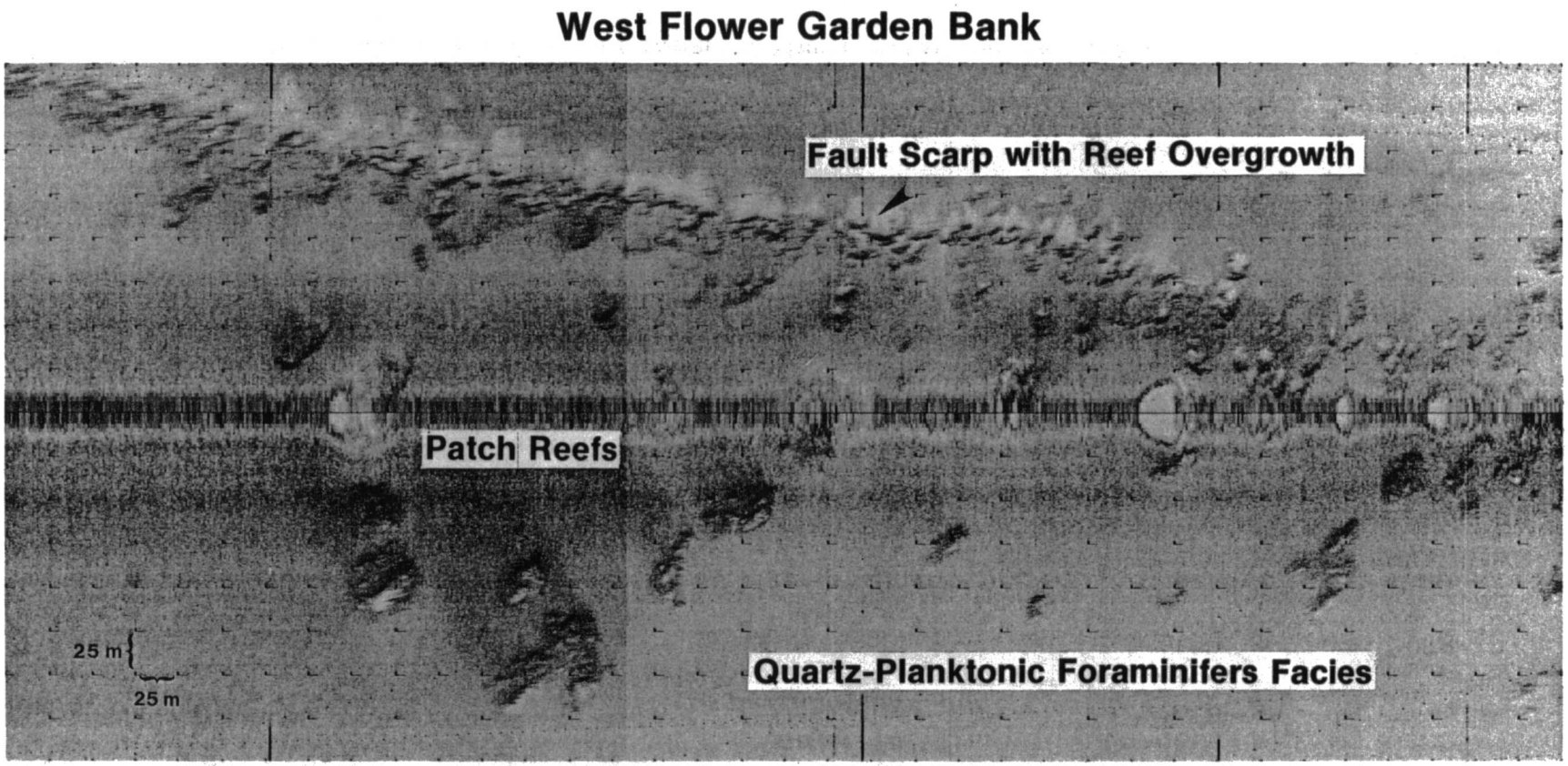

Figure 4.16 Side-Scan sonar record showing fault scarp with reef overgrowth in the northern part of the West Flower Garden Bank (Lease Block A-384; indexed in Figure 4.3). Water depth is about 105 m.

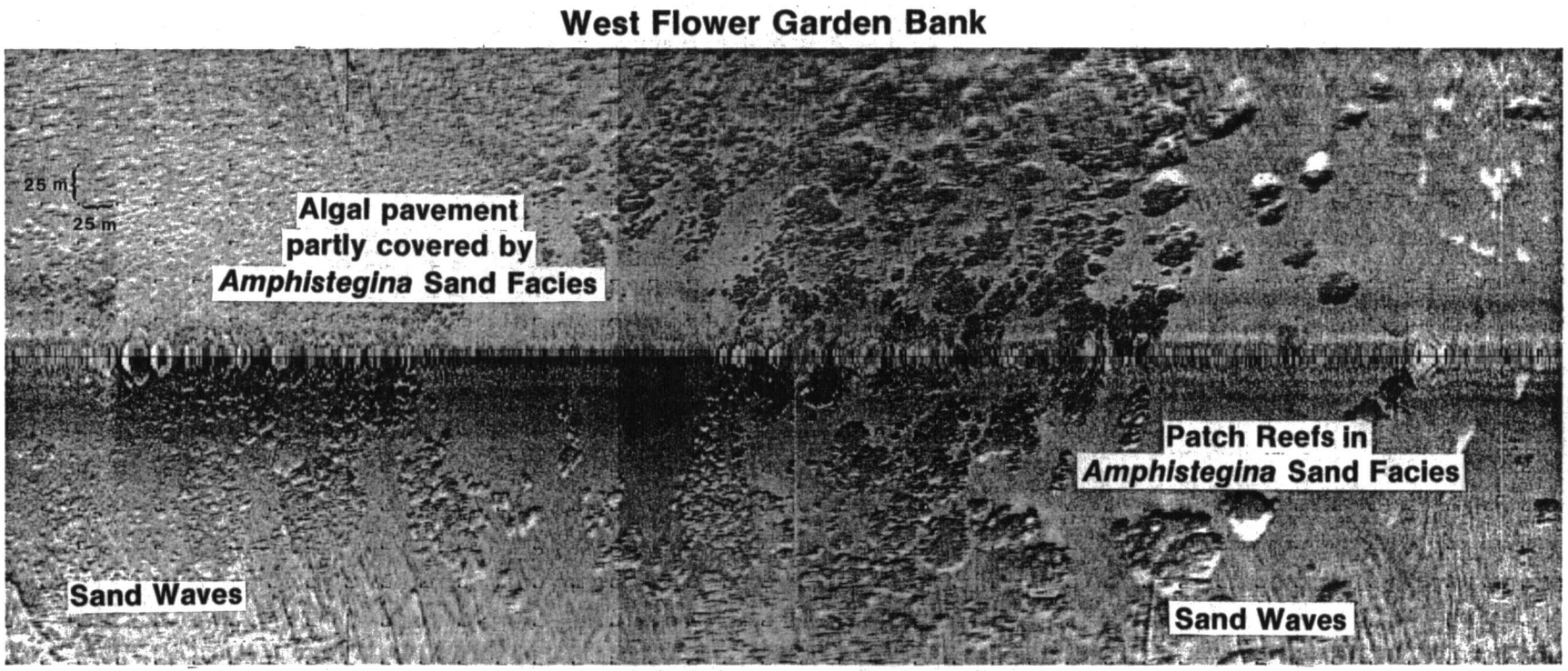

Figure 4.17 Side-Scan sonar record showing patch reefs in the Amphistegina Sand Facies at the West Flower Garden Bank (Lease Block A-398; indexed in Figure 4.3). Depth is about 85 m.

SEDIMENTARY FACIES

General Description

Sediment facies at the West Flower Garden Bank were first described by Edwards (1971). Subsequent sampling augmented by direct observations of the bottom from the Texas A&M submersible DRV DIAPHUS confirm Edwards' facies delineation and extend coverage to the East Flower Garden. The map of sediment distribution in the Flower Garden Banks area (Figure 4.18) is based on 43 samples from Edwards' study of the West Flower Garden Bank, 35 samples taken at the East Flower Garden in 1979, 51 samples from selected areas away from the banks (these were selected from a large collection donated by Tenneco), and 10 additional samples taken in December 1979 in order to fill in the gaps in the off-bank areas.

The sediments of the two banks differ markedly in origin from the sediments of the open shelf surrounding the banks. Bank sediments are all derived from the skeletons of organisms that are living on the banks. The open shelf sediments in the area of the banks, however, are sands and muds that have been eroded from the North American continent and mechanically transported to the Gulf of Mexico by streams such as the Mississippi, Trinity, Sabine, and Brazos Rivers. These sands and muds do not occur at depths shallower than 75 m at the Flower Garden Banks. The sediments above the 75 m level are all coarse sands and gravels and the rocky, limestone structure built by the corals and other reef-dwelling organisms. The loose sediments around the reef reflect the depth zonation of the biological communities that are present on the two banks. Table 4.1 illustrates the relationship between the biological zones and the sediment facies.

As may be seen in Table 4.1, the sediment facies are intimately related to the biological zonation and hydrological conditions at each bank. However, the sediment boundaries do not coincide with the biotic boundaries. This is partly due to the downslope movement of loose sediment by the force of gravity and partly due to the use of soft-bodied organisms in delineating the biotic zonation. In Table 4.1, for example, the lower boundary of the Algal-Sponge biotic zone is based upon the lower depth limit of *Neofibularia*, a colonial, soft-bodied sponge which also grows in the upper part of the *Amphistegina* Sand Facies.

Knowing the distribution of living, lime-secreting, skeletal organisms, one can demonstrate that the direction of sediment transport on the banks is downslope. The Coral Debris Facies accumulates between coral heads of the Living Reef Facies and in a narrow band around the base of the living reef (Figure 4.14). The *Gypsina*-*Lithothamnium* Facies consists of coarse gravel and massive limestone that are forming *in situ* due to the growth of calcareous

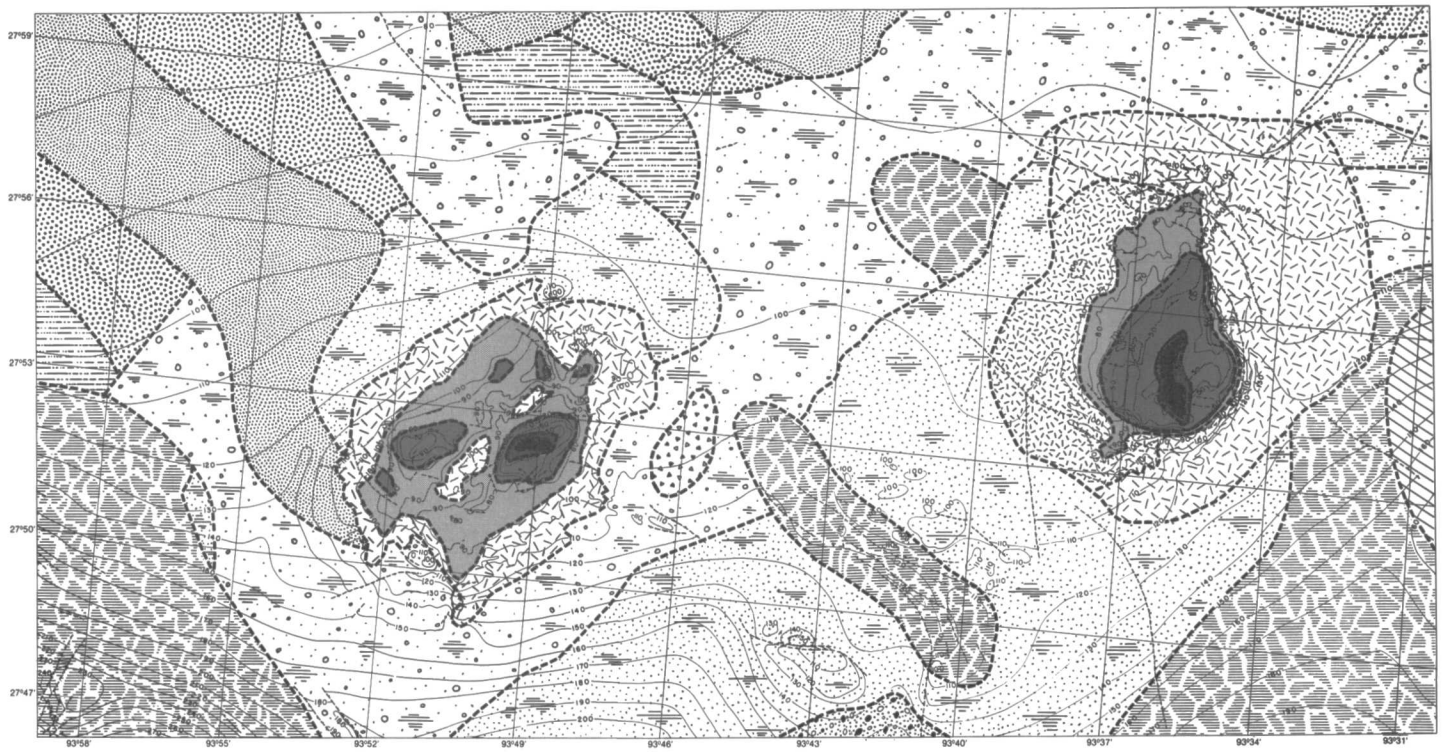

SEDIMENTARY FACIES

Carbonates	Terrigenous	
Living Reef	Mud	M
Coral Debris	Gravelly Mud	gM
Gypsina - Lithothamnium	Slightly Gravelly Mud	(g)M
Amphistegina Sand	Slightly Gravelly Sandy Mud	(g)sM
Molluscan Hash	Clay	C
Quartz-Planktonic Foraminifers	Sandy Silt	sZ
	Gravelly Muddy Sand	gmS
	Slightly Gravelly Muddy Sand	(g)mS
	Muddy Gravel	mG

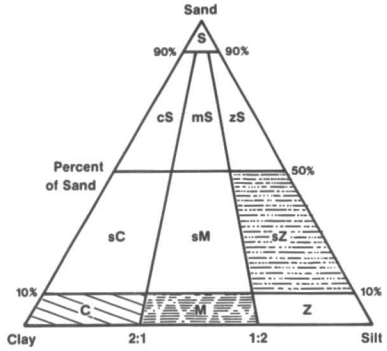

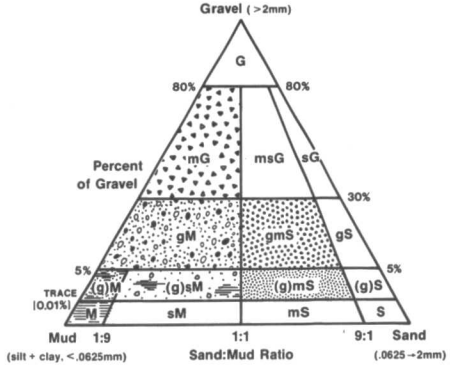

Figure 4.18 Sediment facies in the Flower Garden Banks area.

Table 4.1 Relationship Between Sediment Facies and Biological Zones at the East Flower Garden Bank

SEDIMENT FACIES	DEPTH (m)	BIOLOGICAL ZONE	DEPTH (m)
1. Coral Reef	15-50	1. *Montastrea-Diploria-Porites*	15-36
a. Living Reef (massive limestone)	15-45		
b. Coral Debris (coarse sand and gravel)	25-50	2. *Madracis*	28-46
		3. *Stephanocoenia*	36-52
2. *Gypsina-Lithothamnium* (coarse gravel and massive limestone)	50-75	4. Algal-Sponge	46-88
3. *Amphistegina* Sand (medium to coarse sand, muddy at depths greater than 85 m)	75-90	5. Transition	88-89
4. Quartz-Planktonic Forminifers (sandy mud)	90+	6. Nepheloid	89
5. Molluscan Hash (muddy sand)	90+		

algae and encrusting calcareous protozoans. However, the Amphistegina Sand Facies is composed of the recently dead skeletons of a small protozoan that lives and grows abundantly in the the Gypsina-Lithothamnium Facies. Upon dying, the sand size skeletons of these protozoans are moved downslope by gravity to form the Amphistegina Sand. At depths less than 75 m, the sediments of the banks are medium to coarse, calcareous sands and gravels (Figure 4.18). The living reef and the Gypsina-Lithothamnium Facies are natural sediment traps due to their highly irregular surfaces. Any fine sediments, such as occur below the 75 m depth, would be trapped in the irregular topography of these facies if they were ever carried to the top of the reef by either physical or biological processes. The surface irregularities would act as baffles that retard the velocity of the currents and cause deposition of fine sediment in nooks and crannies on the reef and in the Gypsina-Lithothamnium Facies. This process is analogous to a snow fence that traps snow away from highways and railroad tracks.

As indicated above, there is no land-derived mud in the bottom sediments above a depth of 75 m (Figure 4.19). This fact substantiates the conclusion from water and sediment dynamics studies that the nepheloid layer rarely rises to depths of 75 m (see below, Chapter 5.) If the nepheloid layer were able to cover more of the bank, then one would find land-derived muds mixed with coarser sediments at shallower depths. Moreover, the 80 m isobath is a major boundary in the biolgical zonation. That depth separates the turbid water fauna below from the clear water fauna and flora above. If the nepheloid layer were able to rise to shallower depths, the lower limits of the clear water assemblages would also be raised by the same number of metres (Bright and Rezak, 1978b; Rezak and Bright 1981a, Vol. 3).

The boundary between the areas of carbonate and terrigenous sedimentation is an artifact caused by the use of two different classification systems, carbonate (genetic) and terrigenous (textural). A discussion of the problems created by the use of these two classifications systems is presented in Chapter 1.

Description of Facies

Coral Debris Facies

As indicated in Table 4.1, the Coral Debris Facies ranges in depth from 25 m to 50 m. It overlaps with the living reef, which has a depth range from 15 to 45 m. Where they overlap, the Coral Debris Facies consists of coarse sand and gravel lying between coral heads and in valleys or canyons leading down to the sediment apron around the reef (Figure 4.14). The narrow band of this facies around the living reefs at both the East and West Flower Garden

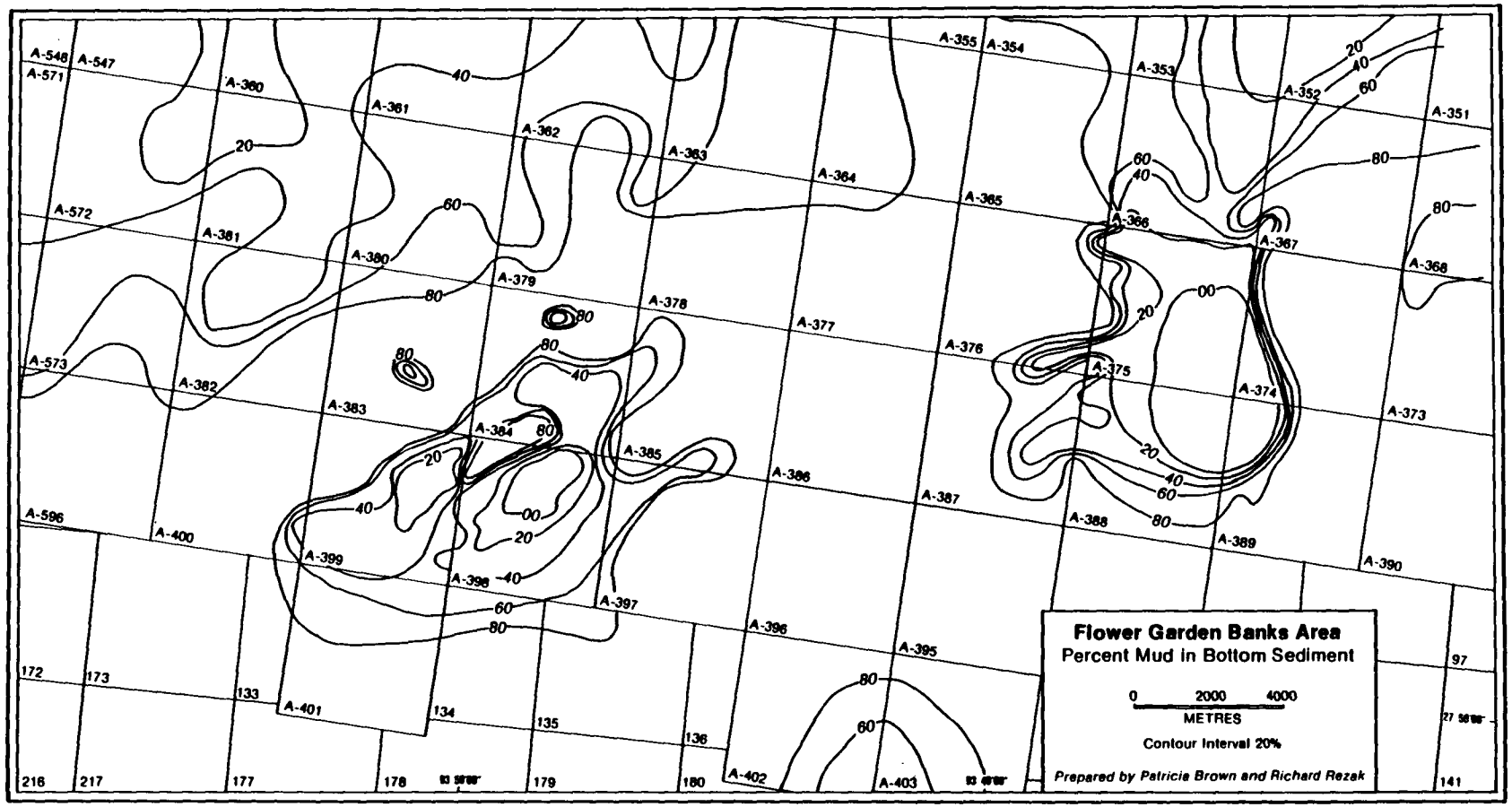

Figure 4.19 Percent mud (silt and clay) in bottom sediment in the Flower Garden Banks area.

Banks attests to the minimal amount of transportation of coral debris. The dominant particle types are 1) coral fragments, 60 to 68%; 2) coralline alage, 16 to 30%; and 3) Gypsina plana, an encrusting foraminifer, 3 to 7%. Textural analysis of samples from this facies shows that 99.83% of the sample is coarser than coarse silt (0.062 mm).

Gypsina-Lithothamnium Facies

This facies ranges in depth from 50 to 75 m. The boundary between this facies and the Coral Debris Facies is transitional and of variable width, both algal nodules and coral sand covering the bottom. The numbers of algal nodules increases with depth until the entire seafloor is covered with nodules. The sediment particles range from sand to cobble size, with up to 48.31% gravel and 49.9% sand. As much as 1.78% mud has been reported from this facies. However, the mud has been analysed using an electron microprobe and found to be carbonate mud produced in situ by boring organisms within the algal nodules (G. Minnery, pers. comm.).

The major contributors to this facies are: 1) coralline algae, 50 to 79%; 2) coral, up to 45%; 3) worm tubes, up to 21%; 4) Gypsina plana, up to 18%; 5) Amphistegina sp., up to 22%. The gravels are sediments that have been created by organisms with encrusting growth habits. Coralline algae, the major contributors to this facies, encrust skeletal grains (whole or fragmented molluscs or corals) or lithoclasts. The grains are rolled around by currents and grow by the addition of successive, more or less concentric layers of coralline algae to form coralline algae nodules similar to those described by Logan et al. (1969) from the Campeche Bank. The nodules attain diameters of 10 to 12 cm. A detailed description of the biota of the nodules is given in Chapter 6. One geologically important organism, the benthonic foraminifer Amphistegina gibbosa, grows profusely on the surfaces of the algal nodules. The whole skeletons of this foraminifer contribute to the coarse sand and granule fractions of the Gypsina-Lithothamnium Facies. In addition, the abandoned tests of A. gibbosa are transported downslope to accumulate in the Amphistegina Sand Facies. These grains are transported farther than any other skeletal grains at the Flower Garden Banks. The algal nodules, as displayed by the giant gravel waves on the side-scan sonar records of the West Flower Garden Bank (Figures 4.14 and 4.15), move in a direction parallel to the isobaths with little or no transport downslope.

Amphistegina Sand Facies

The Amphistegina sand ranges in depth from 75 to 90 m. Both the upper and lower boundaries of this facies are transitional. The

sediment varies in its texture from a clean sand in shallower depths to a sand containing 34.29% mud at a depth of 94 m at the East Flower Garden Bank. At the West Flower Garden, the Amphistegina Sand is 2.24% mud at 75 m and 18.9% mud at 90 m. Amphistegina tests form up to 32% of the sediment in this facies at both banks. Other major contributors include: 1) coralline algae, 17 to 40%; 2) molluscs, 13 to 20%; and 3) lithoclasts, 6 to 16%. The lithoclasts are the result of bioerosion of drowned reefs within this facies.

Quartz-Planktonic Foraminifers Facies

This is the deepest facies in the area (> 90 m depth) and represents the most common sediment on the northwestern Gulf of Mexico Outer Continental Shelf. However, owing to its proximity to the banks, elements derived from the bioerosion of drowned reefs are also present. The facies consists of: 1) quartz grains, 3.5 to 67%; and 2) planktonic foraminifers 9 to 77%. Samples with low percentages of quartz grains have high percentages of planktonic foraminifers and vice versa. Added together, these components range from 53 to 83%. The silt-plus-clay fraction varies from 24 to 100%, with an average of 82%. The facies completely encircles the West Flower Garden Bank but only occurs on the north, east and south sides of the East Flower Garden Bank. On the southeast margin of the East Flower Garden, where the steepest slopes occur, this facies is in direct contact with the Gypsina-Lithothamnium Facies.

Molluscan Hash Facies

This facies occurs on the western and southwestern margins of the East Flower Garden Bank. Edwards (1971) did not recognize the facies on the West Flower Garden Bank owing to the lack of samples far enough to the south and southwest of the bank. The facies is composed of from 15 to 54% sand size mollusc fragments and from 0 to 34.5% quartz grains. The silt-plus-clay fraction ranges from 5 to 26%, with an average of 22%. It is easily distinguished from the Quartz-Planktonic Foraminifers Facies by its low content of planktonic foraminifers (0.5 to 13.3%) and its low mud content. Also, the percentage of molluscs in the Quartz-Planktonic Foraminifers Facies is much lower, ranging from 1.0 to 14.6%.

Patch Reefs

Both living and dead (drowned) patch reefs occur scattered over the seafloor below a depth of 50 m (Figures 4.16 and 4.17). Direct observations of drowned reefs have been made in depths slightly greater than 150 m. Living coralline algae cover substantial areas on these patch reefs down to depths of 85 to 90 m. Studies of the diagenesis of carbonates from patch reefs and algal crusts show a recrystallization of spherulitic aragonite cement to blocky, low-magnesian calcite cement. This recrystallization is not accompanied by a depletion of strontium in the calcite lattice (Stafford, 1982). We originally thought that the patch reefs at the 128 m depth were exposed during the low stand of sea level between 14,000 and 18,000 years B.P. (Figure 1.8, Chapter 1) because of the presence of blocky calcite cement in samples from those depths (Rezak, 1977). Absence of calcite cement in the shallower reefs indicated that those reefs formed during the subsequent rise in sea level. Figure 4.20 illustrates the probable configuration of the West Flower Garden Bank during the 121 to 134 m sea level stillstand (Edwards, 1971).

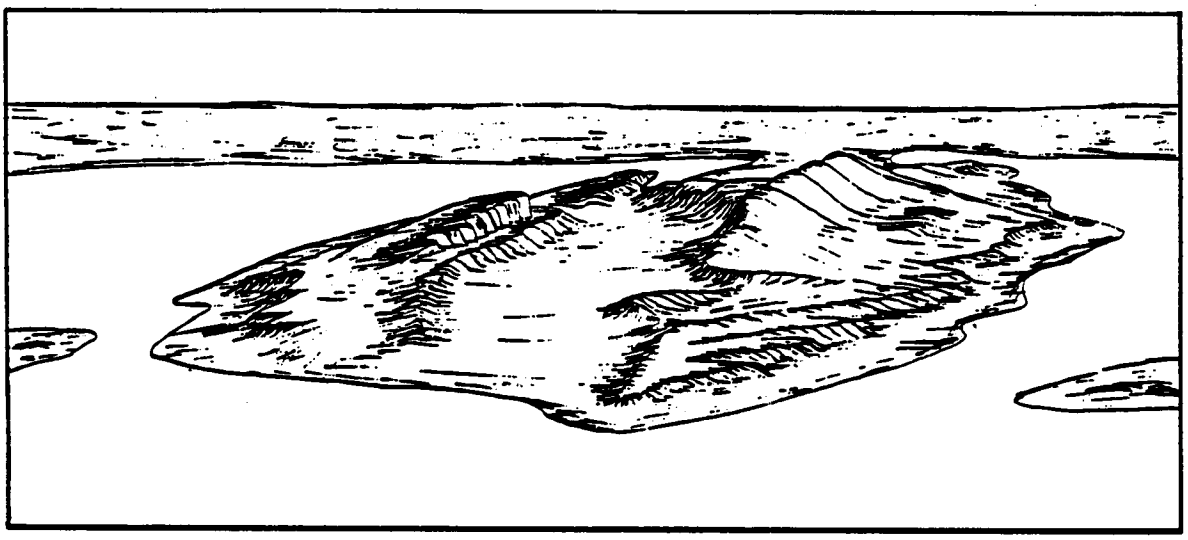

Figure 4.20 Sketch of the West Flower Garden Bank as it may have looked during the 121 to 134 m stillstand of the Gulf of Mexico (Edwards, 1971).

SUMMARY

The East and West Flower Garden Banks (Figures 4.1 to 4.3) are bathymetric prominences caused by salt diapirs. Bedrock outcrops on the seafloor at the crests of these prominences, caused by fracturing of the rocks overlying the salt diapir (Figure 4.10) served as substrates for the initial growth of reef-building organisms.. Because the conditions of water depth, temperature, salinity, and water clarity were favorable, a complex of reef communities developed (Figure 4.15) and drastically changed the nature of the bottom sediments in the area of the banks.

The normal sediments on the open shelf surrounding the banks are sands and muds that have been eroded from the North American continent and mechanically transported to the Gulf of Mexico by streams such as the Mississippi, Trinity, Sabine, and Brazos Rivers. The banks rise from surrounding shelf depths of from 100 to 180 m to crests as shallow as 20 m. The normal shelf sands and muds do not occur at depths shallower than 75 to 80 m. The sediments above the 75 m level are all coarse, skeletal sands and gravels and rocky, limestone structures built by corals and other lime-secreting, reef-dwelling organisms. The loose sediments around the reef reflect the depth zonation of the biological communities that are present on the two banks. However, the distribution of sediment types does not coincide with the boundaries between biotic communities due mainly to the downslope movement of sediment by the force of gravity.

The downslope movement of sediment produced on the banks, together with the absence of land-derived muds in the bottom sediments above a depth of 75 m and the major biological boundary at approximately 80 m, substantiate the conclusion from water and sediment dynamics that the currents flow around the banks rather than up and over them. The nepheloid layer rarely rises to depths of 75 m.

The presence of a series of brine seeps and a brine lake has been documented, indicating the removal by dissolution of prodigious amounts of solid salt from the crest of the salt diapir. The removal of large volumes of solid salt from the shallow sub-bottom beneath the crests of the reefs creates hazardous seafloor instability in those areas.

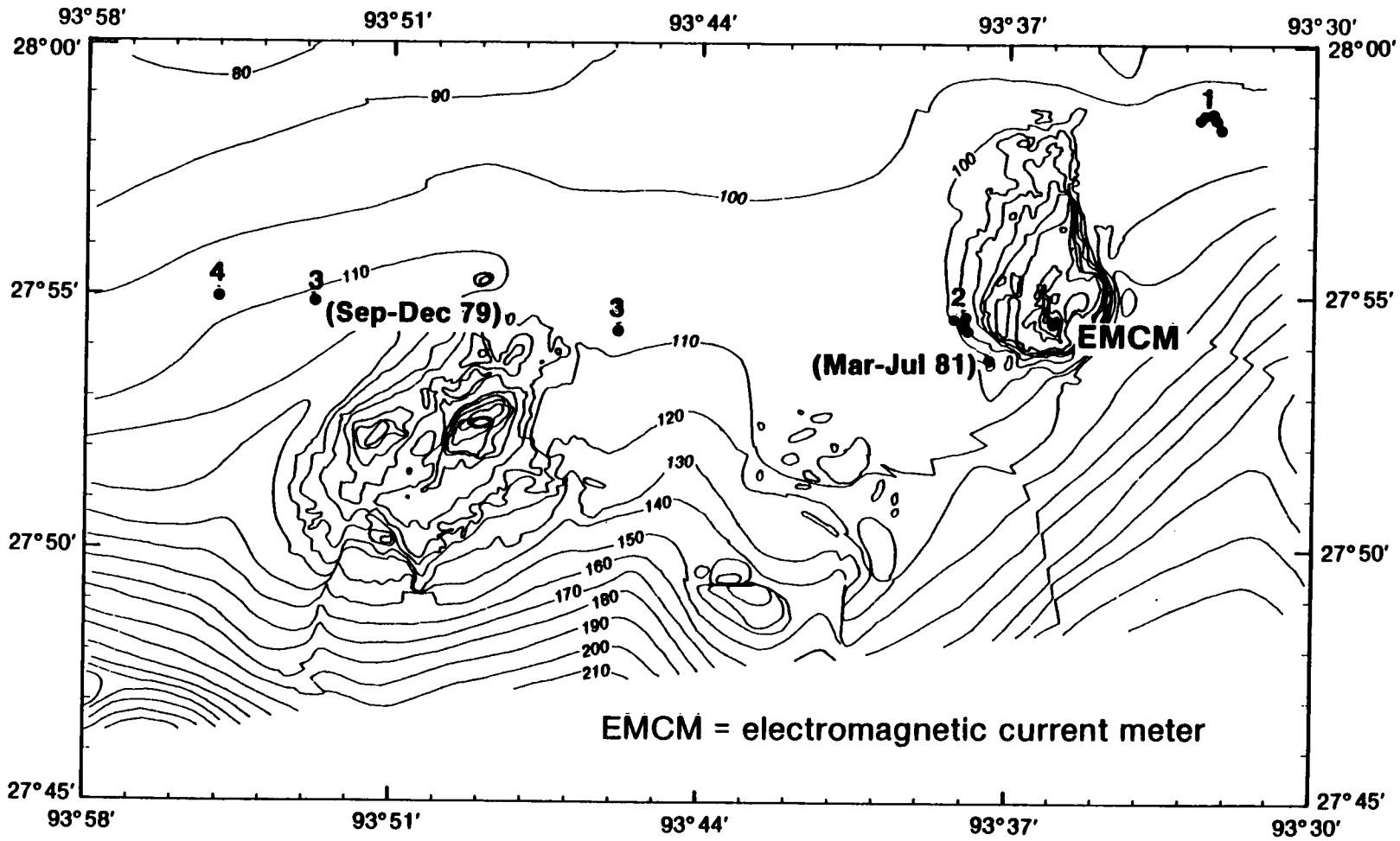

Figure 5.1 Mooring positions for all six current meter array deployments from January 1979 to July 1981. The two cases where a mooring position was significantly changed are indicated by the deployment dates in parentheses.

CHAPTER 5

FLOW, BOUNDARY LAYERS, AND SUSPENDED SEDIMENT AT THE FLOWER GARDEN BANKS

There are two reasons for using the East and West Flower Garden Banks as model systems with which to compare the other banks of the northwestern Gulf of Mexico. First, these two banks have the most complete sequence of depth zonations of biotic communities and sedimentary facies known to exist on the Texas-Louisiana shelf. Second, they are the most intensively studied of the banks. They were the site of a multifaceted monitoring program from January 1979 through July 1981.

It is the living coral reefs at the crests of the East and West Flower Garden Banks which set them apart from otherwise similar banks in the region. By determining why these banks possess the reef and why they are zoned as they are, one is well on the way to understanding the conditions governing the zonation on all of the banks in the northwestern Gulf of Mexico. The biotic zones, sedimentary facies, and depth relationship between the two at the Flower Garden Banks are shown above in Table 4.1.

In this chapter, the East and West Flower Garden Banks will be placed in their physical context. That is, the two banks will be discussed in terms of the temperature, salinity, flow, and suspended sediment of the waters that bathe them and the relationship of those variables to the banks' zonation.

GENERAL SETTING

The Flower Garden Banks lie between 93°30'W and 94°W just south of 28°N. The banks rise above a mud substrate at the shelf edge at the widest point of the continental shelf in the northwestern Gulf of Mexico (Figure 1.5 above). They lie in the eastward flowing shelf-slope current (See Chapter 2) and rise in water that does not mix all the way to the bottom in the winter. It should be remembered that these are high relief banks which extend 80 to 100 m above the surrounding seafloor.

The fact that the banks are at the outermost edge of the widest point on the Gulf of Mexico continental shelf has two important implications. The first is that the volume of water on the shelf decreases both east and west of the longitude of the banks. Therefore, continuity demands that alongshelf flow in either direction must either diverge and slow in the vicinity of the banks, or additional water must be drawn in from offshore to accommodate this increase in volume. The distribution of surface isotherms in Figures 2.22 and 2.27 (above) implies that additional water was

drawn in from offshore in February and April of 1982. In both instances, warmer offshore waters appear to have been drawn up into the arch of the coastline. The second implication of the location of the Flower Garden Banks is that they are at a maximum distance from the turbid surface water of the coast. They should, therefore, receive maximum solar irradiance for shelf-edge banks in the northwestern Gulf of Mexico.

The high relief of the banks, combined with the fact that even in deep winter the waters do not mix to the bottom, precludes the possibility of resuspended sediment from the adjacent seafloor rising to the top of the banks.

METHODS

In January 1979, time series measurements of currents and temperature were established at moorings to the northeast of the East Flower Garden Bank (mooring 1), at the crest of the reef (EMCM), and at the southwest margin of the bank (mooring 2) (see Figure 5.1 for locations). In September 1979 a third mooring was added just northwest of the West Flower Garden Bank (Figure 5.1). Later, in April 1980, the third mooring was moved to the northeast of the West Flower Garden Bank and a fourth mooring was established to the northwest of the bank (Figure 5.1). Statistics regarding the position of moorings, depth of the instruments, sampling intervals, and duration of the recordings appear in Table 5.1.

In addition to the time series measurements, two other types of data were collected. Profiles of temperature, salinity, transmissivity, and horizontal current velocities were obtained on seasonal cruises. At first, this was accomplished by separate lowerings of a salinity, temperature and depth (STD) sensor, a transmissometer, and a profiling current meter. In 1980 we developed an instrument which contained a conductivity, temperature, depth (CTD) probe, 25 cm pathlength transmissometer (XMS), and electromagnetic profiling current meter in a single instrument package. Data from the instrument package is fed up a 7 conductor armored cable to a Z-80 based microcomputer deck unit which is also interfaced with a Loran C receiver for continuous acquisition of position data. The system was named the Profiling Hardwired Instrumented System for Hydrography, or PHISH. On all cruises after October 1980, the PHISH was used for acquisition of station data. Seasonal sampling cruises were made in April, July, and October of 1979, October 1980, March 1981, and July 1981. Additional stations were taken near the West Flower Garden Bank in March 1982.

The third type of data are dye emission observations made in the bottom boundary layer on and adjacent to the Flower Garden Banks. These observations were carried out *in situ* from the DR/V DIAPHUS, a two-man submersible. The design of the dye emitters used

Table 5.1 Current Meter and Associated Time Series Data Inventory, East and West Flower Garden Banks, All Deployments From January 1979 to July 1981. Mooring locations are shown in Figure 5.1

INSTRUMENT DISK FILE CODE	MONTH AND YEAR OF RECOVERY	LOCATION	DEPTH (m) METER/BOTTOM	DATE AND TIME (GMT) BEGINNING		END	
		Savonius Rotor Current Meter					
Mor1Met1	Apr 79	27°58.63'N, 93°32.42'W	56/96	1/16/79	10:34	3/26/79	23:52
Mor2Met1	Apr 79	27°54.65'N, 93°38.02'W	60/100	1/17/79	21:16	4/10/79	19:22
Mor2Met3	Apr 79	27°54.65'N, 93°38.02'W	96/100	1/17/79	21:52	3/25/79	22:46
Mor1Met1	Sep 79	27°58.38'N, 93°32.19'W	60/100	7/12/79	18:05	9/4/79	19:11
Mor1Met2	Sep 79	27°58.38'N, 93°32.19'W	94/100	7/12/79	18:21	9/5/79	11:15
Mor1Met3	Sep 79	27°58.38'N, 93°32.19'W	96/100	7/12/79	18:38	9/1/79	21:26
Mor2Met1	Sep 79	27°54.57'N, 93°38.23'W	60/100	7/11/79	22:05	9/3/79	14:41
Mor2Met2	Sep 79	27°54.57'N, 93°38.23'W	94/100	7/12/79	02:09	9/4/79	12:21
Mor2Met3	Sep 79	27°54.57'N, 93°38.23'W	96/100	7/11/79	21:41	9/4/79	07:47
Mor1Met1	Dec 79	27°58.55'N, 93°32.32'W	53/99	9/9/79	15:01	12/10/79	04:19
Mor1Met2	Dec 79	27°58.55'N, 93°32.32'W	95/99	9/9/79	15:10	11/25/79	07:10
Mor2Met1	Dec 79	27°54.60'N, 93°38.23'W	53/99	9/11/79	16:19	11/28/79	14:19
Mor2Met2	Dec 79	27°54.60'N, 93°38.23'W	95/99	9/11/79	16:20	12/13/79	05:44
Mor3Met1	Dec 79	27°54.93'N, 93°52.79'W	61/107	9/11/79	18:15	12/9/79	22:39
Mor1Met1	Sep 80	27°58.56'N, 93°32.61'W	53/99	4/22/80	23:20	8/12/80	20:20
Mor1Met2	Sep 80	27°58.56'N, 93°32.61'W	95/99	4/23/80	18:00	9/7/80	04:20
Mor2Met1	Sep 80	27°54.43'N, 93°38.00'W	49/95	4/23/80	20:00	10/5/80	17:20
Mor2Met2	Sep 80	27°54.43'N, 93°38.00'W	90/95	4/23/80	20:00	8/20/80	07:40
Mor3Met1	Sep 80	27°54.35'N, 93°45.90'W	58/104	4/23/80	16:00	9/7/80	04:20
Mor3Met2	Sep 80	27°54.35'N, 93°45.90'W	100/104	4/23/80	16:00	8/20/80	06:00
Mor1Met1	Jan 81	27°58.63'N, 93°32.52'W	54/96	10/13/80	19:40	1/19/81	21:20
Mor1Met2	Jan 81	27°58.63'N, 93°32.52'W	80/96	10/13/80	17:40	1/23/81	18:00
Mor2Met1	Feb 81	27°54.39'N, 93°37.95'W	32/99	10/25/80	09:35	2/11/81	15:15
Mor2Met2	Feb 81	27°54.39'N, 93°37.95'W	57/99	10/25/80	08:15	2/9/81	16:35
Mor2Met3	Feb 81	27°54.39'N, 93°37.95'W	83/99	10/25/80	09:15	2/10/81	03:55
Mor2Met4	Feb 81	27°54.39'N, 93°37.95'W	95/99	10/25/80	09:55	2/10/81	11:35
Mor3Met1	Feb 81	27°54.34'N, 93°45.89'W	52/101	10/20/80	17:50	2/9/81	17:11
Mor3Met2	Feb 81	27°54.34'N, 93°45.89'W	63/101	10/20/80	21:10	2/11/81	20:10
Mor3Met3	Feb 81	27°54.34'N, 93°45.89'W	90/101	10/20/80	21:10	2/10/81	06:50
Mor3Met4	Feb 81	27°54.34'N, 93°45.89'W	97/101	10/20/80	21:30	12/5/80	05:50
Mor1Met1	Jul 81	27°58.58'N, 93°32.53'W	47/97	3/6/81	00:40	7/16/81	00:00
Mor1Met2	Jul 81	27°58.58'N, 93°32.53'W	58/97	3/6/81	00:00	7/11/81	10:00
Mor1Met3	Jul 81	27°58.58'N, 93°32.53'W	85/97	3/6/81	00:20	7/16/81	00:00
Mor1Met4	Jul 81	27°58.58'N, 93°32.53'W	91/97	3/6/81	00:20	7/16/81	00:00
Mor2Met1	Jul 81	27°53.79'N, 93°37.47'W	50/103	3/5/81	22:20	6/3/81	21:40
Mor2Met2	Jul 81	27°53.79'N, 93°37.47'W	72/103	3/5/81	22:20	7/15/81	16:00
Mor2Met3	Jul 81	27°53.79'N, 93°37.47'W	85/103	3/5/81	22:20	7/15/81	16:40
Mor2Met4	Jul 81	27°53.79'N, 93°37.47'W	97/103	3/5/81	22:20	4/14/81	03:20
Mor3Met1	Jul 81	27°54.38'N, 93°45.90'W	53/103	3/5/81	17:40	7/16/81	05:40
Mor3Met2	Jul 81	27°54.38'N, 93°45.90'W	64/103	3/5/81	17:20	7/15/81	16:20
Mor3Met3	Jul 81	27°54.38'N, 93°45.90'W	91/103	3/5/81	17:20	7/15/81	15:00
Mor3Met4	Jul 81	27°54.38'N, 93°45.90'W	97/103	3/5/81	17:20	7/15/81	15:00
Mor4Met1	Jul 81	27°55.01'N, 93°55.01'W	47/97	3/5/81	22:20	7/15/81	15:00
Mor4Met2	Jul 81	27°55.01'N, 93°55.01'W	58/97	3/5/81	16:20	7/15/81	22:40
Mor4Met3	Jul 81	27°55.01'N, 93°55.01'W	85/97	3/5/81	16:20	7/15/81	13:40
Mor4Met4	Jul 81	27°55.01'N, 93°55.01'W	91/97	3/5/81	16:00	7/15/81	13:20
		Electromagnetic Current Meter					
		The first four deployments were made on top of the East Flower Garden Bank. The last three deployments were on mooring 2, near the southwest edge of the East Flower Garden Bank.					
EMCM.EMA	Apr 79	27°54.65'N, 93°35.92'W	28/30	2/10/79	18:00	4/16/79	05:30
EMCM.EMA	Jul 79	27°54.65'N, 93°35.92'W	28/30	4/29/79	18:00	7/07/79	05:20
EMCM.EMA	Sep 79	27°54.65'N, 93°35.92'W	28/30	7/14/79	23:30	8/29/79	14:20
EMCM.EMA	Dec 79	27°54.65'N, 93°35.92'W	28/30	9/25/79	00:00	10/16/79	13:50
MOR2.EMCM	Sep 80	27°54.43'N, 93°38.00'W	15/95	4/17/80	15:40	5/08/80	00:40
MOR2.EMCM	Feb 81	27°54.39'N, 93°37.95'W	20/99	10/24/80	22:25	1/11/81	19:54
MOR2.EMCM	Jul 81	27°53.79'N, 93°37.47'W	38/103	3/05/81	16:53	4/06/81	13:13
		Temperature Probe					
		Deployed on mooring line adjacent to the Marsh-McBirney electromagnetic current meter. The first three deployments were on top of the East Flower Garden Bank. The last deployment was on mooring 2, near the southwest edge of the East Flower Garden Bank.					
CONTMP.EMA	Apr 79	27°54.65'N, 93°35.92'W	27/30	2/10/79	16:44	4/24/79	09:10
CONTP.EMA.	Jul 79	27°54.65'N, 93°35.92'W	27/30	4/29/79	13:40	7/10/79	18:46
CONTMP.EMA	Sep 79	27°54.65'N, 93°35.92'W	27/30	7/16/79	14:10	8/30/79	25:22
CONTMP.EMA	Sep 80	27°54.43'N, 93°38.00'W	14/95	4/23/80	20:00	6/8/80	04:00

in the October 1980 experiments is shown in Figure 5.2. They consisted of: a plexiglass canister, open at the top with a small screen-covered orifice in the bottom; an electromagnet; a timing circuit; a rubber diaphragm; and a battery pack. The electromagnet consisted of a carriage bolt wound with a thin copper wire. This was screwed into the bottom of the plexiglass canister so that the head of the bolt was just below the top of the canister. A metal disk was attached to the middle of the rubber diaphragm so that it would be over the head of the carriage bolt when the diaphragm was stretched over the top of the canister. The leads from the electromagnet were attached to a timing circuit. The timing circuit could be set to pulse at intervals from 4 to 10 seconds. Powdered fluorescent dye was placed in the emitter so that when the emitter was placed in water a concentrated dye filled the canister. When the timing circuit pulsed, the electromagnet was powered, attracting the metal disk on the diaphragm. This caused the diaphragm to depress, expelling a puff of dye through the orifice in the bottom of the canister.

Four of these devices were placed on a length of aircraft wire as shown in Figure 5.3. Below each emitter a fiberglass rod was fitted on the wire in a manner which permitted it to rotate freely. The rod, a fishing rod blank, was marked every 5 cm with brightly colored reflecting tape and terminated with a vane. Before the array was deployed, the emitters were turned on and synchronized so that they all pulsed at the same time. A buoy was attached to the upper end of the aircraft wire for flotation and a weight of about 80 pounds to the bottom to serve as an anchor. An acoustic release was attached to the buoy at the top of the array and it, in turn, was attached to a bright yellow line 10 m longer than the water depth at the dive site. At the other end of the bright yellow line was yet another buoy.

At the beginning of an experiment, the whole array was put over the side of the tending vessel; then the submersible was launched. It maneuvered over to the surface float and followed the yellow line down to the dye emitters. The acoustic release was then triggered so that the emitter array was separated from any surface motion that might have been carried by the yellow line. Once on the bottom, the submersible moved so that it was perpendicular to the flow and in front of the emitter array. The dye emission was then recorded on super 8 mm color film and color video tape cassettes. While these observations were taking place, PHISH profiles were taken from the surface ship.

The recorded data were used to calculate velocity profiles, Reynolds stresses, and diffusivity. It was also used, qualitatively, to examine various flow phenomena in the bottom boundary layer (BBL).

DYE EMITTER

Interior View

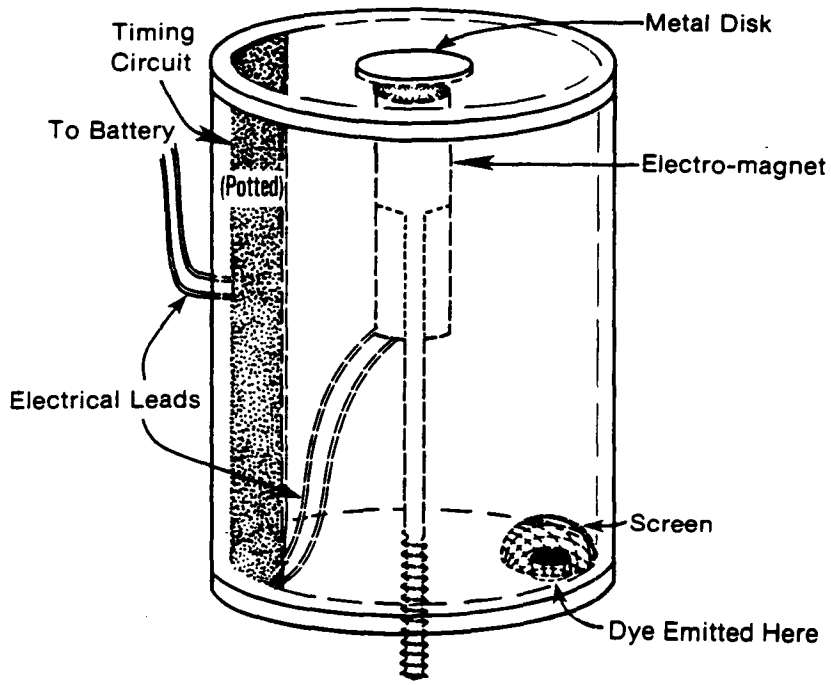

Top View

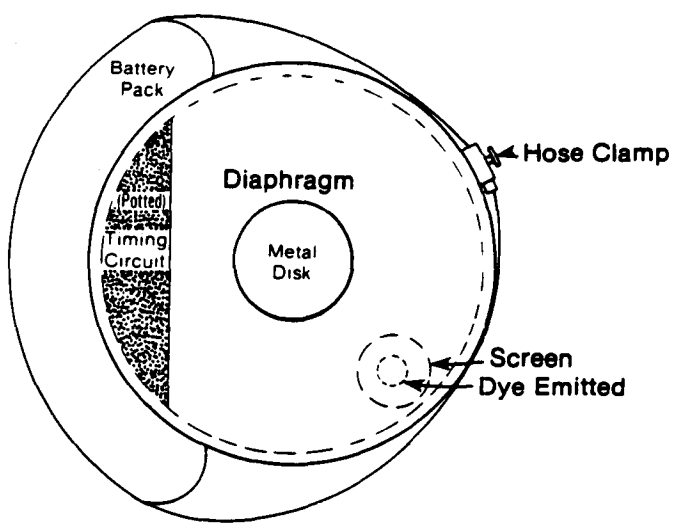

Figure 5.2 Diagrammatic representation of dye emitter apparatus used in October 1980 boundary layer experiments at the Flower Garden Banks.

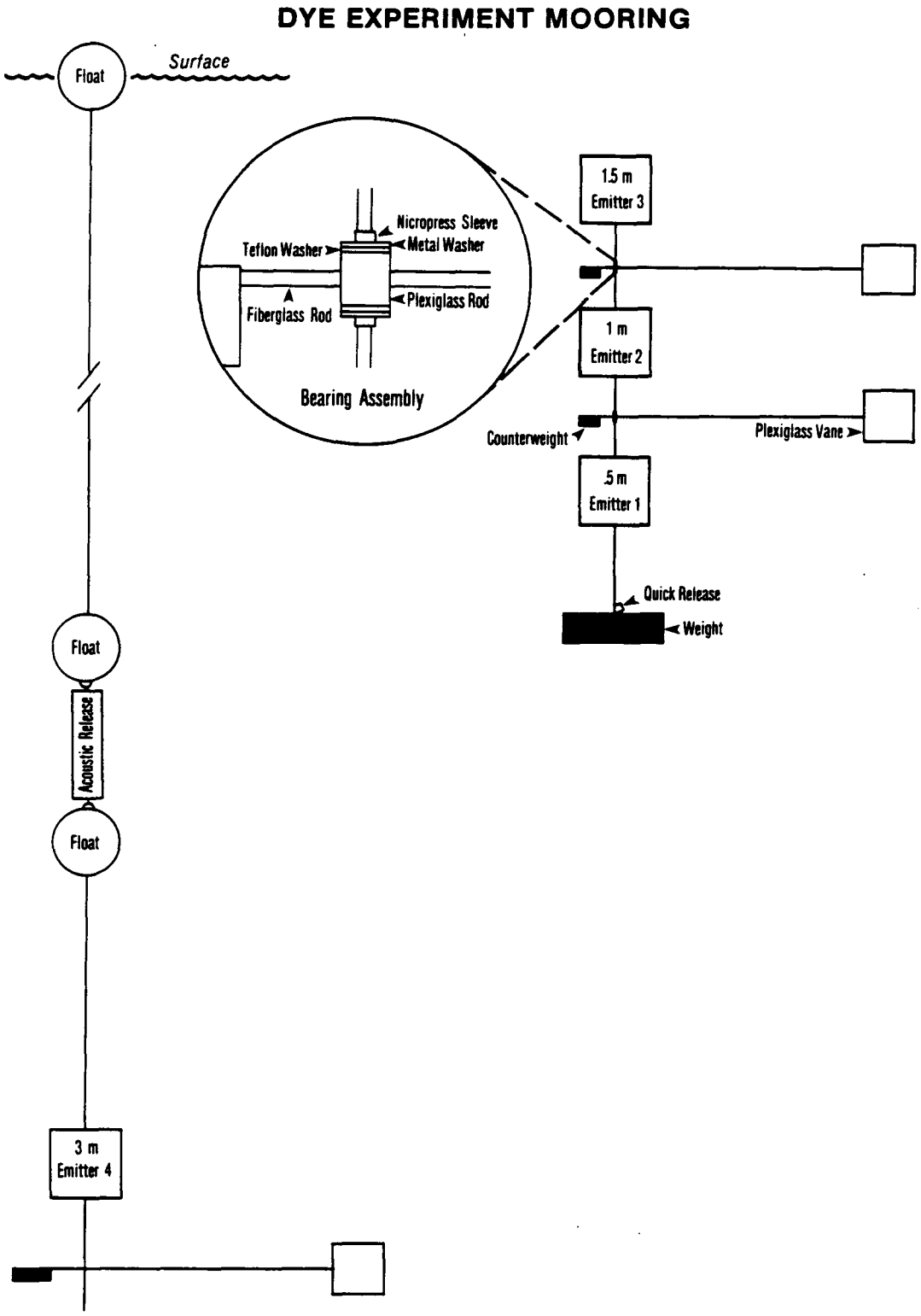

Figure 5.3 Diagrammatic representation of tautline mooring on which vanes and dye emitters were assembled for 1979 and 1980 boundary layer experiments at the Flower Garden Banks.

TEMPERATURE AND SALINITY

The annual cycles of temperature and salinity (T-S) at the Flower Garden Banks are best illustrated by reexamining the mean annual cycle of density (Figure 5.4) and comparing it to composite T-S profiles for early fall, late winter, and midsummer (Figure 5.5). The location of the stations used in the composites is shown in Figures 5.6 to 5.9.

In the winter, repeated cold air outbreaks cool the surface waters and mix them down to approximately 70 m by January. Minimum temperatures in this layer, as recorded by an instrument on the reef at the East Flower Garden (27 m depth), are on the order of 19.5°C. The thickness of the mixed layer decreases through the spring as the number and intensity of the polar cold air outbreaks decline. Rapid warming begins in April, so that by June there is a strong thermocline with a surface mixed layer of minimal thickness. As surface heating continues through the summer, the surface mixed layer thickens and temperature increases from about 28°C in June to about 30°C in August. In late September or early October the polar fronts again push their way out to the region of the Flower Garden Banks. Wind mixing and destabilization of the density structure by surface cooling cause the surface mixed layer to thicken and decrease in temperature once again.

Angelovic (1976) reports that the minimum vertical temperature gradient in the vicinity of the Flower Garden Banks occurs in late February. At that time the surface mixed layer is 30 to 50 m thick with temperatures in the range of 19 to 20°C. Temperatures at the bottom (125 m) at that time are 17 to 18°C. The progression of the temperature cycle at 27 m for the period from deep winter to spring is shown in Figure 5.10. From February through late March the mean temperature remains near 20°C with very modest variance. About 22 March the temperature rises above 20°C and begins to climb toward 20.5°C. At that same time there is an onset of rather large one-and two-day oscillations in the temperature. This is at the very time the base of the mixed layer rises above 30 m so that the top of the Flower Garden Banks is in the thermocline. The large excursions in temperature are the result of vertical oscillations of the thermocline isotherms past the fixed measurement point. Such excursions are caused by inertial currents, shelf waves, and tides.

The composite profiles from October 1980 (Figure 5.5 a,b) show a mean mixed layer depth of about 35 m. Those stations possessing significantly thicker mixed surface layers were all located just downstream of the East Flower Garden Bank, and the thickening appears to be an orographic effect. The temperature in the surface mixed layer is on the order of 27°C. Below the mixed layer there was a strong thermocline. The spread of the envelope around the profiles is also due to orographic effects, as will be shown.

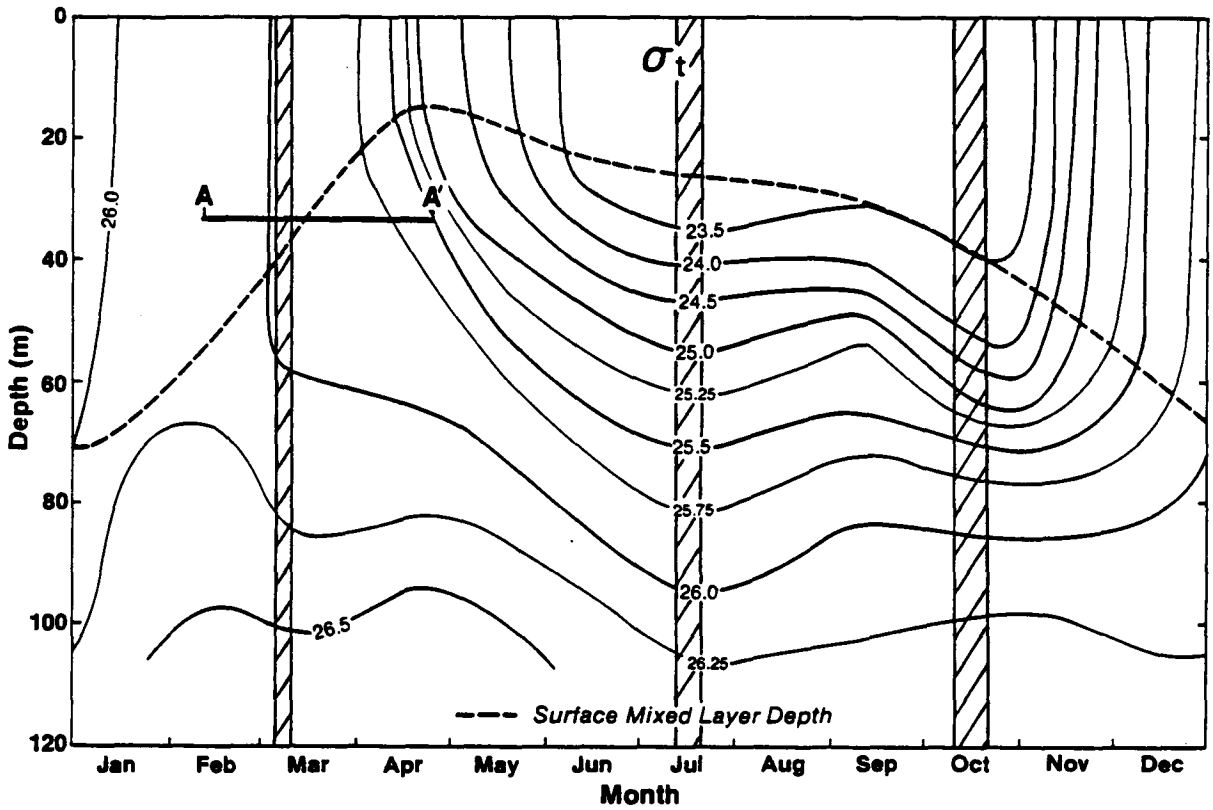

Figure 5.4 Seasonal progression of sigma-t versus depth near the Flower Garden Banks, as in Figure 2.26. A to A' represents period of the temperature recording shown in Figure 5.10. The crosshatched portions indicate periods of survey data shown in Figure 5.5.

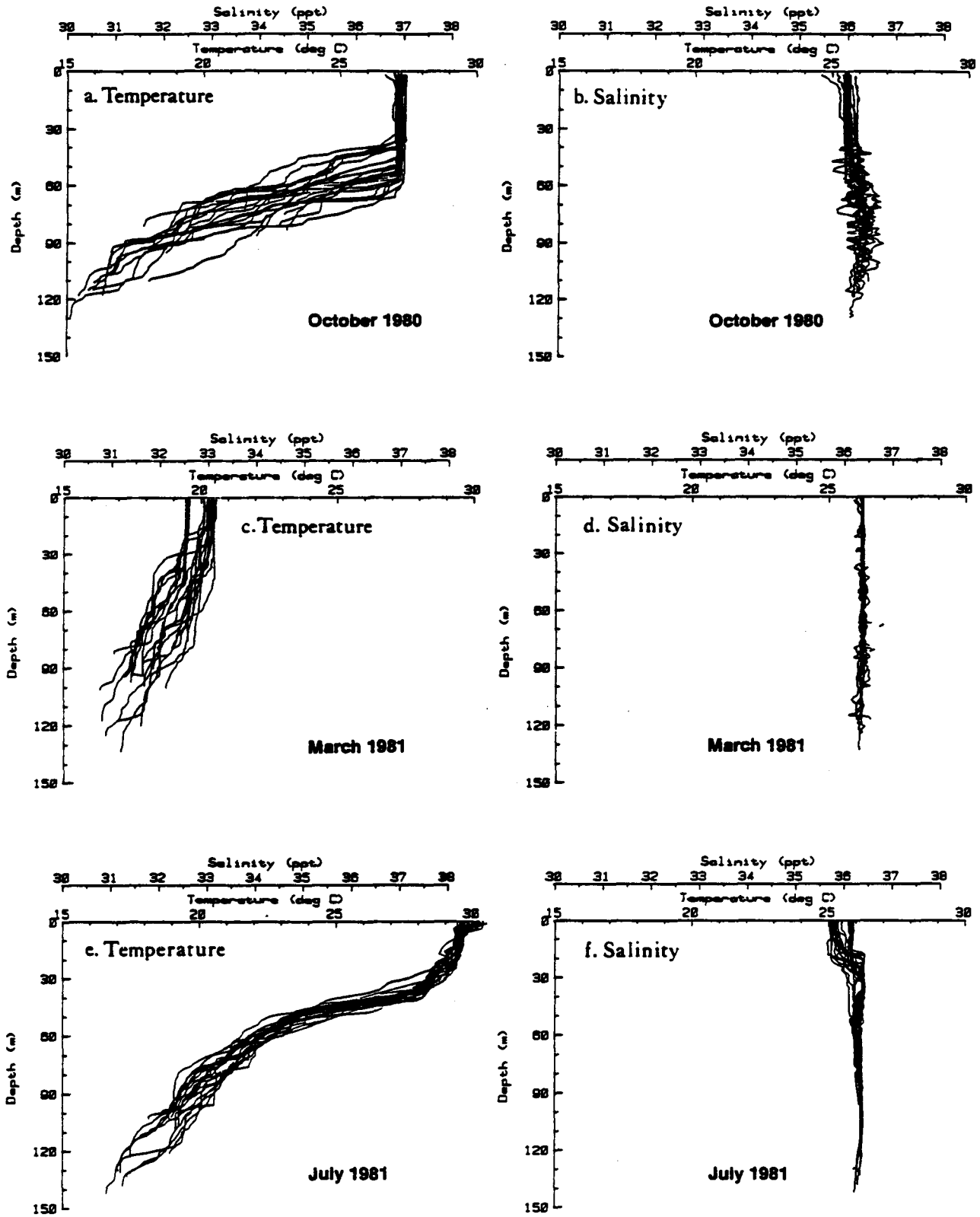

Figure 5.5 Composite plots of temperature and salinity profiles taken near the East and West Flower Garden Banks on three cruises.

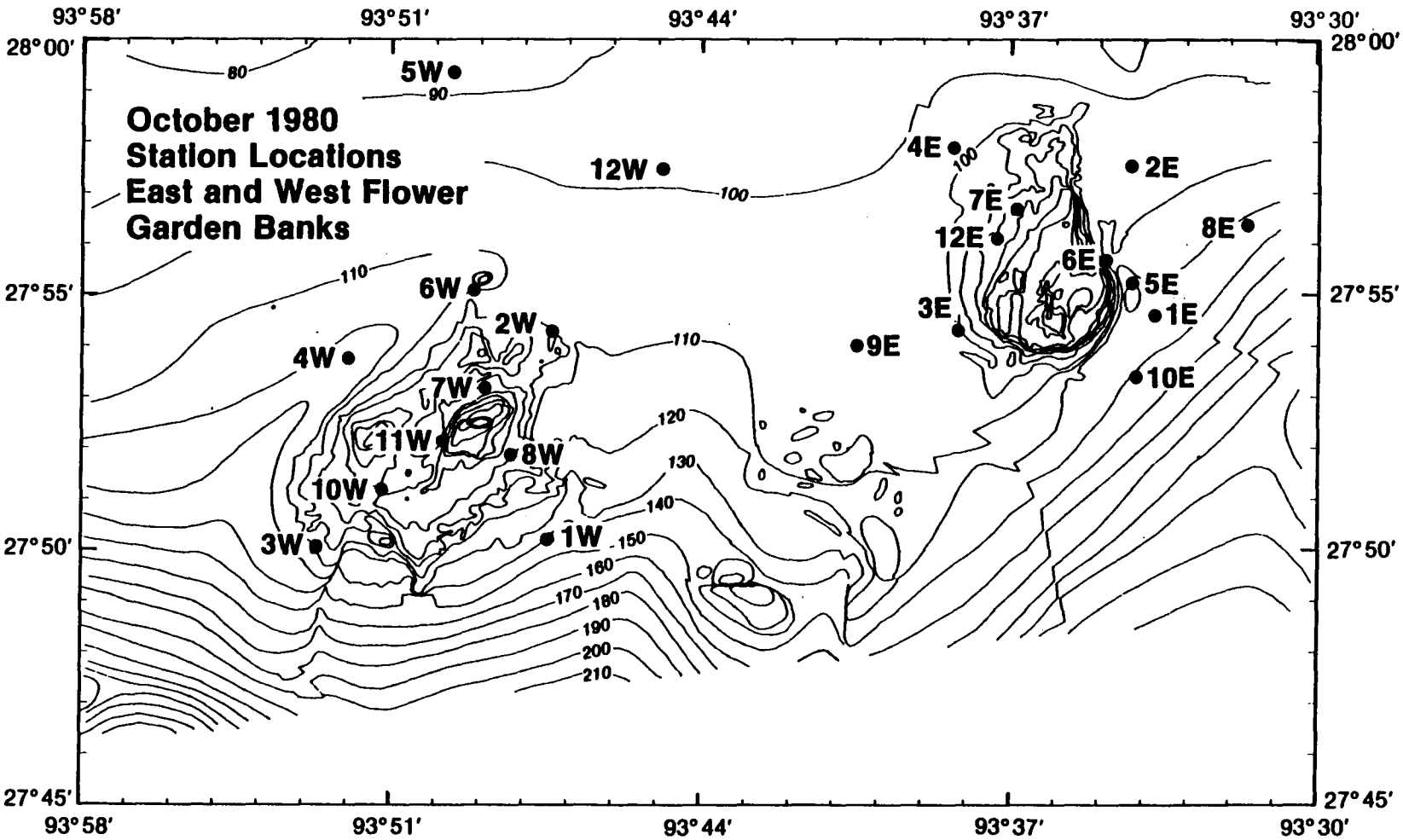

Figure 5.6 Hydrographic station location map for the BALTIC SEAL cruise, October 10-20, 1980.

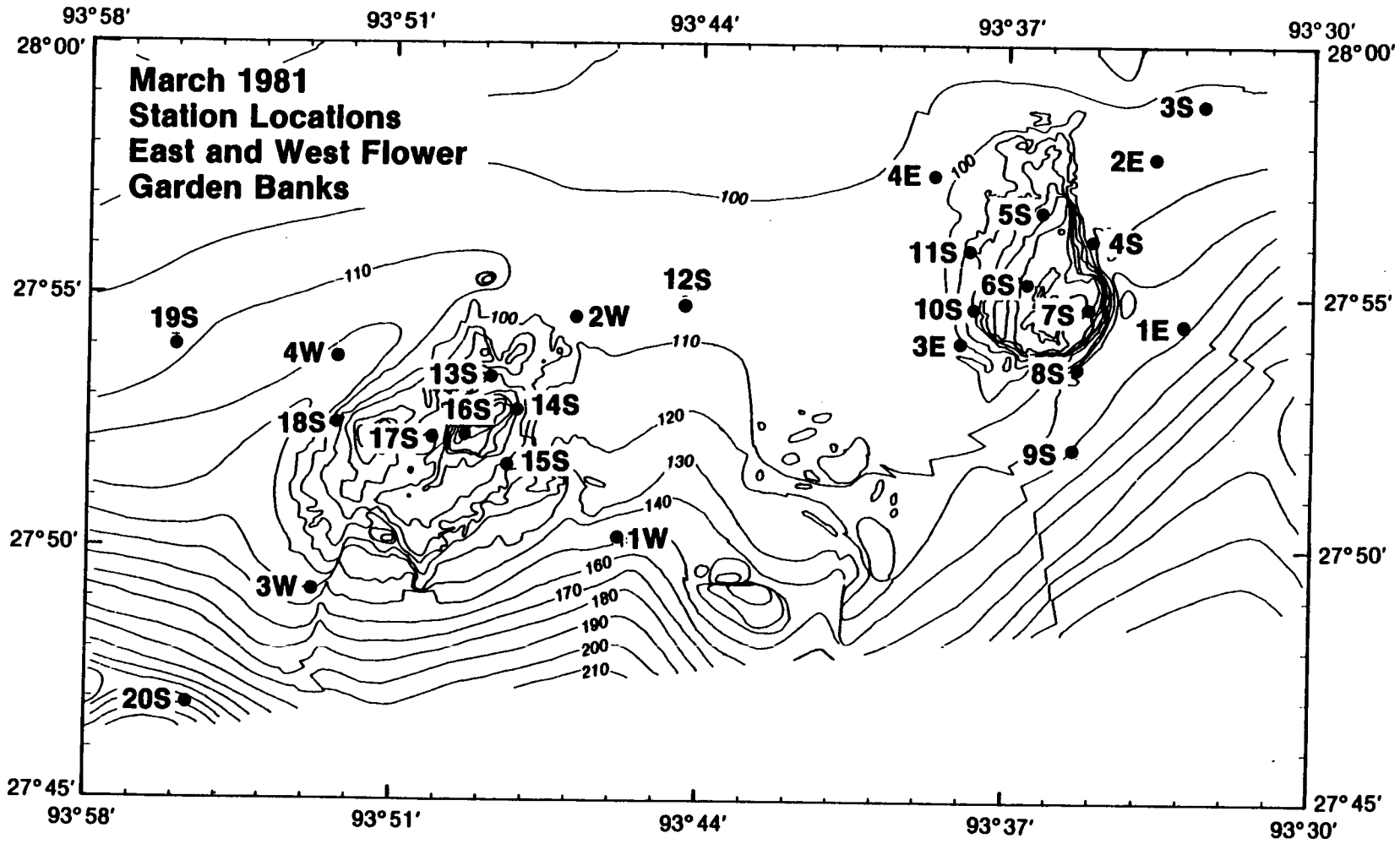

Figure 5.7 Hydrographic station location map for the GYRE cruise, March 3-8, 1981.

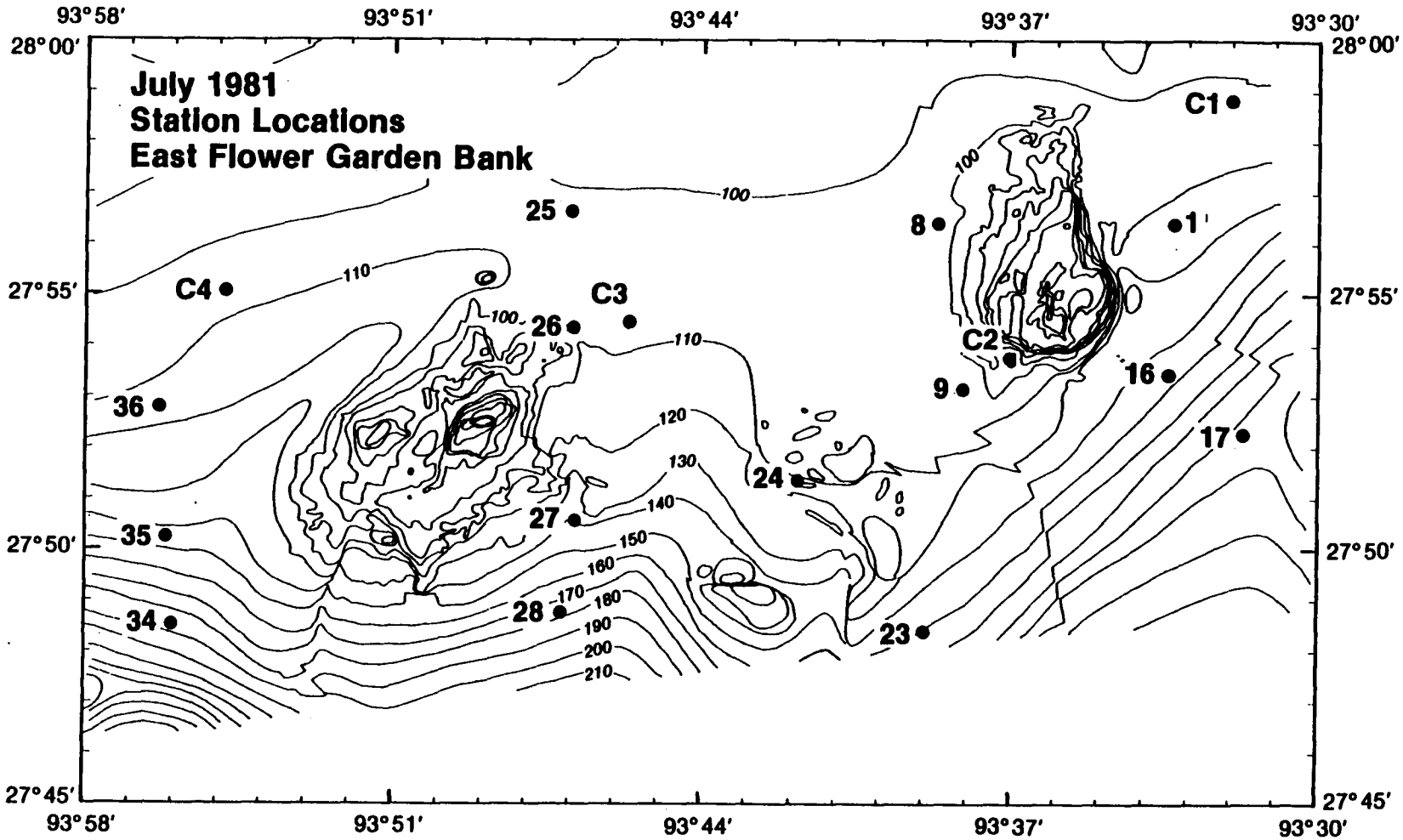

Figure 5.8 Hydrographic station location map for the NORTH SEAL cruise, July 13-17, 1981. (For complete East Flower Garden stations, see Figure 5.9).

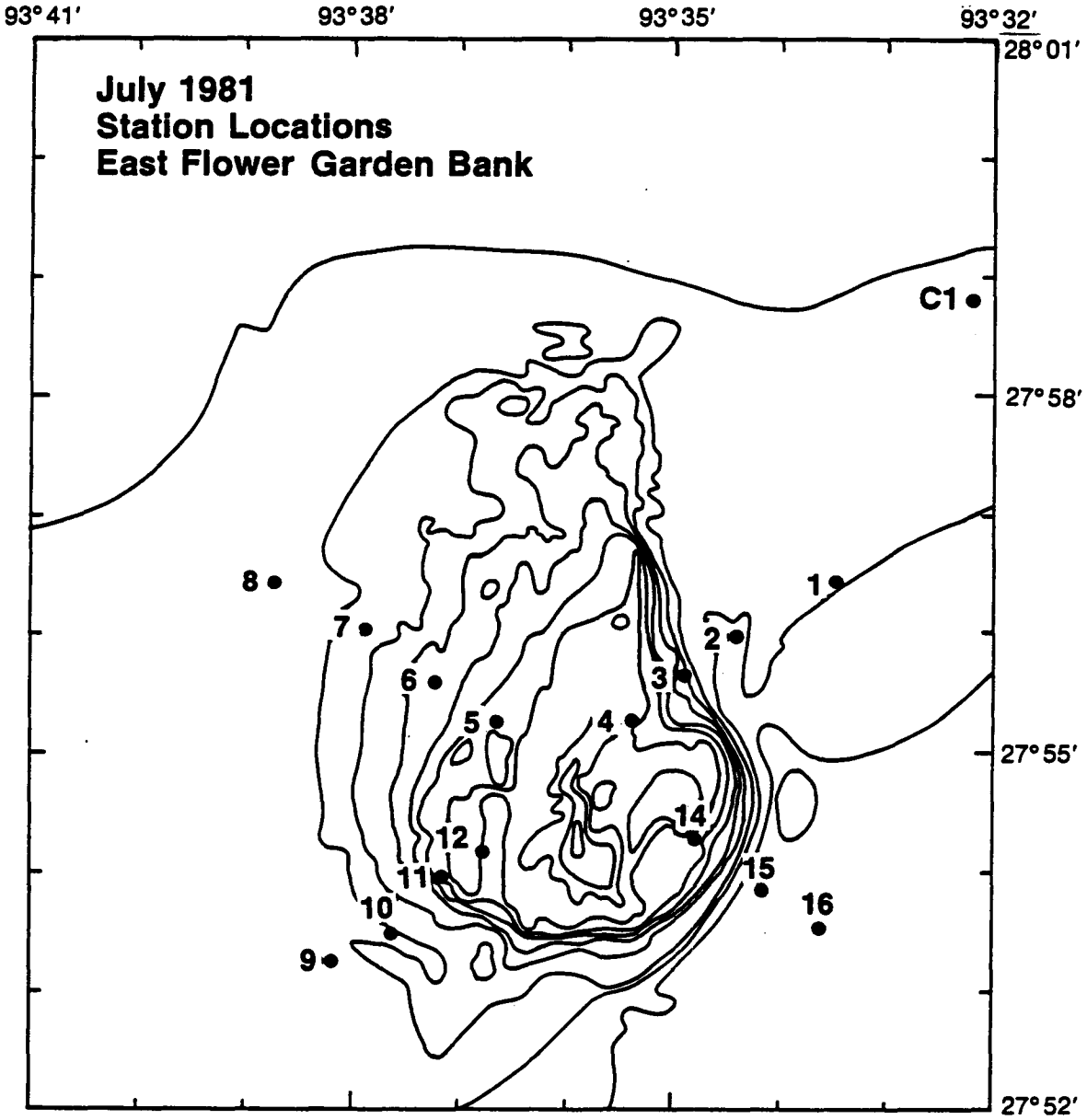

Figure 5.9 Hydrographic stations at the East Flower Garden Bank for the NORTH SEAL Cruise, July 13-17, 1981.

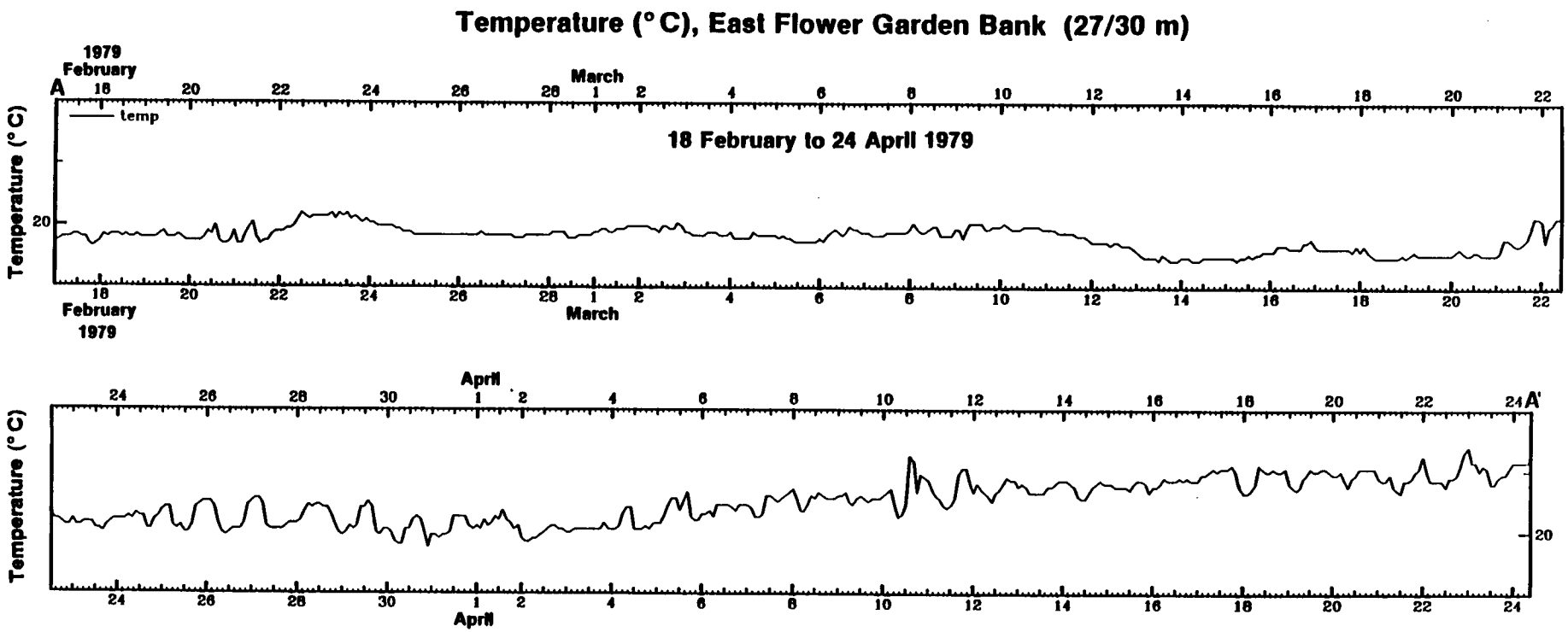

Figure 5.10 Temperature on the East Flower Garden reef at 27 m, representing the transition from deep winter conditions to those of spring. The base of the mixed layer apparently reached this level on 22 March. Thereafter the instrument was in the thermocline. Compare this with the mean annual conditions shown in Figure 5.4.

The March 1981 profiles illustrate the minimum thermal gradient reported by Angelovic (1976). The variations in salinity during both of these cruises were caused by a slight mismatch in the time response of the temperature and conductivity sensors. This was cured before the July 1981 cruise by attaching a pump to the conductivity sensor so that it did not lag the temperature sensor.

The July profiles reveal a warm (30°C), thin (13 m) surface mixed layer with a strong thermocline beneath it. At the time of the survey, water of 25°C or warmer extended to a depth of 50 m.

In October and March, profiles are essentially isohaline with salinities slightly over 36 ppt. The July profiles, however, display a slight depression of the salinity in the 13 m thick surface mixed layer to about 35.5 ppt. This is consistent with the annual pattern of surface salinities shown in Figure 2.17 (above). There are, however, major year-to-year variations in midsummer surface salinities at the shelf edge as shown by the profiles taken at the southwest margin of the East Flower Garden Bank in July 1979 (Figure 5.11). Notice that even though the surface salinity in that profile was near 31.5 ppt, salinity at 15 m was over 35.5 ppt. Or, to state it more emphatically, the water of relatively low salinity did not reach the level of the reef crest at the Flower Garden Banks.

Bottom temperatures at the shelf edge near the Flower Garden Banks undergo a peculiar double yearly cycle of minimums (17°C) and maximums (20°C). The minimums occur in spring (March-April) and midsummer (July-August), whereas the maximums occur in early summer (May-June) and mid-winter (November-January) (Angelovic, 1976).

FLOW FIELD AROUND THE BANKS

Monthly Mean Current Vectors

Vector means were computed, on a calendar month basis, for each current meter record available in the January 1979 to July 1981 interval. The monthly mean vectors were then segregated into three groups by depth. The first group (Figure 5.12a) represents instruments that were near the middle of the water column (32 to 64 m). The second group (Figure 5.12b) represents flow at levels between 11 m and 18 m above the bottom. The third group (Figure 5.12c) was derived from instruments deployed 8 m or less from the bottom. Bottom depths for all of the moorings ranged from 95 to 107 m. The monthly mean vectors are also shown as current roses in Figure 5.13. The time sense of the vectors is lost in this presentation, but the orientation of the vectors is more easily perceived.

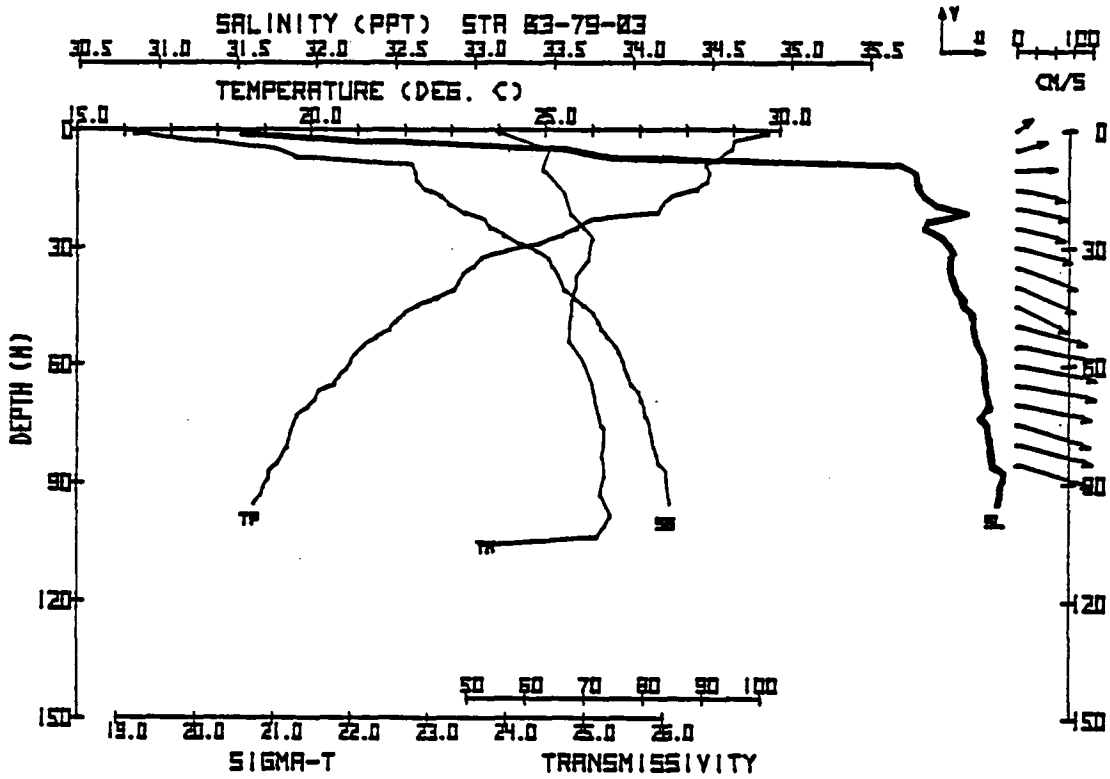

Figure 5.11 Plot of salinity (SL), temperature (TP), transmissivity (TR), and sigma-t (SG) from the East Flower Garden (July 1979). Note the surface salinity minimum near 31.5 ppt. Normal salinities (> 35.5 ppt) occur at depths of 15 m and greater.

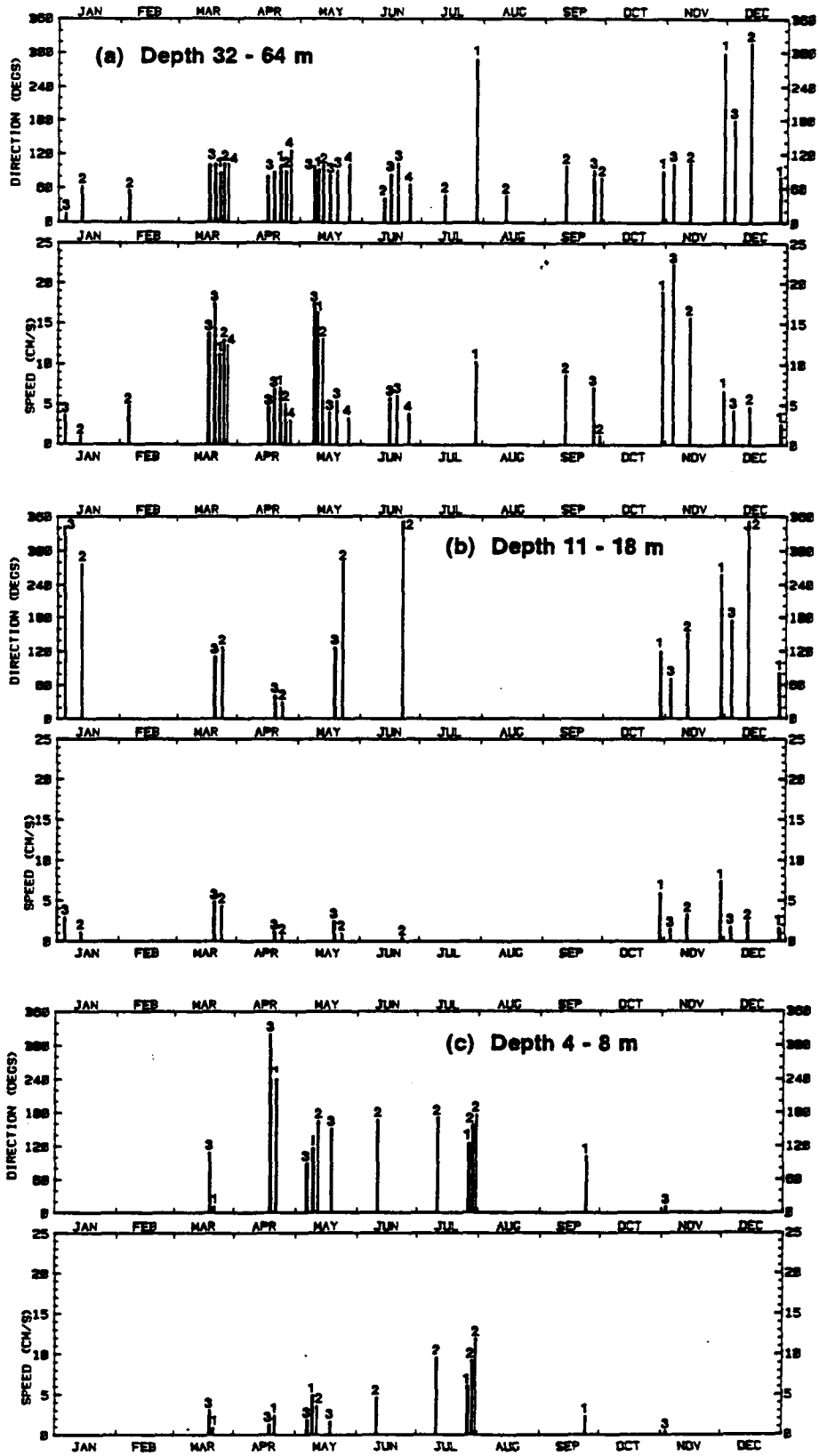

Figure 5.12 One-month averages of speed and direction for current meters in three depth ranges. The mooring number is printed above each average.

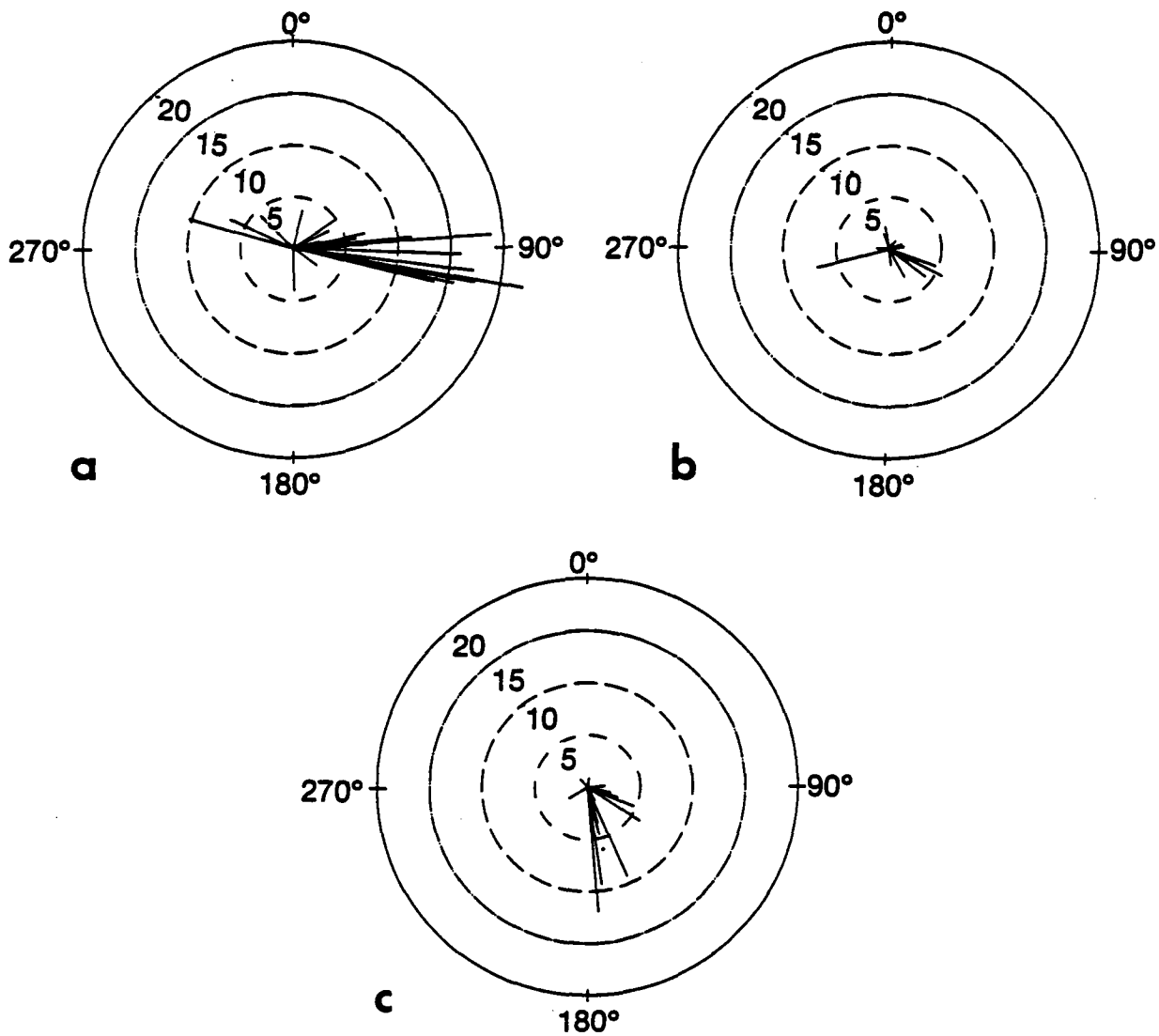

Figure 5.13 Monthly mean current vectors for all deployments and all moorings. Speed labels are in cm/s. Data set divided into three depth ranges: (a) 32 m to 64 m depth (all measurements but one were taken in the depth interval from 47 m to 64 m; (b) 11 m to 18 m from bottom; (c) 4 m to 8 m from bottom.

With the exception of two periods, the mean monthly flow at mid-depths was directed toward the east, often at speeds exceeding 15 cm/s (Figure 5.12a). More modest speeds (on the order of 5 cm/s) were recorded in late winter (December-January) and midsummer (June). The two periods wherein the monthly vector averages possessed a westerly component were July of 1979 and December of 1980.

During July 1979, a major tropical storm, Claudette, crossed over the Flower Garden Banks, then stalled over the coast. This storm produced sustained, high velocity southerly winds as far out as NDBO buoy 42002 (Figure 2.13, above) for a period of five days. Also, just prior to Claudette, a major hurricane, Bob, passed approximately 200 km to the southeast of the banks. Bob seems to have induced the reversals in the summer of 1979 and set up weak westerly flow along the shelf break; then Claudette produced very intense northwesterly flow from 24 July through the end of the month (Figure 5.14). During December 1980, mid-depth currents had an average velocity vector toward the northwest. The reason for this anomalous flow pattern appears to be the cumulative effect of a long series of cold fronts which show up in the wind field as strong winds with northerly components (Figure 5.14). The reversal of the mean flow for this period should not be pictured as a simple phenomenon. The progressive vector diagrams for the Flower Garden deployments from 25 October through 9 February are shown in Figure 5.15. The vectors for December are marked as weeks 5 through 9 on that figure.

With these two notable exceptions, flow at mid-depths in the vicinity of the Flower Garden Banks conforms to the model described in Chapter 2. That is, the flow at the shelf edge off the Texas-Louisiana segment is persistently to the east. The salinity of this water implies that it is of oceanic rather than coastal origin. From the midsummer profiles (Figures 5.5 and 5.11), it is apparent that coastal waters can become entrained at the surface.

Near-bottom currents (Figures 5.12 b,c and 5.13 b,c) tend to flow toward the east or southeast. In general, the stronger the flow was, the more southerly it tended to be. The overall average for records in the 11 to 18 m above the bottom group was toward the southeast. Speeds for this level clustered between 1 and 5 cm/s. The large magnitude vectors pointing toward the south-southeast in Figure 5.13 c are from mooring 2. As will be shown, these vectors are the result of strong topographic steering. If records for mooring 2 are removed for the very near bottom group, the overall average is toward the east-southeast at 1.6 cm/s. The monthly mean vectors are only rarely toward the north. It did happen in March and January at 11 to 18 m above bottom and March, April, and November in the very near bottom flow. It is interesting to note that moorings 1 and 3 do not indicate near-bottom flow in the same directions at these times.

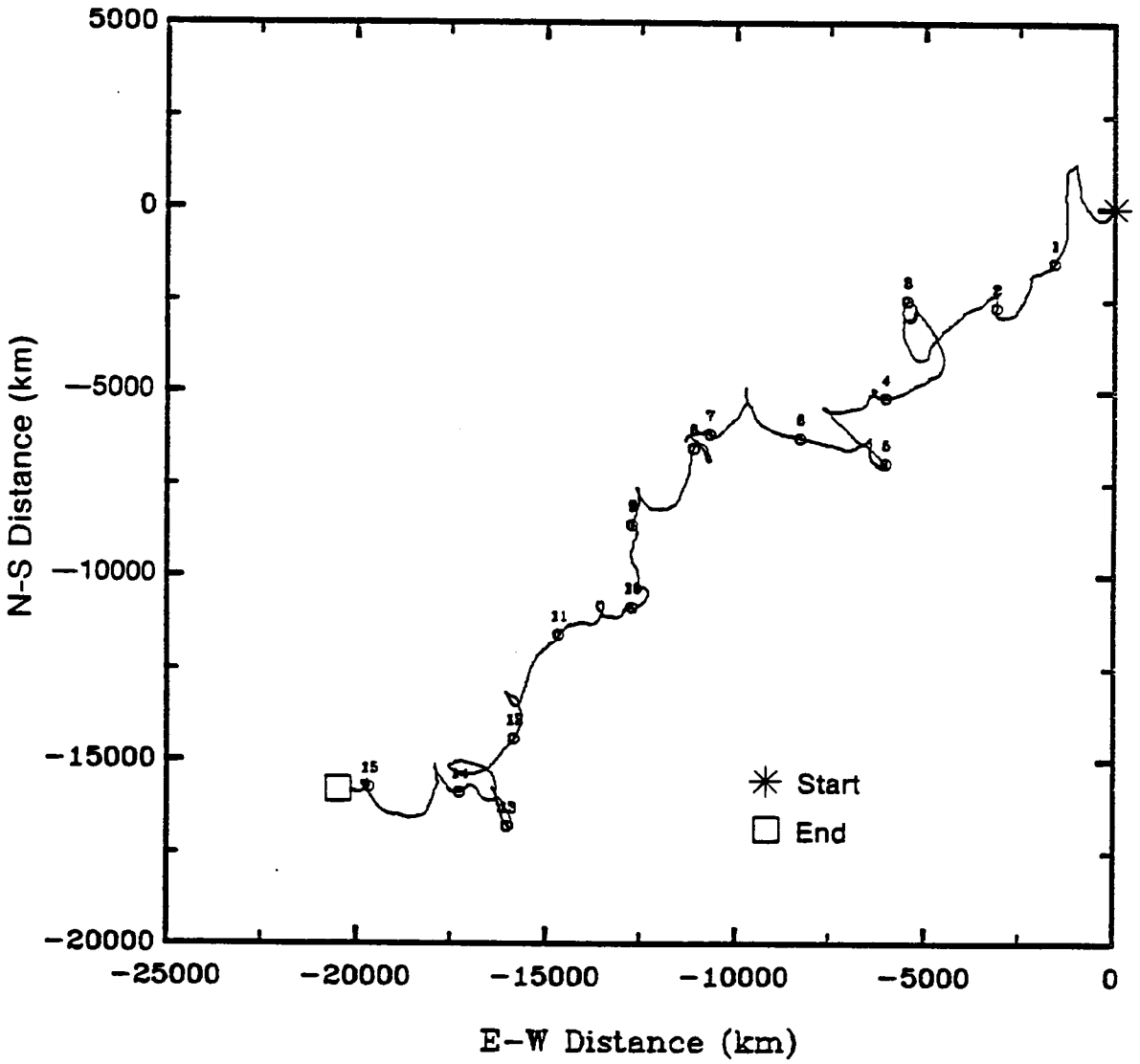

Figure 5.14 Progressive vector diagram, winds at NDBO Buoy 42002, 25 Oct 80 - 9 Feb 81.

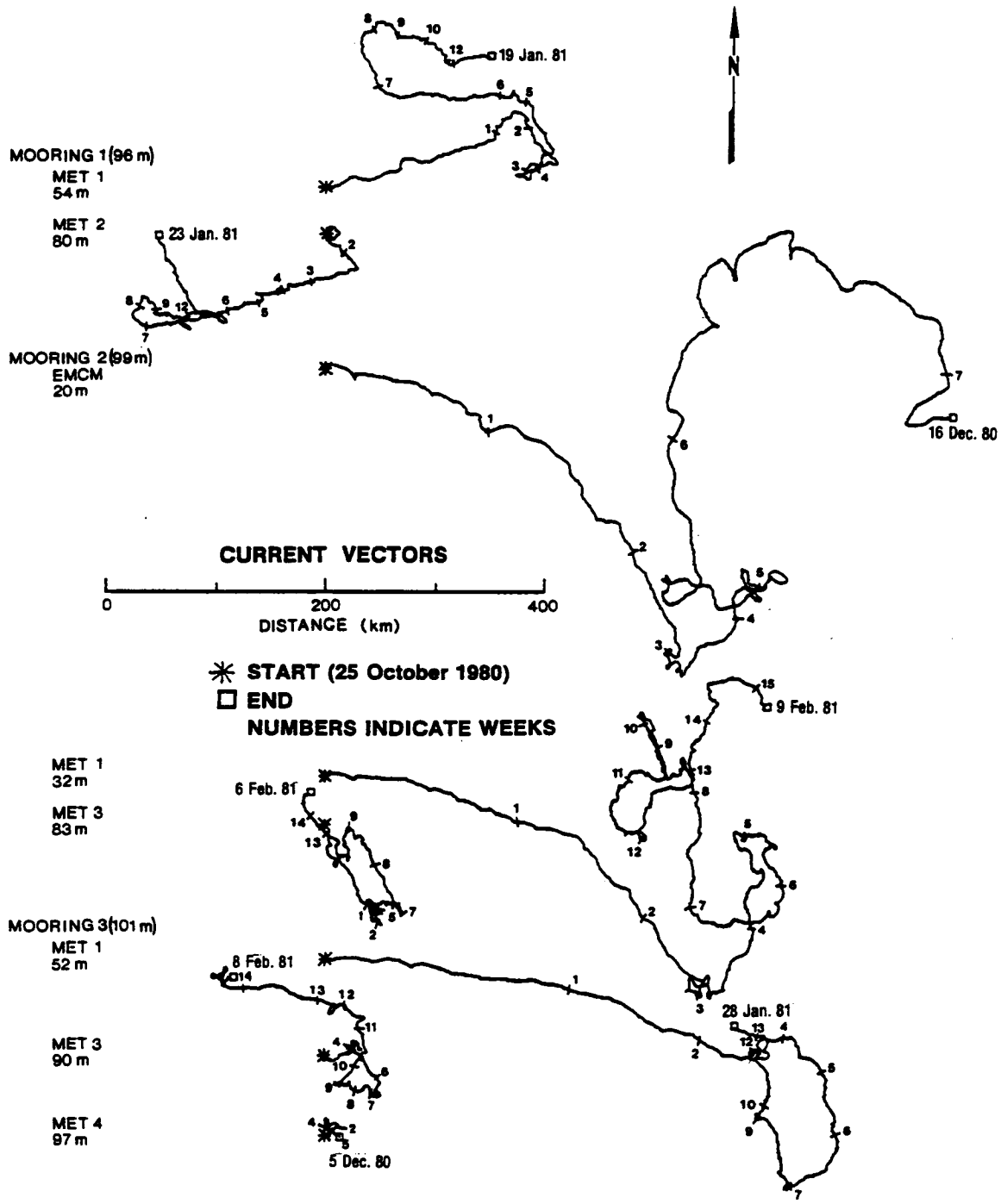

Figure 5.15 Progressive vector diagrams, currents at the Flower Garden Banks, October 80 - February 81.

If one uses the estimate of Ekman boundary layer thickness given by Weatherly et al. (1980)

$$\delta = k \quad \frac{U^*}{f}$$

where k is von Karman's constant, approx. 0.4
U* is the square root of the shear stress at the wall divided by the density of the fluid
f is the Coriolis parameter,

and uses the values we obtained for U* in the boundary layer dye studies, thickness (δ) is roughly 18 m. Therefore, both of the near-bottom velocity groups should have been in the Ekman bottom boundary layer. However, eastward flowing geostrophic currents should produce a boundary layer flow which is rotated counter clockwise (looking down) to the northeast. The monthly mean vectors for the bottom flow are not representative of such a rotation. There is some possibility that even moorings 1 and 3 were within the region of flow deformed by the banks so that centrifugal accelerations may have contributed to the clockwise rotation of the near-bottom vectors. It is also possible that, during the winter, the cold, dense water which is formed on the mid and inner shelf during cold frontal passages (Nowlin and Parker, 1974), tends to produce an offshore deflection of the bottom waters. It is more likely however that the rotation is just due to baroclinic shearing. The idea that the near-bottom flow does go offshore, is certainly consistent with the transects shown in Chapter 2 (Figures 2.34, 2.36, and 2.37). The transmissivity measurements on those transects clearly show offshelf transport of fine sediment in every case.

Variations on the Mean Currents

Each velocity (v) recording in a current meter record consists of the mean (v)--where the mean is taken over a period on the order of a month for example and a fluctuating component (v'). That is:

$$v = \bar{v} + v'.$$

It is not at all unusual to find that the fluctuating parts of the velocity have magnitudes larger than that of the mean flow. These variations about the mean velocity consist of periodic or nearly periodic oscillations and random white noise. A great deal of information regarding the nature of the flow at any given location can be extracted from a current meter record by examining these fluctuating components.

The most common method for studying the oscillations in current meter records is that of spectral analysis. Usually the record is resolved into two orthogonal vector components, u (east-west) and v (north-south). Then the mean is subtracted from each series and the amplitude of the variance (cm^2/s^2) within frequency bands is calculated for frequencies ranging between half the sampling frequency and the inverse of the record length. Typically these analyses are accomplished by means of Fourier transforms of the series. A detailed description of the techniques used on the data collected at the Flower Garden Banks is given in McGrail et al., 1982a.

In addition to being able to resolve how much variance is concentrated at a given frequency, it is also possible to determine the coherence and phase relationship between two time series over the same range of frequencies as above. In the following example, series y and series x have a coherency squared of 1 at the frequency shown because they contain the same sinusoidal oscillation. However, the x series has a phase lag of 90° relative to the y series.

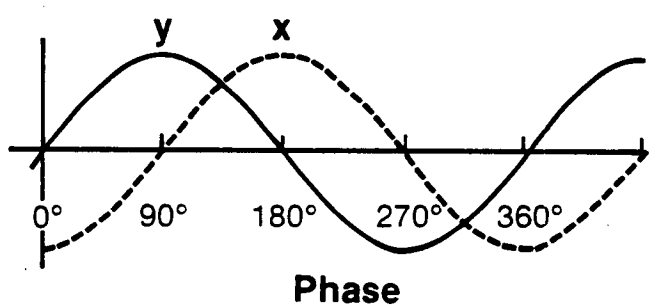

Such a situation might exist between the v velocity components from two current meters for a tidal oscillation if the two instruments were separated by one-fourth of the tidal wavelength in the direction of propagation.

It is possible, therefore, to determine (in a statistical sense) if two time series are oscillating coherently at a common frequency. This is a great aid in determining whether two series are responding to the same forcing mechanism or whether two series are causally related (one forcing the other) at some frequency, although it is not possible to distinguish between the two processes.

Finally, a technique called rotary spectral analysis is used to determine whether an oscillation in the velocity record of a time series is rotational or not, and if it is rotational what the sense of rotation is (clockwise or counterclockwise). This is helpful in determining the kind of phenomena causing the oscillation.

Inertial oscillations, for example, can only rotate in a clockwise sense (in the northern hemisphere).

Spectral analyses were performed on all of the time series records obtained from the moorings at the Flower Garden Banks. These records include velocity, temperature, and transmissivity series. Time series records of wind velocity from the nearby NDBO buoy (42002) were also subjected to spectral analyses.

Examples of these spectra are shown in Figures 5.16 through 5.24 to aid in illustrating the behavior of the flow at the Flower Garden Banks. Figures 5.16 and 5.17 are the spectra for mooring 1, mid-depth and near bottom meters, respectively, during the summer. Figures 5.18 through 5.20 are spectra for the mid-depth and two near-bottom current meter records from mooring 3 (see Figure 5.1 for location) during late spring through midsummer. Spectra for the winter period at mooring 3 appear in Figures 5.21 through 5.23. Figure 5.24 represents the spectra of velocity fluctuations at 32 m, in the winter, at mooring 2.

Velocity Spectra

The contribution of random velocity fluctuation to the autospectra of u and v may be found in the slope of spectral density, G(F), with respect to frequency, F, on the log-log plots (Figures 5.16 to 5.24). The relationship is:

$$G(F) = AF^{-a},$$

where the slope parameter, a, is a positive number.

It can be observed from these spectra that, in general, the value of A decreases with depth. This means that the amplitude of random fluctuations over all frequencies is smaller near bottom than in the upper portion of the water column. There are probably two reasons for this: 1) almost all driving mechanisms for the fluctuations are input through the surface, and 2) random fluctuations are attenuated by friction near the bottom.

Notice that in almost all of the spectra but particularly in those from instruments deployed near the bottom, there is a change in the slope of G(F) near the one cycle per day (cpd) frequency. Above 1 cpd the slope parameter, a, is relatively large, but below 1 cpd the slope flattens out. This suggests that long period random fluctuations are suppressed, particularly near the bottom. The one spectral set that does not exhibit any noticeable break in slope at 1 cpd is that for mooring 2 meter 1 (Figure 5.24). This record comes from the shallowest instrument, during the winter, and very close to the East Flower Garden Bank. Proximity to the bank suggests that interaction of the flow with the bank may be a local

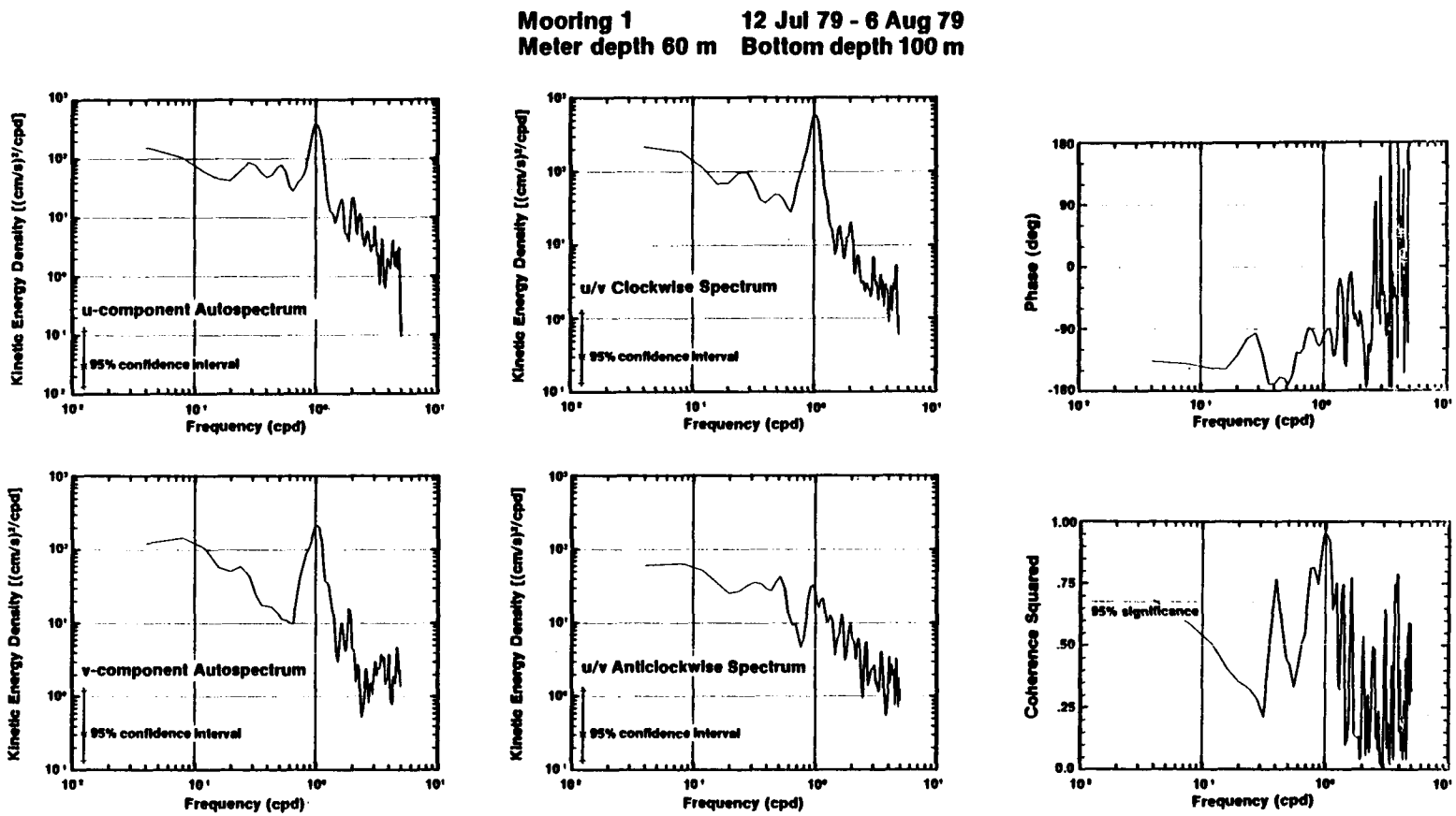

Figure 5.16 Spectral representations of the mid-depth currents at mooring 1 illustrating summer conditions.

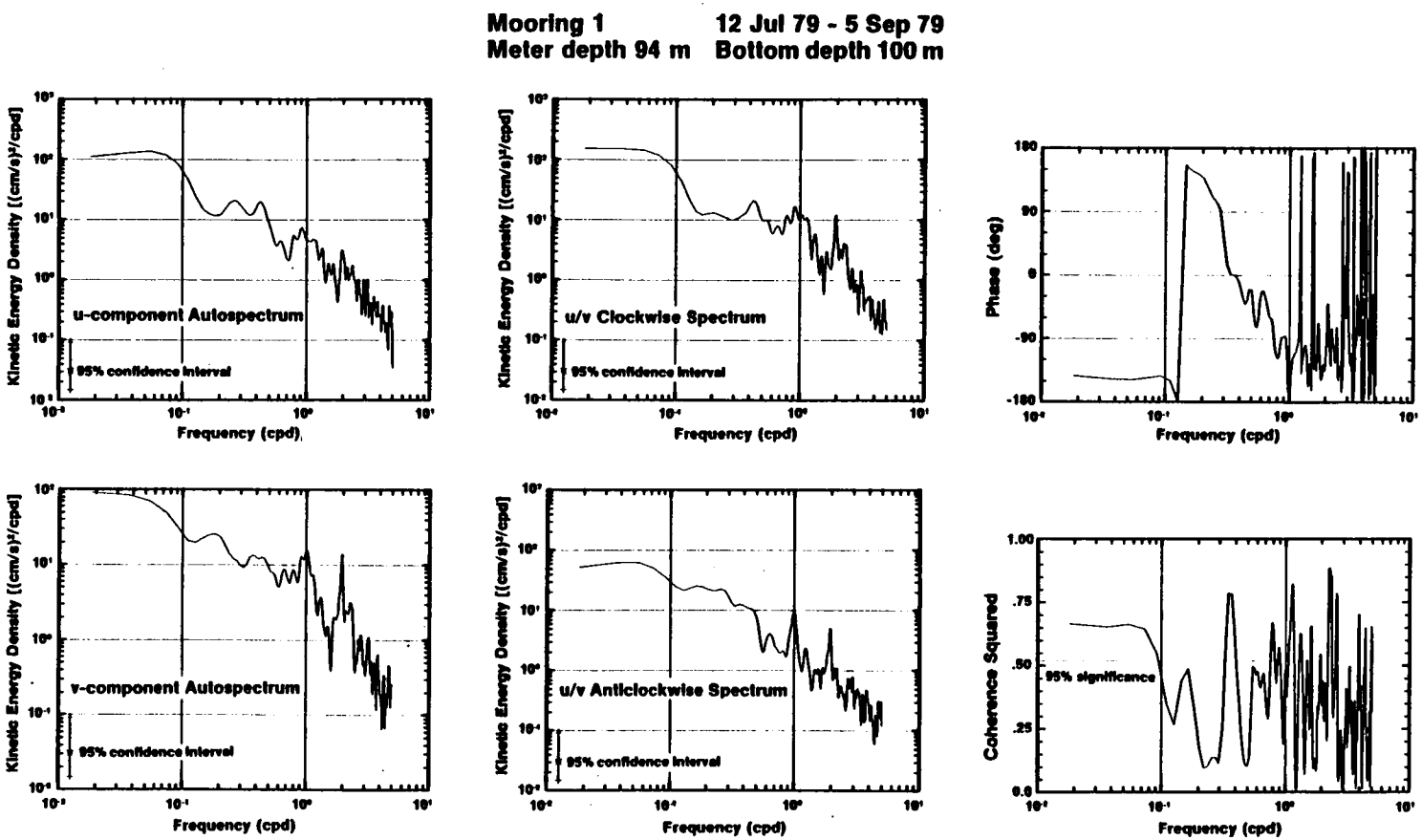

Figure 5.17 Spectral representations of the near-bottom currents at mooring 1 illustrating summer conditions.

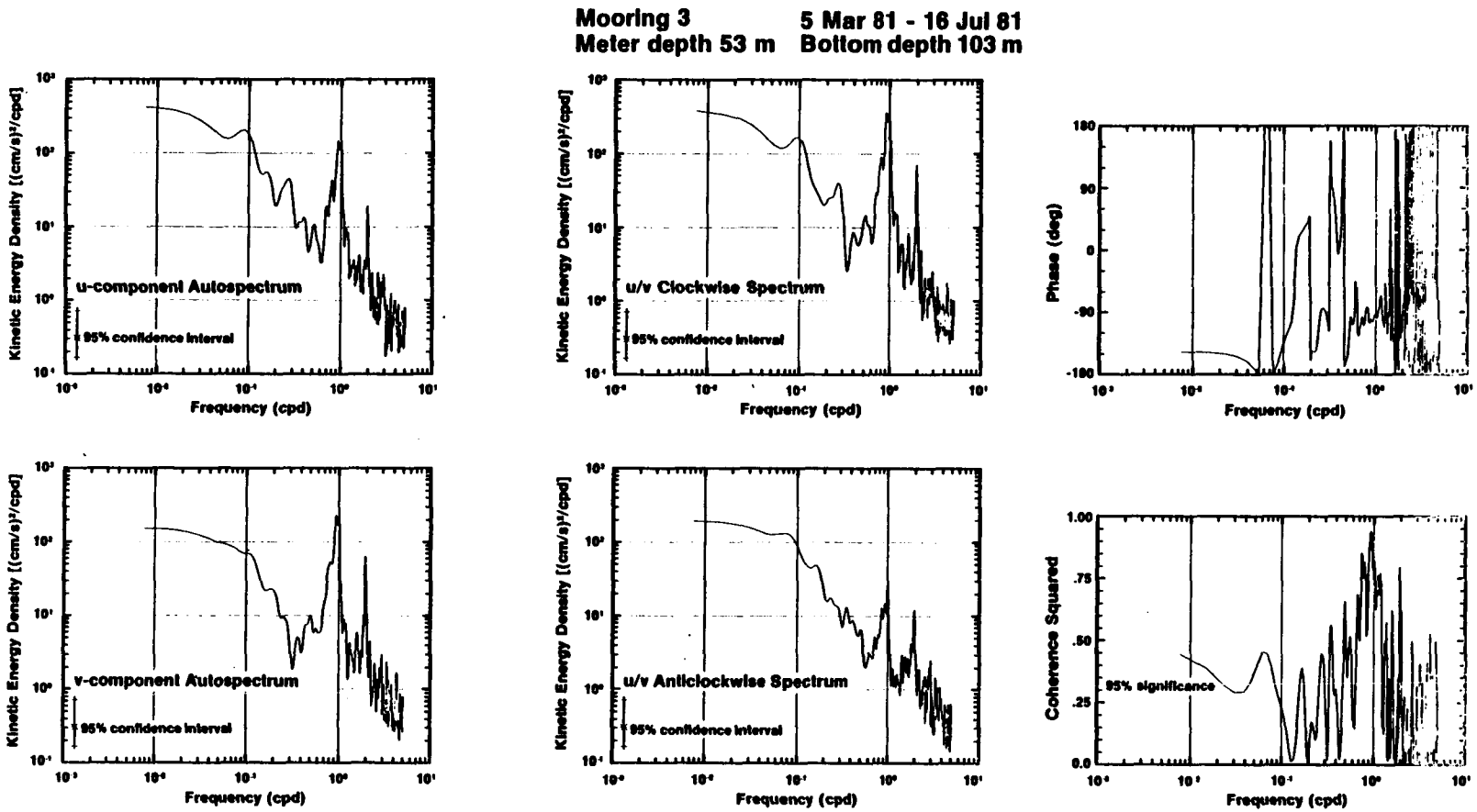

Figure 5.18 Spectral representations of the mid-depth currents at mooring 3 illustrating spring/summer conditions.

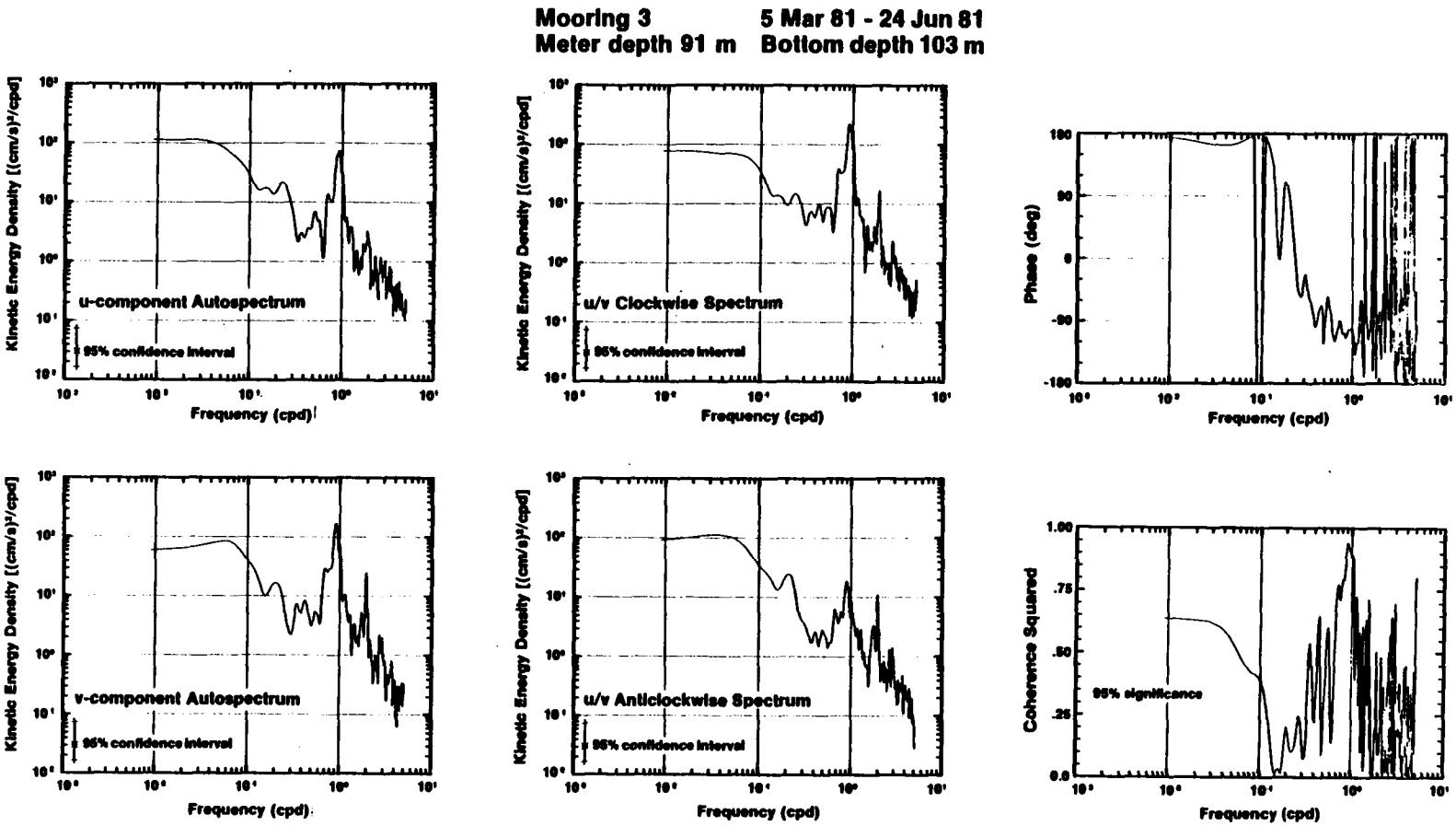

Figure 5.19 Spectral representations of the near-bottom currents at mooring 3 illustrating spring/summer conditions.

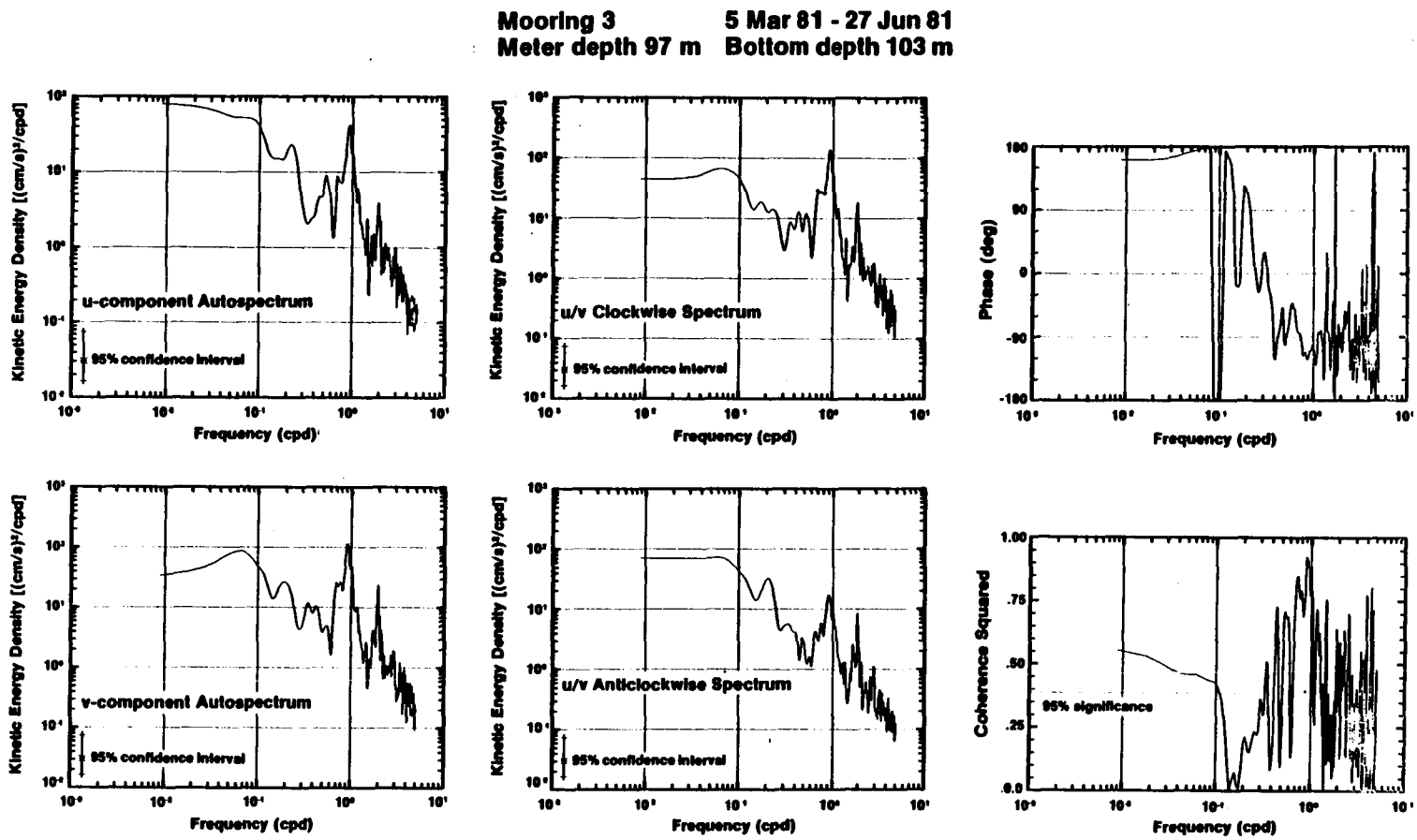

Figure 5.20 Spectral representations of the very near-bottom currents at mooring 3 illustrating spring/summer conditions.

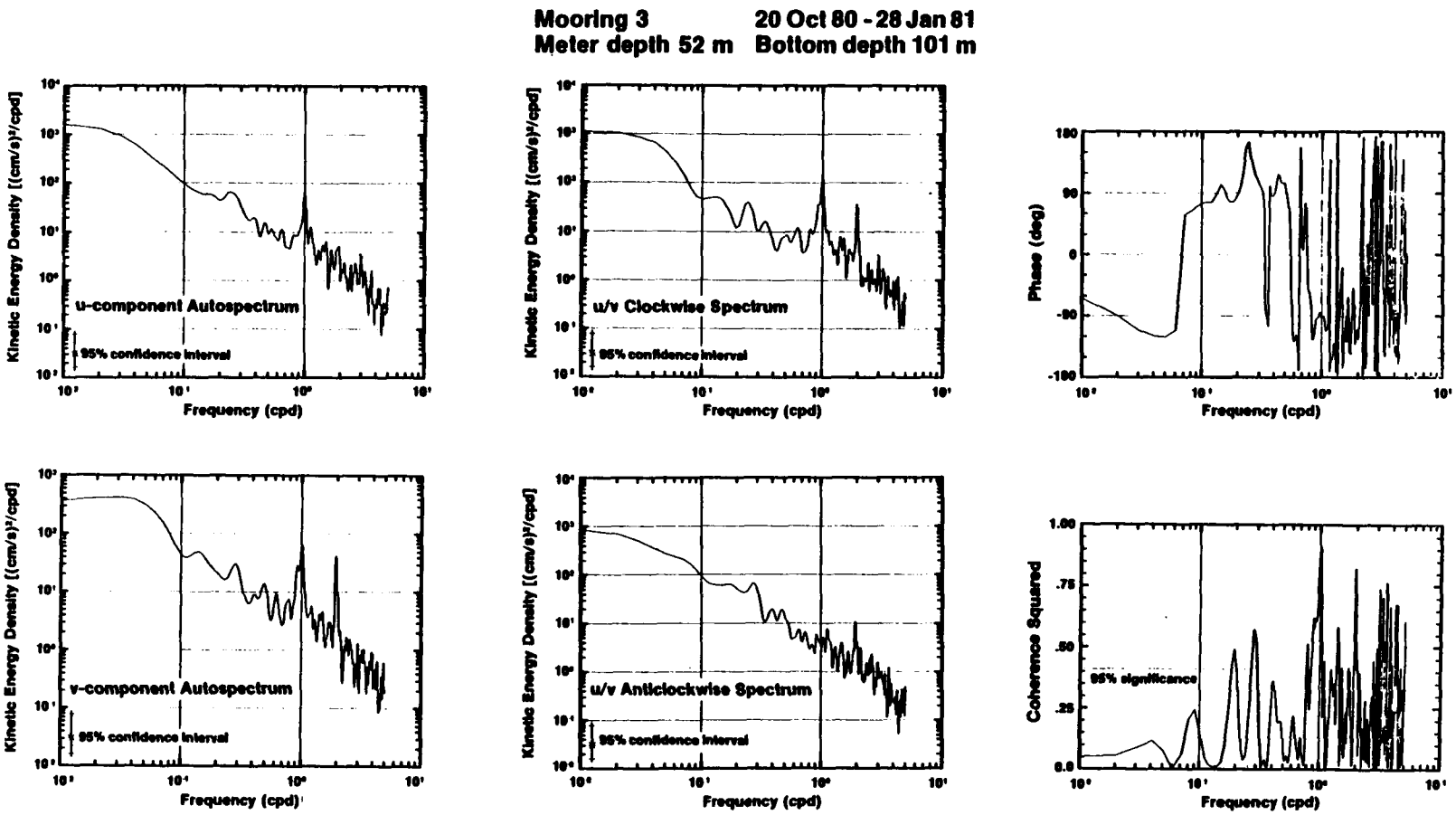

Figure 5.21 Spectral representations of the mid-depth currents at mooring 3 illustrating winter conditions.

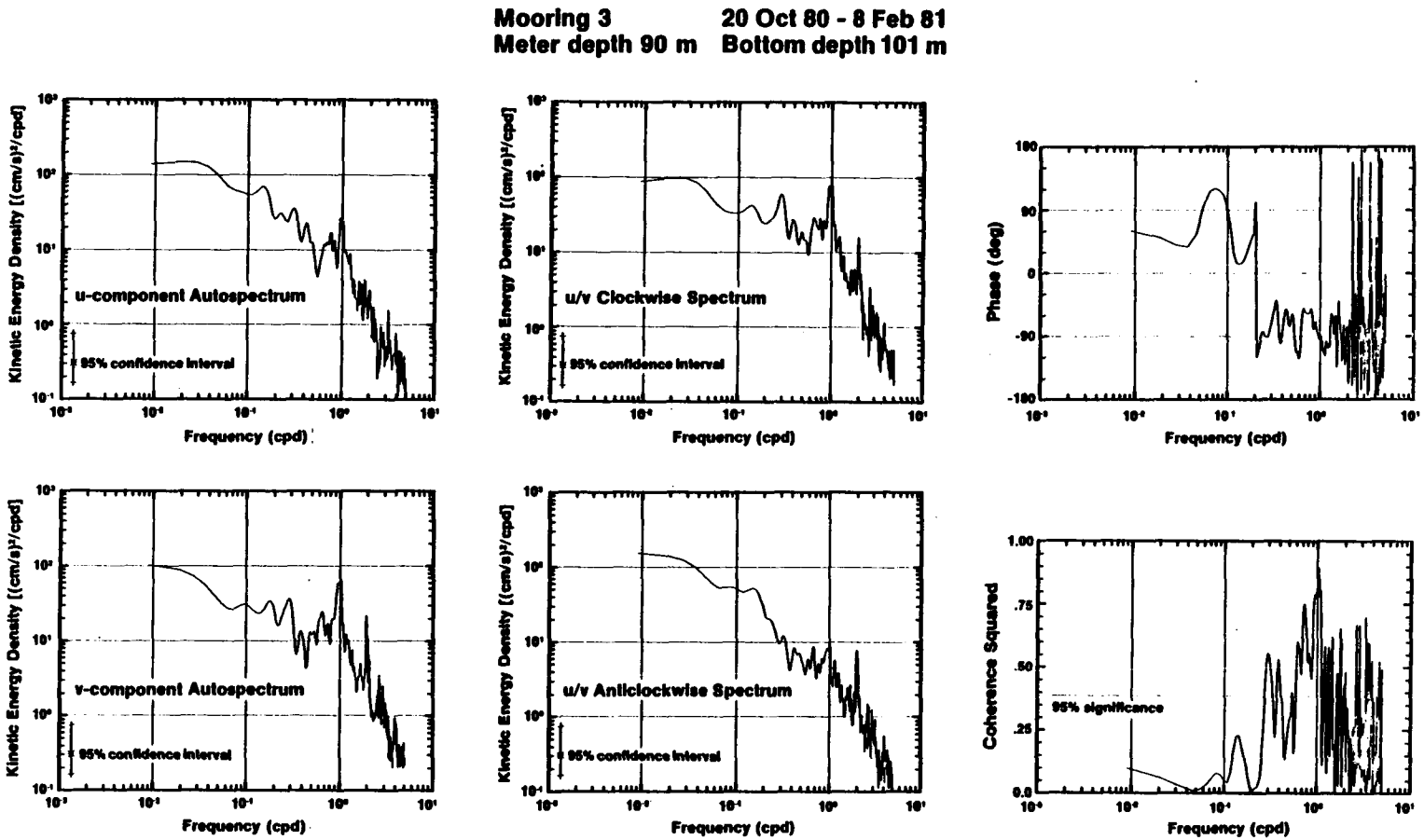

Figure 5.22 Spectral representations of the near-bottom currents at mooring 3 illustrating winter conditions.

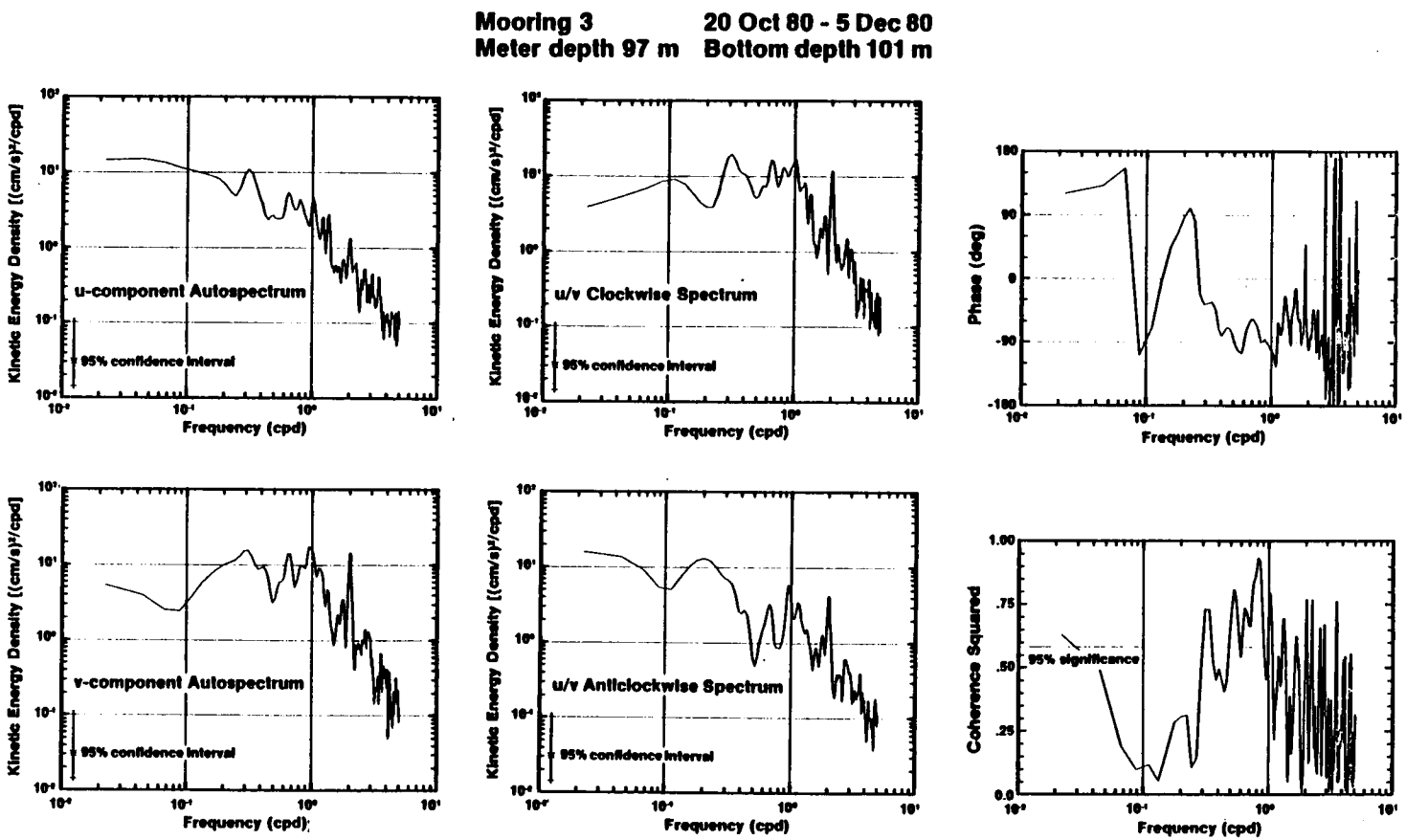

Figure 5.23 Spectral representations of the very near-bottom currents at mooring 3 illustrating winter conditions.

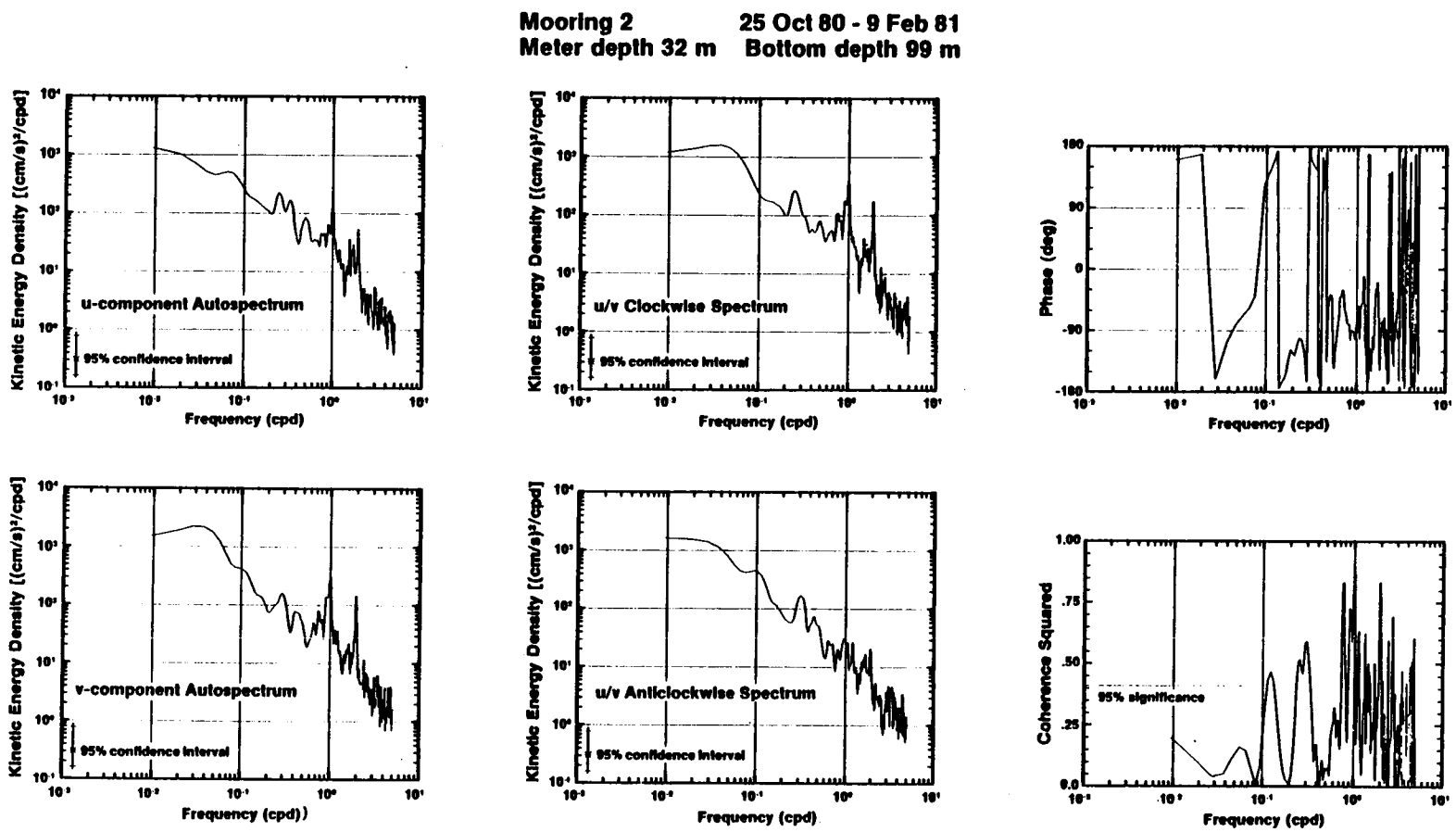

Figure 5.24 Spectral representations of the mid-depth currents at mooring 2 illustrating winter conditions.

source for large scale turbulence. These three factors--proximity to the surface, energetic input during the winter, and proximity to the bank--probably account for the undiminished low-frequency noise in the record.

Periodic and nearly periodic fluctuations appear in the velocity spectra as peaks in the spectral density rising above the baseline noise at the frequency of the oscillation. These periodic fluctuations are due to perturbations imposed on the mean flow by the tide, inertial currents, and what appear to be quasi-geostrophic shelf waves. The periods and frequencies of the major tidal constituents and the local inertial period for the latitude of the Flower Garden Banks are shown in Table 5.2.

Table 5.2 Theoretical Frequency and Period of Major Tidal Constituents and of Inertial Currents

Darwin Name of Tidal Harmonic	Period (hrs)	Frequency (cpd)
S_2	12.00	2.0000
M_2	12.42	1.9324
K_1	23.93	1.0029
O_1	25.82	0.9295
Inertial Currents at 27°55'N Latitude	25.56	0.9390

Tidal Currents

The tides at Galveston Bay, Texas are classified as mixed diurnal. That is, there are two highs and two lows to the water height each lunar day (24.84 hours) but with a large inequality between either the two highs or the two lows. The amplitudes of the three major constituents (K_1, O_1, M_2) range from 9 cm to 12 cm (McGrail et al., 1982a).

In all of the spectra of the currents near the Flower Garden Banks, shown in Figures 5.16 to 5.24, there are prominent peaks at, and close to, the inertial frequency and the K_1 and O_1 tidal frequencies (Table 5.2). The peaks near 2 cpd are due to the S_2 and M_2 semidiurnal tidal constituents. Because of the very small frequency difference between the inertial oscillations and the O_1 tidal constituent, it is not possible to separate them in the autospectra.

A few basic features of the tidal currents can be derived from the velocity spectra. The diurnal and semidiurnal tidal currents

rotate clockwise at all depths. The v (north-south) velocity components of the semidiurnal tidal currents are significantly larger than the u (east-west) components, indicating that the semidiurnal tide is elliptical, with major axis oriented north-south. The ellipticity is enhanced near the bottom. However, the tidal orbits of the K_1 tide are more nearly circular, even near the bottom. Because of the difference in bandwidths of the different spectra, which are a function of the lengths of the time series and the amount of smoothing applied to the spectra, it is difficult to access from them the changes in amplitude with depth or season. Amplitudes and phases of the tidal currents have therefore been computed by harmonic analysis of 29-day segments of the velocity time-series records.

Table 5.3 gives a typical set of amplitudes of the currents computed by harmonic analysis for the K_1 and M_2 tidal constituents (combined baroclinic and barotropic). The S_2 amplitudes tend to be substantially smaller. Tidal current speeds throughout the year generally range from 1 to 3 cm/s for the M_2 constituent and from 2 to 5 cm/s, but sometimes as high as 9 cm/s, for the K_1 constituent.

Table 5.3 Tidal Current Amplitudes (in cm/s) at Mooring 3 for 6 March to 4 April 1981

Meter #	Depth (m)	Tidal Constituent			
		K_1		M_2	
		u	v	u	v
1	53	2.2	3.2	1.4	2.7
2	64	1.8	2.2	0.7	2.4
3	91	1.2	0.8	0.1	2.2
4	97	0.3	0.3	0.2	1.9

All three constituents of the tidal currents (K_1, M_2, and S_2) were found to be strongly baroclinic. Harmonic analysis of a large number of 29-day current record segments shows a large temporal variation in the phase and amplitude that would not occur if the tides were barotropic. The K_1 tidal currents are two to three times larger in the summer than in winter. The other two constituents have no apparent seasonal modulation, but rather are characterized by a scatter in both their amplitudes and their phases relative to the tide potential.

There are also significant reductions in the amplitudes of the tidal currents near the bottom. The amplitude reductions are due to attenuation by bottom friction and to the baroclinicity.

Because the tides do have a significant baroclinic component, the amplitude of the vertical displacements within the water column

was estimated. To do this, the same harmonic analysis used on the u and v components of velocity was applied to the temperature records. Estimates of vertical displacements were then made by dividing the temperature fluctuations by the average vertical temperature gradient appropriate for the time of year and depth of the instrument from which the temperature record was obtained. The K_1 displacements were primarily between 1 and 4 m, with a few between 8 and 10 m in the winter. The larger amplitudes are suspect because it is very likely that horizontal advection in the cross-shelf direction contributes to the winter temperature fluctuations. The M_2 and S_2 also possess larger winter displacements but average between 0.25 m and 1.5 m for the M_2 and between 0.1 and 1.2 for the S_2 constituents.

Inertial Currents

Inertial currents are those that oscillate at or near the local inertial frequency:

$$\omega_I = 2\pi \sin\phi$$

where π is the angular velocity of the earth at the equator, in radians per second (7.27×10^{-5}/s), and ϕ is the latitude of the observations. Dynamically, the Coriolis acceleration $v\omega_I$ is balanced by the centrifugal acceleration v^2/L where L is the radius of the inertial circle.

These currents are usually initiated by an impulse of the wind at the sea surface. Basically, what happens is that the water is accelerated up to some mean velocity. The Coriolis acceleration then deflects the current to the right (in the northern hemisphere) in an ever tighter spiral until the centrifugal acceleration of the curving flow balances the Coriolis acceleration. In a current meter record an inertial oscillation would be seen as a clockwise rotation of the velocity vectors with a period of $2\pi/\omega_I$. As shown in Table 5.2, the inertial period at the Flower Garden Banks is 25.56 hours.

The inertial oscillations observed in the current meter records occur episodically in conjunction with hurricanes and major winter storms. They reach maximum velocities of 20 to 30 cm/s near the surface and decay toward the bottom except at the location of mooring 2 (Figure 5.1). The phase relationship between the surface and bottom changes from season to season apparently as a result of variations in stratification and variations in the wind field generating the inertial currents. The oscillations appear to persist for about 3 to 5 days after initiation but occasionally last as long as 10 days. Figure 5.25 shows a period of strong inertial oscillations at mid-depth and bottom for three moorings during May of 1980.

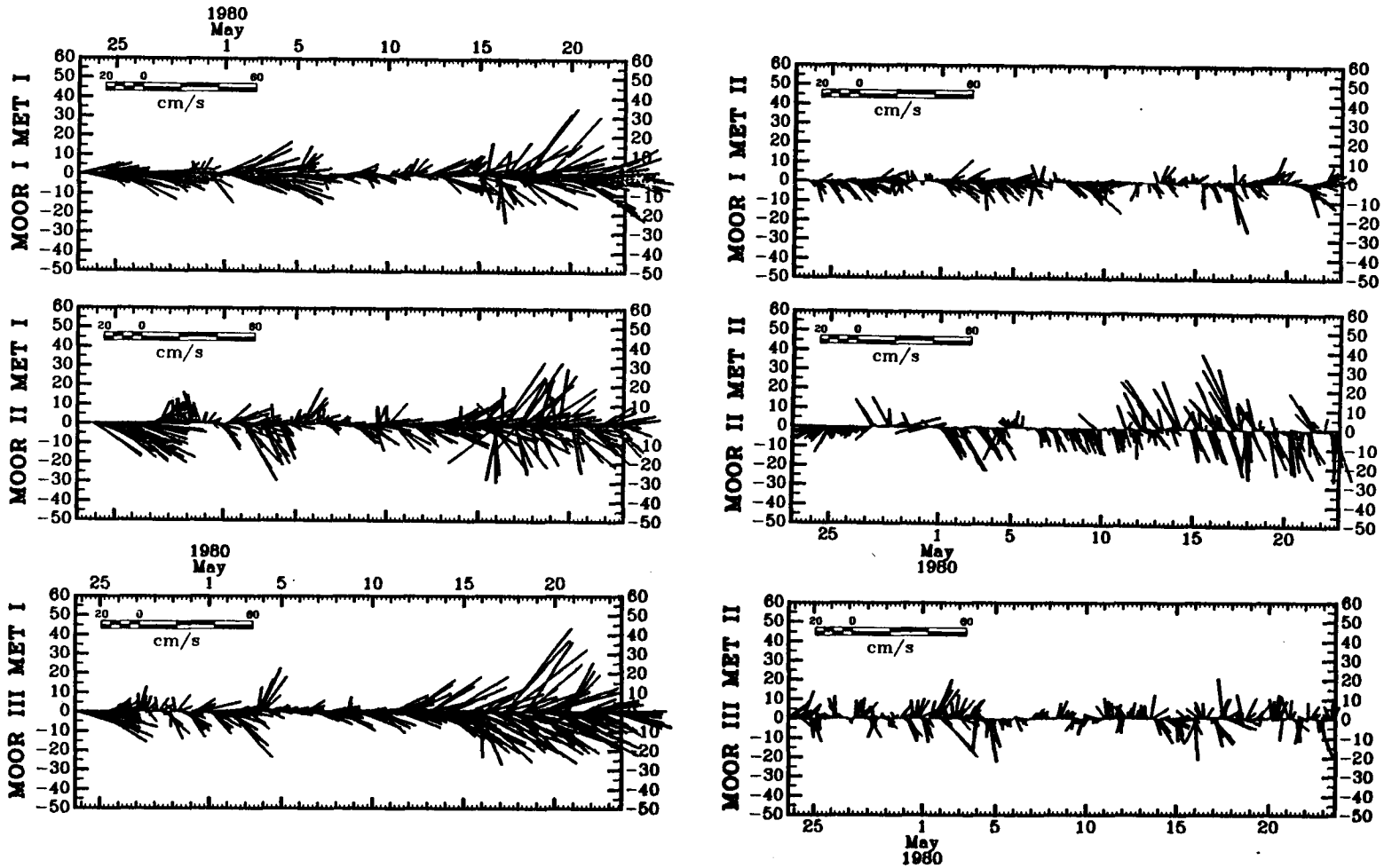

Figure 5.25 Time series of horizontal currents at the upper and lower meters of moorings 1, 2, and 3. Strong inertial currents are observed 15-19 May 1980.

Shelf Waves

When flow on the continental shelf is perturbed at a frequency lower then inertial, waves can be generated which are trapped on the continental shelf by vorticity. These waves travel with their crest normal to the coast and are right bounded. That is, they are constrained to propagate in only one direction such that an observer standing on the crest of the wave and facing in the direction of propagation would have his right shoulder to the coast (in the northern hemisphere). They are quasi-geostrophic in the sense that, to within a few percent, the dynamic balance is between the pressure gradient and the Coriolis acceleration. Shelf waves may be barotropic (surface waves) or baroclinic (internal waves), and they decay exponentially in the offshore direction. Perhaps the most thorough discourse on shelf waves is given by LeBlond and Mysak (1978).

The dispersion relationship for shelf waves (speed of propagation relative to frequency and wavelength) is governed by the slope of the shelf and the latitude for barotropic waves, complicated by the nature of the density distribution for baroclinic waves. Stated differently, for any given wavelength, latitude, and shelf slope, there is only one possible frequency (for each mode) of the barotropic wave.

The most common frequencies for what appear to be shelf waves in the Flower Garden current meter data are 33 hours, 2 days, and 4 days. All of these have clockwise rotation of the velocity vectors and relatively good coherence between the u and v velocity components.

The shelf wave at the two-day period is intermittent and seems to be generated by storms. The coherency between the v components of velocity was determined for meter 1 on moorings 1 and 3 (Figure 5.51, below). At the two-day period, mooring 1 leads mooring 3 by approximately 100°, which means that the meters are about 28% of a wavelength apart for a two-day wave. Because the moorings are approximately 22 km apart, in the east-west direction, the wave must have a wavelength of about 79 km. In the sea surface thermal data for 23 February 1982, there are wave-like features all the way from 90°W to 95°W between about 28° and 28°30'N (Figure 5.26). These waves have an approximate wave length of 83 km, which is just 5% greater than the estimate from the spectral analysis.

Perhaps one possibility is that these waves are generated by the topographic disturbance of the Mississippi Canyon, then propagate to the west. But, it is then not clear why they should only be generated during periods of storms. The amplitude of the current oscillation occasionally gets as high as 15 cm/s, but normally is on the order of 4 cm/s.

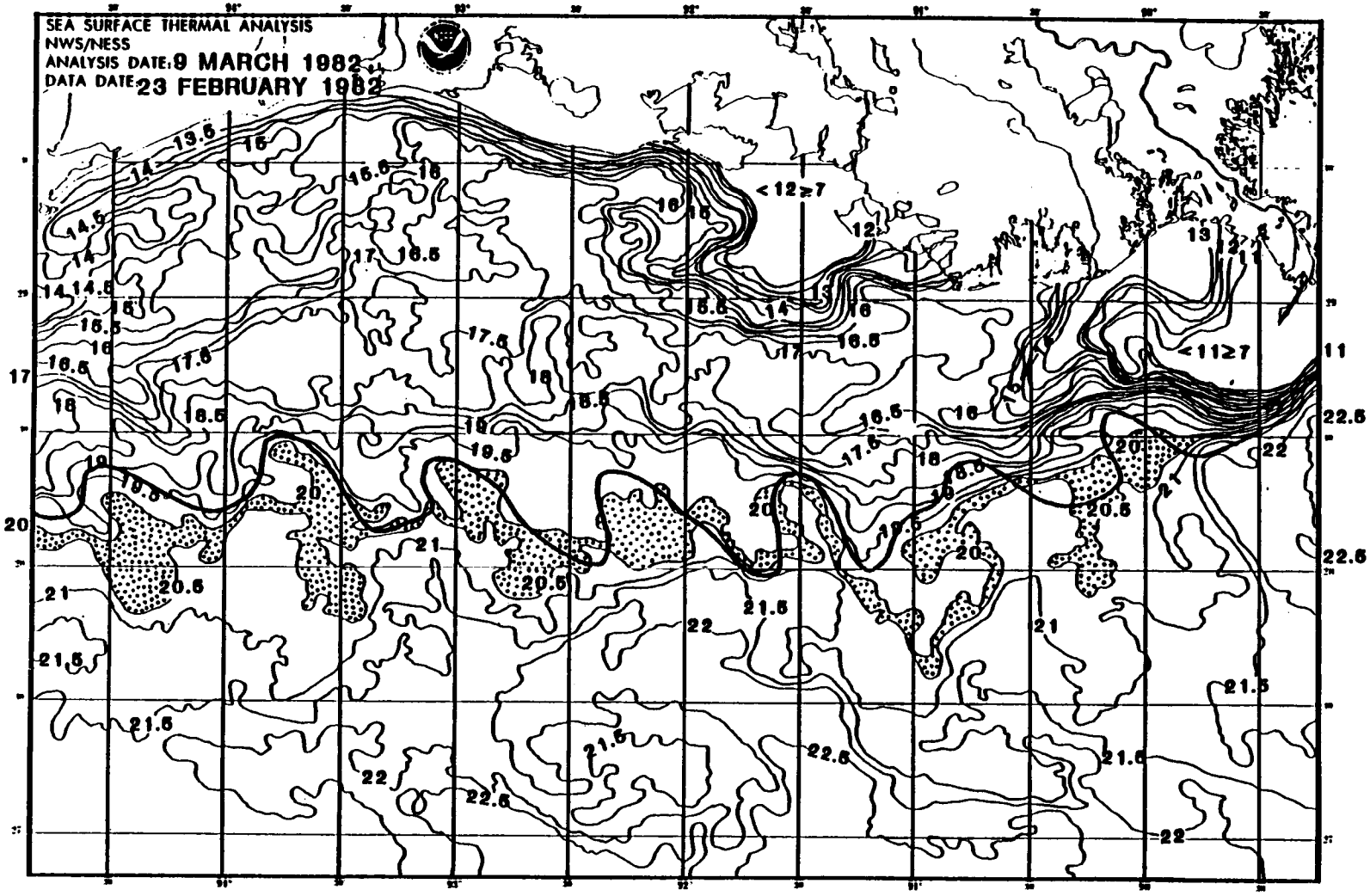

Figure 5.26 Wave-like perturbations in the sea surface isotherms at the shelf edge outlined with a heavy line. The wavelength of these distributions is approximately 80 km. These are probably shelf waves with a two-day period.

The four-day oscillation is very near the three- to five-day period spectral peak found in the wind spectra that represents cold frontal passages. This could be a directly forced oscillation, but it appears more likely that it is a free shelf wave excited by impulses of the wind stress around this preferred frequency.

Hurricanes and Tropical Storms

During the course of the deployment of current meters at the Flower Garden Banks, several hurricanes and tropical storms passed close enough to the banks to generate a recognizable response in the water column. In 1979, three of the five hurricanes that entered the Gulf of Mexico came relatively close to the banks. These were, Bob (9-11 July), Claudette (21-24 July), and Elena (29 August - 1 September). In 1980, Hurricane Allen passed very close to the banks, causing damage to the reefs and monitoring equipment on the banks. Though Allen was the most severe storm, the best records of a storm passage are from Claudette. The response to Allen was recorded by but a single current meter, near the bottom on mooring 2. That will be discussed under "Orographic Effects."

The normal eastern flow of the shelf appears to have been reversed by Hurricane Bob. The early portion of the current meter records (Figure 5.27) reflects both the reversal of the current and the "spin down" or decay of the flow field set up by Bob. Particularly noticeable are the strong inertial oscillations and the two-day shelf waves at mid-depth. Near-bottom currents were relatively strong (> 20 cm/s) and toward the southeast with weak inertial oscillations. The two-day shelf waves are present in the near-bottom flow but are very subtle.

Claudette passed directly over both the NDBO buoy 42002 and the Flower Garden Banks (see Figure 2.13, above, for location of the buoy relative to the banks). By the time Claudette passed over this area she had been reduced to a tropical storm with maximum recorded winds of only 20 m/s (39 knots). After making landfall, the storm became nearly stationary. Unusually strong southerly winds persisted at buoy 42002 through 29 July. The recorded wind at NDBO 42002 for 13 July through 1 August 1979 is shown in Figure 5.27 along with the current and temperature response at mid-depth and near bottom at mooring 1.

The approach of Claudette was heralded by a wind shift from southeast to northeast in the early morning hours of 21 July. As the storm approached, the wind vectors swung in a counterclockwise direction and increased in magnitude. When the storm passed over, the winds rotated to southwesterly and increased further in magnitude.

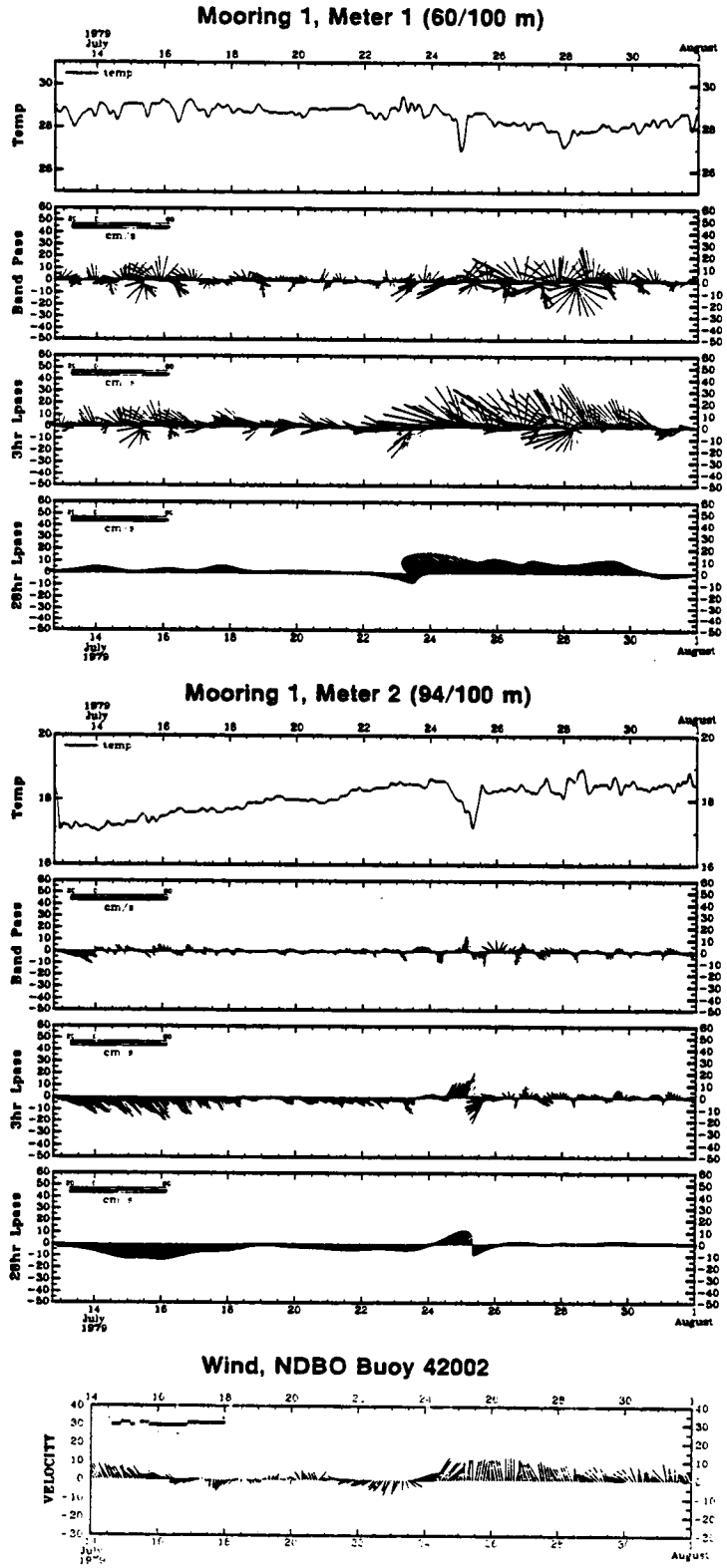

Figure 5.27 Wind and current meter records during the passage of Tropical Storm Claudette.

Little effect from Claudette was seen at the Flower Garden Banks at 60 m depth until late on 22 July when the current started to rotate counterclockwise toward the southwest and to increase in speed. When the storm passed, near midnight (local time) on 23 July, the current abruptly turned toward the northwest at 60 m (Figure 5.27) and accelerated to speeds of over 60 cm/s. This could not have been a direct frictional response because the current vectors would have been oriented either in the direction of the wind or to the right of it. Inertial oscillations started to grow on 23 July, reached a maximum on 28 July, then decayed rapidly.

Near the bottom, the first response to Claudette was a weak rotation of the current late on 23 July, then a major pulse (> 20 cm/s) to the northeast. This was followed by a sudden reversal about mid-day on 25 July. By early on 26 July the mean flow at the bottom had become very weak (about 2 cm/s) in the onshore direction. It was modulated by inertial oscillations of about 10 cm/s amplitude through 28 July. The major onshore pulse at the bottom was accompanied by a sudden drop in temperature which was probably caused by cold water upwelling over the shelf break near the bottom.

Because the banks represent major obstructions to the flow, it is quite likely that the currents would have been accelerated across the reef by the Venturi effect. Also, flow at the level of the reef would probably have been directly driven by the wind stress. The currents would therefore have followed the direction of the wind vectors more closely, though leading them in a clockwise sense.

Surface gravity waves generated by the wind stress would also have been important contributors to the effects felt at the level of the reef. To estimate the maximum oscillatory velocities likely to be generated, wave orbital velocities were computed from Airy wave theory for both the deep and shallow water approximations. Both estimates are given because it is not clear that the waves could make the transformation from deep to shallow water characteristics over the steep slopes of the banks. Only deep water estimates are given for 100 m depths.

Two waves, both exceptionally large for the Gulf of Mexico, were chosen to approximate storm conditions. The first is a wave with a 10-second period and a 5 m height (2.5 m amplitude), and the second is a 12-second wave with a 7 m height.

The equations for these calculations are:

Deep water

$$|u_{max}| = a\sigma e^{-kz}$$

where a = wave amplitude
σ = wave radian frequency
k = wave number

Shallow water

$$|u_{max}| = \frac{a\sigma}{kz}$$

The results of these calculations appear in Table 5.4.

Table 5.4 Results of Airy Wave Theory Calculations

Water Depth	Wave Period, Height		Maximum Orbital Velocity (cm/s) Shallow water Approximation	Deep Water Approximation
20 m	10 s,	5 m	175	70
20 m	12 s,	7 m	245	105
100 m	10 s,	5 m	---	1
100 m	12 s,	7 m	---	11

In general, then, during the passage of a hurricane over the banks, one should expect a three-layer response. A direct wind-driven current down to about the thermocline, an indirectly-forced flow extending from the thermocline to within about 10 m of the bottom, and a near-bottom flow, probably compensatory to a large degree, to that at the surface. In addition, strong oscillatory velocities would be experienced at the level of the reef from surface gravity waves. The surface gravity waves would, however, have little effect near the base of the bank. As will be shown, it also appears that the inertial oscillations are intensified on the bank and penetrate to the bottom with greater magnitude than at sites away from the bank.

Orographic Distortions of the Flow

"Orographic" comes from the Greek base words "oros," meaning mountain, and "graphos," which means to write or describe. Orographic effects, as they pertain to geophysical fluid dynamics, are those perturbations of flow caused by the presence of mountains or mountain-like features in the flow field. The nature of the flow about an obstacle depends on several variables. Among these are the speed of the flow, the vertical and horizontal scale of the object, the depth of water relative to the height of the obstacle, the turbulent viscosity of the fluid, and the degree of stratification present in the water column. Reviews of orographic effects have been presented by Hogg (1980) and Baines and Davies (1980). Hogg (1980) reviews the theoretical aspects of the field; Baines and Davies (1980) review laboratory investigations of these phenomena.

Theoretical Considerations

An understanding of the orographic effects at the Flower Garden Banks is important to the interpretation of the biotic and sedimentological zonation of the banks. Water at the base of the banks is both turbid and cold (on the order of 17°C) so that if it could be carried up onto the reefs it would have a profound effect on the population dynamics of the bank.

In both theoretical and laboratory investigations, four flow regimes have been studied: irrotational without stratification; irrotational with stratification; rotational without stratification; and rotating stratified.

In the first case, one could consider a two-dimensional object such as a half cylinder at the bottom in a steady flow of speed u.

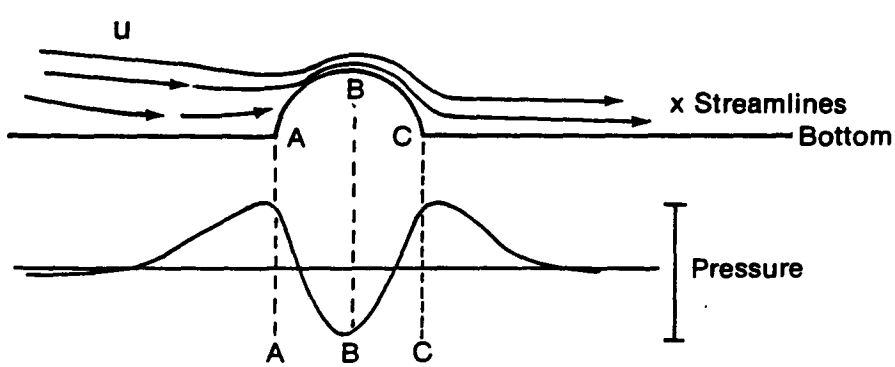

The Bernoulli equation, $P + 1/2\rho u^2 = K$ (where P is pressure, ρ is density, u is the x component of velocity, and K is a constant) may be differentiated with respect to x to give

$$\frac{\partial P}{\partial x} + \rho u \frac{\partial u}{\partial x} = 0$$

As the flow approaches the obstacle, it is blocked and u $\partial u/\partial x$ becomes non-zero and negative (u decreases) so that the pressure rises to a maximum at point A. Then the flow is accelerated over the object causing u $\partial u/\partial x$ to become large and positive so that $\partial P/\partial x$ becomes negative and P reaches a minimum at B. The flow then decelerates in the lee of the object, creating a second pressure maximum. Then the velocity and the pressure return to ambient in the lee of the half cylinder. In essence, the kinetic energy of the flow is converted to potential energy and back again. All this assumes that the fluid is inviscid, extends upward infinitely, and cannot move in the y direction (horizontal direction perpendicular to x).

If the flow is viscid, the water particles traveling over the surface of the object lose energy to friction so that they do not reach the same maximum u at B, and the pressure in the lee of the object drops below ambient. This causes the flow to reverse in the lee of the object and vortices are formed. Also, the lowest level water in front of the object may not have sufficient kinetic energy to rise over the object in the presence of friction. If the water also has a finite depth, then all of the water approaching the obstacle from upstream must be accommodated by accelerating it through the reduced depth over the object. In a viscid fluid, the flow through the reduced aperture cannot accommodate all of the flow from the original cross-section, and a surface wave forms on the upstream side of the object. This causes an adverse pressure gradient and further reduces the rise of the near-bottom water particles in front of the object. Or, to say it differently, the near-bottom flow can become blocked.

If the flow is three-dimensional, so that the fluid is free to move in the y direction, and if the flow is essentially unrestricted on either side of the object, most of the excess fluid blocked by the object will flow around rather than over it. Because both of the Flower Garden Banks occupy about 80% of the water depth, and because their rough surfaces generate considerable turbulence (and therefore make the eddy viscosity large), one would not expect the near-bottom waters to rise very far up their flanks.

Stratification can also reduce the vertical excursion of water impinging on an obstable. Now we return to the two-dimensional model for a moment. The kinetic energy of the oncoming water is converted into potential energy as it moves

vertically, raising the isopycnals and creating an internal wave. The relationship is

$$\rho \frac{u^2}{2} = gh^2 \frac{\partial \rho}{\partial z}$$

where g is the acceleration of gravity and h is the height above equilibrium that a water particle is raised. For any given velocity and stratification, that height is

$$h = \left[\rho \frac{u^2}{2} (g \frac{\partial \rho}{\partial z})^{-1}\right]^{1/2}$$

McGrail and Horne (1981) showed that for a 100 cm/s flow and stratification comparable to that for April at the Flower Garden Banks ($\partial\rho/\partial z = 2 \times 10^{-7}$ gm/cm^4), h is only 50.5 m. This is a worst possible case approach since the velocity is very large and the stratification very low. As with the unstratified model, the introduction of viscosity significantly reduces the actual permissible rise of a water particle. The aperture at the top of the bank would have to accommodate the approximately 20 m of water normally flowing at that depth plus the 50 m of water displaced vertically from below. Because the fluid is incompressible, the velocity through the aperture (U_a) would be

$$U_a = U(1 + h/a)$$

where a is the distance between the top of the bank and the water surface. Using the 100 cm/s value for U, U_a would be 350 cm/s. If friction reduced this by only 29%, U_a would be 250 cm/s and h would be reduced to 30 m. Now, if the flow is permitted to be three-dimensional, the rise would be significantly reduced as the kinetic energy is drained off through horizontal flow around the bank. In the case of a rotating homogeneous flow field, the flow is said to be geostrophic. The x and y components of flow are then

$$+ vf = - \frac{1}{\rho} \frac{\partial P}{\partial x}$$

$$- uf = - \frac{1}{\rho} \frac{\partial P}{\partial y}$$

where v is the y (north-south component of flow)
u is the x (east-west component of flow)
f is the Coriolis parameter $2\omega \sin \phi$.

Under these conditions, the flow is constrained to be two-dimensional in the x-y plane. That is, the vertical velocity, ω, is identically zero everywhere (Hogg, 1980) and the flow is depth independent. When such a flow encounters a bump on the bottom,

the flow at all levels diverges and flows around the bump as if it were a cylinder reaching to the surface. This type of flow is called a Taylor column. In order for the column to form, the flow around the bump must remain reasonably geostrophic and the bump must be relatively large. In order for the flow to remain geostrophic, the horizontal scale of the bump must be large enough so that the Rossby number, ϵ, remains << 1.

$$\epsilon = \frac{u}{Lf}$$

where u is a characteristic velocity
L is a length scale
f is the Coriolis parameter.

If the obstacle has a small radius (L) or the flow has a high velocity (u), then ϵ becomes large, signifying that the inertial accelerations are non-negligible and the flow is ageostrophic. The vertical scale of the obstacle is the ratio of the height of the object (h) to the depth of the water H_o. Hogg (1980) combined the vertical scale and the inverse of ϵ into a single parameter β_T.

$$\beta_T = \frac{h}{H_o} \epsilon^{-1}$$

According to Hogg (1980), a Taylor column can only form when β_T is larger than some number of order 1. Using numbers appropriate to the Flower Garden Banks (u = 20 cm/s), (h/H_o = .8), ($L = 4 \times 10^5$ cm), and ($f = 7 \times 10^{-5}$/s), β_T is equal to 1.12. The number is sufficiently large to indicate that rotational effects are important, but too small to suggest unequivocally that all vertical motion would be suppressed.

When both rotation and stratification are strong, a modification of the Taylor column takes place and cones of deadwater form over the obstacle. The criterion Hogg (1980) gives implies that the cones at the Flower Garden Banks, in the summer, would be more steeply inclined than the sides of the banks. Therefore, the cones could not form. However, the strength of the stratification is so great that little vertical motion is possible as the flow encounters the bank.

In summary, from both theory and order magnitude estimates, one would expect the flow to diverge around the banks with a very modest vertical excursion (on the order of 10 m) on the point of the bank where the flow diverges. Weak vortices and lee waves (internal) probably form on the downstream side of the banks where the flow separates.

Observations

Several types of measurements carried out at the Flower Garden Banks over the period from January 1978 through July 1981 were specifically designed to study orographic effects. The results of these measurements, plus a completely serendipitous set, are consistent with the expectations developed in the last section. The flow is accelerated around rather than over the bank. Vertical excursions on the bank are probably limited to approximately 10 m by rotation, friction, and stratification.

The bottom current directions from velocity profiles taken in July 1979, and a two-day vector mean direction from the lowest meter on mooring 2 are shown in Figure 5.28. By October 1980 the PHISH system was being used. Near-surface (5 m) velocity vectors are shown in Figure 5.29, and the near-bottom (1 m up) are shown in Figure 5.30. It must be remembered that these are instantaneous vectors so they contain random fluctuations as well as the longer term mean signal. Notice, however, the tendency of the vectors to split around the banks on their western (upstream) side and converge on the downstream side. Near bottom, in the lee of the East Flower Garden Bank, there is some indication of a weak return circulation back toward the base of the bank.

Temperature data from some of the same stations shown in Figures 5.29 and 5.30, were used to construct a cross-section of the thermal structure on a line from the northwest to southeast of the East Flower Garden Bank (Figure 5.31). It shows that near-bottom isotherms are deeper on the upstream side of the bank than on the downstream side. This is probably due to centrifugal accelerations on the northwest side of the bank. The centrifugal acceleration would displace the dense cold waters away from the bank. The upper isotherms appear to be displaced upward a few metres on the northwest side of the bank with a sharp drop in the lee of the bank. This latter effect appears to be an internal lee wave which severely compresses the thermocline.

A similar survey around the East and West Flower Garden Banks taken in March of 1981, when the stratification was rather minimal, is shown in Figures 5.32 and 5.33. The velocity vectors at 5 m from the surface (Figure 5.32) appear to be responding to the presence of the banks, particularly at the East Flower Garden Bank. At 1 m from the bottom (Figure 5.33), the flow is sharply attenuated and a little more tangential to the isobaths on the banks. The flow in the lee of the East Flower Garden Bank appears to be weaker and less organized than that to the west of the bank.

In July 1981 another transect across the East Flower Garden Bank from the northwest to southeast was used to construct a thermal cross-section (Figure 5.44). This one also has transmissivity values on it. As usual, the flow was from west to east. In this case, the lower isotherms rise against the bank on

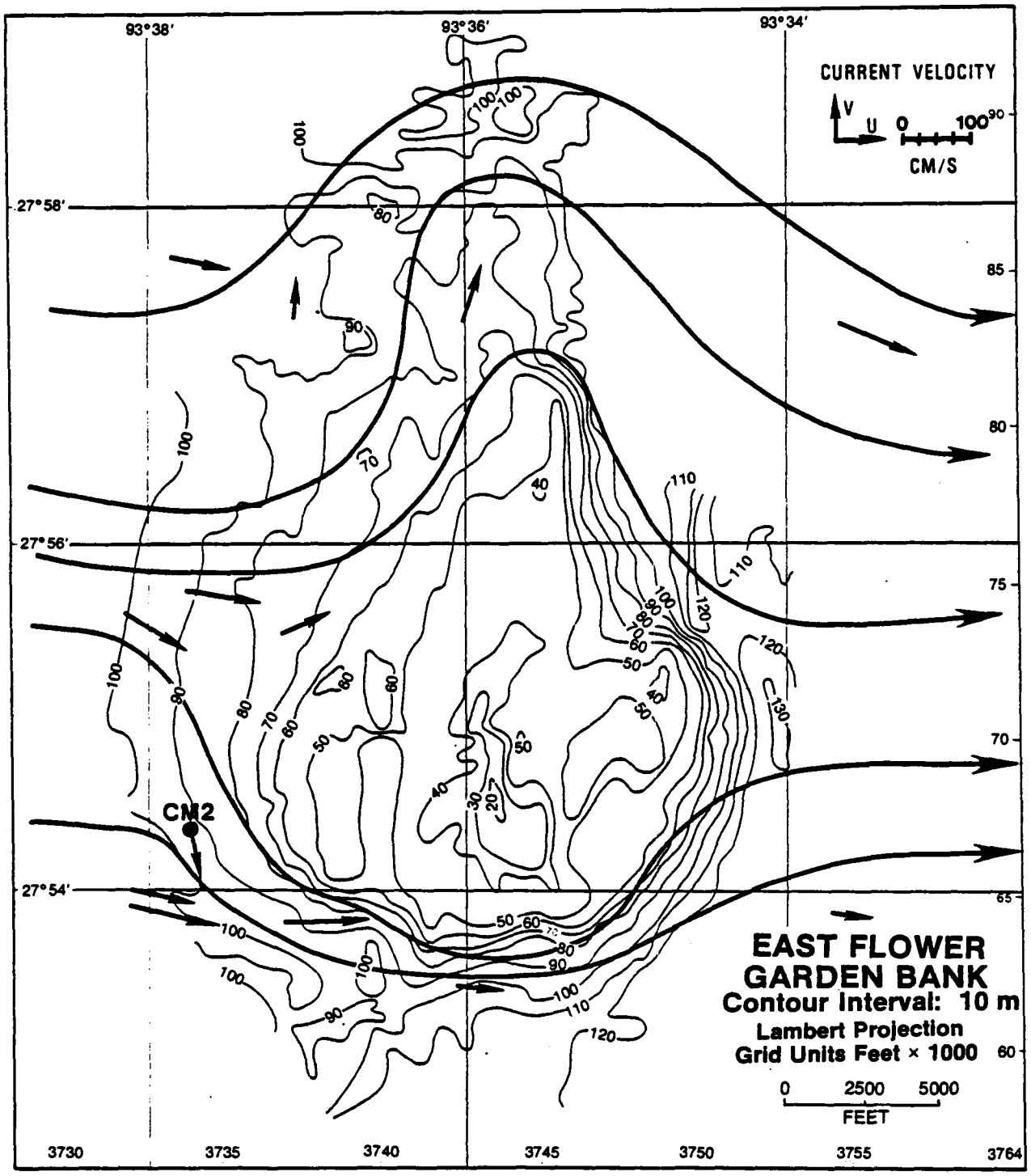

Figure 5.28 Bottom velocity vectors from all July 1979 stations plotted with directional sense only (no magnitude implied). The lines connecting stations of like depth are inferred streamlines. Mean directions for the lowest current meter for 16 to 17 July 1979 are also plotted and demonstrate the consistency of the two types of measurement.

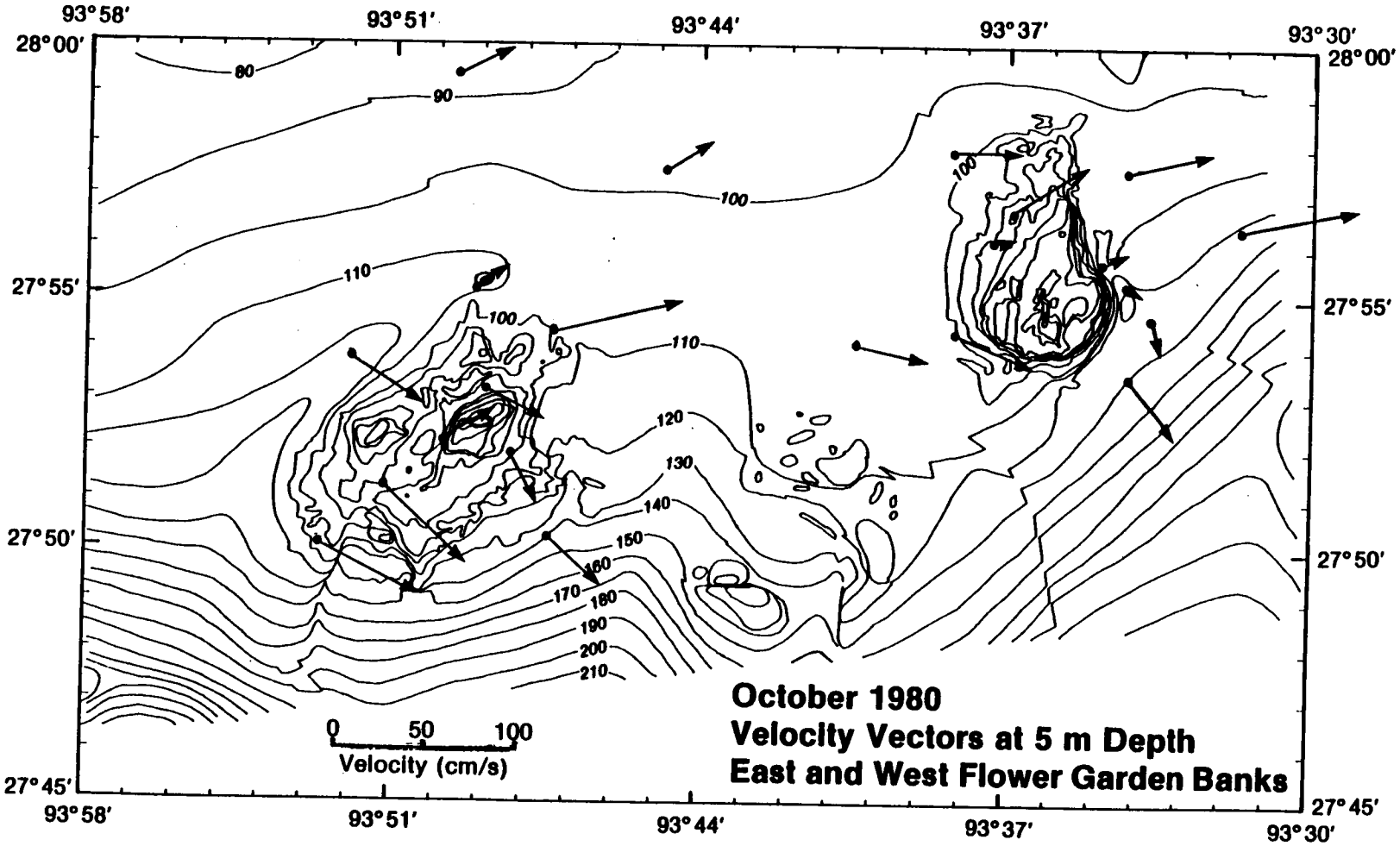

Figure 5.29 Horizontal velocity vectors at a depth of 5 m determined from PHISH stations taken on the October 1980 BALTIC SEAL cruise.

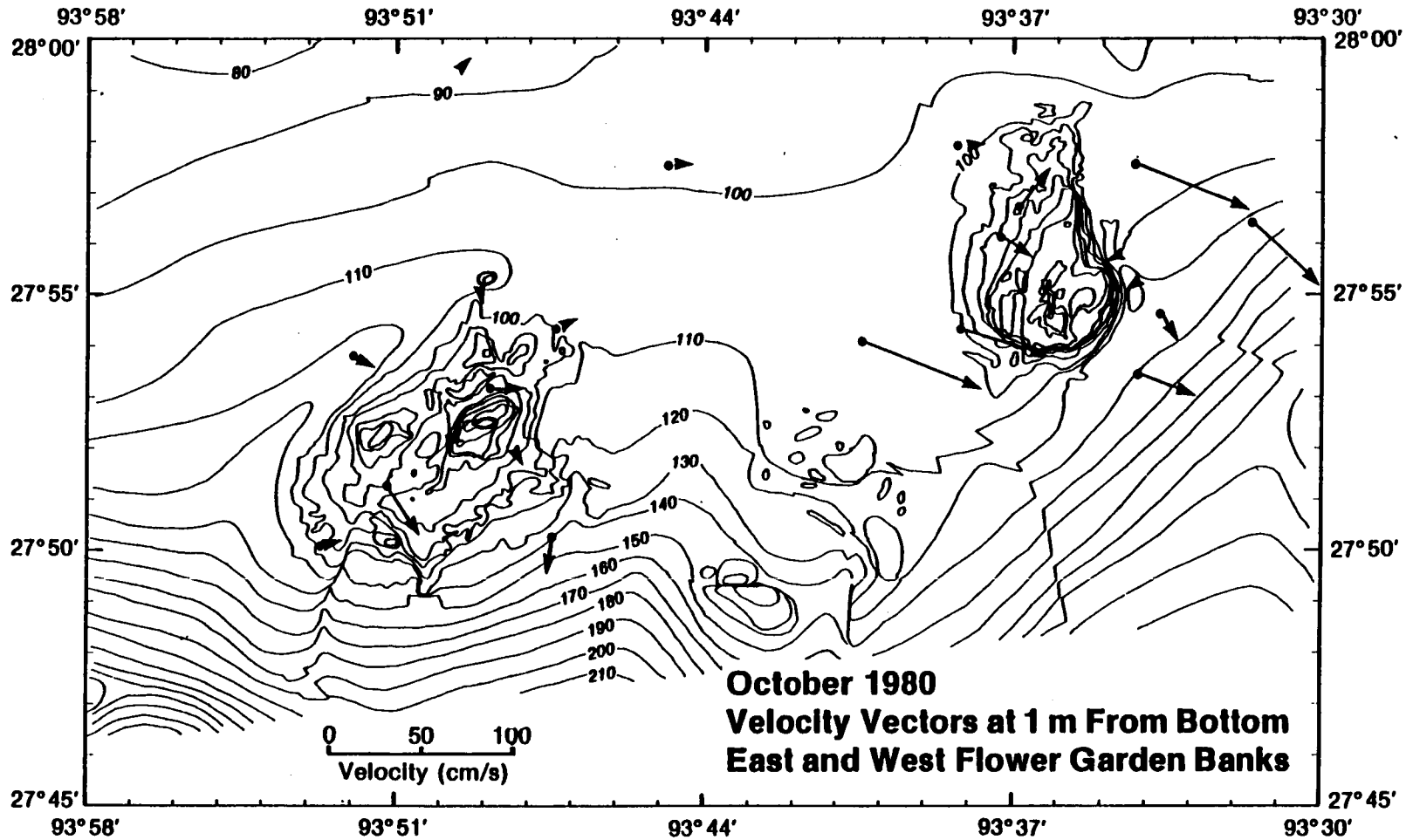

Figure 5.30 Horizontal velocity vectors at 1 m from bottom determined from PHISH stations taken on the October 1980 BALTIC SEAL cruise.

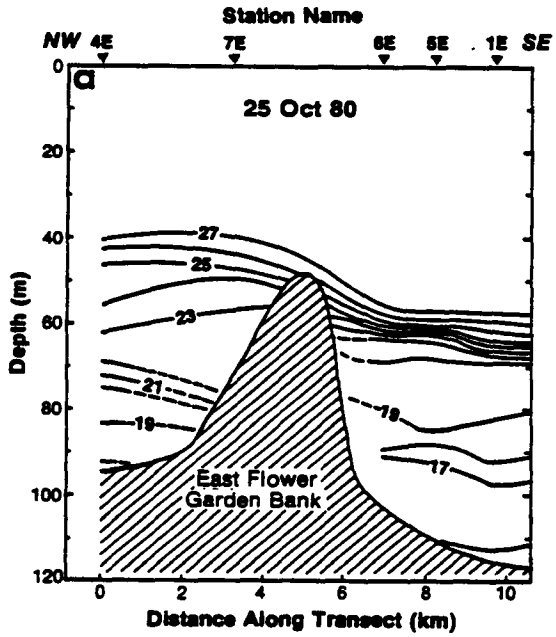

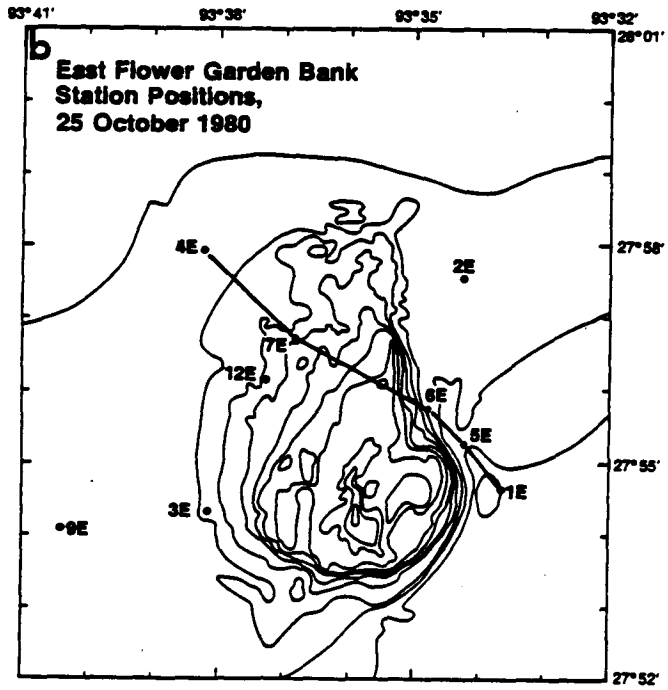

Figure 5.31 a) Vertical section of temperature from northwest to southeast across the East Flower Garden Bank. Stations were taken on 25 October 1980. b) Map of the East Flower Garden Bank showing locations of stations taken on the October 1980 cruise. The heavy line connects the stations used in the vertical section of Figure 5.31a.

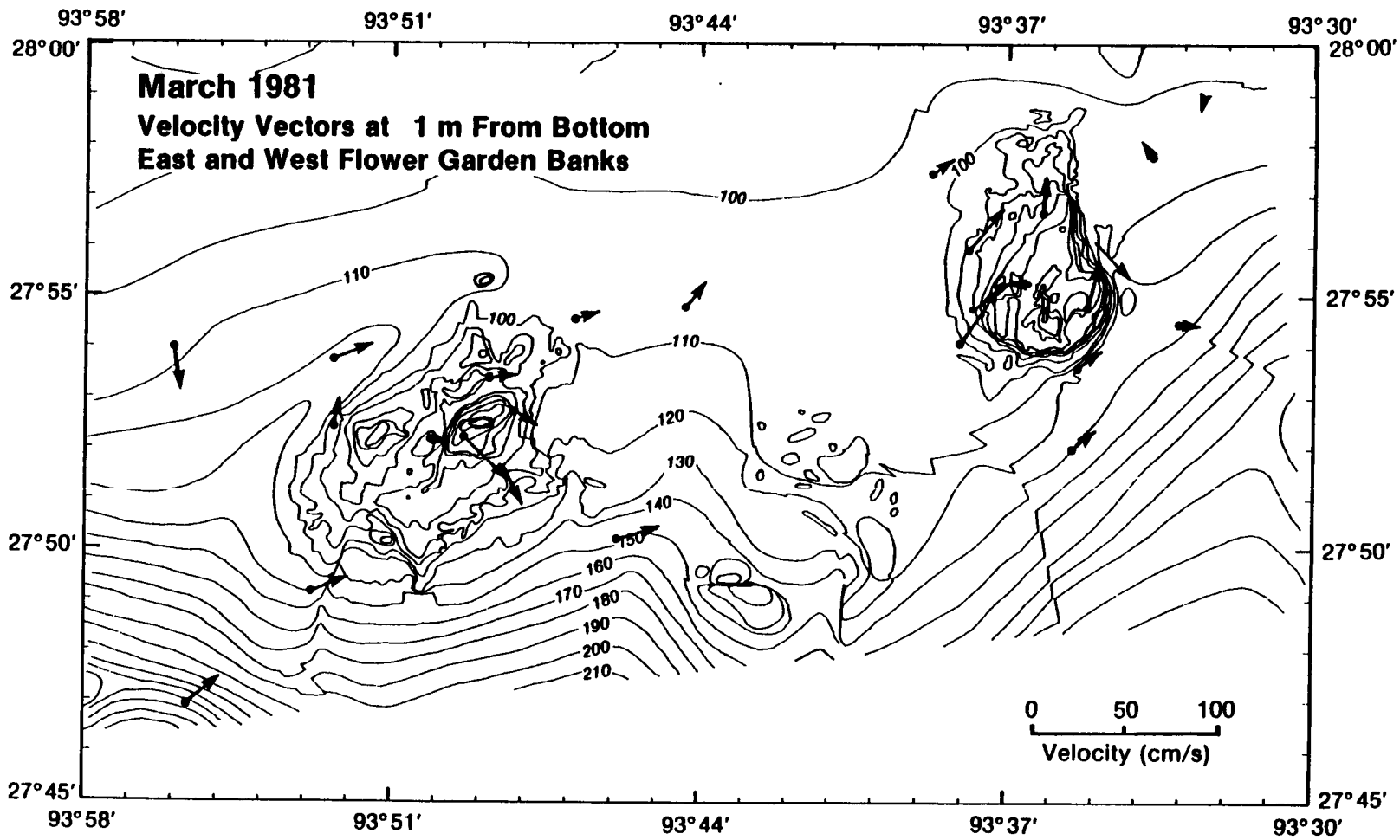

Figure 5.32 Horizontal velocity vectors at 1 m from bottom determined from PHISH stations taken on the March 1981 GYRE cruise.

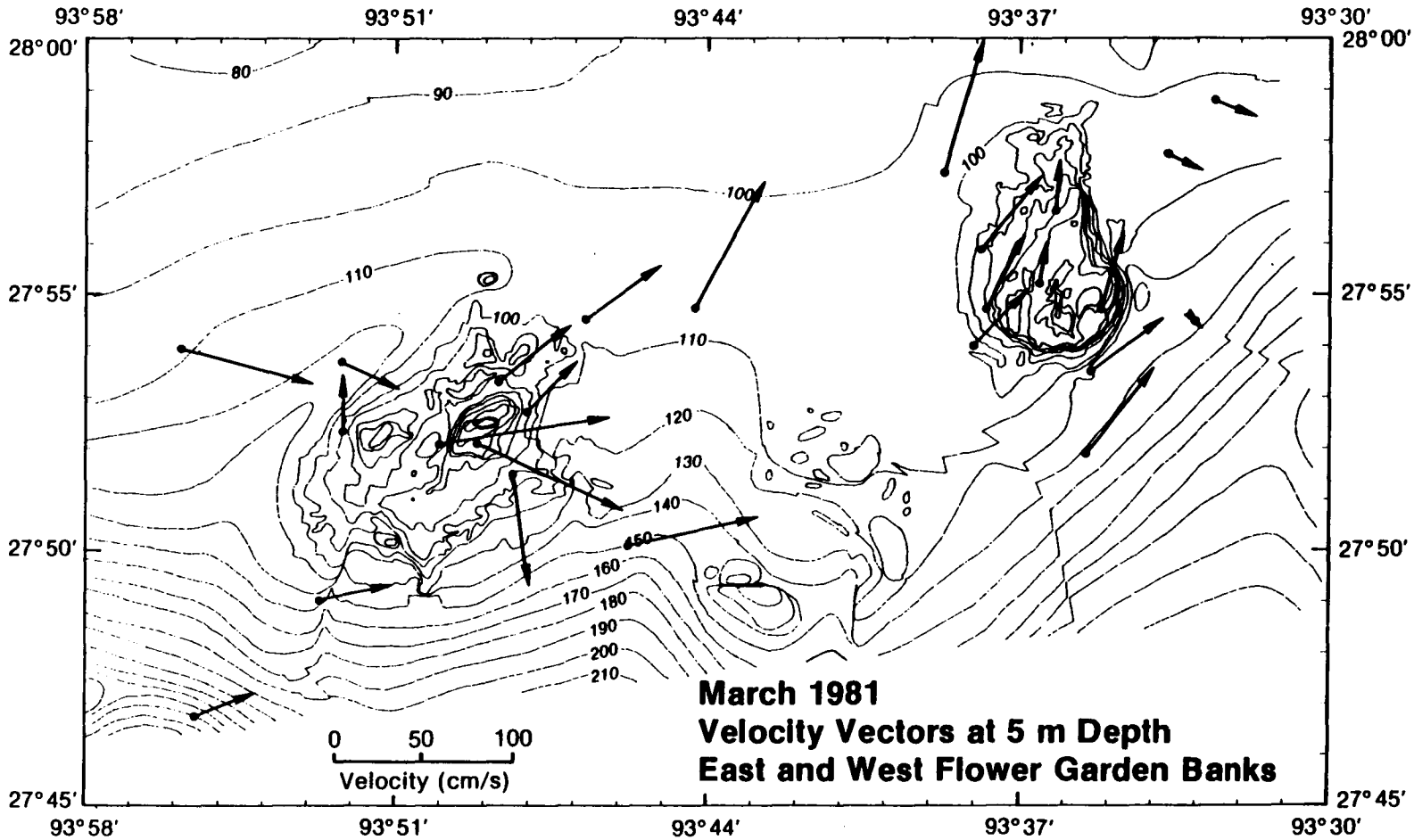

Figure 5.33 Horizontal velocity vectors at a depth of 5 m determined from PHISH stations taken on the March 1981 GYRE cruise.

the upstream side, but the upper isotherms, below 40 m, are depressed. Again, there appears to be a lee wave downstream of the crest of the bank. Very turbid water (< 40%/m transmissivity) is limited to ≥ 80 m depth on the upstream and ≥ 90 m downstream of the bank. Notice the plume of dirty water (< 40%/m transmissivity) between about 90 and 110 m depth on the southeast side of the bank. This appears to be turbid water carried from the bottom on the west side of the bank out across the deeper waters to the south and southeast of the bank.

Another indication of orographic effects generated by the banks is embedded in the time series current meter records. From each record the variance tensor $\bar{\bar{V}}$ was computed where

$$\bar{\bar{V}} = \begin{vmatrix} \overline{u^2} & \overline{uv} \\ \overline{vu} & \overline{v^2} \end{vmatrix}$$

u is the east-west velocity vector
v is the north-south velocity vector.
The single overbar indicates time averaging.

It has been shown that the coordinate axes can be rotated so that $\overline{uv}$ and $\overline{vu}$ become zero. At that orientation $\overline{u^2}$ is a maximum and $\overline{v^2}$ is a minimum. The axes at this orientation, θ, are known as the principal axes, and $\overline{u_o^2}$ and $\overline{v_o^2}$ are the characteristics. These can be computed as follows. The characteristics are the eigenvalues (λ) of the variance tensor, $\bar{\bar{V}}$, and are found from the determinant of

$$\begin{vmatrix} \overline{u^2} - \lambda & \overline{uv} \\ \overline{vu} & \overline{v^2} - \lambda \end{vmatrix} = 0$$

The orientation of the principal axis, θ, is

$$\theta = \frac{1}{2}\tan^{-1}\left(\frac{2\overline{uv}}{\overline{u^2} - \overline{v^2}}\right)$$

Monthly averages of the autocovariance $\overline{u^2}$ and $\overline{v^2}$ and the cross covariances uv were computed for all current meter records containing good quality data. From these values the following were found

1) θ, the orientation of the major axis of variance $\overline{u_o^2}$; θ = 0 is north.

2) $\epsilon = \overline{u_o^2}/\overline{v_o^2}$ is the ratio of the maximum to minimum variance, which is a measure of the ellipticity of variance. The greater the value of ε, the more strongly the

variance of the flow is aligned with the principal axis. The closer ϵ is to 1, the more incoherent the variance is with respect to direction.

Plots of θ versus ϵ were prepared for all moorings and all deployments. The plots for all of the meters on the first five deployments of mooring 2 (the mooring closest to the bank; see Figure 5.1) are shown in Figure 5.34; the plots for all meters on the last deployment appear in Figure 5.35. These were separated because the last deployment of mooring 2 was moved for the purpose of determining the effectiveness of topographic steering. On each plot, the orientation of the local isobaths is shown along with the angles subtended by the East Flower Garden Bank. In general, the records from shallow meters possessed much smaller ϵ values, indicating that the orographic effects, though still present, diminished upward. Near-bottom instruments recorded flow that was sharply polarized along the isobaths, as evidenced by ϵ values of over 12.

Table 5.5 lists the average direction $\overline{\theta}$ for each deployment at mooring 2, the standard deviation of the direction, θ, the orientation of the local isobath (θ isobath), and the difference between them $\Delta\theta$. Two records from shallow meters with small ϵ values were excluded from the averages because θ in such cases has little meaning. The $\Delta\theta$ varies from 5° to 24° but is always positive, meaning the variance is slightly to the right of the isobath, or away from the bank. Considering the location of the mooring, it is possible that this difference is caused by centrifugal acceleration.

For comparison, the θ versus ϵ for the other moorings are shown in Figure 5.35. Notice that at the other moorings the ϵ values were much smaller and less clustered about the orientation of the local isobaths. This is expected because of their greater distances from the banks, relative to mooring 2. What was not expected was the disinclination of the flow at any of these sites to go toward the banks. This is illustrated in Figure 5.36, which shows the range of orientations of the principal axis at each mooring, relative to the bottom topography.

In summary, both the station data and time series current meter data show that the flow goes around the bank rather horizontally, with only low amplitude vertical motions.

An unexpected confirmation of this hypothesis arose upon examination of side-scan sonar records from the East and West Flower Garden Banks. On each of these banks, the sediment in the Algal Nodule Zone and <u>Amphistegina</u> Sand Zone is heaped into giant sand or gravel waves. These waves have amplitudes of 1 to 2 m and wavelengths of 10 to 30 m. Orientation and location of these features are shown for the West Flower Garden Bank (Figure 5.37) and for the East Flower Garden Bank (Figure 5.38).

Formation of bedforms of this size and in sediment of this coarseness would require very high velocity flow. The gravel waves are most prevalent on the west side of both banks. This distribution, together with the orientation of the crests and asymmetry of their form, indicates that the flow forming them comes from the west. With a few exceptions, the crests of the bedforms are nearly perpendicular to the local isobaths. Those exceptions occur on the upstream side of the East Flower Garden Bank, where the flow bifurcates (Figure 5.38). South of this region the bedforms indicate southerly, isobath-parallel flow, and north of it they indicate northerly, isobath-parallel flow. On the West Flower Garden Bank (Figure 5.37), crests of the bedforms are parallel to the isobaths on the downstream (eastern) side of the bank, suggesting a separation point.

The significance of these features is that their formation requires exceptionally high velocities and their orientation is such that even during this extraordinary flow, the currents must remain essentially parallel to the isobaths.

In addition to deforming the mean flow field, it has been demonstrated (Baines and Davies, 1980) that the banks may trap long waves. Evidence of this at the Flower Garden Banks is given by the strong inertial signal in the bottom current meter records at mooring 2. It is only at this site, adjacent to the bank, that inertial oscillations are as strong near the bottom as they are in the upper water column. A segment of the current meter record from 5 m above the bottom at mooring 2 during Hurricane Allen is shown in Figure 5.39.

The very strong polarization of the flow along the isobaths, even as it oscillates in response to a hurricane, is clearly shown. Curiously, the temperature oscillations during this time have a period exactly one-half that of the currents. The vertical lines on Figure 5.39 run through the zero crossings of the velocity vectors and extend through the temperature record to show that these zero crosssings (two per cycle) correspond to temperature minima. These complex relationships are difficult to interpret with respect to the structure and propagation of the waves on the bank. It does appear, however, that these oscillations are concentrated on the slopes of the bank.

The accelerations which attend flow diverging around an obstacle, combined with the trapping of inertial oscillations on the slopes of the banks, should make bottom velocities on the bank surfaces significantly higher than velocities on the adjacent seafloor. Weak flow in the lee of the banks, particularly the East Flower Garden Bank, may contribute to the deposition of fine sediment on the seafloor there.

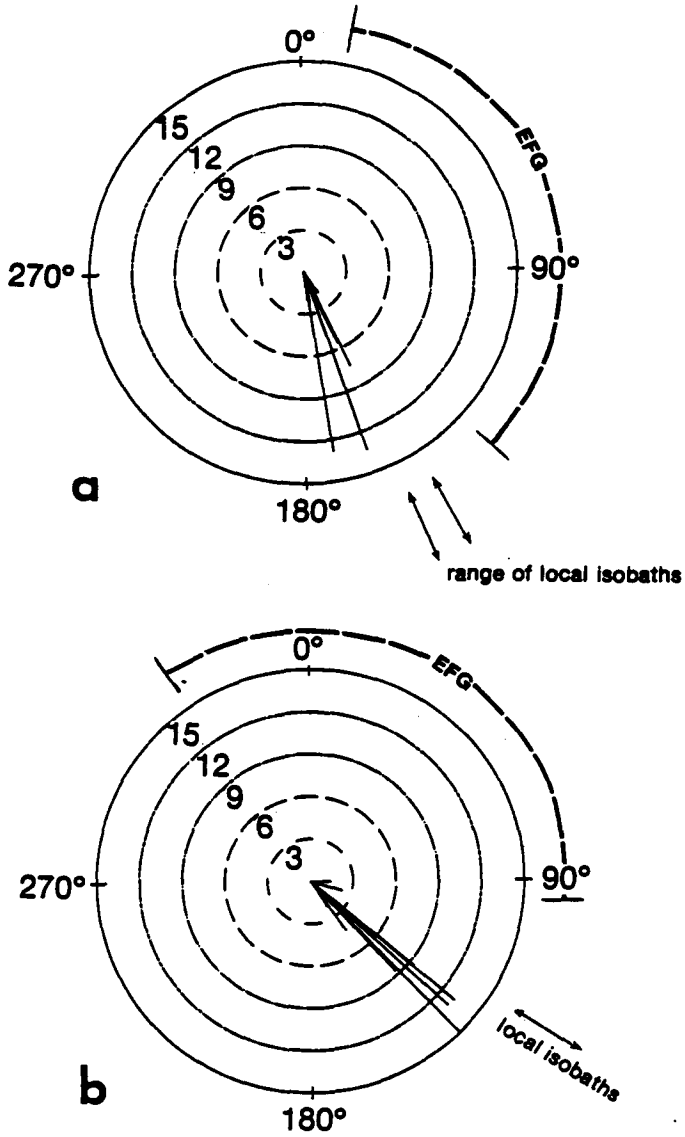

Figure 5.34 Ratio, ϵ, of the variance along the major axis to the variance along the minor axis, plotted in the direction, θ, of the major axis for (a) all meters on mooring 2 deployed before March 1981, and (b) all meters on mooring 2 for the March to July 1981 deployment.

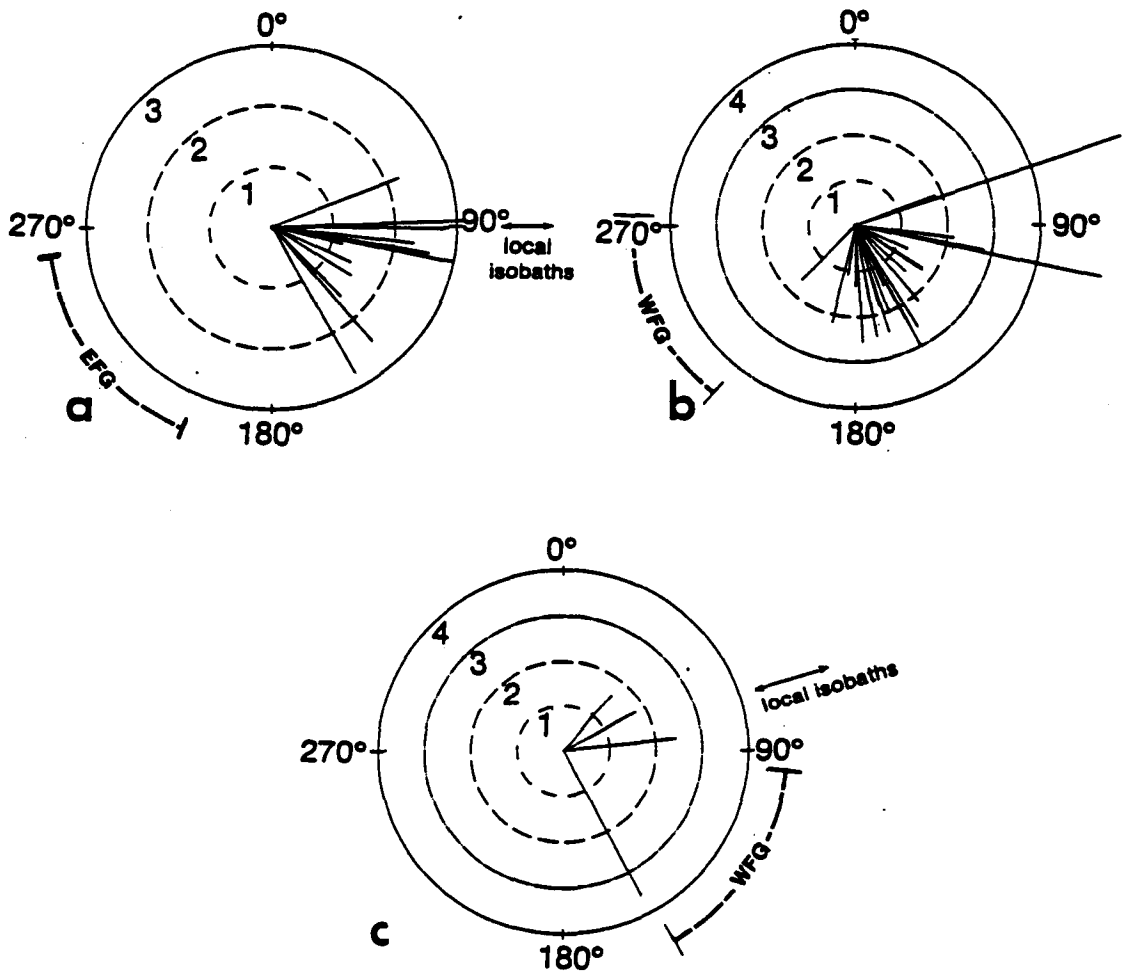

Figure 5.35 Ratio, ϵ, of the variance along the major axis to the variance along the minor axis, plotted in the direction, θ, of the major axis for (a) all meters on mooring 1; (b) all meters on mooring 3; and (c) all meters on mooring 4.

Table 5.5 Average Direction of Major Axis of Variance Compared to Local Isobath Direction

DEPLOYMENT	AVERAGE DIRECTION ($\bar{\theta}$)	LOCAL ISOBATH DIRECTION ($\theta_{isobath}$)	STD. DEV. OF DIRECTION	DIR. $\bar{\theta} - \theta_{isobath}$	NUMBER OF ESTIMATES
1	170.1	156.4	—	13.7°	1
2	166.4	149.4	7.14	17°	2
3	173.5	149.4	—	24°	1
4	157.0	152.0	3.7	5°	3
5	158.2	152.0	7.82	6°	6
6	136.9	122.8	6.9	14°	7

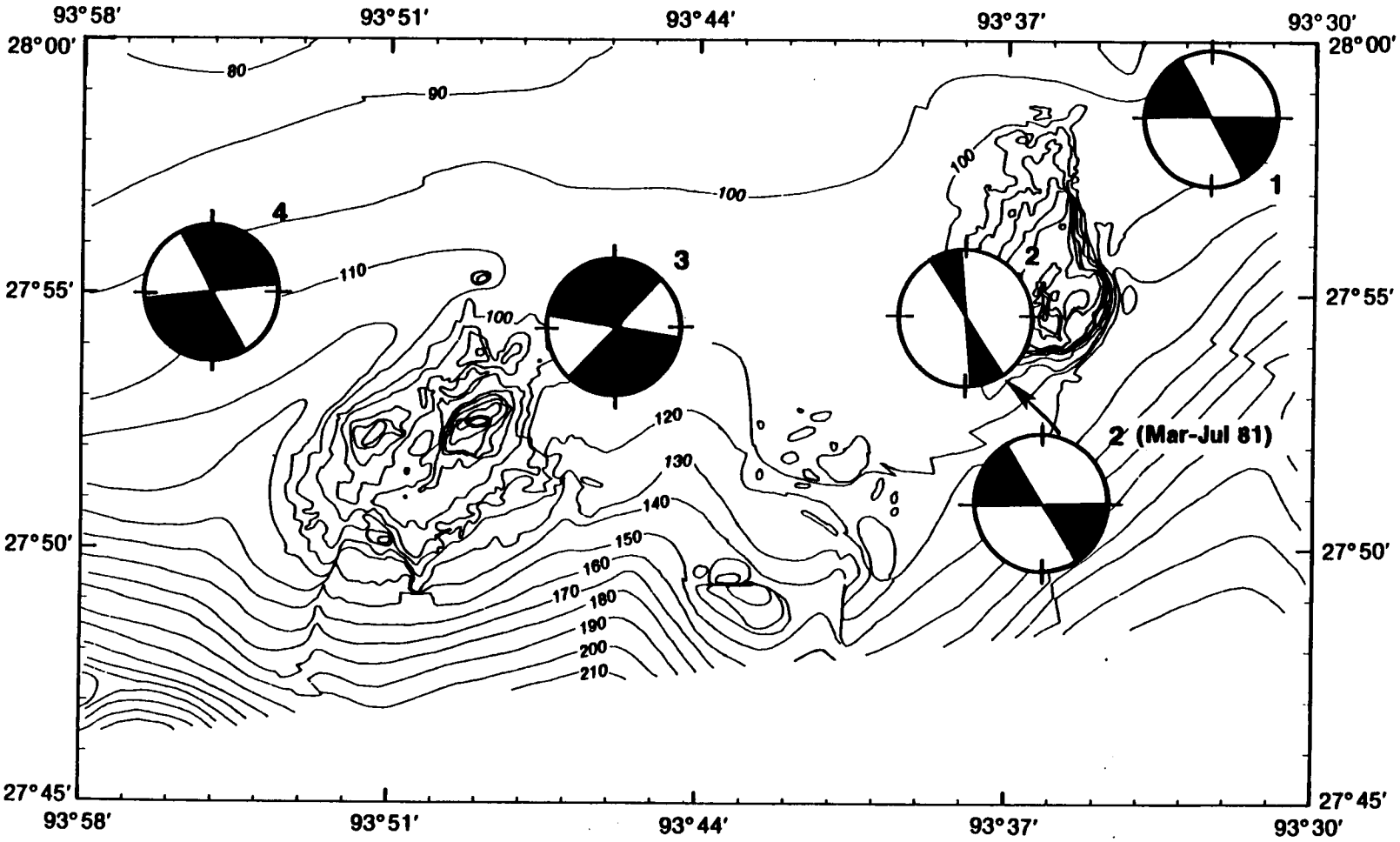

Figure 5.36 Shaded region in each circle shows the range of directions of the major axis of velocity variances for most one-month velocity segments at each mooring (see text for exceptions). Each circle is centered at the mooring position, except for the March to July 1981 deployment of mooring 2. The arrow tip indicates the position of mooring 2 during March through July 1981.

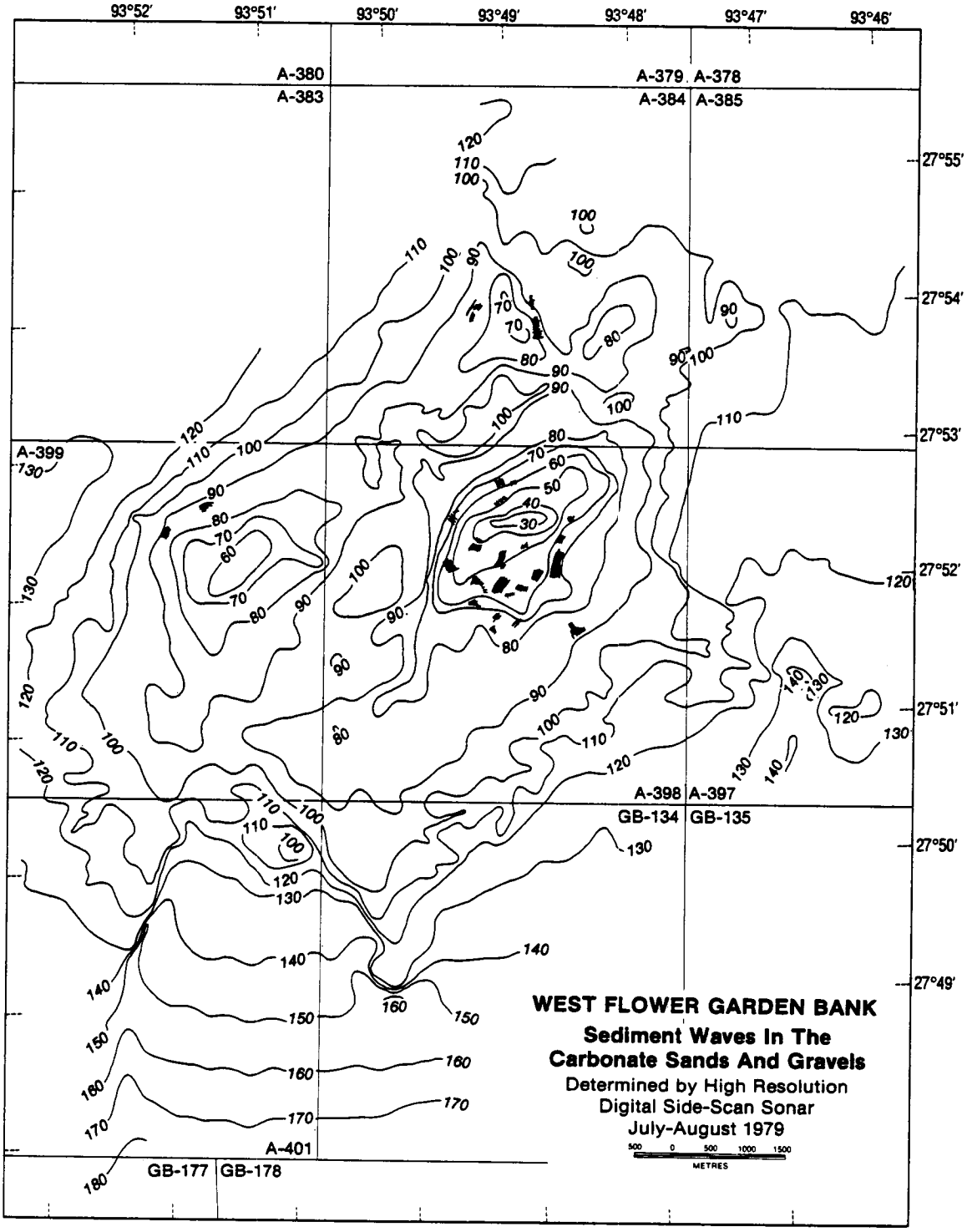

Figure 5.37 Large scale bedforms on the West Flower Garden Bank as determined from a digital side-scan sonar mosaic. Wave lengths and crest lengths are plotted to scale.

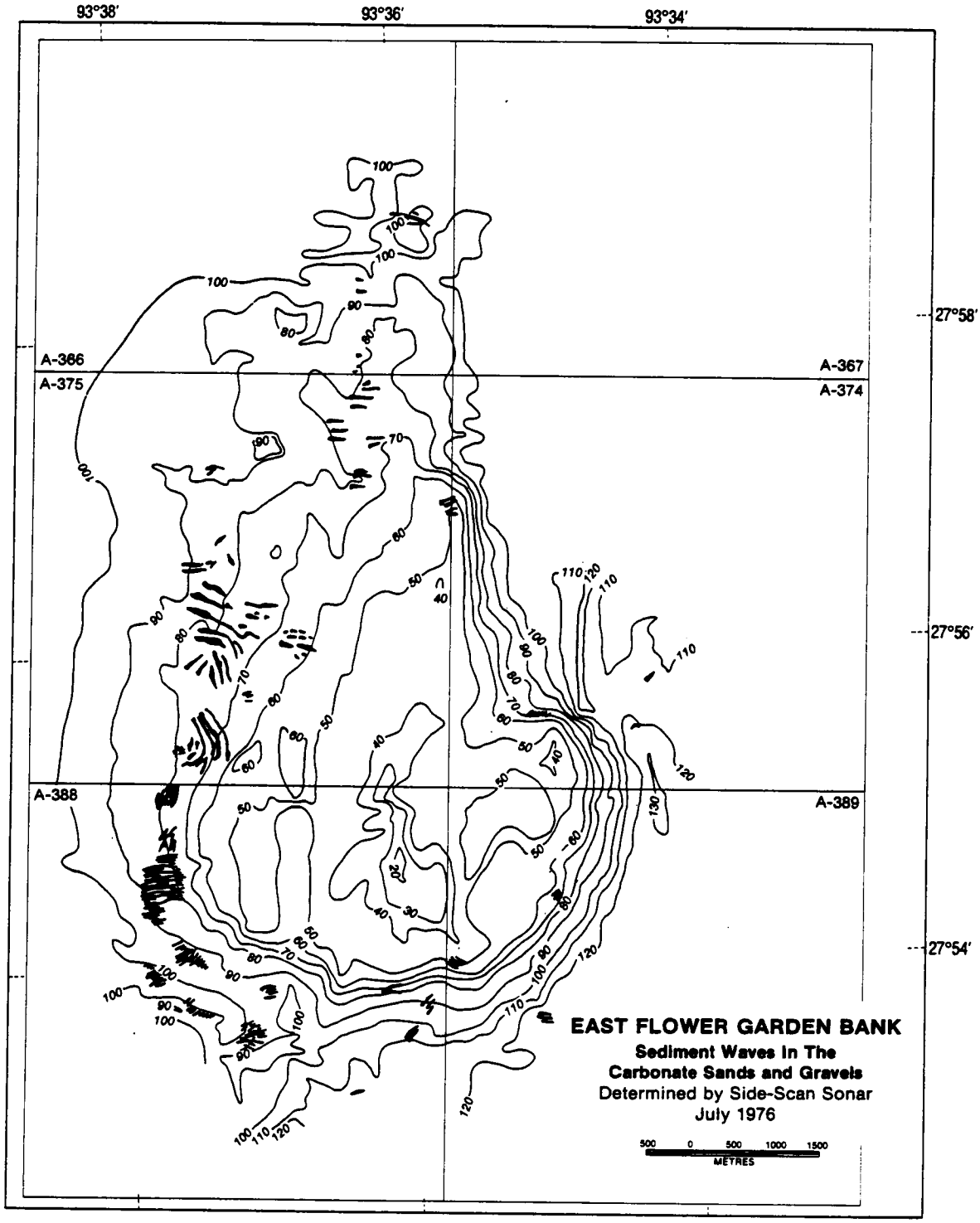

Figure 5.38 Large scale bedforms on the East Flower Garden Bank as determined from side-scan sonar records. Original interpretation by Stephen Viada. Wave lengths and crest lengths are plotted to scale.

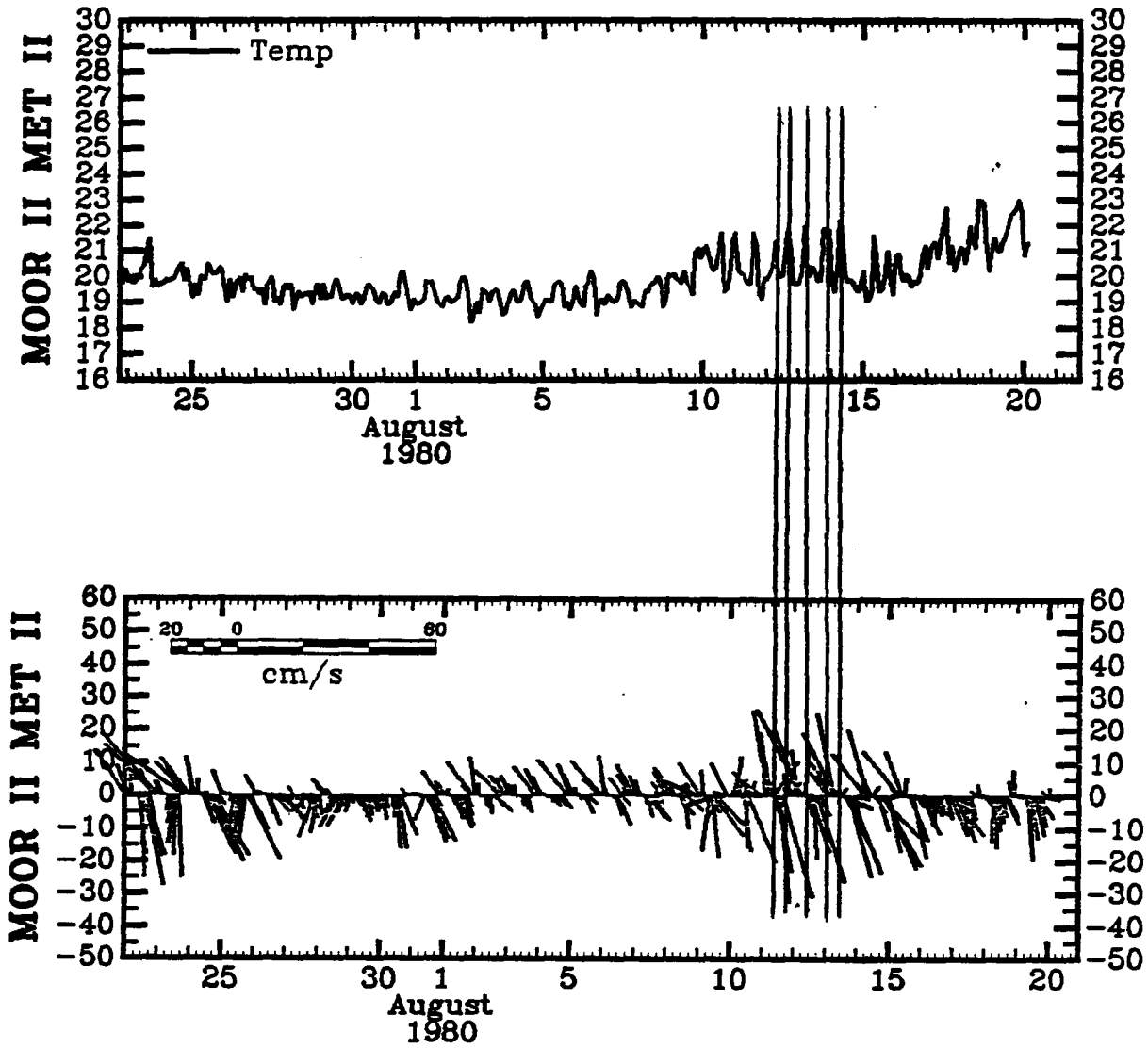

Figure 5.39 Time series of temperature and horizontal velocity from meter 2 of mooring 2, located near the southwest edge of the East Flower Garden Bank at 5 m from the bottom. Hurricane Allen travelled through the Gulf of Mexico during the period of this record (7-10 August 1980).

BOUNDARY LAYERS AND SUSPENDED SEDIMENT

When a viscous fluid flows over any bounding surface, the molecules of the fluid adhere to those of the bounding surface so that on that surface the relative velocity of the fluid becomes zero. This is known as the "no slip" condition. Beyond the immediate bounding surface, the fluid is retarded because of internal friction and the presence of the boundary. At some distance, δ, the flow is unaffected by the presence of the boundary and may, for practical purposes, be considered inviscid. Within the distance δ from the bounding surface, the dynamics of the flow are dominated by viscous and turbulent effects. This zone of δ thickness is known as the boundary layer.

In order to facilitate a discussion of boundary layers it may be useful to introduce the jargon of boundary layer research.

Viscosity (μ) - the internal friction of a fluid, caused by molecular attractions, which produces a resistance to flow or deformation of the fluid. The unit of measure is the poise (1 gm cm^2/s). Viscosity is a characteristic of the fluid.

Turbulent or Eddy Viscosity (η) - the internal friction of a fluid, caused by the presence of turbulence, which produces a resistance to flow or deformation of the fluid. Its magnitude depends on the intensity of turbulence present, but its value is always orders of magnitude greater than molecular viscosity (μ).

Shear Stress (τ) - the force causing two contacting surfaces (or layers) to slide upon each other, moving apart in opposite directions parallel to the plane of their contact. For example, if you had a deck of playing cards neatly stacked on a table, then you placed your finger in the middle of the top card and pushed horizontally, parallel to the table top, you would be exerting a "shear stress" on the cards.

In order to demonstrate the relationship among these variables, consider a small element of fluid at the bottom of a container in which all the fluid is still (see below).

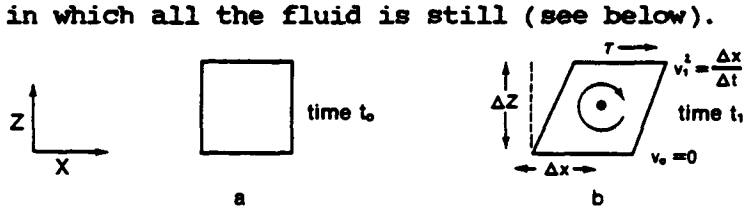

Let t_o be the initial time. Now assume that something far from the bottom sets the fluid in motion parallel to the bottom. The internal friction (viscosity, μ) causes the molecules of fluid to stick together so that those at the top of the element of fluid start to move. But the molecules at the bottom stick to the

container and do not move. Now, over a period of time Δt, the top of the element of fluid, will move a distance Δx, but those at the bottom will not have moved at all. However $\Delta x/\Delta t = v$, a velocity. So, at the top of the fluid element the velocity is $v_1 \neq 0$, and at the bottom $v_o = 0/\Delta t = 0$. Therefore we have a vertical "velocity gradient" where $v_1 - v_o = \Delta v$ and the gradient is $\Delta v/\Delta z$. The force required to make the top of the fluid element move relative to the bottom is the "shear stress" (τ).

Now we can express the relation among these variables mathematically

$$\tau = \mu \frac{\partial v}{\partial z} \qquad (1)$$

From this one can understand how viscosity represents a resistance to flow or deformation because, if τ is held constant and μ is increased in value, $\partial v/\partial z$ must decrease. That is, deformation ($\Delta x/\Delta z$) must decrease.

It should also be clear that for a given viscosity, the application of a large shear stress will cause a large velocity gradient, and the deformation of the fluid element will become so extreme that it will be torn apart. And that is exactly how turbulence begins. Notice that the shearing of the fluid element introduces a rotation about the center of the element. Therefore when the velocity gradient is high, small elements of fluid with a large v are rotated down, and small elements of fluid with a small v are rotated upward. The result is that, in short order, fluid at height Δz is slowed down by the addition of fluid elements with low velocity, and fluid close to the bottom is accelerated by addition of high velocity water from above. Therefore the velocity difference, Δv, per unit height, Δz, is decreased by turbulence. For the same shear stress τ, the effect of turbulence is to reduce the velocity gradient and increase the apparent viscosity.

This apparent viscosity is called the "eddy" or "turbulent" viscosity (η) and the turbulent equivalent of (1) is

$$\tau_t = \eta \frac{\partial v}{\partial z} \qquad (2)$$

τ_t is sometimes referred to as a Reynolds stress.

<u>Diffusion</u> - the transport or mixing of a substance <u>through</u> a medium (like water, for example). The substance diffused may be contaminants, such as sedimentary particles, or some solute. It may, on the other hand, be something like heat, kinetic energy, or momentum that is being diffused. Diffusion always goes "down" the concentration gradient of the diffusing substance; that is, diffusion goes from high concentration toward low concentration. As with viscosity, there is molecular

diffusion and turbulent diffusion. Molecular diffusion is due to the random motions of molecules. Because the length scales of these motions are very small and their speed finite, molecular diffusion is very slow.

Turbulent diffusion, however, proceeds much more rapidly because the motions have much larger length scales. In order to develop an intuitive feel for the difference between the two, remember that we diffuse cream and sugar in coffee by stirring it and thereby inducing turbulence. If we waited for molecular diffusion to accomplish the mixing, the coffee would grow cold long before it were accomplished.

<u>Advection</u> - the transport of a substance from one location to another <u>in</u> the medium. The direction of transport is independent of gradients but dependent on the direction of flow.

The difference between diffusion and advection may be seen in the example of dye poured on the sea surface. Turbulent diffusion causes the patch of dye to grow in size but diminish in concentration, whereas the mean flow advects the patch away from its point of introduction. So it is that sediment is <u>diffused</u> up from the seafloor by turbulence when the shear stress is sufficiently large to cause erosion. However, the sediment is <u>advected</u> from the site of erosion to the site of deposition by the horizontal flow.

In a nonrotating system, the velocity profile is give by:

$$v(z) = \frac{u_*}{\kappa} [\ln (z/z_o)]$$

where $v(z)$ is the horizontal velocity at a height, z, above the boundary.
$u_* = (\tau/\rho)^{1/2}$ is the friction velocity
κ is the von Karman constant, assumed to be 0.4
z_o is a characteristic length scale of a rough boundary, it is the distance above the mean bottom at which $v(z)$ goes to zero.

This is the classic logarithmic velocity profile. The two important variables in this equation are u_* and z_o. The u_* increases with increasing τ. That, in turn, increases with increasing intensity of turbulence. The rougher the bottom is, the larger z_o is and the farther from the wall the velocity is retarded.

Stratification can also affect the boundary layer thickness by extinguishing turbulence. The measure of the strength of the stratification is typically the Brunt-Vaisala frequency (N). It is the frequency at which a particle, displaced from equilibrium and released, would oscillate about its equilibrium position.

Such a particle would act just like a pendulum, first overshooting the equilibrium position as it fell under the acceleration of gravity, then rising past the equilibrium surface on the way up because of buoyant forces. The Brunt-Vaisala frequency (N) is given by:

$$N^2 = -\frac{g}{\rho_o}\frac{\partial \rho}{\partial z}$$

where ρ = density
g = gravitational acceleration.

Remember that energy is required to lift the particle above equilibrium or push it down. The larger the density gradient, the more energy that is required to move the particle vertically. Also remember that in turbulent flow vertical motions are induced by rotation of water parcels under the torque of velocity shear. If the turbulence is very energetic, it will overcome the buoyant forces and mix the stratified water. But, if the stratification is very strong, the turbulence will not be energetic enough to displace the water particles, and the turbulence will be extinguished. The measure of these competing forces is the Richardson number (Ri)

$$Ri = \frac{N^2}{(\partial v/\partial z)^2}$$

It has been found that at a Richardson number of about .25 turbulence is extinguished. If Ri is smaller, it means that $\partial v/\partial z$ is large relative to buoyancy, and turbulence will mix the stratified water. If Ri is greater than .25 it means the N is large relative to the shear forces.

Consider the relation between N and the velocity gradient in the boundary layer of an energetic but stratified flow . At the initial time, the density gradient $\partial \rho/\partial z$ would be constant throughout the boundary layer. Near the bottom $\partial v/\partial z$ tends to be very large but decreases upward to zero at the level of the free stream. Therefore, near the bottom Ri tends to be small and the turbulence mixes the water, rendering its density intermediate between that at the bottom and that at the top of the mixing layer. But that intermediate value is greater than the density of the water originally just below the top of the mixing layer. The density gradient at the top of the mixing layer therefore increases. This continues upward from the bottom until the declining velocity gradient and increasing density gradient reach the point where Ri becomes greater than .25. Then the turbulence is extinguished and no more mixing takes place. That also extinguishes turbulent diffusion out of the bottom boundary layer.

The effect of stratification, then, is to compress the boundary layer by extinguishing turbulent diffusion of momentum (and anything else) at the top. This effectively caps the boundary layer.

If the flow is geostrophic, the boundary layer must adjust both the relative speed and the angular velocity of the fluid to that of the bounding surace. Such a layer is called an Ekman boundary layer. It consists of two parts, an upper part in which the velocity vectors rotate counterclockwise with depth (to the left of the geostrophic velocity [Vg] when looking downstream) and a lower part in which the speed is attenuated logarithmically with no additional angular shearing. According to Weatherly (1972) the thickness of the whole layer is $h = \kappa u_*/f$ and the log layer thickness is

$$\delta_{ln} = 2u_*^2/(f|Vg|).$$

The angular shearing, α, is given by $\sin^2\alpha = A^2(u_*/|Vg|)^2$, where $A^2 = 20$.

However, Weatherly (1972) observed that most of the veering in his experiment did take place in the log layer. He also said that the effect of stratification is to compress the Ekman layer.

Particularly for high velocity flows, the boundary layer on the surface of the banks should not be an Ekman layer. The reason for this is that the flow becomes ageostrophic on the banks because of inertial (centrifugal) accelerations. Also, on the upstream side of the bank, the water encounters the banks suddenly so that the boundary layer is initiated on the leading edge of the bank. The bottom boundary layer is not, therefore, fully developed over the entire surface of the banks.

From three dye experiments carried out on the banks between 49 and 75 m depth it appears that the boundary layer flow did not fit the classic logarithmic profile. The average velocities at three distances above the bottom are shown in Table 5.6.

Locations of the dive sites are shown in Figure 5.40. The failure of these boundary layer velocity profiles to assume the classic logarithmic form is probably due to several factors. The theory assumes that the flow is steady, yet it is clear that the velocity at 30 m above the bottom increased by over 4 cm/s in the four hours between dives D80-17 and D80-18. The bottom at these sites is hydrodynamically rough and inhomogeneous. Algal nodules covering the surface vary from the size of a green pea to that of a grapefruit. Also, the gravel waves introduce yet another scale of roughness. It may well be, therefore, that turbulence due to each scale of these roughness elements is superimposed on the others so that no averaging period will be appropriate for all scales.

At any rate, the reduction of the flow velocity from 15 cm/s to zero over just 30 cm should exert very large stresses on the bottom. This would account for the sphericity of the algal nodules and the transport of sand sized material (Amphistegina tests) out of this zone. Accumulation of silt and clay in such an environment would be out of the question.

Assuming that the boundary layer on the open shelf at the base of the banks is less complicated and using the formulae of Weatherly (1972) to estimate the thickness of the logarithmic layer, one would obtain the following. From a dye emission experiment in 98 m of water it was estimated that u_* was on the order of 0.3 cm/s in a flow that averaged 27 cm/s at a depth of 61 m. From these values, δ_{ln} should be on the order of 95 cm and angular shearing, α, should be on the order of 3°. If the actual velocity were really 15 cm/s just outside the boundary due to baroclinicity δ_{ln} would have been 1.7 m and α would have been about 5°. The Ekman layer thickness h for either case would have been approximately 17 m.

The method of Kundu (1976) was used to compute the mean angular difference between the two meters closest to the bottom on moorings 2 and 3. The results are shown in Table 5.7.

At mooring 2 the angular difference between the two meters is rather large and in the wrong sense for Ekman veering. The lower instrument recorded flow with a clockwise downward spiral. This is undoubtedly due to centrifugal accelerations in the bottom boundary layer (BBL) as the flow accelerates around the East Flower Garden Bank (see Figure 5.1 for locations).

The records from mooring 3 during both deployments rotate in the correct sense for Ekman veering, but they too could be biased by centrifugal accelerations around the northeastern side of the West Flower Garden Bank. The possibility that this veering at mooring 3 is at least partly Ekman type turning cannot be dismissed, however.

The estimates of δ_{ln} and h suggest that for all deployments none of the instruments was in the log layer and only those within 10 m of the bottom were likely to have been in the Ekman layer. This is somewhat reassuring because the mean monthly vectors (Figure 5.13) at mid-depth are oriented just south of east. An Ekman BBL flow under these vectors should turn counterclockwise with depth. However, the instruments 11 to 18 m above the bottom recorded flow that was rotated clockwise, or more southerly. In view of the thinness of the Ekman BBL, this counterclockwise rotation must be attributed to the baroclinicity of the flow rather than some peculiarity of the BBL flow.

The thickness of isohaline and isothermal mixed layers at the bottom is sometimes used to estimate the thickness of the BBL. That is a risky business on a sloping boundary where mixed layers may be stacked by oblique offshore advection. However, all of the

Table 5.6 Boundary Measurements at West Flower Garden Bank

MEASUREMENTS	DIVE		
	D80-17	D80-18	D80-20
Depth (m)	49	50	75
Bottom Type	Algal Nodules	Algal Nodules	Algal Nodules
Mean Flow Direction	150°	140°	115°
Mean Speed (cm/s)/ Height of Emitter (cm)	14.5/130	15.9/130	16.6/150
	12.1/80	15.7/80	16.5/90
	10.8/30	15.1/30	15.6/30
Probability that velocity is independent of height above bottom	.0001	.06	.03

Table 5.7 Measured Angular Shearing in the Bottom Boundary Layer

Moorings	Meters	Dates	Depths(m)	Angle α
2	2 and 3	Jul-Sep 79	94/100, 96/100	-14.5°
3*	3 and 4	Oct-Dec 80	90/101, 97/101	+15.1°
3*	3 and 4	Mar-Jul 81	91/103, 97/103	+ 5.7°

*Records were low-pass filtered first to remove inertial and higher frequencies.

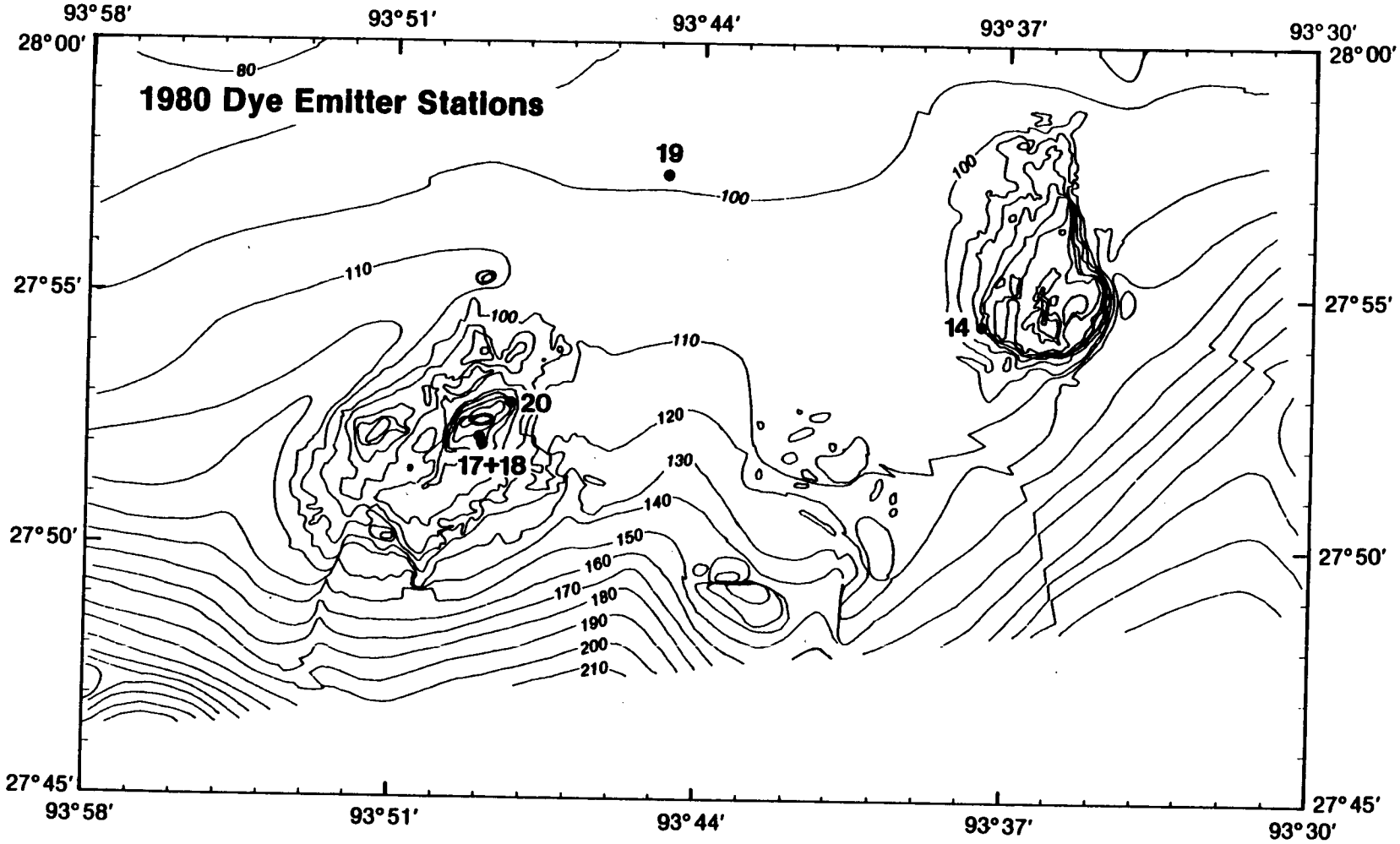

Figure 5.40 Location of October 1980 submersible dive stations where dye emission experiments were made.

stations taken in the vicinity of the Flower Garden Banks on the October 1980, March 1981, and July 1981 cruises were examined for bottom mixed layers. In October and July, fewer than 40% of the stations had bottom mixed layers. The average thickness in July and October was aproximately 6 m, with a standard deviation of 4.1 m in October and 3.4 m in July. In March, 46% of the stations had a bottom mixed layer. The average thickness was 10 m ± 5.1 m. A total of 73 stations were taken during these three surveys.

All but three of the March stations with thick bottom mixed layers (≥ 10 m) were taken on or within one kilometre of the banks. These thickened bottom mixed layers appear to owe their existence to orographic effects rather than increased turbulence and mixing at the bottom. These effects include convergence, baroclinic adjustments to centrifugal accelerations, and bottom intensification of the internal tides and inertial oscillations (I.O.). Michael Carnes (in McGrail et al., 1982) estimated that the I.O.'s at mooring 2, following Hurricane Allen, caused the near-bottom isotherms to oscillate over a vertical distance of 10 to 15 m.

Station 10S (Figure 5.41) from the March survey exemplifies this thickening of the bottom mixed layer. The station was taken on the western slope of the East Flower Garden Bank (Figure 5.7) during a period of strong flow from the southwest. Flow at that location would have been undergoing considerable acceleration (V^2/r) as it encountered the bank. Using 30 cm/s for V and 4.5 km for the radius of curvature yields 2×10^{-3} cm/s^2. The Coriolis acceleration (Vf) for the same velocity flow at this location would have been 2.1×10^{-3} cm/s^2.

A comparable station from the July survey is C2 (Figure 5.41), which was taken on the southwest slope of the East Flower Garden Bank (Figure 5.8). Stations 10 and 11 (Figure 5.42) were taken on either side of C2 but approximately 7.5 and 8 hours later. Notice that neither of these stations have thick bottom mixed layers. Figure 5.43 shows a cross-section of stations 9 through 12, including C2, which runs from southwest toward the northeast (Figure 5.9). It is not clear whether the eight-hour difference in time from C2 to 11 resulted in sampling at different phases of the internal tide or whether orographic effects account for the thickening of the bottom mixed layer. However, local increase in turbulent vertical mixing can be ruled out altogether because that would not have caused the downward flexure of the isotherms in the lower thermocline and it would not have been restricted to this one location.

The bottom mixed layer in station 195 (Figure 5.44) of the March survey is more in line with the scale of δ_{ln} expected from the estimates of 1 to 2 m made above. This station is well away from the influence of the banks so that it is likely that the bottom mixed layer sampled here is due to turbulent mixing in the boundary layer. Notice the sharp transmissivity gradient in the

mixed layer. It suggests active resuspension and upward diffusion of sediment from the bottom that would be commensurate with such mixing.

Station 5W (Figure 5.44) from the October 1980 survey was taken about eight kilometres north of the West Flower Garden Bank (Figure 5.6) and should have been beyond the influence of the bank. The water within two metres of the bottom is not completely isothermal, but the influence of mixing is clearly present. Again the transmissivity spike in this layer implies active resuspension and upward diffusion due to the turbulence in the bottom boundary layer.

Many of the stations taken during these cruises have steplike structures in their near-bottom thermal structure which are associated with increased turbidity. An excellent example of this is station 8E (Figure 5.45) of the October 1980 cruise. This association strongly implies that these steps are boundary layers which have been separated from the continental shelf upslope and advected out over deeper water. This conclusion is consistent with the southwest near-bottom flow, which is obliquely cross-isobathyal. The location of this station is shown in Figure 5.6.

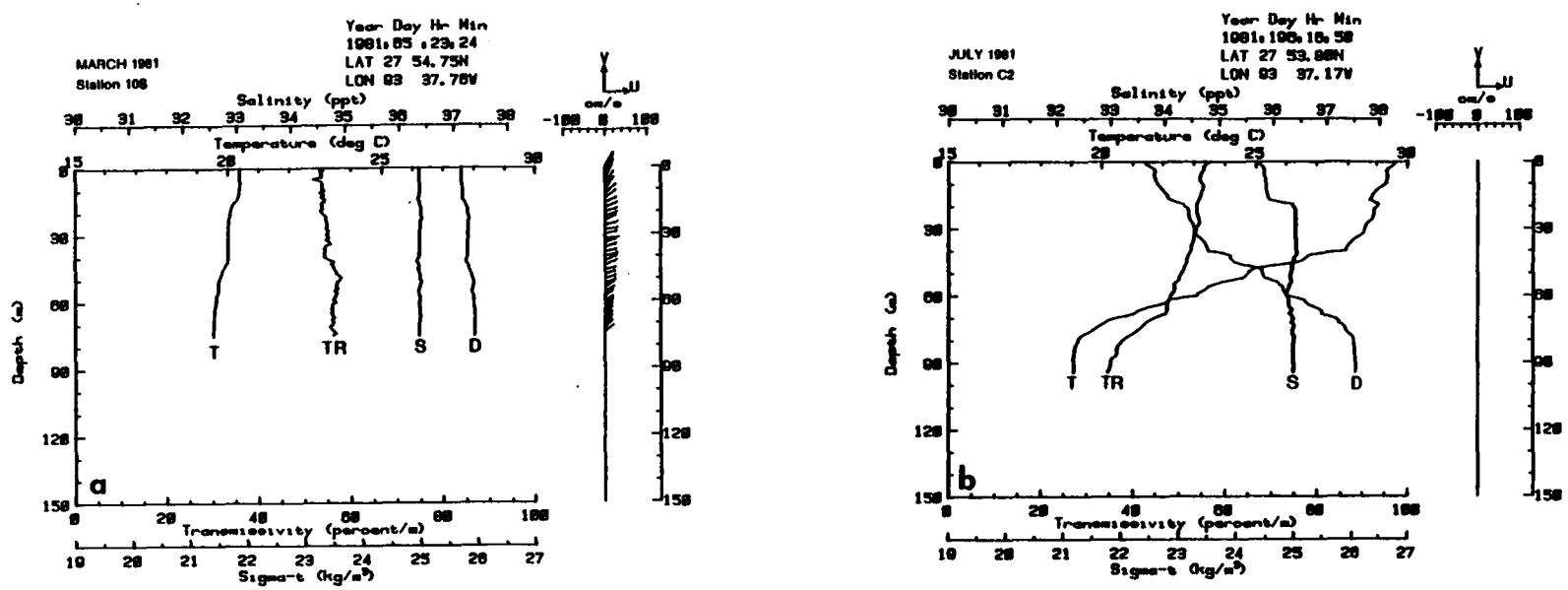

Figure 5.41 Profiles of transmissivity, temperature, salinity, density, and horizontal velocity at stations a) 10S and b) C2. The origin of the velocity vectors is at the depth of the measurement; vectors point in the direction of flow referenced to standard cartographic coordinates (north is toward the top of the page).

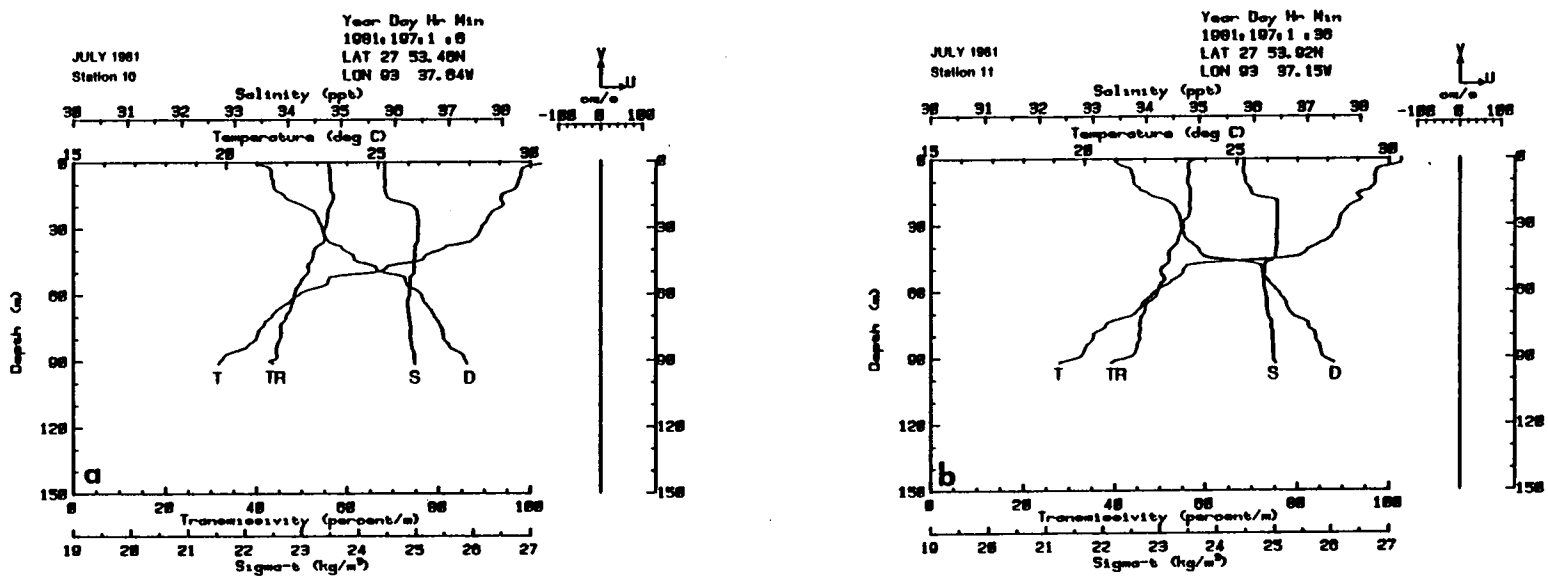

Figure 5.42 Profiles of transmissivity, temperature, salinity, density, and horizontal velocity at stations a) 10 and b) 11. The origin of the velocity vectors is at the depth of the measurement; vectors point in the direction of flow referenced to standard cartographic coordinates (north is toward the top of the page).

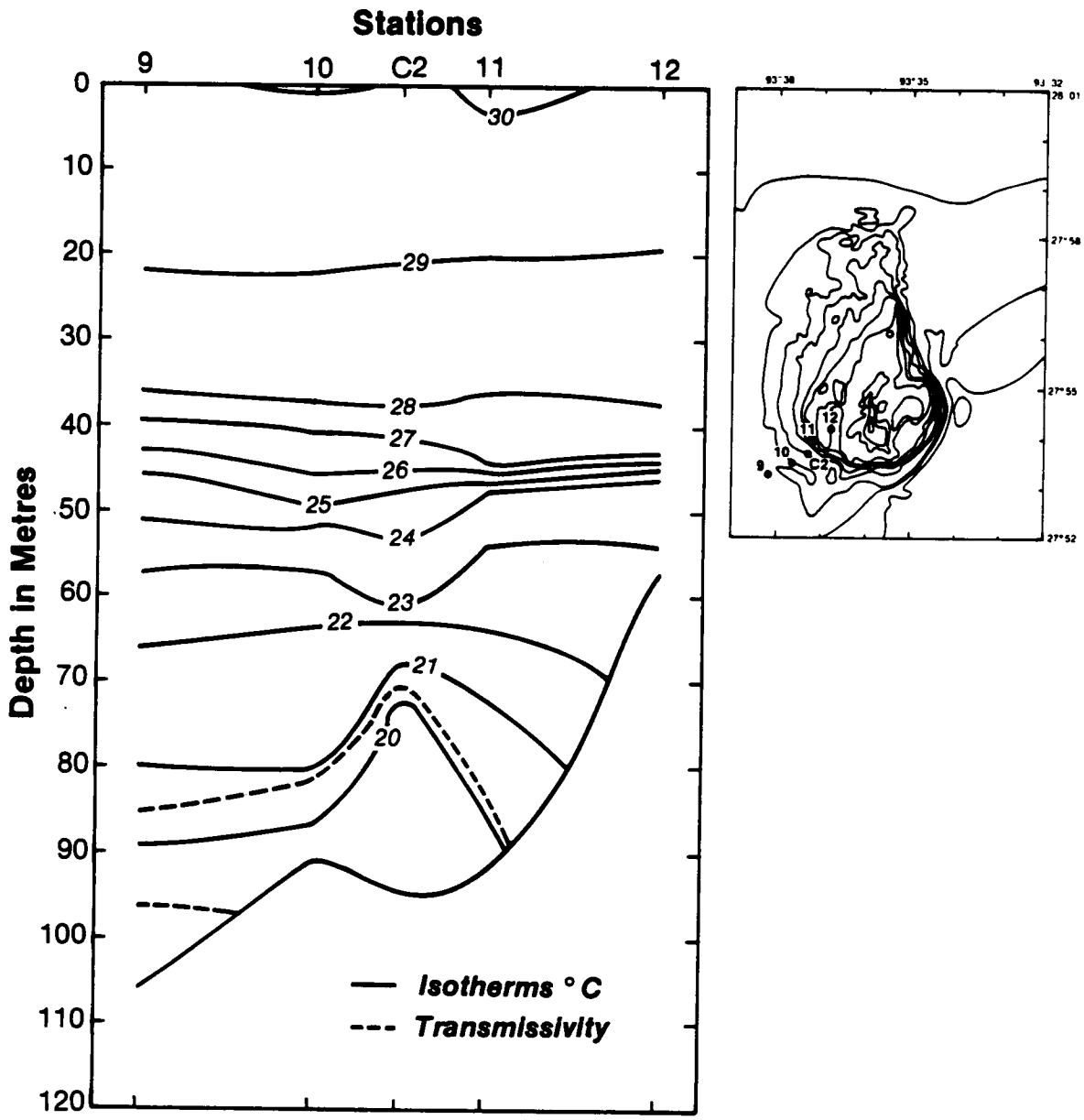

Figure 5.43 Temperature and transmissivity, July 1981, on a southwest transect at the East Flower Garden Bank.

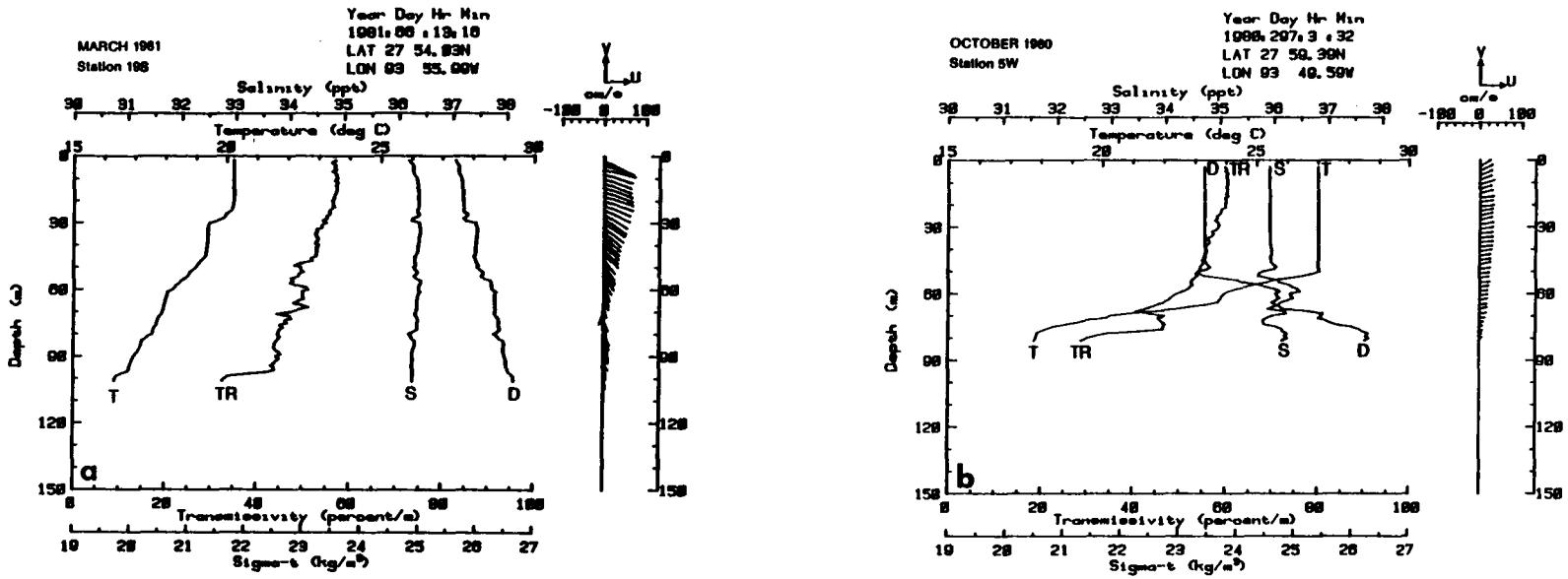

Figure 5.44 Profiles of transmissivity, temperature, salinity, density, and horizontal velocity at stations a) 19S and b) 5W. The origin of the velocity vectors is at the depth of the measurement; vectors point in the direction of flow referenced to standard cartographic coordinates (north is toward the top of the page).

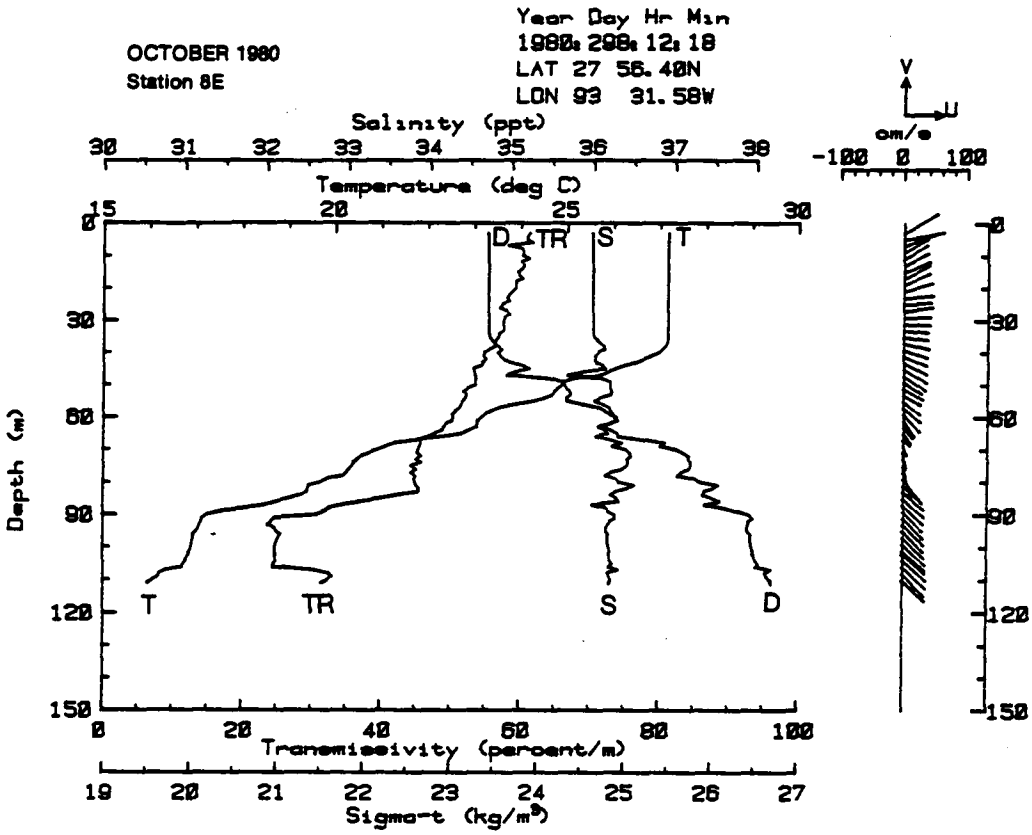

Figure 5.45 Profiles of transmissivity, temperature, salinity, density, and horizontal velocity at station 8E. The origin of the velocity vectors is at the depth of the measurement; vectors point in the direction of flow referenced to standard cartographic coordinates (north is toward the top of the page).

TURBID BOTTOM LAYERS AND SUSPENDED SEDIMENT

The amount of suspended sediment at any height above the bottom is a function of the amount being advected in, the amount being diffused upward by turbulent diffusion, and the amount settling out under the acceleration of gravity. A form of the equation describing this is

$$C(z) = \frac{E}{W\rho}\left(\frac{\partial c}{\partial z}\right)$$

where $C(z)$ is the sediment concentration
ρ is the fluid density
$\frac{\partial c}{\partial z}$ is the vertical sediment concentration
E is the eddy diffusivity
W is the fall velocity of the sediment

The concentration is a delicate balance between the settling velocity and the eddy diffusivity. If turbulence is very intense, the eddy diffusivity will be large and the amount of sediment in suspension at any given height will increase, as long as the shear stress, τ, at the bottom exceeds the critical value (τ_c) required for erosion. When the turbulence is damped and $E/W < 1$, the water will clear at any given height due to settling of the particles.

In the simplest case, $\tau > \tau_c$, so that fine sediment (silt and clay) is being eroded from the bottom. In the log layer the turbulence is rather intense. Beyond the log layer, the turbulence and hence, E, decrease rapidly, but W remains a constant so that near the top of the log layer there is as much sediment lost to settling as is gained by upward diffusion. The sediment cannot penetrate above the point where $W > E$.

The above equation can be integrated from a distance z_1 above the bottom to some other distance, z, to yield

$$\ln \frac{C(z)}{C(z_1)} = -\rho \frac{W}{E}(z - z_1)$$

or

$$C(z) = e^{(-\rho W/E)(z - z_1)} C(z_1)$$

where $C(z_1)$ is the concentration at z_1 (after Shepard, 1963).

Now if z is a substantial distance and E becomes vanishingly small, as in the case above, the concentration at z also becomes vanishingly small. All of this is predicated on a steady state condition.

The transmissivity profile in station 19S (Figure 5.44) is illustrative of what happens during resuspension of fine sediment in a stratified fluid. Near the bottom (z_1), $C(z_1)$ is relatively large. Clay particles are therefore brought together frequently and tend to flocculate so that W is relatively large. On the other hand, E >> W in the mixed layer, where turbulence is undamped. The decrease in C with respect to z is, therefore, relatively small. Above the mixed layer, E becomes very small as the turbulence is extinguished by stratification. Therefore W/E becomes large and C decreases rapidly with respect to increasing height above the bottom, as shown in Figure 5.44 (above).

If a turbid, mixed bottom boundary layer, like that in Figure 5.44, becomes separated from the bottom, there is no longer sediment available from the bottom to replace that lost by diffusion to the water above. In that case z_1 is measured from the base of the separated layer and $C(z_1)$ becomes a function of time. If E remains large, as is often the case, $C(z_1)$ decreases so that $\partial C/\partial z$ becomes small and the fine sediment becomes rather uniformly distributed through the layer. The transmissivity profile in station 8E (Figure 5.45) is illustrative of this point. In this case there appear to be at least two separated layers between 105 and 90 m depth.

On the other hand, if E becomes small in the separated layer and if the layer has flowed out across water of significantly greater density, then $C(z_1)$ can increase with time as the sediment settles onto the density interface. At the interface, W is diminished because of the increased fluid density. Sediment in such a separated layer may be advected over distances of several tens of kilometres before becoming so diffused as to be undetectable in the transmissivity profiles.

From the profiles, dye emission studies, and theoretical estimates, it appears that δ_{1n} on the open shelf around the base of the bank seldom, if ever, exceeds three metres. Also, it appears that the local penetration height of the resuspended sediment is rather limited to that layer. Variations in the concentration of suspended sediment above that height would therefore be a function of advective processes carrying separated boundary layers and associated sediment out over the shelf break.

This hypothesis is consistent with the time series transmissivity and velocity records from the moorings in the vicinity of the banks. Examples of records from moorings 1 and 3 are shown in Figure 5.46. Both meters were five metres above the bottom. The water was consistently clearer at mooring 3 than at mooring 1. This discrepancy may be related to the fact that the bottom to the northwest (upstream) of mooring 3 has less silt and clay in it than that to the northwest of mooring 1 (Figure 5.47).

The velocity, temperature, and transmissivity records for these two instruments were filtered to remove signals with periods equal to or shorter than inertial (Figure 5.48). These show that

at low frequencies, the transmisivity (sediment concentration) is unrelated to speed. That is, some of the highest speed flow is associated with clear water. The records were then high-pass filtered so that the high amplitude, high frequency current and transmissivity signals could be examined (Figures 5.49 and 5.50). These records show that the transmissivity is well correlated with temperature and nearly in phase. Lower temperatures are, in general, also accompanied by lower transmissivities. The transmissivity and velocity components are not quite as well correlated, and there is a phase lag between them.

All of this suggests that at 5 m above the bottom changes in transmissivity at high frequencies (inertial and greater) are related to vertical motions associated with tides and inertial oscillations. This may also be true to some extent in the low frequency signals.

The spectra for the v components of velocity and transmissivity from the moorings discussed are shown in Figures 5.51 to 5.53. The v components of velocity for the upper meters (Figure 5.51) are very coherent in a variety of frequencies, including tidal, inertial, and a broad band encompassing periods of about three to seven days. Notice the strong peaks in those spectra near 1 cpd. The complementary spectra for the lower meters on moorings 1 and 3 (Figure 5.52) are much less coherent, perhaps because the bottom meter at mooring 3 is closer to a bank than the meter at mooring 1. See, for example, how large the signal at 1 cpd is at mooring 3 compared to that at mooring 1. The transmissivity records from these instruments are even more poorly correlated than the v components of velocity (Figure 5.53). In fact, they are only significantly correlated at the semidiurnal frequency. Neither record shows the large peak just below 1 cpd which dominates the velocity spectra of both upper meters and the lower meter of mooring 3.

A review of all of the moored transmissivity and current meter records indicates that during cold front passages, southerly flow causes the transmissivity to decrease. This implies that sediment, resuspended by combined action of wind-driven current and waves in shallower water, is transported to the vicinity of the banks in separated boundary layers.

A similar study of all profiles taken from April 1979 through July 1981 shows that the turbid, separated boundary layers do not extend above approximately 75 m.

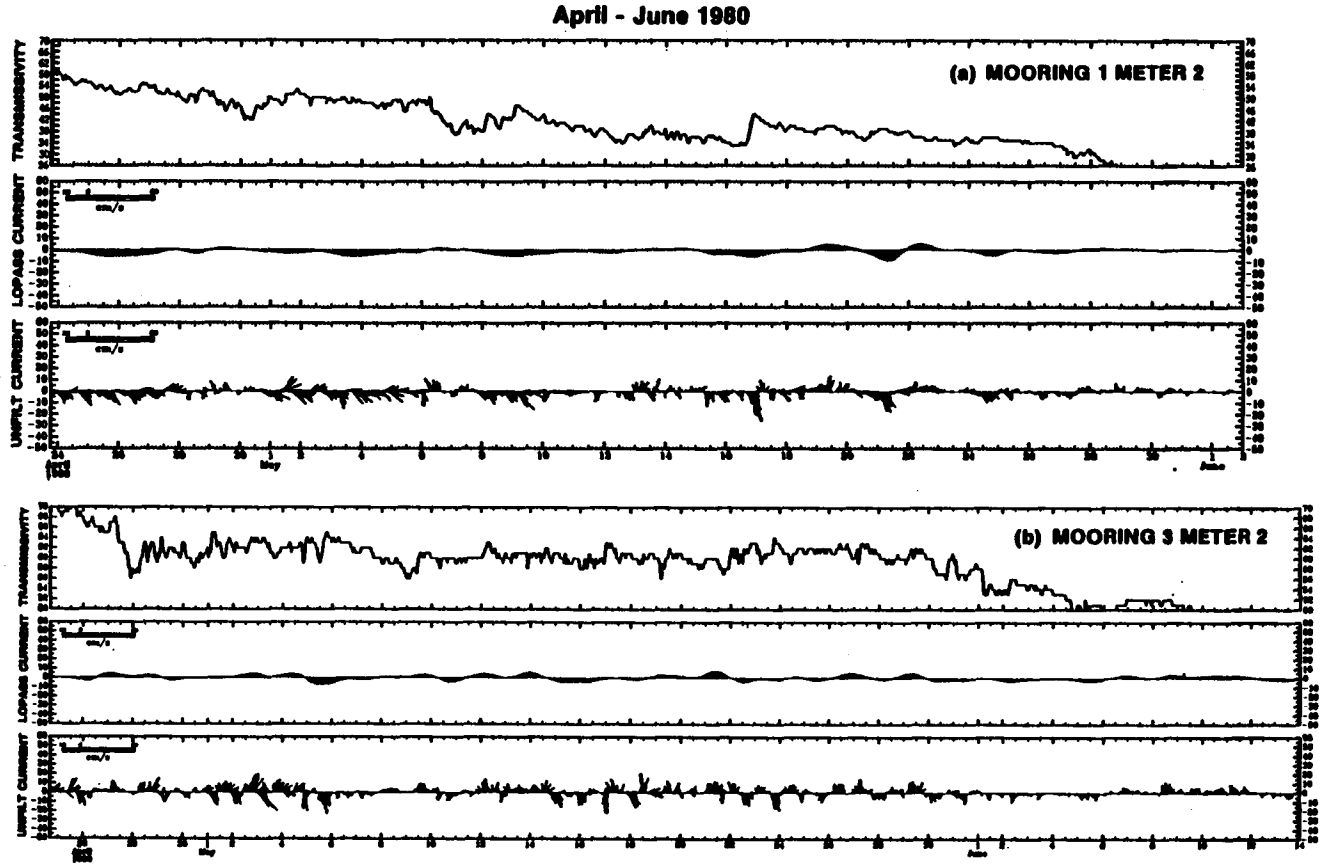

Figure 5.46 Raw velocity and transmissivity (XMS) time series records for April to June 1980 from a) mooring 1 at 95 m depth (bottom depth 99 m), and b) mooring 3 at 100 m depth (bottom depth 109 m). See Figure 5.1 for mooring locations.

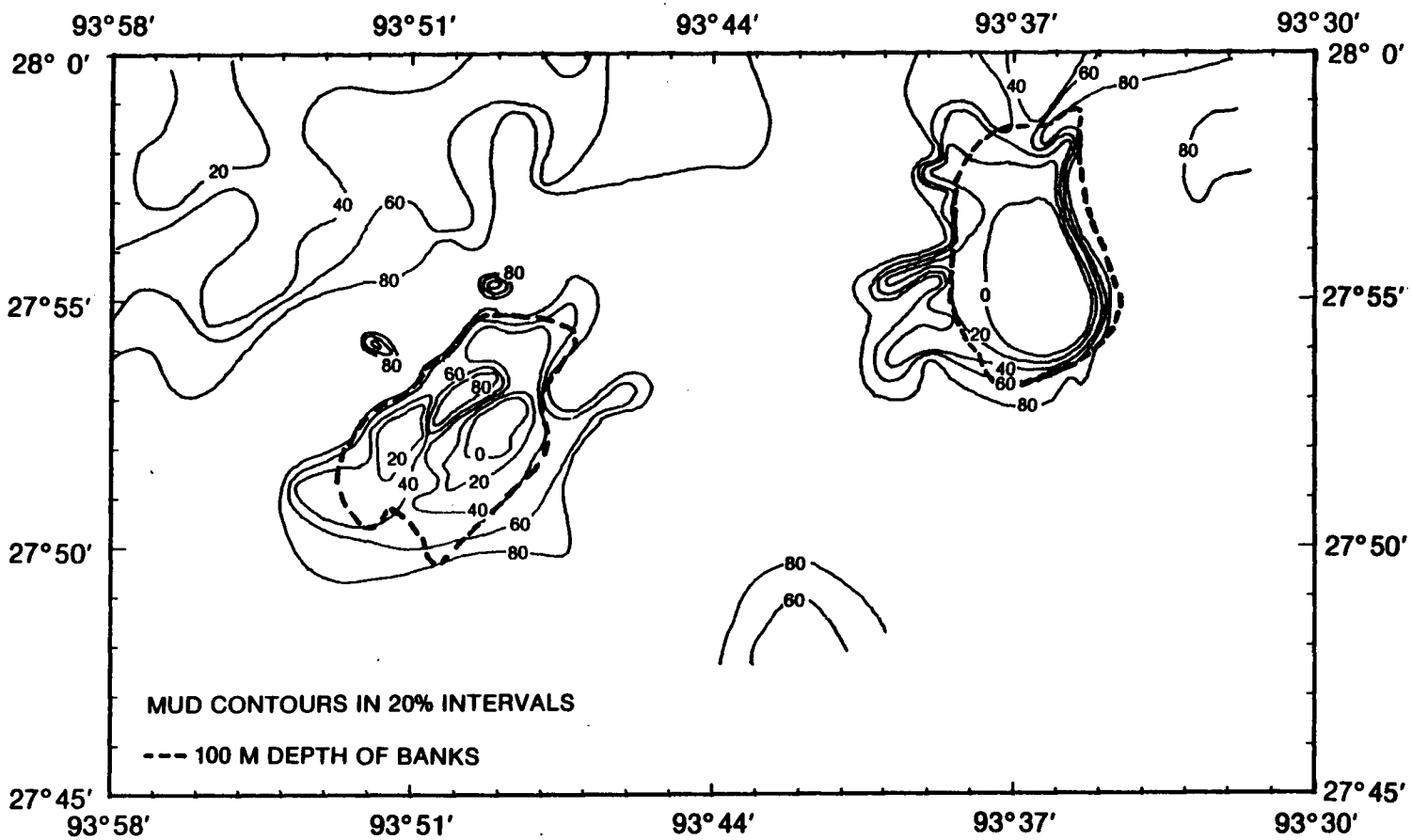

Figure 5.47 Mud contours in 20% intervals.

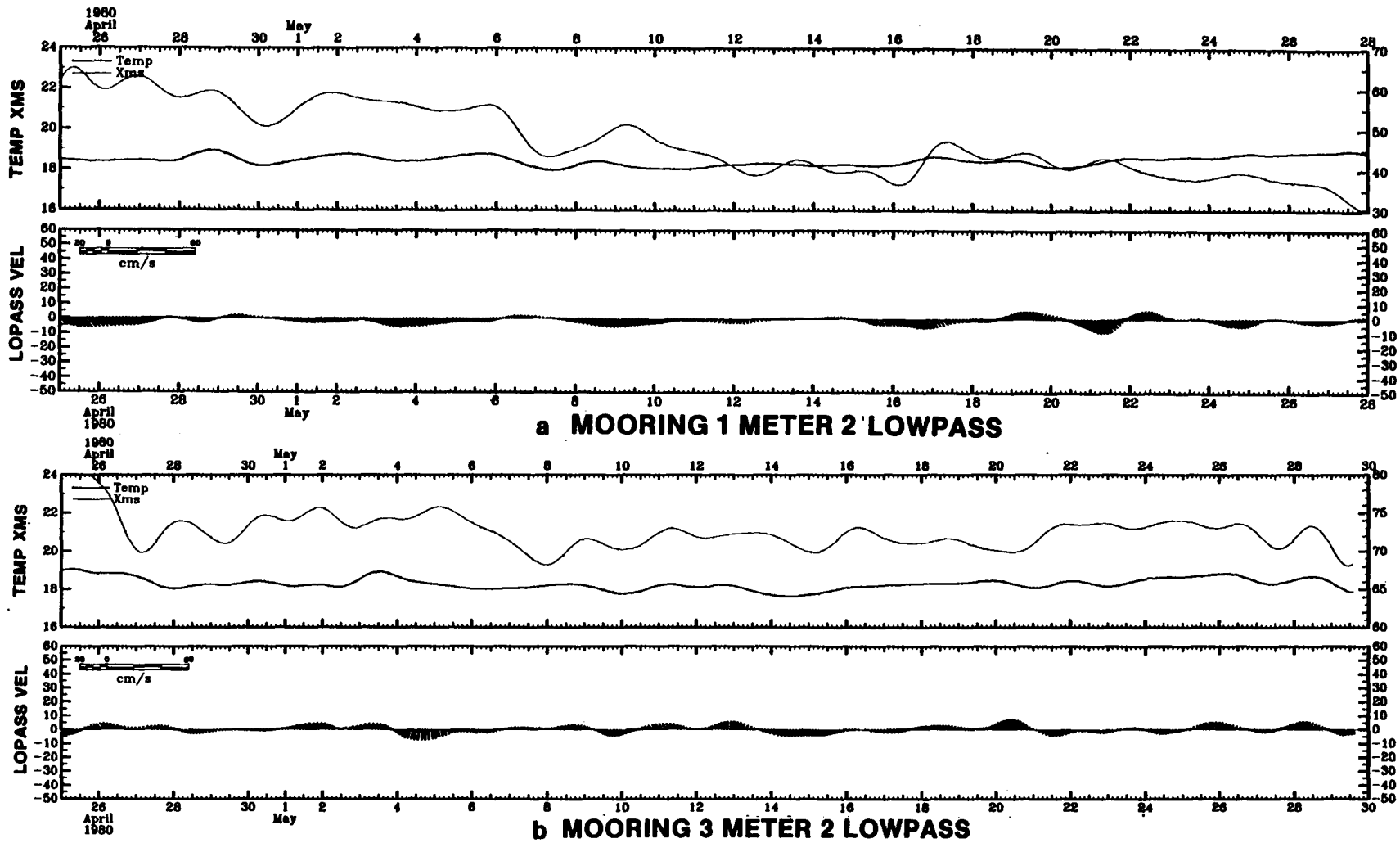

Figure 5.48 Time series of temperature (°C), transmissivity (%/m), and horizontal velocity (stick-plot representation in normal map orientations) lowpassed with a 28-hour filter near the bottom on a) mooring 1 at 95 m depth (bottom depth 99 m) and b) mooring 3 at 100 m depth (bottom depth 109 m) near the Flower Garden Banks.

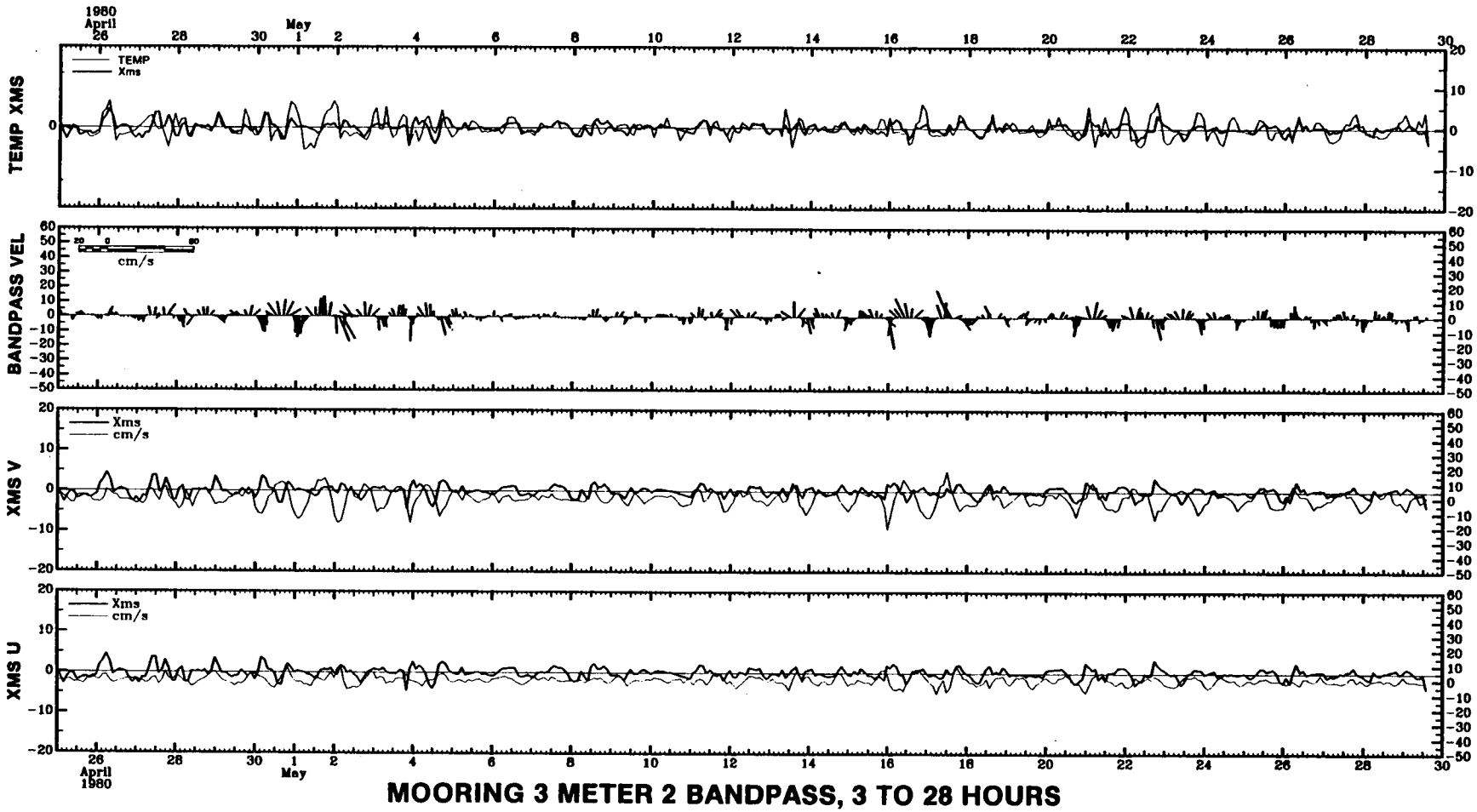

Figure 5.49 Band-Passed time series of temperature, transmissivity, and horizontal velocity, both stick plots and individual orthogonal components near the bottom on mooring 3, northeast of the West Flower Garden Bank. The bandpass eliminates components of the current with periods outside the range of 3 to 28 hours.

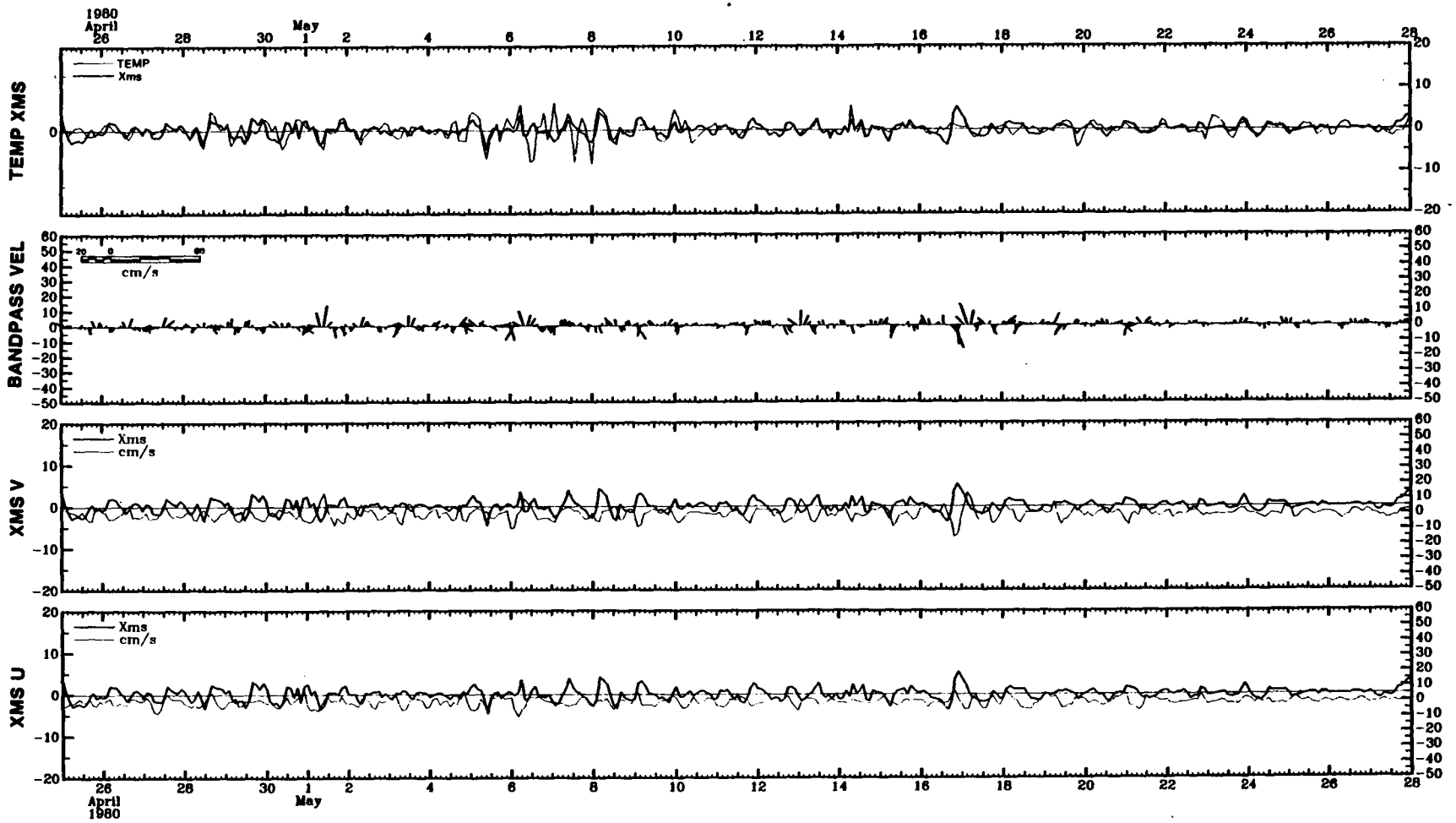

MOORING 1 METER 2 BANDPASS, 3 TO 28 HOURS

Figure 5.50 Band-Passed time series of temperature, transmissivity, and horizontal velocity, both stick plots and individual orthogonal components near the bottom on mooring 1, northeast of the East Flower Garden Bank. The bandpass eliminates components of the current with periods outside the range of 3 to 28 hours.

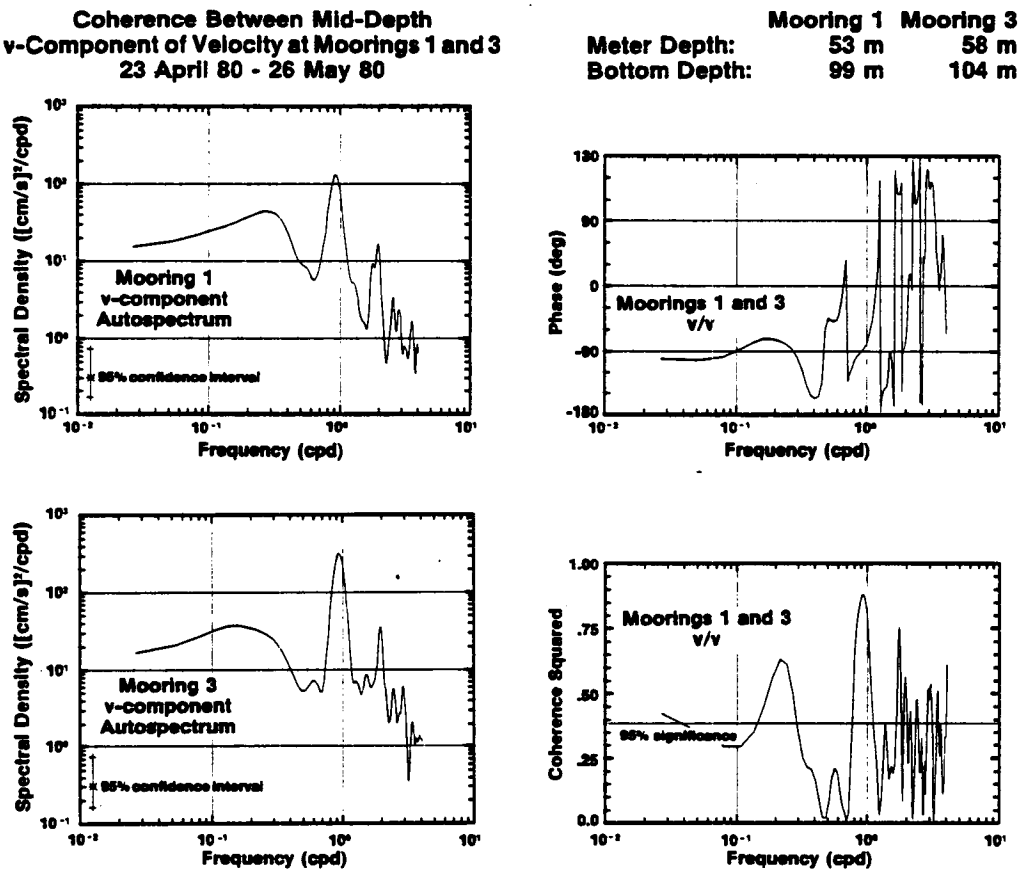

Figure 5.51 Comparison of the mid-depth north-south component of velocity at mooring 1 to that at mooring 3.

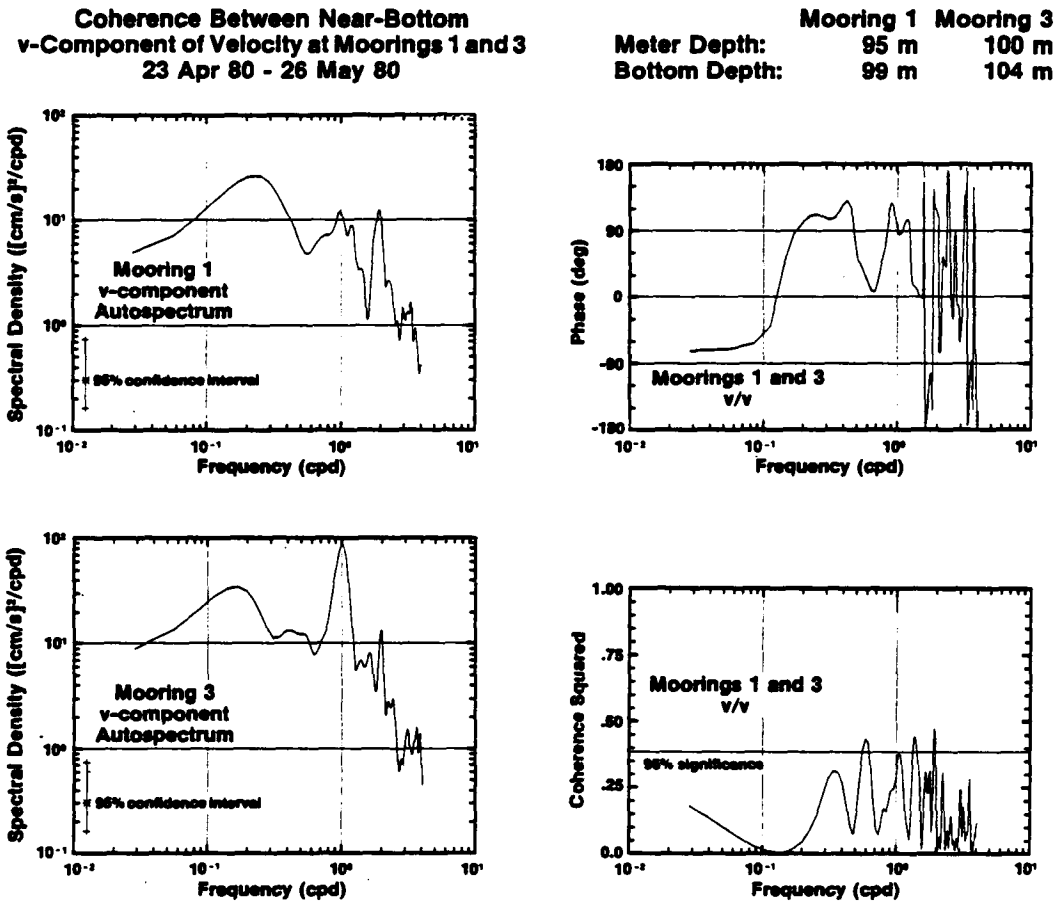

Figure 5.52 Comparison of the near-bottom north-south component of velocity at mooring 1 to that at mooring 3.

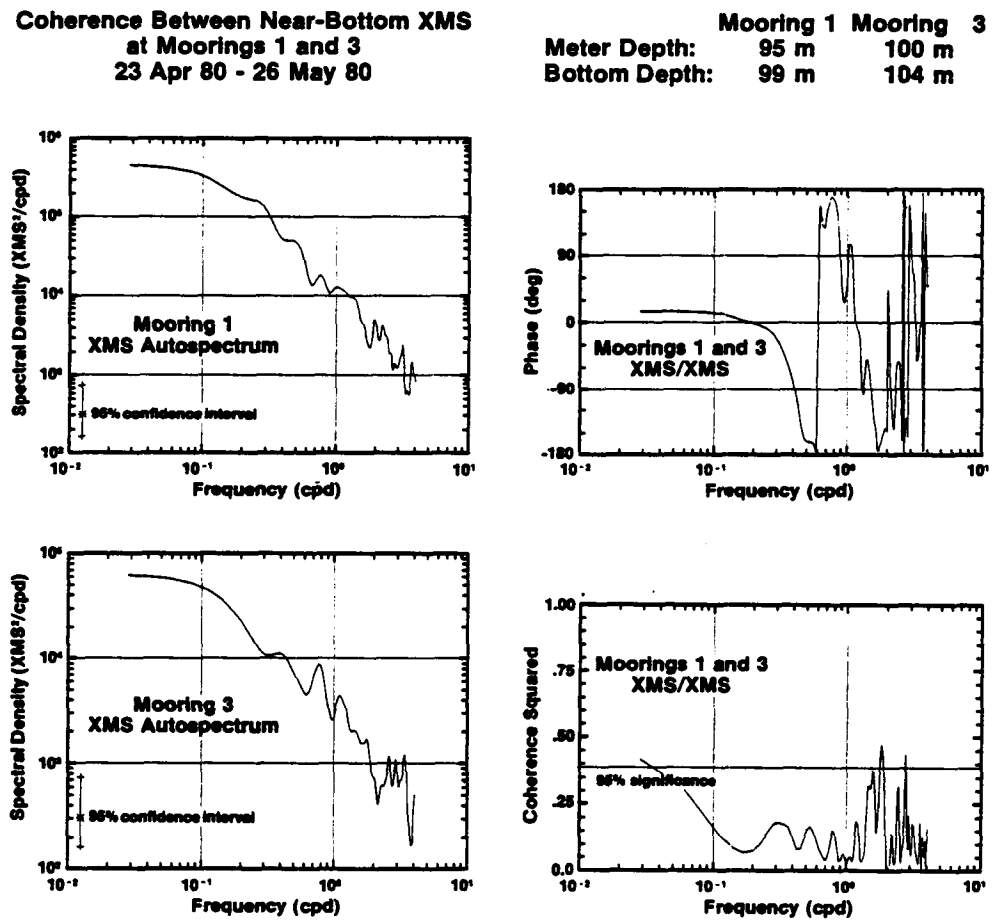

Figure 5.53 Comparison of near-bottom transmissivity measured at mooring 1 to that at mooring 3.

CONCLUSIONS

The reefs at the crests of the East and West Flower Garden Banks are able to exist there because the banks are bathed in warm, clear, saline waters all year round. The depth of surrounding waters is great enough so that modest stratification exists year round and the heat capacity of this thick water column keeps temperatures at the level of the bank above 19°C even during cold frontal passages in the winter. The great distance from shore assures that the surface waters remain relatively free of light-attenuating sediment. Relatively high velocity currents and oscillations from surface gravity waves maintain active circulation over the corals.

The depth of coral reef penetration on the bank may well be correlated with light attenuation, and to some minor extent temperature. At 50 m depth temperatures may drop below 19°C for very brief periods.

Throughout the Algal Nodule Zone current velocities remain high because of orographic effects. This produces large bedforms in the nodules as they are transported over the surface of the bank. The benthonic foraminifers, *Amphistegina*, are winnowed from this zone and swept downslope by gravity.

Currents on the bank surface remain elevated above those away from the bank but are attenuated toward the base of the bank. Deposition of silt and clay on the banks is restricted to depths greater than about 80 m because of two factors. Above this level, the combination of current acceleration by orographic effects, plus trapping of tidal and inertial oscillations, keeps the shear stresses on the bottom sufficiently high to preclude deposition. Also, the bottom boundary layers separated from the seafloor to the northwest do not contain enough fine sediment at this level to contribute significant amounts of fine sediment for deposition.

CHAPTER 6

ZONATION, ABUNDANCE, AND GROWTH OF REEF-BUILDERS AT THE FLOWER GARDEN BANKS

Thomas J. Bright, George S. Kraemer, Gregory A. Minnery, and Stephen T. Viada

HABITAT DESCRIPTION AND ZONATION

The East and West Flower Garden Banks (EFG and WFG), approximately 100 nautical miles southeast of Galveston, Texas, are two of the numerous elevations of the seafloor (banks) in the northwestern Gulf of Mexico produced by intrusion of salt plugs from the Jurassic, Louann evaporite deposits 15 km below the seafloor (Rezak, 1981). Both banks are capped by what are currently considered to be the northernmost thriving tropical coral reefs on the eastern coast of North America. The northern limit of Bahamian reefs is some twenty miles south of the Flower Garden Banks latitude. Reefs of the Bermuda Islands are nearly 300 miles north of the Flower Gardens latitude, but they are situated 570 miles offshore from Cape Hatteras, North Carolina. The ecology of both the Bermudan and Bahamian island systems is influenced greatly by the warm Gulf Stream waters which surround them, and like the Flower Gardens, they harbor elements of the typical Caribbean reef biota.

Within the Gulf of Mexico, the Flower Garden Banks appear to be elements of a discontinuous arc of reefal structures occurring on the continental shelf. The coral reefs closest to the Flower Garden Banks are off Cabo Rojo, about 60 miles south of Tampico, Mexico (Figure 3.1) (Villalobos, 1971). Moore (1958) listed 43 species of Caribbean reef invertebrates from there; many of them are also common at the Flower Gardens. However, certain abundant corals typical of emergent reefs, such as *Acropora palmata* (Elkhorn coral), and *A. cervicornis* (Staghorn coral), do not occur at the submerged Flower Garden reefs. Shallow water octocorals (sea fans and sea whips), which are surprisingly absent from the Flower Gardens, are present at the Cabo Rojo reefs and reefs several miles south near Isla de Lobos (Chamberlain, 1966; Rigby and McIntyre, 1966). Reportedly, octocorals are abundant on Alacran reef (Kornicker et al., 1959) and other reefs on the Yucatan Continental Shelf. Coral reefs off the city of Veracruz were reported by Heilprin (1890). Logan (1969) described the physiography of all reefs and hard-banks on the Yucatan Shelf in some detail (Figure 3.1).

Coral reefs occur in the Tortugas and Florida Keys in the Eastern Gulf of Mexico. Elements of the Caribbean reef biota occupy hard-bottoms and "patch reefs" from Tampa Bay to Sanibel Island on

the West Florida Shelf (Joyce and Williams, 1969; Smith, 1976). Jordan (1952) described aspects of biota from the Florida Middle Ground, approximately 300 square miles of reef formations off Appalachicola Bay, Florida. Grimm and Hopkins (1977) indicate octocoral predominance at the Florida Middle Ground above 28 m, with dominance shifting to the hermatypic corals between 28 and 36 m. Zonation at the Florida Middle Ground differs considerably from that of the aforementioned coral reefs, even though the dominant organisms are components of the Caribbean biota.

The Gulf of Mexico is, therefore, ringed by a combination of thriving coral reefs and scattered hard-banks and patches bearing elements of the Caribbean reef biota. To what extent the Caribbean biota are represented at the Flower Garden Banks with respect to all taxonomic groups is not yet known. Bright and Pequegnat (1974) reported 253 invertebrate species and 103 fishes from the West Flower Garden. Bright and Rezak (1978a) listed over 30 species of benthic algae from the East Flower Garden. The list of species has been substantially expanded through additional research sponsored by the U.S. Bureau of Land Management (Bright and Rezak, 1976; Bright and Rezak, 1978b).

It is not surprising that thriving reefs occur at the locality of the Flower Garden Banks. The environmental conditions there are consistent with the existence of coral reefs (Stoddart, 1969). Positioned at the continental shelf edge, with high vertical relief and surrounding depths of 100 to 140 m, the banks' upper portions are exposed almost continually to tropical-subtropical, clear, oceanic water. Compared to waters closer to shore, clarity is exceptional. Between the surface and 70 m depth, transmissivity is generally above 75%/m for white light (McGrail et al., 1982a), and sunlight penetration is substantial. Salinities typically remain above 35 ppt, but sometimes can be as low as 32 ppt at the surface and 34 ppt at the bank top (20 m depth). Above 25 m depth, water temperature varies annually between 18 and 32°C (Abbott, 1975; Etter and Cochrane, 1975). Under such conditions, the banks have acquired biologically generated carbonate "caps" above approximately 100 m depth. These harbor characteristically Caribbean benthic communities dominated by coralline algae and hermatypic corals (Bright et al., 1974; Bright, 1977; Rezak, 1977).

Biotic zonation is distinct, stringently depth related, and nearly identical on both banks (Figures 6.1-6.3). The characteristics and limits of biotic zones on the banks have been defined primarily on the basis of direct visual observations and selective sampling performed using the Texas A&M research submersible DIAPHUS and scientific SCUBA diving. Such techniques result in basically qualitative judgements. In pursuit of objective insight which may reveal subjectively overlooked subtleties in zonation, we abstracted and analyzed a quasi-quantitative compilation of algae and invertebrate occurrence and abundance observations taken from

videotaped records of all submersible transects. Raw abundance and depth of occurrence values were derived from recorded sightings of the various taxa (except fishes). Each sighting was weighted (ranked 1, 5, 10, or 20) according to the observer's (Bright's) assessment of taxon abundance made at the time. Raw abundances per taxon were then combined within 5 m depth intervals for each bank, and divided by total abundance of all taxa combined within the depth interval (data were converted to relative abundance of each taxon within each depth interval at each bank).

Bray-Curtis cluster techniques were then used to explore relationships between the 10 m depth intervals. Attributes employed were taxon type and square root of relative abundance within intervals. Cluster results (Figures 6.4 and 6.5) indicate strong segregation of taxon type and abundance by depth, implying logical, depth-related biotic zonation on the banks.

The cluster analyses agree with and confirm the authors' qualitative definition of benthic communities and zones at the Flower Gardens. However, the direct qualitative observations, after all, provide a more complete and reliable basis upon which to consider the subtleties of variation in community structure and distribution on the banks -- as described below.

Coral Reefs

Submerged coral reefs constitute the shallowest and largest reefal structures on the East and West Flower Garden Banks, occupying the crests of the banks down to 52 m depth in places (Figures 6.1-6.3). The main reef tops generally vary from 18 to 28 m, but 15 m depths are common and an 11 m depth has been encountered at the East Flower Garden (top of a large coral head). The reefs are made up of closely spaced or crowded coral heads up to 3 m in diameter and height (Figures 6.6 and 6.7). "Patches" of sand or carbonate gravel occur among the coral heads. The heads are frequently very cavernous, showing evidence of substantial internal and surficial bioerosion.

Two biotic zones are recognizable on the coral reefs: a high diversity assemblage (18 hermatypic coral species) limited to depths less than 36 m (*Diploria-Montastrea-Porites* Zone), and a comparatively low diversity assemblage (approximately 12 hermatypic coral species) between 36 and 52 m (*Stephanocoenia-Millepora* Zone) (Table 6.1). The terms "high diversity" and "low diversity" used herein are relative for the northwestern Gulf of Mexico only, and pertain to coral diversity. Coral diversities on reefs in other parts of the Caribbean and southern Gulf of Mexico are substantially higher.

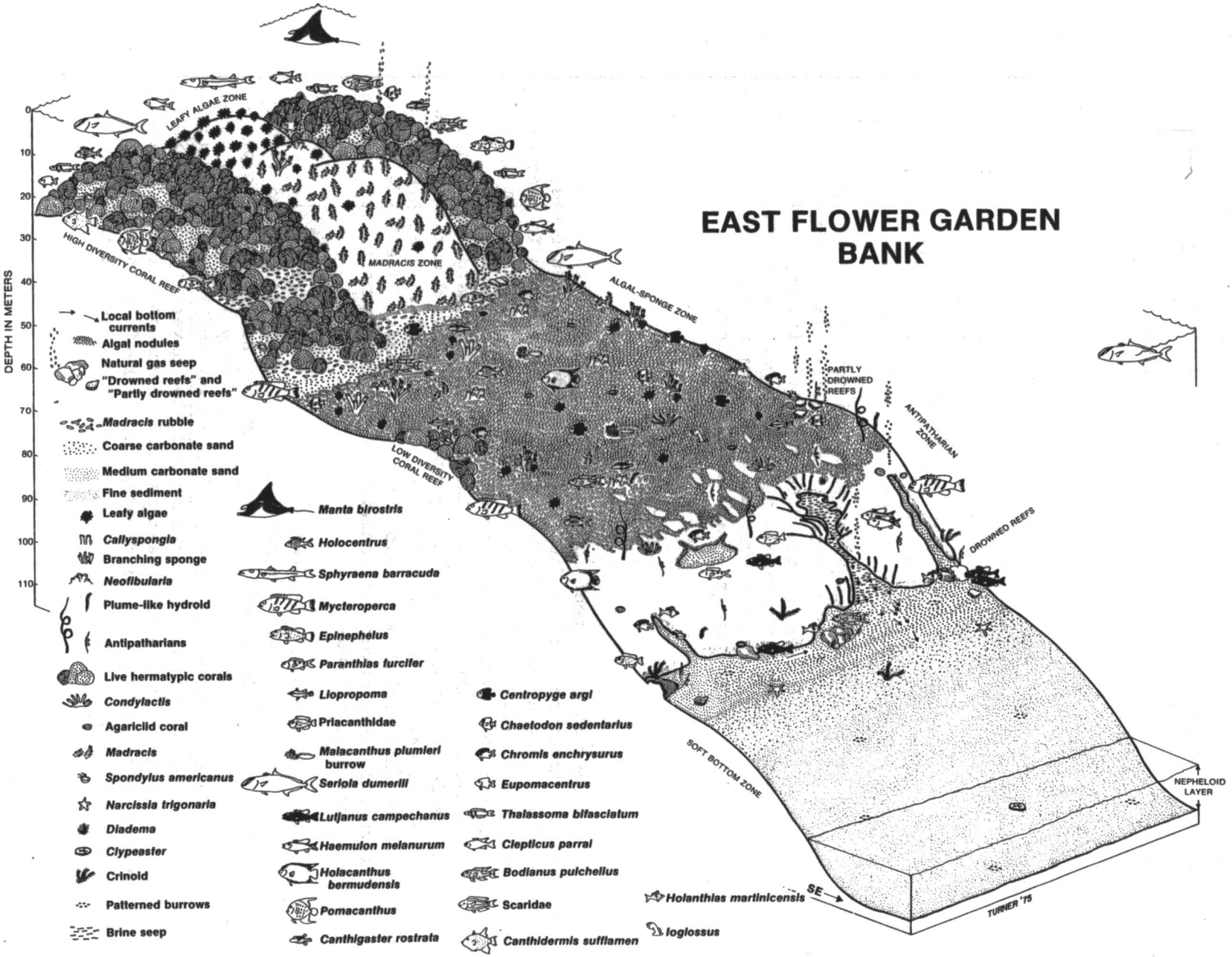
EAST FLOWER GARDEN BANK
DEPTH IN METERS
0
10
20
30
40
50
60
70
80
90
100
110
LEAFY ALGAE ZONE
HIGH DIVERSITY CORAL REEF
MADRACIS ZONE
ALGAL-SPONGE ZONE
PARTLY DROWNED REEFS
ANTIPATHARIAN ZONE
LOW DIVERSITY CORAL REEF
DROWNED REEFS
SOFT BOTTOM ZONE
NEPHELOID LAYER
SE
TURNER '75
Local bottom currents
Algal nodules
Natural gas seep
"Drowned reefs" and "Partly drowned reefs"
Madracis rubble
Coarse carbonate sand
Medium carbonate sand
Fine sediment
Leafy algae
Callyspongia
Branching sponge
Neofibularia
Plume-like hydroid
Antipatharians
Live hermatypic corals
Condylactis
Agaricid coral
Madracis
Spondylus americanus
Narcissia trigonaria
Diadema
Clypeaster
Crinoid
Patterned burrows
Brine seep
Manta birostris
Holocentrus
Sphyraena barracuda
Mycteroperca
Epinephelus
Paranthias furcifer
Liopropoma
Priacanthidae
Malacanthus plumieri burrow
Seriola dumerili
Lutjanus campechanus
Haemulon melanurum
Holacanthus bermudensis
Pomacanthus
Canthigaster rostrata
Centropyge argi
Chaetodon sedentarius
Chromis enchrysurus
Eupomacentrus
Thalassoma bifasciatum
Clepticus parrai
Bodianus pulchellus
Scaridae
Canthidermis sufflamen
Holanthias martinicensis
Ioglossus

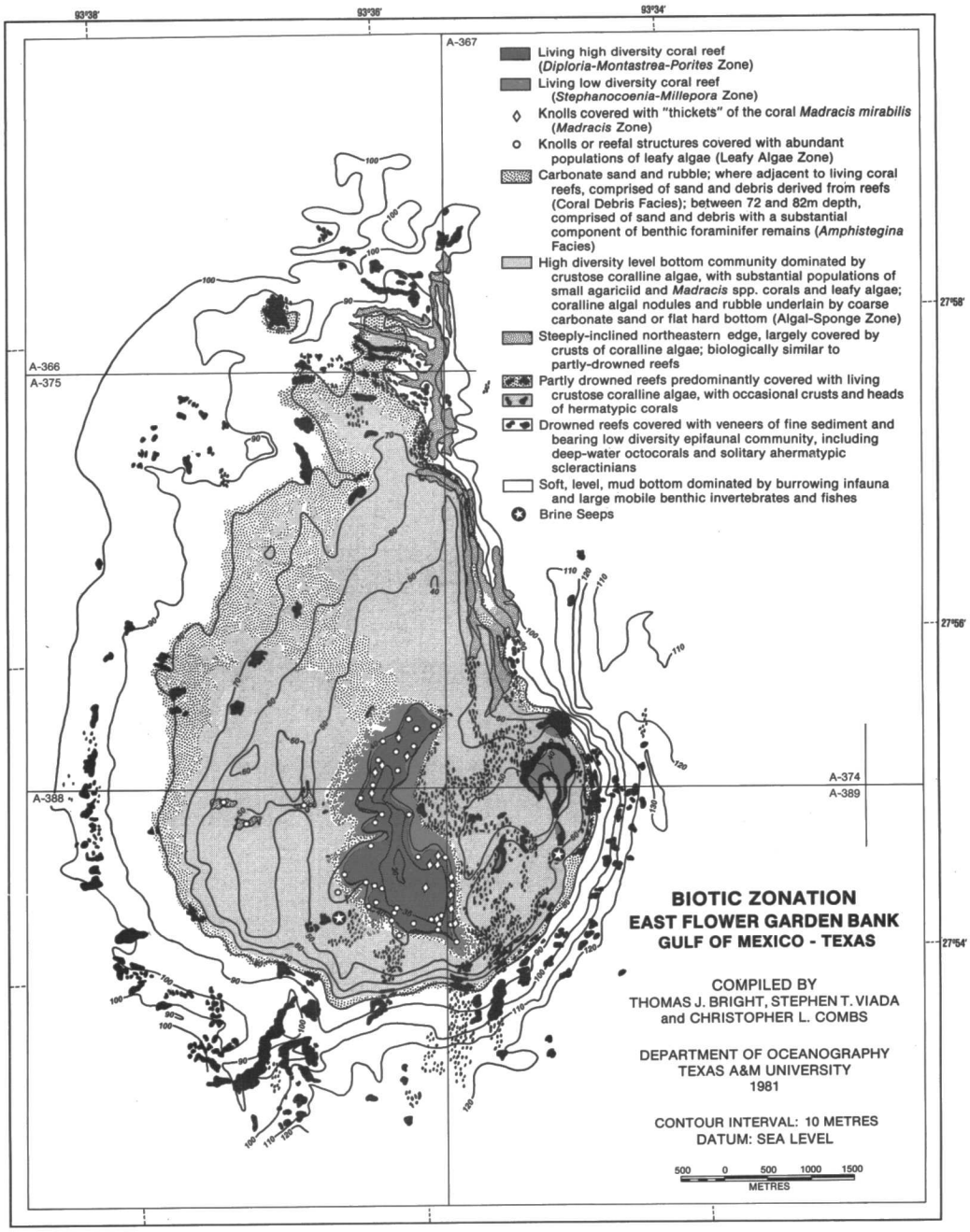

Figure 6.2 Biotic zonation, East Flower Garden Bank.

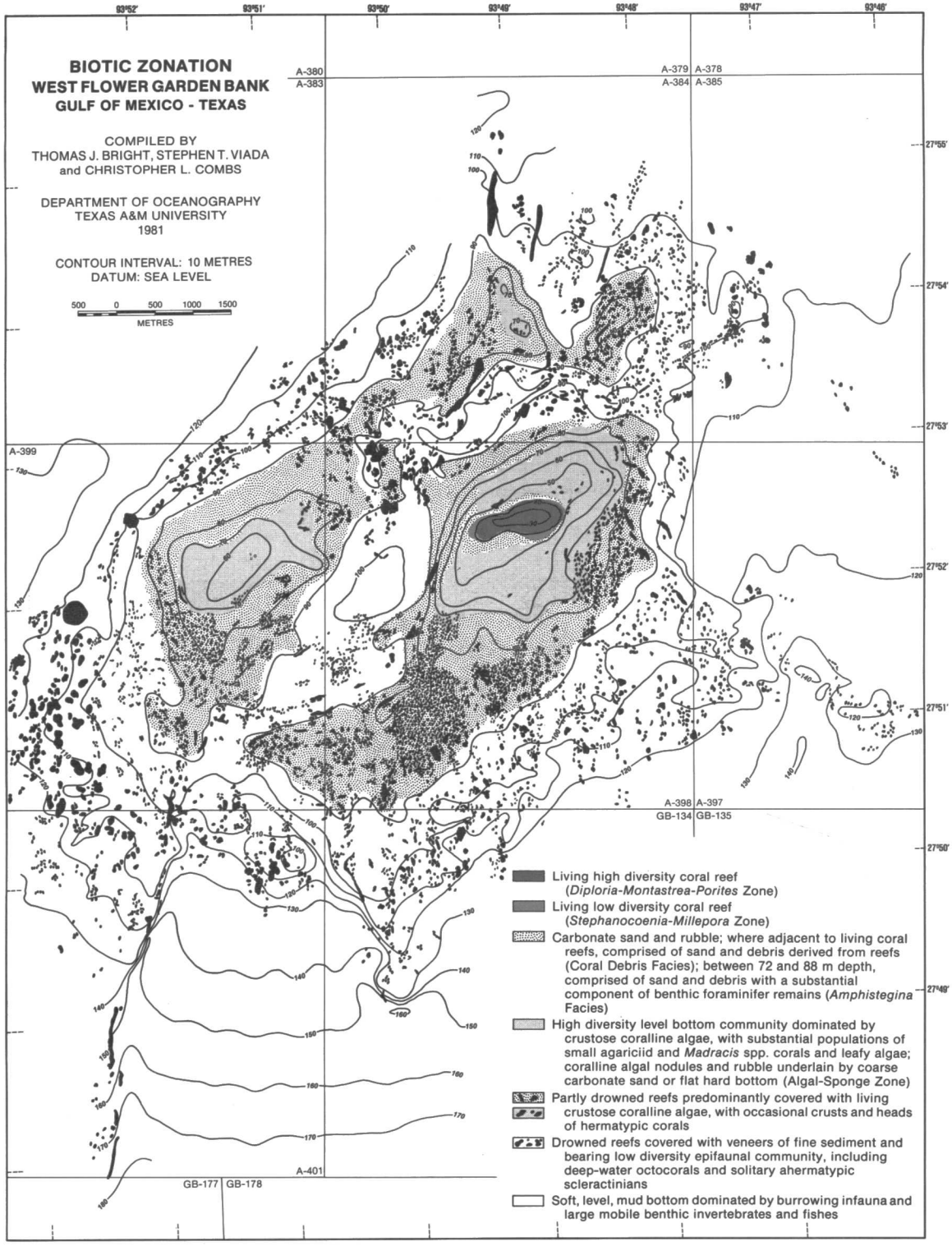

Figure 6.3 Biotic zonation, West Flower Garden Bank. The three "dots" within the 60 m contour on the western-most knoll represent low-diversity coral reefs.

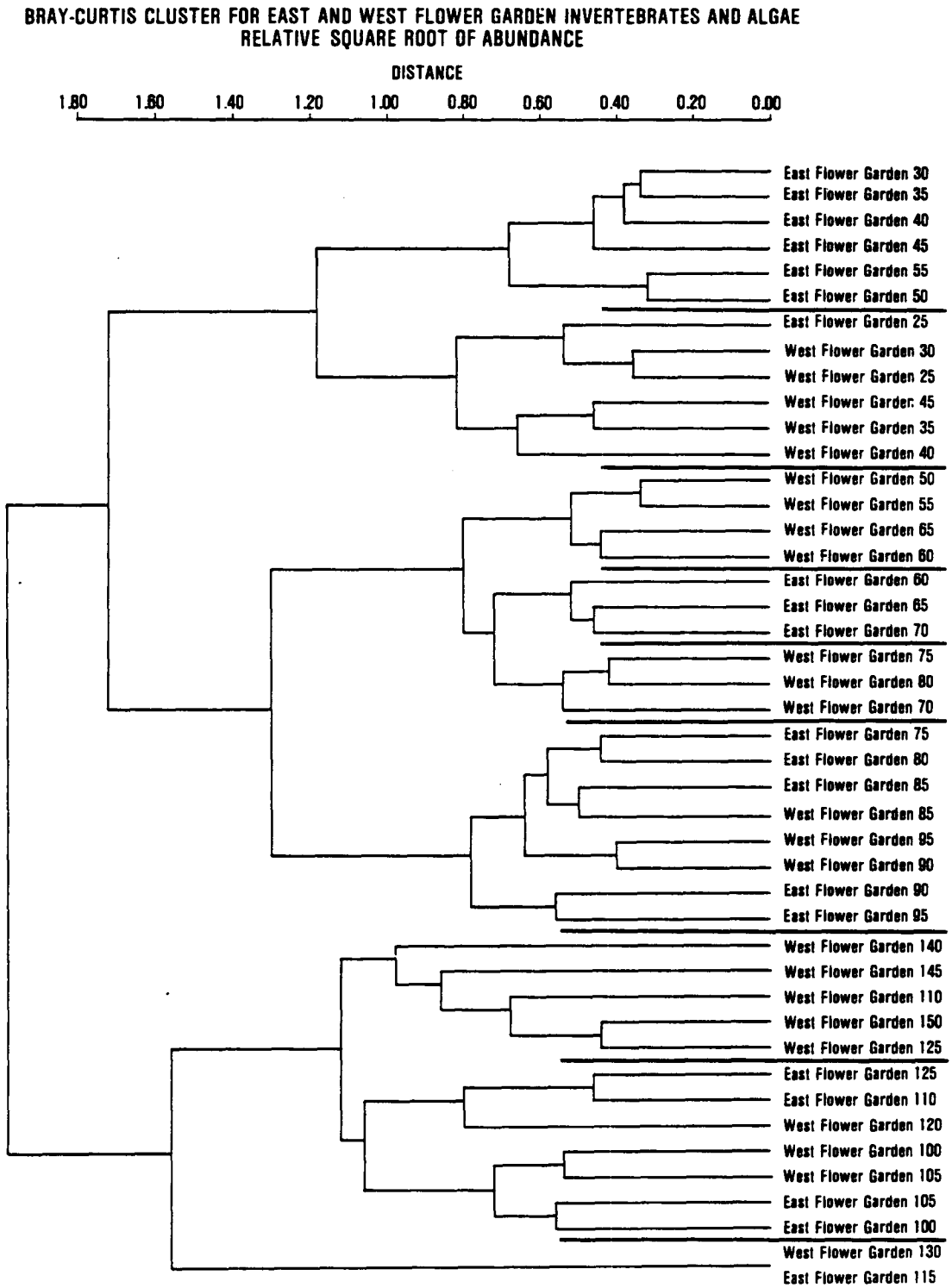

Figure 6.4 Bray-Curtis cluster for 5 m depth intervals at the East and West Flower Garden Banks. Attributes are relative square roots of abundance for invertebrates and algae. The deepest depth in each 5 m interval is indicated for each entity in the clusters (i.e., "West Flower Garden 30" = the depth interval 26 to 30 m at the West Flower Garden Bank).

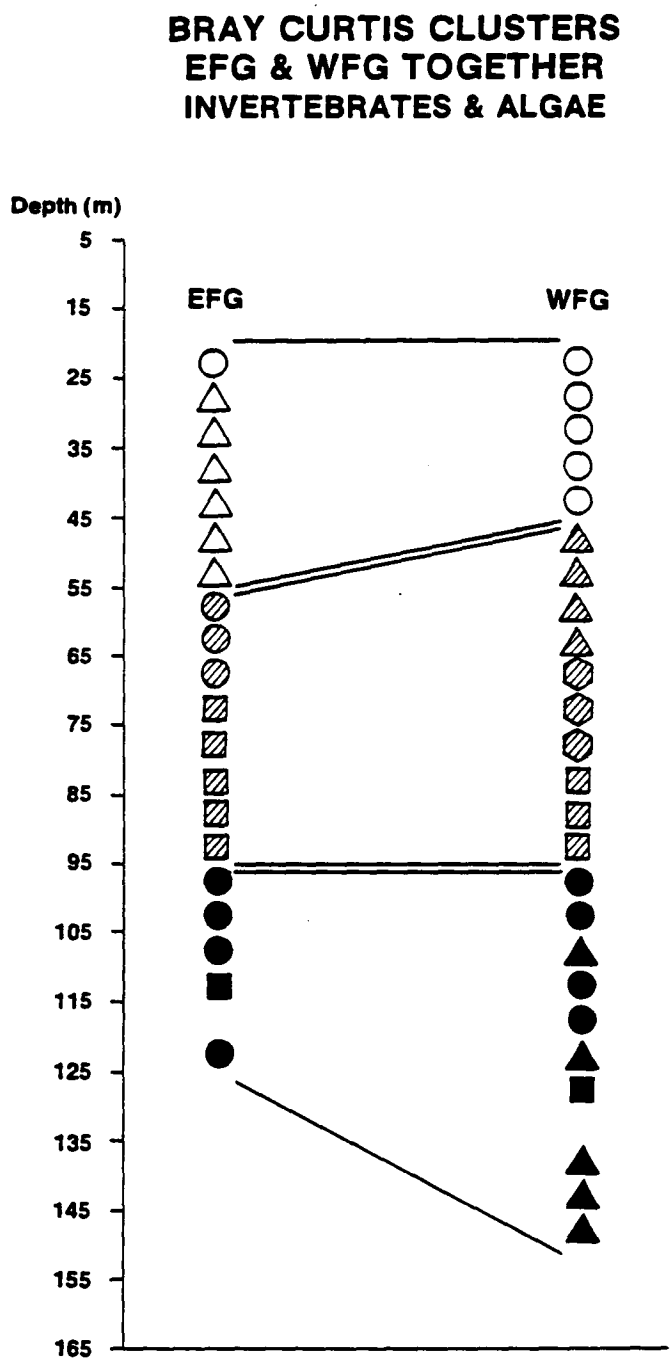

Figure 6.5 Depth zone relationships derived from interpretation of Bray-Curtis clusters (Figure 6.4) for East and West Flower Garden invertebrates and algae. Horizontal and diagonal lines separate major biotic zones as defined by the cluster analysis (clusters separate at Bray-Curtis distance values greater than 1.7). Identically shaped and shaded geometric figures (circles, squares, etc.) indicate locations and depth ranges which clustered together (were most similar in terms of species composition and abundance) within the major zones.

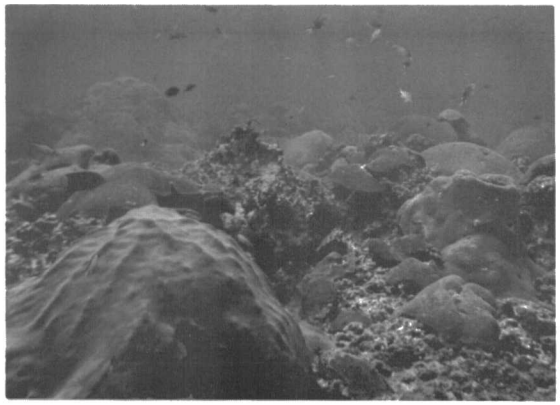

Figure 6.6 Typical Flower Gardens coral reef top (21 m depth).

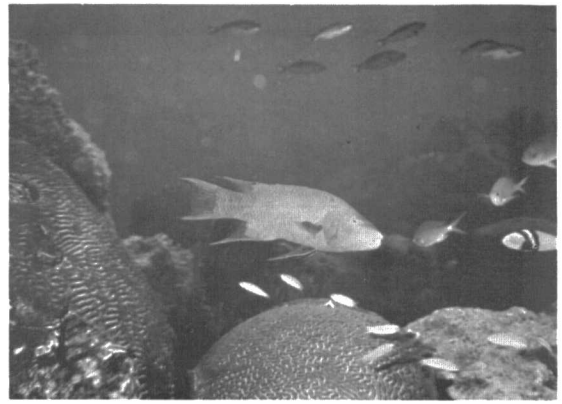

Figure 6.7 Brain corals and reef fishes (*Chromis* sp.; *Bodianus rufus,* Spanish hogfish; *Thalassoma bifasciatum,* Bluehead) at 20 m depth on the West Flower Garden.

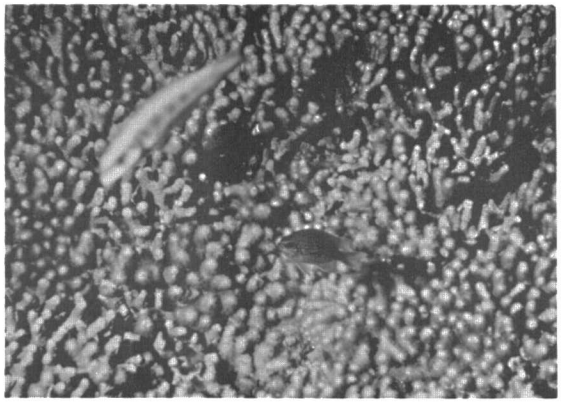

Figure 6.8 *Madracis mirabilis*, dominant coral of *Madracis* zone (28 m depth, East Flower Garden).

Figure 6.9 Leafy algae zone (28 m depth, East Flower Garden).

Table 6.1 Flower Garden Reef Builders. Where information is available, relative abundance is indicated as follows:
**** = very abundant; *** = abundant; ** = common; * = present.
DMP = Diploria-Montrastrea-Porites Zone; Mad = Madracis Zone;
SM = Stephanocoenia-Millepora Zone; AS = Algal-Sponge Zone.
Information concerning occurrences in the Stephanocoenia-Millepora Zone is limited. Probable presence is indicated by a question mark.

Reef Builders	Depths of Collection and/or Observation (m)	Abundance DMP	Mad	SM	AS
RED CALCAREOUS ALGAE					
CORALLINACEAE		****	****	****	****
Porolithon	21-32	**	*		
Hydrolithon	21-65	****	**	?	*
Archeaolithothamnium	21-72	*	*	?	*
Lithophyllum	21-119	***	***	?	**
Lithoporella	21-119	*	*	?	***
Tenarea	21-119	***	**	?	***
Lithothamnium	21-119	*	*	?	****
Mesophyllum	21-119	*	*	?	**
Fosliella?	30-119	*	*	?	*
SQUAMARIACEAE					
Peyssonnelia	21-100	***	***	?	**
GREEN CALCAREOUS ALGAE					
CODIACEAE					
Halimeda	21-91	*	?		**
Halimeda tuna	48-61				*
Udotea	40-64	?			*
Udotea cyathiformis	58				*
FORAMINIFERANS					
Gypsina plana	21-119	**	****	?	***
CORALS					
ASTROCOENIDAE					
Stephanocoenia michelinii	21-52	*		***	
POCILLOPORIDAE					
Madracis	15-92	***			**
Madracis asperula	23-84	*			**
Madracis decactis	15-41	***			
Madracis cf. formosa	62				*
Madracis mirabilis	23-40		****		
Madracis myriaster	113				*

Table 6.1 (Continued)

Reef Builders	Depths of Collection and/or Observation (m)	Abundance DMP	Mad	SM	AS
AGARICIIDAE					
Agariciidae (saucer-shaped)[a]	18-82	*		*	***
Agaricia	15-76	**		**	***
Agaricia agaricites	20-24	*		?	**
Agaricia fragilis?[b]	20-53	*		?	*
Helioseris cucullata	20-84	*		?	**
SIDERASTREIDAE					
Siderastrea siderea	21-50	**		*	
PORITIDAE					
Porites astreoides	21-40	***		*	
Porites furcata	21	*			
FAVIIDAE					
Colpophyllia	21-47	***		**	
Colpophyllia amaranthus	21-26	*		?	
Colpophyllia natans	21-26	**		?	
Diploria strigosa	15-55	***		**	
Montastrea annularis	21-43	****		*	
Montastrea cavernosa	19-60	***		**	*
MUSSIDAE					
Mussa angulosa	21-54	**		*	
Scolymia?[c]	18-46	*		*	
Scolymia cubensis	21-27	*		?	
MILLEPORIDAE					
Millepora alcicornis	15-55	***		***	*
CARYOPHYLLIIDAE					
Oxysmilia?[d]	82-101				
Paracyathus?[e]	19-?	*		?	?

Table 6.1 (Continued)

[a]"Saucer-shaped" Agariciidae are not recognizable to species in situ. Collected specimens are Helioseris cucullata, Agaricia agaricites, and, if the identification is correct (see b), Agaricia fragilis.

[b]Two collected specimens, identification as Agaricia fragilis uncertain.

[c]Possibly only one species, S. cubensis.

[d]In situ sightings only of Oxysmilia?. Oxysmilia rotundifolia is generally abundant on, and has been collected from, deeper parts of shelf-edge carbonate banks in the northwestern Gulf of Mexico. The authors speculate that Flower Garden sightings are this species.

[e]One specimen identified by Dr. S. Cairns as "Paracyathus sp. or Polycyathus sp." Paracyathus pulchellus is common on other banks in the northwestern Gulf of Mexico. The closest collected specimen of P. pulchellus was from 28 Fathom Bank (8 NM due east of the East Flower Garden Bank) at 76 m depth.

Diploria-Montastrea-Porites Zone

More is known of the Diploria-Montastrea-Porites community than of any other at the Flower Garden Banks because it is accessible to research divers using SCUBA. Edwards (1971) considered all coral reefs at the West Flower Garden to belong to this zone, thereby implying a hierarchy of coral dominance (percent cover) similar to that described by Logan (1969) for submerged reefs on the Yucatan Shelf, southwestern Gulf of Mexico. However, subsequent studies by Bright et al. (1974), Tresslar (1974), Viada (1980), and Kraemer (1982) show conclusively that Montastrea annularis is the dominant coral, followed by Diploria strigosa, Montastrea cavernosa, Colpophyllia spp., and Porites astreoides. Convention should therefore dictate a change in zonal designation for high diversity reefs at the Flower Garden Banks to Montastrea-Diploria Zone to reflect the true order of coral dominance above 36 m. For convenience, however, the older designation is retained.

Crustose coralline algae are abundant on the high diversity reefs, and they add substantial amounts of calcium carbonate to the reef substratum. Standing crops of leafy algae on the high diversity reefs are consistently low, possibly kept so by the grazing activities of mobile invertebrates and fishes.

The 253 species of reef invertebrates and 103 reef fishes reported in Bright and Pequegnat (1974) were almost all taken from the Diploria-Montastrea-Porites Zone at the West Flower Garden. Subsequent studies imply a nearly identical community structure and diversity for the Diploria-Montastrea-Porites Zone at the East Flower Garden.

Among the typically caught sport and commercial fishes frequenting the high diversity coral reefs are several species of groupers and hinds, Mycteroperca and Epinephelus; amberjacks, Seriola; Great barracuda, Sphyraena barracuda; Red snapper, Lutjanus campechanus; Vermilion snapper, Rhomboplites aurorubens; Cottonwick, Haemulon melanurum; porgys, Calamus; and Creole fish, Paranthias furcifer.

Spiny lobsters, Panulirus argus, are known to occur on the high diversity reefs at both Flower Garden banks and have been seen by the author on several other banks in the northwestern Gulf of Mexico (Sonnier Bank, 18 Fathom Bank, Bright Bank). Panulirus guttatus has been seen on the shallow coral reefs (26 m) at the East Flower Garden and probably occurs also at the West Flower Garden. The Shovel-nosed lobster, Scyllarides aequinoctialis, is reported from the high diversity reef at the West Flower Garden and undoubtedly occurs also at the East Flower Garden. All of these species of lobsters are probably widely distributed on the Outer Continental Shelf banks in the northwestern Gulf of Mexico, but nothing is known of the magnitude and dynamics of their regional

populations, or whether they could support a commercial lobster fishery.

Stephanocoenia-Millepora Zone

Between 36 and 38 m depth at both banks a transition is apparent from the Diploria-Montastrea-Porites assemblage to a reef zone of lower diversity which extends generally down to 46 m, with components to 52 m. Of the 12 varieties of hermatypic corals known from the zone, 8 are particularly conspicuous: Stephanocoenia michelinii, Millepora sp., Montastrea cavernosa, Colpophyllia spp., Diploria sp., Agaricia spp., Mussa angulosa, and Scolymia sp., probably in that relative order of abundance. Therefore, the designation Stephanocoenia-Millepora Zone is appropriate (Figures 6.2 to 6.3 and 6.10).

Population levels of these corals have not been quantitatively determined, but visual observations indicate considerably lower total live coral cover than in the Diploria-Montastrea-Porites Zone and a great deal of variation in percent cover and relative abundance from place to place. Crustose coralline algae are substantially more conspicuous in the Stephanocoenia-Millepora Zone and are apparently the predominant encrusting forms occupying dead coral reef rock.

Little is known of the assemblage of organisms inhabiting the Stephanocoenia-Millepora Zone. The reef fish populations appear less diverse than in the Diploria-Montastrea-Porites Zone. Population density of the black urchin, Diadema antillarum, which is a significant bioeroder of reef rock, may be similar in both zones. Exceptional numbers of the American thorny oyster, Spondylus americanus, have been seen in the Stephanocoenia-Millepora Zone.

Successional relationships, if any, between the shallower, high diversity Diploria-Montastrea-Porites reefs and deeper, low diversity, Stephanocoenia-Millepora reefs at the Flower Garden Banks cannot be determined from existing information. The low diversity reefs could represent depauperate remnants of high diversity reefs which have been displaced downward to a habitat too deep to support a majority of the contemporary coral species. In this case, much of the dead reef rock upon which the corals of the low diversity reefs now grow would be composed of the remains of coral species now living on the high diversity reefs. Conversely, contemporary high diversity reefs may have developed on the tops of low diversity reefs or other local topographic mounds (possibly accumulations of the coral Madracis mirabilis) whose crests achieved a depth above which high coral diversity and rapid coral growth are possible. To help resolve these questions, more information is needed concerning the nature of the reef rock in both zones, rates of deposition of carbonate rock and sediment, and vertical movements of the

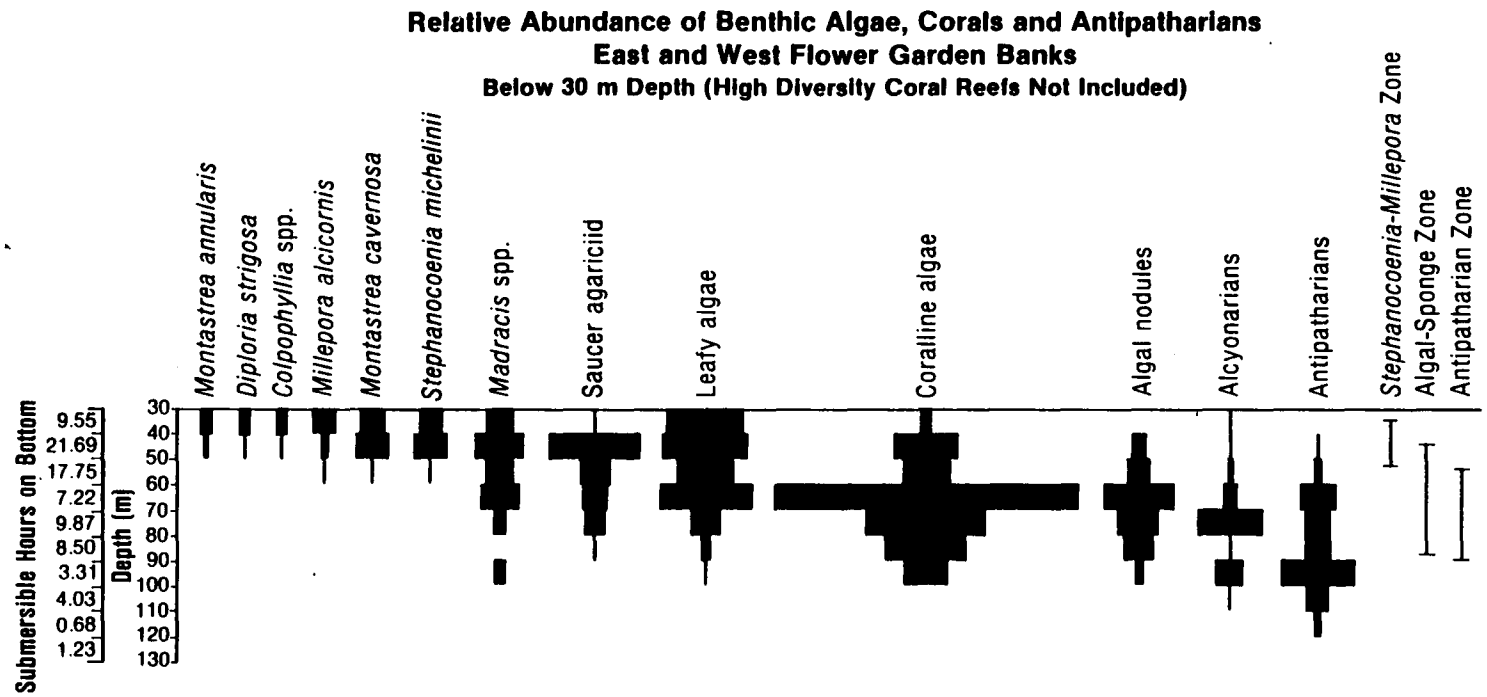

Figure 6.10 Relative abundance of benthic algae, stony corals, alcyonarians, and antipatharians below 30 m depth (high diversity coral reefs excluded). Based on a quasi-quantitative compilation and ranking of observations made from the Texas A&M research submersible DIAPHUS from 1974 through 1980. Raw abundance values were derived from recorded sightings of the various taxa; each sighting was weighted (ranked 1, 5, 10, or 20) according to the observer's (Bright's) assessment of taxon abundance made at the time. Raw abundance values from the East and West Flower Garden were combined within 10 m depth intervals and then divided by the total number of hours spent on bottom making the observations within each depth interval (data were standardized to abundance per hour of observation). Results adequately depict the depth-abundance relationships within taxa. Between-taxon relationships are more approximate, but representative.

substratum and sea level relative to one another in the past several thousand years.

Leafy Algae and *Madracis* Zones

On peripheral parts of the main reefal structure between 28 and 46 m depth at the East Flower Garden, large knolls occur which generally lack significant populations of massive head corals. Certain of these knolls are overwhelmingly dominated by the small branching coral *Madracis mirabilis* (*Madracis* Zone) (Figure 6.8). Other knolls are covered by lush assemblages of leafy algae (Leafy Algae Zone), including species of *Stypopodium*, *Caulerpa*, *Dictyota*, *Chaetomorpha*, *Pocockiella*, *Rhodymenia*, *Valonia*, *Codium*, and others (Figure 6.9). None of these assemblages resembles the adjacent coral reef community in structure although it is likely that most or all of the species found on the knolls also occur on the reefs.

The steeper margins of both main reefs (north, east, and south reef faces) are underlain by thick deposits of coral gravel made up of skeletal remains of *Madracis mirabilis*. Some of these *Madracis* gravel deposits vaguely resemble very large, rounded "spurs and grooves." Others are bluff-like, but many appear to be simply mounds at the reef margins. Living populations of *Madracis mirabilis* occur only at these reef margins, atop the gravel deposits where, standing as thickets a few centimetres high, they are the predominant organisms.

Typically, living *Madracis mirabilis* thickets are accompanied by conspicuous populations of leafy algae and sponges. Elsewhere, the tops of *Madracis* gravel mounds are overgrown by coralline algae, which form a stabilizing, rind-like surface crust beneath which the loose gravel lies. In the grooves and valleys between spurs, hills, or mounds, *Madracis* gravel is frequently shifted by water movements and thrown into large ripple marks, presumably with a resultant net transport of gravel downward and off the reef.

Examples of progressive invasion of the tops of the *Madracis* gravel mounds by hermatypic corals from the high diversity reefs are common. Some mounds harbor a few small heads of *Porites*, *Agaricia*, *Diploria* and other corals superimposed sparsely on the *Madracis* Zone assemblage. Other mounds support larger but scattered heads. Closely spaced heads on the north, east, and south faces of the high diversity reefs (*Diploria*-*Montastrea*-*Porites* Zone) are typically separated by shifting *Madracis* gravel rather than coarse sand, as is the case for most of the reef top.

Thus, it is apparent that, at least in places on the steeper faces of the main reefs, the substratum has been built upward and outward initially through deposition of *Madracis* remains (a massive, roadcut-like anchor scar on the northeastern face of the West Flower

Garden revealed a Madracis gravel thickness of at least 15 m). The Madracis deposits serve as shallow substratum suitable for occupation by the 17 hermatypic coral species of the Diploria-Montastrea-Porites Zone. This successional relationship between the Madracis Zone and the Diploria-Montastrea-Porites Zone probably facilitates the slow spreading of the main reefs onto the adjacent Algal-Sponge Zone.

Algal-Sponge Zone

Though most zones overlap or grade into one another to some extent, they are nevertheless very recognizable and their depth ranges correlate consistently with those of known sedimentological facies (Figure 6.11). The Algal-Sponge Zone includes a number of biotope types occurring between 46 and 82 m at the East Flower Garden and 46 and 88 m at the West Flower Garden. Coarse carbonate sand and gravel surrounding the living coral reefs (Coral Debris Facies) mark a geobiological transition between the coral reefs and the surrounding platform, which is largely covered with carbonate sand, gravel, nodules, and partly drowned reefal structures. In general, the Algal-Sponge Zone is spatially coincident with this platform (Figures 6.1, 6.2, and 6.3).

Large areas on both banks where nodules predominate constitute the Gypsina-Lithothamnium sedimentological facies. The most important contemporary producers of carbonate nodules and crusts on rubble and reefal structures are the coralline algae, and the nodules are typically referred to as rhodoliths or algal nodules (Figure 6.12). Coralline algae are also the overwhelmingly dominant living organisms of the Algal-Sponge Zone.

The algal nodules range in size from less than 1 cm to 10 cm or more, and in most places cover 50 to 80% of the bottom. They create a biotope which harbors an infaunal and epifaunal community which is probably comparable in diversity to the living coral reefs. In addition to coralline algae and the encrusting foraminifer, Gypsina, the nodules themselves house an abundance of boring species and attached epibenthos (Abbott, 1975). Numerous mobile invertebrates and small fishes find shelter under, between, and within the nodules. Beneath the nodules, coarse carbonate sand contains active soft-bottom infaunal populations, as evidenced by the presence of numerous burrows.

Most of the leafy algae at both banks occurs among the algal nodules and on reefal structures within the Algal-Sponge Zone (the aforementioned algae-covered knolls, Leafy Algae Zone, in shallower water are comparatively small in area). Leafy algae are pervasive among the nodules and on hard surfaces within the Algal-Sponge Zone, but are neither uniformly distributed nor uniformly abundant from place to place. At certain locations, lush growths of Stypopodium,

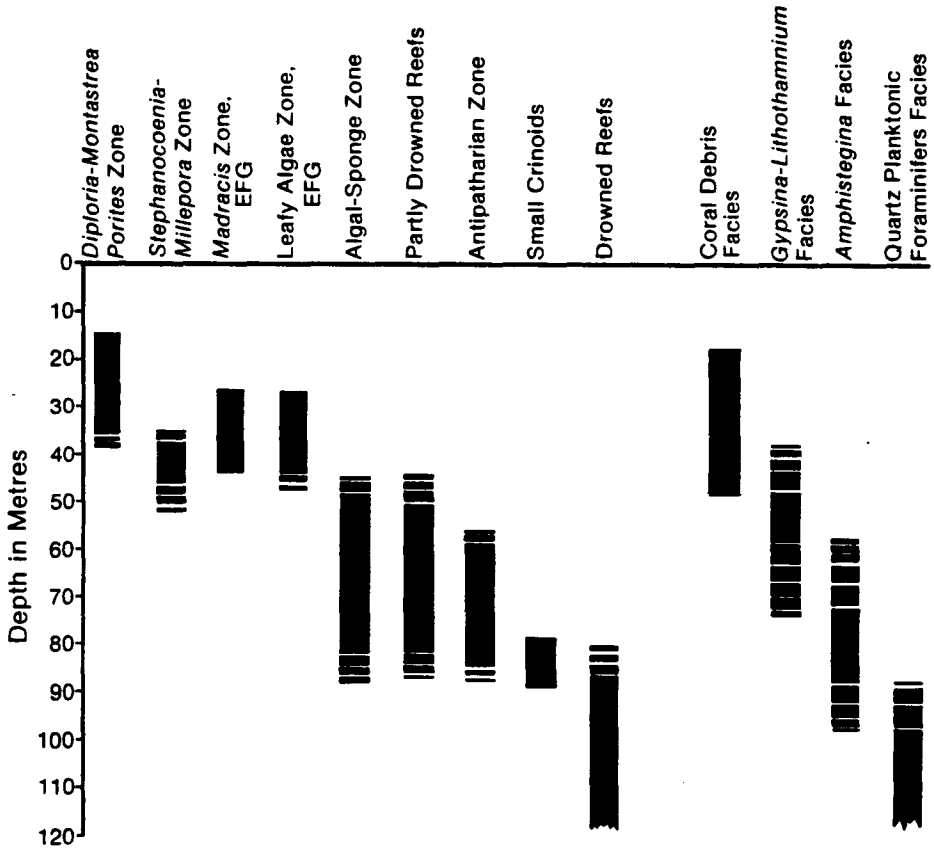

Figure 6.11 Depth ranges of recognizable biotic zones and sedimentary facies (other than hard bottoms) at the Flower Garden Banks. Broken bars indicate varying upper and lower depth extremities for zones, depending on locations.

Peyssonnelia, or Pocockiella may obscure all else on the bottom. The highly productive and rapidly renewable benthic algae populations must furnish substantial amounts of food to the surrounding communities.

Calcareous green algae, Halimeda and Udotea, contribute to sediment production within the Algal-Sponge Zone (Figure 6.13). Patches in excess of 10 m diameter composed almost exclusively of Halimeda have been seen adjacent to algal nodules at both banks. These patches are apparently long-lived, semi-permanent features because the platelike remains of dead Halimeda extend at least several centimetres deep into the substratum. Halimeda also occurs as individual plants among the nodules and on reefal structures.

Several species of hermatypic corals are abundant enough among the algal nodules to be considered major sediment producers within the Algal-Sponge Zone. Saucer-like colonies of Helioseris cucullata and Agaricia are pervasive but unevenly distributed, with populations varying from less than 1 to over 10 colonies per square metre. Several small species of Madracis likewise occur with varying abundance among the algal nodules. Colonies of Montastrea cavernosa have been encountered occasionally in the Algal-Sponge Zone, where, with increasing depth, they tend toward a flat encrusting growth form, presumably in response to decreased light.

Deep-water alcyonarians, primarily Ellisellidae and Paramuriceidae, are abundant in the lower Algal-Sponge Zone. Large, white, coiled, antipatharian whips of the genus Cirrhipathes (= Cirripathes), and bushy colonies of Antipathes are also present in the deeper parts of the zone.

Of the various species of sponges which are conspicuous and abundant within the Algal-Sponge Zone, Neofibularia nolitangere is most distinctive. Crusts of this sponge a metre or so in diameter occur on nodules, sand, or rock within the zone. Fishes and mobile invertebrates are attracted to the sponge, swimming or crawling among its chimney-like spires.

Populations of echinoderms within the Algal-Sponge Zone must add significantly to the carbonate substratum. Sizeable comatulid crinoids and a number of asteroid species are to be found everwhere on the banks except on the living coral reefs. A particularly large population of the asteroid starfish Linckia nodosa and great numbers of the urchins Pseudoboletia maculata (Figure 6.12) and Arbacia punctulata were seen on the algal nodules and reefal structures of the platform west of the main reef at the East Flower Garden. Interestingly, similar concentrations of these particular asteroids and echinoids have not been seen on other parts of either bank.

Small gastropods and pelecypods are abundant on and among the nodules, and gastropod shells are known to be nuclei around which some of the nodules are formed. The largest abundant pelecypod in

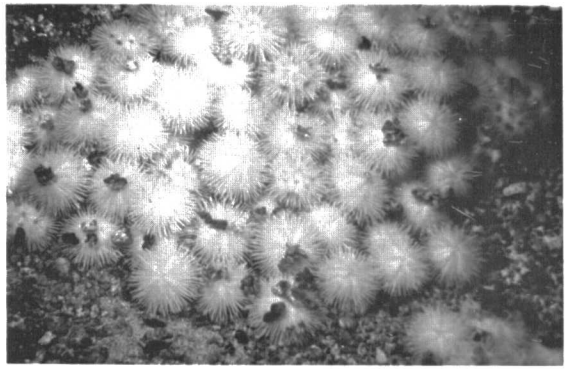

Figure 6.12 Aggregation of white urchins, *Pseudoboletia maculata,* at 59 m depth on bottom covered with very small algal nodules (rhodoliths). Note the nodules displayed on spines of urchins.

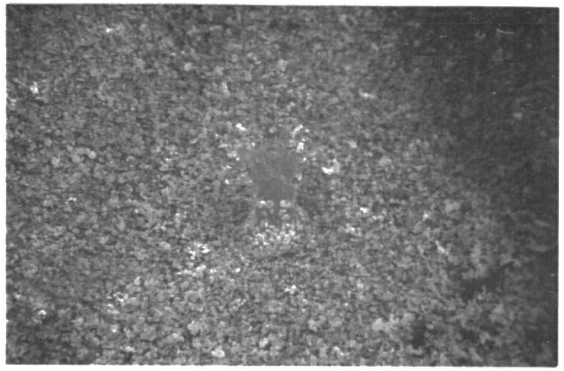

Figure 6.13 Patch of living *Halimeda* sp. at about 55 m depth, East Flower Garden. Large organism in the center is an anemone.

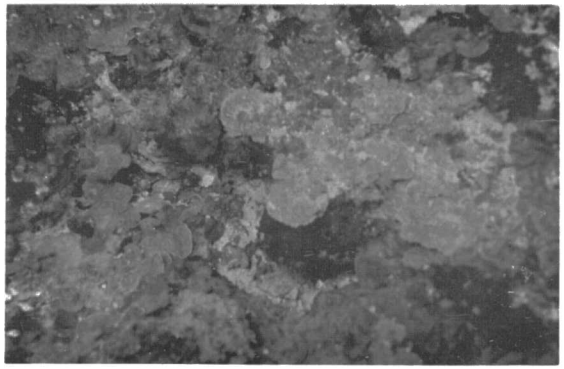

Figure 6.14 Crusts of coralline algae on hard substratum of "partly drowned reef" at the East Flower Garden (60 m depth).

Figure 6.15 Hard sponges attached to carbonate rock coated with veneer of sediment. This is representative of drowned reefs (105 m, Diaphus Bank).

the Algal-Sponge Zone is the American thorny oyster, Spondylus americanus, which occurs attached to nodules as well as reefs. Its distribution, as with many of the conspicuous organisms in the zone, appears irregular and locally contagious (patchy), resulting in a high degree of lateral variation in population levels. Small clumps (approximately one-half metre in diameter) of worm-shell gastropods, Siliquaria modesta, occur infrequently among the nodules and on sand bottoms within the Algal-Sponge Zone. Their contribution to the carbonate sediment is probably minor. The coiled tubes of this species sometimes occur in masses, embedded in the sponge Chelotropella.

Obviously, many species of plants and animals associated with algal nodules within the Algal-Sponge Zone are involved to varied extents in the frame-building processes. Their successful effort in this respect is probably the dynamic factor on which the stability of benthic community structure within the zone depends.

Small Yellowtail reeffishes, Chromis enchrysurus, are the most abundant of the conspicuous fishes congregating around irregularities in the Algal-Sponge Zone. Conical burrows a metre across and one-half metre deep, produced by the Sand tilefish, Malacanthus plumieri, are scattered about the zone from the base of the main coral reef down to at least 70 m. Other particularly characteristic fishes among the algal nodules are the small Cherubfish, Centropyge argi, and Orangeback bass, Serranus annularis.

Partly Drowned Reefs and Drowned Reefs

The nature of both types of living coral reefs has been discussed. As indicated, uncertainty exists concerning the successional relationship, if any, between the high diversity and low diversity coral reefs. The developmental history of the deeper, and presumably older, partly drowned and drowned reefs may be even more complex, possibly involving subaerial exposure of the reef rock (see Rezak, Chapter 4).

The biota now occupying partly drowned and drowned reefs at the Flower Garden Banks probably do not reflect the history of the reefs so much as they do contemporary environmental limitations on depth distributions of the organisms. Accordingly, drowned reefs are defined as those reefal structures now existing at depths too great for hermatypic corals to exist and where crustose coralline algal populations are insignificant (below 82 m at the EFG, below 88 m at the WFG). Partly drowned reefs are those reefal structures covered primarily by living crusts of coralline algae, with occasional crusts and heads of hermatypic corals. They exist now at depths where hermatypic corals have limited capabilities for growth and the

predominance of crustose coralline algae is favored (46 to 82 m at the EFG, 46 to 88 m at the WFG).

Not unexpectedly, partly drowned reefs are generally restricted to the Algal-Sponge Zone, of which they compose a major biotope component. They bear crusts dominated by coralline algae, accompanied by other sessile organisms which are also typical of the algal nodules (Figure 6.14). In addition, they house large anemones such as Condylactis gigantea and Lebrunia danae, an abundance of large comatulid crinoids, occasional basket stars, limited crusts of the hydrozoan coral Millepora, and, infrequently, small colonies of the hermatypic corals Agaricia, Helioseris cucullata, Montastrea cavernosa, and Stephanocoenia michelinii.

The partly drowned reefs attract a number of fish species which also occur on the living coral reefs. Most of these "expatriate" reef fishes are found consistently on similar structures at other banks in the northwestern Gulf which do not support living coral reefs. Therefore, they may not necessarily be recruited from the shallower coral reef fish assemblage at the Flower Garden Banks. The most abundant fish frequenting the partly drowned reefs is the small Yellowtail reeffish, Chromis enchrysurus, which is not often seen on the high diversity coral reefs.

Drowned reefs occur below approximately 82 m at the East Flower Garden and 88 m at the West Flower Garden, where coralline algae do not thrive and hermatypic corals are absent. Comatulid crinoids, small deep-water octocoral whips, Ellisellidae; octocoral fans, Paramuriceidae; antipatharians, Cirrhipathes, Antipathes; encrusting sponges; and solitary ahermatypic corals are the most conspicuous attached organisms (Figure 6.15).

The assemblage of fishes frequenting drowned reefs include Red snappers, Lutjanus campechanus; Spanish flag, Gonioplectrus hispanus; Snowy grouper, Epinephelus niveatus; Bank butterflyfish, Chaetodon aya; scorpionfishes, Scorpaenidae; and, most characteristically, the Roughtongue bass, Holanthias martinicensis. The snappers are highly mobile schooling fish which congregate around reefal structures at all depths on the banks but seem to prefer the deeper "drop-offs" and bank-edge features and show little affinity for the high diversity reef tops. The other fishes listed are commonly found only on the drowned reefs and the deepest partly drowned reefs. The drowned reef ichthyofauna is therefore substantially different in basic species composition from, and of much lower diversity than, that of the partly drowned reefs or the coral reefs.

Drowned reefs at the Flower Garden Banks exist in comparatively turbid water and are generally covered with veneers of fine sediment, the veneers being thicker on the deeper reefs. Light penetration, water turbidity, sedimentation, and temperature are probably the most important factors controlling the present

distribution of hermatypic corals and coralline algae on the banks. It is suspected that, were it not for the chronically turbid bottom water and sedimentation around the peripheries of the banks, the living algal nodules, partly drowned reefs, and other elements of the Algal-Sponge Zones would extend to slightly greater depths, as they do on certain other banks farther offshore where the surrounding soft bottoms are deeper (Rezak and Bright, 1981a, Vol.4).

Transition Zones

White, bedspring-shaped antipatharian whips, *Cirrhipathes*, occur from 52 to over 90 m depth and, where they are most abundant (generally around 60 to 85 m), they mark a transition between biotic assemblages which exhibit distinct shallow-water affinities (leafy algae, abundant coralline algae, hermatypic corals, sizeable shallow water reef fish populations) and those which are deep-water oriented. The upper parts of this supposed "Antipatharian Zone" blend with the Algal-Sponge Zone, and it is impossible to find any sharp demarcation between the two. One might just as well speak of a lower Algal-Sponge Zone which has a sizeable antipatharian population (Figures 6.10 and 6.11).

Deeper parts of the "Antipatharian Zone" (over 80 m) are recognizably less diverse and are characterized by antipatharians, comatulid crinoids, few if any leafy algae, thin to sparse populations of coralline algae, and a distinctly limited fish fauna including *Holanthias martinicensis*, *Bodianus pulchellus*, *Chromis enchrysurus*, *Chaetodon sedentarius*, *Holacanthus bermudensis*, and a few others.

Between 73 and 78 m the nature of the bottom changes, usually rather abruptly, from algal nodules and crusts to a soft, level-bottom of mixed coarse calcareous sand with an abundance of foraminifera (*Amphistegina*) tests and fine silt- to clay-sized particles which are easily stirred up and remain in suspension for a long while. *Amphistegina* is known to live on the algal nodules at both banks. Non-living tests of this protozoan account for a large portion of the *Amphistegina* sands occurring on both banks (Figures 6.2 and 6.3). Presumably, remains of spent *Amphistegina* from the algal nodule biotope are transported downslope to become incorporated into the *Amphistegina* sand.

The *Amphistegina* Sand Facies is characterized by the presence of a conspicuous population of echinoderms, particularly the urchin *Clypeaster ravenelii* and the asteroids *Chaetaster*, *Narcissia trigonaria*, and others. Also, patterned burrows (6 to 12 small burrows in circular aggregations having diameters up to approximately one-half metre) are numerous. In places between 80 and 90 m, a large population of small comatulid crinoids clings to carbonate

gravel and other objects on the Amphistegina sand. These small crinoids do not occur abundantly elsewhere on the banks, and their distribution does not appear to be related to the distribution of larger crinoid species which occupy the lower Algal-Sponge Zone, rocks, and drowned reefs to depths exceeding 120 m. Presence of these crinoids indicates a final transition from shallower, higher diversity, clear-water communities dominated by frame-building corals and coralline algae to subdued, deep-water communities subjected to turbidity, sedimentation, and chronically low light levels. With increasing depth, beyond approximately 90 m, the coarser sediments of the Amphistegina Sand Facies are replaced by mud in the Quartz-Planktonic Foraminifers Facies (Figure 6.11).

The deep-water populations, whether on hard or soft bottom, represent an assemblage of organisms which differs substantially from the clear-water assemblages. Few species of fish and invertebrates occur in both the clear, shallow-water and the turbid deep-water environments on the banks.

POPULATION STUDIES OF HIGH DIVERSITY REEFS

Coral Populations

The Flower Garden Banks harbor 21 species of scleractinian corals and one hydrocoral (Table 6.1). Of these, 18 are considered to be hermatypic (reef-building). Seventeen of the hermatypes occur in the Diploria-Montastrea-Porites Zone. Population levels of the hermatypes identified have been measured using photographic mosaics (Figure 6.16) of 64 transects, each 8 m in length, taken at three sites: 23 transects on the East Flower Garden at 20 m depth on the central reef top (station EFG 20); 23 transects on the East Flower Garden at 26 m depth on the reef top near the reef edge (station EFG 26); 18 transects on the West Flower Garden at 24 m depth on the central reef top (station WFG 24).

Transect positions were restricted to hard-bottom; sand substratum was avoided. Otherwise, no systematic method of transect location was used, and randomness is assumed with substantial subjective confidence. The three samples are considered to be stratified (hard substratum only) and random.

Overlapping photographs were taken along a graduated fiberglass tape transect marker with a Nikonos III camera and electronic strobe mounted to a frame which described an 80 cm X 55 cm field of view on the reef. The resulting color prints were assembled in the laboratory as transect mosaics. A string was stretched along each transect mosaic and the lengths of coral colonies, by species or genera, directly beneath the line were recorded. Metric scale units from the transect tape pictured in the photographs were used for

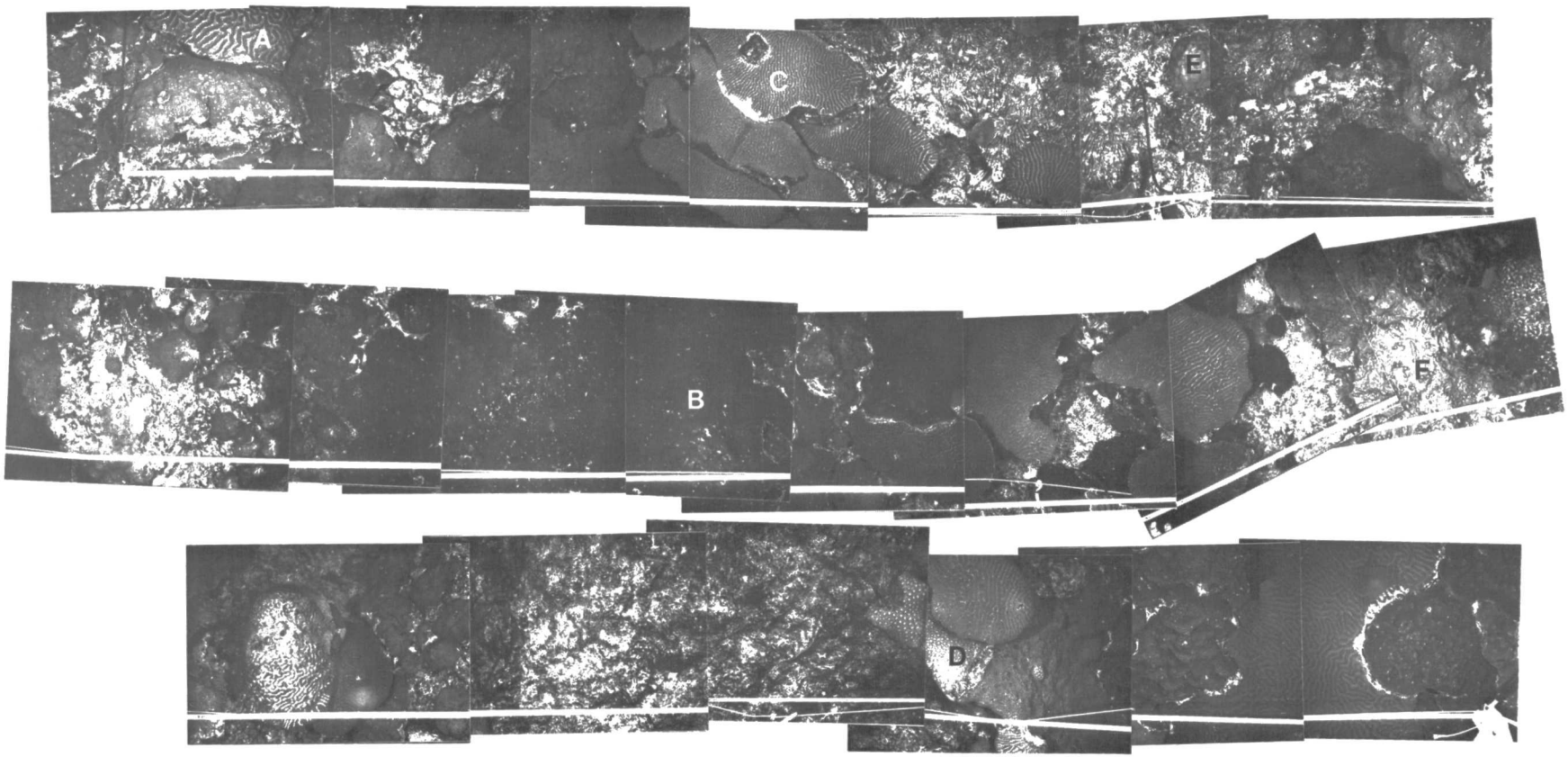

Figure 6.16 Typical photographic mosaic of 10 m long transect at 24 m depth on the West Flower Garden. A = Colpophyllia; B = Montastrea annularis; C = Diploria strigosa; D = Montastrea cavernosa; E = Porites astreoides; F = Millepora alcicornis.

size reference. Most of the 17 hermatypic coral species known to occur on the high diversity reef were identifiable in the photographs, but the two species of Colpophyllia and the three species of Agaricia could not be identified beyond the generic level. The genera were treated as individual taxa in the analyses. Madracis asperula and Porites furcata are so rare that they were never encountered in any of the transects. Failure to detect or resolve these species resulted in 12 measureable taxa (Table 6.2). The determinations are comparable to those achieved using the line transect method reviewed by Loya (1978).

Hard substratum, composed primarily of hermatypic coral reef rock, occupies 85% or more of the bottom within the Diploria-Montastrea-Porites Zone. The remainder is carbonate sand and gravel. This was determined from analysis of wire-line underwater television records of transects traversing the zones at both banks (5 hours at the East Flower Garden, 2.5 hours at the West Flower Garden). On both reefs, somewhat more than half of the hard substratum is covered with living coral (Table 6.2). One-way analyses of variance (ANOVA, 95% confidence level) and Duncan's multiple range tests (DMR) indicate a statistically significant, slightly higher percent coral cover at EFG 26, near the reef edge (65%), than at the other two more central reef top sites (50 to 55%) (Table 6.2). This is consistent with observations by Goreau and Wells (1967) and Porter (1972) of increased coral abundance on reef margins and steep reef slopes in the Caribbean.

Montastrea annularis is the dominant hermatypic species on the high diversity coral reefs, covering 20 to 40% of the hard substratum. ANOVA and DMR analyses imply significantly lower M. annularis population levels at the shallowest site (EFG 20), compared to the other two sites (EFG 26 and WFG 24). Colpophyllia spp. populations were statistically lower at WFG 24. Abundances within each of the other taxa were statistically uniform among the three sites. Therefore, the observed reef edge increase in total coral cover is apparently a reflection of the lower reef top populations of M. annularis at the East Flower Garden and of Colpophyllia spp. at the West Flower Garden.

Corals other than M. annularis cover minor amounts of the substratum, none more than 9%, and most much less (Table 6.2). Together, Diploria strigosa, Colpophyllia spp., Montastrea cavernosa, Millepora alcicornis, and Porites astreoides, in that order of abundance, occupy approximately 20 to 25% of the hard substratum. The importance of the two species of Colpophyllia relative to one another is unresolved, but Colpophyllia amaranthus population levels are probably considerably lower than those of Colpophyllia natans (Tresslar, 1974).

Millepora alcicornis, the only hydrocoral, tends to encrust, spreading rapidly as a thin layer over unoccupied reef rock, with a lateral encrusting growth rate of approximately 2 mm/mo (Bright

Table 6.2 Dominance (% cover) of Major Hermatypic Corals on the Hard Substratum within the Diploria-Montastrea-Porites Zone (high diversity coral reef). Hard substratum constitutes approximately 85% of the bottom within the zone. Determinations are based on 23 transects at each EFG site and 18 at the WFG site. The number of each station is also the depth of collection in metres.

Major Hermatypic Corals	Weighted Averages All Sites Combined	Dominance Expressed as Mean Percent Cover (95% confidence limits of the means)		
		Station EFG 26 (N = 23)	Station EFG 20 (N = 23)	Station WFG 24 (N = 18)
Montastrea annularis	31.80	40.06 (34.88-45.20)	22.88 (17.32-28.51)	32.63 (22.45-42.93)
Diploria strigosa	6.23	4.43 (2.01- 5.03)	8.63 (4.18-13.14)	5.46 (1.93- 8.99)
Colpophyllia spp.	5.33	7.33 (3.49-11.12)	6.62 (3.57- 9.62)	1.11 (0.17- 2.05)
Montastrea cavernosa	3.86	3.68 (1.48- 6.13)	3.84 (2.82- 5.89)	4.10 (1.28- 6.92)
Millepora alcicornis	3.61	3.21 (2.01- 4.38)	3.69 (1.52- 5.94)	4.03 (2.04- 6.20)
Porites astreoides	2.26	2.26 (1.28- 3.24)	1.94 (1.17- 2.72)	2.68 (1.60- 3.76)
Madracis decactis	1.91	3.02 (0.47- 5.61)	0.88 (0.47- 1.31)	1.79 (0.15- 3.43)
Siderastrea siderea	0.90	0.00	1.27 (0- 3.32)	1.56 (0- 3.85)
Agaricia spp.	0.83	0.76 (0.34- 1.19)	0.90 (0.52- 1.28)	0.83 (0.26- 1.40)
Stephanocoenia michelinii	0.30	0.16 (0.02- 0.34)	0.21 (0- 0.57)	0.59 (0- 1.43)
Mussa angulosa	0.26	0.60 (0.19- 1.02)	0.00	0.17 (0.01- 0.33)
Scolymia cubensis	0.03	0.03 (0- 0.06)	0.03 (0- 0.09)	0.03 (0- 0.08)
Total live coral	56.82	64.53 (59.6 -69.46)	50.42 (45.1 -55.74)	55.15 (23.77-86.53)

et al., 1982). This is by far the fastest rate of encrusting growth among the corals at the Flower Garden Banks (see below). Consequently, the species is abundant (Table 6.2). As a primarily opportunistic encrusting form, M. alcicornis may not be nearly as effective a substratum builder in terms of sustained accretionary growth as are dominant scleractinian corals such as Montastrea annularis, which tend to form massive, rounded colonies.

Stephanocoenia michelinii, while not abundant on the high diversity reef tops (Table 6.2), is one of the dominant head-forming species below about 36 m depth on the fringes of the two main reefs, and on outlying low diversity reefs (Figure 6.10).

Although Mussa angulosa and Scolymia cubensis are minor species on the reef, it is likely that they were seriously undersampled in the transects because of their small size and often cryptic occurrence. For these reasons, one may discount the results of ANOVA-DMR comparisons which indicate significantly higher population levels for Mussa angulosa at the deepest site (EFG 26), than at the other two sites. Interestingly, however, M. angulosa is one of the several species whose distribution persists onto the deeper, low diversity reefs.

Shannon-Weaver indices of coral diversity were calculated for the three sites using a method described by Pielou (1966) for estimating the diversity of vegetatively reproducing organisms in large, incompletely censused sample areas using cover as the measure of abundance (Table 6.3). Evenness estimates were derived assuming that a maximum of 13 coral taxa were detectable in the photographic transect mosaics, Porites furcata would have been recognized but not Madracis asperula. Strongly overlapping 95% confidence intervals and similarity of means between the EFG 20 and WFG 24 stations imply that coral diversity and evenness are similar at these central reef locations. Comparatively lower means for EFG 26 may indicate slightly decreased diversity and evenness at the deeper, reef edge station. This would be consistent with the observed increase in dominance of M. annularis at EFG 26 (Table 6.2), which would tend to decrease both diversity and evenness.

Even considering the minor variations in abundance of certain corals from place to place on the East and West Flower Garden Banks, there is a strong impression that the high diversity reef tops of the two banks are essentially similar in coral species composition, cover, dominance hierarchy, diversity, and evenness.

With only 18 species of hermatypic corals (and notably, no acroporids or shallow water alcyonarians), the Flower Garden coral community is less diverse than those of comparable reefs in the southern Gulf of Mexico (34 species), south Florida (51 species), and the Caribbean (55 species). Yet, in spite of the qualitative deficiencies in coral species composition, those hermatypes which occur at the Flower Garden Banks constitute an apparently hardy coral community.

Table 6.3 Shannon-Weaver Indices of Coral Diversity and Eveness[a]. For comparison to other data, see Table 6.7.

Station	Depth (m)	Diversity mean (95% CI)	Evenness	N
EFG 26	26	1.41 (1.24-1.58)	0.55	18
EFG 20	20	1.69 (1.43-1.95)	0.66	22
WFG 24	24	1.62 (1.16-2.09)	0.63	14

Diversity = H'c
Evenness = H'c/H'max
N = number of sets of pooled transects used to estimate Shannon-Weaver index by Pielou's method.

[a]Calculated using the technique of Pielou (1966) for estimating diversity of vegetatively reproducing organisms in communities which cannot be fully censused. Ninety-five percent confidence limits are given in parentheses. Evenness estimates were calculated using the mean Shannon-Weaver diversity values, and assuming 13 recognizable coral taxa within the *Diploria-Montastrea-Porites* Zone (species of *Agaricia* and *Colpophyllia* were not separable in the photographs; *Porites furcata* would have been recognized had it occurred in any of the transect mosaics).

Calcareous Algae and Encrusting Foraminifer Populations

At least nine genera of crustose coralline algae (Corallinaceae) occur at the Flower Garden Banks (Table 6.1). Of these, *Hydrolithon* and *Lithophyllum* are particularly abundant on the high diversity coral reefs. In the deeper Algal-Sponge Zone, *Lithothamnium*, *Tenarea*, *Lithophyllum*, and *Peyssonnelia* (a squamariacean) predominate.

Coverage of crustose coralline algae on hard substratum within the *Diploria-Montastrea-Porites* Zone was estimated from transect mosaics at the EFG 20 and WFG 24 study sites. As a group, crustose corallines occupy approximately 15 to 20% of the hard bottom. The algae tend to inhabit cryptic as well as exposed substratum, and are found abundantly on such things as living gastropod shells, hermit crab shells, attached pelecypods, and shell and coral debris on the sand between coral heads.

Following the mortality of part of a coral colony, the newly exposed reef rock is almost always occupied first by filamentous algae and then by crusts of coralline algae, which tend to persist until overgrown in turn by coral, sponge, or some other superior competitor for space. Observations derived from studies of coral growth and mortality leave the impression that, on the Flower Garden high diversity reefs, the coralline algae are pervasive opportunists, capable of rapidly colonizing and covering exposed reef rock, but incapable of preventing subsequent encroachment by the dominant hermatypic corals. Hence, their importance as frame builders is overshadowed by the corals, which have a competitive advantage at the shallowest depths on the two banks.

The coral's advantage deteriorates with increasing depth, leading to increased, but still secondary, dominance of coralline algae on the low diversity coral reefs, and virtual dominance by coralline algae within the Algal-Sponge Zone, where rhodolith formation is extensive (Figure 6.12). The Algal-Sponge Zone, in fact, occupies considerably more area on the banks than do the coral reefs (Figures 6.2 and 6.3), and the majority of carbonate sediment produced on the banks is of algal origin.

In terms of the banks' overall structure and biology, the coralline algae are extremely important. As with the corals, their patterns of dominance, zonation, and community structure are largely dependent on levels of light intensity and, therefore, depth (Table 6.1). Below approximately 85 m at the Flower Garden Banks, growth of coralline algae is seriously impaired, and reefal development ceases.

As previously indicated, Calcareous green algae, *Halimeda* spp. and *Udotea* spp., contribute to sediment production within the Algal-Sponge Zone (Table 6.1). The encrusting foraminifer *Gypsina plana* is an important contributor to rhodolith formation within the Algal-Sponge Zone. It is also abundant on the high diversity and low diversity coral reefs (Table 6.1).

CORAL GROWTH AND MORTALITY

Accretionary Growth

Coring of living heads of *Montastrea annularis* and *Diploria strigosa* with an underwater pneumatic drill (Stearn and Colassin, 1979), and thin-sectioning of a collected head of *Stephanocoenia michelinii* provided samples for x-radiographic sclerochronological determination of accretionary growth rates (Figure 6.17) using the methods of Hudson et al. (1976). Accretionary growth determinations from the cores were limited to 16 years (1964-1980) due to the core

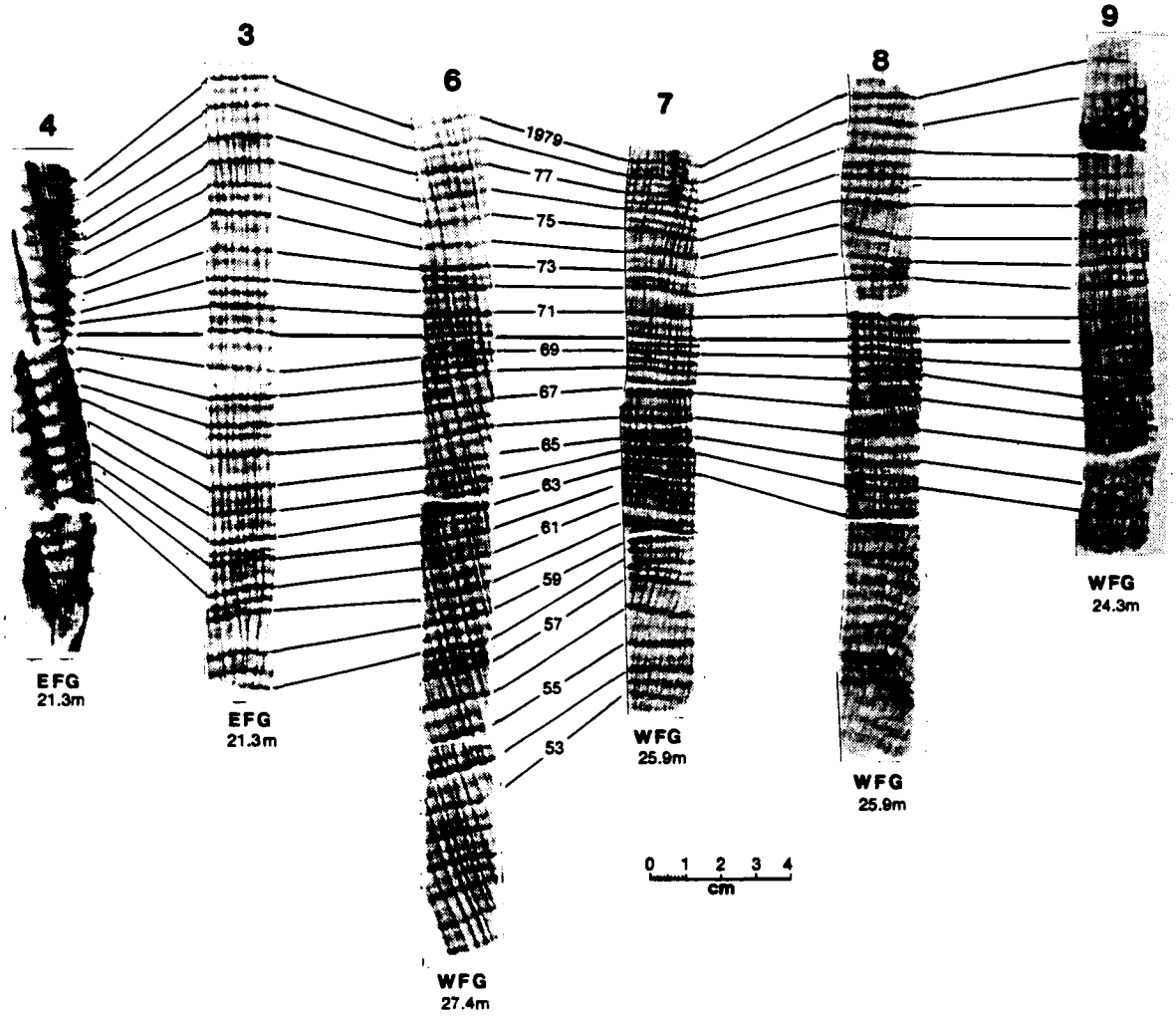

Figure 6.17 X-Radiographs of cores taken from Montastrea annularis and Diploria strigosa at the East and West Flower Garden Banks, showing annual bands. Locations and depths of collection are indicated beneath each core.

lengths. Average growth rates for 4 West Flower Garden heads of M. annularis (collected at 24.3 and 27.4 m depth) appear essentially the same as average rates for 12 East Flower Garden heads (20 m depth) sampled and analyzed by Hudson and Robbin, 1980 (Figure 6.18). Unfortunately, our short cores do not allow comparison beyond 16 years past. Thus, we are unable to say whether the decrease Hudson and Robbin detected in M. annularis growth rate at the East Flower Garden (from a 50-year average of 8.9 mm/yr through 1957 to a subsequent average of 7.2 mm/yr through 1979) also occurred at the West Flower Garden.

Our data suggest a decrease in M. annularis growth rate with increasing depth (Table 6.4). This would not be surprising, but because of the small number of cores it cannot reliably be supported as a conclusion.

The single core of D. strigosa from 21.3 m at the East Flower Garden indicates a substantially lower growth rate for this species (average, 5.2 mm/yr) than for M. annularis (range of averages, 5.9 to 8.4 mm/yr) on the reef top.

Interestingly, the apparent growth rate over 44 years (average, 5.8 mm/yr) of our specimen of S. michelinii (collected in 1974 near the base of the main East Flower Garden reef at 38.5 m depth) is quite comparable to that of D. strigosa. However, considering only the years 1964-1974, the average accretionary growth rate for S. michelinii was only 3.8 mm/yr (Figure 6.18). We suspect that the smaller value is more representative, and that the 44-year average was inflated due to tangential sectioning of growth bands near the central part of the slab which was analyzed. S. michelinii is a dominant coral on the deeper, low diversity coral reefs at both banks. It also survives well on other northwestern Gulf of Mexico banks in water which is often, or chronically, turbid.

Encrusting Growth and Retreat

Encrusting growth is the lateral spreading of thin layers of living tissue and newly secreted corallum across reef rock. Its obverse is lateral retreat of colony borders due to tissue mortality and disintegration. Both encrusting growth and lateral retreat were determined for M. annularis and D. strigosa through planimetric analysis and comparison of seasonal, close-up (MACRO) photographs taken in situ of specific segments of living coral colony borders not in close proximity to other competing colony margins (Kraemer, 1982).

Encrusting growth rates measured for D. strigosa (average, 0.46 mm/mo) were somewhat greater than those of M. annularis (average, 0.33 mm/mo) (Table 6.5). Rates at which disintegrating borders retreated were considerably greater for D. strigosa (average, 0.57 mm/mo) than for M. annularis (average, 0.20 mm/mo).

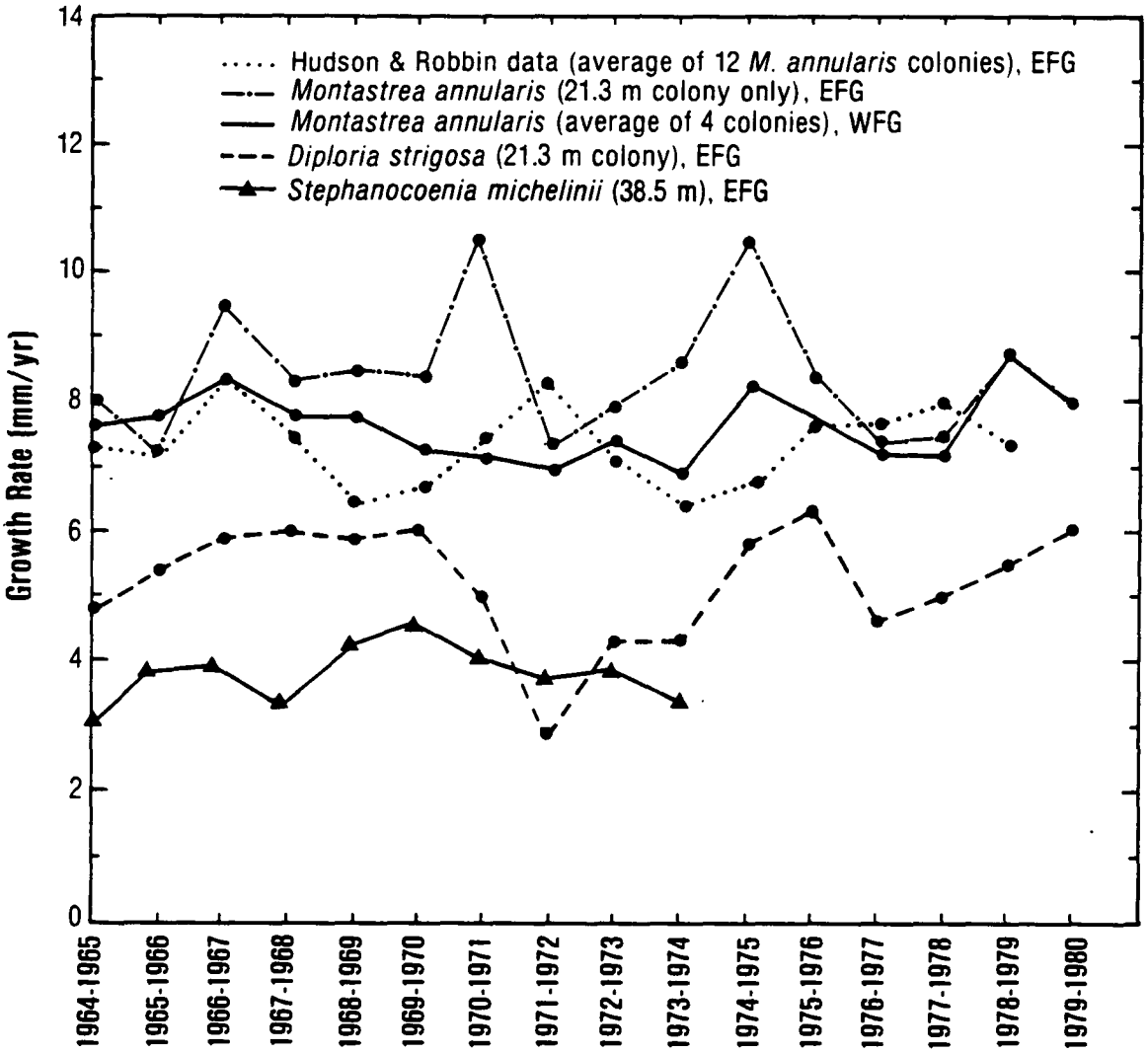

Figure 6.18 Accretionary growth rates for Montastrea annularis, Diploria strigosa, and Stephanocoenia michelinii.

Table 6.4 Accretionary Growth Rates of Corals from the East and West Flower Gardens[a]

Species	Location and Core no.	Depth (m)	Accretionary Growth: Mean (mm/yr)	Accretionary Growth: 95% Confidence Limits of Mean (mm/yr)
D. strigosa	EFG-4	21.3	5.2	4.8 - 5.7
M. annularis	EFG-3	21.3	8.4	7.8 - 8.9
M. annularis	WFG-9	24.4	8.0	7.4 - 8.6
M. annularis	WFG-8	25.9	7.3	6.8 - 7.8
M. annularis	WFG-7	25.9	5.9[b]	5.3 - 6.5
M. annularis	WFG-6	27.4	6.9	6.5 - 7.4
S. michelinii	EFG-s	38.5	?5.8[c]	?5.5 - 6.2

[a]Generated from sclerochronological analyses of sections taken from cores and a collected head.

[b]Core WFG-8 was taken vertically into the top of the head; WFG-7 was taken horizontally into the side of the same head. Results imply that vertically directed accretionary growth on the crest of this head was more rapid than horizontally directed accretionary growth on its flank.

[c]Based on 44 bands in cross section (EFG-s) of head collected in 1974, and interpreted for us by J.H. Hudson. Considering only those bands assumed to be deposited since 1964, the average accretionary growth of *S. michelinii* from 1964-1974 was 3.8 mm/yr.

Table 6.5 Rates of Encrusting Growth and Retreat of Colony Borders Across Underlying Reef Rock at the East and West Flower Garden Reefs

	Species	Mean (mm/mo)	95% Confidence Limits of Mean (mm/mo)	Number of Colonies Measured
Encrusting Growth	M. annularis	0.33	0.16-0.50	13
	D. strigosa	0.46	0.31-0.61	3
Retreat	M. annularis	0.20	0.0-0.43	13
	D. strigosa	0.57	0.0-1.15	6

ANOVA revealed no differences between the East and West Flower Garden in either encrusting growth rates or rates of retreat in M. annularis. Nor were seasonal differences statistically demonstrated. However, simple comparison of the seasonal means (Figure 6.19) hints at a decrease in M. annularis encrusting growth rates during the fall and winter and a possible increase in rates of retreat in the spring.

Coral dominance, as defined here, is dependent on the percent of hard bottom covered by living tissue of the various coral species. The rates at which colonies of coral species can expand their borders when not in direct competition with other colonies, compared to their typical mortality rates in terms of border retreat, are undoubtedly important in determining positions of species in the coral dominance (percent cover) hierarchy (see also Lang, 1973, for concepts of coral dominance based on physiological competition).

As previously indicated, data suggest that D. strigosa encrusts at a slightly greater rate than M. annularis, but D. strigosa typically dies back (retreats) substantially faster than does M. annularis. In addition, D. strigosa is particularly susceptible to disease-related mortality at the Flower Garden reefs (Abbott, 1979). Rates of border retreat in apparently diseased D. strigosa heads are as great as 6.5 mm/mo, an order of magnitude larger than the average rates of retreat for either species. Thus, hypothetically, the net balance between encrusting growth and retreat at colony margins on the Flower Garden reefs could favor M. annularis over D. strigosa, and, if so, would give M. annularis a competitive advantage.

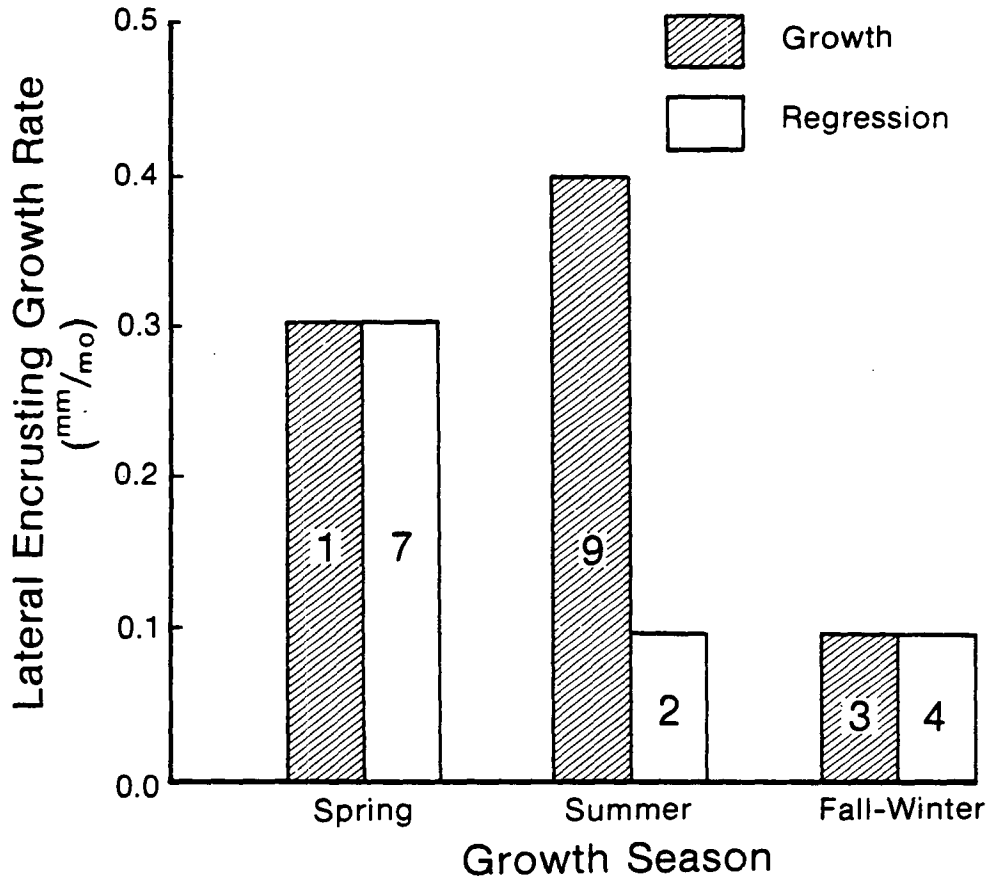

Figure 6.19 Seasonal averages of Montastrea annularis encrusting growth and retreat measurements made between September 1978 and September 1980. Spring = mid-February to early June; summer = early June to early September; fall/winter = early September to mid-February. Numbers of coral colonies measured are indicated on the histogram bars. Although the differences are interesting, one-way analysis of variance did not indicate that they were statistically significant.

DISCUSSION

Assemblages of stony corals occupying the Flower Garden reefs are similar to those of submerged reefs and deep forereefs in the Caribbean and the southern Gulf of Mexico (Goreau, 1959; Bak, 1977; MacIntyre, 1972; Logan, 1969; Kornicker et al., 1959; Rigby and McIntyre, 1966). However, of the approximately 55 species of shallow-water hermatypic scleractinian and hydrozoan corals in the Caribbean, Bahamas, and south Florida, only 18 occur at the Flower Garden Banks (Table 6.6). In comparison, 24 hermatypic species are known from Bermuda, 16 from the northeastern Gulf of Mexico (Florida Middle Ground), and 34 from the southern Gulf of Mexico (Campeche Bank and the Gulf of Campeche).

Bermuda, the Florida Middle Ground, and the Flower Garden Banks represent three separate, northern, biogeographic "end points" in the contemporary distribution of tropical Atlantic coral reefs and coral-dominated assemblages derived from the Caribbean biota. All are depauperate in hermatypic corals, harboring only 29 to 44% of the known tropical Atlantic species (Table 6.6).

Interestingly, coral reefs at the Flower Garden Banks and Bermuda are more closely related to each other in terms of community structure and coral dominance patterns than either are to the Florida Middle Ground assemblages, which are not considered true coral reefs. The Florida Middle Ground has only 6 hermatypic coral species in common with the Flower Garden Banks, and 8 in common with Bermuda, whereas 10 species occur on both the Bermudan and Flower Garden reefs. Only 3 scleractinians and 1 hydrocoral occur at all three locations (Table 6.6).

Primary dominants common to the Flower Garden Banks and Bermuda (*Montastrea annularis*, *Diploria strigosa*, and *Porites astreoides*) are absent from the Florida Middle Ground, where *Madracis decactis*, *Millepora* spp., and *Dichocoenia* spp. are the important stony corals (Hopkins et al., 1977; Grimm and Hopkins, 1977). On the other hand, shallow water alcyonarians and *Dichocoenia* spp. are abundant at the Florida Middle Ground and Bermuda, but are absent from the Flower Garden Banks. In fact, shallow water alcyonarians are abundant on all Atlantic coral reefs other than the Flower Gardens. This discrepancy alone is enough to distinguish the Flower Garden Banks biogeographically. All three northern localities lack *Acropora palmata* and *Acropora cervicornis*, species of material importance on emergent reefs in the Caribbean, south Florida, Bahamas, and the southern Gulf of Mexico.

A distributional link between the Flower Garden reefs and the more diverse Campeche reefs is implied by the fact that only three hermatypes occurring at the Flower Garden reefs are not known from the southern Gulf (*Madracis asperula*, *Madracis mirabilis*, and *Helioseris cucullata*). These species tend to be rare or cryptic on

Table 6.6 Occurrence of Hermatypic Corals in the Western Atlantic

Present *** (no abundance implied)
Absent ---

Hermatypic Corals	CARIBBEAN	BAHAMAS & SOUTH FLORIDA	SOUTH GULF	BERMUDA	EAST & WEST FLOWER GARDEN	FLORIDA MIDDLE GROUND
Stephanocoenia michelinii	***	***	***	***	***	***
Madracis decactis	***	***	***	***	***	***
Madracis asperula[a]	***	***	---	---	***	---
Madracis mirabilis	***	***	---	***	***	---
Acropora palmata	***	***	***	---	---	---
Acropora cervicornis	***	***	***	---	---	---
Acropora prolifera	***	***	***	---	---	---
Agaricia agaricites	***	***	***	---	***	---
Agaricia tenuifolia	***	---	***	---	---	---
Agaricia undata	***	***	---	---	---	---
Agaricia lamarcki	***	***	***	---	---	---
Agaricia grahamae	***	***	---	---	---	---
Agaricia fragilis	***	***	***	***	***	***
Helioseris cuculiata	***	***	---	---	***	---
Siderastrea siderea	***	***	***	***	***	---
Siderastrea radians	***	***	***	***	---	***
Porites astreoides	***	***	***	***	***	---
Porites branneri	***	***	***	---	---	***
Porites porites	***	***	***	***	---	---
Porites divaricata	***	***	***	---	---	***
Porites furcata	***	***	***	---	***	---
Favia fragum	***	***	***	***	---	---
Diploria clivosa	***	***	***	***	---	---
Diploria labyrinthiformis	***	***	***	***	---	---
Diploria strigosa	***	***	***	***	***	---
Manicina areolata	***	***	***	***	---	***
Colpophyllia natans	***	***	***	---	***	---
Colpophyllia amaranthus	***	***	***	---	***	---
Colpophyllia breviserialis	***	***	---	---	---	---
Cladocora arbuscula	***	***	***	---	---	***
Montastrea annularis	***	***	***	***	***	---
Montastrea cavernosa	***	***	***	***	***	---

Table 6.6 (Continued)

Hermatypic Corals	CARIBBEAN	BAHAMAS & SOUTH FLORIDA	SOUTH GULF	BERMUDA	EAST & WEST FLOWER GARDEN	FLORIDA MIDDLE GROUND
Solenastrea hyades	***	***	---	---	---	---
Solenastrea bournoni	***	***	---	---	---	---
Meandrina meandrites	***	***	***	***	---	***
Meandrina brasiliensis	***	***	---	***	---	---
Dichocoenia stokesi	***	***	---	***	---	***
Dichocoenia stellaris	***	***	---	---	---	***
Dendrogyra cylindrus	***	***	***	---	---	---
Mussa angulosa	***	***	***	---	***	***
Scolymia lacera	***	***	---	---	---	***
Scolymia cubensis	***	***	***	---	***	***
Isophyllia sinuosa	***	***	---	***	---	---
Isophyllia multiflora	***	***	***	***	---	---
Isophyllastrea rigida	***	***	---	***	---	---
Mycetophyllia lamarckiana	***	***	***	***	---	---
Mycetophyllia danaana	***	***	---	---	---	---
Mycetophyllia ferox	***	***	---	---	---	---
Mycetophyllia aliciae	***	***	---	---	---	---
Mycetophyllia reesi	***	---	---	---	---	---
Eusmilia fastigiata	***	***	***	***	---	---
Millepora alcicornis	***	***	***	***	***	***
Millepora monliliformis	***	---	---	---	---	---
Millepora complanata	***	***	---	---	---	***
Millepora squarrosa	***	---	---	---	---	---

[a]*Madracis asperula* is considered "hermatypic" because of its apparent importance as a substratum producer in the Algal-Sponge Zone at the Flower Gardens and other shelf edge banks in the northwestern Gulf of Mexico.

Sources: Davis (1982), Dodge et al. (1982), Goreau and Wells (1967), Wells (1973), Porter (1972), Rannefeld (1972), Roos (1964, 1971), Chavez et al. (1970), Chavez (1973), Villalobos (1971), Moore (1958), Fandino (unpublished), Cairns (1977), Jameson (1981), Smith (1971), Hopkins et al. (1977), Grimm and Hopkins (1977), Ginsberg et al. (1970), Wilson (1969).

reefs dominated by head corals or Acropora, and one suspects that they occur in the Gulf of Campeche but have not been reported.

Considering the similarity of the Flower Garden reefs to those in the southern Gulf, and their dissimilarity to tropical hard bottom assemblages in the northeastern Gulf of Mexico, we hypothesize that the Flower Garden biota represent a northward extension of the reefal communities in the southern Gulf of Mexico. The Florida Middle Ground assemblages must be molded by factors inherent in the eastern Gulf, possibly with little direct biological exchange between them and reef systems in the northwestern Gulf. The general patterns of surface currents within the Gulf of Mexico are not inconsistent with this idea (Nowlin, 1972; Merrell and Morrison, 1981). Specifically, epipelagic currents passing the Flower Garden Banks are predominantly from the southwest, and are tropical, oceanic in character (McGrail et al., 1982a). Oceanic currents passing the Florida Middle Ground come directly from the Yucatan Channel and are generally restricted to the eastern Gulf of Mexico. Moreover, the Florida Middle Ground, located on an extensive carbonate shelf, with numerous exposures of hard substratum occupied by tropical epibenthos, is not as geographically isolated from other components of the Caribbean biota as are the Flower Garden Banks, which occur at the edge of a continental shelf of terrigenous clays and sand. Thus, probabilities relating to larval transport and recruitment of Caribbean biota may differ drastically in the two regions.

Midshelf hydrographic conditions at the Florida Middle Ground are more neritic than are the shelf-edge conditions at the Flower Garden Banks and Bermuda. It is likely, therefore, that the similarity between coral populations at the Flower Garden Banks and Bermuda, and the dissimilarity between these two localities and the Florida Middle Ground, is related to winter water temperature minima. During February-March, surface temperatures drop to about 19°C in Bermuda (Bosellini and Ginsburg, 1971), and to approximately 18°C at the Flower Garden reef crest (Etter and Cochrane, 1975). Winter temperatures at the Florida Middle Ground dip to 15.7°C (Hopkins and Schroeder, 1981). The accepted miminum for vigorous coral reef development is 18°C (Stoddart, 1969); 16°C is considered a low temperature stress threshold, below which most hermatypic corals lose their ability to capture food (Mayor, 1915; Roberts et al., 1982).

Cool winter temperatures at all three locations relative to south Florida and the Caribbean are likely factors contributing to the absence of acroporids on the northern reefs. Although the 15 to 23 m water depths at the Flower Garden Banks and the Florida Middle Ground approach the depth limits for Acropora palmata and A. cervicornis, these same species have been observed at similar depths in the warmer waters of Belize and St. Croix in the Caribbean.

Selective exclusion of coral species by unfavorably low water temperatures is generally accepted (Wells, 1957). Bermudan, Flower Garden, and Florida Middle Ground reefs illustrate this well. The Florida Middle Ground in particular, having the lowest winter temperatures, no well-developed aggregations of massive coral heads, and a dominance structure not typical of Caribbean reef communities, is probably existing in quite marginal environmental conditions. The absence of true tropical coral reefs on outcrops and banks closer to shore than the Flower Gardens off Texas and Louisiana is certainly due to the comparatively drastic variations in temperature, salinity, and turbidity on the river-influenced inner and middle continental shelf compared to the basically oceanic shelf edge.

Shannon-Weaver diversity index values from the Flower Garden reefs and several other roughly comparable Atlantic reefs were assessed (Table 6.7). Diversities measured on Panamanian (Porter, 1972) and Puerto Rican reefs (Loya, 1976) were, predictably, higher than those from Bermuda (Dodge et al., 1982) and the Flower Garden reefs. The correspondence between Bermudan and Flower Garden values is interesting in view of the qualitative similarity of these isolated, northern reef communities. Considering the number of possible species in the various regions, it is surprising that there was not a greater discrepancy between the Caribbean diversity values and the values from Bermuda and the Flower Garden reefs.

Total coral cover at the Flower Garden reefs compares favorably with reefs elsewhere in the western Atlantic (Table 6.7). Based on assessments of reefs in south Florida, the Bahamas, the Virgin Islands, and the Caymans, the Flower Garden reefs rate high in terms of apparent vitality and amount of substratum occupied by living coral.

Accretionary growth rates for corals at the Flower Garden reefs are similar to growth rates for the same species on other Atlantic coral reefs. Hudson (1981) determined growth rates for Montastrea annularis at 12 locations off Key Largo, Florida, finding most rapid growth on shallow (1 to 2 m depth), midshore patch reefs in fairly clear water (average growth 11.2 mm/yr). He found slowest growth in the forereef zones of offshore barrier-type reefs in water depths of 6 to 12 m (average, 6.3 mm/yr). This latter value corresponds closely to that obtained by Baker and Weber (1975) at 20 m depth in St. Croix, U.S. Virgin Islands (6.5 mm/yr). Our measurements for the same species (5.9 to 8.0 mm/yr at the WFG and 8.4 mm/yr at the EFG) and those of Hudson and Robbin (1980) (7.4 mm/yr on the EFG between 1964 and 1979) indicate rapid growth, considering the depths of sampling at the Flower Garden reefs (20 to 27 m).

For Diploria strigosa, our estimate of 5.2 mm/yr average accretionary growth at 21 m depth on the East Flower Garden falls between estimates made by Vaughan (1916) for the Dry Tortugas (6.9 mm/yr) and by Shinn (1975) for Carysfort reef off Key Largo

Table 6.7 Comparison of Coral Abundances and Shannon-Weaver Diversity Values from this and Other Atlantic Reef Studies which Employed Similar Techniques[a]

Atlantic Reef Studies	Depth(m)	Total Coral Cover(%)	Diversity H'n	Diversity H'c	Evenness (H'c/H'max)	Number of Hermatypic Corals: In Depth Range	Number of Hermatypic Corals: Known From Area
Panama	17-24			1.5-2.1		28	49
Neth. Antilles	15-40	30-35				27	50
Puerto Rico	11-17	42-79	2.0-2.2	2.5-2.6(?)	.81-.83	20	35
Veracruz	10-17	20				15	34
Bermuda	3-5	14-22		1.3-1.7	.77-.82	16	22
Flower Gard.	20-26	43-55[b]	1.5	1.4-1.7	.55-.66[c]	17	18

[a]H'c is the Shannon-Weaver diversity index, using amount of bottom covered as the measure of coral abundance. H'n is the Shannon-Weaver diversity index, using number of colonies as the measure of coral abundance. In our opinion, only H'c is appropriate for encrusting or head-forming organisms exhibiting variable colony size, such as the corals. The diversity indices for Panama were converted to natural log format for purposes of comparison. Loya (1976) reported H'c/H'max, but not H'c. The H'c values for Puerto Rico were therefore derived from his H'c/H'max using the maximum number of species (22) he encountered.

[b]Derived by multiplying our values for live coral cover on hard bottom by 0.85, which is the approximate proportion of hard bottom within the *Diploria-Montastrea-Porites* Zone.

[c]Calculated using 13 as the number of coral taxa recognizable in photographic transects (H'max=ln 13).

References: Panama, Porter (1972); Netherlands Antilles, Bak (1977); Puerto Rico, Loya (1976); Veracruz, Rannefeld (1972); Bermuda, Dodge et al. (1982); Flower Gardens, Viada (1980) and herein.

(5.0 mm/yr). Our minimal estimate of Stephanocoenia michelinii growth at 38.5 m depth on the East Flower Garden (3.8 mm/yr) implies healthy accretion even at considerable depths.

Baker and Weber (1975) recognized a substantial decrease in growth rate of M. annularis with depth at St. Croix, U.S Virgin Islands (6.5 mm/yr at 20 m depth; 2.1 mm/yr at 25 m depth; 1.6 mm/yr at 30 m depth). Our data also indicate a decrease in growth rate with increasing depth for M. annularis at the Flower Garden reefs, but of a much lesser magnitude (8.4 mm/yr at 21.3 m depth; 7.3 mm/yr at 25.9 m depth; 6.9 mm/yr at 27.4 m depth).

Accounts of encrusting growth of corals are rare in the literature. Only that of Dustan (1975) seems directly comparable to ours. Using Alizarin staining techniques, Dustan measured encrusting growth of M. annularis between 15 and 28 m depth on Jamaican reefs. His values (0.36 to 0.40 mm/mo) are very close to ours (average, 0.33 mm/mo) for the same species at the Flower Garden reefs.

The exceptional water clarity and consequently high light penetration at the Flower Garden reefs may be the important factors favoring rapid coral growth on the reefs between 20 and 30 m depth. There seems to be no evidence of inhibition of accretionary growth due to the northern location of the Flower Garden Banks.

CONCLUSIONS

The Flower Garden Banks (northwestern Gulf of Mexico), Florida Middle Ground (northeastern Gulf of Mexico), and Bermuda (western Atlantic) represent separate biogeographic extremes in the northward distribution of tropical Atlantic coral reefs and hard bottom communities dominated by corals. Coral diversity is considerably less in these northern reefal communities than on reefs in the Caribbean, south Florida, Bahamas, and the southern Gulf of Mexico.

In terms of species composition and dominance of stony corals, the Flower Garden reefs resemble the Bermuda reefs more than they do the Florida Middle Ground. The Flower Garden reefs seem most closely linked biologically to reefs in the southern Gulf of Mexico. They probably are the northernmost elements of an arc of reefal communities of common origin extending from the Campeche Bank to Veracruz, Tuxpan, and the Texas-Louisiana Outer Continental Shelf in the western Gulf.

CHAPTER 7

THE EAST FLOWER GARDEN BRINE SEEP, A UNIQUE ECOSYSTEM

Thomas J. Bright and Eric N. Powell

Sulfide-rich brine (approximately 200 ppt) issues from coarse carbonate sand in the floor of a small depression at 71 m depth on the eastern edge of the East Flower Garden (EFG) Bank, Texas Continental Shelf, approximately 195 km southeast of Galveston, Texas (27°54'31.64"N, 93°34'53.27"W) (Figure 7.1). Other reported oceanic brines are abyssal, occurring at 2000 m depth in the Red Sea (Degens and Ross, 1969) and 2100 m in the Orca Basin, northwestern Gulf of Mexico (Shokes et al., 1977). These occur in restricted basins within larger bodies of water and derive their high salinity from the dissolution of salt domes (Bright, 1977) or other evaporite deposits (Craig, 1969).

Naturally occurring brine and hypersaline systems have also been described from a variety of coastal and lacustrine environments (e.g., Kinne, 1964; Copeland and Nixon, 1974; Moseley and Copeland, 1974), and include large bodies of water, such as the Laguna Madre and Baffin Bay in Texas, and small bodies of water, such as Solar Lake, Sinai (Cohen et al., 1977a), in which the salinity is determined by local evaporation-precipitation regimes and local hydrodynamic conditions.

DESCRIPTION, DYNAMICS AND ORIGIN OF SEEP

Discovered in 1974 during a research submersible survey of the East Flower Garden, the brine seep has subsequently been studied using the research submersibles DIAPHUS (Texas A&M University) and JOHNSON SEA-LINK (Harbor Branch Foundation). Numerous videotaped descriptions, water samples, substratum samples, organisms, current measurements and temperatures were taken during 1976, 1977, 1978, and 1980.

The amphitheater-shaped basin into which the brine flows is 60 m from the edge of the bank, 4 m deep, roughly oval, approximately 50 m across from west-northwest to east-southeast, and 30 m from north-northeast to south-southwest (Figures 7.1 and 6.1). Its wall slope varies from 25° on the north-northwest to almost vertical on the south-southeast. A brine lake (Gollum's Lake) approximately 25 cm deep with an irregular shoreline occupies the

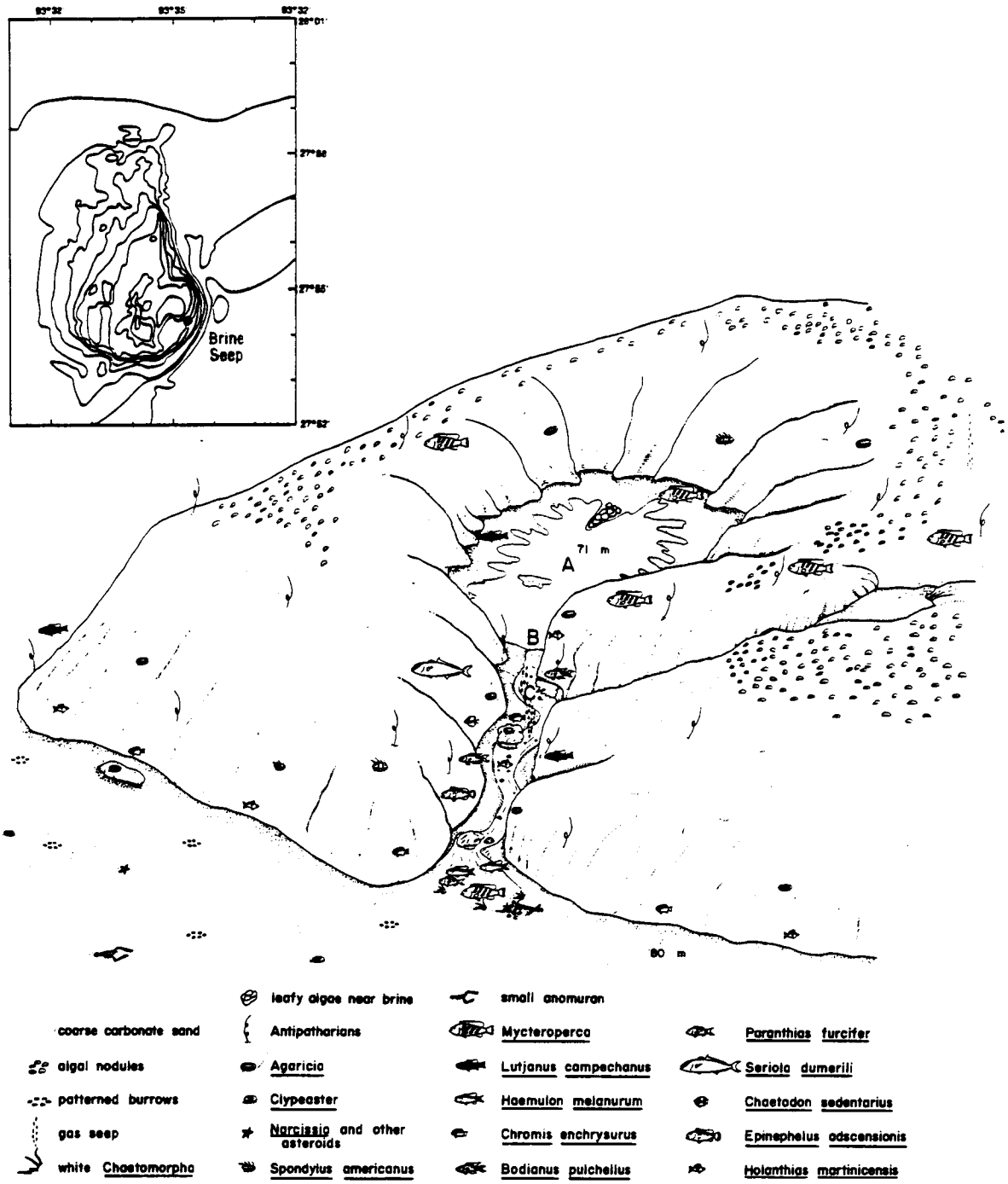

Figure 7.1 Brine seep, eastern edge of East Flower Garden Bank. (A) Brine lake (Gollum's Lake), (B) overflow from lake (71 m depth), (C) stream of mixing brine and seawater. Arrow to right of (C) points to small brine pool (Corner Pool) below overflow. In text: mid-canyon is between the two large boulders shown in the axis of the stream; canyon mouth is the area near the anchor at the edge of the bank (79 m depth). Area indicated as Chaetomorpha may be mixtures of Chaetomorpha and/or Cladophora.

slightly lower eastern and central basin floor (Figure 7.1, A). Large sand waves occur in the lake sediments, probably formed during the passage of major storms (Figure 7.2). Brine from the lake overflows into a mixing stream which runs along the axis of a canyon (Gollum's Canyon). The canyon is approximately 10 m wide at the bottom, 15 m wide at the top, and 96 m in length, and extends from the east-southeast margin of the basin to the edge of the bank at 79 m depth (Figures 7.3 and 7.4).

Chemical aspects of the East Flower Garden brine have been reported by Brooks et al. (1979), Bright et al. (1981), and Powell et al. (1983). The brine is denser than seawater, anoxic, and contains exceptionally high levels of dissolved hydrocarbon gases (methane, ethane, and propane) and hydrogen sulfide (Table 7.1). The density differential inhibits mixing of lake brine with overlying seawater, although diffusion of dissolved components, particularly hydrocarbon gases, across the brine-seawater interface is implied (Table 7.1). Because of the lack of mixing, chemical characteristics of water above and below the interface differ drastically over a vertical distance of less than 2 cm (e.g., salinity approximately 36 ppt vs. 200 ppt) (Table 7.1, Figure 7.6).

Normally, the lake's interface is perfectly flat. Small internal waves (less than 1 cm high) were created by movements of the research submersible. The waves were visible because of the presence of thin, white bacterially derived sulfur flakes (Lauer, 1979) floating at the interface. No irregular light refraction indicative of mixing was observed at the interface as the waves moved slowly back and forth across the lake.

Residence time of brine in the basin is approximately one day. The lake, 25 to 30 m long, 15 to 20 m wide and generally less than 0.25 m deep, and contains about 465 m^3 (465,000 litres) of brine (Table 7.2). The overflow rate of brine from the lake into the canyon was estimated to be 355 to 718 m^3/day. Residence time is therefore 0.65 to 1.3 days. The brine depth and overflow rate appeared similar during six years of observation (1974 to 1980).

Mixing starts immediately as the brine spills out of the lake in turbulent flow down a 0.5 m fall (Figure 7.1, directly below B). Salinity in the overflow was 55 ppt in 1976, representing an initial entrainment of approximately seven parts seawater to one part brine. A small pool (Corner Pool) in a depression 2 m downstream from the overflow contains undiluted brine (Figure 7.1, C). Corner Pool may represent a secondary seepage of brine from the substratum at a level slightly below the main seep.

Mixing continues as brine flows at a rate of 10 to 25 cm/s down a 1 to 3 m wide channelized depression in the canyon axis. Near mid-canyon (45 m from outflow) the salinity is 48 ppt (dilution factor of 14), and near the canyon mouth (90 m from outflow) it is 30 to 40 ppt (dilution factor about 50). Due to entrainment of

Table 7.1 Chemical Characteristics of Brine, Brine-Seawater Mixture, and Seawater Near the East Flower Garden Brine Lake. Samples taken 1976, 1977, 1978, and 1980.

	Brine Lake				Small Brine Pool Below Overflow		Lake Overflow		Mixing Stream Mid-Canyon		Mixing Stream Canyon Mouth			20 cm Above Brine Lake			20 cm Above Small Brine Pool		Local Sea Water at 75 m Depth	Orca Basin Brine	Red Sea Brine
Year	76	77	78	80	77	80	78	80	76	80	76	78	80	76	77	80	76	77			
Salinity* (g/kg)	180	195.2	--	200.1	190	220	--	88.6	48.4	41.9	39.6	--	37.4	--	36.7	36.1	--	36.1	36	258.1	256.4
Salinosity* (g/l)	211	215.6	196	--	219	--	55.5	--	48.5	--	39.7	38.0	--	--	36.7	--	--	36.1	36	--	--
Salinity (sum of ionic species) (g/kg)	191.4	217.8	--	--	219.1	--	--	--	46.0	--	40.6	--	--	--	36.4	--	--	35.8	36	--	--
Potassium (g/kg)	0.375	0.363	--	--	0.353	--	--	--	0.426	--	0.421	--	--	--	0.407	--	--	0.391	0.40	0.63	2.16
Calcium (g/kg)	1.509	1.617	--	--	1.653	--	--	--	0.513	--	0.446	--	--	--	0.441	--	--	0.423	0.41	1.04	4.71
Sodium (g/kg)	81.1	79.3	--	--	75.8	--	--	--	12.7	--	13.3	--	--	--	11.5	--	--	11.2	10.8	91.5	92.4
Magnesium (g/kg)	1.153	1.067	--	--	1.018	--	--	--	1.387	--	1.421	--	--	--	1.327	--	--	1.326	1.29	1.05	0.81
Chloride (g/kg)	122.8	131.0	--	--	135.9	--	--	--	28.2	--	22.2	--	--	--	20.1	--	--	19.7	19.4	149.5	155.3
Sulfate (g/kg)	4.70	4.42	--	--	4.37	--	--	--	2.81	--	2.82	--	--	--	2.77	--	--	2.75	2.7	3.66	0.75
(mmol/l)	59.4	52.1	--	--	51.5	--	--	--	29.4	--	29.4	--	--	--	29.6	--	--	29.3	--	--	--
Sulfide (umol/l)	P	P	2200	1607	P	2175	300	761.9	P	85.9	P	70	32.5	--	N	1.7	--	N	0.0	< 1	--
ΣCO_2 (mgC/l)	35.5	25.0	53.3	--	48.0	--	23.2	--	22.3	--	20.6	27.0	--	--	20.2	--	--	21.0	25	55	--
Methane (ul/l)	2000	2730	1040	--	8900	--	690	--	140	--	42	1.75	--	--	940	--	--	--	50	24,000	--
Ethane (ul/l)	240	414	99	--	500	--	41	--	9.5	--	2.0	0.32	--	--	54	--	--	--	0.5	29	--
Propane (ul/l)	1210	14.7	--	--	18.6	--	--	--	< 10	--	< 10	--	--	--	70	--	--	--	0.5	--	--
Iso-butane (ul/l)	--	2.6	--	--	3.4	--	--	--	--	--	--	--	--	--	--	--	--	--	--	--	--
n-butane (ul/l)	--	0.45	--	--	< 0.3	--	--	--	--	--	--	--	--	--	--	--	--	--	--	--	--
$\overline{C_1}:(C_2+C_3)$	8.3	6.4	--	--	17.2	--	--	--	15	--	15	--	--	--	15.4	--	--	--	50	800	--
Delta C-13 [CH_4](ppt)	-42.5	-40.0	-44.6	--	-47.1	--	-52.4	--	--	--	--	--	--	--	--	--	--	--	--	-74	--
Delta C-13 [DOC](ppt)	--	--	--	--	--	--	--	--	--	--	--	--	--	--	--	--	--	--	-22	-23	--
Delta C-13 [ΣCO_2]	--	--	-23†	--	--	--	--	--	--	--	--	--	--	--	--	--	--	--	0	-16	--
Phosphate (umol/l)	7.5	2.36	--	--	4.00	--	--	--	3.13	--	1.89	--	--	--	0.31	--	--	0.47	2.5	81.5	--
Nitrate (umol/l)	3.6	0.0	--	--	0.3	--	--	--	7.9	--	8.1	--	--	--	1.1	--	--	1.3	23	0.0	0.0
Silicate (umol/l)	16.3	205	--	--	192	--	--	--	5.3	--	5.8	--	--	--	27.2	--	--	30.6	29	235	235
ATP (ng/l)	--	85.3	--	--	--	--	--	--	--	--	--	--	--	--	45.5	--	--	38.5	2.0	5-15	--
Radium-226 (dpm/l)	--	2.9±0.2	--	--	--	--	--	--	--	--	--	--	--	--	--	--	--	--	0.2	5	--
Helium (ul/l)	--	0.6	--	--	--	--	--	--	--	--	--	--	--	--	--	--	--	--	0.04	--	--
DOC (mgC/l)	4.56	--	--	--	--	--	--	--	1.37	--	1.62	--	--	--	--	--	--	--	0.0	3.5	--
Oxygen (ml/l)	--	0.0	--	0.0	0.0	--	--	4.77	--	3.6	--	--	2.5	--	3.0	5.11	--	4.4	5.0	0.0	0.0
Temp. (°C)	--	--	--	--	22.5	--	--	--	20.0	--	19.9	22.2	--	20.2	22.2	--	20.0	22.2	19.0-22.2	5.0	--
Density (kg/l)	--	1.104	--	--	1.106	--	1.040	--	1.034	--	1.028	1.027	--	--	1.026	--	--	1.026	1.025	1.185	--
Dilution Seawater/brine	0.0	0.0	0.0	--	0.0	0.0	7.2	--	13.1	--	47.6	> 90	--	--	--	--	--	--	--	0.0	0.0

* Estimated by refractometer. P = presence indicated by sample odor; N = absence indicated by lack of odor. † Average of three samples.
Compiled in part from Bright (1977), Brooks et al. (1979-1), and Powell et al. (1982).

Figure 7.2 Sand waves in brine lake. Depressions contain brine, with its typical dark, fine, flocculent sediment. Light areas are crests of sand waves rising above the brine. Note the very thin white line representing sulfur bacterial populations along the "shoreline." Manipulator arm of submersible is visible at right.

Figure 7.4 Sulfur bacteria-diatom "mat" covering substratum in stream. Water flow is from upper right to lower left.

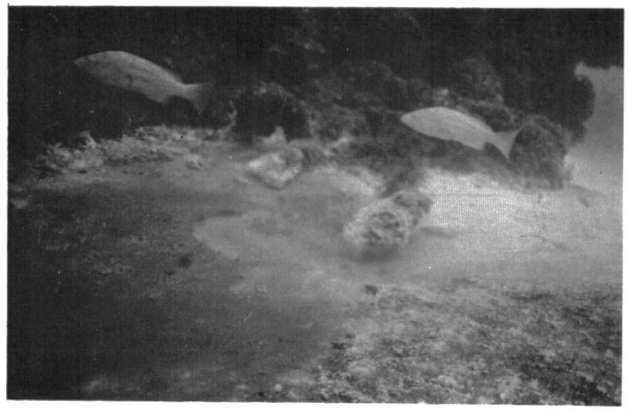

Figure 7.3 Overflow from Gollum's Lake (lower left) into the mixing stream (white stream bed curves to left and disappears behind cliff) in Gollum's Canyon.

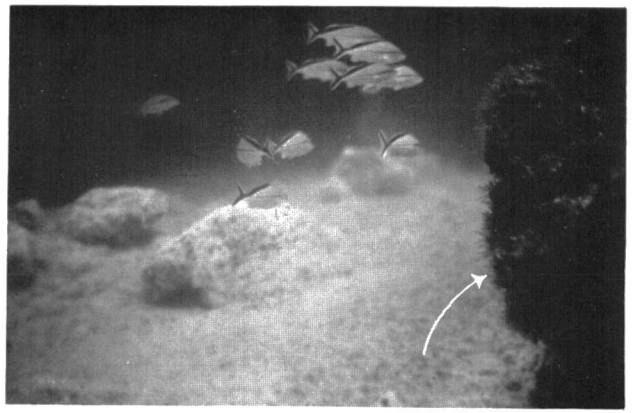

Figure 7.5 Cottonwick (*Haemulon melanurum*) hovering just above and in the mixing stream near Cottonwick rock. Note abundance of suspension-feeding polychaetes attached to rocks at right.

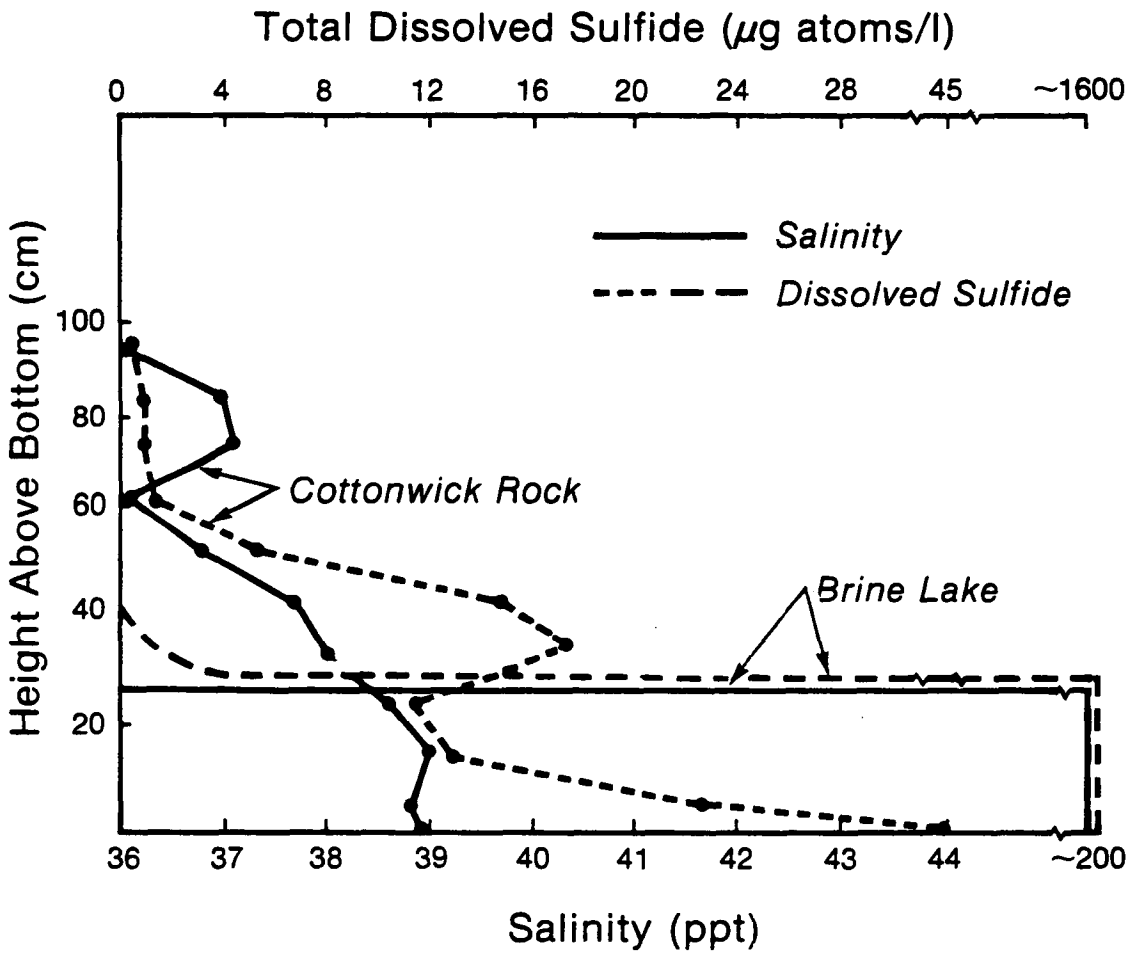

Figure 7.6 Profiles of sulfide and salinity both in the brine lake and along a vertical transect at the Cottonwick Rock.

Table 7.2 Estimations of Residence Time, Volumes of Brine Produced, and Total Salt and Sulfide Production by the East Flower Garden Brine Seep

---

Approximate depth of Gollum's Lake = 25.4 cm

Approximate area of Gollum's Lake = 1.83×10^7 cm^2

Approximate volume of Gollum's Lake = 4.66×10^5 litres

Current speed at overflow = 5.1 to 10.3 cm/sec

Cross-sectional area of outflow = 806.5 cm^2

Volume of outflow = 3.55×10^5 to 7.18×10^5 l/day

Residence time of brine in Gollum's Lake = 0.65 to 1.3 days

Residence time of brine in Gollum's Canyon = < 15 min.
(11 min. assuming an average speed of 11 cm/sec)

Volume of solid salt dissolved per year from salt dome to feed Gollum's Lake (assume salinity of 200 ppt) = 1.08×10^4 to 2.17×10^4 m^3

Amount of sulfide (as $[S^{-2}]$) produced by EFG brine seep per year (assume $[S^{-2}]$ = 1606 to 2173 μg-atoms/l in the brine)
= 6.66×10^3 to 1.82×10^4 kg

increasing amounts of seawater in the downstream direction, the volume of recognizable brine is considerably more at the canyon mouth (stream 1.0 m thick) than it is near the lake overflow (stream 0.3 m thick) (Figures 7.3 and 7.5). At the canyon mouth the brine stream leaves its channel, spreads laterally, decreases substantially in height, and dissipates as it moves onto the level bottom adjacent to the bank.

Figure 7.6 shows a salinity and total dissolved sulfide profile of the stream taken at a large rock (Cottonwick Rock) just upstream of the canyon mouth. The salinity and sulfide concentrations decreased from the bottom to the top, but contained many local heterogeneities, which are probably manifestations of the dynamic mixing associated with the brine stream. Highest concentrations were associated with highest current velocities. Compare the profiles at the Cottonwick Rock (Figure 7.6) with the current profile at the "Anchor," slightly below the canyon mouth (Figure 7.7). Lowest salinities at 95 cm from the bottom approximate the point of no flow on the current profile.

Total dissolved sulfide in 1980 was 1607 ug-atoms/l in the lake. This is distinctly lower than the value obtained by Brooks et al. (1979) and suggests a greater year to year variability in sulfide concentration than in salt concentration. In the canyon, sulfide concentration varied from 80 ug-atoms/l just downstream of Corner Pool to 32 ug-atoms/l at the Anchor.

Salinity and total dissolved sulfide in the brine stream decreased considerably at two places during the stream's travel down the canyon: one in the overflow between Gollum's Lake and Corner Pool and the second between a downstream narrowing of the canyon (Constriction) and the Anchor, in the vicinity of the Cottonwick Rock (Figure 7.7). Elsewhere in the canyon, sulfide concentrations and salinity were remarkably stable, considering the flow and mixing regimes present.

It is assumed that the only significant source of sulfide in the East Flower Garden brine seep area is Gollum's Lake. Therefore dilution is the only significant factor controlling sulfide concentrations in the canyon. The travel time for water down the canyon is sufficiently fast to make physical oxidation insignificant, even with substantial quantities of oxygen available, because of the slow speed at which sulfide is oxidized relative to the hydrodynamics involved (O'Brien and Birkner, 1977; Cline and Richards, 1967).

The sand and rubble substratum of the canyon has obviously been affected by the flow. In 1976 coarse, carbonate sand had been piled in levee-like deposits on either side of the stream channel and along the bases of the canyon walls. By contrast, in 1980 the channel contained large ripple marks and showed evidence of substantial flushing and sediment transport. The stream channel

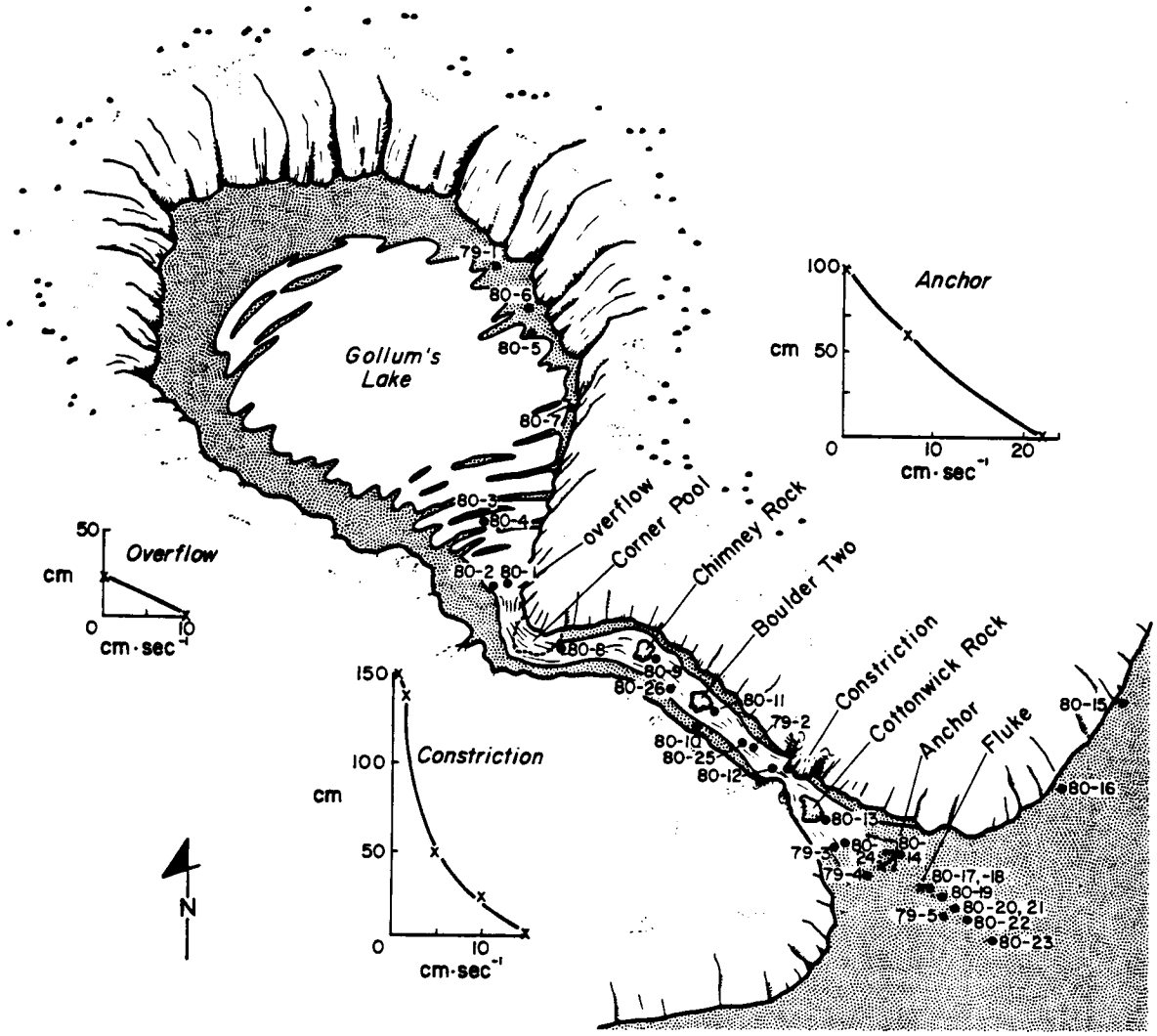

Figure 7.7 The East Flower Garden brine seep area with location of soft-bottom stations sampled and current profiles of the brine stream at three stations, measured by a Savonius rotor placed on the manipulator arm of the submersible. Stations labeled 80- were sampled in 1980 by the research submersible JOHNSON SEA-LINK. Stations labeled 79- were sampled in 1979 by the research submersible DIAPHUS and reported by Powell and Bright (1981).

bed, though basically sand, is relatively rough, containing rubble, sizeable boulders, mollusk shells, and even a stick of waterlogged wood. Scour and erosional undercutting of carbonate rock is apparent where large boulders occur in the stream or where the stream contacts the canyon wall.

Most sediments are very coarse to granular sands, and poorly sorted. Sediment grain sizes are quite uniform over the entire area, being slightly coarser in the canyon and around Gollum's Lake, slightly finer below the Cottonwick Rock and just downstream of the canyon mouth, and intermediate at the farthest downstream stations (Powell et al., 1982).

Geothermal warming of the brine is mininal. There was no noticeable difference in brine temperature compared to that of water above the brine-seawater interface (22.2°C in 1977, 20.3°C in 1976).

Other brine seepages may exist at the East Flower Garden. Several small (1 m diameter) volcano-shaped structures were observed on the soft bottom at 100 m depth on the northeastern flank of the bank. These are probably degassing features such as are seen on sub-bottom profiles and side-scan sonar records over a large part of the Louisiana shelf (Rezak, pers. comm.). The coloration of the substratum and associated surficial deposits suggest that brine seepage may accompany the degassing at these particular sites. In 1980, while traversing the East Flower Garden towing an underwater television system, scientists from LGL Ecological Research Associates, Inc., of Bryan, Texas, located a small brine seep and pool on sandy bottom at 44 m water depth southwest of the main coral reef (Figure 6.2). No rocky substratum or brine overflow was seen, and it is probable that at this seep the brine percolates laterally as interstitial water and is exposed only in depressions in the sand. Presence of these additional brine seeps at the East Flower Garden is strong evidence that the salt is very close to the seafloor beneath much of the bank, and in places actually extends to just beneath the base of the East Flower Garden coral reef (40 to 50 m beneath the sea surface).

Although the salt concentration of the East Flower Garden brine is about 25% less than that of the Orca Basin and Red Sea brines (Table 7.1), all have similar ionic ratios. However, differences in geomorphological setting and heat (from igneous activity) content between the Gulf of Mexico (Orca Basin and East Flower Garden) and Red Sea brines indicate different modes of origin. The Red Sea brines are evidently formed by seawater percolating though evaporite deposits, obtaining heat from igneous activity and dissolved solids, and then surfacing in the deep depressions of the central Red Sea (Craig, 1969). Shokes et al. (1977) have postulated that the Orca Basin brine originates from dissolution of near-surface salt deposits not far beneath the seafloor. Their hypothesis is based on small temperature increases in the brine relative to seawater,

apparent lack of sulfate depletion, and small increases in K^+ and Ca^{2+} relative to Na^+. The East Flower Garden brine also has a very small thermal difference from the overlying seawater, is depleted in K^+ and Mg^{2+} relative to seawater, and has only small enrichments of the other major ions relative to NaCl.

Natural gas seeps (primarily methane, with small amounts of ethane and propane) occur along the axis of Gollum's canyon and elsewhere in the vicinity. Typically, they emit series of small bubbles in intermittent bursts lasting several seconds. Such gas seeps are not unique to the brine flow area and are common over the entire East Flower Garden Bank (Bright, 1977), and on most other banks in the northwestern Gulf of Mexico (Bernard et al., 1976). The molecular and isotopic composition of gaseous hydrocarbons dissolved in the East Flower Garden brine indicates a thermocatalytic origin (Brooks et al., 1979) and, therefore, the presence of stratigraphic hydrocarbon traps.

These observations all suggest that the East Flower Garden brine seep is the product of dynamic dissolution of salt by percolating seawater at the crest of a dome surrounded by stratigraphic hydrocarbon traps which contribute thermocatalytic hydrocarbons. The East Flower Garden and Orca Basin brines (Table 7.1) both originate from evaporite deposits, but have different histories, the Orca Basin brine containing more biologically produced dissolved hydrocarbons (Brooks et al., 1979).

At the East Flower Garden the dense brines flow by gravity through porous substratum to the shores of Gollum's Lake and other points of emission, where they emerge and are diluted into the surrounding seawater within a day or so. We suspect that similar gravity flows are involved in the creation and maintenance of the much larger Orca Basin lake, but the Orca brine, contained in an enclosed basin, remains intact on the seafloor for many years, thereby allowing biological processes, primarily bacterial, to impact measurably the brine's composition (Brooks et al., 1979).

BIOTA

Bacteria and Microflora

The dominant organisms in Gollum's Lake are bacteria. ATP values (Table 7.1), indicative of the level of bacterial activity, are 10 to 20 times greater than those expected in the Gulf water at comparable depths and are equivalent to bacteria values obtained from surface waters in portions of the Gulf of Mexico (Bright et al., 1980a).

The substratum within the lake has a distinctive color zonation which suggests the presence of a sulfuretum (a habitat in which sulfur bacteria are dominant, producing visible white patches of dense cell masses and elemental sulfur, Jorgensen, 1977b). During all submersible dives, such white patches were observed floating at the brine-seawater interface and adhering to the substratum everywhere the interface intersected the bottom (Figure 7.2).

The interface between brine and overlying oxygenated seawater is sharp, with sulfide-rich anoxic water below and sulfide-deficient, oxygen-rich water above (Table 7.1). This interface, or transition zone, is favorable for growth of sulfide-oxidizing bacteria, which require both sulfide and oxygen for active development. A culture of sulfide-oxidizing, mixotrophic, sulfur-producing bacteria isolated from the 1977 East Flower Garden brine samples produced sulfur deposits in the laboratory (Lauer, 1979). Evidence strongly indicates, therefore, that the white material in the lake is a sulfur bacterial mat.

Directly beneath and bordering the interface-related white mats in the lake there is typically a narrow, dark-olive colored mat. Deeper in the brine, covering nearly all of the bottom of the lake, is a deposit of light-olive colored material of loose, fine, particulate consistency which is easily resuspended. This deposit is several centimetres thick in the deeper parts of the lake, and of organic origin. In 1976, thin, diffuse patches of purple were observed on the light-olive particulate deposit directly adjacent to the dark-olive mats near the lake borders. The purple color was absent in 1977 and thereafter. The olive mats and purple coloration are thought to be bacterial, the purple probably being photosynthetic bacteria.

White mats also cover the bottom of the canyon where the stream of mixing water touches the substratum (Figures 7.3, 7.4 and 7.5). Sulfide levels in the mixing water are high, even at the canyon mouth (Table 7.1). But the stream water is also oxygenated due to the admixture of seawater. Thus the entire mixing stream represents a flowing zone of water a few metres wide and up to one metre thick, containing both oxygen and sulfide. The existence of sulfide-oxidizing organisms should be favored wherever this water contacts the substratum.

The white mat in Gollum's Canyon (Figure 7.4) was dominated by Beggiatoa (a sulfide oxidizer) with some Oscillatoria filaments, as well as numerous pennate diatoms and bacteria (Powell et al., 1982). These organisms were embedded in a mucilaginous matrix of uncertain origin, though it was probably mostly bacterial.

Diatoms were common and much more abundant in the mat than in other benthic samples collected away from the seep at similar depths on the bank. Though diatoms are not normally considered important members of the sulfuretum flora, other workers have found benthic

diatoms capable of living in areas with relatively high sulfide concentrations (Admiraal and Peletier, 1979; Round, 1979).

The East Flower Garden brine has higher concentrations of both organic and inorganic carbon than seawater. The dissolved organic carbon (DOC) concentration of the brine is three to five times higher than that of overlying shelf waters. There are three possible origins for the elevated DOC in the brine. First, the organic matter could come from the dissolving salt and be seeping into the pool along with the brine (Wilson, 1963). Second, the dissolved organic carbon could be derived from bacterial action on particulate organic carbon contributed to the brine lake by the highly productive surrounding benthic and and planktonic communities. A great deal of organic detritus is swept into the lake from the bank itself, as evidenced by the presence of chunks of sponges, algae, mollusc shells, and other detritus. Third, organic matter could be produced in the brine by chemosynthetic bacteria. Since the brine lake is well within the photic zone, bacteria could use inorganic hydrogen (e.g., H_2S, H_2) to convert the energy of radiation directly into energy-rich compounds; for example,

$$2H_2S + CO_2 \xrightarrow{h\nu} (CH_2O) + 2S^0 + H_2O. \qquad (1)$$

With the available data, it is impossible to estimate the relative contributions of these sources.

There is an excess of total carbon dioxide in the brine lake over that in normal seawater (Table 7.1). This could come from dissolution of the salt deposit, or bacterial oxidation of organic matter in the brine, or both (Brooks et al., 1979). One mechanism of bacterial oxidation of organic matter is anaerobic sulfate reduction:

$$2(CH_2O) + SO_4^{2-} \rightarrow 2HCO_3^- + H_2S. \qquad (2)$$

The presumed presence of elemental sulfur floating on the brine pool implies the presence of heterotrophic sulfide-oxidizing bacteria (reaction 3), or photosynthetic sulfur bacteria (reaction 1), or both:

$$H_2S + \tfrac{1}{2}O_2 \rightarrow S^0 + H_2O. \qquad (3)$$

Heterotrophic sulfide-oxidizing bacteria have been isolated and cultured from the brine pool (Lauer, 1979). Bacteria such as Beggiatoa need both hydrogen sulfide and oxygen (O_2), and therefore can only grow at a diffusion gradient (or in a mixing zone) where both these gases are present (Jorgensen, 1977a). The

brine interface apparently provides excellent conditions for sulfide oxidation.

Soft-Bottom Infauna

Whereas bacteria are the only living components of the sulfuretum community in the full-strength, anoxic, sulfide-rich brine of Gollum's Lake, assemblages in the canyon's mixing stream are considerably more diverse, comprising not only sulfur bacteria but also plants and metazoans. In considering canyon communities it is useful to recognize two classes of biota which are defined by the proportions of sulfide and oxygen present in their environment.

The "thiobios" is a community of organisms inhabiting a sulfide-dependent chemocline and depending on sulfide as well as oxygen for existence (Powell and Bright, 1981; Boaden, 1980; Riese and Ax, 1980). Conversely, the "oxybios" comprise those communities which are much less tolerant, or intolerant, of sulfide in the environment and which require oxygen. The thiobios comprises not only the sulfuretum community but also assemblages dominated by plants and animals, including specialized metazoans, which are tolerant of or dependent upon the presence of sulfide.

Numbers of organisms collected in soft-sediment samples from the brine seep system are shown in Figures 7.8 to 7.10 (see Figure 7.7 for locations). Control stations and stations associated with the sandy bottom between Gollum's Lake and the carbonate bank were dominated by copepods, with numerous turbellarians, nematodes, and annelids. This is presumably representative of normal infaunal populations in the absence of brine. No living metazoans occurred in the sediment from the bottom of Gollum's Lake. Between these faunal and environmental extremes, some interesting ecotonal assemblages exist, occupying the coarse carbonate sand bed of the canyon stream where progressive mixing of brine and sea water occurs as the water flows downhill.

Throughout the upper canyon, from below Corner Pool to the Constriction, the stream bed infauna was dominated by gnathostomulids, nematodes, annelids, gastrotrichs, and turbellarians (Figures 7.8, 7.9, and 7.10). The upper canyon, between the Overflow and Chimney Rock was depauperate. No living organisms were collected at station 80-2 at the Overflow, and only a few turbellarians were collected at station 80-8 just below Corner Pool. Mid-canyon stations near Chimney Rock and Boulder Two had relatively more gastrotrichs and copepods, while stations just above the Constriction had more gnathostomulids and amphipods.

Below the Constriction, the fauna was composed primarily of annelids, ostracods, copepods, tanaids, amphipods, turbellarians, and nematodes. Cottonwick Rock marks a significant ecotonal

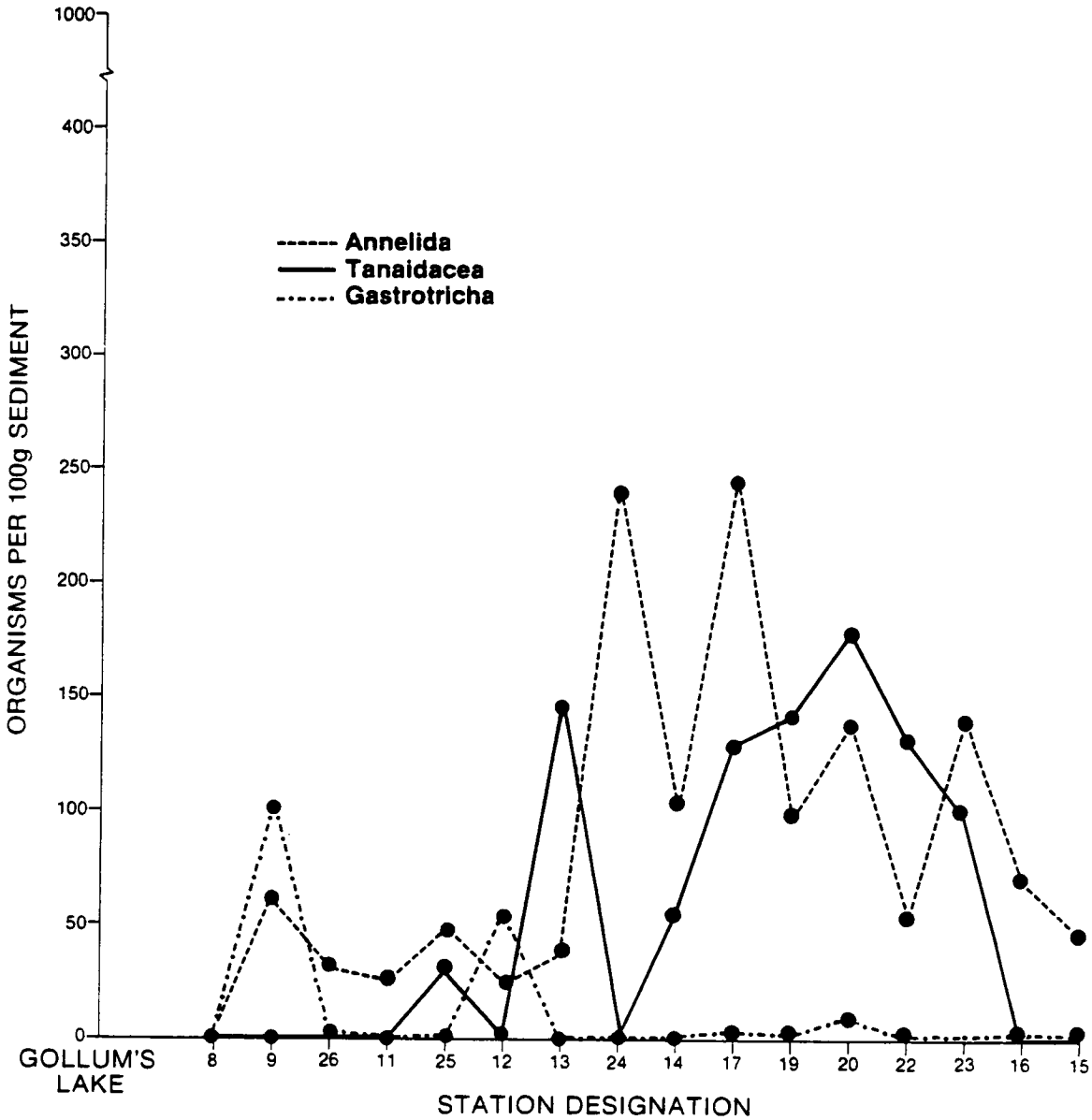

Figure 7.8 Numbers of annelids, tanaids, and gastrotrichs found in September 1980 along a transect from Gollum's Lake down Gollum's Canyon and out onto the sandy bottom adjacent to the canyon mouth. Soft bottom only; see Figure 7.7 for station locations.

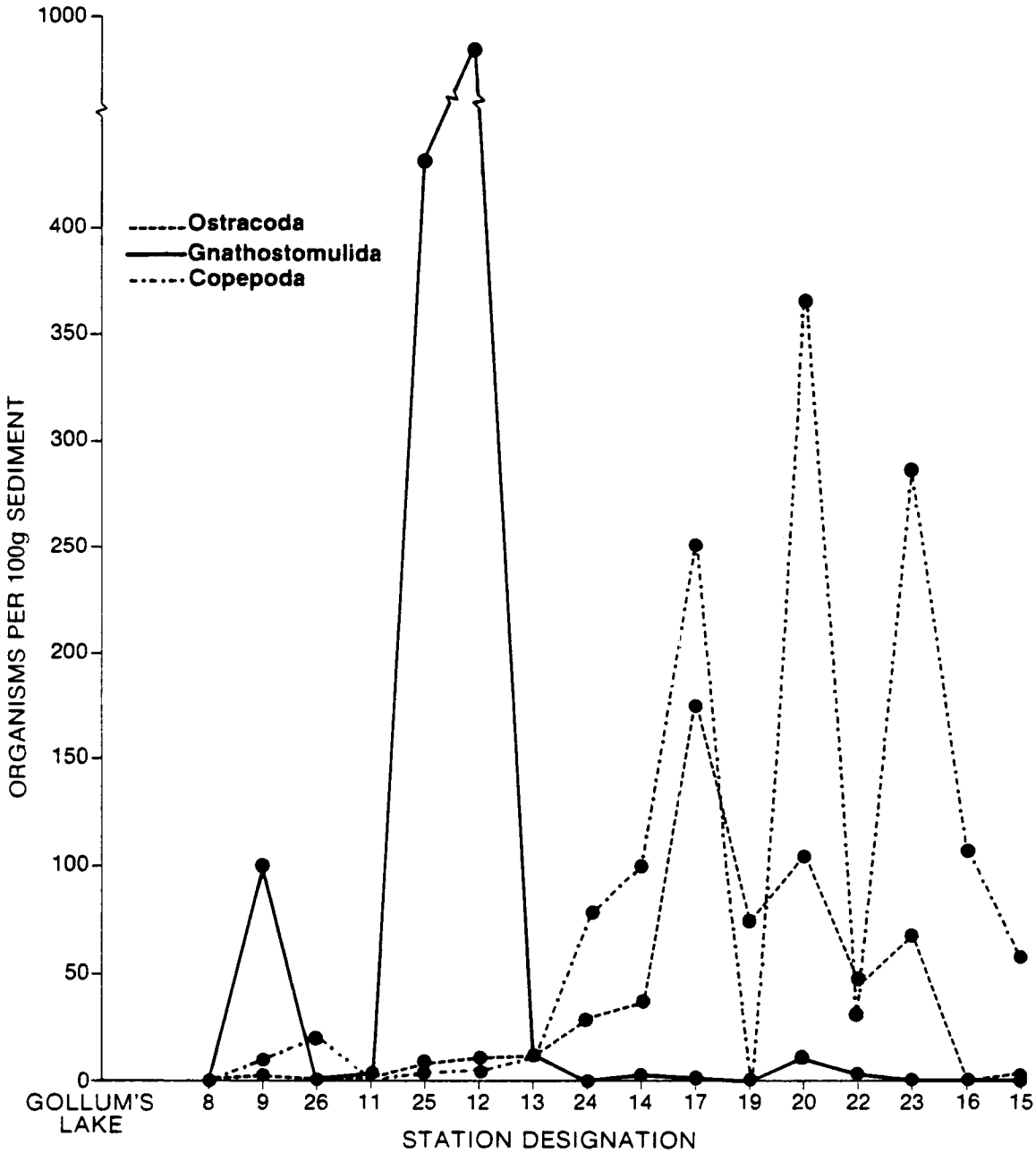

Figure 7.9 Numbers of copepods, ostracods, and gnathostomulids found in September 1980 along a transect from Gollum's Lake down Gollum's Canyon to the Anchor and out onto the sandy bottom adjacent to the canyon mouth.

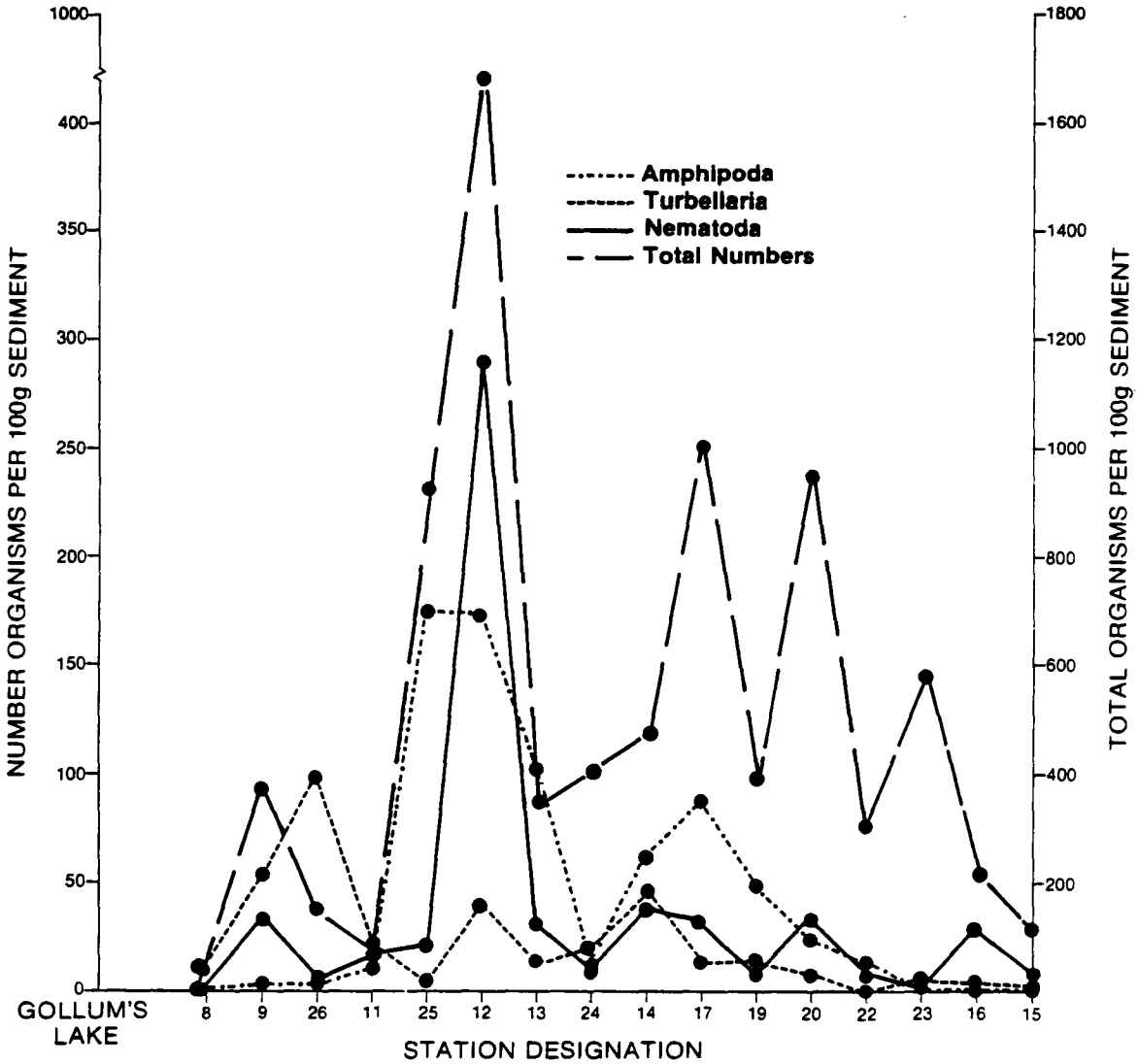

Figure 7.10 Numbers of turbellarians, nematodes, amphipods, and total biota along a transect from Gollum's Lake down Gollum's Canyon to the Anchor and out onto the sandy bottom adjacent to the canyon mouth.

transition between upstream infaunal populations which, as will be shown below, are especially tolerant of or dependent upon the presence of dissolved sulfide (thiobios), and downstream infauna much less tolerant of sulfide (oxybios). Some sulfide tolerant gnathostomulids were still present at Cottonwick Rock. Tanaids and annelids constituted a larger portion of the total infauna in this area than farther downstream mainly because copepods and ostracods were less abundant than at most downstream stations.

Stations below the canyon mouth were dominated by one or more of the following more oxybiotic groups: copepods, ostracods, tanaids, amphipods, and annelids. Molluscs (which were more abundant at these stations than elsewhere), turbellarians, and nematodes were also present in large numbers. Stations 80-17 to 80-23, downstream of the Fluke, resembled control stations (copepods were usually the dominant groups and annelids, turbellarians, and nematodes were common), but were readily distinguished by the presence of high numbers of ostracods, tanaids, and amphipods, which were practically absent from control stations.

Changes in total numbers of organisms (Figure 7.10) were closely associated with physically controlled community boundaries. The abundance of sulfide-dependent thiobios reached a peak in mid-canyon at the Constriction and was generally lower upstream. Ecotone stations below Cottonwick Rock (80-13, 80-14, and 80-24) had comparatively low abundances. Thiobios were no longer abundant at these stations, but only a portion of the oxybios (the tanaids and the annelids) were present in high numbers. The abundance of oxybios reached a peak at station 80-17 with the increase in abundance of copepods and ostracods and the continued importance of the tanaids and annelids. Total faunal abundance gradually decreased downstream of station 80-17, but total numbers at the farthest downstream station (80-23) were still high in comparison to control stations and most stations in the basin between Gollum's Lake and the hard substratum.

Hard-Bottom Epibenthos and Infauna

The brine and brine-seawater mixtures which favor substantial specialized bacterial populations are obviously toxic to most marine organisms. Hydrogen sulfide is lethal to many fishes and invertebrates at concentrations less than 1 ppm (Powell et al., 1979). However, the effects of the East Flower Garden brine on the distribution of epibenthic, hard-bottom macrobiota are very localized and may not extend beyond several metres from the hypersaline brine lake or mixing stream (Bright et al., 1980a).

Coralline algae (*Lithothamnium*, *Lithophyllum*, and others) are the dominant organisms on the East Flower Garden at the depth of the brine flow (Bright and Rezak, 1977). Coralline algae crusts cover

50 to 90% of the exposed rock, nodules, and rubble (which are deposited primarily by the algae). As the primary substratum producers, coralline algae create and maintain the essential habitat for attached and mobile benthic organisms associated with the periphery of the hard-bank. The distribution and apparent health of coralline algae adjacent to the brine flow are, therefore, of some importance.

Interestingly, it appears that coralline algae populations are affected to a greater extent in the overflow canyon than in the basin containing undiluted brine. One nodule that was only partly immersed in the brine lake was collected. That part of the nodule that had been below the brine-seawater interface housed no live macroscopic organisms. However, the upper surface of the nodule, 1 to 4 cm above the interface, was encrusted with healthy coralline algae. Visual observations of the lake indicate that coralline algae populations are apparently normal a few centimetres above the lake interface wherever it contacts hard substratum.

In the overflow canyon there is no stable, sharp interface between the mixing stream and adjacent seawater. The lower limit of apparent healthy encrustations of coralline algae on the walls of the canyon corresponds generally to the rather diffuse top of the mixing stream.

Soft algae occur immediately above the lake's brine-seawater interface. The top of the algal nodule collected from the lake harbored, a few centimetres above the brine, species of filamentous and leafy algae belonging to the genera Cladophora, Dictyota, and Microdictyon. In September 1976, a substantial population of Microdictyon, Chaetomorpha, Rhizoclonium, and other species of soft algae were collected from a slight elevation of the sandy substratum along the "shoreline" of the brine lake. The algae were growing in seemingly healthy condition only 2 cm away from the brine. Such populations must be subject to substantial seasonal and/or year-to-year variation. The same location was devoid of algae in September 1977; algae were present in 1979 but gone again in 1980.

Effects of the brine seep on distribution of epibenthic invertebrates are apparently similar to those described for algae. Live foraminifers, sponges, bryozoans, anemones, polychaetes, sipunculids, amphipods, and pelecypods were found on nodules one or two centimetres above the brine-seawater interface. Small, healthy, saucer-shaped colonies of hermatypic, agariciid corals were observed within 3 m lateral distance and 0.5 m above the edge of the brine lake. The same corals occur on top of Cottonwick Rock in the axis of the canyon less than 1 m above the upper limit of the mixing stream. Sponges were seen on the canyon walls less than 1 m from the mixing stream.

Hard-bottom infauna from quantitative samples taken in 1980 at the Cottonwick Rock and adjacent to Gollum's Lake (Figure 7.11) were

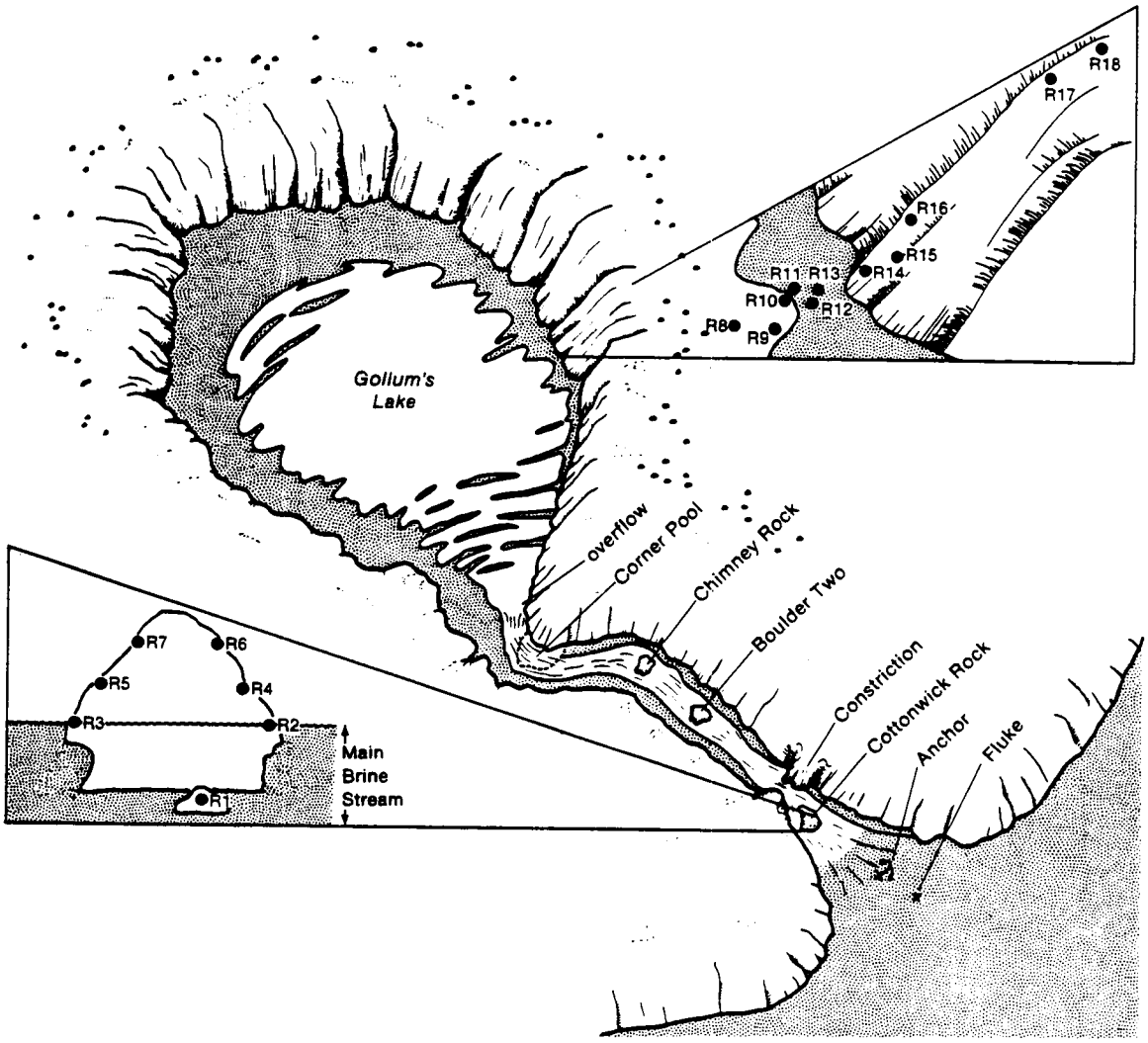

Figure 7.11 Locations of the hard-bottom stations sampled in the East Flower Garden brine seep area. Hard-bottom stations are distinguished from soft-bottom stations (Figure 7.7) by the prefix R.

dominated by tanaids, isopods, annelids, scyphozoans, sipunculids, and amphipods (Figures 7.12 and 7.13) (Gittings, 1983).

On the hard-bottom adjacent to Gollum's Lake, most infaunal taxa have abundance peaks near the lake (Figure 7.12) decreasing rapidly with distance from its edge. Control stations (R17 and R18) from the nearby hard bank have similar biotic composition but fewer numbers.

The sharp brine-seawater interface and the fact that diffusion is the primary mechanism by which material moves across the interface limit the distance over which the brine, while in the lake, can have an effect on the local biota. The brine stream-seawater interface in the canyon, however, is spread out vertically over several metres or more by the turbulent nature of the stream. The entire Cottonwick Rock is, therefore, influenced by the brine stream even though the main body of the stream covers only its lower portion.

Cottonwick Rock station R1 is located within the main body of the brine stream and is probably thiobiotic. Amphipods were abundant in the main brine stream and at the nearby stream bed soft-bottom stations. Stations R2 and R3 were located at the upper boundary of the main brine stream and are oxybiotic. The white bacterial-algal mat of the canyon covers the Cottonwick Rock below R2 and R3. At and above these stations, the rock is covered by more normal carbonate bank biota. Tanaids, scyphozoan scyphostomae, annelids, and isopods were most abundant just above the main brine stream, whereas sipunculids were most abundant near the top of the rock and farthest from the brine stream (Figure 7.13).

Total numbers reached a peak near the brine stream interface at stations R2 and R3, but dropped off less rapidly with distance than in the Gollum's Lake stations, supporting the hypothesis that the brine stream affects a considerably larger area of the nearby hard bank than does the brine lake.

Fishes

Bright et al. (1980a) reported 29 species of fish, and the distinctive burrow of one more, within the brine seep basin and canyon. All are typical inhabitants of the Flower Gardens at the depths in question. Groupers (mostly *Mycteroperca phenax*) and members of a large school (100 or more) of Cottonwick, *Haemulon melanurum*, were the most frequently encountered fish in the canyon.

Of the 29 species, 21 were observed within 1 m distance of the mixing stream, usually on the canyon wall near its base. All behaved in apparently normal fashion. Only four species were seen

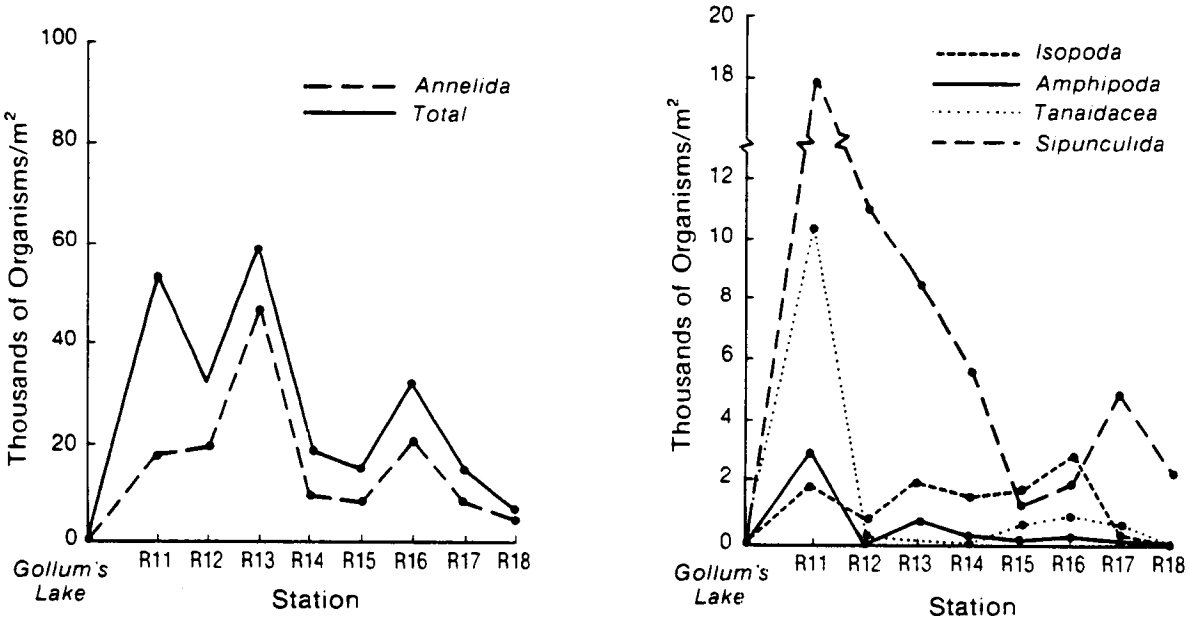

Figure 7.12 Abundances of important taxa and total fauna on the Gollum's Lake transect. Rocks R8, R9, and R10 were totally immersed in the brine of Gollum's Lake and were devoid of fauna; R17 and R18 were controls. Locations of the stations are given in Figure 7.11.

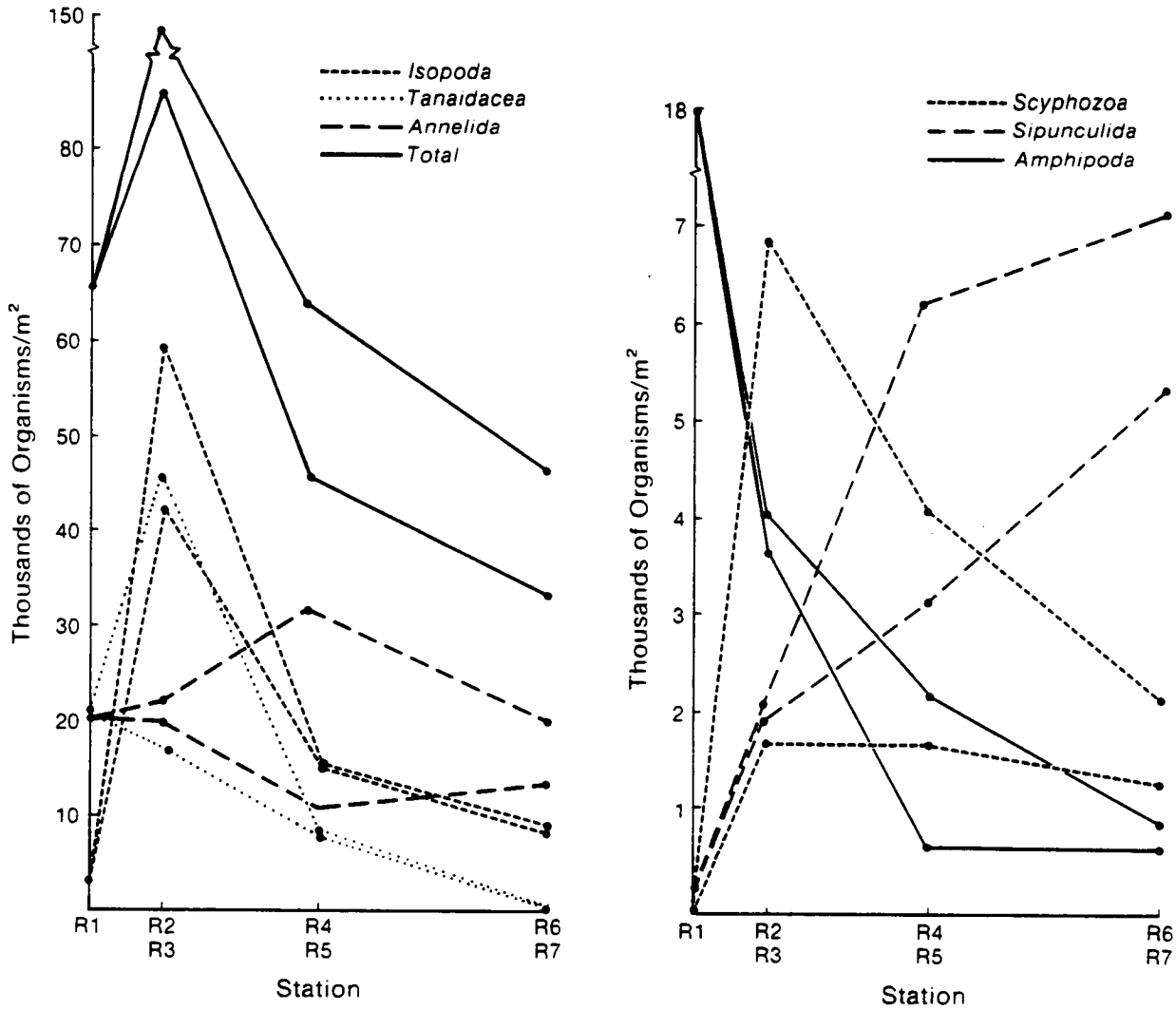

Figure 7.13 Total numbers of selected taxa from the Cottonwick Rock stations. Station locations are given in Figure 7.11. Values for the station pairs R2-R3, R4-R5, and R6-R7 are plotted as maximum and minimum values for stations located at similar positions relative to the brine stream. No statistical relevance (e.g., standard deviation) should be inferred.

within 1 m of the lake's brine-seawater interface. The lake, however, being surrounded by sand for the most part, is rather isolated from the basin walls and rocky substratum which would attract reef fishes. A Sand tilefish, Malacanthus plumieri, had constructed a burrow in the sandy bottom near the western wall of the basin, 15 or 20 m away from the lake margin.

Nine species of fish entered the mixing stream. Most of these occurrences were near mid-canyon at a 2 m high boulder, the lower half of which was immersed in the stream. Salinity in the stream axis at this location was 48 ppt, with dissolved sulfide, methane, and oxygen present (Table 7.1). The smaller fishes (several Holanthias martinicensis, a young Gonioplectrus hispanus, and Bodianus pulchellus) swam along the surface of the boulder, repeatedly entering and leaving the mixed water, with no apparent change in behavior as they did so. One large Blue angelfish, Holacanthus bermudensis, swam completely across the axis of the stream along the bottom, taking two bites from the stream bed, as if feeding. This fish then swam over the surface of the boulder, entering and leaving the mixed water several times, apparently ignoring the difference in water types.

Several fishes exhibited behavior which could be interpreted as purposeful entry into the water of the mixing stream and hypersaline brine of the lake. From mid-canyon to the canyon mouth, groupers and Cottonwicks swam in and out of the mixed water, usually with no particular behavioral changes other than a tendency to turn upstream, swimming gently against the current while holding their positions (Figure 7.5). Frequently, however, individual Cottonwicks were observed to swoop downward into the stream axis and swim quickly and somewhat erratically upstream for a short distance and then leave the stream. This maneuver, which lasted only one or two seconds, was repeated frequently by individuals. The fishes may have been responding primarily to the presence of a bottom current rather than chemical characteristics of the approximately 48 ppt water.

On three occasions, large Greater amberjack, Seriola dumerili, swam rapidly downward toward the brine-seawater interface of Gollum's Lake, turned on their sides as they approached the bottom, entered the hypersaline brine (200 ppt), flapped violently along the bottom on their sides for a few strokes, and then swam upward. One large snapper, Lutjanus sp., apparently performed a similar action. It was seen swimming quickly away from a stirred-up spot in the lake. This is typical behavior for jacks and other large fishes on sandy bottoms in the absence of brine, and may not have been elicited by the presence of the brine. Nevertheless, these fish did briefly enter the hypersaline, anoxic, sulfide-rich water, stirring it up considerably. Such is probably a frequent occurrence.

BRINE SEEP ECOSYSTEM FUNCTION

The Thiobios Hypothesis

All marine sediments, with the exception of wave stressed beaches and some areas of the deep sea, possess three vertical zones: a surface oxidized layer, usually 1 to 10 cm deep; a reduced deeper layer characterized, in clastic sediments, by its distinctive black coloration; and the boundary between the two, where the redox potential changes dramatically from about +200 mv to about -200 mv. This change was termed the redox potential discontinuity (RPD) by Fenchel and Riedl (1970) but it will be referred to herein as the chemocline. The reduced sediments are characterized by the absence of oxygen, hydrogen sulfide concentrations around 30 to 9000 ug-atom/l (about 1 to 300 ppm), nitrogen in the form of ammonia, and high concentrations of reduced organic compounds such as methane.

Fenchel and Riedl described the environmental conditions and biota of the reduced sediments underlying most shallow-water marine sediments. They called this biotope the sulfide system and described a group of interstitial organisms associated with it. These included various micro-metazoans such as gnathostomulids, gastrotrichs, nematodes, and turbellarians. Boaden and Platt (1971) later suggested the term "thiobios" to describe the biota of the sulfide system. Although the discovery of the thiobios was unexpected because the environmental parameters associated with the sulfide system (e.g., high H_2S concentrations and very low to zero O_2 levels) were generally considered inimical to metazoan life, subsequent work has corroborated Fenchel and Riedl's claim that a thiobios does exist. Thus, in most sandy marine sediments, two distinct groups of interstitial organisms are present. One inhabits the surface oxic sediment. The other, the thiobios of Boaden and Platt (1971), inhabits both the deeper reducing sediment and the chemocline between them (e.g., Crezee, 1976; Ehlers, 1973; Ott, 1972). Among the meiofauna, some taxonomic groups, such as the solenofilomophids (Crezee, 1976), the catenulids (Sterrer and Rieger, 1974), and the gnathostomulids (Farris, 1976) are nearly or totally restricted to the thiobiotic environment. Other groups, such as the harpacticoid copepods are rarely encountered in it (Fenchel and Riedl, 1970; Wieser et al., 1974).

The importance of the sulfide system and the thiobios in structuring benthic communities has recently become an area of great interest in benthic ecology and paleoecology. Meiobenthologists are now questioning the chemical-ecological boundaries of the thiobiotic environment and the role of thiobiotic micro-metazoans in meiofauna community structure and function (Fenchel and Riedl, 1970; Reise and Ax, 1979, 1980; Boaden, 1980). Reise and Ax (1979, 1980) and Reise (1981), for example, have demonstrated an association of many supposed thiobios with the micro-oxic zones of the burrow walls of

macroinfauna. They point out that the distributional maxima of most thiobios are consistently associated with low-oxygen regions such as the micro-oxic zones of animal burrow walls and the chemocline at the upper boundary of the sulfide system rather than with the black, reducing sediments below the chemocline.

Deep sea ecologists are now involved with a major investigation of newly discovered communities in the vicinity of warm water "vents" issuing from igneous rock on the Galapagos Rift. These depend trophically on a sulfide system (e.g., Rau and Hedges, 1979; Corliss et al., 1979; Rau, 1981; Felbeck et al., 1981) and provide an excellent example of the potential for the sulfide system as a food source for macrofauna (and, presumably, meiofauna as well).

Paleoecologists are attempting to reconstruct Precambrian and Paleozoic community structure. A number of recent hypotheses and models implicate the sulfide system as a particularly important component of the early Phanerozoic (Cambrian to Present) benthos (Fenchel and Riedl, 1970; Boaden, 1975, 1977) since oxygen levels were considerably lower than today in many areas of the ocean (Cloud, 1968; Berry and Wilde, 1978).

The chemical gradient from the oxic, oxidized environment to the sulfide-rich, reduced environment in normal marine sediments occurs over a vertical distance of about 1 to 10 cm. The importance within the benthic ecosystem of a specialized micro- and meiofaunal community, termed the thiobios (Boaden and Platt, 1971), associated with the reduced sediments, is now a matter of significant controversy primarily because of the small vertical extent over which this chemical gradient occurs. The presence of animal burrows crossing this gradient makes biological and chemical investigation of this problem very difficult.

The East Flower Garden brine seep system provides an unusually good opportunity to study the impact of a sulfide system on eukaryotic community structure. During the brine's travel down Gollum's Canyon, both the hydrogen sulfide concentration (actually total dissolved sulfide) and the salt content are diluted. At the same time oxygen is continually added to the brine stream. Oxygen and hydrogen sulfide coexist within the brine stream throughout the canyon's length, while the concentration of sulfide decreases. Thus, in and downstream of Gollum's Canyon, the chemical gradient is spread out over more than 96 m horizontally, rather than a few centimetres vertically, as is the case in most marine sediments.

The canyon infaunal communities are unique in that they exist totally in and below the chemocline that begins at the top of the brine stream. The animals are bathed continuously with sulfide-rich water. Should any of the biota attempt to reach the normal oxidized seawater above the stream by leaving the sediment, the stream would immediately flush them out of the canyon. The biota are, therefore, restricted to the chemocline and below. Gollum's Canyon has

provided the opportunity to examine, in more detail than previously possible, the effects on and changes in eukaryotic community composition that occur during the transition from reducing, sulfide-dominated conditions to oxidizing, oxygen-dominated ones and to determine what chemical criteria delimit the thiobios from normal oxic communities.

Factors Affecting Faunal Distribution

The soft-bottom stations sampled in the East Flower Garden brine seep system fall into three main groups: stations adjacent to Gollum's Lake and the control stations; middle canyon stations; and stations at and below the canyon mouth. The latter group can be divided into two subgroups: one, an ecotone subgroup, is located between the Cottonwick Rock and the Anchor; the other subgroup is located from the Anchor downstream. These observations based on the taxonomic groups enumerated do not imply, of course, that all species within the groups have similar distributions. The data are sufficient, however, to delineate the major faunal boundaries present in the system.

Although sediment grain size is commonly observed to be an important factor determining boundaries for infaunal communities (McNulty et al., 1962; Pollock, 1971; Hulings and Gray, 1976), it is unlikely that variations in grain size distribution can explain any of the faunal shifts observed here. All soft-bottom stations were coarse to very coarse sands. Between-station variability is small and is not associated with changes in faunal composition.

Although salinity is important in structuring benthic communities (Kinne, 1964; Carpelan, 1967), changes in salinity are unlikely to have produced the faunal boundaries observed in this system except in the brine lake and in the overflow region, where salinities remain high enough to prevent most metazoan life. The significant changes in community composition in the canyon below Corner Pool occur over a salinity range of no more than 2 ppt in an area that may have yearly salinity changes of that magnitude in the overlying seawater (McGrail and Horne, 1981). Low abundances in the canyon near Corner Pool and Boulder Two occur at salinities essentially equivalent to that of the high abundance stations near the Constriction (station 80-12). Salinity change between the Constriction and the canyon mouth, where the greatest change in faunal composition occurs, is no more than 1 ppt, whereas sulfide concentration changes by over 50%. Since most of the taxa involved are known to have euryhaline representatives in hypersaline areas, changes in taxonomic composition, at the taxonomic levels dealt with here, induced by such small variations in salinity, should not even be expected.

The data allow a choice between oxygen and sulfide as the component chiefly responsible for the faunal boundaries observed. Oxygen is not limiting in the brine seep area exclusive of Gollum's Lake. Typically, oxygen concentration must drop below 1 ppm to cause significant changes in community composition of the type observed here (Rhoads and Morse, 1971; Gallardo, 1977; Rosenberg, 1977; Jorgensen, 1980). Values in Gollum's Canyon below Corner Pool never drop low enough to produce such changes since over 95% of the brine stream is entrained oxic seawater. Thus, although there probably is an oxygen gradient in the canyon, it is not ecologically meaningful.

Changes in sulfide concentration, on the other hand, are ecologically meaningful. Gnathostomulids are present throughout the canyon where sulfide concentrations are above 40 ug-atoms/l. Nematodes, gastrotrichs, and amphipods show peak abundances under these conditions as well. Loss of the gnathostomulids as a principal component of the community coincides with a substantial drop in sulfide concentration in the area between the Constriction and the Cottonwick Rock. Copepods and ostracods are found in significant numbers only where sulfide concentrations are considerably lower (e.g., 1 to 5 ug-atoms/l) above Gollum's Lake at stations 80-3, 80-5, and 80-6, and below the Anchor at stations 80-17 to 80-23, where sulfide concentrations are approximately 2 ug-atoms/l.

Between the Cottonwick Rock and the Anchor, where sulfide drops by a factor of at least 3, is a transition community. Tanaid and annelid abundances in this area are near the peak values found downstream, but neither the thiobiotic gnathostomulids nor the oxybiotic copepods are as common as elsewhere.

Thus, in the area of transition from thiobios to oxybios, the ecologically significant change in brine stream chemistry is in sulfide concentration. It is likely that the ability to detoxify sulfide is of considerable adaptive importance to the thiobios (Powell et al., 1979, 1980).

Interestingly, certain members of the oxybios, such as the tanaids and annelids, approach the thiobiotic-oxybiotic boundary closer than others. The decrease in total abundance at the canyon mouth is caused by the reduction of thiobiotic organisms and the failure of all groups of the oxybios to be well represented. Jacubowa and Malm (1931), Theede et al. (1969), and Powell et al. (1979) demonstrate substantial variability in sulfide tolerance among oxybiotic metazoans. Some oxybiotic organisms withstand relatively high concentrations of sulfide, particularly for short time periods. Therefore, the thiobiotic-oxybiotic boundary is not necessarily at 0 ug-atoms/l sulfide, but probably at some value above zero, as determined by the oxygen and sulfide flux rates and the biota's sulfide detoxification capabilities.

Values for total dissolved sulfide in the brine stream are within the 96-hr lethal dose values for many oxybiotic organisms (Oseid and Smith, 1974a,b). Since high oxygen concentrations increase the oxybiota's ability to detoxify sulfide (Oseid and Smith, 1974a; Powell et al., 1980), it is likely that the sulfide concentration at the thiobiotic-oxybiotic boundary in the canyon is higher than in most areas (the faunal shift takes place around 20 to 40 ug atoms/l sulfide). In normal marine sediments, where oxygen concentrations may be considerably lower in the chemocline (Revsbech et al., 1980a,b), the sulfide concentration may also be considerably lower at the boundary.

Trophic Relationships

A bacterially productive sulfuretum exists in the brine lake and in the canyon. The brine provides a continuous sulfide source for the growth of the sulfide-oxidizing organisms which form a luxuriant white bacterial-algal mat that covers the bottom of the canyon throughout its length. Significant quantities of white particulate matter produced by the sulfuretum organisms are swept out of the canyon constantly (Figure 7.14). Potentially these all provide a significant food source for the canyon community and communities adjacent to and downstream of it. The trophic structure may be, to this extent, similar to the thermal vent communities recently reported from mid-ocean rift valleys (Ballard and Grassle, 1979; Rau and Hedges, 1979; Karl et al., 1980).

Sulfide-based food sources are likely to be important in the trophic structure of many marine communities (Jorgensen, 1977a,b; Gallardo, 1977; Kepkay et al., 1979). Since the current regime in Gollum's Canyon continuously flushes sulfur bacteria and other organic matter out of the lake and canyon to the adjacent and downstream communities, the East Flower Garden brine seep system provides an opportunity to assess the impact of a significant sulfur-based food source on shallow-water soft and hard-bottom benthic communities.

Most benthic systems, including the brine seep, receive organic carbon input from detritus, bio-deposition, and autotrophy (Figure 7.14). A portion of this organic carbon is digestible if eaten by the oxybios; a portion is not. The bacterial and plant components of the suluretum and thiobios may function as organic carbon recyclers, transforming refractory carbon into useable plant and animal carbon by both sulfate reduction and sulfide oxidation processes (and other thiobiotic heterotrophy).

Bacterial oxidation of organic matter through anaerobic sulfate reduction produces bacterial carbon and hydrogen sulfide (Equation 2, Bacteria and Microflora section, above). In the presence of oxygen, heterotrophic sulfide oxidizing bacteria use hydrogen

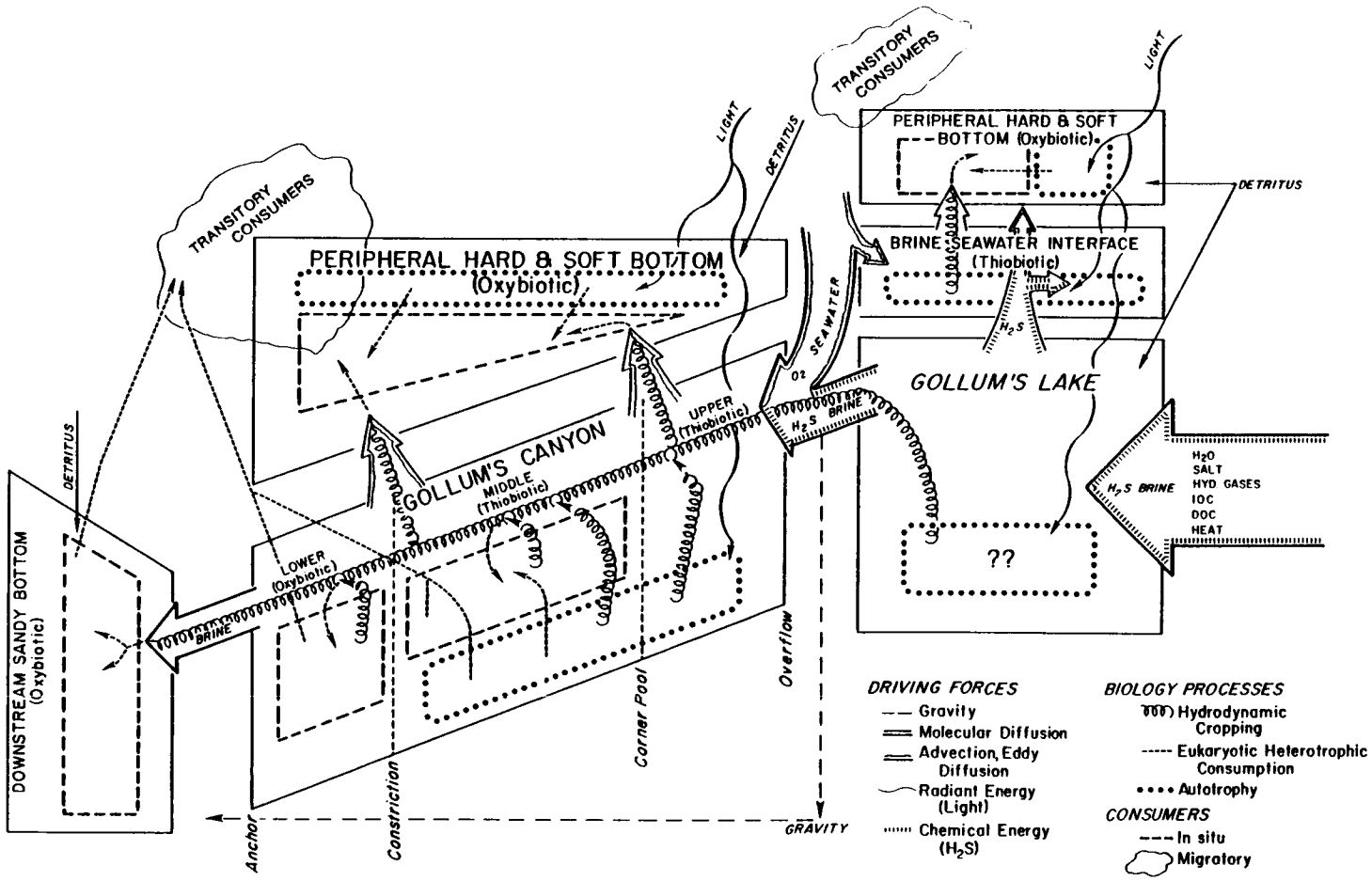

Figure 7.14 The East Flower Garden brine seep system: driving forces and biological processes. Thiobiotic autotrophy includes sulfide-oxidizing heterotrophy (including Beggiatoa) as well as true autotrophy. Other bacterial heterotrophy occurs in all systems and can be expected to provide a food source for metazoans but is not included in the diagram. Box and arrow size are not meant to imply any quantitative relationships. Question mark indicates some degree of doubt as to the occurrence of autotrophic prokaryotes (photosynthetic bacteria) in the lake sediments below the interface. DOC = dissolved organic carbon, IOC = inorganic carbon, Hyd Gases = hydrocarbon gases.

sulfide to produce organic carbon at the brine-seawater interface and in the stream (Equation 3). Insofar as sufficient light is present, another important source of consumable organic carbon is probably bacterial chemosynthetic autotrophy (Equation 1) through the oxidation of hydrogen sulfide in both the anoxic brine and the mixing stream. This thiobiotically transformed carbon is then available again for heterotrophic consumption by the oxybiotic and thiobiotic metazoans.

The trophic base for the East Flower Garden brine seep system is probably dependent primarily on organic carbon produced at the lake interface and in the canyon by autotrophic and heterotrophic sulfide oxidation. It is unlikely that sulfate reduction in the lake and canyon is nearly as important either as a source of digestible organic carbon or hydrogen sulfide. (Nearly all of the hydrogen sulfide entering the system is preformed and comes in with the brine.)

In general, sulfide oxidizing organisms are limited by either light or sulfide concentration (e.g., Takahashi and Ichimura, 1970; Matsuyama, 1979; Pfennig, 1975). Sulfide is not a limiting factor in this system insofar as its concentration changes significantly only by dilution in the canyon. Thus, the sulfide supply is greater than the capacity for its use by the organisms. Light is quite ample for plant growth and is favorable for prokaryotic photosynthesis as well (Figure 7.14). Data from other workers reviewed by Bright et al. (1980a) show that primary production rates can exceed 1 $gm \cdot m^{-2}$/day in sulfide-oxidizing systems. The primary producers present in the Gollum's Lake area may be expected to have growth rates of this order.

The standing crop is limited primarily by the continual removal of these organisms by the gravity-driven water currents and mixing processes associated with the brine. Current speeds can be over 20 cm/s in the canyon, and the entire lake is replaced about once per day. Observations over several years have consistently noted pieces of the white benthic mat being swept out of the lake and the canyon mouth. In addition, mixing processes in the canyon and in the seawater above Gollum's Lake transfer food to the hard-bank biota from both the canyon thibios and lake sulfureta. This advective entrainment of plant and animal material from Gollum's Lake and Canyon will be hereafter referred to as hydrodynamic cropping (Figure 7.14).

The oxybiotic communities of the peripheral soft- and hard-bottom, the lower canyon downstream of the Cottonwick Rock, and the sandy-bottom downstream of the canyon's mouth are primarily heterotrophic and are dependent on production derived elsewhere in the system (plus in situ bacterial heterotrophy). Heterotrophic, eukaryotic consumption occurs in three ways.

1. Resident heterotrophs consume produced carbon at its source. This occurs in all oxybiotic habitats and in the middle canyon thiobios.

2. Migrating heterotrophs composed of mobile organisms such as fish (Bright et al., 1980a) and possibly some benthic invertebrates, enter the canyon and downstream communities periodically to feed, then leave.

3. Hydrodynamic cropping sweeps autotrophic and heterotrophic organisms from the lake and canyon downstream, or mixes them up into the peripheral hard-bank and soft-bottom communities for consumption there by heterotrophs.

It is likely that hydrodynamic cropping is the most important of these processes and that much of the food used by heterotrophic communities contiguous to the lake and canyon thiobios is that which is washed out of the seep.

Carbon isotope analyses support this hypothesis. Brooks et al. (1979) reported that inorganic carbon derived from the brine seep had a Delta C-13 value much more negative than normal seawater (Table 7.1). Since this carbon provides part of the carbon for thiobiotic production and since many sulfur bacteria also fractionate carbon (Wong et al., 1975), carbon isotope analysis might be used to trace thiobiotically fixed carbon in this system. Nevertheless, three of five samples of the canyon's bacterial mat (Powell et al., 1982) provided Delta C-13 more negative than local benthic algae and Gulf of Mexico plankton (Fry and Parker, 1979). Most Delta C-13 values for animals in the brine seep area were more negative than would be expected if the carbon source were either local benthic algae or plankton. For example, sponges from control stations had Delta C-13 values higher than sponges from stations near the Gollum's Lake and Canyon thiobios. Most of the values for polychaetes and crustaceans within the seep system were more negative than for local benthic algae or plankton away from the seep, suggesting that thiobiotically fixed carbon from the seep is the primary source for them as well. Numbers of metazoans below the canyon mouth, where the brine stream discharges its suspended particulate load, are five to ten times the number present at control stations. In general, past these peripheral zones of enrichment, numbers tend to decrease with distance from the lake and canyon on both the hard- and soft-bottom. The high abundances obtained in the canyon and lake area and the carbon isotope analyses suggest that the oxybios is quite capable of utilizing the thiobiotically transformed or produced organic carbon brought to it by the seep's water currents.

CONCLUSIONS

The East Flower Garden brine seeps are unlike any other known to science insofar as they exist in an offshore marine environment which is well supplied with light. The dense, very salty (200 ppt), anoxic, sulfide-rich brine is formed when seawater, percolating through the porous rocks of the banks, dissolves portions of a salt dome, the top of which must be within 44 m of the sea surface.

Populations of sulfide-oxidizing and sulfate-reducing bacteria occupy the brine seep system, autotrophically producing and heterotrophically recycling organic carbon in substantial quantities. This material is apparently utilized as food by sulfide-tolerant thiobiotic infauna and epifauna which live on the bed of a flowing stream of mixing brine and seawater (oxic, but with high levels of dissolved sulfide). Oxybiotic infauna and epifauna directly adjacent to the seep, though intolerant of sulfide, derive food from the system and exist in greater abundance than do similar populations elsewhere on the bank at similar depths.

CHAPTER 8

CLASSIFICATION AND CHARACTERIZATION OF BANKS

Richard Rezak and Thomas J. Bright

Submarine banks may be classified in a variety of ways both geologically and biologically. We have settled on a classification based upon the general location on the shelf (i.e., midshelf or outer shelf) and the nature of the geological structure expressed in them. From this very general beginning we may then look at details of the geology and biology of the banks in order to further characterize them and to develop groupings of banks with similar attributes. The relationship of the geology, biology, and hydrology of the banks will be developed in this chapter, with the ultimate aim of providing a basis for predicting the geological and biological environments on less studied banks from limited amounts of remotely sensed data.

SYSTEM OF CLASSIFICATION

Geological categorization is based upon structural expression; that is, did the bank or reef develop on relatively undisturbed strata, like the banks off South Texas, or did it grow on a diapiric structure, like the banks off East Texas and Louisiana? A further subdivision may be made on the basis of the nature of the structure underlying the bank. Is the structure that which we normally associate with salt diapirs or is the structure inherited from early Jurassic and Triassic tectonic features? The nature of the substrate also is involved in the categorization. Is the substrate made up of bedded Mesozoic and/or Cenozoic sandstones, siltstones, or claystones? Or is the substrate a carbonate cap (reef) that totally conceals the original bedrock substrate? Based on these considerations, the geological classification of the banks identifies two categories: midshelf bedrock banks, and outer shelf bedrock banks with carbonate reef caps.

The most appropriate means of categorizing the banks biologically involves recognition of a number of distinct benthic biotic zones characteristic of hard banks in the northwestern Gulf of Mexico, with an indication of the banks on which each zone occurs, and the depth range of each zone on each bank. Seven characteristic benthic biotic zones have been identified. These are classified within four general categories depending on degree of reef-building activity and primary production as follows:

A. Zones of Major Reef-Building Activity and Primary Production.

I. Diploria-Montastrea-Porites Zone: A zone consisting of living, high-diversity coral reefs. Hermatypic corals dominant. Coralline algae abundant. Leafy algae limited.

II. Madracis Zone and Leafy Algae Zone: The Madracis Zone is dominated by the small branching coral Madracis mirabilis, which produces large amounts of carbonate sediment. In places, large (possibly ephemeral) populations of leafy algae dominate the Madracis gravel substratum (Leafy Algae Zone).

III. Stephanocoenia-Millepora Zone: A zone consisting of living, low diversity coral reefs. Hermatypic corals dominant. Coralline algae abundant. Leafy algae limited.

IV. Algal-Sponge Zone: A zone dominated by crustose coralline algae actively producing large quantities of carbonate substratum, including rhodoliths (algal nodules). The zone extends downward, past the depth at which algal nodules diminish in abundance, to the greatest depth at which coralline algal crusts are known to cover a substantial percentage of the hard substratum. This is the largest of the reef-building zones in terms of area of sea bottom. Leafy algae are very abundant.

B. Zone of Minor Reef-Building Activity.

V. Millepora-Sponge Zone: A zone where crusts of the hydrozoan coral Millepora share the tops of siltstone, claystone, or sandstone outcrops with sponges and other epifauna. Isolated scleractinian coral heads may be present, but rare. Coralline algae are rare.

C. Transitional Zones Wherein Reef-Building Activity May Range from Minor to Negligible.

VI. Antipatharian Zone: Limited crusts of coralline algae and several species of coral exist within a zone typified by sizeable populations of antipatharians. Banks supporting Algal-Sponge Zones (A, IV above) generally possess something comparable to an Antipatharian Zone as a "transition" between the Algal-Sponge Zone and the deeper, turbid-water, Nepheloid Zone of the lower bank.

D. Zone of No Reef-Building Activity.

VII. Nepheloid Zone: A zone wherein high turbidity, sedimentation, resuspension of sediments, and resedimentation dominate. Rocks and drowned reefs here are generally covered with veneers of fine sediment. Epifauna are depauperate and variable; deep-water octocorals and solitary stony corals are often conspicuous. This zone occurs in some form on lower parts of all banks below the depths of the Antipatharian or Transitional Zones.

This scheme does not represent a final word on benthic zonation on hard banks in the northwestern Gulf of Mexico. The supposed "Antipatharian Zone" and "Nepheloid Zone" are particularly problematic and may not be valid designations in the biological sense. Each surely represents several biotic assemblages of superficial similarity which could all ultimately be given separate zonal designations. No single bank off Texas-Louisiana possesses all of the zones indicated above, though the East and West Flower Garden Banks lack only the *Millepora*-Sponge Zone (Table 8.1 and Figure 8.1). The two Flower Garden Banks harbor the most diverse and thoroughly developed offshore hard-bottom epibenthic communities in the region. They differ from other shelf-edge carbonate banks primarily in the degree of development of coral reefs. High diversity coral reefs (*Diploria*-*Montastrea*-*Porites* Zone) are not present on any other northern Gulf banks. Lower diversity coral reefs (*Stephanocoenia*- *Millepora* Zone) are present at the Flower Gardens and also at two other shelf-edge banks, 18 Fathom and Bright.

The *Millepora*-Sponge Zone, occupying depths comparable to the *Diploria*-*Montastrea*-*Porites* Zone, is characteristic of the Tertiary bedrock substrata of the Texas-Louisiana midshelf banks. Interestingly, the zone is present on one shelf-edge carbonate bank (Geyer) but only on a bedrock prominence at the bank's crest.

Upper parts of the relict Pleistocene carbonate reefs of the South Texas midshelf banks and certain midshelf carbonate banks off North Texas and Louisiana are occupied by benthic assemblages comparable to those of the supposed *Antipatharian* Zone found at somewhat greater depths on the north Texas-Louisiana shelf-edge carbonate banks (Table 8.1).

Thus, as further detailed below, the basic geological categories of northwestern Gulf Outer Continental Shelf banks are also broadly distinguishable from one another in terms of benthic community structure. The biotic differences between bank types are probably explicable in terms of lateral and depth-related variations in substratum type, water temperature, turbidity, and sedimentation.

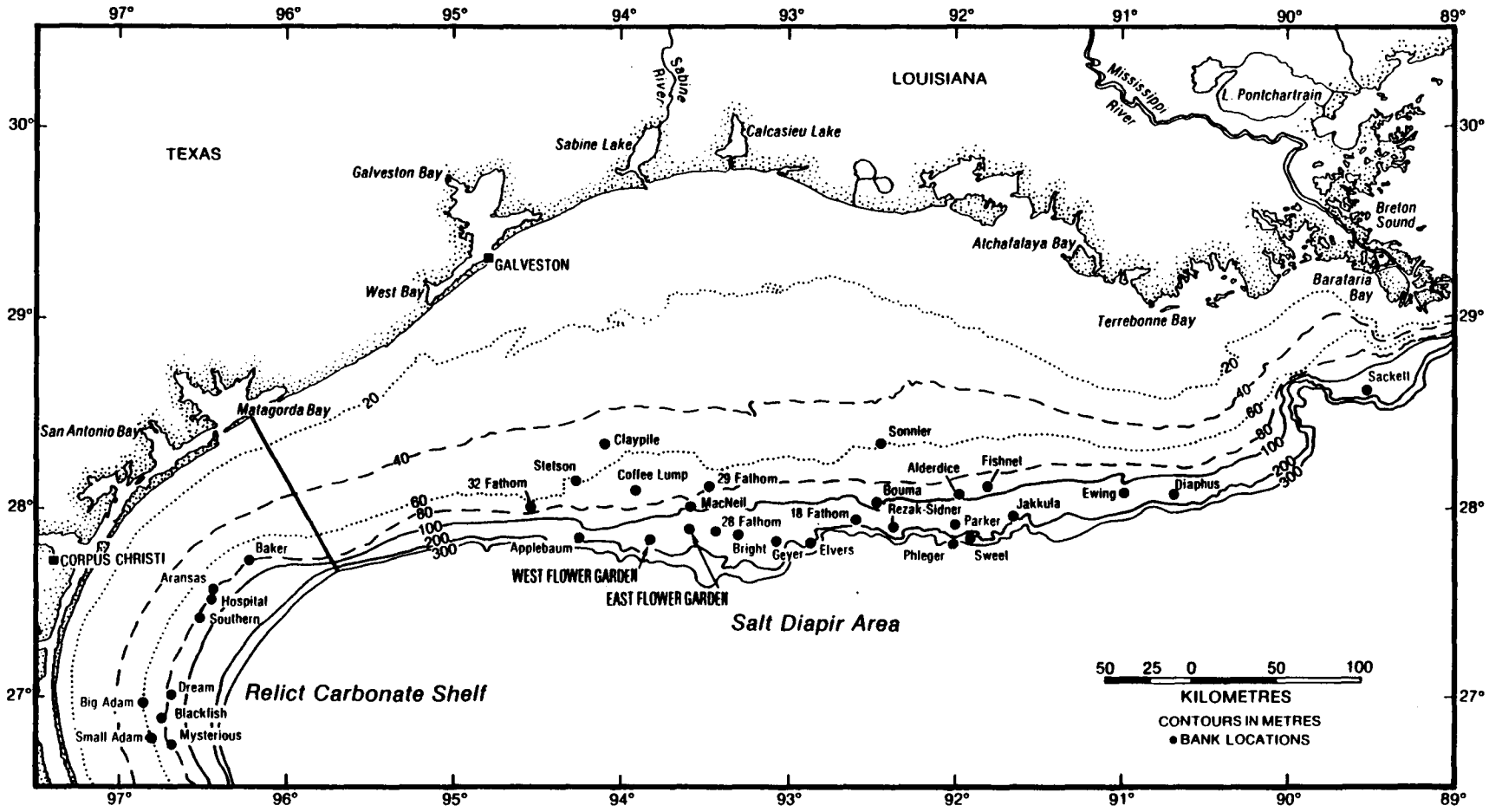
97°
96°
95°
94°
93°
92°
91°
90°
89°
30°
29°
28°
27°
TEXAS
LOUISIANA
Sabine River
Sabine Lake
Calcasieu Lake
Mississippi River
L. Pontchartrain
Galveston Bay
GALVESTON
West Bay
Atchafalaya Bay
Terrebonne Bay
Breton Sound
Barataria Bay
Sackett
San Antonio Bay
Matagorda Bay
20
40
60
80
100
200
300
Claypile
Sonnier
Stetson
Coffee Lump
32 Fathom
29 Fathom
Alderdice
Fishnet
Bouma
MacNeil
Ewing
Diaphus
Rezak-Sidner
Jakkula
18 Fathom
28 Fathom
Parker
Bright
Geyer
Elvers
Phleger
Sweet
Applebaum
Baker
CORPUS CHRISTI
Aransas
Hospital
Southern
WEST FLOWER GARDEN
EAST FLOWER GARDEN
Salt Diapir Area
Relict Carbonate Shelf
Big Adam
Small Adam
Dream
Blacklish
Mysterious
50 25 0 50 100
KILOMETRES
CONTOURS IN METRES
• BANK LOCATIONS

Table 8.1 Depth ranges (in metres) of biotic zones on Outer Continental Shelf hard banks in the northwestern Gulf of Mexico. P = Zone present, but depth range uncertain.

BANKS	BIOTIC ZONES							
	MILLEPORA SPONGE	DIPLORIA-MONTASTREA-PORITES	MADRACIS	STEPHANO-COENIA	ALGAL-SPONGE	ANTIPATHARIAN-TRANSITIONAL	NEPHELOID	SOFT BOTTOM
Clayplle	40-45	-	-	-	-	-	45+	50+
Sonnier	18-52	-	-	-	-	-	52+	60+
Stetson	20-52	-	-	-	-	-	52+	62-64+
Small Adam	-	-	-	-	-	60?	P	64+
Big Adam	-	-	-	-	-	60?	P	66+
North Hospital	-	-	-	-	-	58-70	70+	68-70+
Aransas	-	-	-	-	-	57-70	70+	70-72+
Baker	-	-	-	-	-	56-70	70+	70-74+
Blackfish	-	-	-	-	-	60?	P	70-74+
Hospital Rock	-	-	-	-	-	59-70	70+	70-78+
Mysterious	-	-	-	-	-	70?	P	74-86+
Southern	-	-	-	-	-	58-70	70+	80+
Dream	-	-	-	-	-	62-70	70+	80+
South Baker	-	-	-	-	-	59-70	70+	80-84+
32 Fathom	-	-	-	-	-	52?	P	55+
Coffee Lump	-	-	-	-	-	62-68	68+	70+
Fishnet	-	-	-	-	-	66-73	73+	78+
Alderdice	-	-	-	-	55-67	67-82	82+	84-90+
Ewing	-	-	-	-	56-72	72-80	80+	85-100+
Bouma	-	-	-	-	60-75	75-84	84+	90-100+
Parker	-	-	-	-	60-82	82-?	P	100+
Sackett	-	-	-	-	**67-82	65-85	85+	100+
East Flower Garden	-	15-36	28-46	36-52	46-82	82-86	86+	100-120+
Applebaum	-	-	-	-	76?	P	P	100-120+
Bright	-	-	-	37	52-74	74-?	P	110+
West Flower Garden	-	20-36	P	36-50	46-88	88-89	89+	110-130+
Diaphus	-	-	-	-	-	73-98	98+	110-130+
18 Fathom	-	-	-	45-47	45-82	82-?	P	110-130+
28 Fathom	-	-	-	-	52-92	92-100	100+	110-140+
Jakkula	-	-	-	-	59-90	90-98	98+	120-140+
Rezak-Sidner	-	-	-	-	55-93	93-100	100+	120-150+
Sweet	-	-	-	-	75-80+	P	P	130-200+
Elvers	-	-	-	-	60-97	97-123?	123+	180+
Geyer	37-52	-	-	-	60-98	98-123?	123+	190-210+
Phleger	-	-	-	-	-	?	*122+	200+

*Clear water, but biota typical of nepheloid zone
**Weakly represented, environmentally stressed

SOUTH TEXAS RELICT CARBONATE SHELF REEFS

Geology

A line drawn from Matagorda Bay to the shelf break (Figure 8.1) divides the Texas continental shelf into an area of drowned reefs on a relict carbonate shelf and an area of banks situated on salt diapirs. Figure 8.2 illustrates a seismic profile across Baker Bank. The only apparent structure involved is normal faulting with very little displacement of the shallow reflectors. The shallow reflectors are horizontal and continuous beneath the bank. The keystone fault system displayed in Figure 8.2 is typical of the faulting over shale or salt ridges due to extension in the strata overlying the ridge. Berryhill et al. (1976) illustrate seismic profiles across three other banks on the South Texas shelf, and these also show no signs of association with salt diapirs.

There is no doubt that the banks on the South Texas shelf are drowned coralgal reefs. Rock dredging by the U.S. Geological Survey (Berryhill et al., 1976) and Texas A&M University (Bright and Rezak, 1976) recovered coralline material from Southern Bank and samples of dead coral from Dream Bank. Radiocarbon (C^{14}) dating yielded ages of 18,000 and 10,580 years B.P., respectively. These banks are dead reefs that were living close to a Late Pleistocene to Early Holocene shoreline.

The banks vary in relief from 1 to 22 m. The flanks of all of these banks are immersed in a layer of turbid water (nepheloid layer) that varies in thickness from 15 to 20 m. Many of the banks are totally immersed in the nepheloid layer. Hospital and Southern Banks have the greatest relief, and their crests are generally at or slightly higher than the top of the nepheloid layer. Rock samples have been taken from Baker, South Baker, Southern, Dream, Big Adam, and Small Adam Banks. All of the samples consisted of either dead coral or dead coralline algae nodules.

The coral from Dream Bank that was dated at 10,580 $\pm$ 155 years B.P. yields a maximum date for the viability of the reef. Some event that caused the death of corals and most of the coralline algae occurred soon after that time.

Southern Bank is a good example of the relict reefs (Figure 8.3) on the South Texas shelf. The bank is circular in plan view, approximately 1300 m in diameter, and rises from a depth of 80 m to a crest of 60 m. Four geomorphic features are discernible on the bathymetric map (Figure 8.3): 1) a north-south trending marginal depression up to 4 m deep situated on the east side of the bank; 2) steep slopes extending along the northeast and northwest perimeter of the bank; 3) a flat terrace located between the 68 and 72 m

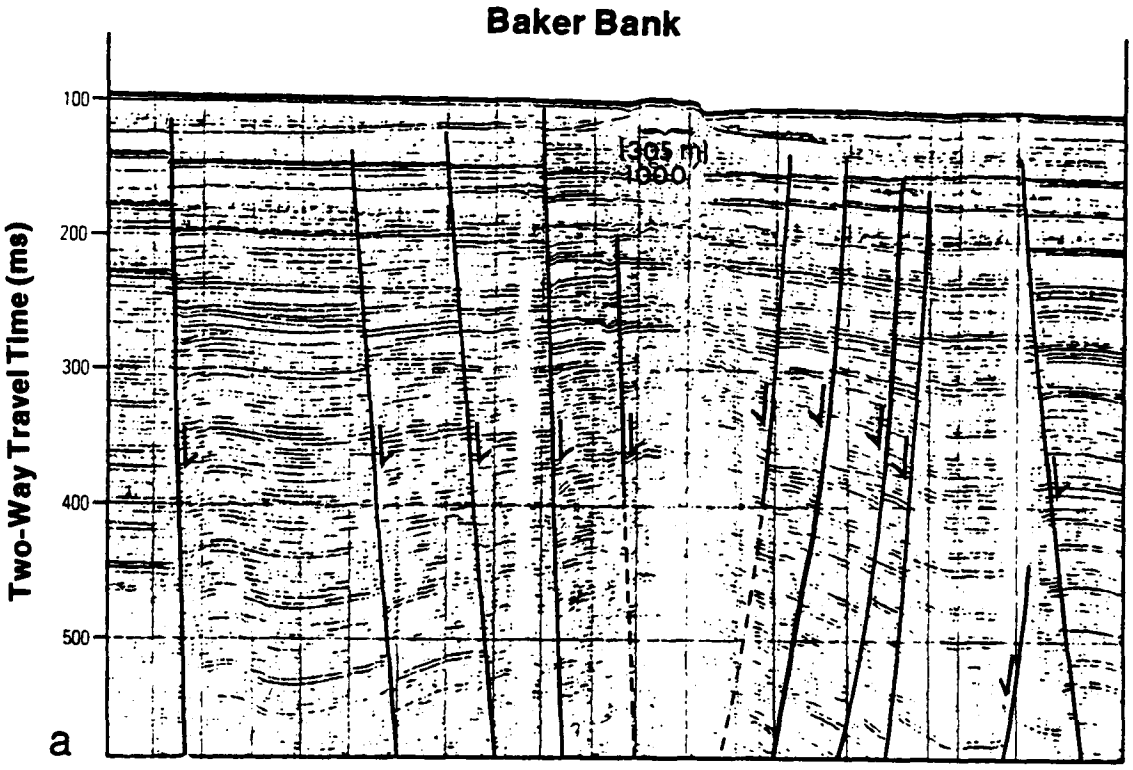

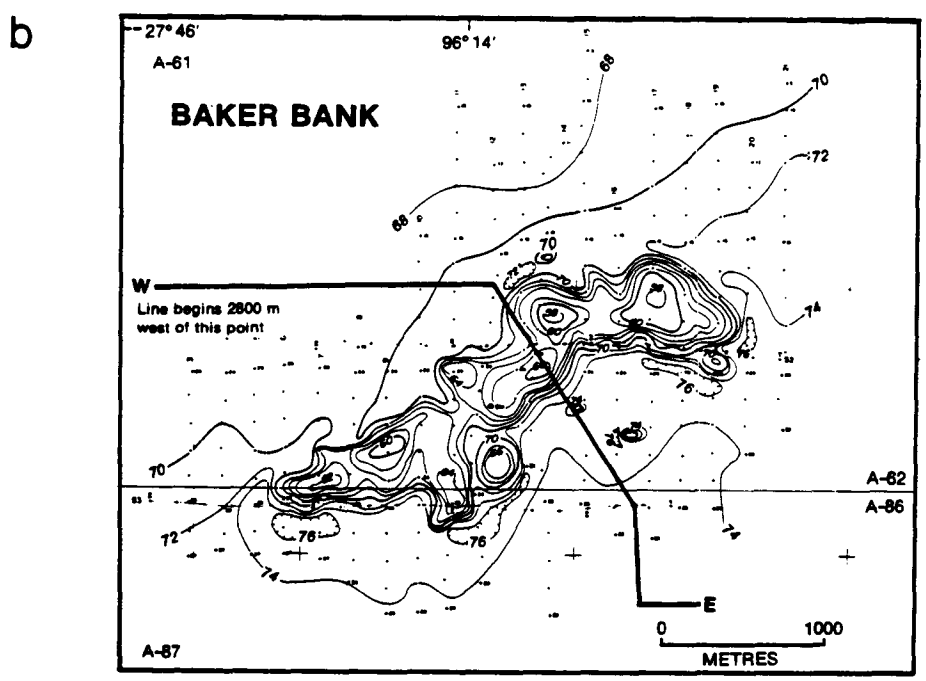

Figure 8.2 (a) USGS Del Norte model 561 sparker profile across Baker Bank (after Trippett and Berryhill, 1976, Map I-1287-F); b) bathymetric map of Baker Bank showing location of sparker profile.

contours; and 4) two peaks rising from the terrace to depths of 60 to 62 m.

Submersible observations allow for detailed description of the various characteristics of these geomorphic features. The observations show several features. The marginal depression is bounded on its west side by one to two metre high cliffs of coralgal reef rock. The center of the depression contains an accumulation of fine-grained sediment whose surface is dotted with numerous patterned burrows 1 to 2 cm in diameter. No observations were made over the depression's east side. The steep slopes on the bank consist of a step-like progression of one to two metre high coralgal cliffs topped by small, irregularly-shaped terraces. The terraces consist of coralgal outcrops separated by rubble-filled channels. Proceeding up the bank from the edge of the marginal depression, the terraces become progressively wider. Channels on the terraces are approximately one metre deep and up to several metres wide, and are aligned parallel to the slope of the banks. The major terrace at 66 m consists of a relatively flat, rubble-covered coralgal substrate bounded by coralgal cliffs at its outer perimeter. On the substrate, in the sand- and gravel-sized rubble, and ripple beds with parallel to sub-parallel symmetrical crests, approximately 5 cm in height and approximately 1 m in wavelength. The crests have a northeast-southwest lineation. Proceeding across the flat portions of the terrace toward the peaks, one finds coralgal outcrops approximately 50 to 75 cm high becoming more common. The peaks are relatively flat-topped and consist of large, rubble-covered coralgal outcrops separated by channels and depressions. The channels decrease in width and depth toward the crests of the peaks. At the crest of the largest peak, several groups of small cone-shaped pinnacles appear to have been eroded from the coralgal reef rock. They are approximately 75 cm high and vary from 10 to 50 cm in diameter. Near the crest of this peak, several small, intermittent gas seeps were seen emanating from small holes in the substrate, which are rimmed with a white precipitate.

The surficial sediments consist of varying proportions of three main components: clay, silt, and coarse carbonate detritus. Four dominant sediment types can be recognized on and around the bank: 1) a fine grained poorly sorted silty clay whose > 62 um fraction, when present, consists of 20% quartz grains, 53% foraminifera tests, and 24% miscellaneous carbonate grains; 2) a medium-grained very poorly sorted clayey silt whose > 62 um fraction consists of 75% quartz grains and 15% foraminifera tests; 3) a coarse-grained extremely poorly sorted shelly mud whose > 62 um fraction consists of 25% quartz grains, 24% foraminifera, 25% miscellaneous carbonate grains, and 19% shell fragments; and 4) a very coarse-grained carbonate rubble that was not sampled on Southern Bank due to the hard coralgal substrate beneath the rubble. Samples from a similar facies on other banks were found to be very poorly sorted and consisted of 10% quartz grains, 9% foraminifera tests, 30% shell, coral and algal grains, and 51% miscellaneous carbonate grains.

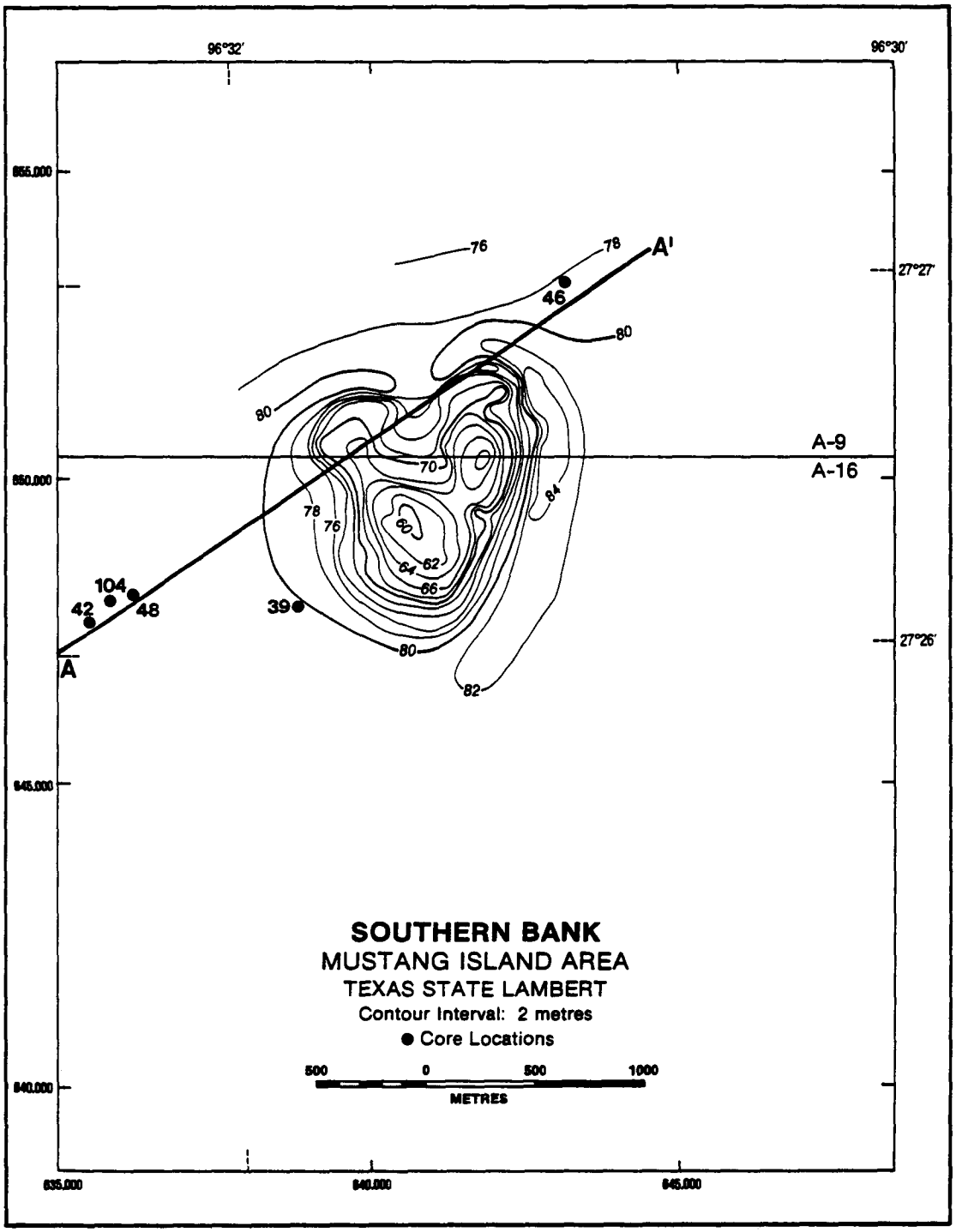

Figure 8.3 Bathymetry of Southern Bank showing locations of cores and cross section in Figure 8.4.

Submersible observations show it to consist of sand- and gravel-sized grains of shell, coral, and miscellaneous carbonate detritus mixed with cobble-sized algal nodules.

The four dominant sediment types exhibit a distinctive surficial distribution pattern. The surficial sediments of the shelf in the area where the South Texas shelf banks are located consist largely of clayey silts (Berryhill et al., 1976). These clayey silts are predominant in the sediments immediately surrounding the western half of the bank, with the exception of a 600 m wide zone of shelly muds adjacent to the western perimeter of the bank. In a core from station 39 (Figure 8.3), 2.5 m of shelly mud was recovered. The sediments surrounding the eastern half of the bank are silty clays with occasional shell fragments or sand-silt layers. The bank is blanketed by a veneer of fine-grained sediment, which gradually decreases from an approximate thickness of 20 cm on the bank's edge to a trace on its crest. Carbonate rubble is the predominant sediment on the terrace and peaks.

The 3.5 kHz sub-bottom profiles reveal several reflectors terminating against the bank. The shallowest of these reflectors can be traced into the surrounding shelf sediments at a depth of about 10 m and is believed to be the Pleistocene-Holocene boundary, termed reflector A by Berryhill et al. (1976). It is the shallowest continous reflector depicted in Figure 8.4 and is directly overlain by a seismically transparent sediment designated as Unit 4 (Berryhill et al., 1976). Unit 3 (Berryhill et al., 1976) is the shelly mud unit shown in Figure 8.4. Its absence to the east of the bank is simply due to the fact that none of the cores penetrated reflector A, which is the upper surface of Unit 3. On the southwest side of the bank, reflector A intersects the seafloor about 600 m to the west of the bank, leaving Unit 3 exposed on the seafloor between that point and the bank.

The coralgal reef rock could not be traced into the subsurface to any significant depth due to the shallow penetration of the 3.5 kHz energy source and the generally poor record quality. However, Berryhill et al. (1976) illustrates several banks in sparker seismic profiles, and the surface of the bank coincides with the surface of Unit 3 in the subsurface (Figure 8.2a). We propose that the terrace formed by Unit 3 represents a carbonate shelf that existed during Late Wisconsin time. It seems very likely that the event that caused the demise of the reefs was not a rapid rise in sea level but the inception of the nepheloid layer on the South Texas continental shelf. The presence of the nepheloid layer has not only caused the death of the once thriving reefs but also controls the present day fauna and flora of the South Texas midshelf banks.

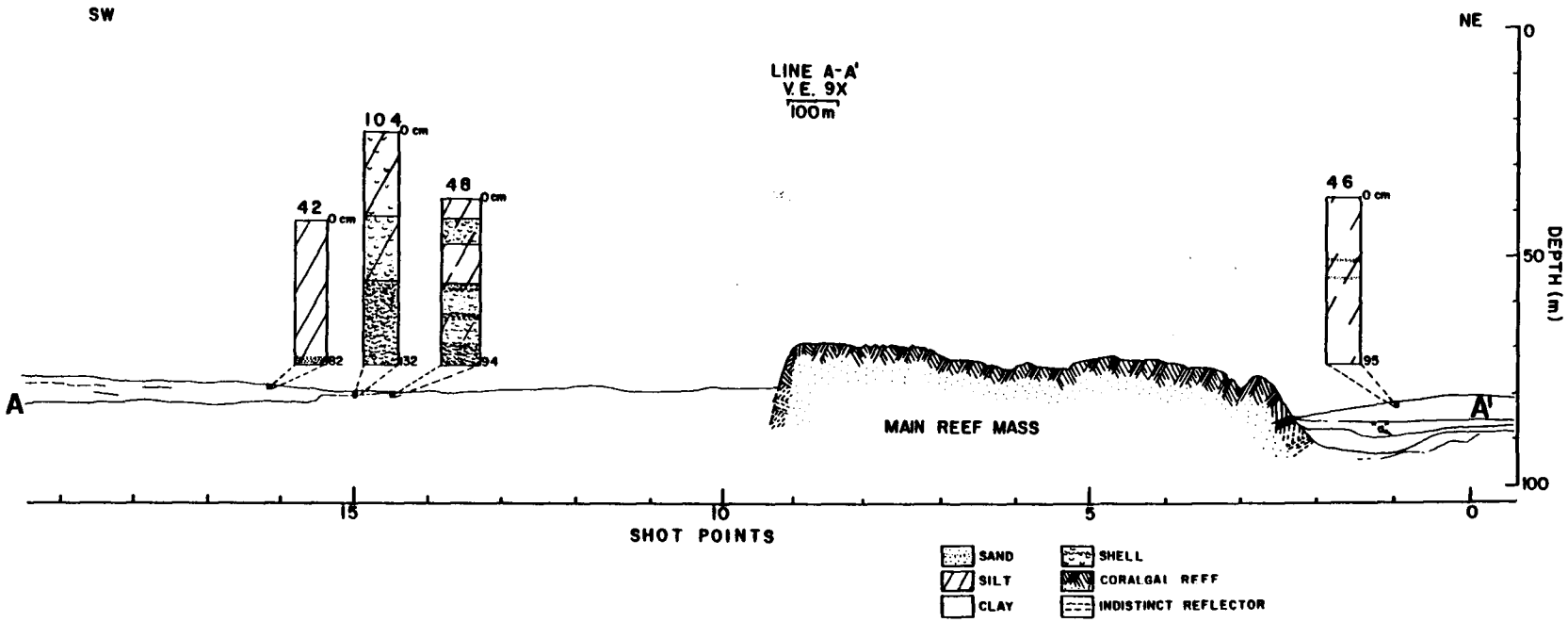

Figure 8.4 Cross-Section through Southern Bank with locations of four cores showing sediment types around the bank.

Biology

The South Texas mid-shelf banks are composed of carbonate substrata overlain by fine sediment veneers of varying thicknesses. Carbonate patch reefs up to 1.5 or 2 m high occur on the banks and are seemingly clustered at particular depths (Figure 8.5) It is on these structures, which provide at least some local relief above the generally sediment-covered carbonate rock bottoms of the banks, that the epifaunal communities are best developed. And it is around them that the greatest number of fishes congregate.

Though there are bank-to-bank variations in population levels, virtually all of the South Texas banks examined are inhabited by fishes and epibenthic invertebrates typical of the Antipatharian Zone (so named because of the conspicuousness and abundance of the large, white, spiraled sea whip-like coelenterates Cirrhipathes, of the Order Antipatharia). A zone similar in biotic composition to the Antipatharian Zone is present in the same depth range on midshelf carbonate banks off north Texas and Louisiana (32 Fathom, Coffee Lump, Fishnet Banks), and somewhat deeper on the Texas-Louisiana shelf-edge carbonate banks (Table 8.1). Except for the shelf-edge banks, this zone grades into one of exceptionally high and chronic turbidity and sedimentation near the bases of the banks (Nepheloid Zone). Population levels and diversity of epifauna decrease sharply below approximately 70 m depth, because of chronic turbidity and sedimentation.

Antipatharian Zone assemblages occupying Southern Bank (Figure 8.5) are representative of those of all the South Texas midshelf banks. Cirrhipathes is the most conspicuous epifaunal organism on these banks. An almost equally conspicuous macrobenthic organism is the white, somewhat vase-like sponge Ircinia campana, which, interestingly, is not particularly noticeable within the Antipatharian Zone on banks off north Texas and Louisiana. Comatulid crinoids are abundant and easily seen everywhere on the upper portion of the bank.

Large white sea fans, Thesea, though apparently less abundant than the organisms mentioned above, were frequently seen because of their size. Other deep-water alcyonarians, mostly paramuriceids, occur on Southern Bank, other South Texas banks, and deep parts of the midshelf and shelf-edge carbonate banks farther north. Alcyonarian fans in particular seem to be restricted to the Antipatharian Zone and deeper zones in the northwestern Gulf of Mexico.

The only conspicuous stony corals on Southern Bank are saucer-shaped agariciid colonies near the top of the bank in relatively clear water. These small coral patches are not particularly abundant but were encountered several times during submersible dives. Other corals collected included the small,

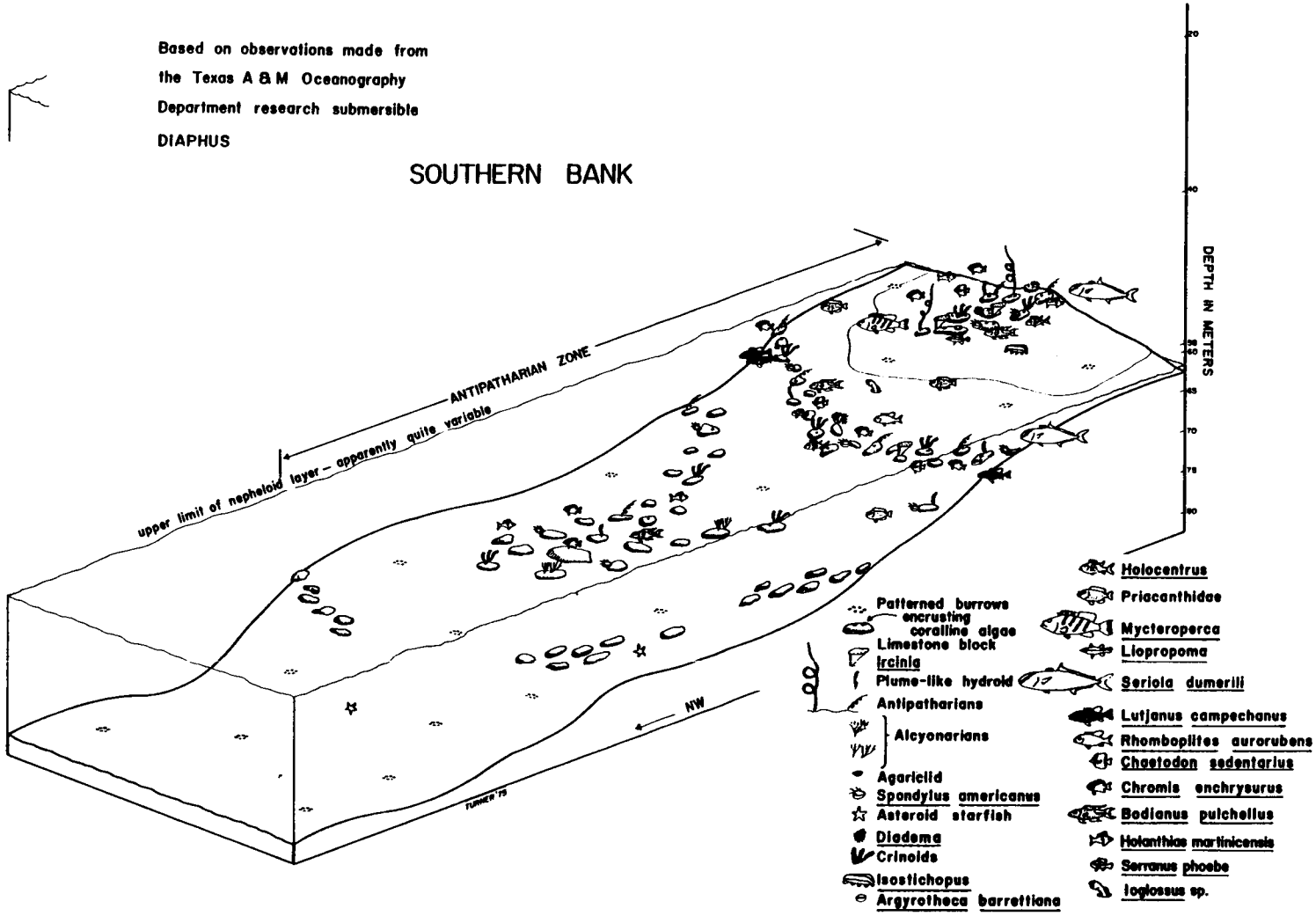

Figure 8.5 Diagrammatic representation of biota at Southern Bank.

branching Madracis brueggemanni and a number of solitary species in moderate abundance. We speculate that there may be a moderate population of the solitary corals, but they are individually quite small. The encrusting coralline algae population on Southern Bank is sparse, occurring most extensively at the very crest of the bank where it not only forms isolated patches on the carbonate blocks but also encrusts the tops of pieces of rubble on the sediment-covered bottom between blocks. At best, the current carbonate producing capacity of these limited populations of corals and coralline algae is feeble and possibly rivaled by that of the mollusks and echinoderms.

The American thorny oyster, Spondylus americanus, appears to thrive in substantial numbers not only in the clearer waters at the crests of the banks but also within the nepheloid layer farther down. It was observed in apparent good health attached to sediment-covered hard bottoms, itself bearing a significant veneer of fine sediment. Another very small species of calcium carbonate secreting organism, the brachiopod Argyrotheca barrettiana, is present cemented to the rocks, but due to its size is certainly not a major substratum builder.

Leafy algae, though present at least at the very crest of Southern Bank, are not abundant. A larger population of leafy algae was detected on the crest of Southern Bank in September 1976 than was the case in June 1975. Year to year and seasonal variation in leafy algae populations on offshore banks is a virtual certainty. We presume that small, variable populations of leafy algae similarly exist on most of the South Texas banks.

Conspicuous among the larger mobile benthic invertebrates are the arrow crab, Stenorynchus seticornis; hermit crabs; the black urchin, Diadema antillarum; the sea cucumber, Isostichopus; and fireworms, Hermodice.

Burrows in the sediment on all parts of the bank, and adjacent to it, are obviously of biological origin, though the nature of the organisms responsible is unknown. The distinctive clusters of holes designated as "patterned burrows" have a form that may indicate involvement of a mobile species, but the authors have no observations that would confirm it.

Groundfish populations at Southern Bank, and all the South Texas banks, are strikingly similar in composition and apparent magnitude per unit area to those frequenting the Antipatharian Zones at the Flower Garden Banks and other northwestern Gulf banks. The most characteristic resident species are Chromis enchrysurus, Holanthias martinicensis, Bodianus pulchellus, Chaetodon sedentarius, Liopropoma eukrines, Priacanthus, Serranus phoebe, Ioglossus, and Holacanthus bermudensis, in apparent order of abundance. Chromis enchrysurus, the Yellowtail reeffish, is particularly abundant, occurring not only in schools of up to a

hundred or more, but also in small groups and singly. Holanthias martinicensis, the Roughtongue bass, is perhaps most characteristic of the Antipatharian Zone because it is not typically observed in any of the shallower zones found on banks farther north. It seems to be strictly a deep-water variety. All of the other fishes mentioned above, except possibly Serranus phoebe, Tattler, are also fairly abundant on the coral reefs and in the Algal-Sponge Zones at the Flower Garden Banks. Surprisingly few large groupers of the genus Mycteroperca or hinds of the genus Epinephelus have been observed on Southern and the other South Texas midshelf banks.

Most of the fishes prefer to congregate around the carbonate reefal structures. However, the bigeyes, Priacanthus arenatus and Pristigenys altus, seem also to favor locations on the flatter portions of the bank, particularly over small potholes in the bottom into which they can retreat. The Hovering goby, Ioglossus calliurus, likewise favors the level sediment-covered bottom, where it digs a hole to occupy when not hanging suspended in the water directly above.

Larger migratory fishes which cannot be considered residents of any particular bank occur at Southern, and include the most important game and commercial fishes: schools of Red snapper and Vermilion snapper, Lutjanus campechanus and Rhomboplites aurorubens; the Greater amberjack, Seriola dumerili; the Great barracuda, Sphyraena barracuda; small carcharhinid sharks, and the Cobia, Rachycentron canadum.

Benthic communities occupying Baker, South Baker, Aransas, Hospital, North Hospital, and Dream banks are similar in content and abundance to those of Southern Bank. South Baker Bank may be a bit more profuse biologically. Populations of branching antipatharians, Antipathes, and gorgonocephalan basket stars are sizeable at Baker Bank and a Spanish lobster, Scyllarides sp., was seen. These are, however, typical components of the regional Antipatharian Zone.

Because of their relatively low relief above surrounding mud bottom, the southernmost midshelf carbonate banks on the South Texas shelf (Small Adam, Big Adam, Blackfish, and Mysterious) apparently suffer from chronic high turbidity and sedimentation from crest to base, and all rocks are heavily laden with fine sediment. Consequently, the epibenthic communities on these banks, though derived from Antipatharian Zone and upper Nepheloid Zone assemblages, are severely limited in diversity and abundance. Cirrhipathes is abundant and basket stars are frequent, clinging to the upper extremities of the Cirrhipathes whips. Red and Vermilion snapper, large groupers, amberjack, and barracuda were observed. Little else could be determined visually concerning the communities on these low relief banks because of the extremely poor visibility.

NORTH TEXAS-LOUISIANA REEFS AND BANKS ON DIAPIRIC STRUCTURES

Midshelf Banks

Midshelf banks are defined as banks rising from depths of 80 m or less and having a relief of from about 15 m to about 50 m. Banks on the North Texas-Louisiana shelf that fall into this category are Stetson, Claypile, Coffee Lump, Sonnier, and Fishnet. These banks are similar to each other in that they are all associated with salt diapirs and are outcrops of relatively bare, bedded Tertiary limestones, sandstones, claystones, and siltstones. The geology of two of these banks will be described as representative of the group.

Geology

Sonnier Banks

Sonnier Banks are located at 28°20'N latitude 92°27'W longitude (Figures 8.1 and 8.6). In Lease Block 305 of the Vermilion Area, South Addition, several peaks arranged in an arcuate pattern rise from a depth of about 60 m to crest at from 20 to 58 m. The individual peaks are apparent fault blocks that have been created by the collapse of the crest of the salt diapir (Figure 8.7). The two highest peaks, near the center of Lease Block 305 (Figure 8.6), have been observed from the submersible. The northern "twin" peak consists of steeply dipping Tertiary sandstones, siltstones, and claystones. The strike of the beds varies from 300° to 330°, and the dip varies from 45° to 90°. The side-scan sonar record (Figure 8.8) shows linear patterns of outcrops converging towards the east and diverging towards the peak just west of the survey line (Figure 8.6). The sub-bottom profile (Figure 8.7) shows a central area of no sub-bottom reflectors, flanked by beds dipping to the north and south. We know from submersible observations and the side-scan sonar records that the peaks and surrounding areas are composed of steeply dipping bedded rocks. The absence of sub-bottom reflectors in the central area of Sonnier Banks is due to dips that are too steep to return a bedding plane reflected sound wave to the transducer. The strong surface return in that area is due to reflections from the upturned edges of beds. The predominant unconformity on the north side of the diapir is absent on the south side of the diapir. This may be due to the uncomformity being below the lowest reflecting horizon on the south side of the diapir.

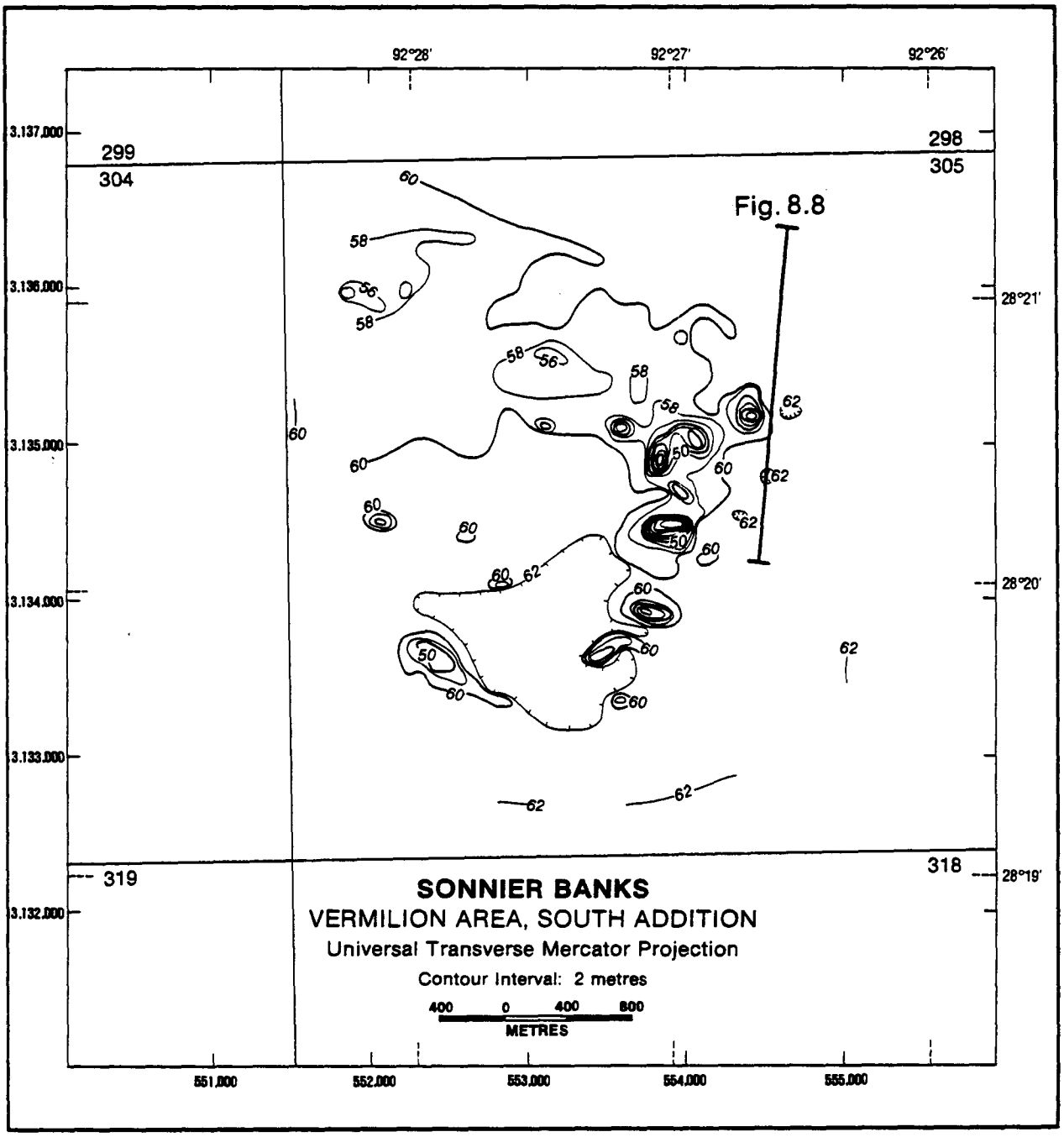

Figure 8.6 Bathymetry at Sonnier Banks, showing location of the sub-bottom profile and side-scan record shown in Figure 8.7.

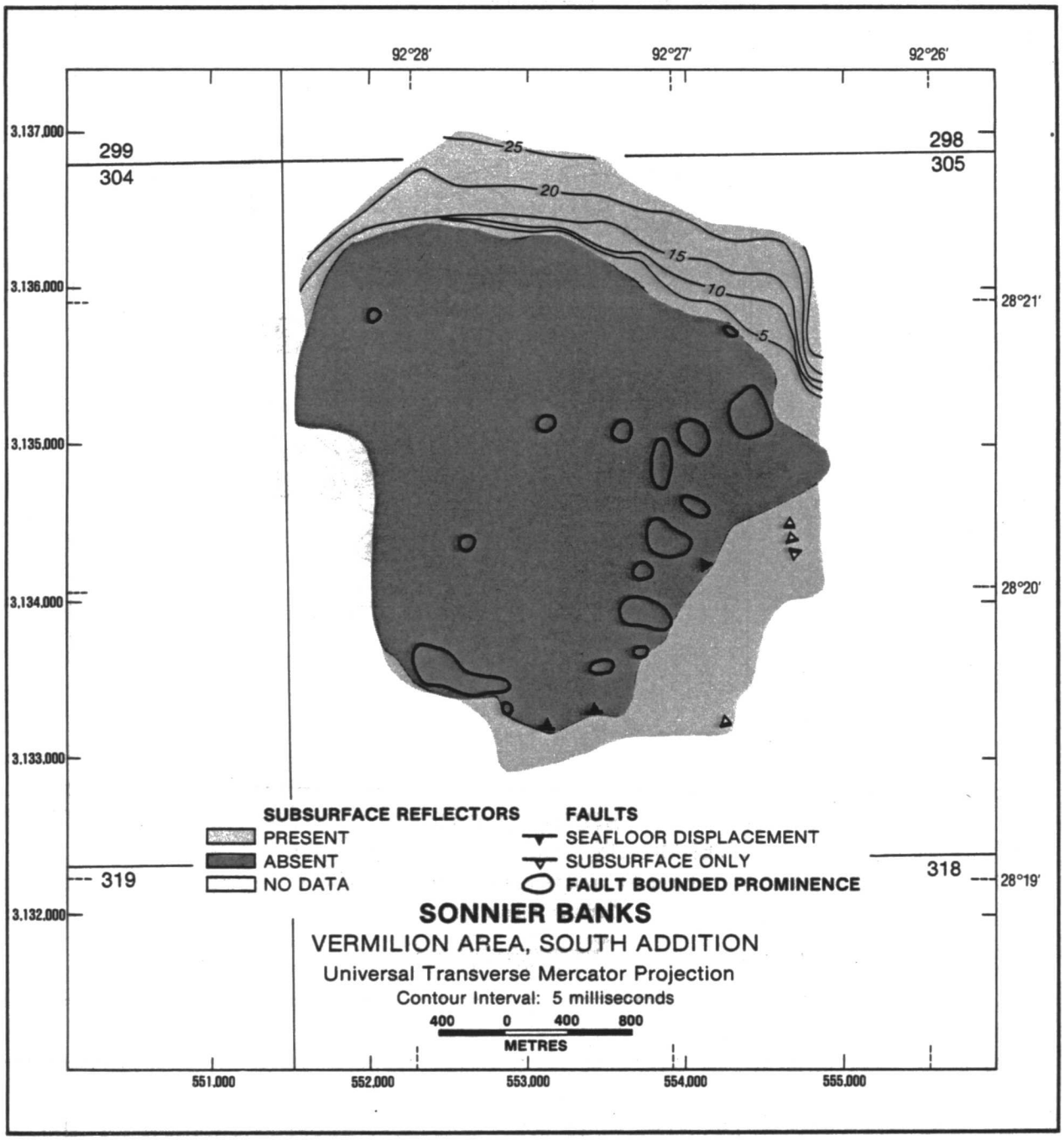

Figure 8.7 Structure/Isopach map of Sonnier Banks. Contours are isopachs (sediment thickness) from the seafloor to the unconformity on Figure 8.8.

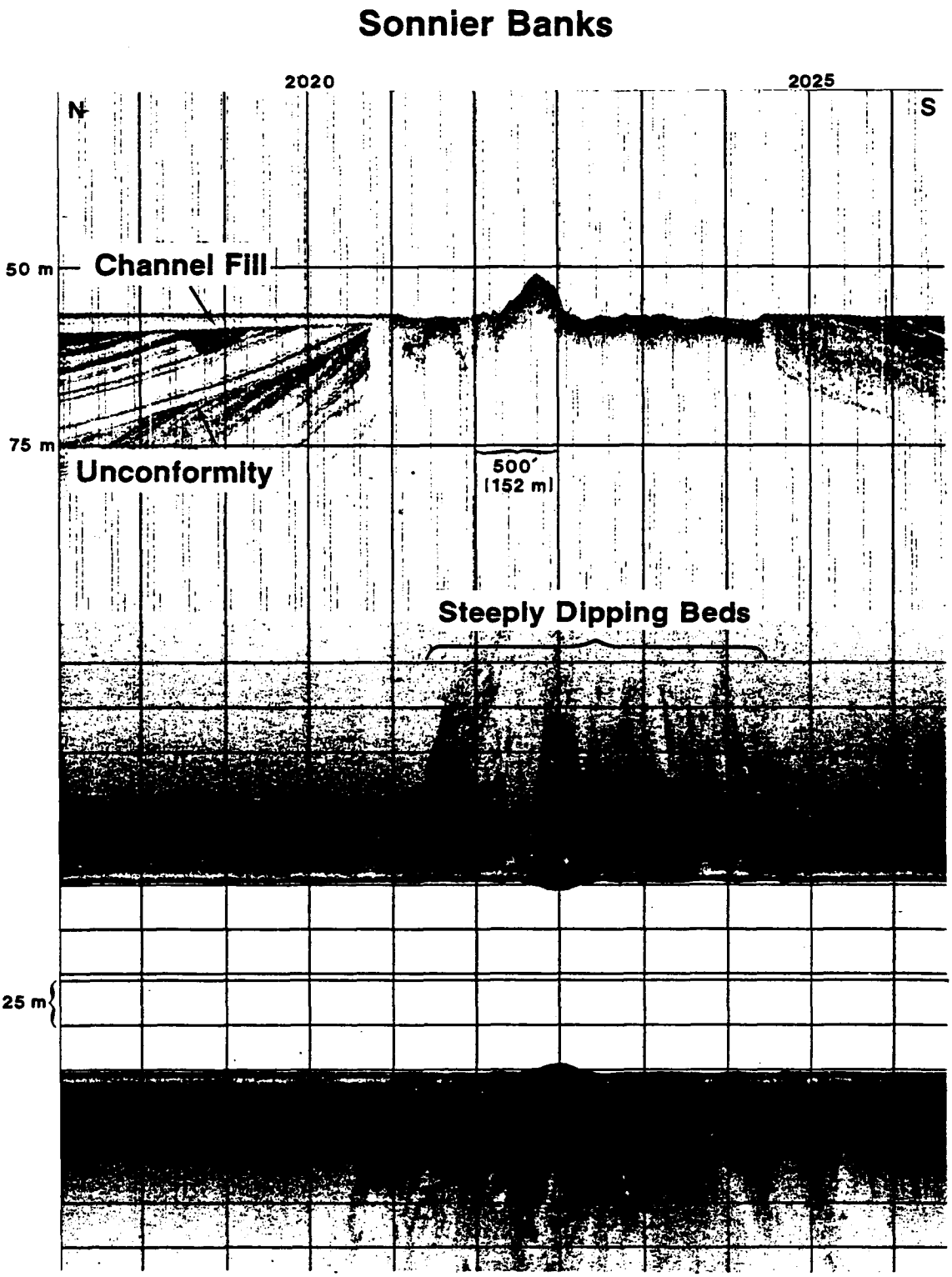

Figure 8.8 A 7 kHz sub-bottom profile and side-scan sonar record across the east side of the Sonnier Banks area. Location is indexed on Figure 8.6.

Fishnet Bank

Fishnet Bank is located at 28°09'N latitude and 91°48'30"W longitude (Figure 8.1). The bank lies in the northeastern quarter of Lease Block 356 in the Eugene Island Area. It is a small bank, covering only 1.9 km^2. The bank is nearly circular, with a relatively flat crest that lies at depths of 66 to 70 m. A raised rim along the southeastern and southern margins of the bank may be a reef build-up. Three separate peaks on the rim attain minimum depths of just greater than 60 m. Surrounding water depths are about 78 m on all sides of the bank. An east-west channel, 78 to 79 m deep, extends along the base of the north side of the bank (Figure 8.9).

Two patterns of local relief are found atop Fishnet Bank: 1) a pattern along the southern and southeastern perimeter of the bank, which may be a fringing reef but is more likely an outcrop of a more massive rock unit, and 2) ellipsoidal patterns of outcrops resulting from the truncation of the domal uplift. The fringing reef or outcrop of massive rock occupies the break in slope at the margins of the relatively flat top of the bank. The ellipsoidal outcrop patterns are caused by steeply dipping, erosionally truncated sedimentary beds in the central part of the bank. These features have less than one metre of relief.

Two seismic units were mapped on Fishnet Bank: 1) an area where subsurface reflectors are absent, which is the main body of the bank, and 2) the surrounding, uppermost sedimentary unit (Figures 8.10 and 8.11). The sediment sequence mapped around the margins of the bank onlaps the bank and underlying sediments, and appears to be only slightly tilted upward towards the bank (Figure 8.11). This suggests that uplift of the bank was nearly completed prior to deposition of the last sequence.

The sequence below the mapped unit is truncated by an angular unconformity that appears to have formed at the same time as the truncation of the beds that crop out on the top of the bank. This sequence is severely fractured by a pattern of radial faults. Many of the faults extend into the non-reflective unit of the bank proper. These faults were formed due to the doming of the strata overlying the salt diapir as it was rising. The faults and their associated sediments were truncated during the Late Wisconsin low stand of sea level. With the beginning of the Holocene transgression, deposition of the overlying sediments began to bury the unconformity. Renewed movement on the faults in Recent time has displaced the unconformity and created broad, shallow depressions on the seafloor (Figure 8.12).

A diffuse pattern of reflections within the water column over the bank proper is observed in all of the boomer crossings of the bank (Figure 8.11). This is in sharp contrast to those crossings

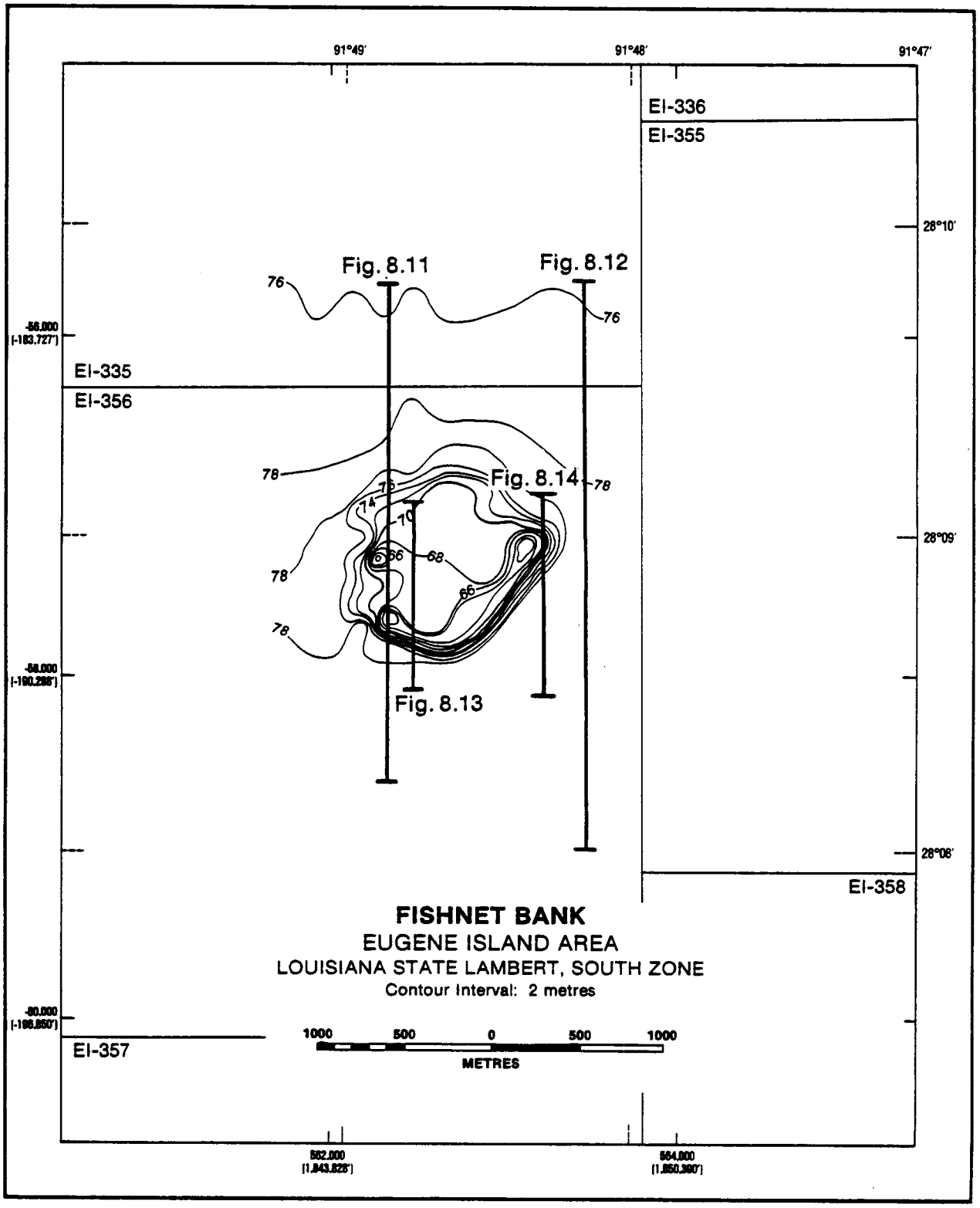

Figure 8.9 Bathymetry of Fishnet Bank, indexing location of profiles shown in Figures 8.11 and 8.12, and side-scan sonar records shown in Figures 8.13 and 8.14.

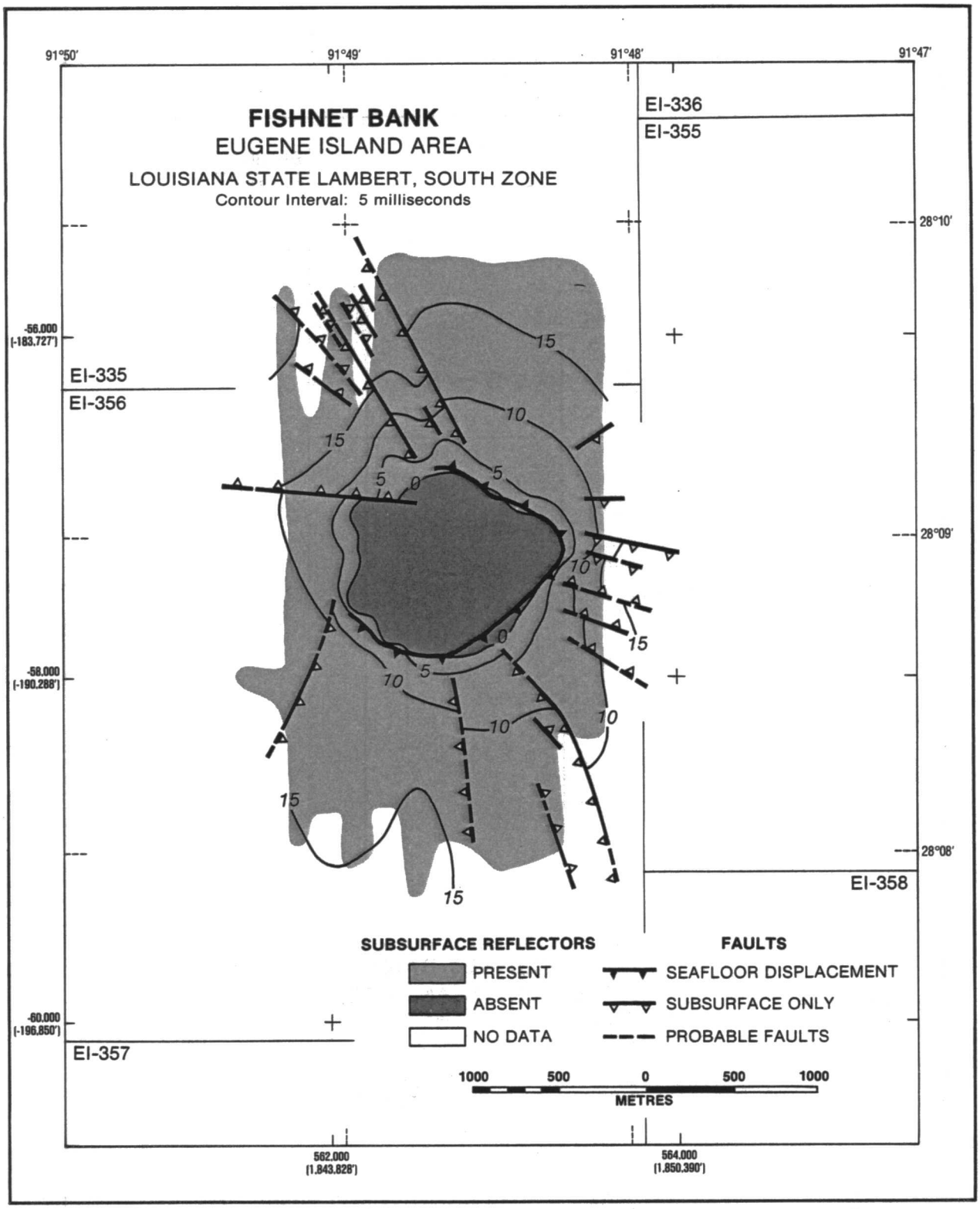

Figure 8.10 Structure/Isopach map of Fishnet Bank. Isopachs indicate the thickness of sediments from the surface to horizon H shown in Figure 8.11.

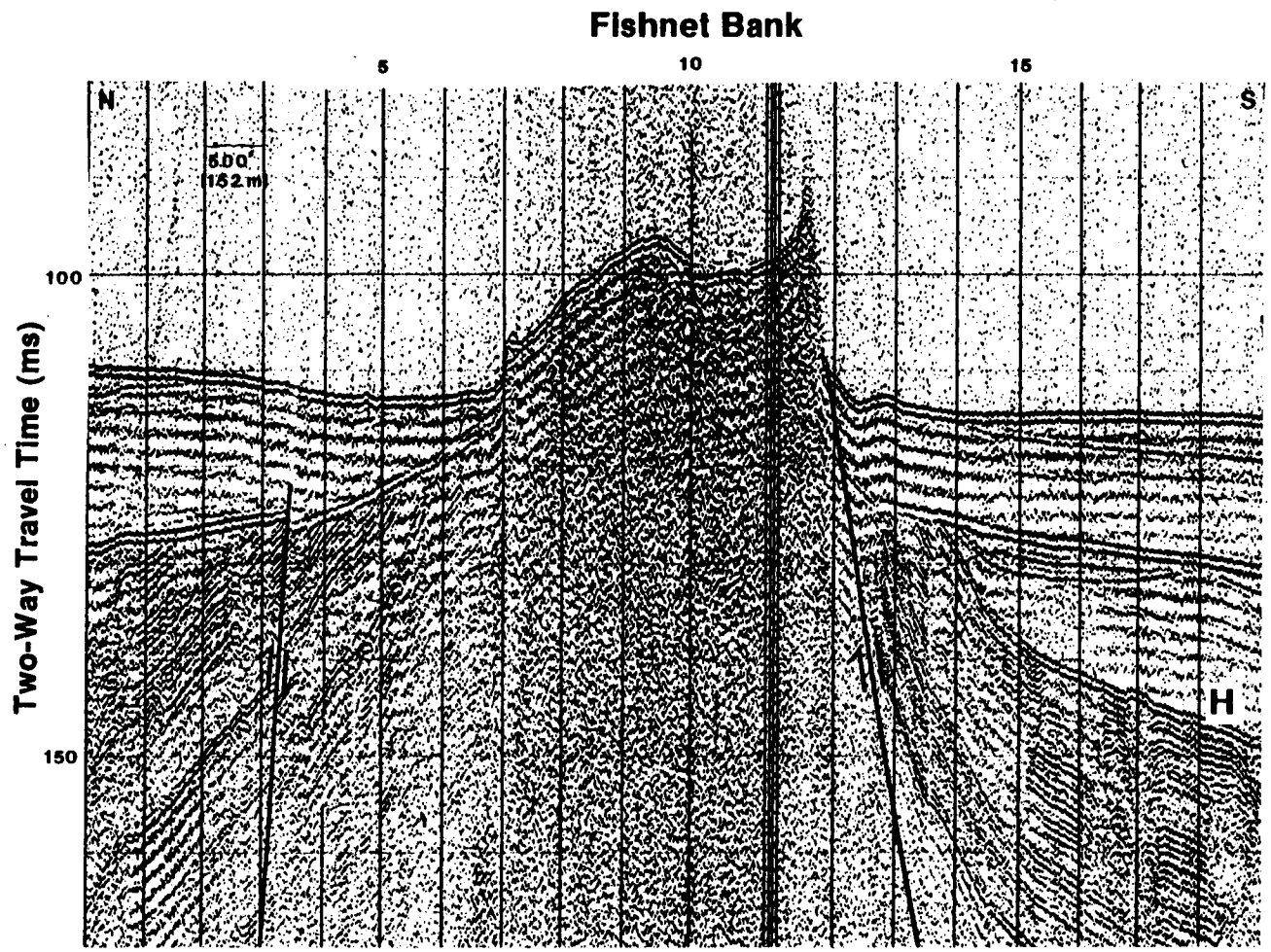

Figure 8.11 Boomer profile across Fishnet Bank. Location is indexed on Figure 8.9.

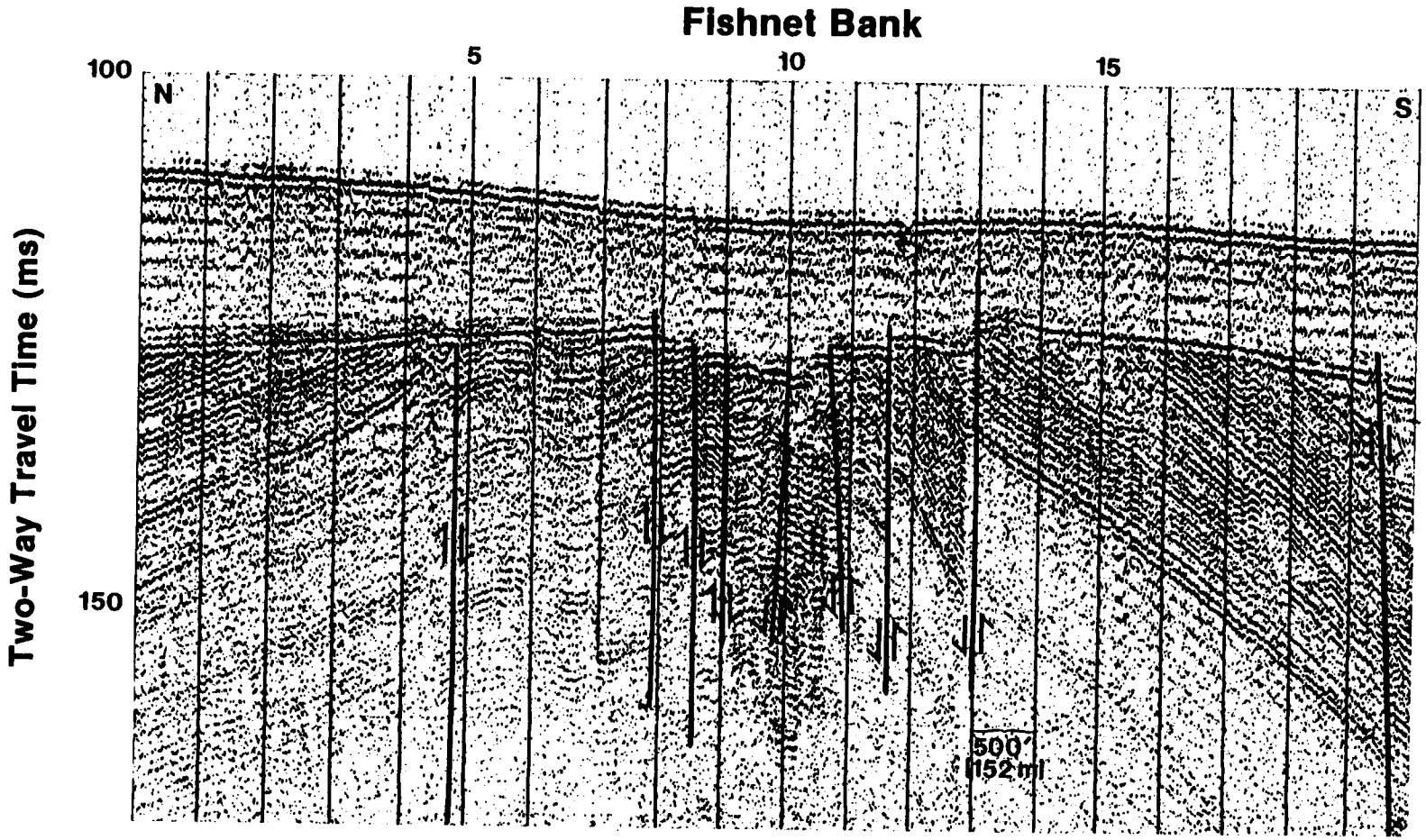

Figure 8.12 A 3.5 kHz sub-bottom profile across the eastern edge of Fishnet Bank (see Figure 8.9).

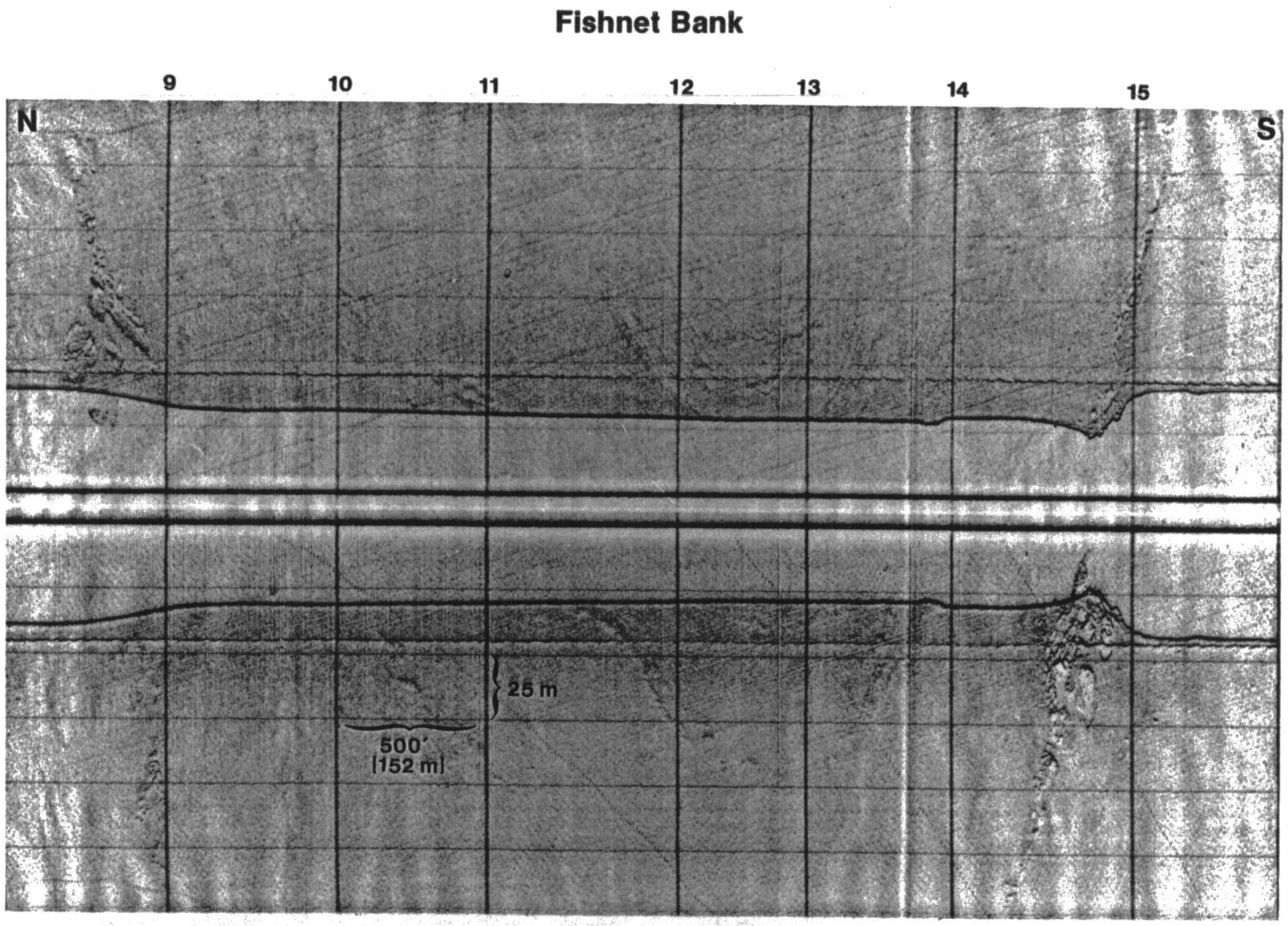

Figure 8.13 Side-Scan sonar record showing the pattern of outcrops at Fishnet Bank. Location is indexed in Figure 8.9.

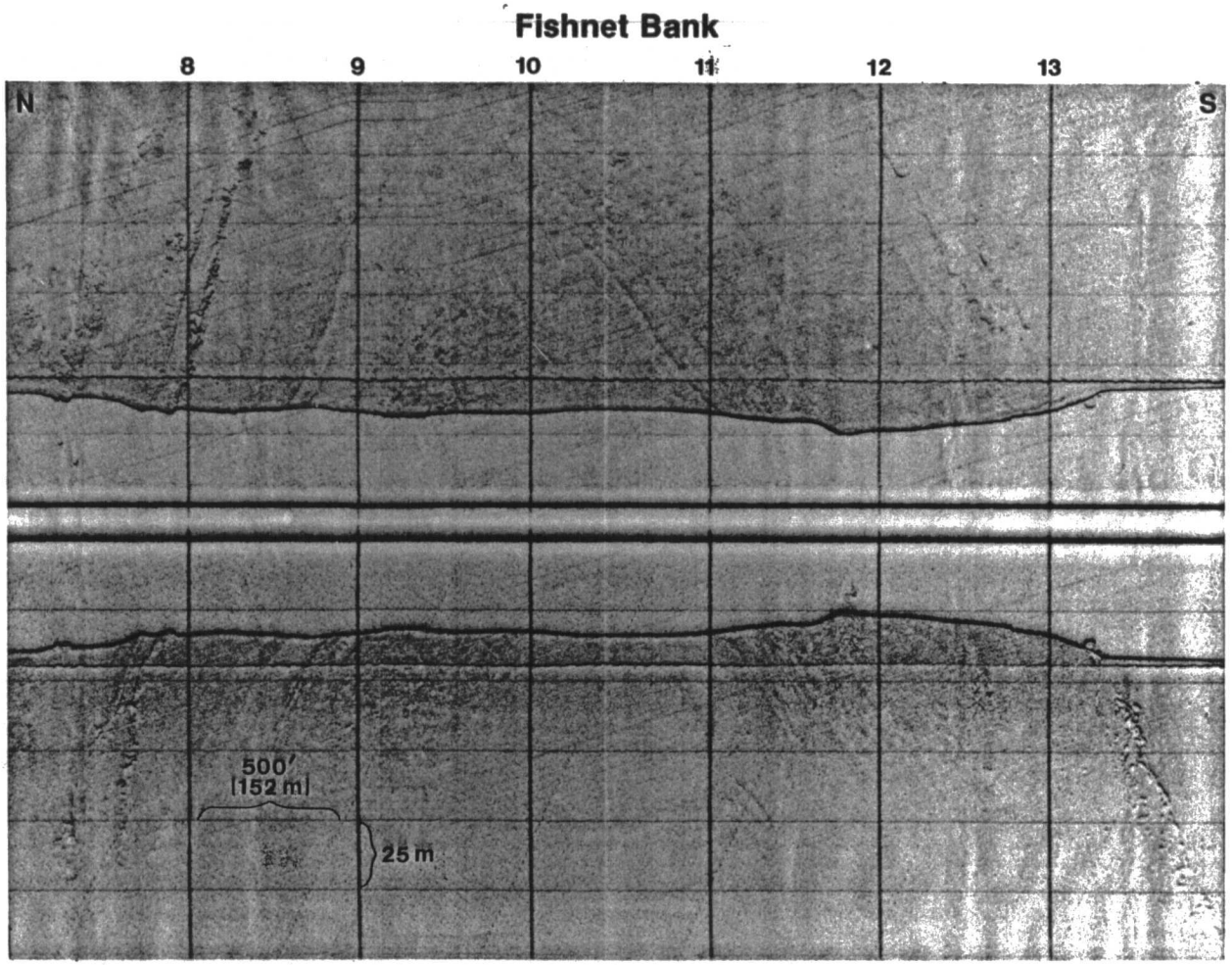

Figure 8.14 Side-Scan sonar records showing outcrop patterns on Fishnet Bank. Location is indexed in Figure 8.9.

off the margins of the bank, which show considerably less of this pattern. Wipe-out of bedding reflectors due to the presence of gas is also displayed on the sub-bottom profiles. While there are no obvious vents, it does appear that Fishnet Bank is seeping a considerable amount of gas into the water column. In June 1974, W.E. Sweet observed gas seeps on the bottom (unpublished data).

The 3.5 kHz profiles and side-scan sonar records (Figures 8.13 and 8.14) indicate a lack of sediment cover at Fishnet Bank. W.E. Sweet's log of a submersible dive on 20 June 1974 indicates that along the southwest side of the bank, where maximum relief occurs, there is a high blocky ridge (unpublished data). Numerous large blocks had broken off the ridge and slumped down the flanks of the bank. Other discontinuous ridges were noted on the bank. On the top of the bank, a thin veneer of fine sediment overlies a fairly hard substrate composed of shale. Sweet reported that the top of the nepheloid layer was encountered at a depth of 79 m and that the visibility at 82 m was about one metre.

During our submersible dive on 13 October 1978, the top of the nepheloid layer was at a depth of 61 m. The bottom at the beginning of the dive was at 78 m and consisted of a very fine, easily suspended mud with shell hash and finger coral fragments on the surface. On the way up the slope, large blocks of rock were encountered, similar to those described by Sweet. The top of the talus slope lies at 70 m depth. From that point to the top of the ridge, at a depth of 64 m, the rock forms a vertical cliff. All of the rocks encountered during this dive were Tertiary bedrock. On a second dive that day, two peaks were observed that are quite different from the ones seen on the previous dive. The peaks consist of cavernous rocks that resemble the drowned reefs that have been observed on other banks.

Biology

The biotic assemblages occupying north Texas-Louisiana midshelf banks with surrounding depths of 62 m or less (Sonnier, Claypile, and Stetson) are distinct and compose a *Millepora*-Sponge Zone dominated by hydrozoan fire corals (*Millepora*) and various sponges. The biota are best developed on Sonnier Banks, which will be discussed below .

The crest of Sonnier (20 to 21 m depth) is almost entirely encrusted with fire coral (*Millepora alcicornis*) and the sponges *Neofibularia nolitangere* and *Ircina* (Figure 8.15). The fire coral population extends downward to 40 m depth, but is severely diminished below the bank's crest. Dead branches and broken pieces of fire coral occur abundantly in the unconsolidated sediment at the bases of the shallower outcrops along with siltstone chips and fine silt- and clay-sized particles. The coral must, therefore,

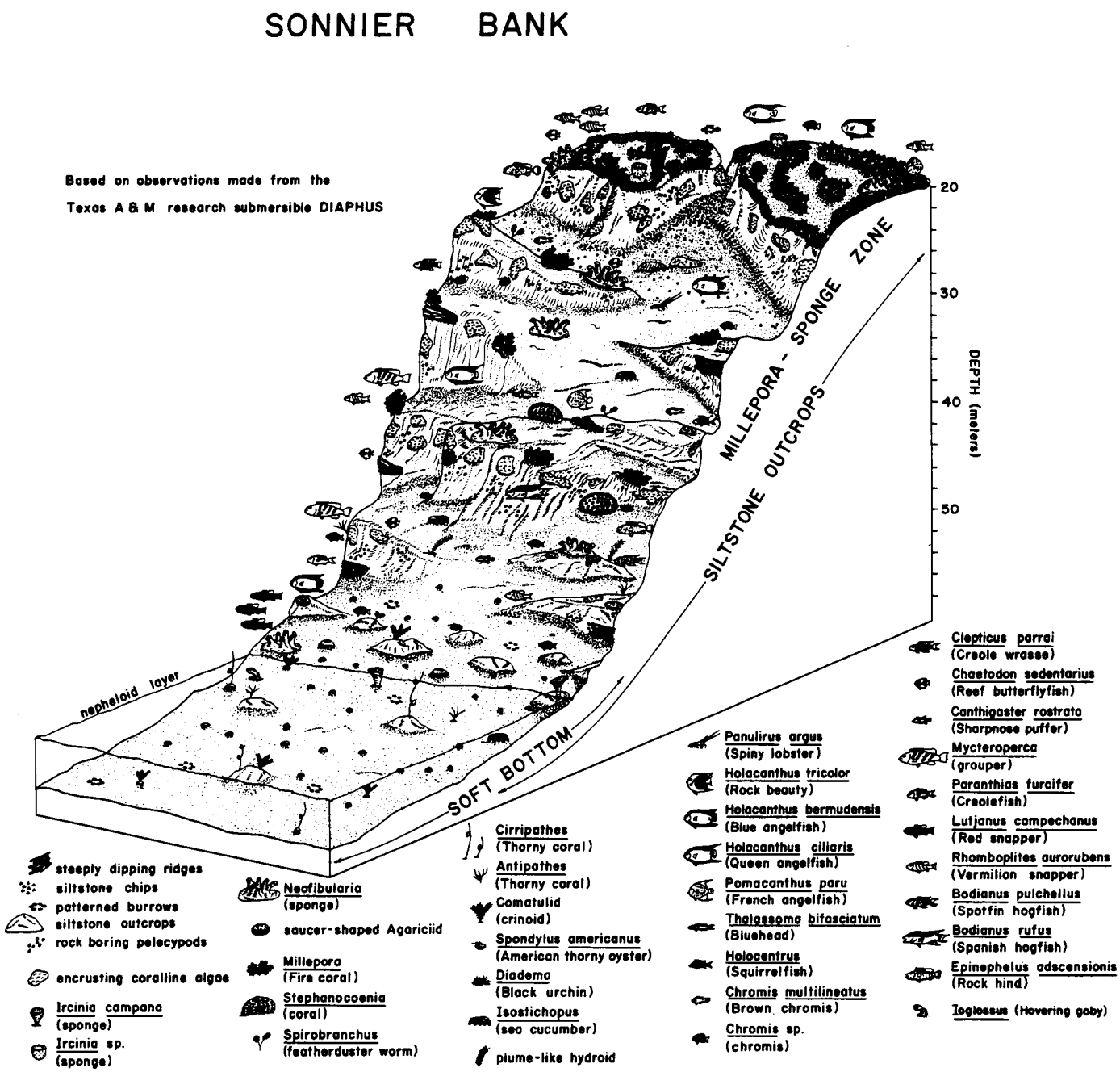

Figure 8.15 Diagrammatic representation of biota at Sonnier Banks.

contribute significantly to the sediment which is produced on the bank and ultimately transported to the surrounding level-bottom.

Heads of the hermatypic anthozoan coral Stephanocoenia michelinii were seen at 36, 38, and 41 m depth. None of these heads was over one metre in diameter. Dead patches on the deepest one possibly indicate periodic mortality and regrowth. Stephanocoenia michelinii is widespread on the midshelf and shelf-edge banks off North Texas and Louisiana. It appears to tolerate conditions of low light intensity and moderate turbidity better than other types of reef-building corals in the northwestern Gulf (Stephanocoenia also occurs at Stetson Bank as deep as 50 m). The only other stony coral encountered at Sonnier Banks was the saucer-shaped agariciid, which seems to be even more tolerant of such conditions than Stephanocoenia and was seen at 52 m depth. Encrusting coralline algae occur on Sonnier Banks down to 47 m depth. Its abundance is moderate above 40 m, becoming sparser with increasing depth.

Populations of fishes and conspicuous, mobile invertebrates at Sonnier Banks are diverse and abundant above 45 m depth, and very comparable to populations at Stetson Bank. Among the more numerous reef fishes are several species of large angelfishes and butterflyfishes, Chaetodontidae; damselfishes, Pomacentridae; Bluehead, Thalassoma bifasciatum; hogfishes, Bodianus; Creolefishes, Paranthias furcifer; Rock hind, Epinephelus adscensionis; groupers, Mycteroperca; and others typical of submerged reefs and banks in the northwestern Gulf. Large schools of Vermilion snapper, Rhomboplites aurorubens, were seen above 35 m depth, and Red snapper schools, Lutjanus campechanus, were encountered near the base of the bank. A species of Chromis similar in shape, size, and habit to Chromis enchrysurus is extremely abundant above 50 m depth. Chromis enchrysurus, which is abundant on most of the other banks in the northwestern Gulf, was not observed at Sonnier Banks during the dives made in September 1977.

A sizeable population of the large sea cucumber Isostichopus is present between 35 and 45 m depth. The molt of a spiny lobster, Panulirus, was seen at 27 m depth.

A correlation between the depth distribution and abundance of epibenthic communities and patterns of chronic turbidity at Sonnier Banks is probable. During the September 1977 submersible dive, observers noted that water turbidity at Sonnier Banks was greater below 42 m than above, although a highly turbid nepheloid layer was not encountered above 52 m depth. The abundance of Millepora, sponges, coralline algae, and most of the other encrusting epifauna is greatly reduced below 40 m depth.

The base of Sonnier Banks lies at approximately 52 m depth. With increasing distance away from the largest bank structures, outcrops become smaller and give way to a mud bottom with loose sandstone and siltstone boulders and cobbles, all covered with

veneers of sediment. At 58 m depth, mud is the predominant sediment, with few rocks on the sediment surface.

Although certain species which are abundant on the banks extend some distance out onto the surrounding level bottom (Neofibularia nolitangere and Isostichopus were seen down to 54 m depth), benthic communities occupying this turbid water, rock strewn, soft-bottom differ considerably from those found on the bank. Conspicuous organisms present adjacent to the bank, but not on it, include the antipatharians Cirrhipathes and Antipathes, comatulid crinoids, the sponge Ircinia campana, and the Hovering goby, Ioglossus calliurus. Abundant burrows, tracks, and trails in the mud attest to a substantial population of large infaunal and mobile benthic organisms.

Biotic communities on Sonnier and Stetson Banks are basically the same, and above 52 m depth represent a distinct Millepora-Sponge Zone. Sonnier populations are somewhat more abundant. A well developed Millepora-Sponge Zone is present between 37 and 52 m depth on a claystone-siltstone pinnacle protruding from the carbonate crest of Geyer Bank at the continental shelf edge. This offshore manifestation of an otherwise midshelf hard-bank assemblage implies either that substratum type is the primary factor controlling community structure in the Millepora-Sponge Zone, or that the Millepora-Sponge Zone is a pioneer community that populates newly exposed bedrock.

Relatively clear water is probably a necessary requirement for healthy development of this assemblage. Claypile Bank, a Tertiary bedrock structure farther inshore, with a greater crest depth and less vertical relief than the others, harbors a depauperate Millepora-Sponge Zone. This is probably due to conditions of higher average turbidity and sedimentation than occur at Sonnier and Stetson, and certainly Geyer Bank, the crest of which is in perpetually clear, oceanic water.

A few sizeable heads of Stephanocoenia michelinii were encountered at Claypile Bank, in depths to 42 m, further indicating this species' resistance to turbidity, sedimentation, and reduced light. Light intensity at the crest of Claypile Bank is, nevertheless, adequate to support significant populations of leafy and filamentous algae. In fact, the predominant organisms occupying the broad top platform of the bank in September 1976 were low-growing mats and clumps of soft algae. Extensive meadows of attached Sargassum were observed on the bank in June 1972. These algal populations are certainly seasonal and irregular, as is the case on other offshore banks in the northern Gulf.

Farther offshore than Stetson, Sonnier, or Claypile, there exists a series of midshelf banks inhabited by transitional assemblages roughly comparable to those of the Antipatharian Zone. These "transitional" banks (Fishnet, Coffee Lump, and 32 Fathom

Bank) have surrounding depths in excess of 65 m but less than 80 m. They are most similar in biotic structure to the South Texas midshelf banks, which, though of different geologic origin, arise from approximately the same surrounding depths.

General characteristics of Coffee Lump are illustrative of the "transitional" midshelf banks. Most of the bottom at Coffee Lump is composed of an unconsolidated mixture of clay, silt, sand, shell, and rubble (64.0 to 67.7 m depth), with occasional large boulders a metre or so across and a half a metre high. Major hard-bottom features examined included a reef-like carbonate rock ledge (62.5 to 65.5 m depth) and the other a large, almost horizontal, slabby outcrop of siltstone (59.5 to 64.0 m depth).

Where the soft bottom consists of substantial amounts of sand, shell, and rubble there is a predominance of antipatharian whips, Cirrhipathes; comatulid crinoids; large asteroids such as Narcissia trigonaria and Goniaster; the urchin, Clypeaster ravenelii; the sea cucumber, Isostichopus badianotus; small branching corals; small benthic fishes; and an enormous population of minute crustaceans, including pagurid (hermit) crabs, "decorator" crabs, other brachyuran crabs, and small anomurans.

The extremely large populations of small fishes and crustaceans on the soft bottom above 68 m are significant. These organisms may be the most abundant on Coffee Lump. They are closely associated with the innumerable small burrows on the bank and were seen producing tracks and trails in the sediment. These animals must be a major source of food for larger fishes and other predators occupying the bank.

The assemblage of organisms inhabiting hard bottoms above 68 m depth at Coffee Lump is similar in composition and structure to assemblages encountered on South Texas midshelf banks such as Southern and South Baker Banks. The most conspicuous, predominant, and abundant organisms are antipatharian whips, Cirrhipathes; comatulid crinoids; encrusting coralline algae; sponges (including a large population of Ircinia campana); large hydroids; and fragile white "bushes" of serpulid worms, Filograna.

Coralline algae cover up to 30% of the rocks at the tops of outcrops or ledges. Cobble-sized rocks lying on the soft bottom frequently bear small patches of coralline algae on their upper surfaces.

A significant population of hermatypic agariciid corals was detected on the shallower parts of the larger hard-rock structures (59.5 to 64 m depth). Other small branching corals were seen on the hard bottom, and solitary corals almost certainly occur there. Those parts of the rocks not covered by corals, coralline algae, or encrusting sponges are generally laden with sediment veneers or a sediment-epifauna mat.

Most of the larger fishes seen were associated with the hard bottom. Predictably, the Yellowtail reeffish, Chromis enchrysurus, was the most abundant. Schools of Vermilion snapper, Rhomboplites aurorubens, were present. Other fishes encountered were typical of hard bottom at these depths throughout the northwestern Gulf of Mexico.

Shelf-Edge Carbonate Banks and Reefs

The shelf-edge carbonate banks and reefs are located on complex diapiric structures. Several of these banks are described in the following pages to illustrate the complexity of the structures and the similarity of the biotic zonation. Although all of the shelf-edge banks have well developed carbonate caps, there are local areas of bare bedded rocks that have been exposed by recent faulting.

Geology

Geyer Bank

Geyer Bank is located at 27°51'17"N latitude and 93°04'09"W longitude (Figure 8.1). The bank lies in the Garden Banks Area, Lease Blocks 105, 106, 149, 150, 193, and 194 (Figure 8.16).

Situated just south of the shelf break on the upper continental slope, the bank rises from depths of 210 m on the north and 190 m on the south. It is a north-south elongated structure covering about 55 km^2 in area. The steepest slopes are found at the northern end of the bank, with gentle slopes on the east and west sides and moderately steep slopes on the southeast and southwest sides. The bank is "hamshaped" with the "shank" end to the north. The top of the bank is broad and relatively flat, with prominences on the north and south ends rising to depths of less than 60 m and separated by a saddle around 90 m depth.

The unusual distribution of depths surrounding the bank is due to the fact that Geyer Bank is the northeastern part of an arcuate salt diapir complex. The southern boundary of Geyer Bank is on a saddle between the bank and the next diapir to the southwest.

The internal structure of the core on Geyer Bank is difficult to interpret because the surface of the bank reflects a large part of the seismic energy. This difficulty is well illustrated on the profile in Figure 8.17 by the strong surface return and the presence of a strong multiple. However, the surface configuration of the bank, as shown on Figures 8.17 and 8.18 gives some clues to the

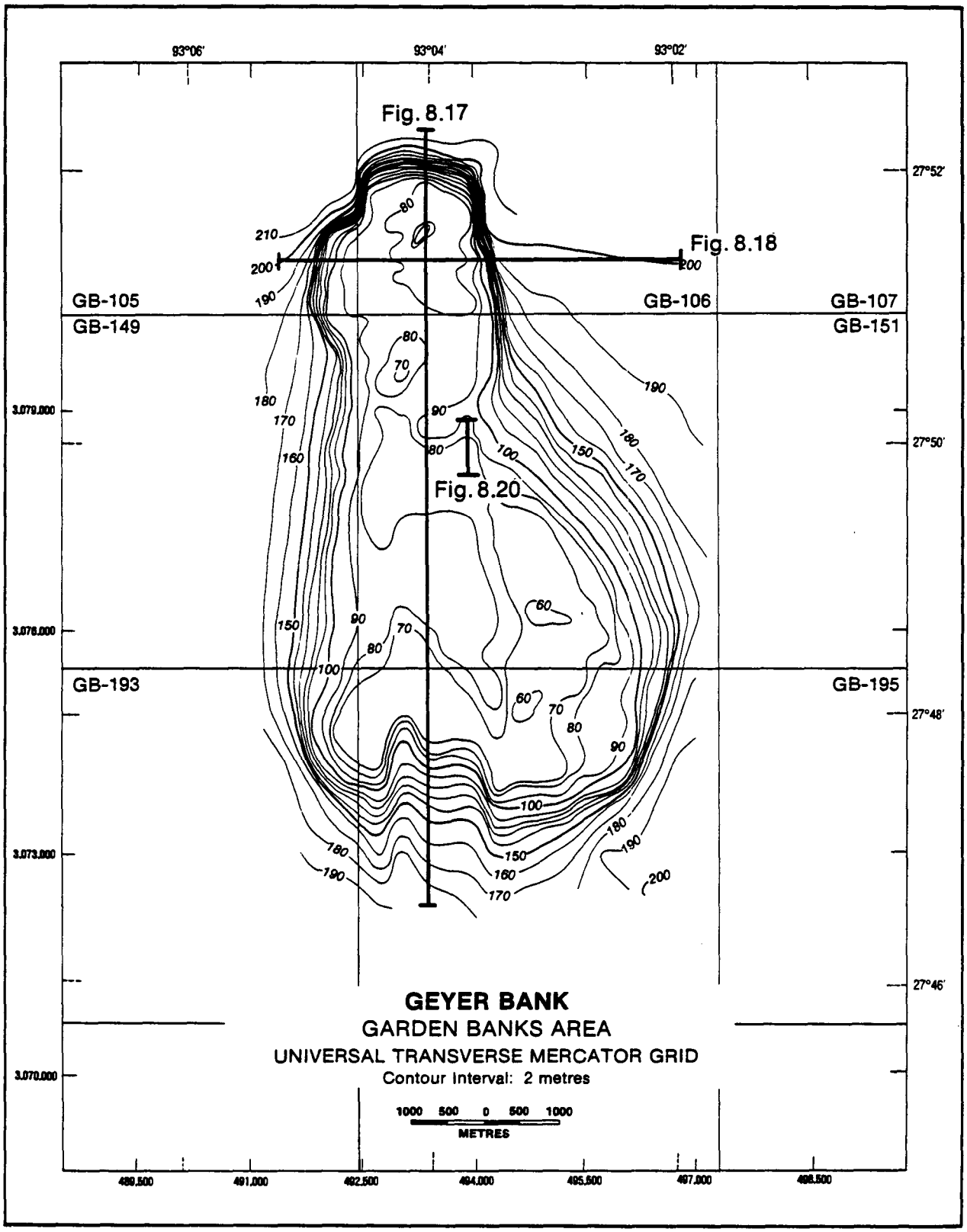

Figure 8.16 Bathymetry of Geyer Bank, showing location of boomer profiles and side-scan sonar records shown in Figures 8.17, 8.18, and 8.20.

structure. These are substantiated by direct observations of the bottom from the submersible during a dive made 21 October 1978.

Two structural units were mapped on the basis of the seismic profiles: 1) the non-reflective area, which underlies most of the bank proper; and 2) the surrounding stratified and tilted sedimentary sequence. The non-reflective area displays very weak internal reflective patterns due to the loss of signal strength by reflection from the hard surface of the bank and the nearly vertical bedding surfaces within the bank proper. Outcrops of nearly vertical beds were observed from the submersible on 21 October 1978. The overlying stratified unit, seen on the flanks of the bank, is bounded above by the seafloor and below by a more steeply dipping sequence upon which the mapped unit overlaps (Figure 8.17 and 8.18). Contours of this sequence are isopachs representing thickness of the unit or depth below the seafloor to its boundary.

The steep slopes on the margins of the bank are most likely fault scarps. Only one major and a few minor faults have been mapped on the basis of sub-bottom data. However, the numerous nearly vertical slopes on the upper surface of the bank are probably fault scarps, indicating that the upper part of the non-reflective unit is more extensively block faulted than appears on the structural map (Figure 8.19). The areas mapped as slumps on that figure may also be fault blocks.

The entire bank is essentially fault bounded. The zero isopach or limit of the non-reflective unit may be considered to be a series of interconnected faults caused by the upward thrust of the salt diapir. The faults on the top of the bank, those inferred from topographic expression and direct observation of nearly vertically oriented beds, are most probably normal faults caused by collapse of the crest of the bank due to the removal of salt by dissolution.

It should be noted that the darker subsurface area, just beneath the surface at the top of the bank on each of the boomer profiles, is an artifact created by a malfunction of the recorder signal gain control. It does not represent real structure.

The seismic profiles indicate little evidence for gas either being vented or within the sediments at Geyer Bank. However, during a submersible dive 12 October 1978, an area of gas seeps was encountered at a depth of 82 m. The entire upper surface of the bank could potentially collapse. Recent movement along faults at the top of the bank is suspected because of the presence of bare rock outcrops along with outcrops that are relatively heavily encrusted by coralline algae and other organisms. If all outcrops on the bank had been exposed at the same time, then all of them should now be encrusted with nearly the same amount of reef-building organisms.

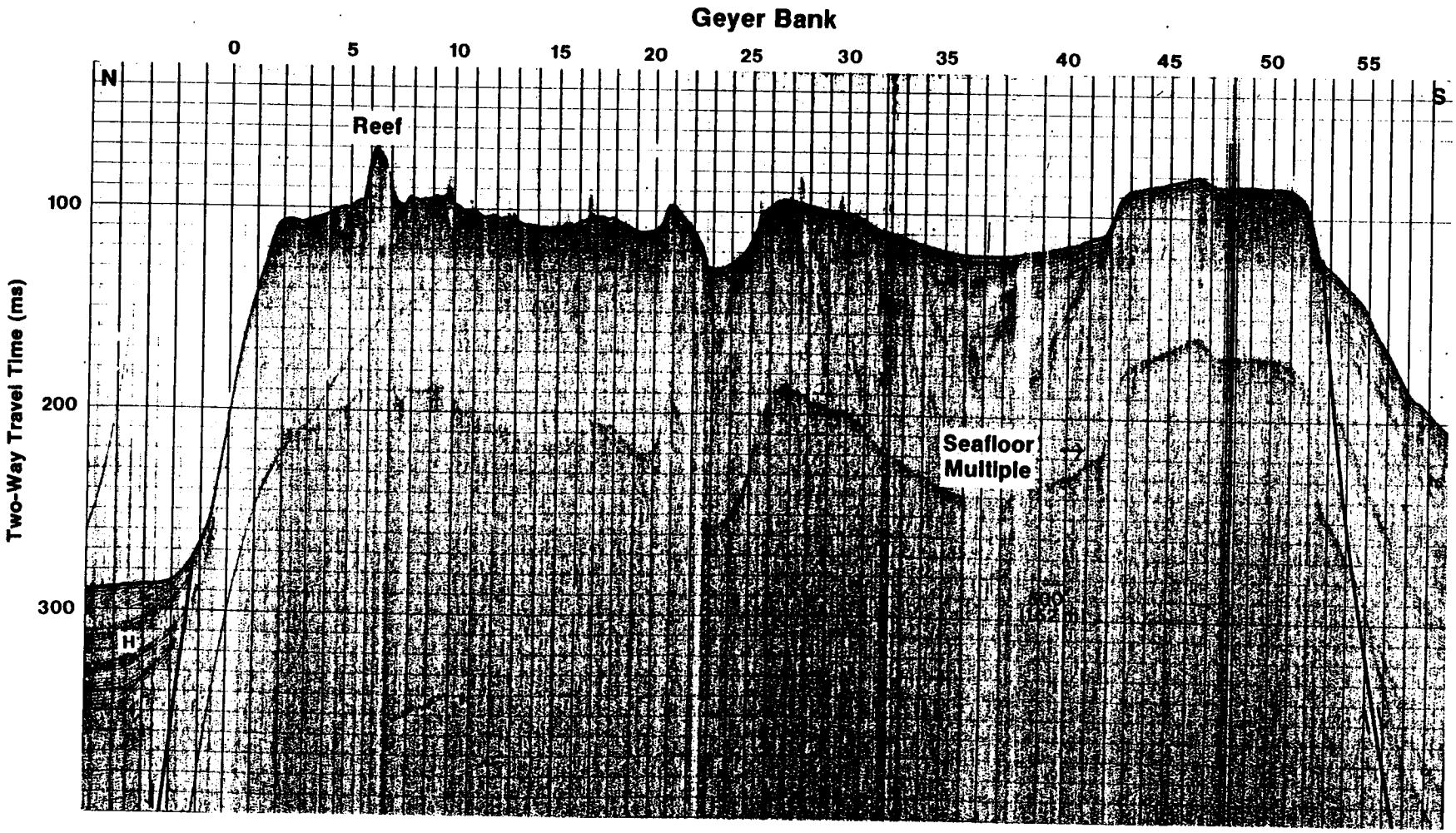

Figure 8.17 North-South boomer profile across Geyer Bank. Location is indexed in Figure 8.16.

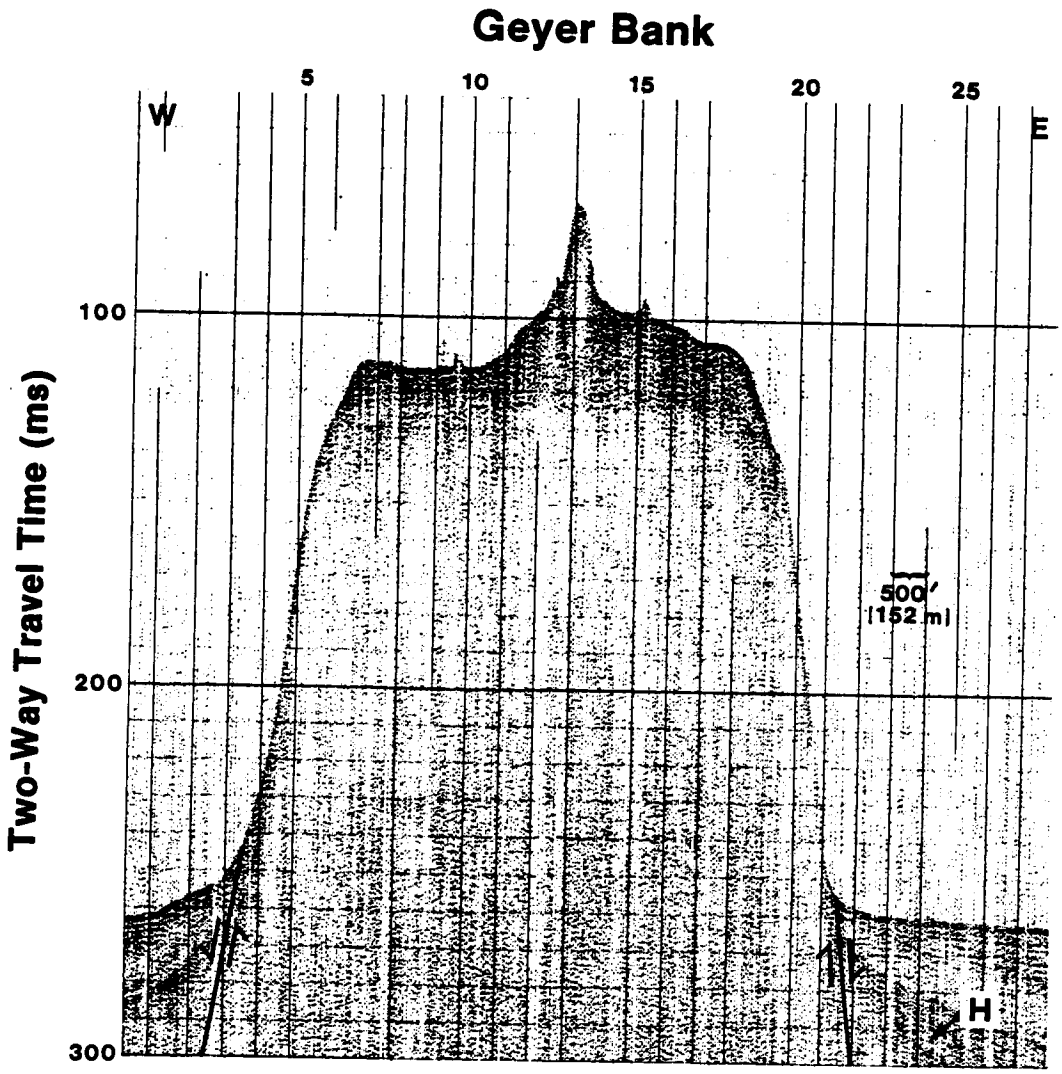

Figure 8.18 East-West boomer profile across Geyer Bank. Location is indexed in Figure 8.16.

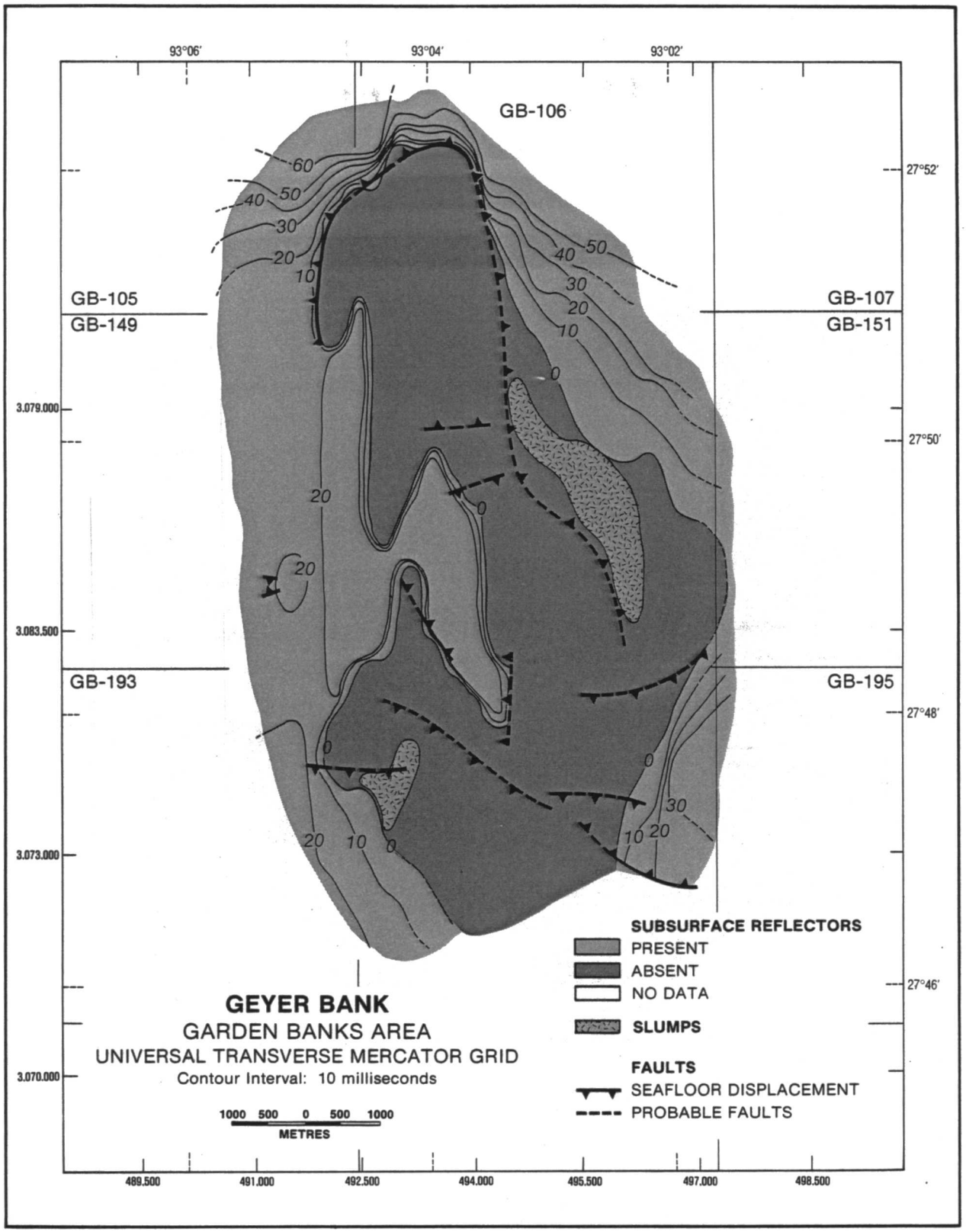

Figure 8.19 Structure/isopach map of Geyer Bank. Isopachs indicate the thickness of sediments from the surface to horizon H (Figure 8.18).

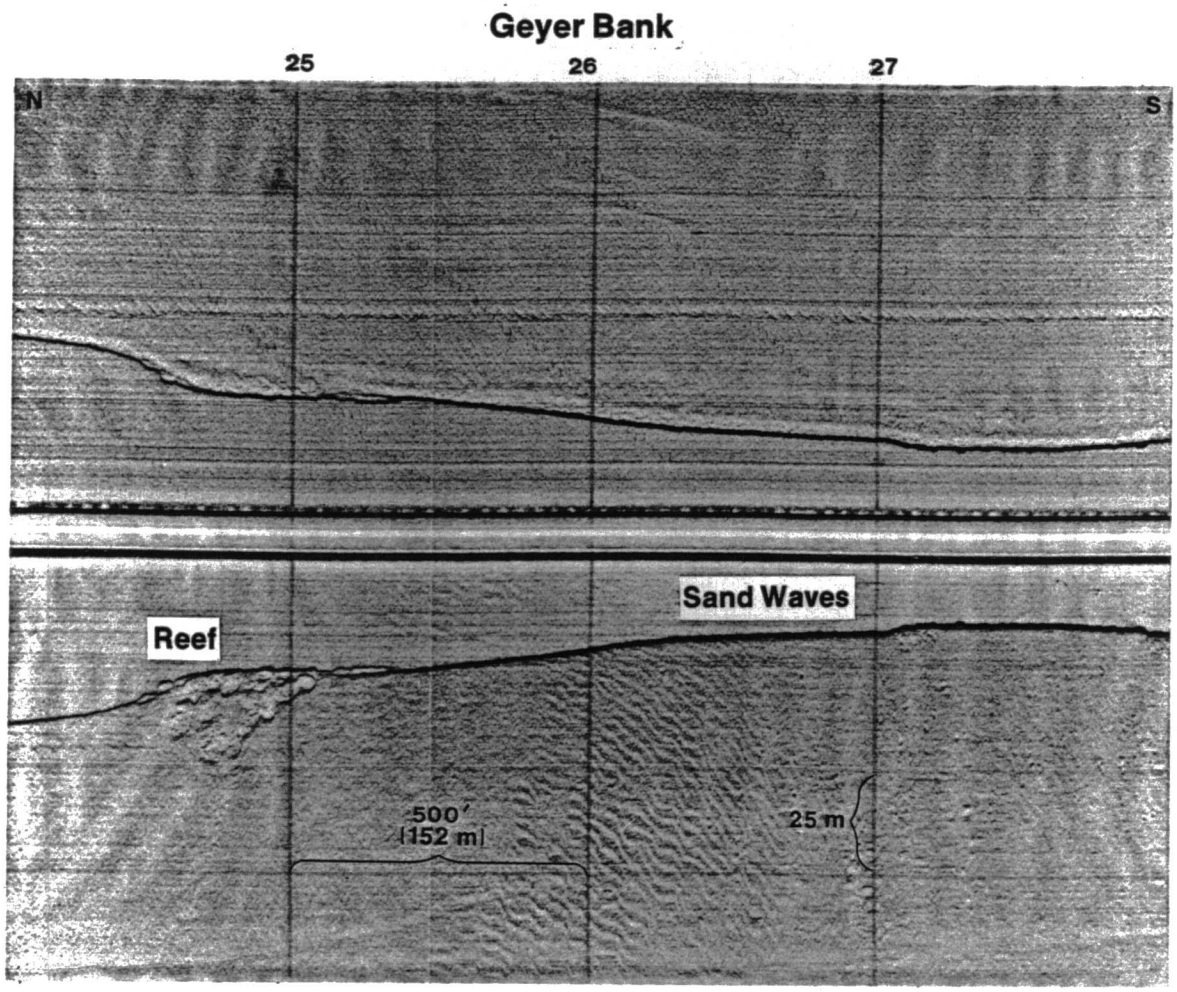

Figure 8.20 Side-Scan sonar record showing sand waves and reef. Location is indexed in Figure 8.16.

Although no sediment samples were taken on Geyer Bank, seismic and side-scan sonar data together with direct observations of the bottom from the submersible give a general idea of the nature of the sediments on the bank. There is little or no evidence on the boomer and 3.5 kHz records for recent sediment cover on top of the bank. However, the side-scan sonar records show large areas of sand waves in the central and southern parts of the bank (Figure 8.20). The wave patterns toward the perimeter of the bank appear to have a general wave structure, regularly spaced with nearly uniform amplitude, and with the trend of the crest nearly at right angles to the isobaths.

The sediment descriptions on video tapes of the 12 October 1978 dive indicate large areas of algal nodules and carbonate sand between depths of 60 and 75 m. Large scale sand waves are probably composed of algal nodules, and the sand waves (Figure 8.20) are probably equivalent to the Amphistegina Sand Facies at the Flower Garden Banks.

The sediment at 213 m depth on the north side of the bank is a very cohesive clay. Large angular fragments of clay were thrown up into a pile ahead of the battery pod of the submersible as it plowed into the bottom. At a depth of 187 m, coralline algal nodules were observed lying on the muddy bottom. These must have rolled from the top, where they grew, down the steep slope of the bank. Drowned reefs were observed at 98 to 94 m, 87 m, 78 m, 76 m, and 70 m depths.

Diaphus Bank

Diaphus Bank is located at 28°05'18"N latitude and 90°42'26"W longitude (Figure 8.1) in Lease Blocks 314 to 317 of the South Timbalier Area. It lies close to the shelf edge and is about 50 miles west of the Mississippi Trough. The bank is rectangular and covers an area of about 33 km^2. Superimposed upon this rectangle are two ridges that intersect at nearly right angles to form a rough cross. The surrounding water depths range from 110 m on the north to 130 m on the south, with increasing depths to the south, down the upper continental slope. The bank stands about 40 m above the surrounding shelf, with the shallowest depth at a peak in the center of the bank lying at 73 m (Figure 8.21).

The most prominent feature of the bank is an east-west ridge which has an extremely steep (locally about 90 m/km) and linear south side. The slope on the north side is much gentler, being only about 20 m/km. A smaller ridge extends to the north (about 2.5 km) and to the south (about 1.7 km) from the center of the east-west structure.

Local relief on the bank is concentrated along the crests of the intersecting ridges. This relief is primarily related to the normal faulting that is so evident in the north-south seismic profiles (Figure 8.22).

The seismic reflection records reveal that Diaphus Bank is a domal diapiric structure that has been breeched by a major down-to-the-sea, normal fault, creating the massive, south-facing scarp that is so prominent on the bank. Radial faults have created the less prominent north-south ridge.

Two seismic sequences were mapped (Figure 8.23): 1) the exposed acoustic basement unit, which is highly reflective and consists of well stratified sedimentary rock; and 2) a poorly reflective sedimentary unit which surrounds the bank and can be seen to overlie and unconformably onlap the basement unit (Figure 8.22). The distribution and thickness of the upper unit are shown by isopach contours in Figure 8.23. The upper boundary of this unit is the seafloor, and the lower boundary is the unconformity. Unlike many of the banks, the overlying sediments are not steeply tilted upward where they onlap the basement unit. This fact suggests that the doming which produced the primary uplift and tilting of the basement unit took place prior to deposition of the surrounding sediments.

The dominant sediment at the crest of the western peak (76 m depth) is a coarse, carbonate sand with scattered algal nodules on its surface. This sediment occurs between large coralline algae encrusted reef masses 4 to 6 m high (Figure 8.24). The dominant particle types in this sediment are coralline algae and *Amphistegina*. The depth at that peak is close to the lower limit of the *Gypsina-Lithothamnium* Facies at the West Flower Garden Bank. At Diaphus Bank, both the *Gypsina-Lithothamnium* Facies and the *Amphistegina* Sand Facies occur together. This combination is typical of the transition zone between the two facies at the West Flower Garden Bank.

Alderdice Bank

Alderdice Bank is located at 28°04'40"N latitude and 91°59'36"W longitude (Figure 8.1) in Lease Blocks 170, 171, 178, and 179 of the South Marsh Island Area (Figure 8.25). The bank is an oval, elongate in an east-west direction, and covers an area of about 16 km^2. The top of the bank is relatively flat, with depths ranging from 78 to 82 m. Superimposed upon this broad surface is a smaller scale relief formed by ridges and peaks. The shallowest bank depths (59 m) are two of these peaks. Depth of the seafloor surrounding the bank on the south, west, and northwest sides is about 92 to 94 m, while on the northeast and east sides it is about 84 m. Although the relief is not great along the margins of the bank

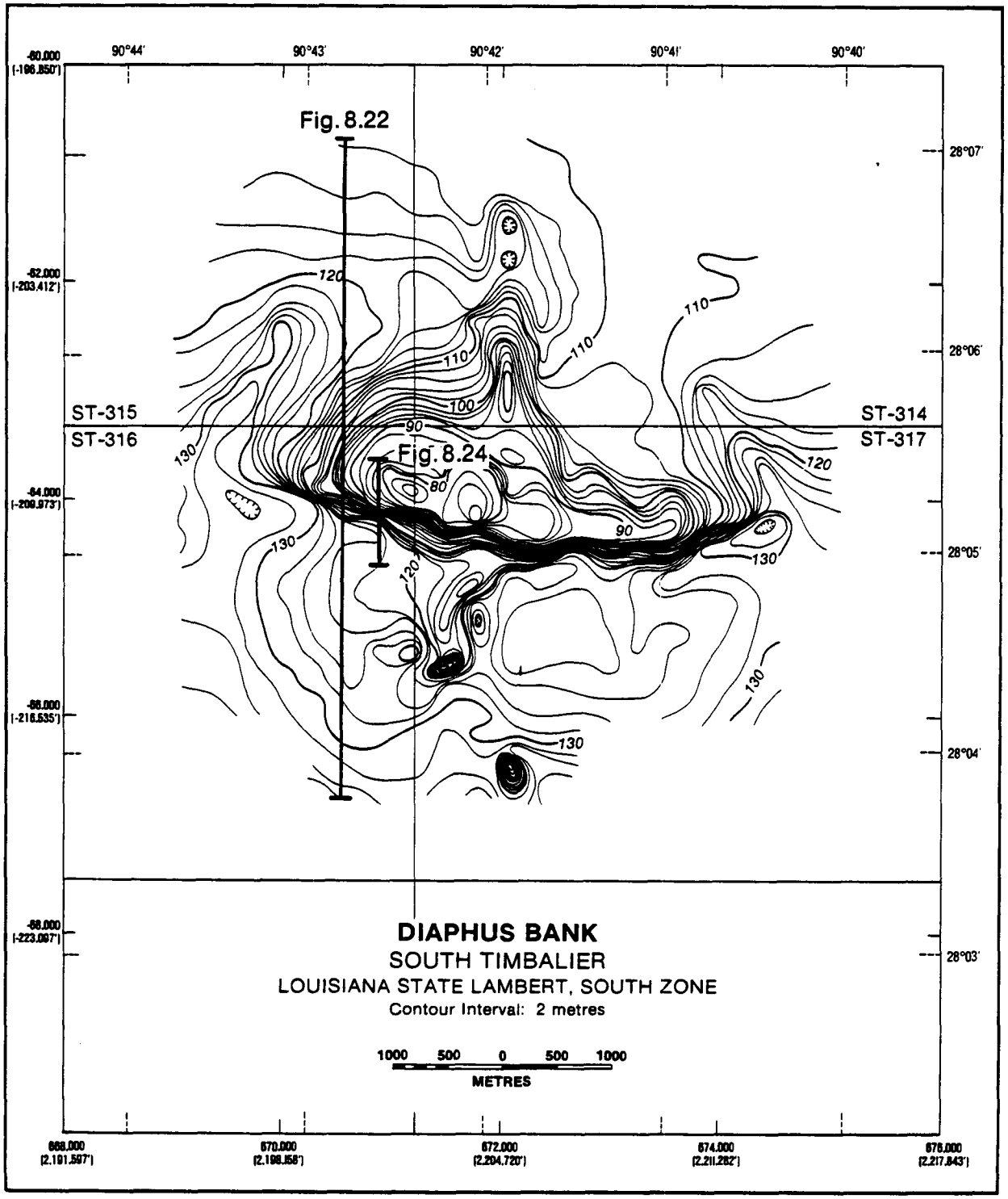

Figure 8.21 Bathymetry at Diaphus Bank, indexing location of boomer profile and side-scan sonar record shown in Figures 8.22 and 8.24.

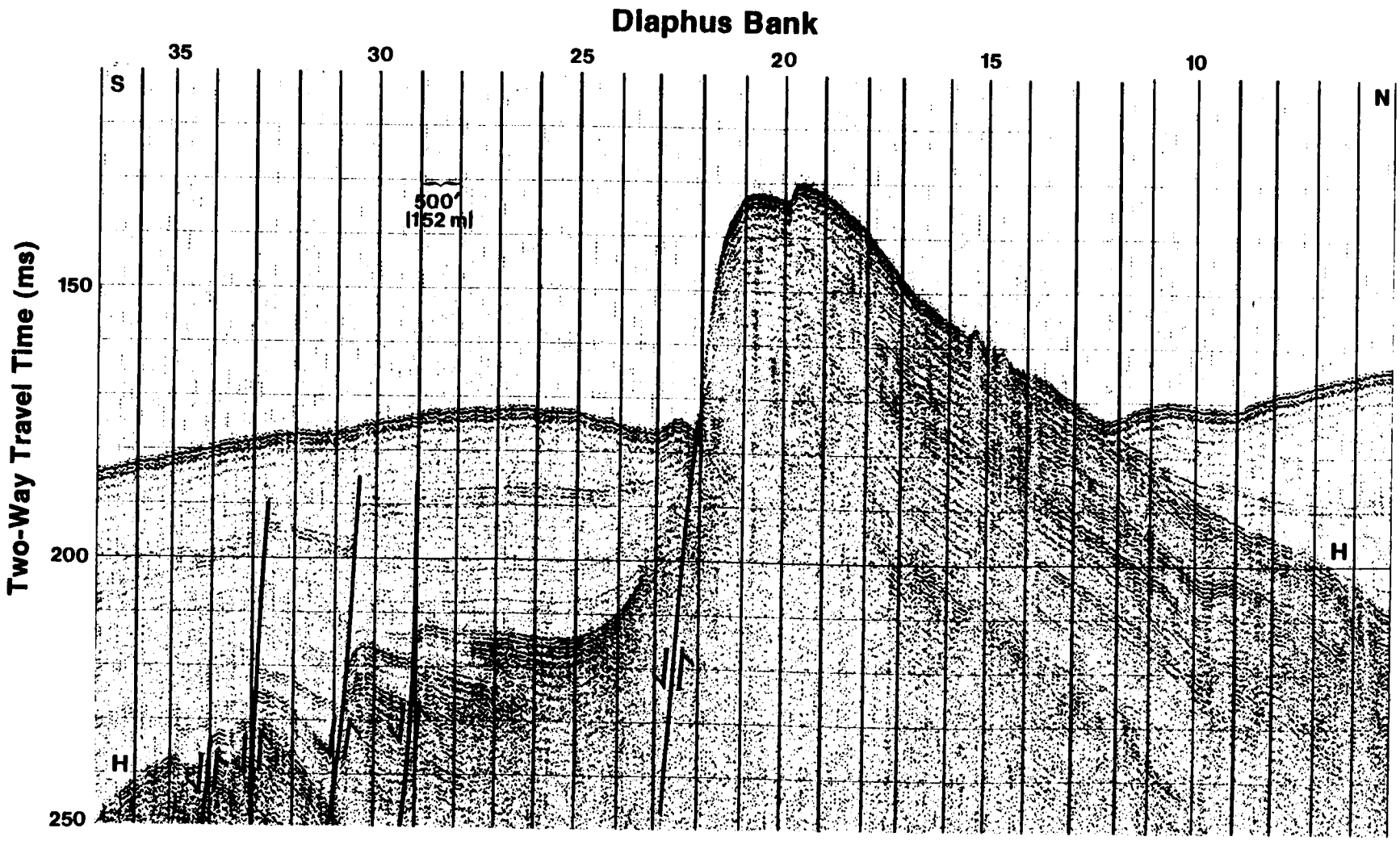

Figure 8.22 North-South boomer profile across Diaphus Bank. Location is indexed in Figure 8.21.

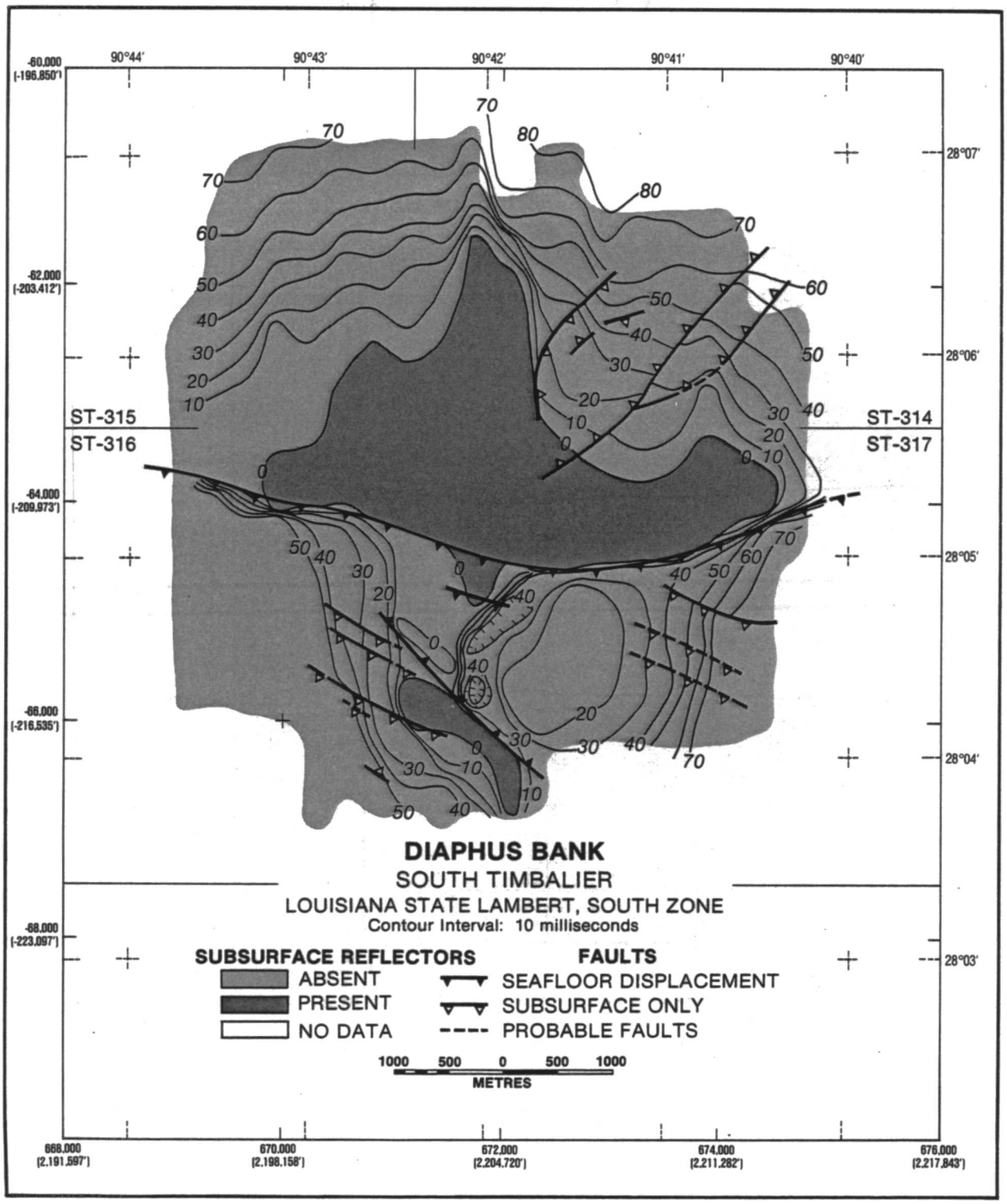

Figure 8.23 Structure/Isopach map of Diaphus Bank. Isopachs indicate the thickness of sediments from the surface to horizon H (see Figure 8.22).

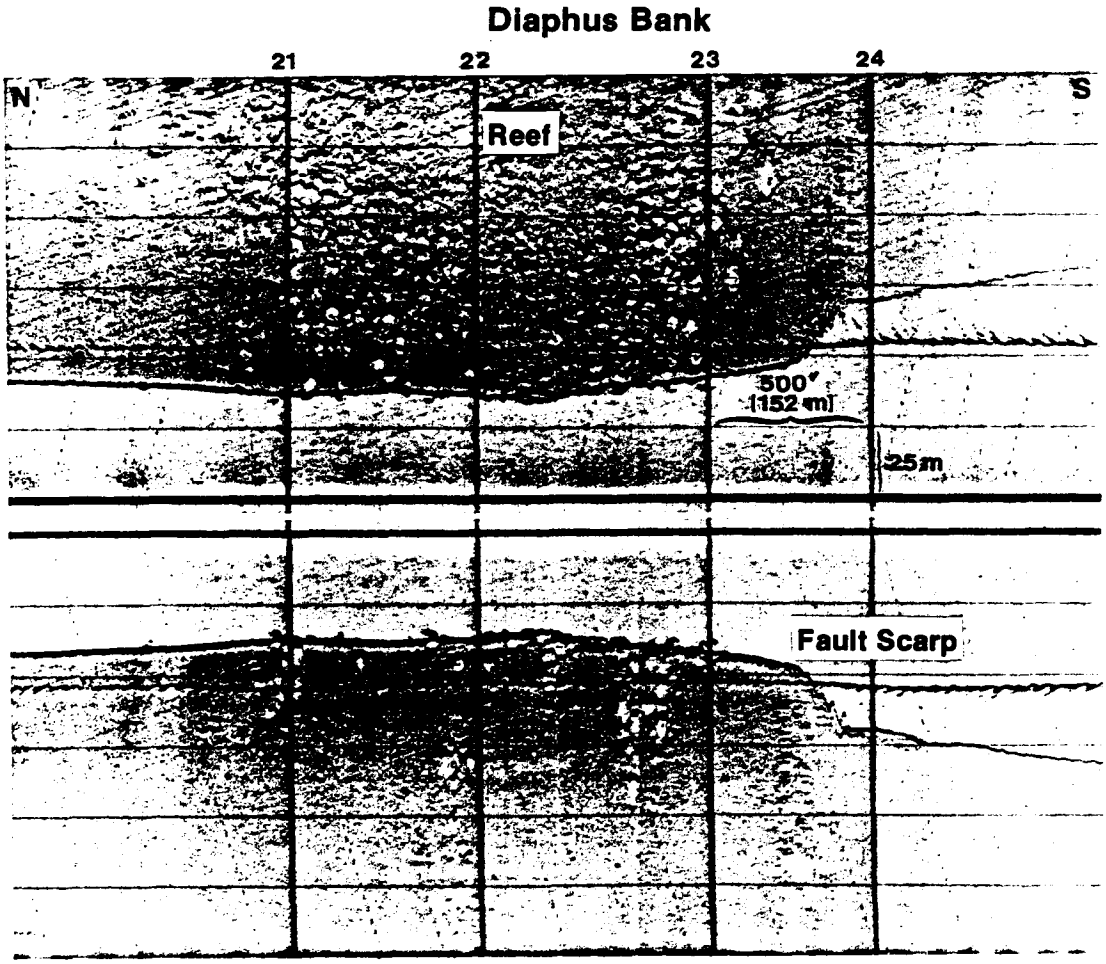

Figure 8.24 Side-Scan sonar record across Diaphus Bank. Location is indexed in Figure 8.21.

(generally less than 10 m), the margins are rather steep around the western half of the bank. The features on top of the western part of the bank have a rather random distribution. However, the eastern part of the bank displays a dominant north-south ridge. There is also a gentle north-south oriented swell on the seafloor extending northward from the eastern part of the bank (Figure 8.25). The gentle depression on the northwest margin of the bank is the head of a north-south oriented valley that curves around the western margin of the bank. This valley was probably eroded during a lower stand of sea level during Late Pleistocene or Early Holocene time.

Structurally, Alderdice Bank is a uniformly uplifted salt dome with a non-reflective core and surrounded by onlapping sediments that are tilted upward along the margins of the bank and are progressively more steeply tilted with depth (Figures 8.26 and 8.27). The main body of the bank has been mapped (Figure 8.28) as non-reflective core, which may be cap rock and salt.

The sequences mapped in Figure 8.28 are: 1) non-reflective core; 2) a reflector on the east end of the bank which has been uplifted with the non-reflective core of the bank and may represent the top of the salt; and 3) the onlapping, more recent sediment around the rest of the bank. Contours in Figure 8.28 represent thickness of the sedimentary sequences down to the deepest reflector that can be interpreted as a sequence boundary. The lower boundaries are marked near the margins of the boomer profiles shown in Figures 8.26 and 8.27.

The surrounding sedimentary sequences, mapped in Figure 8.28 contain two prominent erosional unconformities with clear truncation of bedding reflectors upon which the overlying sediments onlap towards the bank. The base of the mapped sequence is also an unconformity. The presence of the angular unconformities, together with the increasing dips with depth, indicate that the bank has been in the process of uplift over a long period of time including several periods of erosion and subsequent deposition.

Two patterns of faults are present on the bank: 1) the annular fault that encircles the bank; and 2) the radial faults. All show evidence of Recent activity as seen by displacement, such as in Figure 8.27. Along the eastern margin of the bank it appears that the seafloor and sub-bottom structure have opposite displacements along the same faults--and that is actually the case. The central block is a graben that was formed during the last regression of sea level. With renewed sedimentation following the subsequent transgression, the surface relief on this part of the bank was buried. In very recent time, upward movement of salt has reversed the relative movement along these faults and the Recent sediments have been bowed upward over the graben. The directional sense of this movement can be seen where each of the faults intersects the seafloor.

Several seismic profiles and side-scan sonar records show peaks that were suspected of being outcrops of bedrock covered by some thickness of carbonate reef growth (Figures 8.26, 8.29, and 8.30). One such ridge (Figure 8.30) on the southwestern peak of the bank was examined using the submersible DRV DIAPHUS. The ridge is about 100 m long, 24 m high, and 5 m wide at the base, and lies at a depth of about 77 m. It is a massive ledge of nearly bare basalt that strikes 055° and dips about 80° to the south-southeast. Petrographic analysis of the rock indicates that it is an alkalic basalt (Rezak and Tieh, 1980). K-AR age determination of the bulk rock by Geochron Laboratories yielded an age of 76.8 $\pm$ 3.3 m.y. (Senonian). This is the oldest known rock exposed on the continental shelf off Louisiana and Texas.

The feature is interpreted as a dike or sill that has been rafted to the surface by the salt diapir. It has been exposed at the seafloor due to dissolution of the surrounding salt and the subsequent collapse of the adjacent cap rock on either side of the feature. This implies a sizeable root zone still embedded in the salt. Similar features have been observed on Red Sea salt domes in East Africa and in the Zechstein region of Germany. Mounting evidence of Late Mesozoic igneous activity, together with published multi-channel seismic data (Martin, 1978; Humphris, 1978), strongly indicate a rifted origin for the Gulf of Mexico.

Faulting occurs over the entire bank and surrounding seafloor, as evidenced by the discontinuous outcrop patterns on the side-scan sonar record (Figure 8.29 and 8.30) and by displacement of reflectors in the boomer records (Figure 8.27). Evidence for Recent movement along faults may be found in the outcrop of basalt and on boomer records. The basalt outcrop is covered by a rather thin crust of coralline algae, sponges, and bryozoans. If this rock had been exposed at the seafloor since Late Pleistocene time, one would expect more massive encrustations over the bedrock outcrops, such as those on the peak just to the east, and on other banks such as the Flower Gardens. The presence of such thin crusts suggests a relatively short time span for colonization by encrusting organisms.

A diffuse pattern of reflections in the water column over most of the bank, particularly the western half, is probably due to general gas seepage from nearly vertical beds seen on the side-scan records. Specific vents are also evident over the western part of the bank (Figure 8.28). One of these is just to the east of the basalt outcrop.

Submersible observations indicate that below 82 m the sediment is primarily fine mud. The bank sediments above 75 m consist of carbonate sands and gravels that are representative of the *Gypsina-Lithothamnium* Facies and the *Amphistegina* Sand Facies. Below that depth and down to 82 m the sands and gravels are mixed with silt- and clay-sized sediment.

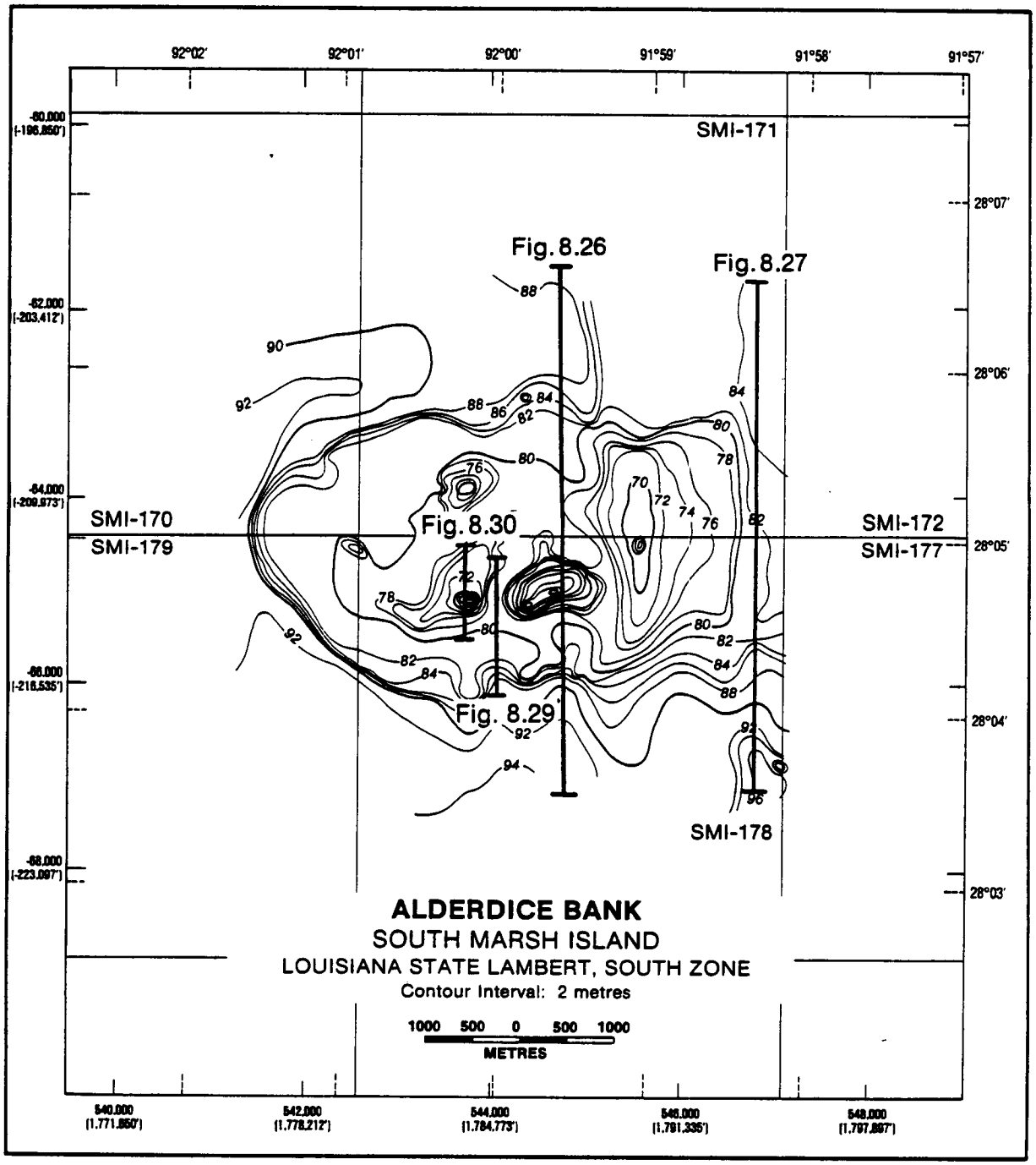

Figure 8.25 Bathymetry of Alderdice Bank, indexing boomer and seismic reflection profiles shown in Figures 8.26 and 8.27, and side-scan sonar records shown in Figures 8.29 and 8.30.

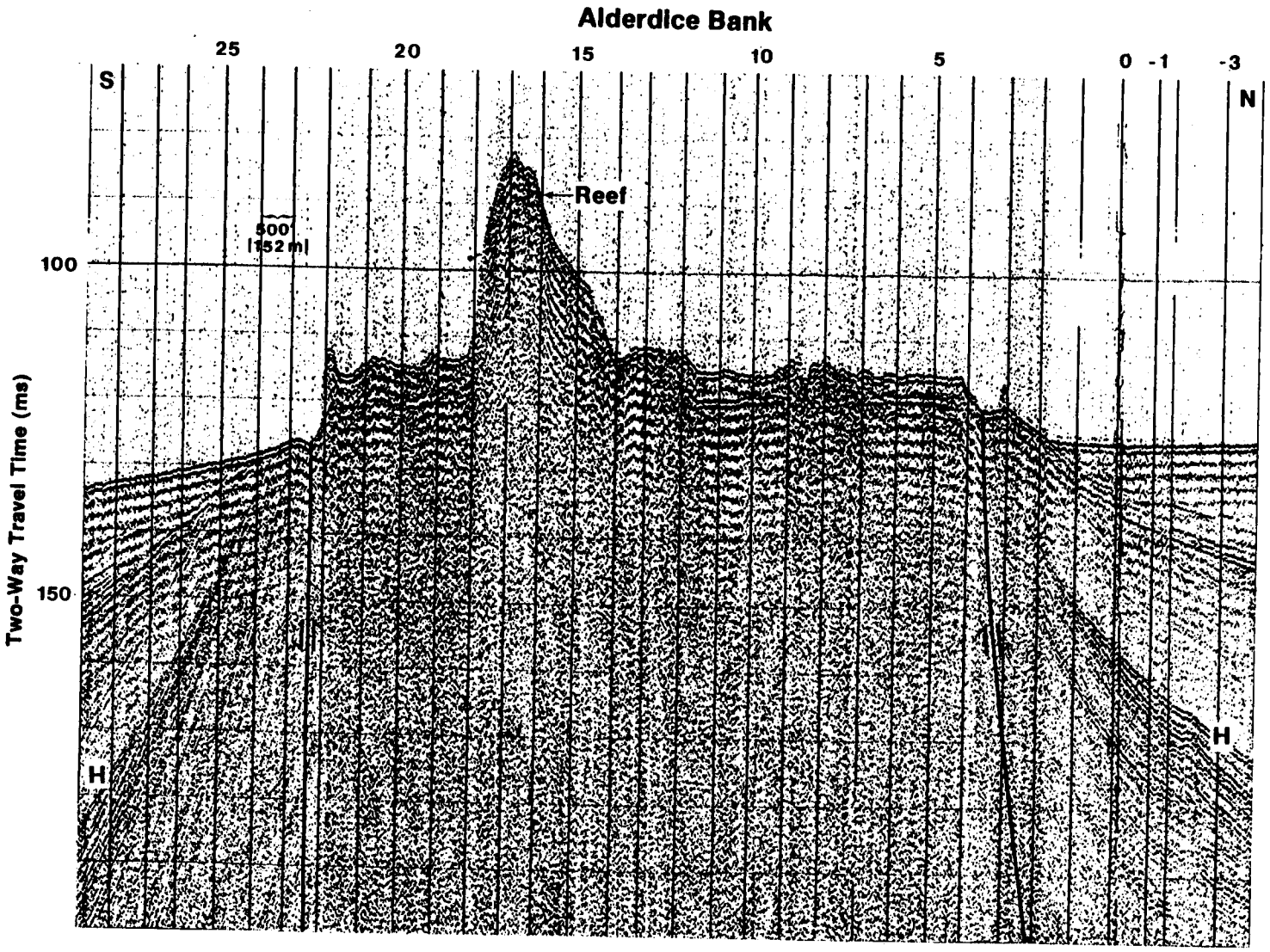

Figure 8.26 North-South boomer profile across the main peak at Alderdice Bank (see Figure 8.25 for location).

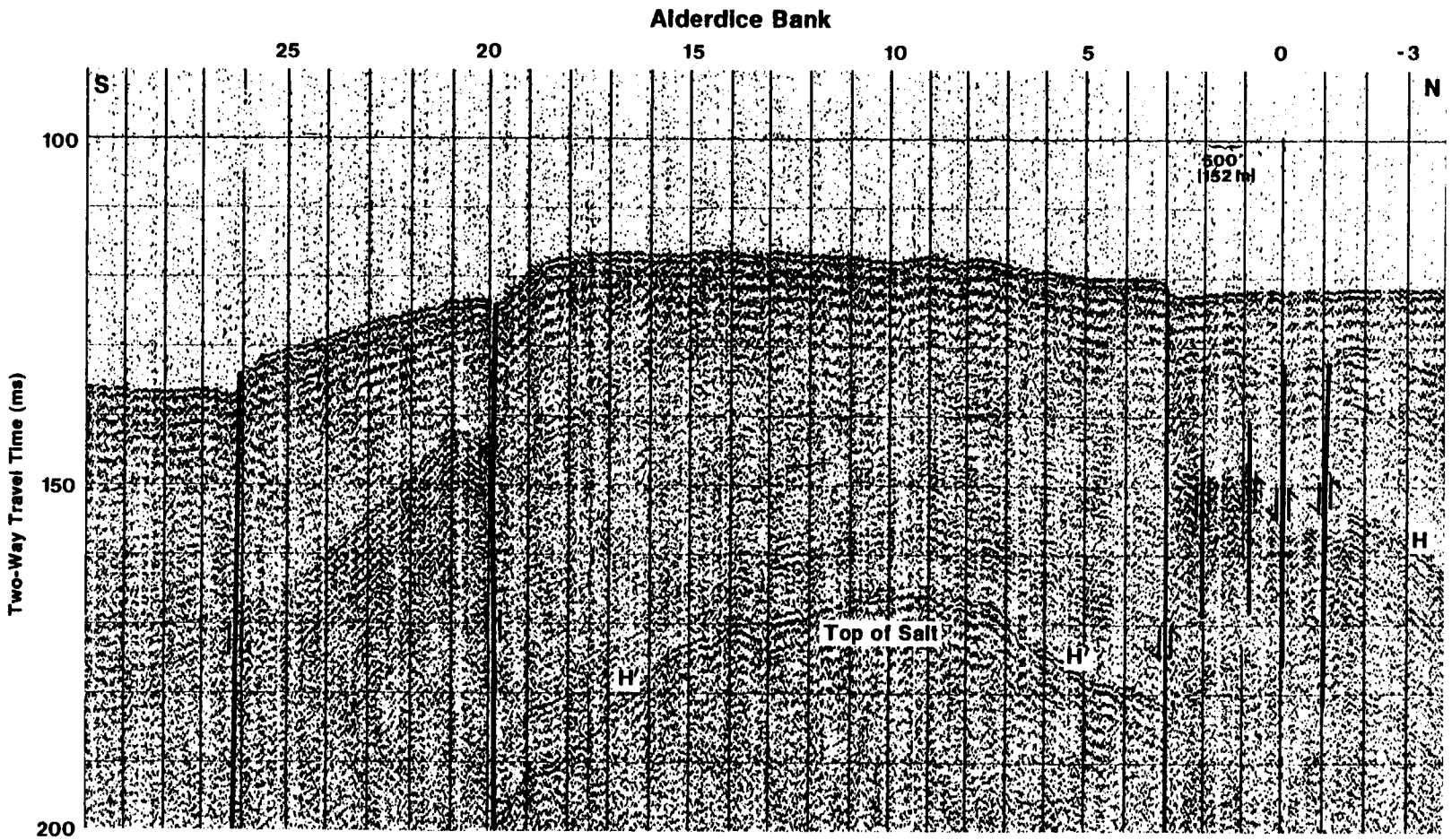

Figure 8.27 North-South profile across the east side of Alderdice Bank showing renewed uplift of salt. H represents the base of the upper sedimentary sequence; H' is the base of the lower sedimentary sequence.

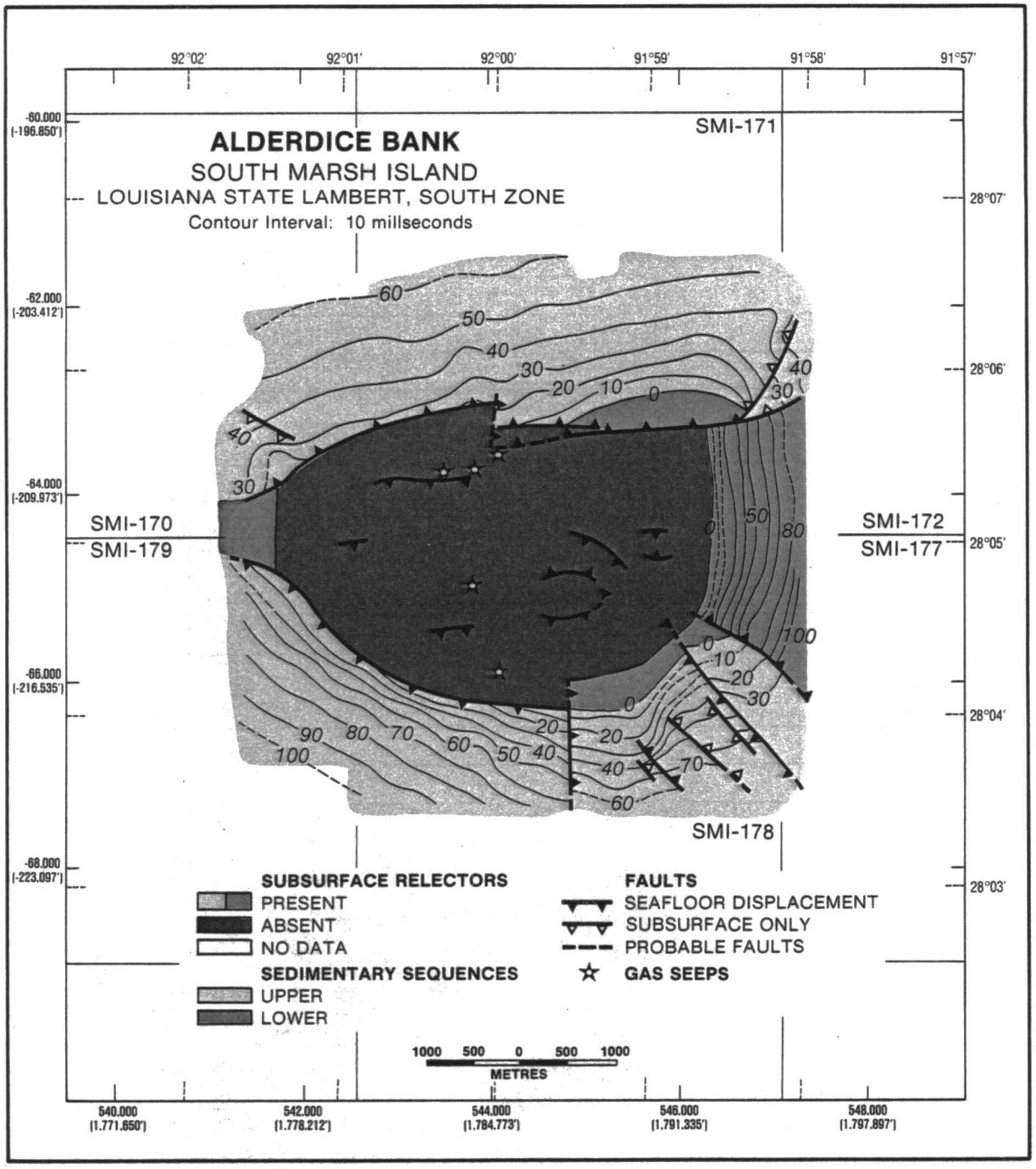

Figure 8.28 Structure/Isopach map of Alderdice Bank. Isopachs are thickness of sediment from the surface to horizons H and H' (Figure 8.27).

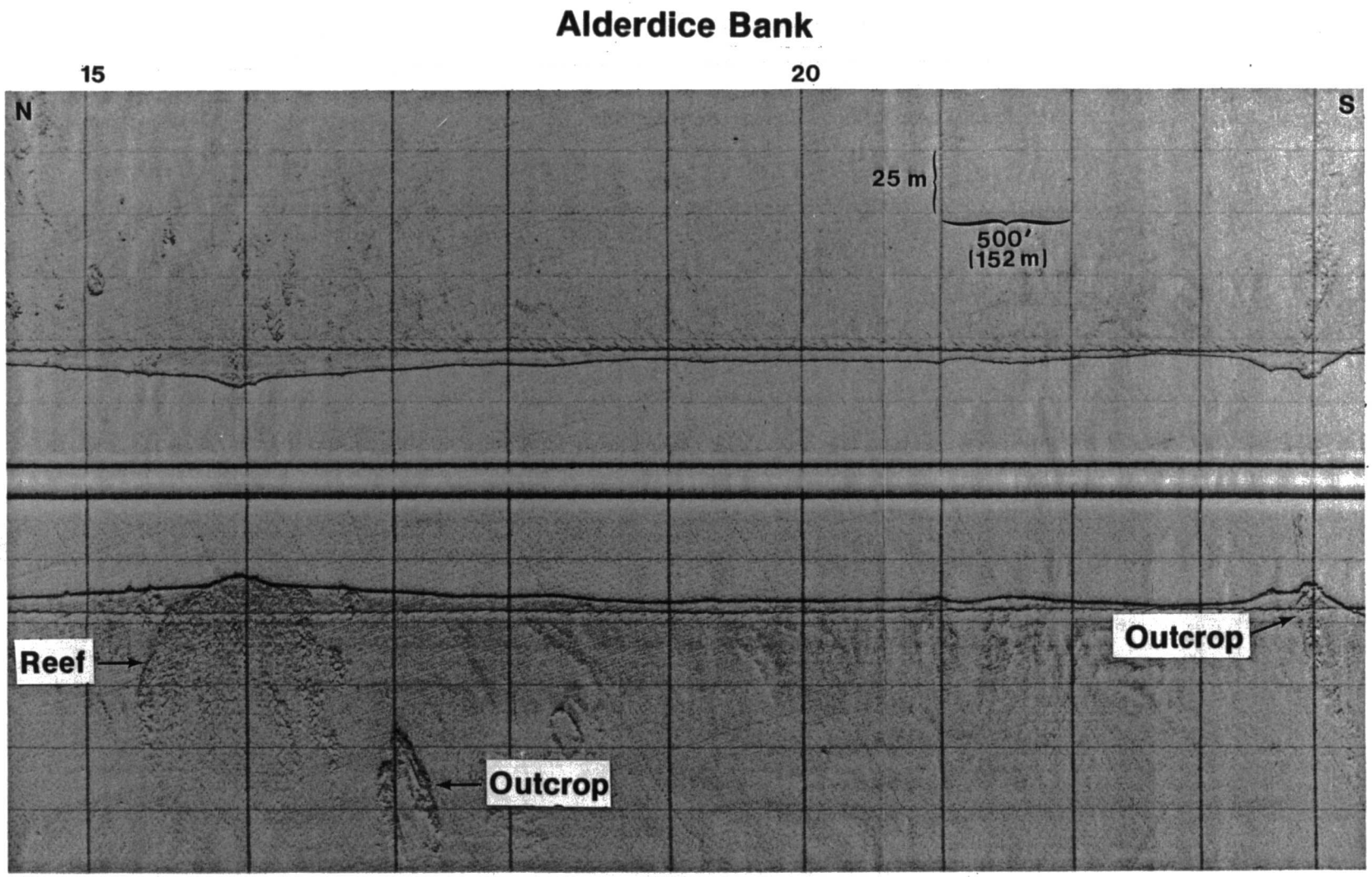

Figure 8.29 Side-Scan sonar record across outcrops and reefs at Alderdice Bank (see Figure 8.25 for location).

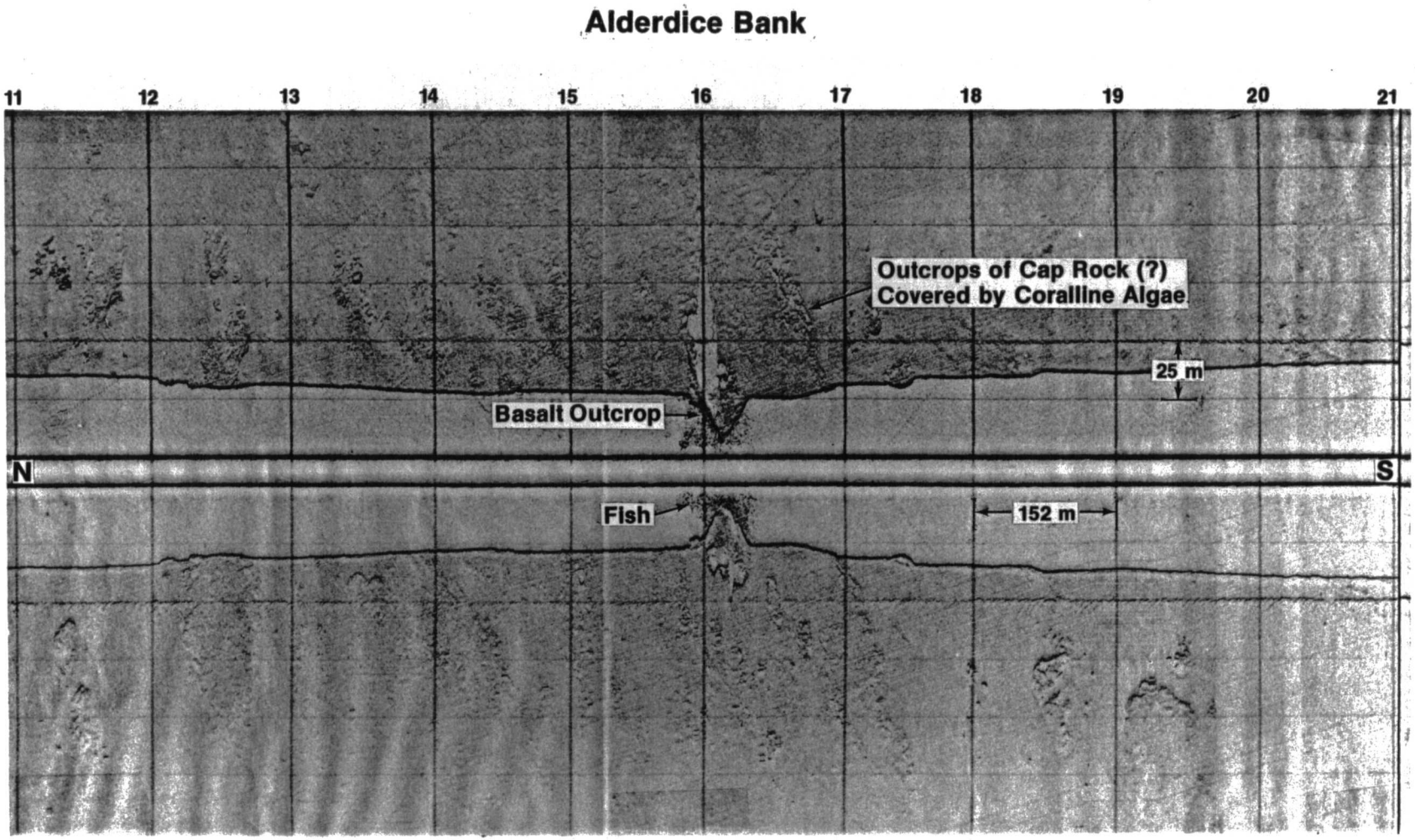

Figure 8.30 Side-Scan sonar record across basalt outcrop at Alderdice Bank.

Sackett Bank

Sackett Bank is located at 28°38'01" latitude and 89°33'22"W longitude (Figure 8.1) in Lease Block 148 of the West Delta Area (Figure 8.31). It lies close to the shelf edge and is about 12 miles east of the Mississippi Canyon. The bank is nearly circular and covers an area of 7.07 km^2. The crest of the bank is broad and relatively flat at a depth of 63 m. The base of the bank lies at a depth of about 100 m.

Structurally, the bank is a nearly symmetrical diapir with a non-reflective core and well stratified and faulted upturned beds on its flanks (Figure 8.32 and 8.33). The boomer profile (Figure 8.32) shows very hazy reflectors in the subsurface which are evidence for gas-charged sediments. Figure 8.32 also shows two active gas seeps in the core of the bank. Figure 8.33 shows gassy zones on the north side of the bank and a gas seep on the south side of the core of the bank. The fault patterns on Sackett are mostly oriented in a near east-west direction except for the southwest flank of the bank where they are oriented northwest-southeast (Figure 8.34). Most of the faults do not displace the seafloor, indicating that Sackett is relatively stable.

Above 65 m depth the bottom sediment is predominantly sandy, with scattered algal nodules. Scattered about on this upper terrace are drowned patch reefs and pinnacles up to 3 m high and 12 m across. Limited amounts of living coralline algae occur on the patch reefs, tops of nodules, and pieces of rubble. The substrate of the 67 to 73 m terrace is basically a carbonate rubble strewn sandy bottom with significant amounts of silt and clay.

At about 72 m depth a small outcrop of siltstone or claystone was encountered, similar in appearance to the rocks at Stetson and Sonnier Banks. The presence of bored and relatively unencrusted bedrocks at Sackett does not imply recent exposure, as the carbonate productivity at Sackett has been severely retarded due to the turbid conditions in this area owing to the outflow of the Mississippi River. Below a depth of 82 m the sediment is primarily silt and clay. In September 1977, when Sackett was explored with the submersible, the top of the nepheloid layer was roughly coincident with the break in slope at 72 to 74 m depth. This accounts for the increased mud content of the sediment with increasing depth.

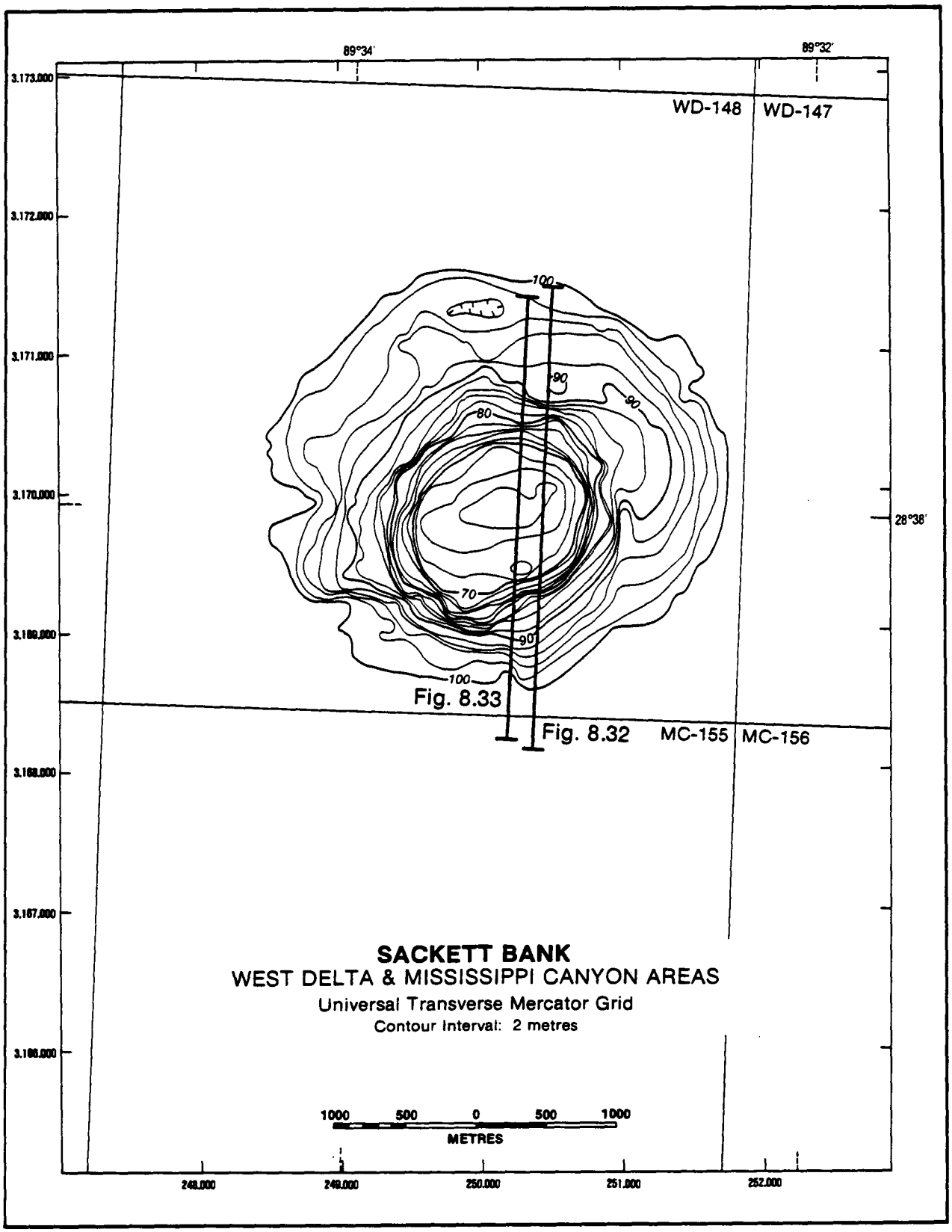

Figure 8.31 Bathymetry of Sackett Bank, indexing location of boomer profiles and side-scan sonar records shown in Figures 8.32 to 8.33.

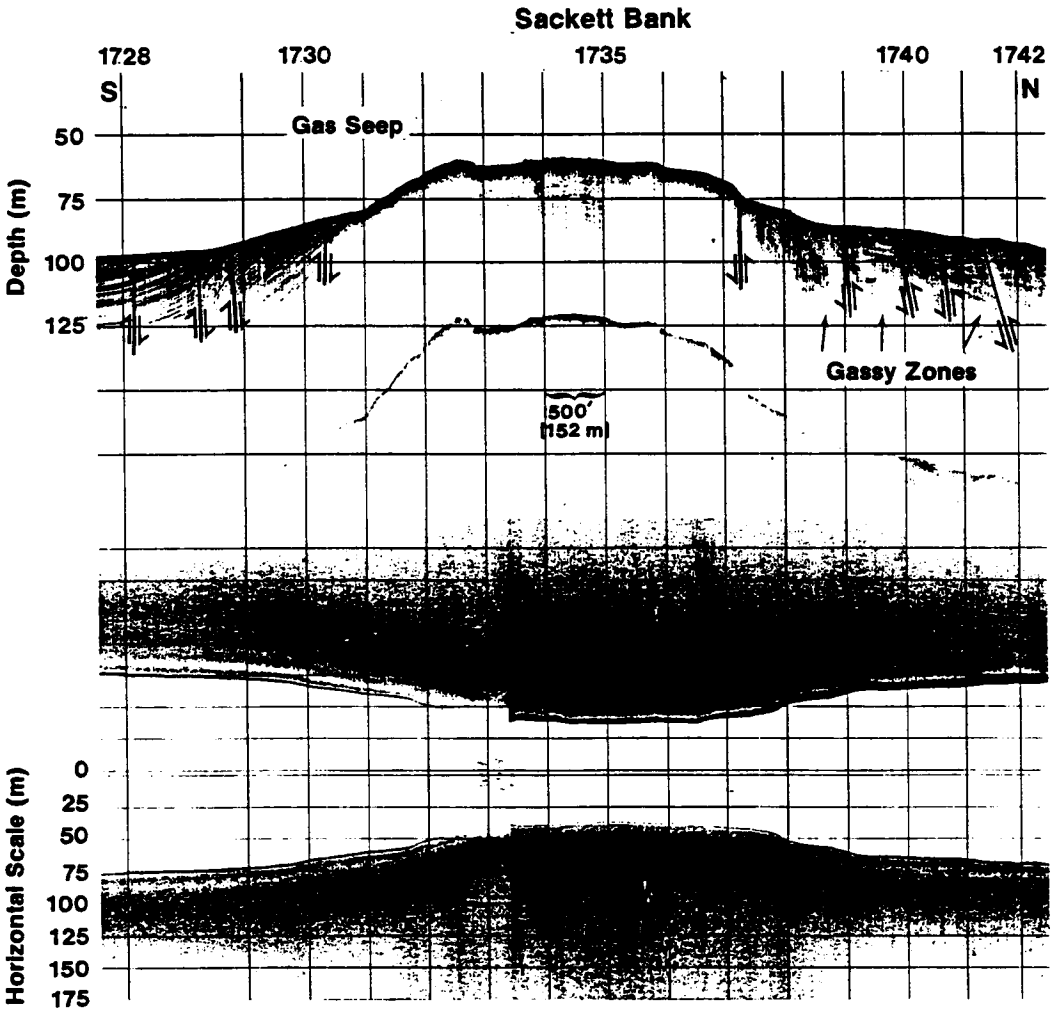

Figure 8.32 Boomer seismic profile across Sackett Bank (see Figure 8.31 for location).

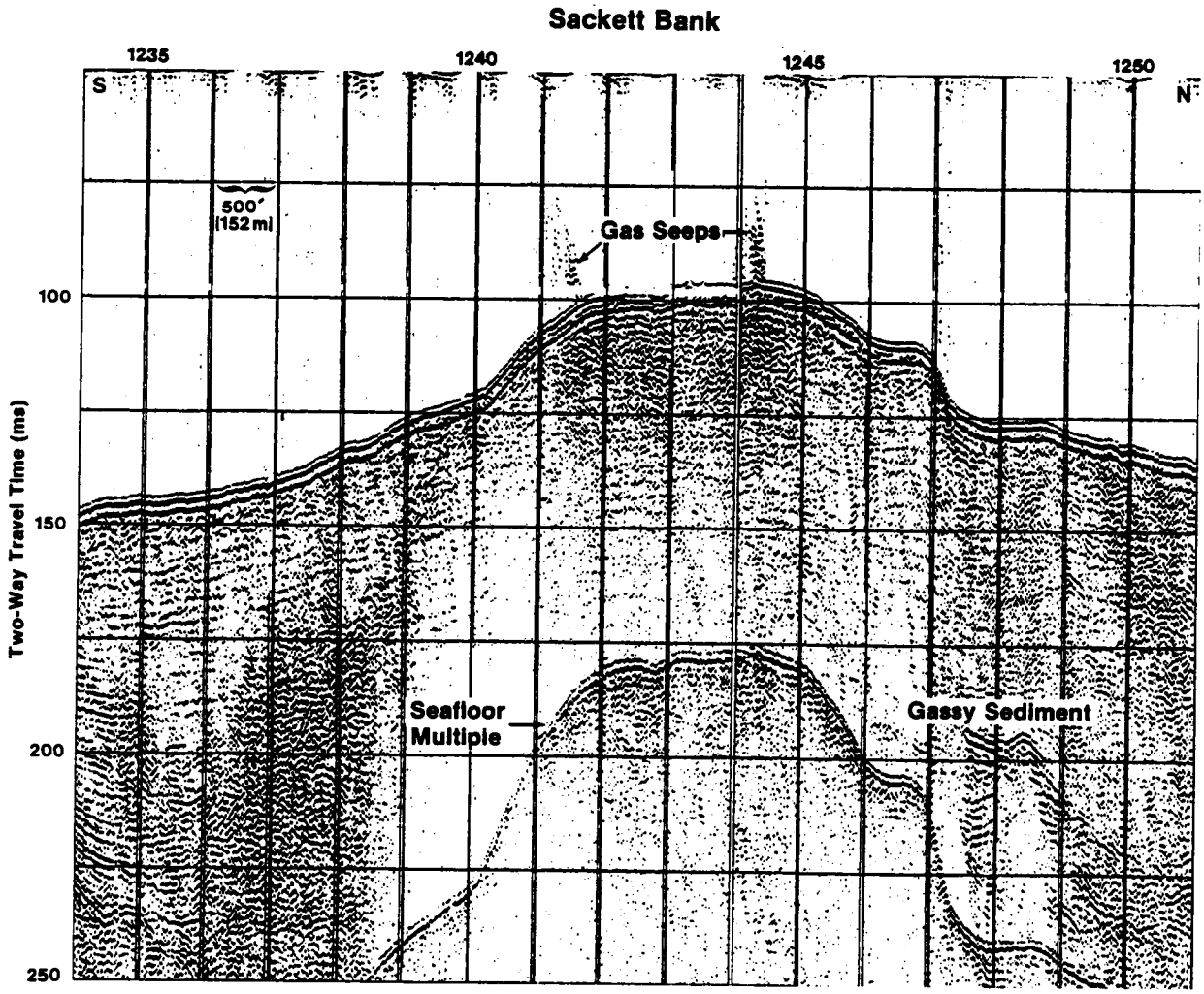

Figure 8.33 A 7 kHz profile and side-scan sonar record across Sackett Bank (see Figure 8.31 for location).

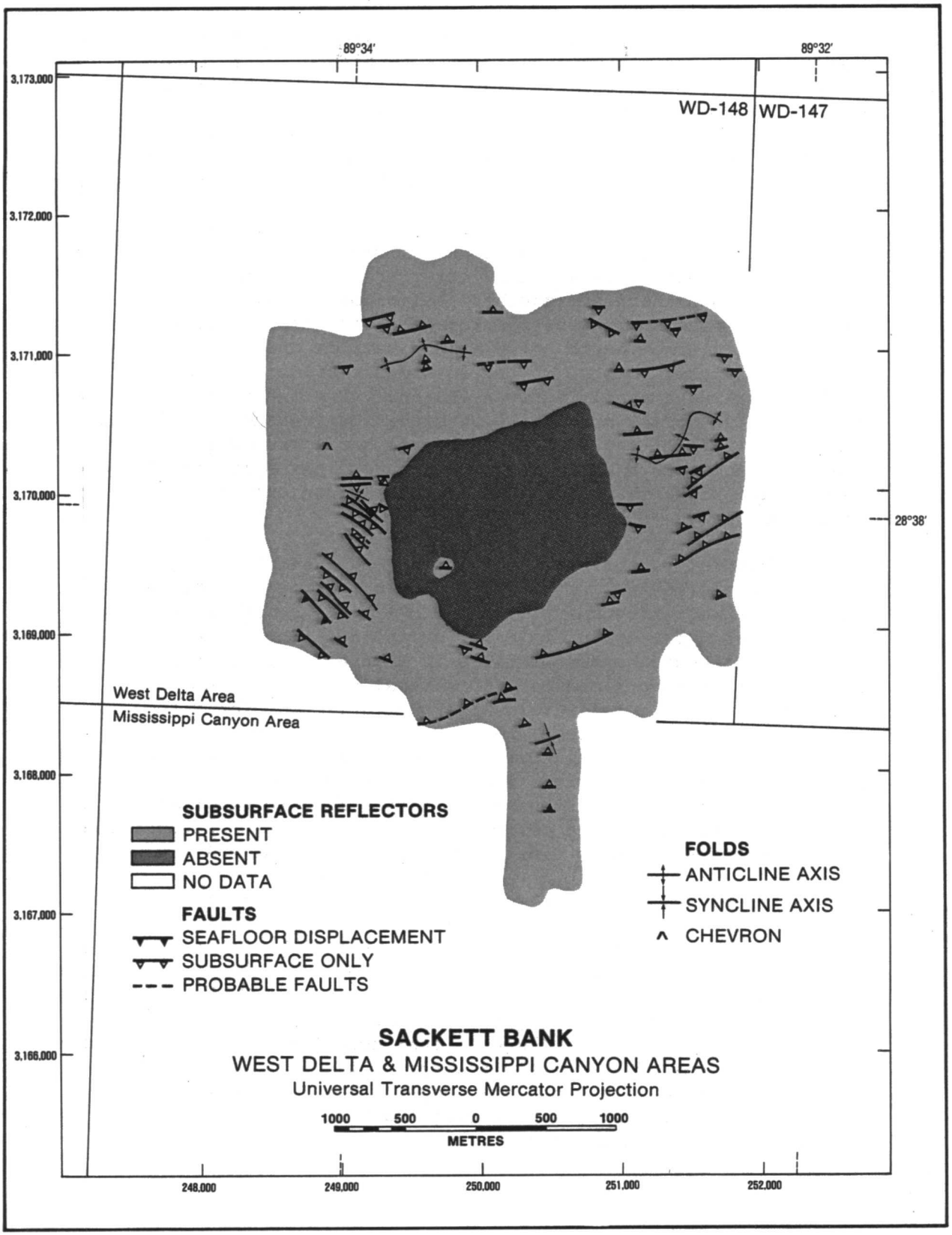

Figure 8.34 Structure map of Sackett Bank.

Rezak-Sidner Bank

Rezak and Sidner Banks are described as a single unit because they are parts of a single geological structure. The center of the structure that forms the two banks is located at 27°57'N latitude and 92°23'W longitude (Figure 8.1) in Lease Blocks 404, 405, 411, and 412 of the Vermilion Area (Figure 8.35). The Rezak-Sidner structure is rectangular in shape and covers an area of 78 km^2. It is bounded by steep slopes on the north, east, and south sides, with a more gentle slope to the west (Figure 8.35). Local depressions are abundant at the base of the northern, eastern, and southern slopes. The eastern slope has very irregular and complex relief. Although it is a single structural unit, the bank can be divided into northern and southern halves on the basis of bathymetry. The shallowest portion of the northern half (Rezak Bank) has a minimum depth of 60 m on a peak at the northeast corner of the structure. Depths of the adjacent seafloor around the northern half are mostly between 120 and 140 m on the north and east sides, and 98 to 110 m on the west side. The northern half is about twice the width of the southern half and has a very gentle slope to the west (about 10 m/km). The southern half has a minimum depth of 55 m on the ridge that forms the eastern margin and has surrounding depths of 140 to 180 m.

Structurally, the bank is a tilted fault block of well stratified sedimentary rock that has been uplifted on the east and dips to the west (Figures 8.36 and 8.37). It is bounded by steeply dipping normal faults on its east, north, and south sides. As seen in the north-south boomer profiles in Figure 8.36, the shallow structure of the bank consists of several seismic sequences separated by strong reflectors interpreted as unconformities. The stratification in each sequence is represented by weak yet recognizable reflections. Care must be taken not to confuse the bedding reflections with the strong ringing of the seismic source. Despite the troublesome ringing, it is possible to see reflection termination patterns that define erosional truncation, depositional onlap, and truncation by faulting (Figures 8.36 and 8.37).

Seafloor relief on the top of the bank is due to faulting, erosion, and, to a lesser extent, carbonate reef growth. The reflectors within the fault block are truncated by faulting on the north and south sides of the bank. The saddle in the middle of the bank appears to be both a structural and erosional feature. A large part of the upper seismic sequence has been removed by erosion (Figures 8.37 and 8.38). The erosional unconformities, the surface erosion, and the progressively greater tilt of the individual seismic sequences with depth all suggest that this bank has experienced several stages of uplift and tilting during a period of several rises and falls of sea level.

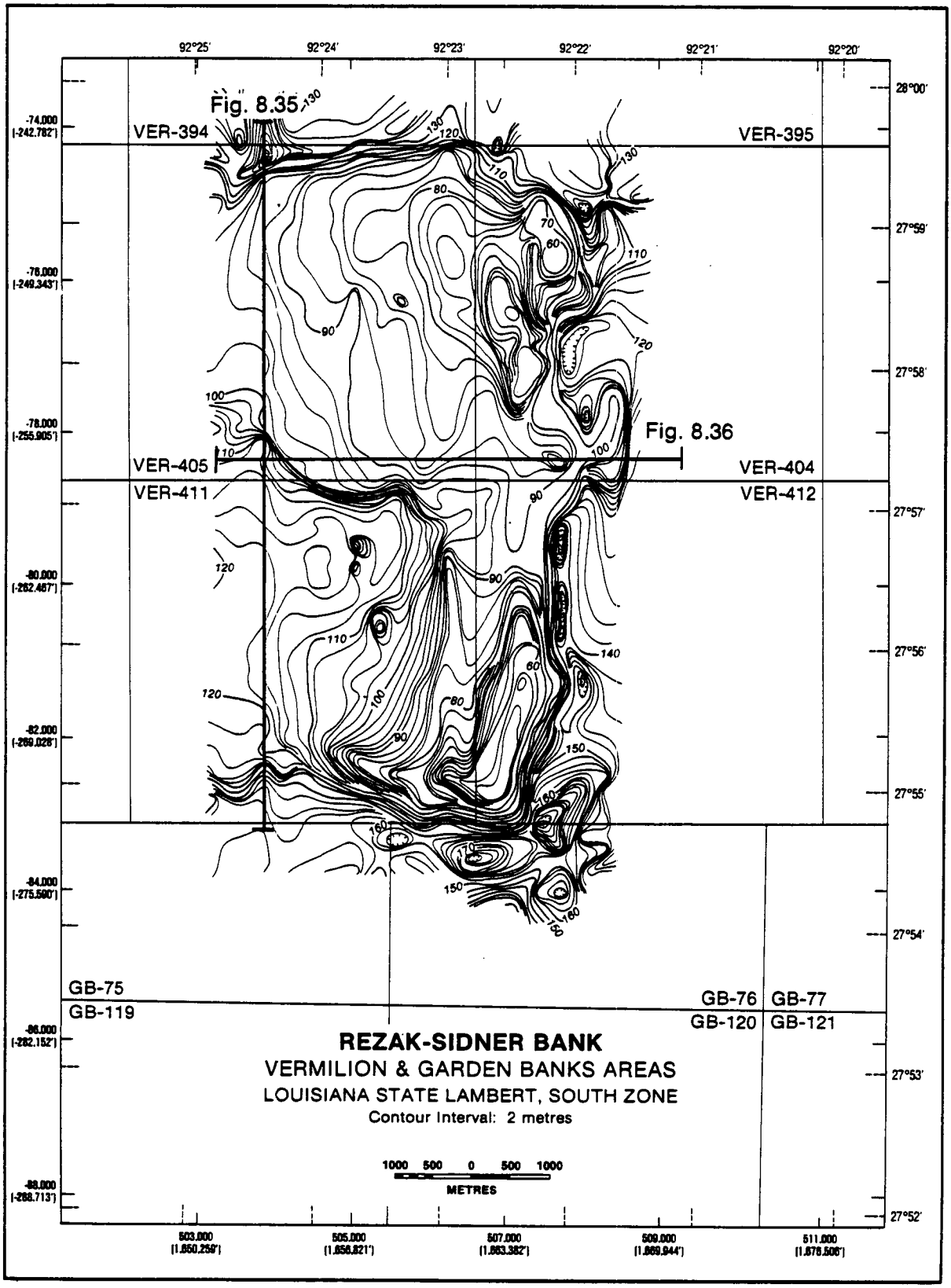

Figure 8.35 Bathymetry at Rezak-Sidner Bank, indexing location of boomer profiles shown in Figures 8.36 and 8.37.

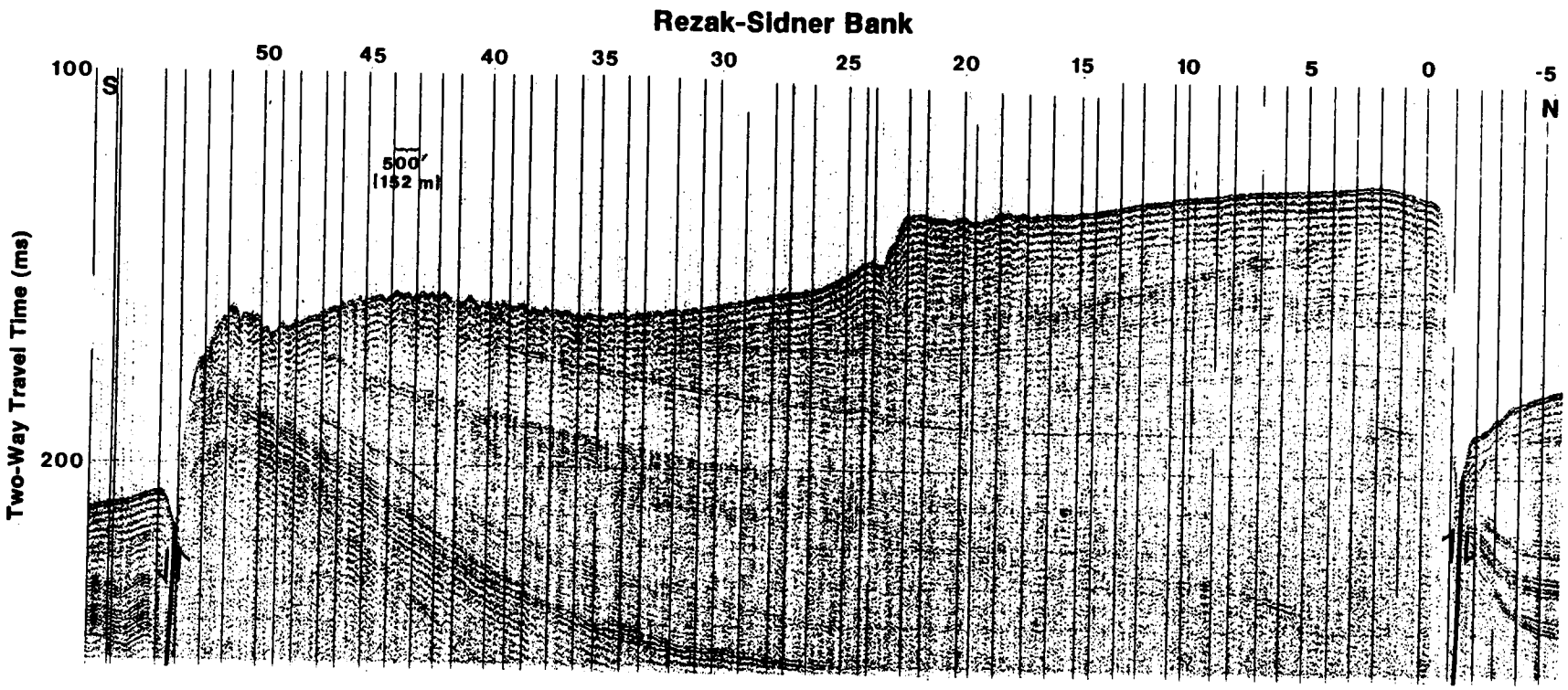

Figure 8.36 North-South boomer profile across Rezak-Sidner Bank (see Figure 8.35 for location).

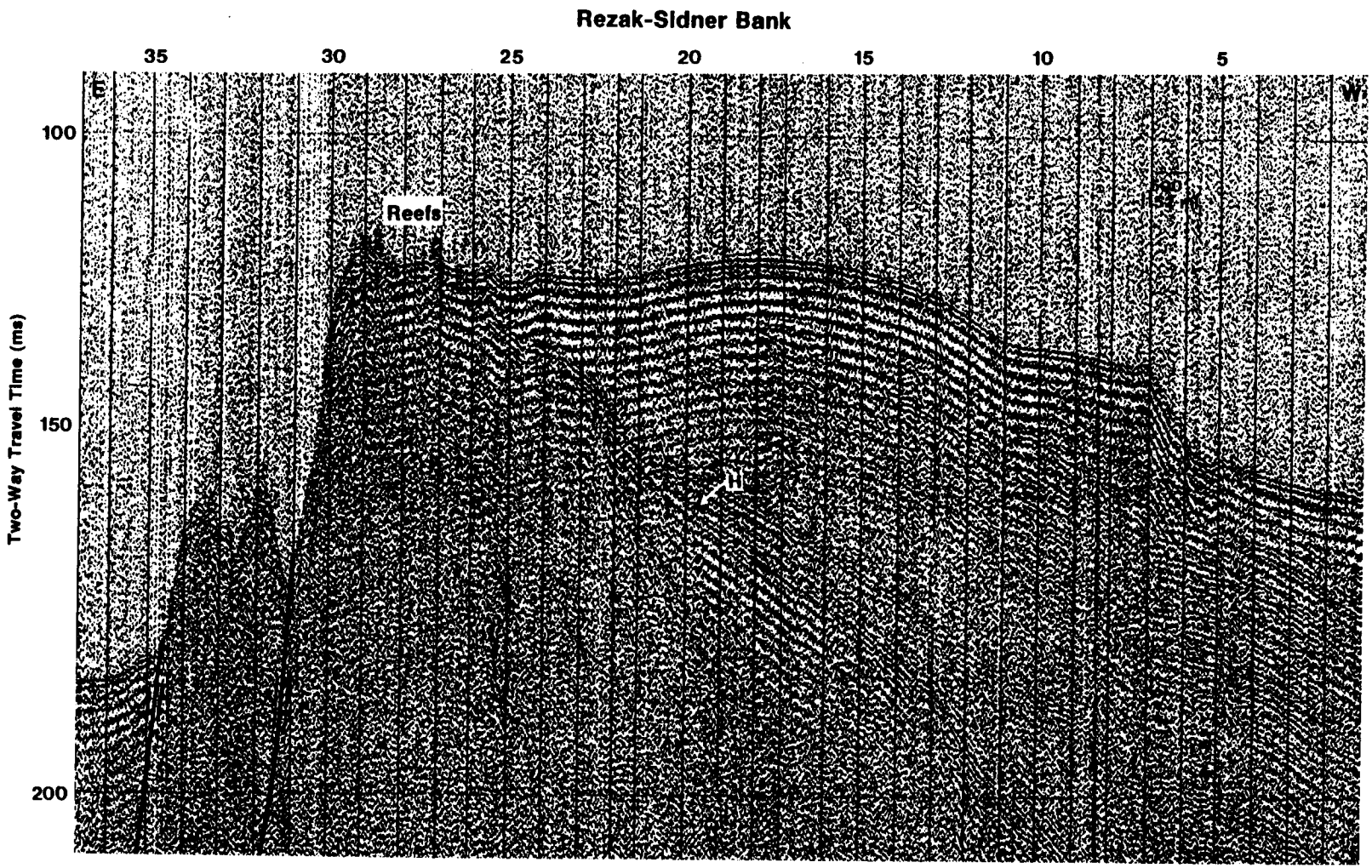

Figure 8.37 East-West boomer profile across Rezak-Sidner Bank (location indexed in Figure 8.35).

Faulting has been active in Recent time as evidenced by the numerous faults that displace the seafloor along the margins of the bank. Faults are not common within the main body of the bank, but two normal faults control the topography of the saddle in the middle of the bank.

One apparent gas vent exists in the southwest corner of the bank (Figure 8.38) and another was observed during a submersible dive at a depth of 69 m just south of the 62 m peak in the southwest part of Lease Block 404.

Submersible observations indicate that the dominant sediments on the top of the bank are coralline algae nodules and a coarse carbonate sand. These sediments are equivalent to the *Gypsina-Lithothamnium* Facies and the *Amphistegina* Sand Facies at the Flower Garden Banks.

Summary of Structural Geology

The complexity and variety of structural style in the banks described here and in Chapter 4 are due to a number of factors. The most important of these factors are: 1) the regional stress field; 2) the shape of the dome (circular or elliptical); and 3) structures inherited from Late Triassic to Early Jurassic tectonics.

The influences of outline shape and regional strain on salt dome fault patterns have been amply demonstrated by Withjack and Scheiner (1982), using both experimental and analytical models. They found that circular domes in the absence of regional stresses developed radial fault patterns such as we have observed at Fishnet Bank (Figure 8.11) and possibly Sonnier and Sackett Banks. With regional extension, most normal faults on the crests of circular domes trend in a direction perpendicular to the direction of regional extension. Diaphus Bank (Figures 8.22 and 8.23) is a good example of this kind of fracture pattern. Diaphus lies close to the shelf edge. The major fault on the bank parallels the shelf edge.

With regional compression during doming, most normal faults on the crests and flanks of circular domes strike parallel with the regional compression direction. Strike slip faults that trend 30° from the regional compression direction may form on the flanks. Thrust faults that strike approximately perpendicular to the regional compression may develop on the peripheries. None of the salt domes that we have mapped shows evidence of regional compression. This is most likely due to the location of our study area on the middle and outer continental shelf, where regional compressive stresses are absent. Regional compressive stresses are more apt to be found on the middle to lower continental slope.

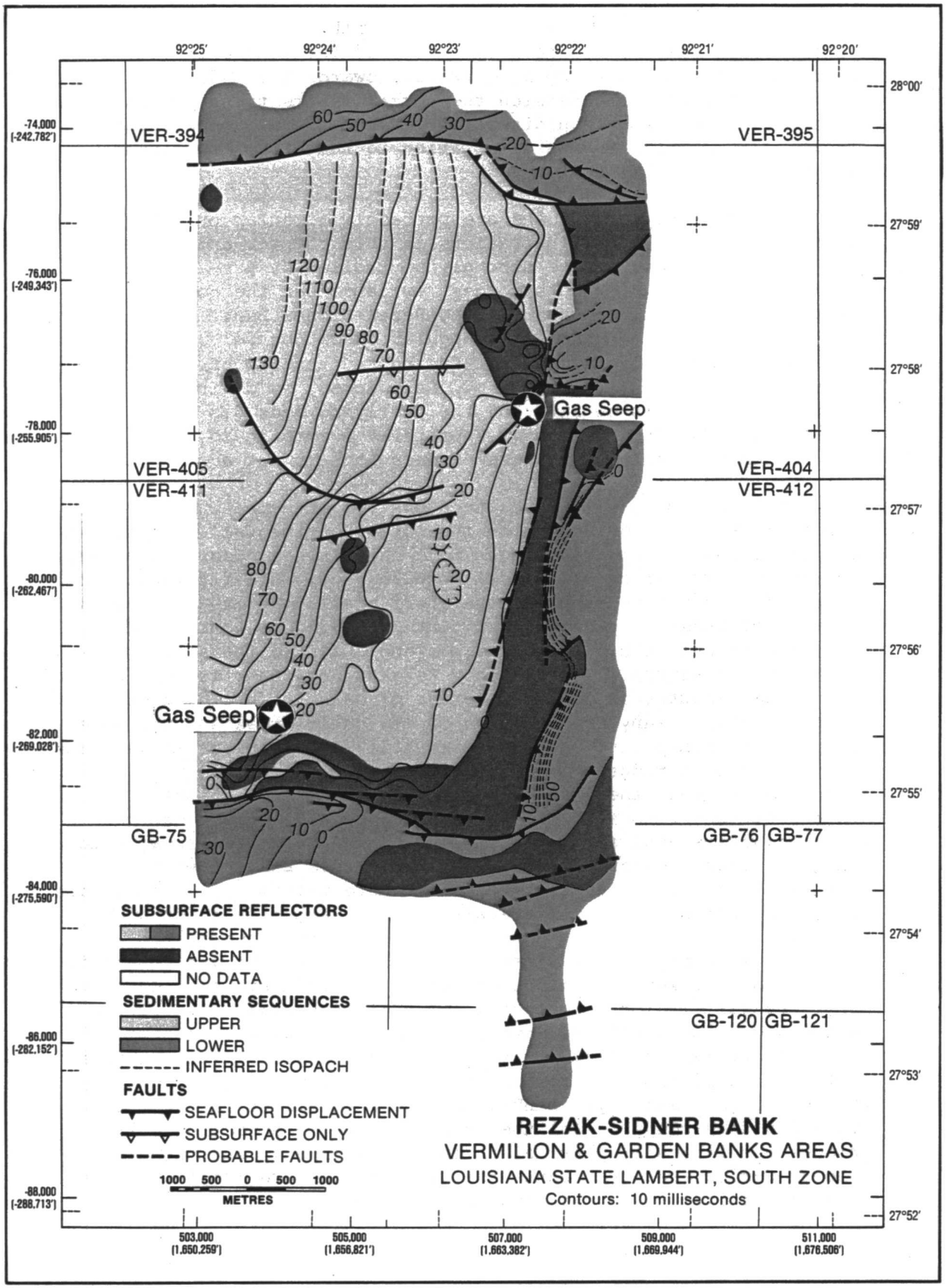

Figure 8.38 Structure/Isopach map of Rezak-Sidner Bank. Isopachs indicate thickness of sediment from the surface to horizon H shown in Figure 8.37.

With elliptical domes not involved with external stresses, the pattern of normal faults roughly parallels the long axis of the ellipse, but the faults splay outwards towards the ends of the long axis. With regional extension the normal faults trend perpendicular to the regional extension direction. For regional compression, the faulting is similar in its orientation to that found in circular banks.

Unfortunately, few domes are perfectly circular or elliptical, as can be seen in the illustrations in this chapter and Chapter 4. The shapes of domes may be strongly controlled by pre-existing regional structures. The strongest evidence for the control of shape by pre-existing structures is Rezak-Sidner Bank. The structure of that bank is a rectangular block bounded by normal faults on three sides. The east-facing fault scarp of the bank has a displacement of at least 130 m. Salt domes, by definition, are roughly circular in outline and the overlying beds dip in all directions away from a point. Therefore, according to the definition of a salt dome, Rezak-Sidner Bank is not a salt dome.

If it is not a salt dome, then what is it? The only tectonic processes known to be active on the Outer Continental Shelf are salt diapirism and gravity faulting. Salt diapirs, as described above, should be circular or elliptical in plan view. Gravity faults are linear features that parallel the shelf break. Rezak-Sidner Bank is neither of these. The major fault at Rezak-Sidner Bank trends north-south and is approximately perpendicular to the shelf break. Trippett and Berryhill (1982) show Rezak-Sidner Bank to be a part of a northwest-southeast trending series of banks formed by a ridge of salt at depth. Many of the banks on the shelf break and the upper slope on this map (Trippett and Berryhill, 1982) appear to be parts of complex salt ridges with arcuate patterns. Figure 4.4 demonstrates that the East Flower Garden is located at the intersection of two salt ridges, and Figure 4.10 shows that the non-reflective area at the West Flower Garden Bank is linear rather than circular. Geyer (Figure 8.19) and Elvers Banks (Rezak and Bright, 1981a) are also situated on arcuate bathymetric prominences. Their non-reflective cores are also linear rather than circular. The linearity of these cores must be due to the presence of pre-intrusion zones of weakness along which the salt was intruded. These zones of weakness might be joints or fault systems inherited from pre salt tectonic features. Many of the banks on the upper slope and outer shelf are complicated due to regional extension. Parallel normal faulting, oriented at right angles to the regional extension direction, is common on the East Flower Garden, West Flower Garden, and Geyer Banks. At the East Flower Garden the faulting does not parallel the crests of the intersecting salt ridges but is nearly parallel to the shelf break. At the West Flower Garden and Geyer Banks the faulting is more complex. Some faults parallel the shelf break and some parallel the salt ridge crest.

Consequently, the patterns of faulting will vary depending upon the developmental history of a salt diapir. Those diapirs that are not associated with pre-injection tectonic features will be circular or elliptical in plan view. Those that are associated with pre-injection tectonic features will assume the pattern of those features. These two forms are extreme end members in a spectrum of structural styles that lies between them. These styles are controlled by the history of changes in the regional stress field at a given location on the shelf or slope.

Biology

Fundamentals of biotic zonation on shelf-edge carbonate banks and reefs were presented in Chapter 6, describing the East and West Flower Garden Banks. The Flower Gardens differ from the other banks insofar as they alone possess relatively shallow (15 to 36 m) high diversity coral reefs (*Diploria-Montastrea-Porites* Zone). Lower diversity coral reefs occur at the Flower Garden Banks (*Stephanocoenia-Millepora* Zone) and also on 18 Fathom Bank (*Stephanocoenia-Montastrea-Agaricia* Zone) and Bright Banks between 36 and 52 m depth (Table 8.1). The heartier corals of this zone (*Stephanocoenia michelinii* and *Millepora alcicornis*) have been observed on many of the other banks, and probably occur on most.

In terms of amount of substratum occupied, however, the Algal-Sponge Zone assemblage is the most important clear-water community on shelf-edge banks. Its presence is indicative of year-round tropical-subtropical oceanic conditions. Its lateral and vertical distribution and apparent diversity and abundance provide important clues to the degree to which the warm, clear oceanic water mass which facilitates its development is modified by more turbid, less saline, and seasonally cooler neritic waters. All of the shelf-edge banks possess transitional zones (roughly equivalent to the Antipatharian Zone of the South Texas midshelf banks) which grade downward from the Algal-Sponge Zone (where present) into turbid deep-water communities (Nepheloid Zone) at the bases of the banks.

To supplement the previous description of the Flower Garden zonal pattern, the biota of four additional banks will be depicted. Geyer Bank represents a system which is located as far offshore as possible on the continental shelf. Therefore it is subject to minimal neritic influence and has maximal surrounding depths (approximately 200 m). The high relief of this bank, and of its neighbor Elvers Bank, above the deep surrounding mud bottom prevents chronically turbid waters from rising much shallower than 100 m on the bank, where they could interfere with development of the Algal-Sponge Zone.

Alderdice Bank represents the other extreme, existing as far inshore as a bank may and still support an Algal-Sponge Zone. Unlike Geyer Bank, it is more exposed to the influence of neritic water masses, and, due to shallow surrounding depths (85 to 90 m), turbid bottom waters frequently approach its crest, to which the Algal-Sponge Zone is restricted.

Sackett Bank is a special case insofar as it is closest to the mouth of the Mississippi River. Algal-Sponge Zone assemblages, though present, are weakly developed on this bank. Diaphus Bank, being the next shelf-edge bank west of Sackett, apparently is subject to some degree of coastal influence. Consequently, reef building is diminished and biotic communities are less well developed compared to those of the shelf-edge banks farther west. These factors and others will be assessed pursuant to the bank descriptions in an effort to explain regional patterns of biotic community structure and abundance on Outer Continental Shelf hard banks in the northwestern Gulf of Mexico.

Geyer Bank

Zonation of benthic biota on Geyer Bank is correlated with substratum type and depth. The community established on rock outcrops at the crest of the bank bears a substantial resemblance to those occupying outcrops at similar depths on Stetson and Sonnier Banks and is recognizable as a *Millepora*-Sponge community (Figure 8.39). The hydrocoral *Millepora* is particularly conspicuous near the crests of bedrock peaks and outcrops (peak crests examined were at 37 m and 49 to 52 m). Sponges, including *Neofibularia nolitangere*, *Agelas*, and various massive demosponges, are possibly more evenly distributed, and predominate on the steeper slopes or cliffs. Coralline algae occur as crusts and patches on the rock, but are not significant reef builders in the *Millepora*-Sponge Zone. Leafy algae are locally abundant on the outcrops, particularly on their crests. Only two small colonies of hermatypic corals were seen, one a platelike crust of an agariciid and the other a monocentric variety with small polyps. The large anemone *Condylactis gigantea* is conspicuous and abundant on the bedrock (in places it is the prevalent invertebrate), and *Diadema antillarum* and *Spondylus americanus* populations are substantial.

The most abundant fish frequenting the outcrops are Yellowtail reeffish, *Chromis enchrysurus*, and Creole fish, *Paranthias furcifer*. Other conspicuous species include the Marbled grouper, *Epinephelus inermis*; Rock beauty, *Holacanthus tricolor*; and, at the 37 m peak, the Brown chromis, *Chromis multilineatus*. At least 28 additional species of fish were encountered.

Much of the rock is not occupied by epifauna, possibly because it is poorly cemented and apparently disintegrates easily. The rock

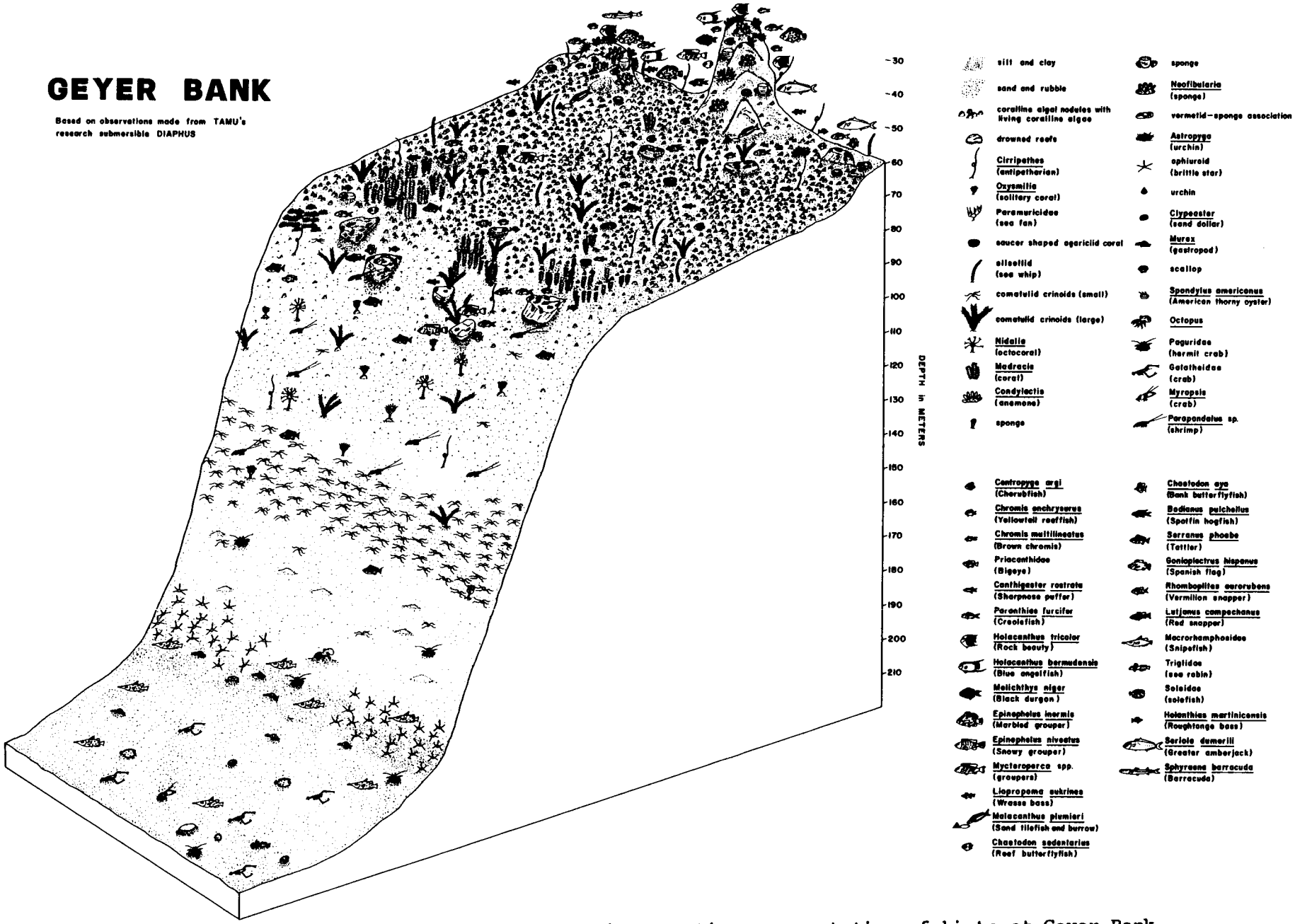

Figure 8.39 Diagrammatic representation of biota at Geyer Bank.

is riddled by holes, probably produced by rock-boring pelecypods. Unconsolidated sediments on the tops of the peaks are composed primarily of rock chips, Millepora rubble, and shell fragments. Finer erosional products occur in "channels" on the less steep slopes of the bedrock peaks. Near the slope bases, talus aprons of cobbles and chips occur, the lower portions of which (64 m or so) are mixed with carbonate rubble and algal nodules derived from the surrounding terrace.

Between 64 and 83 m, the biotic communities and surficial sediments are dominated by calcium carbonate producing organisms. These are primarily coralline algae, but also small branching corals of the genus Madracis. Coralline algal nodules and rubble underlain by coarse carbonate sand constitute most of the substratum between 64 and 76 m depth. The nodules in this range are generally large and their exposed surfaces are almost totally covered with growing coralline algae engaged in the production of carbonate substratum.

Patch reef-like structures occur on Geyer Bank from 64 to at least 98 m depth. The largest of these were encountered at 64 to 67 m near the bedrock outcrops and at 87 to 95 m at the edge of the upper platform of the bank. Some of these structures were 3 to 5 m in height. Smaller patches one-third to one metre high were seen between 70 and 98 m. All were covered with healthy populations of living coralline algae, but the abundance of coralline algae decreased substantially below 90 m.

Although coralline algae are certainly the most important substratum producers and reef builders on Geyer Bank, immense populations of the small hermatypic branching coral Madracis were encountered between 76 and 82 m depth. On the reconnaissance transect, live Madracis and Madracis remains composed almost all of the substratum from 79 to 82 m depth. Where such populations occur, Madracis must be the dominant frame-building organism.

Associated with the Madracis populations are extensive covers of a flattish, maroon-colored, leafy, calcareous alga, Peyssonnelia, which in places occupies 50 to 90% of the bottom on top of Madracis remains. This alga is an effective competitor for bottom space that otherwise would probably be occupied by living Madracis, and consequently may locally retard substratum production by the corals. Other leafy algae occur on the bank at all depths down to 107 m. Clusters and individual stalks of the calcareous green alga Halimeda were seen from 61 m on the bedrock outcrops down to 76 m on the nodule terrace.

Other conspicuous and abundant invertebrates on the part of the bank dominated by coralline algae or Madracis include: small saucer-shaped agariciid coral colonies (down to 82 m); ellisellid sea whips (72 to 77 m); Cirrhipathes (throughout the zone, as well as shallower and deeper); clusters of "worm-shell" gastropods embedded in the sponge Chelotropella (abundant from 72 to 79 m,

attaining the size of a bushel basket); large crinoids (72 m and deeper, tremendous populations between 75 and 81 m); and small yellow sponges of unknown identity which are extremely abundant between 76 and 78 m depth. The diversity and abundance of invertebrates is probably greater among the algal nodules and Madracis (67 to 82 m) than elsewhere on the bank.

The fishes most frequently seen on the nodule and Madracis bottom were small: Sharpnose puffer, Canthigaster rostrata; Orangeback bass, Serranus annularis; Cherubfish, Centropyge argi; and Yellowtail reeffish, Chromis enchrysurus. Many very small fishes were seen darting about among the algal nodules, but none could be identified. Evidence of burrowing by the Sand tilefish, Malacanthus plumieri, was seen above 72 m.

Where reefal structures occur, more and larger fishes congregate: numerous Creole fish, Paranthias furcifer; Reef butterflyfish, Chaetodon sedentarius; Roughtougue bass, Holanthias martinicensis; and 25 additional species, including snappers (Lutjanus and Rhomboplites aurorubens), groupers of the genus Mycteroperca and, at 97 m, Snowy groupers, Epinephelus niveatus.

At approximately the lower limit of the profuse growth of small Madracis, 82 m, the slope increases to 5° or so. An additional, and greater, slope increase occurs at 91 m. These breaks in slope mark the edge of the upper bank platform and also the upper part of an interesting zone of sedimentological and biological transition on the bank slope extending downward to the mud bottom near 189 m. Scattered algal nodules and sizeable carbonate gravel were found as deep at 197 m, but it is felt that most of such material encountered below 91 m has been carried downslope from the upper platform. Generally, below 82 m, the unconsolidated bottom contains less and less coarse carbonate gravel and sand. At 104 m the sediment is a combination of sand and finer grained material with a 30 to 40% cover of carbonate gravel. At 128 m it has graded to a mixture of silt-clay-sand-gravel, and at 177 m it is mostly muddy, with silt- and clay-sized particles and some remaining coarser material. At 198 m the bottom is sticky, coherent mud, and the slope is slight compared to that existing between 91 and 189 m. Although the few sizeable algal nodules found on this slope appear to be washed down from above, they were observed in places to be spaced as closely as one or two metres, even at 128 m depth. No living coralline algae were seen on these nodules below 113 m.

A rather diverse and abundant assemblage of attached epifauna is established on the parts of these nodules not covered by coralline algae. This richness and diversity extends down to over 140 m, and substantial epifauna were seen on nodules as deep as 162 m. The organisms found on the nodules of the bank slope are not the types which would occur on hard substrata on the upper bank platform. They are typical of hard substrata on the deeper flanks of other banks in the northwestern Gulf at similar depths. The most

conspicuous attached invertebrates associated with these nodules are small sponges (generally more abundant above 110 m); solitary corals, probably Oxysmilia (100 to 160 m); branching corals having the appearance of Oculina (123 to 152 m); the octocoral, Nidalia (105 to 131 m); and small octocoral fans. The fans are generally oriented parallel to the slope of the bank, indicating a predominance of currents running horizontally.

The bank slope harbors impressive populations of echinoderms. At 91 m an aggregation of several hundred (possibly 700 or more) very large black urchins, Astropyga magnifica, was seen on the sand and rubble bottom. These aggregations occur on other banks in the northwestern Gulf at similar depths on similar bottoms. They continually cycle surficial sediment through their guts, egesting small spherical fecal pellets through the dorsal aboral pore. During the examination of this urchin aggregation, at least two were observed to emit apparent reproductive products from five pores surrounding the aboral gut opening. The white reproductive fluid was shed by one urchin after being touched by the submarine's manipulator arm. Subsequently, an adjacent undisturbed urchin also emitted the white fluid, as if some cue from the first urchin had triggered a similar response in the second. As at other banks, several young Marbled grouper (Epinephelus inermis) accompanied the Astropyga aggregation, swimming above and between the urchins and often contacting their spines.

Another colorful, large, spiny urchin, Coelopleurus floridanus, was seen on the slope between 143 and 178 m. Its population must be significant insofar as four sightings were recorded within that narrow depth range. Two of these sightings, however, were of the remains of urchins, apparently recently eaten. Only one Stylocidaris urchin was seen (151 m) on the transect, even though at other banks these organisms are often very abundant on such bottoms.

Small crinoids capable of rather graceful swimming actions occur on the slope from 91 to 175 m clinging to rubble or any other object on the bottom. Between 136 and 160 m, the population of these organisms is phenomenal, peaking at about 137 to 146 m.

The most frequently encountered fish on the steeper bank slope was the Tattler, Serranus phoebe, seen down to 175 m, but more abundant around 107 m. Numbers of Bank butterflyfish, Chaetodon aya, Spanish flag, Gonioplectrus hispanus, and Snowy grouper, Epinephelus niveatus, were seen on the large reefal structures between 91 and 98 m at the top of the slope, but not elsewhere. It is suspected that the range of the snowy grouper extends considerably deeper.

The slope of the bank decreases below approximately 189 m. Even at that depth a substantial amount of carbonate gravel is mixed with the basically muddy sediment. The gravel content of the

sediment decreases below 193 m, leaving a very sticky, coherent mud bottom with a thin veneer of loose, easily stirred fine material which probably undergoes repeated disturbance by the active community of mobile benthic animals existing there. Tracks, trails, burrows, depressions, large holes and small mounds are the recognizable features on this bottom. They reflect movements or excavating activities of the limited number of species of echinoderms, molluscs, crustaceans, and fishes which appear to be the main components of the soft-bottom biota.

The most numerous organisms seen between 189 and 197 m were small ophiuroids, five centimetres or so in length, which covered the bottom in places almost arm tip to arm tip (several hundred per m^2). Hermit crabs, mostly occupying Murex shells, are frequent below 165 m. Several other types of crabs occur on the mud bottom. Small galatheid crustaceans are rather abundant, being frequently observed in burrows and small holes between 201 and 213 m. They were particularly apparent in the openings of numerous small burrows in the sticky mud rims of larger (one-third metre diameter) holes, some of which were occupied by groupers.

An octopus was seen in its hole at 186 m. Swimming scallops were seen at 207 and 213 m. A sizeable populations of Murex occurs around 197 m. One was seen in the apparent act of preying upon a Clypeaster sand dollar at 201 m. Remains of dead urchins were seen a number of times between 151 and 213 m. They must be prime forage for more active benthic predators on the bank slope and deeper mud bottom.

The urchins, crabs, and gastropods are certainly responsible for many of the fresh tracks and trails seen on the soft bottom. One of the more distictive tracks seen was produced by flatfishes Pleuronectiformes, dragging their bodies along the bottom by undulations of the dorsal and anal fins, leaving a series of small indentations on either side of the linear track produced by the central part of the fish.

The distinctiveness, variability, abundance, and freshness of the tracks, trails, and burrows are indicative of a very active assemblage of organisms on the deep, soft bottom. Some are probably deposit or detritus feeders (the urchins and ophiuroids primarily, possibly some of the crabs and galatheids). Four suspension or filter feeding types were seen, a penshell (dead but in place) at 206 m, stalked colonial coelenterates (sea pens) at 204 m, worms (apparently sabellids) with tentacles extended above the bottom between 193 and 204 m, and the aforementioned scallops. Benthic predators (fishes, crabs, gastropods, octopods, asteroids) are probably the most active group and may be responsible for a majority of the tracks and trails.

At least nine different types of fishes were seen on the mud bottom below 189 m. Some lurk in the bottoms of large, steep-sided

holes, and one was seen inside a dead penshell. Flatfish and sea robins rested on the sediment. The most interesting and abundant fish, however, was the Snipefish, Macrorhamphosus scolopax, which hovered above the bottom, nose down, at a steep angle (also observed at Elvers Bank). These fish, seen from 189 to 213 m, were most abundant between 189 and 197 m and numerous at least down to 204 m. Plankton abundance adjacent to the bottom appeared greater than in the water some distance above. It is possible that the Snipefishes make a good living in the narrow bentho-pelagic realm near the bottom by feeding on planktonic organisms.

Sackett Bank

Sackett Bank is a shelf-edge topographic feature capped by carbonate sediments, including sand, debris, algal nodules, rock ledges and drowned algal reefs (Figure 8.40). Biotic communities here, though composed of species found commonly on the other shelf-edge banks in the northwestern Gulf, are much less diverse, and less abundant than are those of the other banks. In terms of community structure, the epibenthic biota of Sackett Bank seem to occupy a position somewhere between those of the South Texas fishing banks (such as Southern and South Baker Banks) and those of the other shelf-edge carbonate banks in the northwestern Gulf of Mexico (such as 18 Fathom Bank and the Flower Garden Banks).

The topmost part of Sackett Bank (64 to 65 m depth) is rather flat and sandy with carbonate rubble, a few scattered coralline algal nodules, and drowned coralline algal reef patches. On this upper terrace, limited amounts of live coralline algae occur on the reef patches, nodules, and tops of pieces of rubble. However, the present degree of carbonate production by coralline algal populations on Sackett Bank does not appear to be substantial.

Some of the drowned reef patches are quite large, up to 3 m high and 12 m across (the largest we have seen crest at 61 m depth). All are covered with thin veneers of fine, easily stirred sediment and harbor surprisingly sparse populations of epibenthos and fishes. The primary invertebrates clinging to or encrusting the drowned reefs are comatulid crinoids, encrusting sponges, Diadema, Cirrhipathes, Spondylus americanus, the saucer-shaped agariciid, and small patches of coralline algae. Fish are not particularly abundant on the drowned reefs, though the following types are frequent: Chromis enchrysurus, Yellowtail reeffish; Bodianus pulchellus, Spotfin hogfish; Equetus umbrosus, Cubbyu; Seriola dumerili, Greater amberjack; Priacanthus, bigeye; Serranus phoebe, Tattler; Apogon, cardinalfish; Chaetodon sedentarius, Reef butterflyfish; Chaetodon aya, Bank butterflyfish; Paranthias furcifer, Creole fish; and Holanthias martinicensis, Roughtongue bass. These are generally the same species seen over the entire upper portion of the bank above 73 m depth. The population of

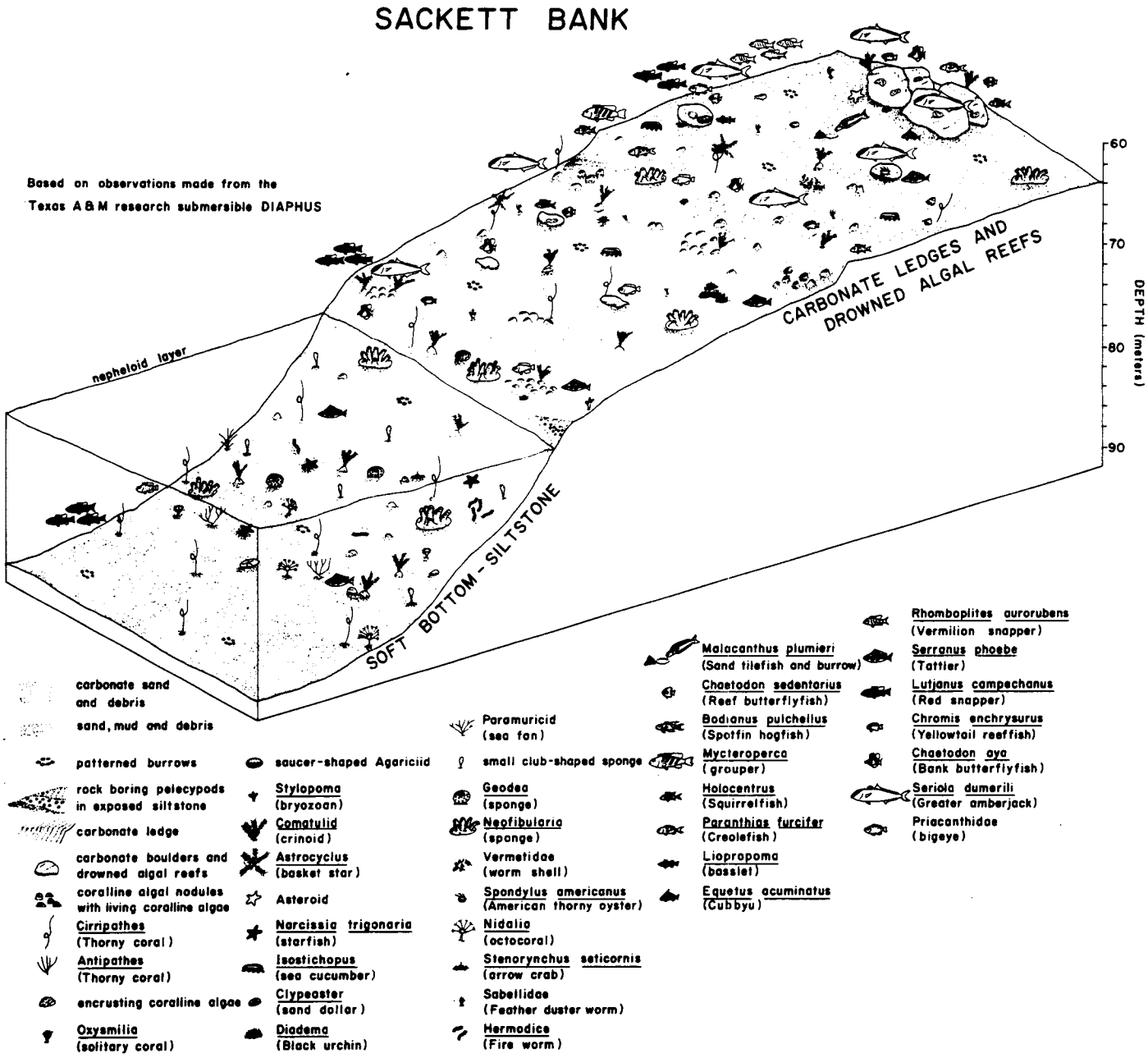

Figure 8.40 Diagrammatic representation of biota at Sackett Bank.

Chaetodon aya seemed large in comparison to other banks examined. Schools of Vermilion snapper, Rhomboplites aurorubens, were seen near the drowned reefs.

The predominantly sandy bottom, occupying most of the upper platform of the bank above 65 m depth, houses a relatively depauperate assemblage of macroepifauna compared to those occurring at similar depths on other shelf-edge banks in the northwestern Gulf. However, clusters of burrowing sabellid polychaete worms are, rather abundant. Comatulid crinoids are frequent on rubble and nodules, and the population of the sponge Neofibularia nolitangere is significant. Diademid urchins and the large sea cucumber Isostichopus are conspicuous.

Small mounds of "tangled" worm-shell gastropod tubes (probably Siliquaria modesta) were seen on the upper terrace (64 m depth). These organisms have been observed also on several other shelf-edge banks. They may be important contributors to carbonate sediment on Sackett Bank.

Burrows produced by the Sand tilefish, Malacanthus plumieri, are interesting in terms of what they may indicate concerning the nature of the surficial sediments covering the top of Sackett Bank. These conical burrows, about one metre in diameter, were seen in what appeared to be basically sandy bottom with some rubble and few nodules. Adjacent to the burrows, however, were piles of algal nodules, presumably removed from the burrows by the fishes during construction. This would imply that, even though the visible sediment surface is mostly sand, there are significant amounts of coarse material and dead algal nodules buried just beneath. Considering this, and the fact that fair-sized drowned reefs are present on the uppermost part of the bank, it is hypothesized that in the past Sackett Bank must have supported a rather active reef-building community dominated by coralline algae.

Actually, living coralline algal nodules are more abundant near the bases of small carbonate ledges and on low mounds on a 67 to 73 m depth terrace bordering the upper platform (Figure 8.40). The carbonate ledges, one to two metres high, separate the upper platform from the terrace in places. The ledges are generally of relatively gentle slope with algal nodules scattered on them. Near their bases, nodules extend sparsely for some distance out onto the terrace. Populations of epibenthos and fishes are somewhat more diverse and abundant on and adjacent to these ledges than is the case for the shallower drowned reefs. Crinoids, sponges, diademid urchins, sabellid worms, and the same types of fishes listed above for drowned reefs occur on the ledges and among the nodules. Large groupers appeared to prefer the ledges.

The substratum of the 67 to 73 m depth terrace is basically a rubble-strewn sandy bottom with significant amounts of silt and clay. Very few algal nodules were found on the central part of the

terrace. Clusters of them occur more frequently on small mounds toward the break in slope around 70 to 72 m depth. Sabellid worms are abundant on the terrace, and in general the conspicuous soft-bottom epifaunal populations are similar to those on the upper platform except for some significant additions. The antipatharian, Cirrhipathes, becomes abundant near the outer margin of the terrace. Basket stars are associated with Cirrhipathes. Substantial populations of the large urchin Astropyga magnifica were observed on the central part of the terrace.

At approximately 72 m depth the slope increases considerably. At this depth also was encountered a small outcrop of claystone bedrock similar in appearance to the rocks at Stetson and Sonnier Banks, and to outcrops seen in a basin at Bouma Bank and at the crest of Geyer Bank. These rocks are generally rather soft, and probably disintegrate rapidly where they are exposed directly to water. Chips and fine sediment obviously derived from the bedrock were seen around the base of the outcrop. Small bore holes in the exposed claystone rock at Sackett Bank are identical in appearance to holes in the outcrops at Stetson Bank, where they are considered to be produced by rock-boring pelecypods. The occurrence of claystone-siltstone outcrops at midshelf banks such as Stetson and Sonnier, and the less conspicuous occurrence of similar outcrops on deeper parts of the shelf-edge carbonate banks, is interesting. One might speculate that the substantial carbonate reefal communities on the shelf-edge banks have developed on, and almost totally overgrown or buried, a basic substratum of upthrust claystone and siltstone. In all cases, the unconsolidated sediments on the flanks of the shelf-edge carbonate banks grade outward from coarse carbonate sand to mixtures of sand, silt, and clay and finally to a fine mud. A one metre deep grouper hole in the soft mud bottom at 90 m depth at Sackett Bank was observed to have either claystone or siltstone at its bottom.

When Sackett Bank was explored with the submersible, the top of the nepheloid layer was roughly coincident with the break in slope at 72 to 74 m depth. A substantial change in the composition of the benthic epifaunal community is apparent between 73 and 76 m depth. The comatulid crinoid population becomes "tremendous"; Neofibularia sponges are abundant and, surprisingly, white rather than the normal reddish brown; fire worms, Hermodice, are exceedingly numerous; Asteroid starfishes, particularly Narcissia trigonaria and Astropecten-like forms, are conspicuous; Cirrhipathes become somewhat more abundant; the globular, white sponge Geodea and small, yellow, club-shaped sponges appear as major components of the soft-bottom community. These conditions persist to at least 85 m depth. In addition, at around 80 m depth, Antipathes (a branching antipatharian), the club-shaped octocoral Nidalia occidentalis, small paramuriceid sea fans, and large solitary stony corals, probably Oxysmilia, are found. The paramuriceids, Nidalia, and the large solitary corals are abundant down to around 88 m depth. Interestingly the large polyps of Nidalia were contracted and

inconspicuous above 83 m depth but well expanded below 85 m depth (daytime observation).

Below 90 m depth almost nothing was visible on the mud surface, the conspicuous epifaunal organisms having nearly disappeared. However, holes 20 cm to one metre wide and deep were seen. One contained a large eel, and a grouper occupied another. A school of Red snapper, Lutjanus campechanus, was cruising near the bottom.

The fact that the epibenthic communities on the upper part of Sackett Bank are poorly developed compared to those on shelf-edge banks to the west makes Sackett Bank very interesting ecologically. Its topography, depth, and location would seem to favor development of clear-water carbonate reefal communities, were it not for the proximity of the Mississippi River. Indeed, the presence of large drowned coralline algal reefs and large numbers of dead algal nodules buried under carbonate sand indicates that a substantial, active reef-building community existed on the bank some time in the past, dominated by coralline algae.

The small population of living coralline algae existing on the bank suggests that environmental conditions do not now altogether preclude limited carbonate substratum production. It is hypothesized, however, that the conditions of water quality, hydrography, and turbidity associated with Mississippi River outflow are responsible for limiting the contemporary development and growth of substantial carbonate reefal communities at Sackett Bank.

Such communities, which are basically dependent on photosynthetic organisms, require adequate levels of light throughout the year. The water overlying Sackett Bank was much more turbid when observed than the water above any of the other shelf-edge banks. The upper 10 m of the water column (above the thermocline) was very green and contained an enormous amount of organic matter in the form of plankton and seston (floating, non-living organic material, often mucus-like). At the thermocline (approximately 10 m depth) large, horizontal "sheets" of mucus-like white organic matter were seen. Mucus "strands," accompanied by very large zooplankton populations, extended down past 30 m depth. All this suspended material, substantially the result of enormous phytoplankton and zooplankton production, effectively blocks out much of the downwelling light, even though the water between the organically turbid surface layers and the bottom nepheloid layers may be quite clear. It is possible, therefore, that the benthic reefal communities of Sackett Bank are held in check partly by the tremendous productivity of nutrient rich, near-surface marine waters in the vicinity of the Mississippi Delta. Long-term observations of light penetration, salinity, temperature, nutrients, suspended organics, and water column productivity at Sackett Bank and shelf-edge banks supporting substantial Algal-Sponge Zones could reveal much concerning the environmental factors limiting

development of clear-water carbonate reef-building communities in the northwestern Gulf of Mexico.

The structure and abundance of biotic communities at Sackett Bank is intermediate between those described for shelf-edge carbonate banks (such as Geyer Bank and the Flower Garden Banks) and South Texas fishing banks (such as Southern Bank). Living coralline algae populations at Sackett Bank are more substantial than those found on the South Texas banks but much less developed than those of most other shelf-edge banks. Sackett Bank's closest shelf-edge neighbor, Diaphus Bank, exhibits similar limitations in the degree of development of clear water, reef-building zones.

Diaphus Bank

Although scleractinian corals and coralline algae live on Diaphus Bank, no substantial populations of either were encountered during the survey. Reef-building appears to be arrested at present, but drowned reef patches occur at least down to 107 m depth. These currently inactive (non-growing) reefs are covered with fine sediment or sediment-epifauna mats and sponges with small amounts of coralline algae.

The largest drowned reefs (2.5 to 3 m high) were seen between 85 and 95 m depths, marking the break in slope at the edge of the bank's upper platform (Figure 8.41). This is presumably the level of most active past reef building. Progressing from the bank edge toward the top central portion of the bank (82 m depth), the drowned reefs become increasingly less elevated above the bottom (some only 0.5 m high), but their lateral dimensions (averaging 3 to 6 m across) and spacing (generally 3 to 9 m or more apart) are fairly uniform. Below 95 m, the drowned reefs are smaller and more heavily laden with fine sediment.

Sediment cover on the drowned reefs is somewhat less above 88 m depth, but even at 82 m it is substantial, sometimes occurring on 90 to 95% of the rock surface. Above 95 m, at least, the sediment on rocks is most often entrapped by low-growing populations of attached epibenthic organisms forming a mat. At greater depths, the fine sediment cover may be so great as to obscure or preclude most small attached benthos.

Coralline algal cover on the drowned reefs on top of the bank generally varies from nil to 10 or 15% and probably averages 3 to 5%. The greatest cover (20 to 30%) was encountered on a very large reef (3 m high) at 88 m on the bank edge. Although a few living patches of coralline algae were seen down to 107 m depth, very little occurred below 98 m. In general, the contemporary coralline algae population is incidental on the part of the bank surveyed and

cannot be considered to constitute an effective reef-building population.

It is possible that on the shallowest peaks (74 to 78 m depth) there is some degree of expression of the Algal-Sponge Zone. Between 80 and 98 m, however, the assemblages are comparable to those of the Antipatharian Zone. The remainder of the shelf-edge carbonate banks which have crest depths above 80 m are occupied by well developed Algal-Sponge Zones (Ewing, Jakkula, Sweet, Alderdice, Parker, Rezak-Sidner, Bouma, 18 Fathom, Elvers, Geyer, Bright, 28 Fathom, East Flower Garden, West Flower Garden, and probably Applebaum). The crest of Phleger Bank is too deep, 122 m, to support Algal-Sponge or Antipatharian Zones. The hard-bottom biota atop Phleger, though apparently existing in clear water (Continental Shelf Associates, 1980), are types found in turbid water (Nepheloid Zones) near the bases of the shelf-edge banks slightly farther inshore.

Clear water assemblages of the Algal-Sponge Zone, dominated by coralline algae, extend downward to nearly 100 m on those banks which are positioned at the extreme edge of the continental shelf and surrounded by depths in excess of 180 m (Geyer, Elvers, and probably Sweet). At the other extreme, on those shelf-edge carbonate banks (such as Alderdice) that are substantially inshore from the shelf break and surrounded by depths less than 100 m, the Algal-Sponge assemblages are restricted to shallower depths (generally less than 75 m, Table 8.1).

Alderdice Bank

The 85 m depth contour can be taken as an inshore limit for the distribution of shelf-edge carbonate banks bearing reefal communities. Alderdice Bank exists at this inshore limit, and were it not for the several peaks rising into clear water above 65 m depth, probably would not support even an Algal-Sponge Zone.

The bank is composed of four major topographic peaks on a flattish platform of about 80 m depth. In addition, a spectacular basalt outcrop juts vertically out of the bottom at 76 m, cresting at 55 m (Figure 8.42). Reconnaissance of one of the major peaks, the basalt outcrop, and a good part of the 80 m platform, revealed basic differences in biotic communities occupying the three structural zones.

Healthy, growing coralline algal nodules underlain by carbonate sand occur at the crest of the large southeastern peak (58 to 67 m depth). The nodules are accompanied here and there by very small reefal structures and carbonate blocks covered with the dominant coralline algae. The extreme variability in size of nodules, blocks, and firmly affixed reef rock gives the substratum an

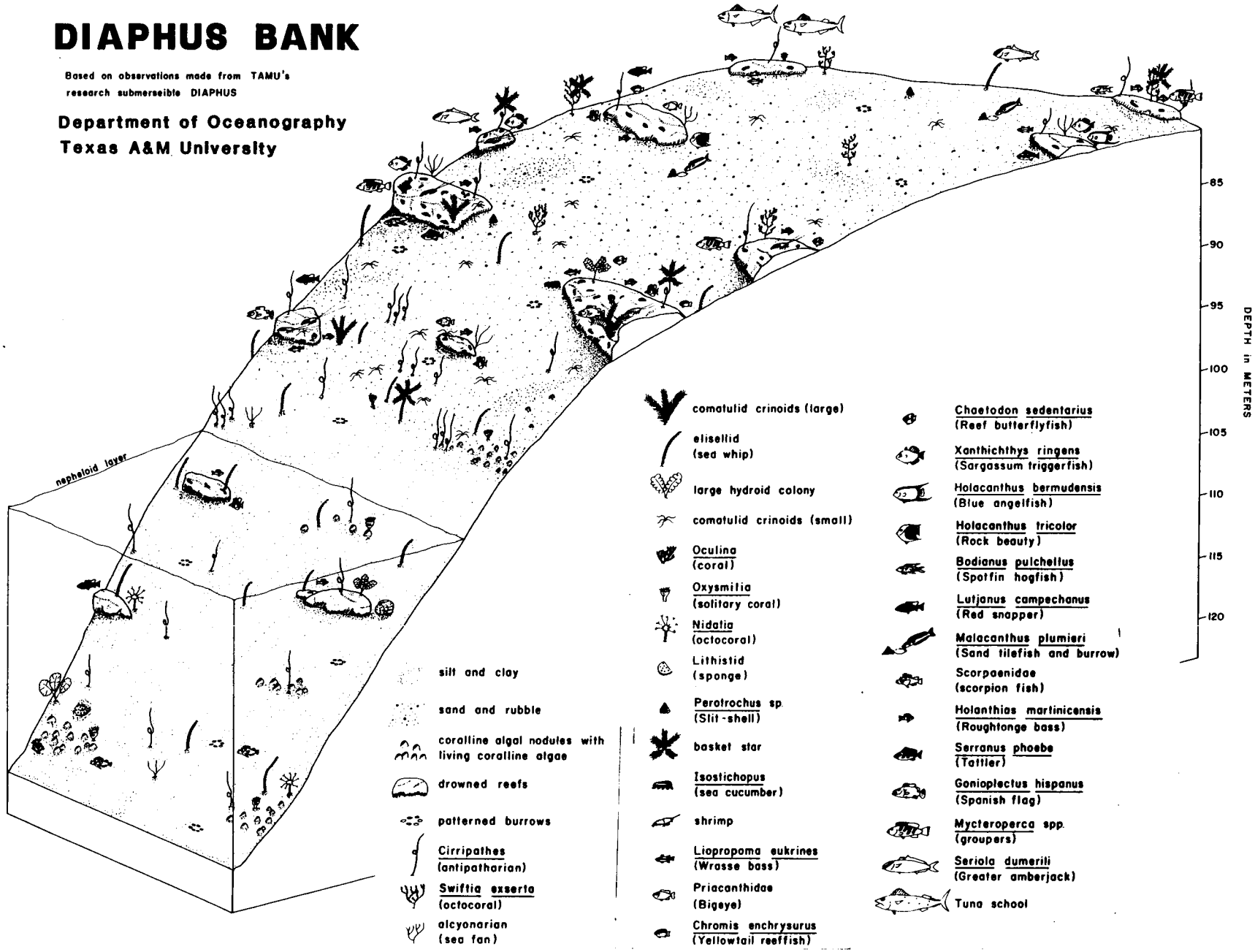

Figure 8.41 Diagrammatic representation of biota at Diaphus Bank.

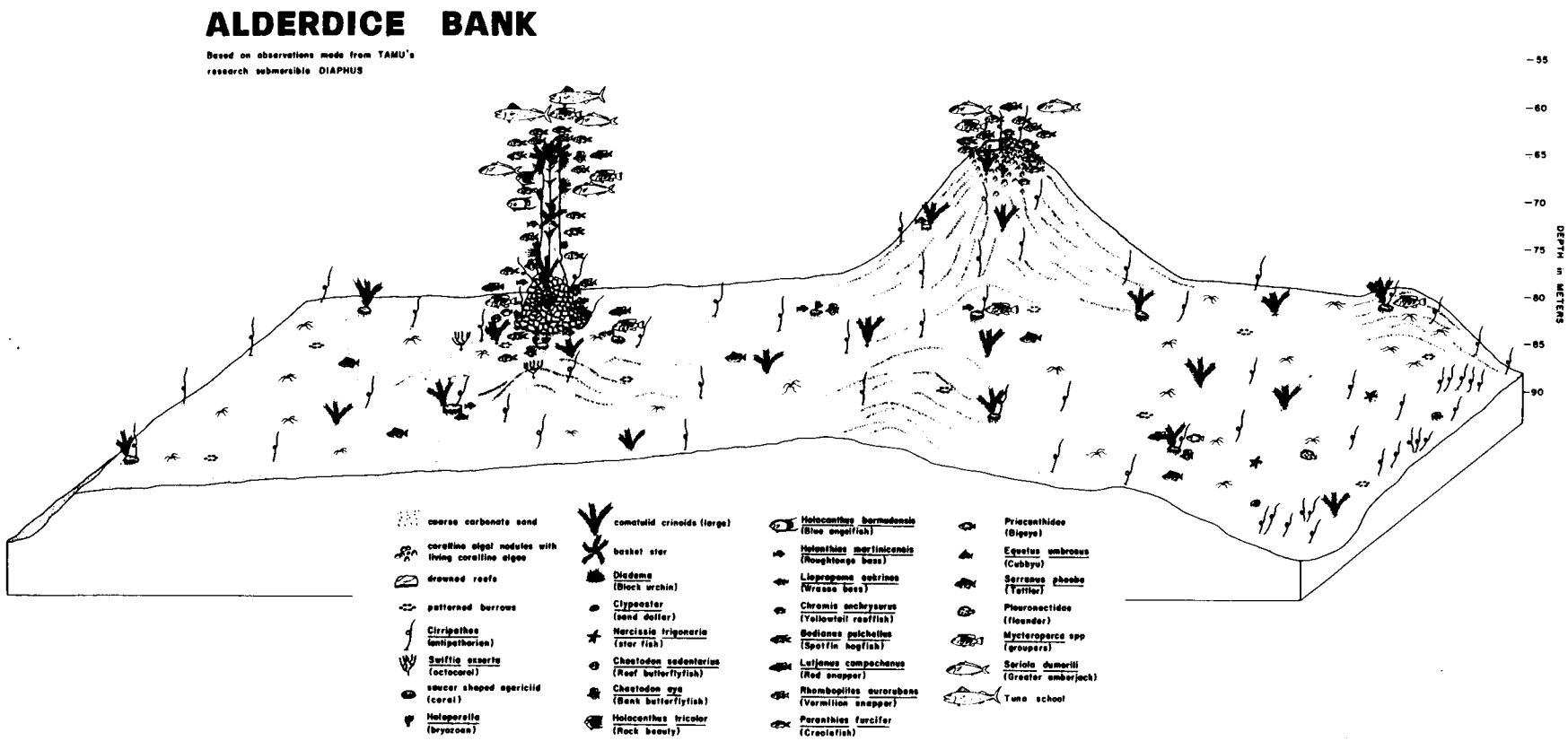

Figure 8.42 Diagrammatic representation of biota at Alderdice Bank. Basalt outcrop at left appears here as a pinnacle, but is actually a 100 m long ridge (see Figure 8.30)

irregular appearance not typical of other algal nodule zones. Contributing to the irregularity is the "lumpy" nature of the highly bioturbated sand, where it is exposed.

The most conspicuous invertebrates on the peak are Cirrhipathes, massive sponges of several species, and large branching bryozoan colonies, Holoporella. An exceptionally large number of Yellowtail reeffish, Chromis enchrysurus, was encountered above 67 m; the peak was literally swarming with them. Creolefish, Paranthias furcifer, were numerous; groupers, Mycteroperca, congregated on top; schools of snappers, Lutjanus and Rhomboplites aurorubens, and Greater amberjack, Seriola dumerili, were seen.

The Algal-Sponge Zone described above is probably restricted to crests of the several peaks at Alderdice Bank and, therefore, is of limited areal extent. It is nevertheless a zone of active reef-building and carbonate substratum production.

Small "drowned" reefal structures occur on the bank down to at least 85 m depth. They are surrounded by the large expanse of unconsolidated sediment which constitutes most of the bank. With increasing depth, the sediment grades from carbonate sand, gravel, and nodular material (75 m), to mixtures of sand, silt, clay, and gravel (79 m), to soft, primarily fine sediment (82 m). Reefal structures below the Algal-Sponge Zone are typically laden with veneers of sediment entrapped by mats of low epifaunal growth. Below 82 m the drowned reefs are almost totally covered with thin layers of fine sediment. Nevertheless, small amounts of coralline algae occur on the drowned reefs down to at least 79 m (5% cover at 76 m). No algae were seen below 79 m.

Cirrhipathes is generally the most conspicuous invertebrate at all depths and is particularly abundant locally below 84 m. Between 76 and 85 m enormous populations of small comatulid crinoids occur on the unconsolidated bottom, clinging to rocks and rubble. Larger crinoids are numerous on rocks and drowned reefs between 76 and 85 m, and were seen to 88 m. Branching colonies of Holoporella are abundant above 76 m. Various alcyonarians occur on the rocks between 76 and 79 m, the largest being white muriceid fans and the orange and white branching form Swiftia exserta.

The deeper, muddy bottoms below 82 m are comparatively barren but are abundantly etched with tracks, trails, and burrows, indicating an active population of mobile benthic invertebrates. The sand dollar, Clypeaster ravenelii, is fairly numerous below 85 m, and the starfish, Narcissia trigonaria, was seen between 82 and 85 m.

Two species of hermatypic corals were encountered at 76 m, saucer-shaped agariciids and a small head of what appeared to be Stephanocoenia. Neither was abundant, and both occurred on drowned reefs.

Holanthias martinicensis was the most frequently seen fish around the drowned reefal structures below 76 m. Others included Yellowtail reeffish, Chromis enchrysurus; Spotfin hogfish, Bodianus pulchellus; Blue angelfish, Holacanthus bermudensis; Reef butterflyfish, Chaetodon sedentarius; Cubbyu, Equetus umbrosus; Spanish flag, Gonioplectrus hispanus; and bigeye, Priacanthus. A school of snappers, Lutjanus, and several groupers, Mycteroperca, were also seen. Tattlers, Serranus phoebe, were numerous on the unconsolidated bottom.

The most impressive feature on Alderdice Bank is the basalt outcrop. It is an elongated narrow ridge extending vertically upward from the 76 m surrounding depth to 55 m crest depth. Spires examined at the crest were two or so metres across at the top, with sheer cliffs extending downward to approximately 67 or 69 m. Below this, large blocks of basalt talus were piled around the base of the outcrop. The hard basalt is covered with crusts of coralline algae, sponges, bryozoans, and other epifauna. Near the top of the outcrop, these crusts are nearly total, up to 50% being coralline algae. At 69 m on the large blocks, coralline algal cover is 70 to 80%, but the cover decreases with increasing depth to small patches at 76 m.

Large Basket stars, Diadema urchins, and branching colonies of the bryozoan Holoporella are particularly abundant and visible on the outcrop and talus slope. Basket stars tend to accumulate at the very peak of the outcrop. Cirrhipathes, Antipathes, large comatulid crinoids, and small branching alcyonarians are numerous on the talus slope surrounding the outcrop.

Fishes swarm around the crests of the outcrops. Frequenting the outcrop crests are large schools of Creole fish, Paranthias furcifer; Vermilion snapper, Rhomboplites aurorubens; Greater amberjack, Seriola dumerili; and tuna; as well as large Red snapper, Lutjanus campechanus, and groupers, Mycteroperca. Creole fish and Vermilion snapper were the most numerous large fishes on the structure at all depths. Holanthias martinicensis was abundant, particularly on the talus slope. Closely associated with the outcrop and talus blocks are the Wrasse bass, Liopropoma eukrines; Spotfin hogfish, Bodianus pulchellus; Bank butterflyfish, Chaetodon aya; Blue angelfish, Holacanthus bermudensis; Rock beauty, Holacanthus tricolor; and a damselfish which resembles Chromis scotti.

ENVIRONMENTAL CONTROLS

Based on the nature, distribution and degree of development of their epibenthic communities, hard-banks on the Texas-Louisiana Outer Continental Shelf can be divided into five environmental groups as follows:

1. South Texas midshelf relict Pleistocene carbonate reefs bearing turbidity tolerant Antipatharian Zones and Nepheloid Zones (surrounding depths of 60 to 80 m; crests 56 to 70 m).

2. North Texas-Louisiana midshelf Tertiary outcrop banks bearing clear water, Millepora-Sponge Zones and turbid water-tolerant Nepheloid Zones (surrounding depths of 50 to 62 m; crests 18 to 40 m).

3. North Texas-Louisiana midshelf banks bearing turbidity tolerant assemblages approximating the Antipatharian Zone (surrounding depths of 65 to 78 m; crests 52 to 66 m).

4. North Texas-Louisiana shelf-edge carbonate banks bearing clear-water coral reefs and Algal Sponge Zones, transitional assemblages approximating the Antipatharian Zone, and Nepheloid Zones (surrounding depths of 84 to 200 m; crests 15 to 75 m).

5. Eastern Louisiana shelf-edge carbonate banks bearing poorly developed elements of the Algal Sponge Zone, transitional Antipatharian Zone assemblages, and Nepheloid Zones (surrounding depths of 100 to 110 m; crests 67 to 73 m).

The clear-water biotic zones on these banks (Millepora-Sponge, several coral reef zones, and Algal-Sponge Zone) are distinctly tropical in faunal and floral content. Biota of the Antipatharian and related transitional zones are largely composed of tropical species apparently more tolerant of turbidity. Environmental factors which can be correlated with and probably control regional patterns of community structure, distribution, abundance, and zonation of tropical epibenthos in the northwestern Gulf are: distance from shore, regional patterns of substratum type, bottom depth, bank relief, water temperature, salinity, river runoff, turbidity, sedimentation, currents, and seasonal variation in the last six of these (Figure 8.43). These factors have been substantially described in Chapters 1 and 2 and this chapter.

Conditions at the shelf edge near and beyond the 80 m depth contour on the broad North Texas-Louisiana shelf west of about 91° longitude are favorable for development of tropical reef communities. Current patterns are such that shelf-edge waters come primarily from the southwest, and are oceanic, with little admixture of neritic water from the Texas-Louisiana shelf (Chapter 2, Figures 2.11, 2.12, 2.39). These currents carry larvae, spores, and juveniles from the Gulf of Campeche, Yucatan shelf, and the Caribbean.

There is a strong tendency for coastal water masses, highly influenced by outflow from the Mississippi and other rivers in Louisiana and North Texas, to be held onshore and shunted west most

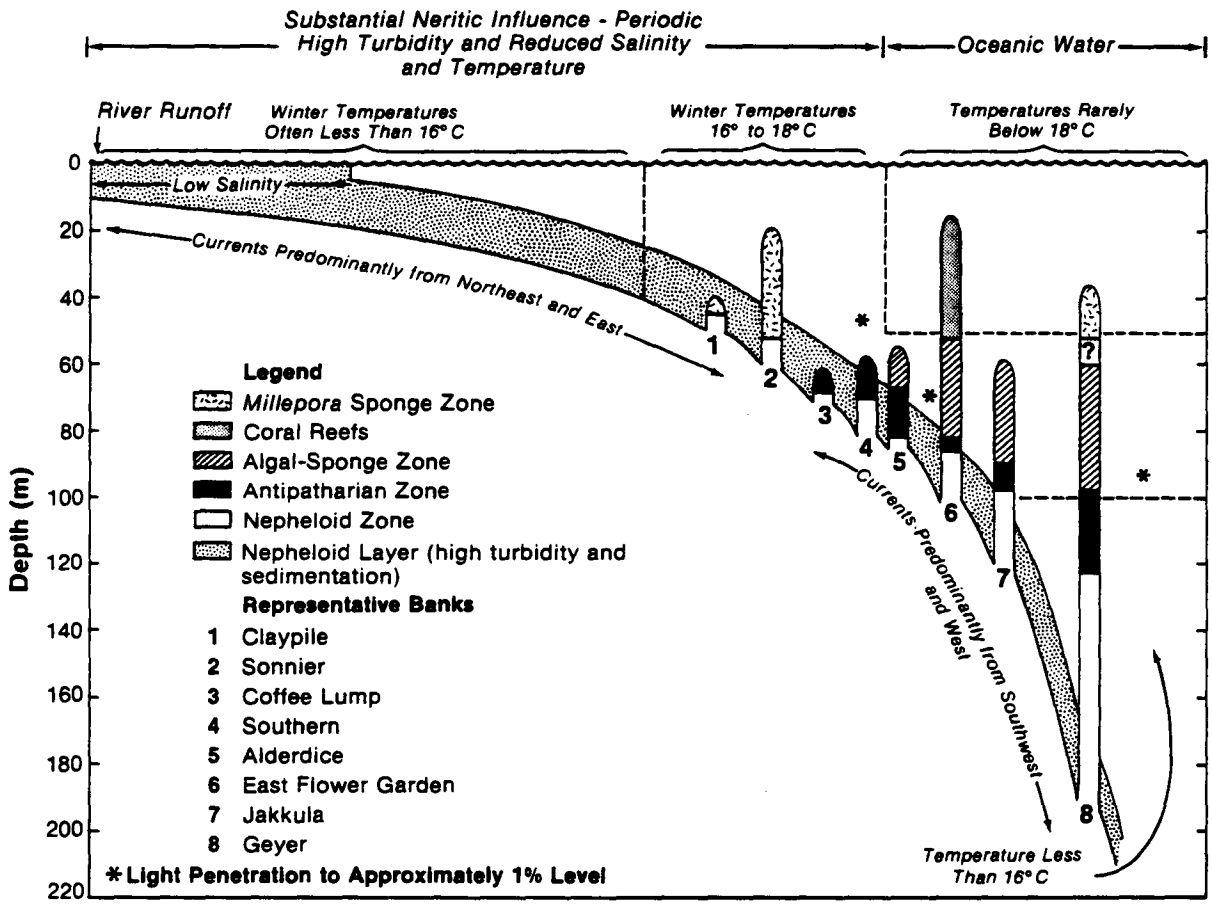

Figure 8.43 Comparison of biotic zones to temperature, salinity, turbidity, and light differences at selected banks.

of the year (particularly during February to May periods of peak runoff) by the general shelf circulation pattern. As a result, turbidity in the shelf-edge waters is usually nil, and salinity averages 36 ppt (Figure 2.17). Where high runoff combines with seasonal disruption of the typical counterclockwise current regime on the shelf (such as may occur in late spring or early summer), lower salinities may occur in shelf-edge waters; however, the lowest surface salinity we have ever measured at the Flower Gardens was 32 ppt, and this was accompanied by 34 ppt at 25 m depth.

For most of the year, near-surface water temperatures throughout the Gulf are tropical to sub-tropical (27 to 30°C) (Chapter 2, Figure 2.20). However, near shore in the northern Gulf, temperatures become warm-temperate from December through March. During the coldest months (January to February) temperatures grade from as low as 10°C in the estuaries to 18°C on the outer shelf edge (Figure 2.19).

Onshore-offshore seasonal movements of the 18° and 16°C surface isotherms probably have very significant influences on distribution of tropical reef biota in the northwestern Gulf. As indicated in Chapter 6, 18°C is considered to be the minimum seasonal temperature limit for vigorous growth of coral reefs. The lower limit, 16°C, is stressful for most reef-building corals. Though reef-building coralline algae and other biotic elements of the tropical reef ecosystem may tolerate somewhat lower temperatures, 16°C is probably near the bottom of their optimal range.

In the northwestern Gulf, the 18°C winter surface isotherm can be expected to occur somewhere between the locations of the 30 and 80 m depth contours, projected upward. The 16°C isotherm occurs between the 20 and 40 m depth contours (see Chapter 2, and Harrington, 1966). The surface isothermal layer during winter extends 50 to 75 m downward (Chapter 2, Figure 2.26), with temperatures only 1 to 3°C less at 100 m. Thus, above 50 m depth off North Texas and Louisiana, and seaward of the general 80 m bottom depth contour, salinities are high and temperatures range annually from approximately 18 to 30°C (Figure 8.43). Where suitable hard substratum exists in the absence of chronically turbid water, conditions on this part of the shelf are favorable for the growth of tropical reef communities dominated by corals or coralline algae, or both.

The degree of light penetration into clear surface waters, and the antagonistic effects of turbidity in bottom nepheloid layers are almost certainly the factors controlling depth ranges for these communities on the various shelf-edge banks. High turbidity decreases light penetration and is therefore inimical to the development of coral and algal reef communities. Sedimentation associated with high turbidity results in smothering of encrusting epibenthos by veneers of silt and clay. In the northwestern Gulf, due to the enormous sediment load entering it from the rivers,

turbidity and sedimentation are major factors limiting development of tropical reef assemblages. It is speculated that reef development at Sackett Bank (Algal-Sponge Zone) is seriously attenuated due in part to increased turbidity in surface waters from admixed Mississippi River outflow. This influence, accompanied by somewhat reduced salinities, diminishes westward but may extend as far as Diaphus Bank (91°W) during periods of particularly high runoff (Figure 2.17).

Midshelf banks (Mysterious to Fishnet) arise from surrounding depths of 60 to 80 m. Their tops, which support Antipatharian Zone type assemblages between 56 and 73 m, exist within a depth range which on shelf-edge banks (Flower Gardens to Elvers) is occupied by diverse, clear-water Algal Sponge Zones. The lack of Algal-Sponge Zones on the midshelf banks, and the occurrence instead of Antipatharian assemblages which are typically found in deeper water at the shelf edge is probably due largely to high turbidity.

The effects of bottom nepheloid layers and associated sedimentation are certainly more pronounced on the midshelf banks than at the shelf-edge banks (Figures 2.36 and 2.37 and associated text). We speculate that most or all of the midshelf banks are frequently totally covered by the nepheloid layer, especially during severe wave conditions. At the Flower Garden Banks, a substantial nepheloid layer has not been observed shallower than about 80 m, and usually the water is fairly clear even at that depth. Fine, terrestrial sediments are not found on shelf-edge carbonate banks above the lower limit of their Algal-Sponge Zones. The midshelf banks, however, are generally coated with thin to thick layers of fine sediment, presumably derived from nepheloid layers.

Relief above the surrounding bottom is of considerable importance in alleviating the negative impacts of bottom nepheloid layers and attendant sedimentation on development of epibenthos. An Algal-Sponge Zone probably will not become established on banks which have less than about 15 m relief above a mud bottom due to the impact of nepheloid layers. At Alderdice Bank, the Algal-Sponge Zone extends downward to only 67 m, which is 17 m above the surrounding mud. Farther offshore, at the East Flower Garden, the Algal-Sponge Zone extends downward to 82 m, about 18 m above the surrounding soft bottom. In even deeper water where surrounding depths are over 180 m (Geyer and Elvers Banks), the vertical extent of the Algal-Sponge Zone is not limited by bottom nepheloid layers because of the high relief. Here, they extend down to over 95 m depth and are probably limited primarily by the degree of light penetration from above (Figure 8.43).

Thus, on the shelf-edge banks, there is a gradual increase in the maximum depth of expression of coralline algae-dominated communities with increasing surrounding depth (Figure 8.43 and 8.44; Table 8.1). A similar trend is apparent for the Antipatharian Zones on these banks (Figure 8.43; Table 8.1). These observations imply

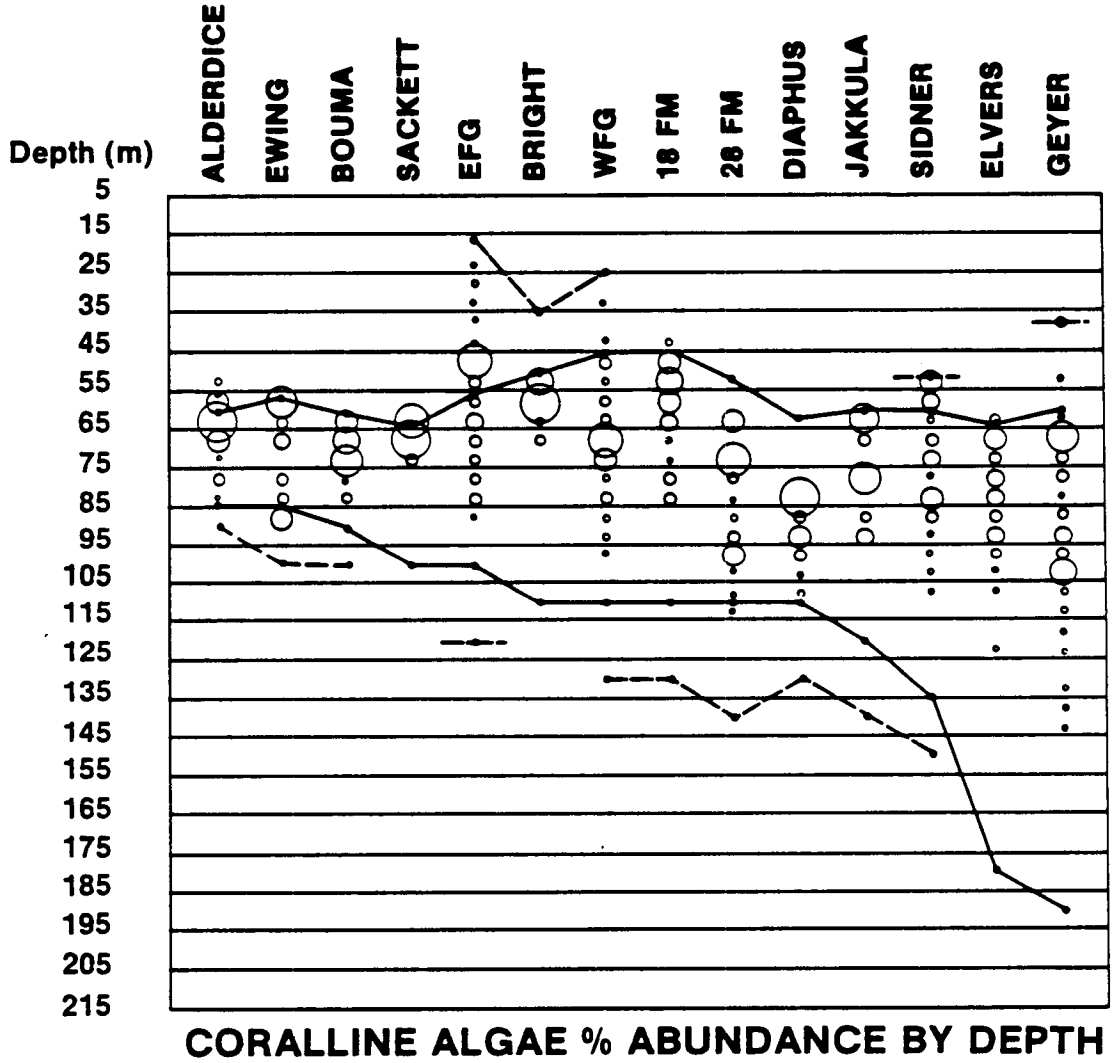

Figure 8.44 Coralline algae relative abundance by depth on shelf-edge OCS carbonate banks in the northwestern Gulf. Sizes of circles represent percentage abundance of coralline algae at various depths within banks only (total area of all circles within one bank equals 100% of the coralline algae population for that bank). Bank to bank variation in abundance is not represented.

Diagonal solid lines between 45 and 65 m depth represent the crest depths of the major carbonate platforms at the various banks. Dashed lines or presence of circle centers above the solid line represent crest depths of reefs or pinnacles. Diagonal solid lines below 85 m depth represent the general depth of the mud bottom surrounding the banks. Lower dashed lines indicate that parts of the surrounding bottom adjacent to the banks extend to the depths of the lines.

that the bottom nepheloid layers are of great importance as ecological limiting factors on the lower 15 to 20 m of the banks.

Thus, the deeper clear-water reefal communities (Algal-Sponge Zones) are excluded from the midshelf carbonate banks by winter low temperatures, high turbidity, reduced light, and sedimentation. They are limited in downward extent on some of the shelf-edge banks by the effects of nepheloid layers. In their place is a less diverse and less abundant "Antipatharian Zone" assemblage made up of epibenthic forms which, though basically tropical in origin, are tolerant of the stresses imposed.

Coral reefs would not be expected on the midshelf carbonate banks because the depths of the bank crests are too great (over 52 m). Even if shallower hard substratum were present, the aforementioned conditions of midshelf water qualities would probably preclude active coral reef development on these banks. Hard substratum exists within suitable depths for coral reef development in the form of midshelf claystone-siltstone banks arising from surrounding depths of 52 m and extending upward to 18 m (Sonnier Bank) and 20 m (Stetson). The Millepora-Sponge Zones of these banks are undoubtedly subject to seasonal temperatures somewhat less than the 18°C minimum for vigorous reef growth, but probably not much less than 16°C (Chapter 2).

The crests of Stetson and Sonnier Banks may, however, be fairly well isolated from the effects of bottom nepheloid layers due to their relief (40 to 42 m) above the surrounding mud bottom. The other midshelf claystone-siltstone bank, Claypile, with only 10 m relief, is certainly often covered by the nepheloid layer. Consequently, the abundance of dominant epibenthos is least at Claypile (lowest relief) and greatest at Sonnier (highest relief).

Speculation on environmental factors governing the development of the Millepora-Sponge Zone is complicated by the fact that the zone also occurs on shelf-edge bedrock outcrops, protruding from the crest of Geyer Bank between 37 and 52 m depth. The implication here is that development of this zone is dependent upon the presence of newly exposed bedrock outcrops, and vigorous development of the biota is favored by clear water and winter minimum temperatures above 16°C.

The question is why have tropical coral reefs not developed on the claystone-siltstone outcrops on Geyer Bank, which are exposed to the same oceanic conditions as are the coral reefs at the Flower Garden Banks? Hypothetically, the claystone, which is very soft and disintegrates readily upon exposure to water, may be unsuitable substratum for most reef-building corals. Indeed, the epifauna inhabiting the Millepora-Sponge Zone obviously "prefer" the thin beds of rock-hard siltstone which protrude from the softer but more extensive claystone on these outcrops. One can imagine a faunal succession on shelf-edge banks which results in: 1) recruitment of

reproductively prolific hydrozoan corals (Millepora) to exposed, hard siltstone beds; 2) spreading of these to adjacent claystone to create a carbonate veneer over the outcrop; 3) partial mortality of Millepora and subsequent recruitment of anthozoan hermatypic corals on the carbonate skeletal crust; 4) crowding out of the hydrozoan corals by the more competitive anthozoans; resulting in 5) transformation to a tropical coral reef.

The distributions of major epibenthic biotic zones in relation to the environmental factors discussed above are summarized in Figures 8.43 and 2.39). Correlations exist between regional patterns of winter temperature, turbidity, and light penetration in shelf waters and distribution patterns of the recognized biotic zones on Outer Continental Shelf banks. Coral reefs are restricted to clear oceanic water where temperatures rarely drop below 18°C. Most of the other bank zones may experience lowest winter temperatures of around 16°C. Neritic seasonal variability in temperature and salinity is greatest along the coast and diminishes offshore to roughly the 80 to 85 m depth contour, beyond which more stable, oceanic conditions predominate. Neritic influences on the midshelf are greatest in the upper 10 m of the water column. Deep tropical reef zones dominated by coralline algae are restricted to the clear, oceanic, shelf-edge waters beyond the 85 m depth contour. Neritic influences extending to the edge of the narrow shelf off the Mississippi delta limit reefal development on nearby banks.

Chronic turbidity of bottom water (nepheloid layers) and associated sedimentation severely limit epibenthos on the lower 15 to 20 m of most banks. Vigorous reef development is restricted to those parts of banks well above the effects of nepheloid layers. Continual turbidity and sedimentation on low relief banks substantially reduces diversity and abundance of the assemblages present. Penetration of sunlight into the water decreases toward shore due to generally increasing turbidity. This, combined with the light blocking and smothering effects of bottom nepheloid layers and suspended sediment around the bases of the banks, tends to "displace" zones upward on the banks closer to shore.

CHAPTER 9

ECOSYSTEM DYNAMICS

R. Darnell and T.J. Bright

The most effective method of describing the functional relationships of an ecosystem is through the development and use of various types of models. In effect, a model is a sophisticated simplification of the system under consideration. It must be a simplification because the diversity of the components and the complexity of their interrelations make the entire system otherwise unmanageable and, really, inconceivable. It must be sophisticated because only through intelligent and informed judgement can the model be made to focus upon the key elements and interrelations, providing enough information to be truly representational without clouding by excessive detail.

The coral reef and Algal-Sponge Zone (essentially an algal reef) are interesting systems to model. A portion of each system is sessile and attached. A portion flows through. Yet another portion hovers around, and among the hoverers, some are resident, while others are transient. Several groups of producers are present. Carbon flow is complicated by the relationships between organic and inorganic states. Yet, the whole system displays a functional unity and a steady-state or dynamic equilibrium.

DEVELOPMENT OF FUNCTIONAL MODELS OF THE EAST FLOWER GARDEN CORAL REEF SYSTEM

The Modeling Process

Any model consists of a series of internal compartments or reservoirs connected to one another by pathways which represent directional flows from one compartment to another. These pathways are often indicated by arrows. Also included in the model are various external factors or forcing functions which contribute to the system or which influence flow rates. In addition, the model may include internal storage compartments and pathways by which materials are lost from the system.

The development of an effective functional model of any ecological system must proceed through a series of logical stages. The first stage is the development of the conceptual model. Major steps in the development of this model include the following:

§Definition of the limits of the system to be modeled.

§Determination of how the myriad system components can be effectively grouped into a small number of compartments.

§Definition of the internal and external factors affecting each compartment.

§Determination of what flows are to be modeled, that is, the exchange medium or "currency" of the system. For an economic model it could be dollars. For an ecological system it should be calories or some chemical element such as carbon or nitrogen. The same basic model could be employed to represent the flow of different currencies.

§Development of the integrated flow diagram or conceptual model which ties together all the compartments into a logical framework representing the components and pathways as they interact and as they relate to the external milieu.

The second stage (which could be by-passed, but which is generally important in the development of an ecosystem model) is development of the graphical model. Most biological and ecological data from field and laboratory studies can be represented graphically, and most biologists or ecologists are quite comfortable when dealing with graphs. In the graphical model each pathway or arrow is now represented by one or more graphs indicating the nature of the relationships and the factors influencing the flow rates.

The third stage is development of the mathematical model in which each pathway or arrow is represented by one or more equations or by quantitative statements which can be handled by a computer. It should be clear that once a given pathway has been represented by a graphical function, the general nature of the equation describing the relationship is automatically determined. Although values for the various constants remain to be set, the form of the equations is already known. In the final version of the model, all the equations representing a given pathway must be integrated, and equations for the various pathways must be appropriately coupled.

The final stage is development of the applied model. That is, all the constants must be fixed so that the model represents the actual system under study. Values may be drawn from the same or related systems, and for some purposes approximations will suffice. Put another way, the model itself is an approximate representation, and full evaluation of all constants could prove a lengthy and costly enterprise. In any event, the applied model is, at worst, a rough representation of the actual field ecological system.

Once the applied model has been developed, it is ready for evaluation. This is accomplished through repeated computer runs employing alternative values for the constants and, if necessary,

making minor adjustments in some equations. Additional field and laboratory studies may be required to provide more realistic values for some constants. These activities fall into the category of "fine-tuning" the model.

Conceptual Model

The East Flower Garden Reef covers the crest and upper flanks of a high topographic feature on the Outer Continental Shelf. Although well submerged, the reef is within the euphotic zone, and therefore receives sunlight sufficient for photosynthesis. It is bathed by oceanic water and is subject to advective import and export of materials which are dissolved and suspended in the water column. Larger organisms move through the area, and some become temporary or permanent residents. Attached forms of the reef proper include corals, leafy algae, and coralline algae, as well as a variety of animal consumers such as sponges, worms, pelecypods, and the like. Many animal species constituting the infauna, epifauna, and nekton are found in association with the reef. The coral polyps are subject to pathological disturbance. Considerable calcareous debris falls into the crevices and around the base of the reef. Particulate organic detritus is added by all plants (through death) and all animals (through egestion, death, etc.). Hundreds of species are now known from the reef area.

Despite the taxonomic diversity, it has been determined that the reef ecosystem can be adequately represented by a sixteen-compartment model. Definitions of the advective imports/exports and composition of the sixteen compartments are provided in Table 9.1. Among the advected nutrients, nitrogen, phosphorous, and calcium are considered to be most important, the latter because of its role in the formation of calcareous skeletons. Among the model compartments, four represent photosynthetic producer groups, ten are consumer groups, and two are storage compartments. Three of the above compartments are associated with advective imports/exports. Although a certain amount of subjective judgement has been employed in determining the exact disposition of individual species or groups, the basic categories are clear enough.

As a preliminary to the determination of pathways of flow through the system, it is necessary to establish the input-output characteristics of each compartment of the model. This information is presented in Table 9.2. A full justification of each item will not be attempted here, but a number of major points of clarification are presented below.

Nitrogen and phosphorous are considered essential for the zooxanthellae, leafy algae, and coralline algae. These elements plus silicon are also essential for phytoplankton, but since phytoplankton is simply being swept through the system, it is best

TABLE 9.1 Definition and Composition of Categories in the Conceptual Model of the East Flower Garden Coral Reef Ecosystem. The compositional lists are indicative rather than exhaustive, and generally only the most important elements are included.

Category	Composition
	Import/Export
Advective import	Nutrients (N, P, Ca), phytoplankton, zooplankton, transient predators, particulate organic detritus.
Advective export	Nutrients, phytoplankton, zooplankton, transient predators, particulate organic detritus.
	Compartments of Model
Producers	
X_1 Phytoplankton	Marine phytoplankton in waters bathing the reef.
X_2 Zooxanthellae	Symbionts within hermatypic corals. Some are periodically released to become phytoplankton.
X_3 Leafy algae	*Caulerpa*, *Chaetomorpha*, *Codium*, *Dictyota*, *Pocockiella*, *Rhodymenia*, *Stypopodium*, *Valonia*, and others.
X_4 Coralline algae	*Archaeolithothamnium*, *Hydrolithon*, *Lithophyllum*, *Lithoporella*, *Lithothamnium*, *Mesophyllum*, *Porolithon*, *Tenarea*, and others.
Consumers	
X_5 Zooplankton	Marine zooplankton in waters bathing the reef.
X_6 Coral polyps	*Agaricia*, *Colpophyllia*, *Diploria*, *Helioseris*, *Madracis*, *Millepora*, *Montastrea*, *Porites*, *Stephanocoenia*, and others.
X_7 Plankton feeders	Sponges, sea anemones, pelecypods, some annelids, crinoids, tunicates.
X_8 Pathogens	Probably blue-green algae.

TABLE 9.1 (Continued)

Category		Composition
X_9	Coralivores	*Hermodice*, *Diadema*, *Coralliophaga*, some crabs, some fishes (butterflyfishes, parrotfishes, and wrasses).
X_{10}	Herbivores	Some mollusks, small crustaceans, butterflyfishes, and parrotfishes.
X_{11}	Detritivores	Meiofauna, small macrofauna, some annelids, mollusks, echinoderms (sea urchins, sea cucumbers, brittle stars, some starfishes), some fishes.
X_{12}	Omnivores	Some mollusks, annelids, crustaceans, and fishes (butterflyfishes, damselfishes, filefishes, squirrelfishes, surgeonfishes, grunts, puffers, triggerfishes, and trunkfishes).
X_{13}	Transient predators	Sharks, some rays, dolphins, jacks, barracudas, mackerels, tunas, and others.
X_{14}	Resident predators	Some mollusks (*Conus*), some annelids (nereids) some crustaceans (crabs), some fishes (eels, snappers, groupers, goatfishes, gobies).
Storage Compartments		
X_{15}	Particulate organic detritus	Decomposing organic matter (including dead plants and animals plus secretions and egestions). Bacteria, fungi, and other decomposing microbes are also included in this group.
X_{16}	Calcareous substratum	Reef rock and pieces of calcareous material derived from mechanical breaking of stony corals, calcareous algae, mollusks, echinoderms, serpulid worms, and barnacles.

Table 9.2 Input-Output Characteristics of Reservoirs of the East Flower Garden Coral Reef Conceptual Model

Reservoir	Receives input from	Gives output to
X_1 Phytoplankton	Advective import Zooxanthellae	Zooplankton Particulate organic detritus Export
X_2 Zooxanthellae	Light Nutrients (N,P) Coral polyps	Phytoplankton Coral polyps
X_3 Soft algae	Light Nutrients (N,P)	Herbivores Particulate organic detritus
X_4 Coralline algae	Light Nutrients (N,P,Ca)	Particulate organic detritus Calcareous debris
X_5 Zooplankton	Advective import Phytoplankton	Plankton feeders Coral polyps Particulate organic detritus Export Respiration
X_6 Coral polyps	Zooxanthellae Zooplankton Nutrients (Ca)	Zooxanthellae Pathogens Coralivores Particulate organic detritus Respiration Calcareous debris
X_7 Plankton feeders	Zooplankton	Omnivores Transient predators Resident predators Particulate organic detritus Respiration
X_8 Pathogens	Coral polyps	Respiration Particulate organic detritus

Table 9.2 (Continued)

Reservoir	Receives input from	Gives output to
X_9 Coralivores	Coral polyps	Omnivores Transient predators Resident predators Particulate organic detritus Respiration
X_{10} Herbivores	Soft algae	Omnivores Transient predators Resident predators Particulate organic detritus Respiration
X_{11} Detritivores	Particulate organic detritus	Omnivores Transient predators Resident predators Particulate organic detritus Respiration
X_{12} Omnivores	Plankton feeders Coralivores Herbivores Detritivores Particulate organic detritus	Transient predators Resident predators Particulate organic detritus Respiration
X_{13} Transient predators	Advective import Plankton feeders Coralivores Herbivores Detritivores Omnivores	Export Particulate organic detritus Respiration
X_{14} Resident predators	Plankton feeders Coralivores Herbivores Detritivores Omnivores	Particulate organic detritus Respiration

Table 9.2 (Continued)

Reservoir	Receives input from	Gives output to
X_{15} Particulate organic detritus	Advective imports Phytoplankton Zooplankton Coral polyps Soft algae Coralline algae Plankton feeders Coralivores Herbivores Detritivores Omnivores Transient predators Resident predators	Detritivores Omnivores Respiration Export
X_{16} Calcareous debris	Corals Coralline algae	

considered as an advective input rather than as a resident and locally metabolizing entity. Phytoplankton impinging upon the reef was produced elsewhere.

The nutrient calcium is essential for the formation of calcium carbonate by coralline algae and coral polyps. Sufficient carbon (bicarbonate) is probably derived from internal metabolism, and in any event, the level of inorganic carbon in seawater is sufficiently high so that it would never be considered a limiting nutrient.

A symbiotic relationship between zooxanthellae and coral polyps is shown by the fact that each of these compartments both gives and receives from the other.

Calcareous debris, derived from coralline algae and coral polyps, is a dead-end storage which contributes to no other compartment.

Particulate organic detritus is contributed by every living compartment except zooxanthellae, and the latter contribute through the phytoplankton. The detritus compartment is here defined to include all microbial organisms associated with particulate organic material. This is reasonable insofar as virtually all of the decomposers are adherent to detritus. Eliminating the necessity for a special decomposer compartment greatly simplifies the model.

All animal groups show respiratory loss. Although respiration may exceed photosynthesis in the producer groups, consideration of their respiratory loss is not essential to the success of the model, and it is, therefore, ignored. The nature of the pathogens has not been clearly established, so they are shown to have respiratory loss. Since microbes are included in the particulate organic detritus category, this compartment also exhibits a respiratory loss.

The remaining input-output functions should be fairly obvious and require no further comment.

The resulting flow diagram or conceptual model is presented in Figure 9.1. This model has been kept as general as possible so that it could be used to model the flow of calories or of specific chemical elements. Shapes of the various symbols follow the energy circuit language of Odum (1972). Features of the conceptual model are discussed below.

The primary attached reef structure consisting of corals (with zooxanthellae), leafy algae, and coralline algae is shown within the heavy rectangle. Although some of the animal species (sponges, tunicates, etc.) are also attached, no good purpose is served by placing some of each consumer group inside and some outside of the rectangle.

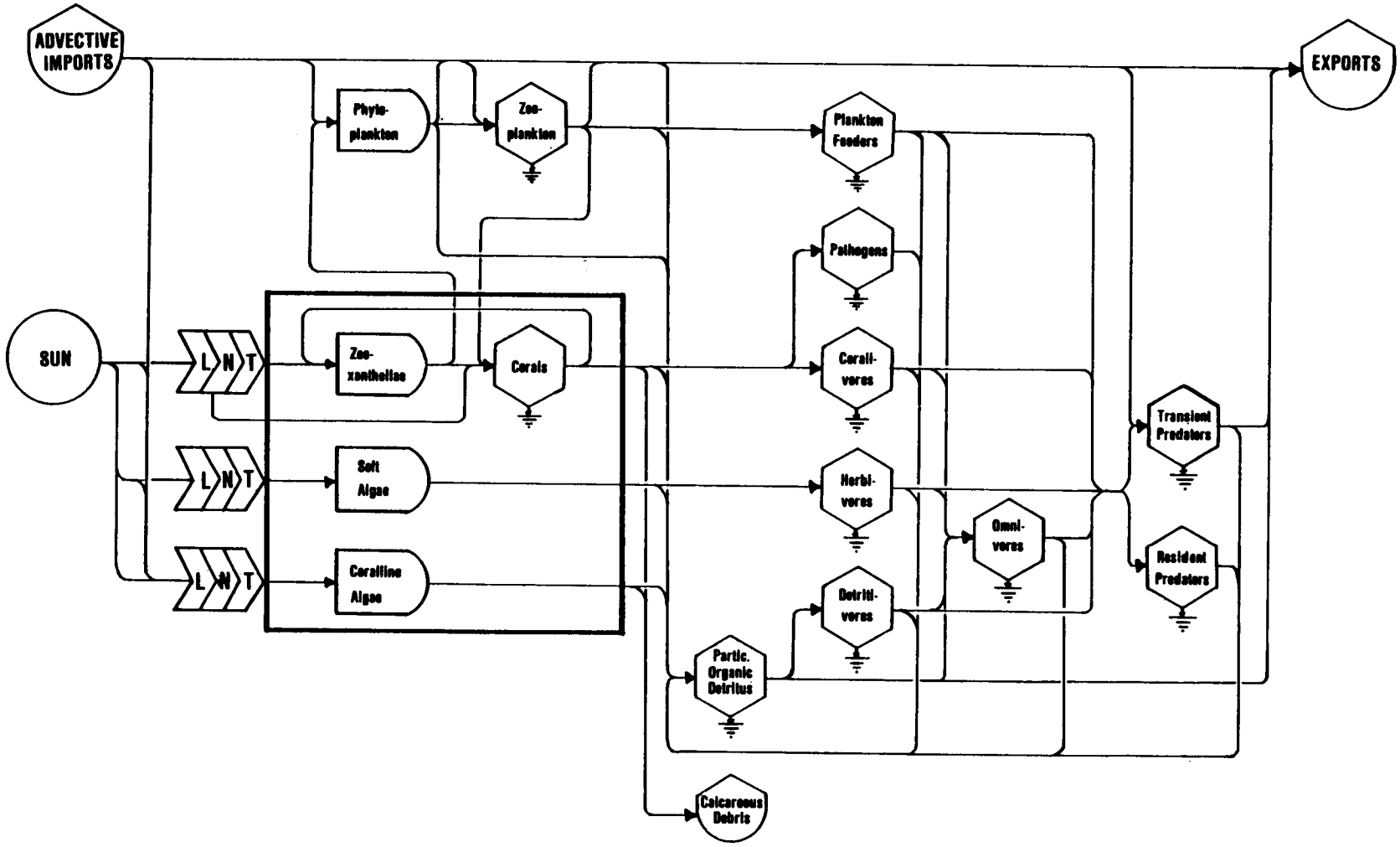

Figure 9.1 East Flower Garden reef - conceptual model.

Advective imports are shown sweeping over the reef, contributing materials, picking up materials, and passing away as advective exports.

Radiant energy from sunlight is shown as an external forcing function giving input to the producers of the reef.

Light (L), nutrients (N), and temperature (T) are shown as determinants of photosynthesis by the producers of the reef, but not by the phytoplankton because of its brief residence in the area (as mentioned earlier).

The four producer compartments are lined up in a single vertical column for ease of visualization.

One nutrient, calcium, is shown as an input to the coral polyps, which require this element for skeletal formation.

The symbiotic relationship between zooxanthellae and coral polyps is indicated.

Respiratory loss (which is an energy and carbon sink) is depicted by the electrical "ground" symbol at the bottom of each consumer compartment, as well as the particulate organic detritus compartment.

Calcareous debris is shown receiving input from corals and coralline algae.

Particulate organic detritus, which receives input from most other compartments (and advected imports), contributes to the detritivores and omnivores (and advective exports).

Consumer species are lined up vertically in columns roughly representing trophic levels.

Omnivores are shown receiving input from the various lower trophic levels and from particulate organic detritus.

Transient predators are shown associated with both import and export; together with the resident predators they receive input from the various lower trophic levels.

An effort has been made to line up a food resource and its consumer groups on the same horizontal line to facilitate visual comprehension.

In order to arrive at a visually simple model, it has been necessary to omit certain compartments and pathways, and some of these intentional omissions should be addressed.

Phytoplankton dependence upon light and nutrients has been omitted because it is not needed. As mentioned above, phytoplankton consumed on the reef was produced elsewhere.

Producer respiration has not been included because one is more interested in net rather than gross primary production. For very precise model evaluation it could easily be included.

Two intentional but potentially serious omissions are the recruitment of young from external sources and production, and loss of reproductive products (gametes, eggs, larvae, etc.) by the various living compartments. These could easily be depicted in the model by showing advective import into each of these compartments and advective export from each. However, to include all these imports and exports would considerably increase the number of pathways depicted, and this, in turn, would obscure the chief features for which the model was constructed. Any detailed attempt to evaluate the model would have to take these inputs and outputs into account.

For some purposes it might be desirable to divide the consumer species differently or to increase the number of consumer compartments (e.g., sedentary vs. mobile plankton feeders). In the present context, this appears to be unnecessary proliferation.

The particulate organic detritus compartment might well have been allocated to two different compartments (i.e., microbes in one and substrate in another). However, considering the intimacy of the association, little is to be gained by such a separation.

As it stands, the conceptual model displays the key features of trophic flow through the coral reef system and the relationships of the system with the ambient water column. In the opinion of the authors it is also the simplest, clearest, and most economical expression of the underlying relationships of the total functioning ecosystem.

Graphical Model

With the conceptual model developed, it becomes necessary to establish how the flows take place along each pathway. Throughout, it must be kept in mind that the actual quantity of flow along a given pathway will relate not only to how the flow occurs but also to the size of each compartment. For example, the flow from phytoplankton to zooplankton might be characterized by a certain graphical function, but the quantity of flow would also relate to the standing stock of phytoplankton and the standing stock of zooplankton. In the present section, interest centers only on graphical representation of how flows occur along the pathways. To

avoid dealing in pure abstraction, we will assume that our concern is the flow of calories through the system.

Primary Production

The most complex pathways are associated with primary production because light, temperature, and nutrients are all involved and because analysis of the light factor includes several steps. In effect, light availability sets the maximum possible level of photosynthesis, while nutrient availability and ambient temperature establish the degree to which this maximum can be realized. Each of these factors will be examined, in turn.

Light Limitation

Conceptually we must determine the amount of solar radiation (within the photosynthetically useful spectrum) striking the upper atmosphere on a daily basis throughout the year. Next we must ascertain what portion of this light reaches the sea surface, both as direct illumination and as backscatter, assuming clear days. This is then appropriately modified to take into consideration cloud cover (from cloudy days). Account may be taken of the distribution of light throughout the 24-hour day. Next the light at the level of the reef must be determined by considering light penetration through the water column as modified by suspended matter (including the nepheloid layer, if necessary). Once we know the daily and seasonal distribution of light striking the reef, we must determine how the light is used by the several groups of producers. Each producer group exhibits its own threshold below which light is not useful (i.e., reef-building corals have a higher threshold than leafy algae, and these in turn, have a higher threshold than coralline algae). Above the threshold, but still at low light intensities, light utilization for photosynthesis is nearly linearly related to light intensity. With increase in light intensity there is a leveling off of photosynthesis (in the optimum range), followed at even higher light intensities by a reduction in photosynthesis due to photo-inhibition. Specific characteristics of the light utilization curve vary among the different producer groups.

In the graphical model (Figure 9.2) the essential features of the light limitation function are displayed in seven graphs, four describing light getting to the reef and three showing its utilization by the producer groups. Each of these graphs is described in the following pages.

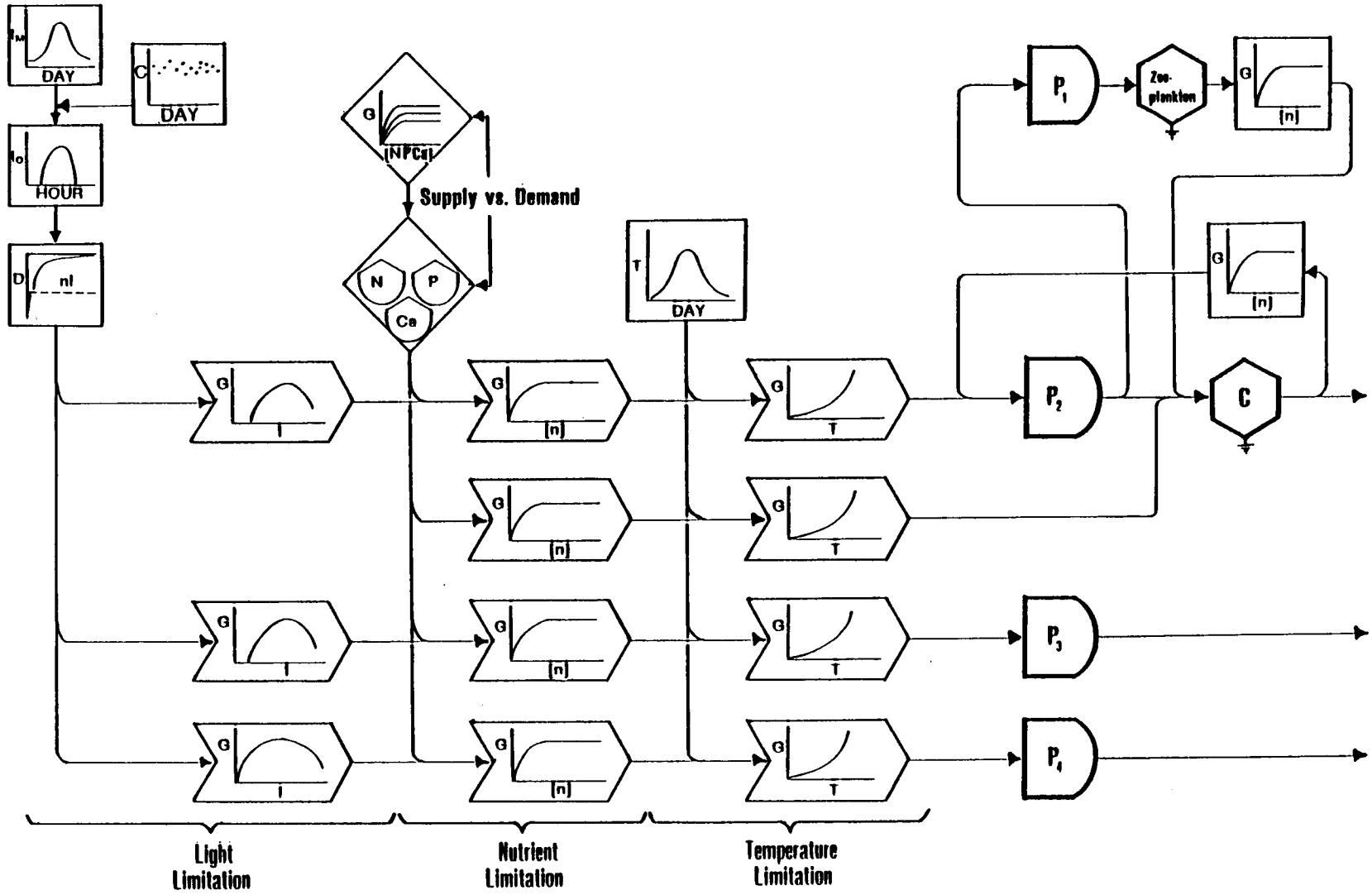

Figure 9.2 East Flower Garden reef - graphical model of producers and coral polyps. Capital letters $P_1 \ldots P_4$ refer to phytoplankton, zooxanthellae, soft algae, and coralline algae, respectively. C refers to coral polyps. Letters on the graphs and the equations for the graphs are explained in Table 9.3.

§Light reaching the sea surface follows a bell-shaped curve beginning and ending with the shortest day of the year (December 21) and peaking on the longest day of the year (June 21).

§Cloud cover is a variable factor. The average number of cloudy days per month can be obtained from meteorological atlases and applied to the local situation.

§The distribution of surface light during the 24-hour period is a truncated bell-shaped curve because there is no effective light between sunset and sunrise.

§Once in the water column light intensity decreases exponentially with depth. Presence of suspended matter in the water column hastens the extinction, and the presence of a nepheloid layer (nl) substantially reduces the light passing through it.

§Photosynthesis (expressed here as net production) of all producer groups is characterized by more-or-less paraboloid curves in which the ascending arm is nearly linear for lower photosynthetically-effective light levels. The light intensity threshold for production is highest for zooxanthellae and lowest for the coralline algae.

Nutrient Limitation

The nutrient factor operates through a supply versus demand relationship. In effect, at low nutrient concentrations nutrient uptake is more-or-less linearly related to availability. Eventually, as saturation is approached, uptake levels off, and further increase in the supply of nutrients does not result in further uptake. Nutrient uptake kinetics follow the classical Michaelis-Menton enzyme-substrate kinetics. Details of uptake rate and saturation level may vary with each type of nutrient, but the nutrient present in least supply (in relation to demand) will be the one which limits the production rate.

Temperature Limitation

The temperature of the sea surface (and presumably, the mid-depth) varies throughout the year in bell-shaped curve fashion (from coldest to warmest and back to coldest periods of the year). Primary production is related to temperature by an exponential function.

Zooxanthellae Dependence Upon Coral Polyps

It is presumed that the coral polyps furnish the zooxanthellae with certain types of nutrients (ammonium, etc.), and the relationship is presumed to follow the supply and demand curve discussed earlier.

Advective Imports and Exports

Graphs have not been drawn for import/export functions, but these relations will be addressed briefly. The availability of passive import materials (nutrients, phytoplankton, zooplankton, and particulate organic detritus) depends upon their concentrations in the water column (at the appropriate depth levels) and the rate of water movement. Water movement, in turn, may reflect current flow and other advective properties of the water masses bathing the reef. Import of transient predators relates to their availability on the continental shelf and in nearby waters as well as their ability to locate the reef system. A first order estimate of their ability to find the reef would be to assume a rate of searching and a random encounter relationship. If olfactory or other cues are assumed, then the reef influence would exhibit considerably greater dimensions in the downstream directions. Recruitment of young to the resident reef populations could take place through the passive zooplankton transport pathway or through the active random search method. Active or passive recruitment could be highly seasonal, depending on the species.

Export of passive materials (phytoplankton, zooplankton, gametes, larvae, and particulate organic detritus) would relate to the quantities and buoyant properties of the materials and to the velocity and persistence of the water flowing over the reef. Export of transient predators would relate to some calculation of their hunting efficiency and patience. At some point a hungry predator will move on.

Secondary Production

Although the various consumer species exhibit a great diversity of life styles, these are all variations on a few basic themes. All must feed, respire, egest, and reproduce. Young may develop and mature locally or be exported from the reef (at any of several developmental stages). On the other hand, the local population may receive recruitment from outside the reef (at any of several developmental stages). Predatory loss may occur at any stage of the life history.

These general life history features of a consumer species are displayed in Figure 9.3. Graphical representation has been provided for the more important pathways, and these graphs are discussed below.

§Food intake follows the same function as nutrient uptake, described earlier. At low food levels intake is linearly related to food availability, but as the consumer approaches satiation there is a leveling off, and increase in food availability does not result in increased food intake. Food intake is also related to temperature, and temperature may show daily and seasonal variation.

§Respiration is exponentially related to temperature for all life stages.

§Eggs neither feed nor egest.

§Hatching of eggs is a function of developmental time; that is, from a given brood the percentage of unhatched eggs decreases with time.

§Growth of larvae and juveniles is exponentially related to temperature.

§Although not depicted graphically, predatory loss is a feeding relationship of the type described above. Food intake increases linearly at first and then levels off when the predators are no longer hungry.

The relationships depicted in Figure 9.3 have been applied to a single consumer species, any consumer species of the reef. However, it should be evident that the same model displays the features of a multi-species consumer compartment as depicted in Figure 9.1. When applied to a multi-species compartment, the pathways of the consumer model take on statistical properties. For example, some species of the compartment may produce eggs, larvae, and juveniles which remain reef-resident, whereas others may engage in export/import, that is, dispersal of young and recruitment from outside the reef. When applying the model to a multi-species compartment, one is concerned with the percentage of species and individuals utilizing each of the available pathways or the percentage of calories flowing along each pathway. Thus, this same consumer model may be used to represent each of the consumer compartments in the general conceptual model of the reef ecosystem.

Elements of a Mathematical Model

In the development of equations for the various pathways of the ecosystem model, an effort has been made to keep the expressions as

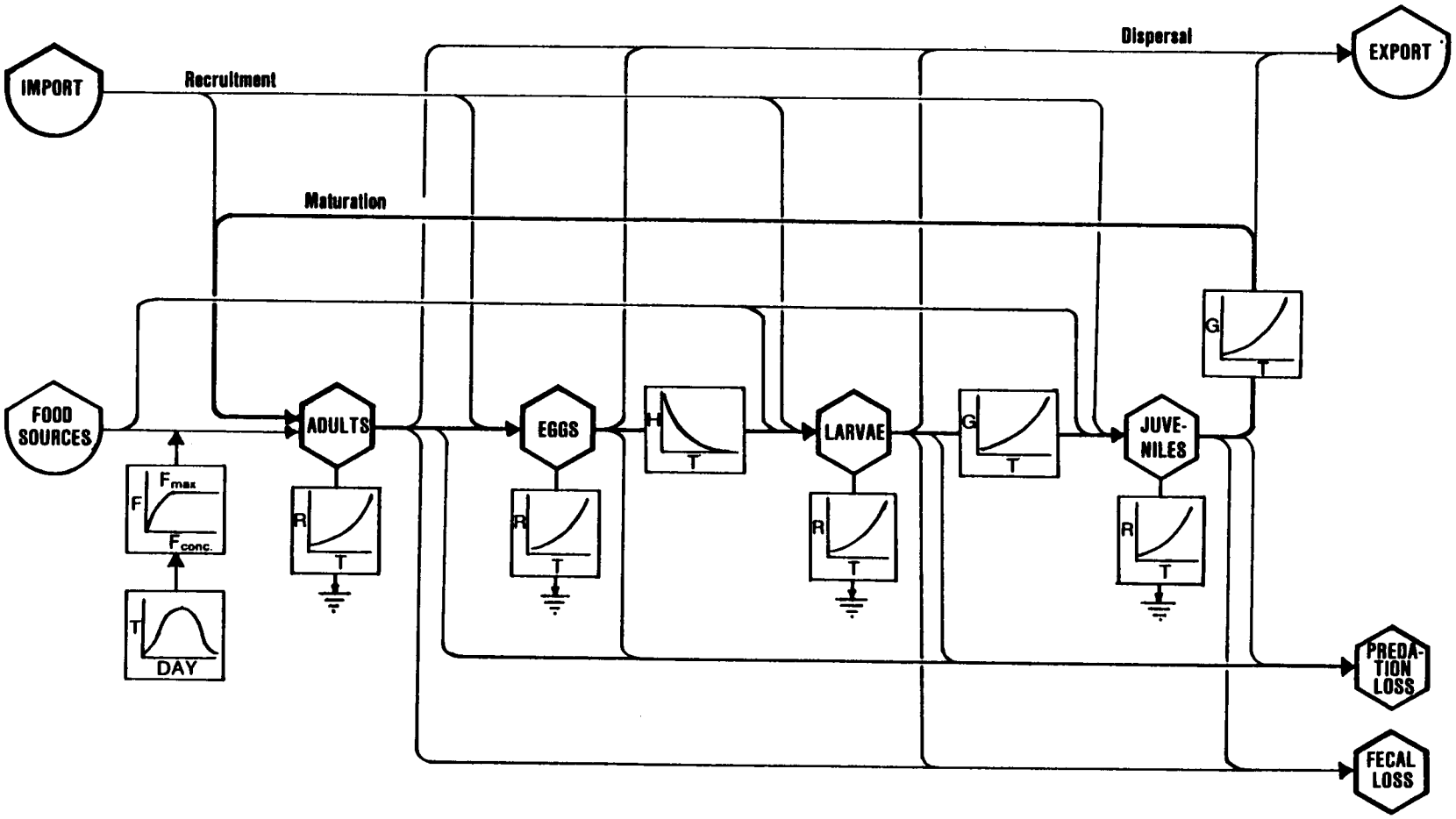

Figure 9.3 East Flower Garden coral reef - conceptual and graphical model of consumer species.

simple as possible while still indicating the general nature of each relationship. For example, growth could be expressed as the addition of increments to the existing population or as the initial population multiplied by a constant incremental function. Addition was chosen because it is generally simpler than multiplication. Where constants are indicated (by Greek letters), they could stand for a single number or a more complex formulation. For a fully effective mathematical model of the Flower Garden ecosystem some of the equations would have to be expanded, but given the present limited data base, the simpler expressions should be sufficient. In the development of the equations the authors have been guided by the work of Kremer and Nixon (1975). Explanatory notes concerning some of the equations follow.

Equations Relating to Primary Production (Table 9.3)

Equations 1 to 5 deal with the problems of getting solar radiation from the upper atmosphere down to the level of the reef.

Equation 1: Several complex steps are involved in getting light from the upper atmosphere to the sea surface; these will be explained in the next section. However the equation, as written, is adequate to express the incident clear-sky radiation at the sea surface.

Equation 2: The number of cloudy days (c) will vary from month to month, and the light reduction factor (γ) varies with the nature of the cloud cover.

Equation 4: The concentration of suspended matter (s) in the water column varies widely, and the light reduction factor (ε) due to the suspended matter likely varies with the nature of the suspended material (e.g., plankton vs. inorganic material). It is assumed that light reduction by the nepheloid layer is a simple function of the concentration of suspended matter.

Equations 6 and 7 relate to how the plants utilize the incident light for photosynthesis. Therefore, the constants in these equations would be different for each group of producers.

Equation 8 concerns the nutrient limitation problem; the constants would vary with each producer group and each nutrient. As stated earlier, the single limiting nutrient for each species is what is really important.

Equation 9 expresses the effect of water temperature on primary production. As in the case of the light factor, water temperature around the reef affects all the producer species, but the actual production response would be species-specific.

Equations 10 and 11: These equations simply bring the effects of light, nutrients, and temperature into single statements related to producer growth and standing crop.

Equations Relating to Secondary Production (Production of Consumer Species) (Table 9.4)

Adults

Equation 12 provides a general expression for the size of any adult consumer population at any time (t). It does not assume a constant growth rate of individuals in a population, but it could be converted to such by expressing the initial part of the equation as follows:

$$A_t = A_o . e^{\omega'[FOOD_A - (FEC_A + RESP_A + EGGS_A)]}$$

where ω is a constant relating food intake and metabolism to population growth.

Equations 13 to 16 deal with metabolism and reproduction. Growth of individual consumers has not been spelled out, but it is indicated by the expression $[FOOD_A - (FEC_A + RESP_A + EGGS_A)]$; that is, food intake minus egestive and metabolic losses gives accumulation.

Equation 13: Two expressions are provided for food intake. The linear relationship (Equation 13a) would apply only under conditions of low to moderate food availability. Such would likely be the case for most consumers most of the time.

Equation 14: Fecal loss may represent loss of a constant percentage of the ingested food, or the relationship may be more complex. In some species, higher feeding rates are accompanied by lower assimilation percentages. In this instance the constant (τ) would represent a variable percentage.

Equation 15: In all species, respiration is a function of temperature. However, it is also a function of body size. In order to keep the model within bounds, the latter relationship has not been indicated, but any detailed modeling effort would have to take

account of the respiration/body size relationship. This equation takes the following form:

$$\text{Respiratory loss} = \sigma' \, W\tau'$$

where W is body weight
and σ' and τ' are constants.

Equation 16: This equation more properly should express total gamete production since males do not produce eggs. However, on a population basis, egg production would be the major drain on energy and material resources.

Equations 17 to 20 concern additions to and losses from the adult population.

Equation 18 requires explanation. Recruitment may involve active searching by mobile individuals (as expressed in the equation) or passive transport of relatively immobile individuals. In either instance the density of individuals in the search area (ϕ) and effective area of the reef influence (κ) would be involved. However, for passive searchers the search factor (ι) would relate to transport by water currents. Since most adults are mobile, they would generally conform to the active search mode.

Eggs, Larvae, and Juveniles

Equations 21 to 27 represent egg production, metabolism, recruitment, and loss phenomena. Eggs do not feed or produce fecal matter. Otherwise, the egg equations parallel those for adults and require no special clarification.

Equations 28 to 36 express larval relations and require no additional comment.

Equations 37 to 45 express juvenile relations and require no comment.

Equations Relating to Storage Compartments (Table 9.5)

Particulate Organic Detritus Compartment (Equations 46 to 60)

Equation 46 provides a general expression for the size of the particulate organic detritus compartment at any time (t). Since this compartment receives contributions from practically all others, the equation contains many additive factors. Losses are due to microbial respiration, consumption by detritivores and omnivores,

and advective export. Much detritus is probably added when turbulent water associated with storms tears up portions of the reef. To include possible storm effects would require additional (and generally unknown) terms in each equation. While recognizing that this might be a significant problem, we have chosen to keep the models and equations simple for the present.

Equation 47: As it stands, this equation states that advective import of particulate organic detritus to the reef system is some function of the concentration of the material in the water column and the velocity of the water flow across the reef. In actuality, the situation is probably far more complex than this, but the present formulation should be a reasonable first order approximation.

Equation 48: The same general comments apply to the addition of phytoplankton to the reef detritus pool.

Equation 49: Zooplankton contributes to the local detritus pool through death and also through production of fecal pellets which are brought to the reef.

Equation 50: Coral polyps contribute both through egestion and mucus production.

Equations 51, 52, and 54: It is assumed that a regular percentage of the soft algae, coralline algae, and pathogens is lost through natural death or incidental to feeding by herbivores. Actually, much is probably lost to the detritus pool through storms, as well.

Equations 53 and 55 to 60 deal with contributions of various consumer groups through fecal loss. Other losses by these groups (through natural mortality, secretions, etc.) are probably negligible by comparison.

Equations 61 to 64 deal with losses from the particulate organic detritus compartment through microbial respiration, consumer feeding, and advective export. Most consumer species probably ingest some organic detritus incidental to other feeding, and collectively this could constitute a significant loss. However, to add a detritus food input factor to each consumer compartment would unduly complicate the models and equations.

Equation 64 concerns detritus loss due to advective export. Here it is assumed that the quantity exported is a simple function of the amount of particulate organic detritus present on the reef and the velocity of the water sweeping the reef. As in the case of advective import, the situation is probably more complex than this, but the present equation is a reasonable first order statement.

Table 9.3 General Form of Equations Used to Describe Pathways Affecting Primary Production in the Models of the East Flower Garden Coral Reef Ecosystem. Letters of the Greek alphabet signify constants which must be evaluated in the development of an applied mathematical model.

<u>Light limitation (LTLIM)</u>

(1)	Total clear sky daily-incident solar radiation at sea surface	$I_M = \alpha + \beta \cos \left[\frac{2\pi\ (\text{day} + 10)}{365} \right]$ where α and β are constants relating to latitude
(2)	Sea surface incident radiation, taking into account reduction due to cloud cover	$I_o = I_M(1.0 - \gamma c)$ where c is the number of cloudy days (calculated on a monthly basis), and γ is the light reduction factor due to clouds
(3)	Light intensity at depth (d) in the water column	$I_d = I_o e^{-\kappa d}$ where d is depth in the water column (in meters), and κ is the extinction coefficient of light in clear oceanic water
(4)	Extinction coefficient corrected for reduced light penetration due to suspended matter	$K_o = \kappa(1 - \epsilon s)$ where s is the concentration of suspended matter, and ϵ is a constant relating suspended matter to light reduction
(5)	Photoperiod description	$I_p = \zeta I_f$ where I_f is the illumination at depth during the daily photoperiod (expressed as a square wave function), and ζ is the correction to a halfwave sinusoidal function

Table 9.3 (Continued)

(6)	Averaging light (over 3-day periods) to account for light acclimation by the producers	$I_{opt} = (\eta I_1' + \theta I_2' + \iota I_3')$ where I_1', I_2', and I_3' are the average light levels at depth for day-1, day-2, and day-3, respectively, and η, θ, and ι are constants for weighting the influence of each of the preceding days
(7)	Plant growth as a function of (weighted) available light	$P = \lambda I_{opt} - \mu$ where P is plant growth, and λ and μ are constants (representing the slope of the line and the y-intercept, respectively)

Nutrient limitation (NUTLIM)

(8)	Plant growth in relation to concentration of a given nutrient	$G = G_M \left[\frac{[\nu]}{K_{s_\nu} + [\nu]} \right]$ where G_M is maximum growth under optimum nutrient concentrations, $[\nu]$ is the actual availability of a given nutrient, and K_s is the half saturation constant for growth (in relation to that particular nutrient)

Temperature limitation (TPLIM)

(9)	Plant growth in relation to temperature	$G_T = e^{\rho T - \sigma}$ where G_T is the daily growth rate at a given temperature, ρ and σ are constants, and T is water temperature, which is assumed to vary on a seasonal basis according to a cosine function: $T = \tau - \nu \cos \left[\frac{2\pi\ (\text{day} - \phi)}{365} \right]$ where τ and ν are constants and ϕ is the average coldest day of the year

Table 9.3 (Continued)

<u>General primary production equations</u>		
(10)	Plant growth (net daily production) for a given producer compartment	$G_p = G_{MAX}(LTLIM)(NUTLIM)(TPLIM)$ where G_{MAX} is the maximum plant growth potential under optimum conditions
(11)	Producer standing crop at any time (t)	$P_t = P_o e^{(G_p - X_{(a,b,c...n)})}$ where P_t is the standing crop of producers in any compartment at time (t), G_p is plant growth (as defined above), and $X_{(a,b,c...n)}$ is losses due to consumers, export, and particulate organic detritus production

Table 9.4 General Form of Equations Used to Describe Pathways Affecting Secondary Production in the Models of the East Flower Garden Coral Reef Ecosystem. Constants which must be evaluated in the development of an applied mathematical model are signified by letters of the Greek alphabet. However, a given Greek letter appearing in this and the preceding table may signify different constants in the two tables.

Adult Consumers

General equation for the size of an adult consumer population at time (t)

$$(12)\quad A_t = A_o + [FOOD_A - (FEC_A + RESP_A + EGGS_A)] + (MAT_J + RECR_A) - (DISP_A + PRED_A)$$

where: A_o is the size of the initial adult population

$FOOD_A$ is food intake

FEC_A is unassimilated food or fecal loss

$RESP_A$ is respiratory loss

$EGGS_A$ is reproductive loss due to egg production

MAT_J is maturation of resident juveniles into the adult population

$RECR_A$ is addition to the adult population by recruitment from outside the reef area

$DISP_A$ is loss of adults through dispersal from the reef

$PRED_A$ is loss of adults through predation

Each of these terms is defined in greater detail below.

Table 9.4 (Continued)

Food, metabolism, and reproduction

(13a) Food intake (daily ration), assuming a linear relationship between feeding and food

$$FOOD_A = \alpha(a + b + c...n)$$

where α is a relationship between feeding rate and food availability and a,b,c,...n are the different food sources utilized (each of which could be modified by availability constants)

(13b) Food intake (daily ration), assuming an Ivlev type feeding relationship

$$FOOD_A = FOOD_{MAX}(1 - e^{-\beta(a + b + c,...n)})$$

where $FOOD_{MAX}$ is the maximum food intake under conditions of food excess, β is a constant relating to feeding rate, and a,b,c,...n are different food sources utilized

(14) Fecal loss

$$FEC_A = \gamma FOOD_A$$

where γ represents a percentage of the ingested food

(15) Respiration in relation to temperature

$$RESP_A = \delta T$$

where δ is the Q_{10} value for adult respiration, and T is the ambient temperature.
Note: T is defined as

$$T = \tau + \nu\cos\left[\frac{2\pi\ (day-\phi)}{365}\right]$$

(see equation 9)

(16) Egg production by adults

$$EGGS_A = \epsilon A$$

where A is the adult population, and ϵ is the rate of egg production by the adults

Population additions and losses

(17) Maturation of juveniles into adults

$$MAT_J = \zeta J - \eta$$

where J is the juvenile population, ζ is the maturation rate of juveniles (as modified by temperature), and η is loss of juveniles (through dispersal and predation)

Table 9.4 (Continued)

(18)	Recruitment of adults from outside the reef area	$RECR_A = \theta\iota\kappa$ where θ is the density of adults in the search area, ι is the rate of searching, and κ is the effective area of reef influence
(19)	Dispersal loss by the adult population	$DISP_A = \lambda A$ where A is the adult population, and λ is the fraction of the adult population which leaves per unit of time
(20)	Predation loss by the adult population	$PRED_A = \mu A$ where A is the adult population, and μ is the average rate of loss due to predation Note: This equation might be written as follows. $PRED_A = Ae^{-\nu P}$ where P is the abundance of predators, and ν is a factor depicting the predation rate. Thus, $\mu = e^{-\nu P}$

Eggs of Consumers

General equation for the size of the consumer egg population at time (t)

(21) $E_t = E_o - RESP_E + (EGGS_A + RECR_E) - (MAT_E + DISP_E + PRED_E)$

where: E_o is the size of the initial egg population

$RESP_E$ is respiratory loss

$EGGS_A$ is the contribution to the egg population by resident adults

Table 9.4 (Continued)

$RECR_E$ is addition to the local egg population by recruitment from outside the reef area

MAT_E is loss of eggs through maturation to larvae

$DISP_E$ is loss of eggs through dispersal from the reef

$PRED_E$ is loss of eggs through predation

Metabolism

(22)	Respiration in relation to temperature	$RESP_E = \delta' T$ (see equation 15)

Population additions and losses

(23)	Contribution of eggs by local adults	$EGGS_A = \epsilon A$ (see equation 16)
(24)	Recruitment of eggs from outside the reef area	$RECR_E = \theta' \iota' \kappa'$ (see equation 18)
(25)	Maturation rate of eggs expressed as hatching time (in days)	$MAT_E = \xi e^{-\rho T}$ where ξ and ρ are rate constants, and T is the temperature
(26)	Dispersal loss by the egg population	$DISP_E = \lambda' E$ (see equation 19)
(27)	Predation loss by the egg population	$PRED_E = \mu' E$ (see equation 20)

Table 9.4 (Continued)

Larvae of Consumers

General equation for the size of the consumer larva population at time (t)

(28) $L_t = L_o + [FOOD_L - (FEC_L + RESP_L)] + (MAT_E + RECR_L) - (MAT_L + DISP_L + PRED_L)$

where: L_o is the size of the initial larval population

$FOOD_L$ is food intake

FEC_L is unassimilated food or fecal loss

$RESP_L$ is respiratory loss

MAT_E is maturation of eggs into the larval population

$RECR_L$ is addition to the local larval population by recruitment from outside the reef area

MAT_L is loss of larvae through maturation to juveniles

$DISP_L$ is loss of larvae through dispersal from the reef

$PRED_L$ is loss of larvae through predation

Food and metabolism

(29) Food intake (daily ration) $FOOD_L = \alpha''(a + b + c...n)$ (see equation 13)

(30) Fecal loss $FEC_L = \gamma''FOOD_L$ (see equation 14)

(31) Respiration in relation to temperature $RESP_L = \delta''T$ (see equation 15)

Population additions and losses

(32) Maturation rate of eggs into larvae $MAT_E = \xi e^{-\rho T}$ (see equation 25)

Table 9.4 (Continued)

(33)	Recruitment of larvae from outside the reef area	$RECR_L = \theta''\iota''\kappa''$ (see equation 18)
(34)	Maturation rate of larvae	$MAT_L = \xi' e^{-\rho' T}$ (see equation 25)
(35)	Dispersal loss by the larval population	$DISP_L = \lambda'' L$ (see equation 19)
(36)	Predation loss by the larval population	$PRED_L = \mu'' L$ (see equation 20)

Juveniles of Consumers

General equation for the size of the consumer juvenile population at time (t)

(37) $$J_t = J_o + [FOOD_J - (FEC_J + RESP_J)] + (MAT_L + RECR_J) - (MAT_J + DISP_J + PRED_J)$$

where: J_o is the size of the initial juvenile population

$FOOD_J$ is food intake

FEC_J is unassimilated food or fecal loss

$RESP_J$ is respiratory loss

MAT_L is maturation of larvae into the juvenile population

$RECR_J$ is addition to the local juvenile population by recruitment from outside the reef area

MAT_J is loss of juveniles through maturation to adults

$DISP_J$ is loss of juveniles through dispersal from the reef

$PRED_J$ is loss of juveniles through predation

Food and metabolism

(38)	Food intake (daily ration)	$FOOD_J = \alpha'''(a + b + c...n)$ (see equation 13)

Table 9.4 (Continued)

(39)	Fecal loss	$FEC_J = \gamma'''FOOD_J$ (see equation 14)
(40)	Respiration in relation to temperature	$RESP_J = \delta'''T$ (see equation 15)
	<u>Population additions and losses</u>	
(41)	Maturation rate of larvae into juveniles	$MAT_L = \zeta'L - \eta'$ (see equation 17)
(42)	Recruitment of juveniles from outside the reef area	$RECR_J = \theta'''\iota'''\kappa'''$ (see equation 18)
(43)	Maturation of juveniles into adults	$MAT_J = \zeta J - \eta$ (see equation 17)
(44)	Dispersal loss by the juvenile population	$DISP_J = \lambda'''J$ (see equation 19)
(45)	Predation loss by the juvenile population	$PRED_J = \mu'''L$ (see equation 20)

Table 9.5 General Form of Equations Used to Describe Pathways Relating to Storage Compartments of the East Flower Garden Coral Reef Ecosystem. Greek letters signifying constants in the present table do not denote the same constants appearing in the two previous tables.

Particulate Organic Detritus Compartment

$$(46)\quad Pd_t = PD_o + (PD_{AI} + PD_{PP} + PD_{ZP} + PD_{CO} + PD_{SA} + PD_{CA} + PD_{PF} + PD_{PA} + PD_{CV} + PD_{HE} + PD_{DV} + PD_{OM} + PD_{TP} + PD_{RP}) - (RESP_{PD} + PDFOOD_{DV} + PDFOOD_{OM} + PD_{AE})$$

where: PD_t is the size of the particulate organic detritus pool at time (t)

PD_o is the initial size of the particulate organic detritus pool

PD_{AI} is the advective import contribution to the PD pool

PD_{PP} is the phytoplankton contribution to the PD pool

PD_{ZP} is the zooplankton contribution to the PD pool

PD_{CO} is the coral polyps contribution to the PD pool

PD_{SA} is the soft algae contribution to the PD pool

PD_{CA} is the coralline algae contribution to the PD pool

PD_{PF} is the plankton feeder contribution to the PD pool

PD_{PA} is the pathogen contribution to the PD pool

PD_{CV} is the coralivore contribution to the PD pool

PD_{HE} is the herbivore contribution to the PD pool

PD_{DV} is the detritivore contribution to the PD pool

PD_{OM} is the omnivore contribution to the PD pool

PD_{TP} is the transient predator contribution to the PD pool

PD_{RP} is the resident predator contribution to the PD pool

Table 9.5 (Continued)

$RESP_{PD}$ is the respiratory loss (due to microbes) from the PD pool

$PDFOOD_{DV}$ is the loss from the PD pool due to feeding by the detritivores

$PDFOOD_{OM}$ is the loss from the PD pool due to feeding by the omnivores

PD_{AE} is the loss from the PD pool due to advective export

Contributions to the particulate organic detritus compartment

(47) Advective import

$$PD_{AI} = \alpha PD_W e^{\beta V}$$

where PD_W is the PD concentration of the water bathing the reef, V is the velocity of the water, and α and β are constants relating settling rate to water velocity

(48) Phytoplankton contribution to the PD pool

$$PD_{PP} = \gamma PPe^{\delta V}$$

(see equation 47)

(49) Zooplankton contribution

$$PD_{ZP} = \epsilon ZPe^{\zeta v} + \eta FEC_{ZP} e^{\theta V}$$

where ZP is the zooplankton concentration of water bathing the reef, V is water velocity, ϵ and ζ are constants relating zooplankton import rate to water velocity, FEC_{ZP} is fecal production by the zooplankton, and η and θ are constants relating the import rate of zooplankton fecal pellets to water velocity

(50) Coral polyp contribution

$$PD_{CO} = \iota FOOD_{CO} + MUC_{CO}$$

where $FOOD_{CO}$ is food intake by coral polyps, ι is a factor relating food intake to fecal production, and MUC_{CO} is mucus production by the corals

Table 9.5 (Continued)

(51)	Soft algae contribution	$PD_{SA} = \kappa SA$ where SA is the soft algae population, and κ is a function representing loss of soft algae to PD
(52)	Coralline algae contribution	$PD_{CA} = \lambda CA$ (see equation 51)
(53)	Plankton feeder contribution	$PD_{PF} = \mu FOOD_{PF}$ where μ is a factor relating food intake to fecal production
(54)	Pathogen contribution	$PD_{PA} = \nu PA$ (see equation 51)
(55)	Coralivore contribution	$PD_{CV} = \xi FOOD_{CV}$ (see equation 53)
(56)	Herbivore contribution	$PD_{HE} = \rho FOOD_{HE}$ (see equation 53)
(57)	Detritivore contribution	$PD_{DV} = \sigma FOOD_{DV}$ (see equation 53)
(58)	Omnivore contribution	$PD_{OM} = \tau FOOD_{OM}$ (see equation 53)
(59)	Transient predator contribution	$PD_{TP} = \upsilon FOOD_{TP}$ (see equation 53)
(60)	Resident predator contribution	$PD_{RP} = \phi FOOD_{RP}$ (see equation 53)

<u>Losses from the particulate organic detritus compartment</u>

(61)	Respiratory loss	$RESP_{PD} = \chi T$ (see equation 15)

Table 9.5 (Continued)

(62)	Loss due to detritivore feeding	$PDFOOD_{DV} = \psi FOOD_{DV}$ where $FOOD_{DV}$ is the total food intake by the detritivores, and ψ is the fraction of the total food which is PD
(63)	Loss due to omnivore feeding	$PDFOOD_{OM} = \omega FOOD_{OM}$ (see equation 62)
(64)	Loss due to advective export	$PD_{AE} = \alpha' PDe^{\beta' V}$ where PD is the particulate organic detritus pool of the reef, V is velocity of the water bathing the reef, and α' and β' are constants relating water velocity to PD export

Calcareous Debris Compartment

(65) $CD_t = CD_o + (CD_{CO} + CD_{CA})$

where: CD_t is the size of the calcareous debris pool at time (t)

CD_o is the size of the initial calcareous debris pool

CD_{CO} is the contribution of the corals to the CD pool

CD_{CA} is the contribution of calcareous algae to the CD pool

(66)	Coral contribution to the CD pool	$CD_{CO} = \gamma' COFOOD_{CV}$ where $COFOOD_{CV}$ is the coral polyps grazed by the coralivores, and γ' is a factor relating coral debris formation to coralivore grazing
(67)	Coralline algae contribution to the CD pool	$CD_{CA} = \delta' CAFOOD_{CV}$ where $CAFOOD_{CV}$ is the coralline algae food of the coralivores, and δ' is a factor relating calcareous algae debris formation to coralivore grazing

Equations 65 to 67 relate to the calcareous debris compartment. In these equations it is assumed that the quantity of calcareous debris formed is a function of the feeding rates of consumers grazing the corals and coralline algae. It is likely that much of the debris comes from structural weakening by the various boring species, followed by mechanical agitation during storms. For more detailed modeling purposes, these factors would have to be evaluated and included.

PARTIAL EVALUATION OF MODEL FROM EXISTING DATA

As a general rule, it is highly desirable to develop the conceptual model prior to the field sampling program so that all the data required for model evaluation will be available. In the present instance the conceptual model was developed after the field work was completed, so the problem now becomes one of fitting available data to the conceptual system. Therefore, data for evaluation of the model are derived, in part, from studies carried out on the East Flower Garden coral reef, but they must be supplemented with information gleaned from the literature dealing with similar systems elsewhere. Considering the unique nature of the East Flower Garden reef, the applicability of transferred data is sometimes less than desirable, and the source of such introduced data is indicated. Thus, we emphasize strongly that the calculated values which appear in the following section are only gross estimates of reality. Standing crops, production, and growth are derived herein as an exercise to partially evaluate the model. Results should not be construed as truly representative of conditions at the Flower Gardens. They should, however, be at least within an order of magnitude of actuality and a base from which to approach second and subsequent approximations.

Environment and Advective Import

Light

In development of the light data the authors have been aided by Dr. Guy Franceschini of the Meteorology Department of Texas A&M University. Data provided in the Smithsonian Meteorological Table (List, 1966) have permitted calculations of the total daily solar radiation reaching the sea surface at the latitude of the East Flower Garden reef (Table 9.6 and Figure 9.4). This calculation includes both direct and indirect radiation, and it is based on the general assumption of 25% absorption by the atmosphere (by moisture and ozone). Cloud cover data were provided in the U.S. Naval Weather Service Summary of Synoptic Meteorological Observations for the Galveston area (Sabine Pass quadrant). Mean monthly cloud cover

Table 9.6 Calculation of Monthly Progression of Solar Radiation at the Sea Surface and at Various Water Depths†

Month	Average Surface Radiation: Cloudless Sky (cal/cm^2/day)	Percentage which Penetrates Cloud Cover	Corrected Average Surface Radiation (cal/cm^2/day)	Radiation which Reaches Various Water Depths (cal/cm^2/day)		
				20 m (68.1% of surface)	45 m (42.0% of surface)	80 m (21.5% of surface)
January	405	54.27	220	150	92	47
February	475	55.06	262	178	110	56
March	587	55.01	323	220	136	69
April	655	59.74	391	267	164	84
May	708	65.68	465	317	195	100
June	727	68.85	501	341	210	108
July	712	70.20	500	340	210	108
August	670	64.81	434	296	182	93
September	590	62.81	371	252	156	80
October	508	65.85	335	228	141	72
November	440	60.69	267	182	112	57
December	370	55.37	205	140	86	44

†Clear sky radiation calculations at the latitude of the reef are based on data from the Smithsonian Meteorological Tables (List, 1966). Cloud cover data for the reef area are based on data from the U.S. Naval Weather Service (1975).

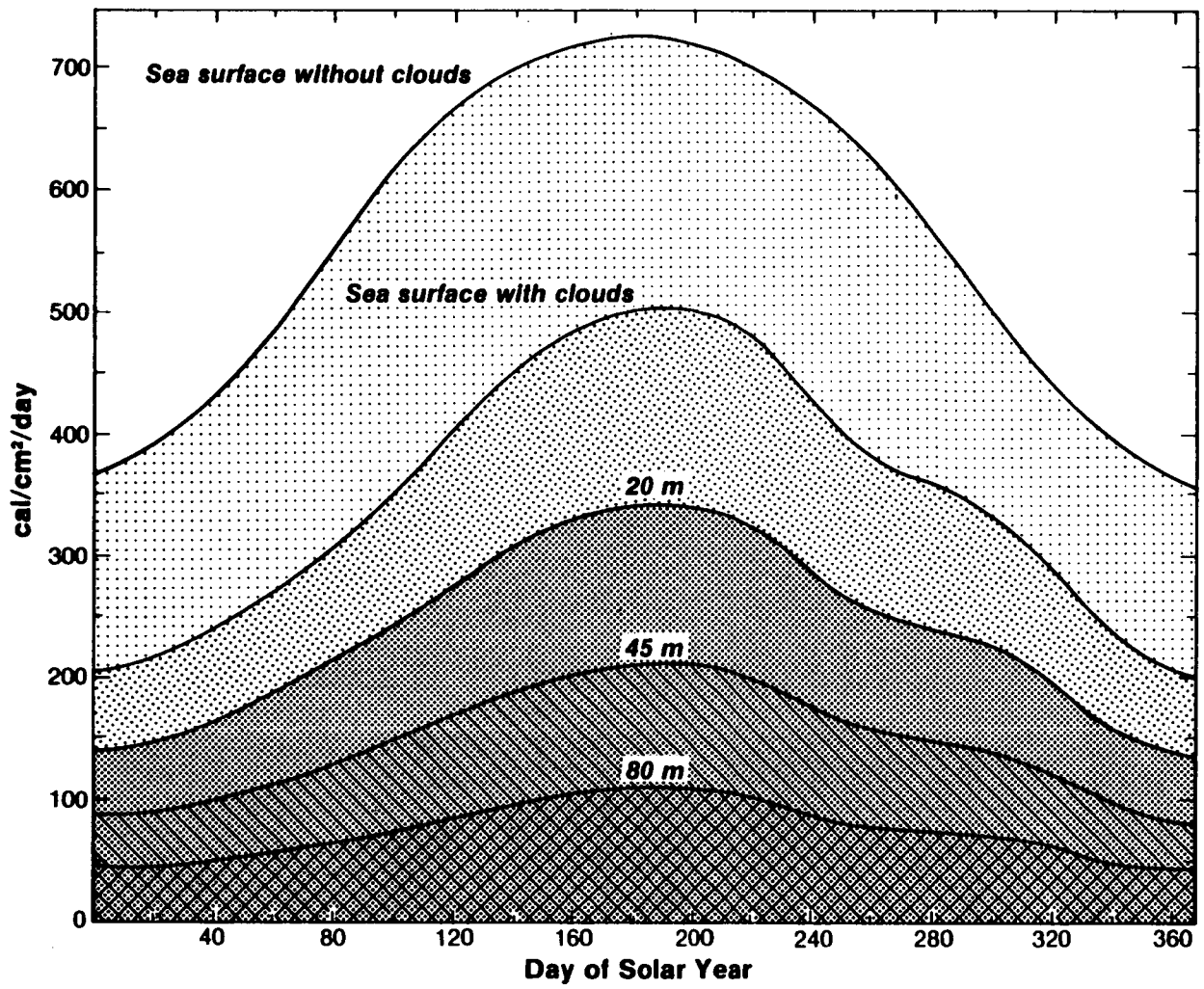

Figure 9.4 Solar radiation reaching the sea surface and various depths at the East Flower Garden Bank.

data were converted to percent transmission by the equation of Angstrom [$I_O = I_M(1 - kc)$] given in Sverdrup et al. (1942). In this equation I_M is the clear sky radiation, c is the cloud cover (expressed in tenths), and k is a factor which relates cloud cover to light transmission. It must be noted that the corrected sea surface radiation values are biased by two factors. The assumption of 25% absorption by the atmosphere over-compensates in the summer and under-compensates in the winter months. Thus, the curves should be lower in the winter and higher in the summer than shown in the figure. The second bias relates to the source of the cloud cover data. The data represent a point midway between shore and the outer shelf, and this point clearly has more cloud cover than the outer shelf where the reef is located. This bias results in over-compensation for cloud cover at all seasons, and the sea surface light at the reef site should be somewhat higher than indicated at all seasons.

Limited data have been taken during the study concerning light penetration at various depths as a percentage of sea surface radiation. By applying these data throughout the year, it has been possible to estimate light levels at the various critical reef depths. However, the annual variability of light penetration in relation to seasonal differences in suspended matter is unknown.

With the reservations noted above, it is possible to reach some interesting general conclusions concerning the light factor. The cloud cover tends to be greatest during the winter months and least during the summer, but the smooth progression is interrupted by the fact that October has less cloud cover than either August or September. Hence, the sea surface radiation curve shows a slight hump during October which is reflected in the curves at all depths. During the winter months, the Live Coral Zone (20 to 45 m depth) generally receives less than 150 cal/m^2/day, but this value more than doubles during the summer. The Algal-Sponge Zone (45 to 80 m) varies from a winter low of about 44 to 86 cal/m^2/day to a summer high of 108 to 210 cal/m^2/day.

Temperature

Temple et al. (1977) provided two years of monthly data on depth distribution of temperature throughout the northwestern Gulf shelf. Their station E-6 was quite close to the East Flower Garden reef, and the monthly averages of the two-year data set are considered to provide excellent information on temperature conditions of the reef area. This information has been plotted in Figure 9.5. At all reef depths the minimum temperature of around 17.5°C was reached in the month of February. Maximum temperature of 29.4°C was observed at reef-top level in August, 27.9°C at the coral reef bottom in September, and 24.2°C at the bottom of the non-coral reef in November. During the warm-up months from March through

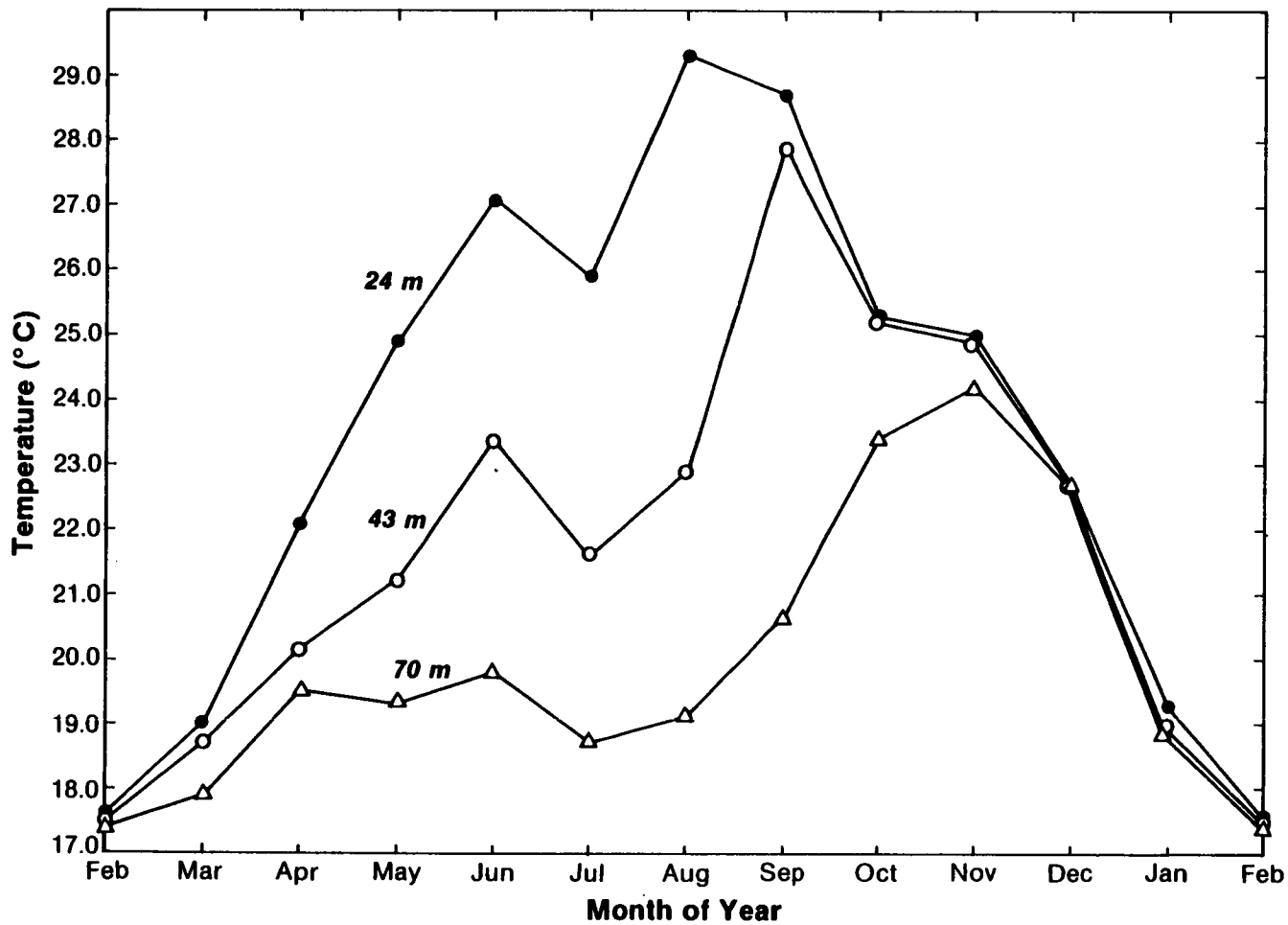

Figure 9.5 Monthly water temperatures at selected depths in the vicinity of the East Flower Garden Bank, based on two-year averages. Data from Temple et al. (1977).

August there developed a remarkable divergence of temperature from the shallowest to the deepest portion of the reefal zones (coral reef 20 to 45 m, Algal-Sponge Zone 45 to 80 m) so that by August the temperature differential exceeded 10°C. Physiologically this would translate to a two or three-fold difference in metabolic rate. By November all three depths were within a range of one degree centigrade, and they remained very close together through February. During both years, the temperatures at all depths dropped in the month of July, probably in response to some shift in current patterns during that month. In general, the data show a steady warming of the shallower waters during the spring and summer months (except for the dip in July) due to solar heating. During the fall months, vertical mixing reduced the difference in October, and thereafter through February the vertical column was essentially isothermal. The data demonstrate that not only does the coral reef receive substantially more light than the Algal-Sponge Zone, but it is on the average considerably warmer and peaks during late summer while there is still sufficient radiation for photosynthesis. Temperatures on the deeper reef peak during the fall when radiation has fallen to a lower level. Considering the combined effects of temperature and light, it appears likely that photosynthesis on both coral and algal reefs is extremely seasonal and that during the winter months the coral-zooxanthellae symbiosis might depend largely upon heterotrophic feeding by the coral polyps.

Import of Nutrients

From data provided by McGrail (this volume) it has been calculated that the average velocity of water bathing the reef is about 7.0 cm/s or 6048 m/24-hour period (Table 9.7). Limited data are available concerning the concentration of nitrogen (as nitrite plus nitrate) and phosphorous (as phosphate) during all seasons except spring (Bright et al., 1981) (Table 9.7). On the basis of nutrient concentrations and water velocity it has been possible to calculate the quantity of nutrients bathing each square metre of the reef, assuming a water column one-half metre thick (which is the average height of most of the large coral heads). In all cases the nutrients were more concentrated at 50 m than at 25 m. For the most part, they were more concentrated in the winter than during other seasons. Quantities of nitrogen carried to the reef daily varied from a maximum of 6713 mmol at 50 m during the winter to 1058 at 25 m during the fall. Phosphate varied from 1421 mmol at 50 m to 816 mmol at 25 m, both extreme values occurring during the fall. Calcium concentration, which is a conservative property of seawater, was assumed to be constant throughout the year at 10 mmol, and the amount carried to the reef daily at all seasons was determined to be of the order of 3024×10^4 mmol.

Table 9.7 Water Column Characteristics†

Average Current Speed: 7.0 cm/s = 252 m/hr = 6,048 m/24-hr

NUTRIENTS

	Concentration (umol)				Nutrients/24-hr period (mmol)			
	W	Sp	Su	F	W	Sp	Su	F
Nitrogen (NO_2+ NO_3)								
25 m	1.06	--	.54	.35	3205	--	1633	1058
50 m	2.22	--	.60	.65	6713	--	1814	1966
Phosphate								
25 m	.36	--	.29	.27	1089	--	877	816
50 m	.41	--	.42	.47	1240	--	1270	1421
Calcium	------ 10,000 ------				-------3024 x 10^4-------			

SUSPENDED MATTER

	mgC/m^3	Conversion Factor	Dry wt. (mg/m^3)	Dry wt./24-hr (kg/m^2 of bottom)
Phytoplankton	452	3.3	1492	4.512
Zooplankton	45	1.7	77	0.233
Other	3	2.0	6	0.018
Total POC	500		1575	4.763

†Twenty-four-hour calculations are based upon water column one-half metre thick and represent material brought to each square metre of reef area.

Import of Suspended Matter

A few data are available for total suspended matter (as organic carbon) in the surface (upper 90 m) waters of the Gulf in the vicinity of the East Flower Garden Reef (Table 9.7), but concentrations at various depths are not known. From knowledge of total suspended matter it has been possible to calculate the amounts of phytoplankton, zooplankton, and other elements bathing the reef (the latter including organic and inorganic seston plus non-photosynthetic bacteria). Standard oceanographic conversion factors have been employed to convert each to the equivalent value in terms of dry weight. As in the case of nutrients, the quantity daily brought to each square metre of reef area (one-half metre deep water column) has been determined from water velocity data. The calculations indicate that during a given 24-hour period about 4.763 kg of particulate matter bathes each square metre of reef, and this includes 4.512 kg of phytoplankton, 0.233 kg of zooplankton, and 0.018 kg of other materials. Depth and seasonal distribution patterns are not available. It should be noted that if the upstream areas of the reef remove significant amounts of material, the downstream areas could be faced with lower concentrations. However, since the reef surface is not smooth, the bottom layer of water is likely quite turbulent, and mixing of near-bottom waters may keep the concentration near the stated level. Furthermore, downstream portions of the reef receive contributions from upstream portions and, as a result, may receive larger particulate concentrations.

Derived Data for the Reef Surface

Area of Reef Bank Surface

In the following discussion it is assumed that the Live Coral Reef Zone extends from about 20 to 45 m and that the non-coral reef zone extends from 45 to 80 m. Planimetry has been employed on the contour maps to determine the actual surface area within each zone. As shown in Table 9.8, the Live Coral Zone covers a surface area of 2.55 km^2, and the Algal-Sponge Zone covers 18.30 km^2. Within the Live Coral Zone, 85%, or 2.16 km^2, is covered by hard bottom. Within the Algal-Sponge Zone, 20.6%, or 3.77 km^2, represents drowned reefs, and 52.9%, or 9.68 km^2, represents live bottom.

Surface Area of Living Cover

If all coral and algae were flat and if distributions were uniform within the zones, then the surface area in each zone should

Table 9.8 Derived Data for the East Flower Garden Reef Surface

Area of Reef Bank Surface

Zone	Depth Range (m)	Surface Area (km^2)
Live Coral Zone	20 - 45	2.55
- Hard bottom in coral reef zone (85% of zone area)		2.16
Algal-Sponge Zone	45 - 80	18.30
- Drowned reefs (20.6% of zone area)		3.77
- Live bottom (52.9% of zone area)		9.68

Surface Area of Living Cover

Group	Assumptions	Surface Area (km^2)
Surface of Live Coral Heads	- In the 20 to 45 m zone, live coral covers 50% of the hard bottom.	1.08-2.16
	- Coral ranges from flat to hemispherical.	
Surface Covered by Soft Algae	- In the 20 to 45 m zone, soft algae cover 3 to 5% of the hard bottom.	0.65-1.08
	- In the 45 to 80 m zone, soft algae cover 6 to 10% of the live bottom.	
Surface of Coralline Algae	- In the 20 to 45 m zone, coralline algae cover 15% of the hard bottom area.	10.55-21.09
	- In the 45 to 80 m zone, coralline algae cover 70% of the drowned reef surface as flat pavement on hemispheric surfaces.	
	- In the 45 to 80 m zone, coralline algae cover 80% of the live bottom area as living hemisphere surfaces.	

indicate the coverage of the living organisms. However, these conditions are not met, and a series of corrections has been necessary to develop estimates of the actual coverage by living organisms. These corrections are based upon the assumptions provided in Table 9.8, and considering the sources of potential error it seems appropriate to include maximum and minimum figures (based upon the assumption of hemispherical vs. flat surfaces). The actual coverage of live coral heads was determined to be 1.08 to 2.16 km^2, that of soft algae to be 0.65 to 1.08 km^2, and that of coralline algae to be 10.55 to 21.09 km^2. These values will be employed in subsequent calculations.

Biomass Data

In the following discussion the biomass of each of the model compartments will be computed in terms of dry weight. These data will then be converted to caloric equivalents, which will be the most useful units for the metabolic considerations which follow.

Zooxanthellae

Odum and Odum (1955) provided data on the density of zooxanthellae in shallow reefs of Eniwetok Atoll. Dustan (1979) discussed variation in zooxanthellae density with depth of the water column. Applying these data to the actual depths of the East Flower Garden coral reef and multiplying by the calculated surface area of living coral, it has been possible to determine the approximate biomass of zooxanthellae inhabiting the reef (Table 9.9). The total value lies in the range of 15,900 to 31,800 kg dry weight, depending upon which value for the surface area of coral heads is employed.

Soft Algae

Soft algae biomass calculations were somewhat complicated, and they are presented in Table 9.10. The soft algae include the leafy algae (for which actual seasonal biomass data are available) and the epipelic (mostly filamentous) algae (for which only crude visual estimates are available). In calculating the epipelic algae it has been assumed that they undergo the same seasonal percentage changes in biomass as the leafy algae. Clearly spring is the season of greatest biomass, followed by summer. Fall and winter levels are nearly identical.

Table 9.9 Biomass Calculations for Zooxanthellae and Coral Tissue†

Zooxanthellae Calculations

Depth Range (m)	Surface Area of Coral Heads (km^2)	Density (dry wt.) (g/m^2)	Density (dry wt.) (kg/km^2)	Total Biomass (kg)
20 - 30	0.23 - 0.45	20.1	20,100	4,600 - 9,000
31 - 40	0.48 - 0.97	14.2	14,200	6,800 - 13,800
41 - 45	0.37 - 0.74	12.1	12,100	4,500 - 9,000
Totals	1.08 - 2.16			15,900 - 31,800

Coral Tissue Calculations

Depth Range (m)	Surface Area of Coral Heads (km^2)	Density (dry wt.) (g/m^2)	Density (dry wt.) (kg/km^2)	Total Biomass (kg)
20 - 30	0.23 - 0.45	152	152,000	35,000 - 68,600
31 - 40	0.48 - 0.97	109	109,000	52,300 - 105,900
41 - 45	0.37 - 0.74	92	92,000	34,000 - 68,100
Totals	1.08 - 2.16			121,300 - 242,600

†These calculations are based upon estimates by Odum and Odum (1955) of 38.0 g/m^2 of zooxanthellae and 250.0 g/m^2 of coral tissue in a reef of 0 to 1 m depth, and they are corrected for depths of the East Flower Garden reef on the basis of data provided by Dustan (1979).

Table 9.10 Soft Algae Biomass Calculations. Coverage of leafy algae is based upon measurements. Coverage of epipelic algae is based upon visual estimates.

Coral Reef Zone (above 45 m)

- Leafy Algae (coverage = 3 to 5% of hard bottoms above 45 m)

Season	Surface Area Covered (km^2)	Density (mean dry wt.) (g/m^2)	Density (mean dry wt.) (kg/km^2)	Total Biomass (kg)
Winter	0.065 - 0.108	33.3	33,300	2,165 - 3,596
Spring	0.065 - 0.108	129.0	129,000	8,385 - 13,932
Summer	0.065 - 0.108	53.9	53,900	3,504 - 5,821
Fall	0.065 - 0.108	34.5	34,500	2,243 - 3,726

- Epipelic Algae (est. = 2% of leafy algae biomass)

Season	Leafy Algae Biomass (kg)	Conversion Factor	Estimated Biomass (kg)
Winter	2,165 - 3,596	0.02	43 - 72
Spring	8,385 - 13,932	0.02	168 - 279
Summer	3,504 - 5,821	0.02	70 - 116
Fall	2,243 - 3,726	0.02	45 - 75

Algal-Sponge Zone (below 45 m)

- Leafy Algae (coverage = 5% of live bottoms and drowned reefs)

Season	Surface Area Covered (km^2)	Density (mean dry wt.) (g/m^2)	Density (mean dry wt.) (kg/km^2)	Total Biomass (kg)
Winter	0.585 - 0.912	33.3	33,300	19,481 - 30,370
Spring	0.585 - 0.912	129.0	129,000	75,465 - 117,648
Summer	0.585 - 0.912	53.9	53,900	31,532 - 49,157
Fall	0.585 - 0.912	34.5	34,500	20,183 - 31,464

- Epipelic Algae (coverage = 6 to 10% of live bottoms and drowned reefs)

Season	Surface Area Covered (km^2)	Density (mean dry wt.) (g/m^2)	Density (mean dry wt.) (kg/km^2)	Total Biomass (kg)
Winter	0.702 - 0.912	13.3	13,300	9,337 - 12,130
Spring	0.702 - 0.912	51.5	51,500	36,153 - 46,968
Summer	0.702 - 0.912	21.5	21,500	15,093 - 19,608
Fall	0.702 - 0.912	13.7	13,700	9,617 - 12,494

Totals

Season	Coral Reef Zone	Algal-Sponge Zone	Both Zones
Winter	2,208 - 3,668	28,818 - 42,500	31,026 - 46,168
Spring	8,553 - 14,211	111,618 - 164,616	120,171 - 178,827
Summer	3,574 - 5,937	46,625 - 65,765	50,199 - 71,702
Fall	2,288 - 3,801	29,800 - 43,958	32,088 - 47,759

Coralline and Endolithic Algae

There is no easy way to separate coralline algae from other calcareous forms (including those which inhabit the live coral heads), so they are grouped together here. The calculations for this combined algal group are provided in Table 9.11. From this table it is seen that the coralline and endolithic algae together are by far the most abundant producers of both zones of the East Flower Garden reef. Odum and Odum (1955) estimated that endolithic algae are 15.5 times the biomass of the zooxanthellae. Whereas this number is probably quite high for the Flower Gardens, in the absence of direct measurements it has been used as a basis for present calculations on the coral reef. In the Algal-Sponge Zone a great deal of the bottom is covered with algal nodules, and to this is added the endolithic algae of the drowned reefs.

Live Coral Tissue

Living coral heads contain coral polyps as well as living tissue between the polyps, and the data from Odum and Odum (1955) express the biomass of living coral tissue on a per-unit-surface area basis which includes both polyp and inter-polyp tissue. Table 9.9 provides the calculations for total coral tissue on the East Flower Garden reef. The resulting values are almost an order of magnitude higher than the values for zooxanthellae.

Plankton Feeders

Population estimates are available for many of the more abundant consumer species of the coral reef zone. By estimating the average size of individuals in the populations, one can calculate wet weight, and by application of standard conversion factors dry weight values may be obtained for most of the populations, for which numerical estimates are available. However, since population estimates for some of the abundant species are lacking, the dry weight values presented represent only partial biomass values for the various consumer groups. For the Algal-Sponge Zone there are no population estimates for the consumer species, and a simple listing of important species by consumer categories must suffice.

In Table 9.12 are presented the biomass calculations for major plankton feeders of the coral reef for which data are available. No conversion factor has been found for sponges, and they are given as wet weight only. Plankton feeders of the Algal-Sponge Zone are listed in Table 9.17.

Table 9.11 Coralline and Endolithic Algae Calculations†

Coral Reef Zone (above 45 m)

- Algae in Live Coral (est. = 15.5 x zooxanthellae biomass)

Zooxanthellae Biomass (dry wt.) (kg)	Conversion Factor	Total Biomass (kg)
15,900 - 31,800	15.5	246,450 - 492,900

- Endolithic Algae Between Coral Heads (est. = 15% coverage of hard bottom)

Surface Area Covered (km^2)	Density (g/m^2)	Density (kg/km^2)	Total Biomass (kg)
0.324 - 0.648	100	100,000	32,400 - 64,800

Total Biomass in Live Coral Zone 278,850 - 557,700

Algal-Sponge Zone (below 45 m)

- Algae on Live Bottom (est. = 80% coverage of live bottom)

Surface Area Covered (km^2)	Density (g/m^2)	Density (kg/km^2)	Total Biomass (kg)
7.74 - 15.49	100	100,000	774,000 - 1,549,000

- Algae on Drowned Reefs (est. = 70% coverage)

Surface Area Covered (km^2)	Density (g/m^2)	Density (kg/km^2)	Total Biomass (kg)
2.64 - 5.28	100	100,000	264,000 - 528,000

Total Biomass in Algal-Sponge Zone 1,038,000 - 2,077,000

Total Biomass in Both Zones 1,667,650 - 3,336,300

†Conversion factors and biomass estimates are based upon Odum and Odum (1955) and modified for the depths of the East Flower Garden reef on the basis of data provided by Dustan (1979).

Table 9.12 Biomass Estimates for Some of the Major Plankton Feeder Groups of the Coral Reef Zone for which Data are Available†

Taxon	Population Estimate	Biomass (wet wt.) Average (kg)	Biomass (wet wt.) Total (kg)	Conversion Factor	Biomass (dry wt.) (kg)
Fishes					
Blue chromis - juv.	143,553	0.0025*	359	0.4	144
- ad.	255,205	0.005*	1,276	0.4	510
Brown chromis	882,584	0.005	4,413	0.4	1,765
Creole fish	196,721	0.300*	59,016	0.4	23,606
Creole wrasse	287,106	0.300*	86,132	0.4	34,453
Red-spotted hawkfish	10,633	0.003*	32	0.4	13
Ocean triggerfish	143,553	0.500	71,777	0.4	28,711
				Total Fishes	89,202+
Invertebrates					
Sponges	861,317	0.02	17,226	--	--
Bivalves	494,474	0.01	4,945	0.11	544
			Total Invertebrates		--

†Population estimates are derived from field census. Average weights are based upon laboratory assessment unless indicated by an asterisk (*) in which case they are estimates made by experienced personnel. Wet weight/dry weight conversion is based upon data provided in Cummins and Wuycheck (1971).

Herbivores

Biomass estimates for some of the major herbivore groups of the live coral zone are provided in Table 9.13. The total dry weight biomass values for this group are only about a third of the total value given for the plankton feeders. It would undoubtedly be a much smaller fraction if estimates of all species (especially the sponges) were available. Some of the herbivores of the Algal-Sponge Zone are listed in Table 9.17.

Omnivores

Biomass estimates for some of the major omnivore groups of the live coral zone are given in Table 9.14. Despite the large number of species listed in this category, the total biomass estimate is close to that of the plankton feeder group. As in the case of the plankton feeder category, the biomass estimate of the omnivore group is probably quite low. Omnivores of the Algal-Sponge Zone are shown in Table 9.17.

Table 9.13 Biomass Estimates for Major Herbivore Groups of the Coral Reef Zone for which Data are Available†

Taxon	Population Estimate	Biomass (wet wt.) Average (kg)	Biomass (wet wt.) Total (kg)	Conversion Factor	Biomass (dry wt.) (kg)
Fishes					
Princess parrotfish	15,950	1.00	15,950	0.4	6,380
Stoplight parrotfish	15,950	1.00	15,950	0.4	6,380
Other parrotfish	63,801	0.75	47,851	0.4	19,140
Redlip blenny	10,633	0.004*	43	0.4	17
				Total Fishes	31,917+
Invertebrates					
--	--	--	--	--	--

†For terminology and data sources see footnote to Table 9.12.

Table 9.14 Biomass Estimates for Major Omnivore Groups of the Coral Reef Zone for which Data are Available.† Total fish biomass is grossly underestimated.

Taxon	Population Estimate	Biomass (wet wt.) Average (kg)	Biomass (wet wt.) Total (kg)	Conversion Factor	Biomass (dry wt.) (kg)
Fishes					
Bicolor damselfish					
- juv.	5,317	--	--	--	--
- ad.	116,969	0.0035	409	0.4	164
Threespot damselfish					
- juv.	15,950	--	--	--	--
- ad.	143,553	0.0035	502	0.4	201
Other damselfish	271,155	--	--	--	--
Bluehead					
- juv.	664,597	0.0008	532	0.4	213
- ad.	186,087	0.0075	1,396	0.4	558
Yellowhead wrasse	15,950	0.05*	797	0.4	319
Clown wrasse	37,217	--	--	--	--
Spanish hogfish	47,851	0.20	9,570	0.4	383
Spotfin hogfish	53,168	0.20	10,634	0.4	4,254
Puddingwife					
- juv.	47,851	--	--	--	--
- ad.	5,317	0.30	1,595	0.4	638
Reef butterflyfish	143,553	--	--	--	--
Longsnout butterflyfish	26,584	--	--	--	--
Rock beauty	21,267	0.20*	4,253	0.4	1,701
Queen angelfish	15,950	0.25	3,987	0.4	1,595
Sharpnose puffer	21,267	0.01	213	0.4	85
Neon goby	154,186	0.001	154	0.4	62
Yellow goatfish	5,317	0.10*	532	0.4	213
Spotted goatfish	5,317	0.10*	532	0.4	213
Knobbed porgy	5,317	0.75	3,988	0.4	1,595
Taillight filefish	10,633	0.20*	2,127	0.4	851
Smooth trunkfish	5,317	0.065	346	0.4	138
				Total Fishes	13,183+
Invertebrates					
Gastropods	4,774,463	0.005	23,872	0.13	3,103
Long-spined sea urchin	2,381,914	0.10	238,191	0.33	78,603
				Total Invertebrates	81,706+

†For terminology and data sources see footnote to Table 9.12.

Transient Predators

Only a single species of transient predator of the live coral zone is represented by a population estimate (Table 9.15). No data concerning transient predators of the Algal-Sponge Zone are available.

Resident Predators

Calculations for biomass of some of the resident predators of the live coral zone are presented in Table 9.15. Although only a few species are involved, they average larger in size and together represent a fairly large biomass. Some of the resident predators of the Algal-Sponge Zone are given in Table 9.17.

Table 9.15 Biomass Estimates for Major Transient and Resident Predator Groups of the Coral Reef Zone for which Data are Available†

Taxon	Population Estimate	Biomass (wet wt.) Average (kg)	Biomass (wet wt.) Total (kg)	Conversion Factor	Biomass (dry wt.) (kg)
Transient Predators					
Bar Jack	31,901	0.75	23,926	0.4	9,570
Resident Predators					
Graysby	21,267	0.6	12,760	0.4	5,104
Rock hind	10,633	0.6	6,380	0.4	2,552
Great barracuda	37,217	1.5	55,826	0.4	22,330
Trumpetfish	5,317	--	--	--	--
			Total Resident Predators		29,986+

†For terminology and data sources see footnote to Table 9.12.

Other Categories

No biomass or mass estimates are available for the following categories: pathogens (X_8), coralivores (X_9), particulate organic detritus (X_{15}), and calcareous debris (X_{16}).

Standing Stock Estimates Based on Caloric Equivalents

The dynamics of any ecosystem are most meaningfully analyzed in energetic terms. Hence, the biomass data are expressed as caloric equivalents. Caloric conversion factors for most groups are found in Cummins and Wuycheck (1971) and Wissing et al. (1973).

Live Coral Zone

Table 9.16 shows calculations and final caloric equivalent estimates for all the Live Coral Zone groups for which data are available. Among the producers, the coralline and endolithic algae greatly predominate, followed by the zooxanthellae and, lastly, the soft algae. The latter show a definite seasonal peak during the spring, and although the zooxanthellae and coralline and endolithic algae may also exhibit some seasonality, we have no information on this point. On a per-square-metre basis, the plankton subsidy appears small, but considered over the surface of the entire hard bottom area of the Live Coral Zone (2.16 km^2) the daily phytoplankton contribution amounts to 45,400 x 10^6 kcal, and to this is added about 2000 x 10^6 kcal of zooplankton. Therefore, nearly 50,000 x 10^6 kcal of plankton energy is brought to the reef daily. This exceeds the standing crop of soft algae and approaches that of the zooxanthellae. Although the figures for many consumer groups are incomplete or lacking, present data suggest that the consumers are dominated by the live coral tissue (which is at least partly "herbivorous" due to its consumption of zooxanthellae photosynthetic products). If the sponge estimates were available, however, the plankton feeder group might be of the same order of magnitude as the coral tissue. Corals, of course, are also plankton feeders, and the abundance of these two groups again points to the importance of plankton as an energy source for the reef consumers. In general, the predator populations seem large in comparison with the prey populations, but many of the predators probably make use of transient prey as well. Data gaps preclude discussion of particulate organic detritus and detritus feeders.

Table 9.16 Biomass Summary and Caloric Conversions for the Live Coral Zone (above 45 m)

Advective Import

Group	Biomass (dry wt.) ($kg/m^2/24$-hr.)	Conversion Factor (kcal/g-dry wt.)	Biomass Equivalent (kcal x 10^6)
x_1 Phytoplankton	4.512	4.477	0.021
x_5 Zooplankton	0.233	4.813	0.001

Reef-Associated Groups

-Producers

Group	Biomass (dry wt.) (kg)	Conversion Factor (kcal/g-dry wt.)	Biomass Equivalent (kcal x 10^6)
x_2 Zooxanthellae	15,900 - 31,800	4.000	63,600 - 127,200
x_3 Soft algae			
- Winter	2,208 - 3,668	4.000	8,832 - 14,672
- Spring	8,553 - 14,211	4.000	34,212 - 56,844
- Summer	3,574 - 5,937	4.000	14,296 - 23,748
- Fall	2,288 - 3,801	4.000	9,152 - 15,204
x_4 Coralline and endolithic algae	278,850 - 557,700	4.000	1,115,400 - 2,230,800

Producer Standing Crop ($X_2 + X_3 + X_4$)	Winter	1,187,832 - 2,372,672
	Spring	1,213,212 - 2,414,844
	Summer	1,193,296 - 2,381,748
	Fall	1,188,152 - 2,373,204

Table 9.16 (Continued)

Reef-Associated Groups (Continued)

-Consumers

Group	Biomass (dry wt.) (kg)	Conversion Factor (kcal/g-dry wt.)	Biomass Equivalent (kcal x 10^6)
x_6 Coral tissue	121,300 - 242,600	3.700	448.810 - 897.620
x_7 Plankton Feeders			
Fishes	89,202+	5.000	446.010+
Inverts.	--	--	--
x_8 Pathogens	--	--	--
x_9 Coralivores	--	--	--
x_{10} Herbivores	31,917+	5.000	159.585+
x_{11} Detritivores	--	--	--
x_{12} Omnivores† - Fishes	13,183+	5.000	65.915+
- Inverts.	81,706+	4.108 0.883	82.153+
x_{13} Transient Predators	9,570+	5.000	47.850+
x_{14} Resident Predators	29,986+	5.000	149.930+
-Storage Compartments	--	--	--

Group	Biomass (dry wt.) (kg)	Conversion Factor (kcal/g-dry wt.)	Biomass Equivalent (kcal)
X_{15} Particulate organic detritus	--	--	--
X_{16} Calcareous debris	--	--	--

†Under omnivores, caloric conversion factors are given for both gastropods and sea urchins.

Algal-Sponge Zone

Calculations and caloric estimates for the Algal-Sponge Zone are provided in Table 9.17. Here again, the coralline and endolithic algae are by far the most abundant producer group, and the soft algae show seasonal abundance patterns. Although no estimates of consumer abundance are available, large populations of sponges suggest that here also, the consumers are dominated by plankton feeders. Compared with the community of the Live Coral Zone, that of the Algal-Sponge Zone is much simplified. It exhibits far fewer species and fewer consumer groups. Snappers and groupers are the primary resident predators of this zone.

Reef Metabolism

Live Coral Zone

In the absence of direct measurements, gross primary production of the Live Coral Zone may be estimated from the amount of radiation in the visible spectrum which impinges on the reef and the assumption of a 5.8% photosynthetic efficiency derived from studies of Odum and Odum (1955) for the coral reef at Eniwetok. Since light extinction is logarithmically related to depth, it has been necessary to compute the log mean depth of the coral reef in order to obtain average light values. From the average daily light values within each month it has been possible to estimate total monthly and total annual gross primary production (Table 9.18). The latter value is 52.02×10^9 (or $52,020 \times 10^6$) kcal/yr. Using data from Odum and Odum (1955) it has also been possible to estimate net production and respiratory loss (Table 9.20). Assuming that net production is 58.3% and respiration is 41.7% of gross production, the respective estimates for the Live Coral Zone system are $30,329 \times 10^6$ kcal for net production and $21,693 \times 10^6$ kcal for respiration. For the coral reef at Eniwetok, Odum and Odum (1955) established a relationship between gross primary production and standing crop biomass of 12.5:1. With admittedly underestimated biomass, the estimated range for the East Flower Garden reef is 18.9 to 11.8:1.

It was noted earlier that the phytoplankton and zooplankton which impinge upon the reef bring to the Live Coral Zone about 50×10^6 kcal per day. On an annual basis this would amount to $18,250 \times 10^9$ kcal. If, through grazing and precipitation, the reef removed only one percent of the plankton from the lower one-half metre of water bathing the reef, this would result in an annual energy subsidy of $185,000 \times 10^6$ kcal. This figure is 3.6 times that of gross and 6.1 times that of net production estimated for the Live Coral Zone. How much of this potential energy resource is

actually utilized is not known, but it cannot be ignored in any consideration of the metabolism of this reef.

Algal-Sponge Zone

Using the methods described above, we estimate the gross primary production of the Algal-Sponge Zone to be 198.86 x 10^9 kcal/yr (Table 9.19). On a per-unit-area basis, the Live Coral Zone is about 1.63 times as productive as the Algal-Sponge Zone (24.08 versus 14.79 x 10^9 kcal/km^2 of productive bottom), and this results from the fact that the live coral reef receives more light and higher temperatures. However, due to the considerably larger surface area, the Algal-Sponge Zone annually produces 3.82 times as much as the Live Coral Zone.

Using data from Smith and Marsh 1973) concerning the algal reef at Eniwetok, it has been possible to estimate net production and respiration for the Algal-Sponge Zone of the East Flower Garden reef. Assuming that net production is 74.2% and respiration is 25.8% of gross production, the estimates for the East Flower Garden are 147,554 x 10^6 kcal for net production and 51,306 x 10^6 kcal for respiratory loss (Table 9.21). Thus, it is estimated that the Algal-Sponge Zone accounts for 4.87 times the net production of the Live Coral Zone, but the respiration is only about 2.37 times as much. It is not possible to estimate the gross production to standing crop ratio since standing crop biomass estimates for the Algal-Sponge Zone are not available.

Coral Growth

From a series of borings of live coral heads (*Montastrea annularis*) it has been possible to estimate the annual rate of skeletal accretion at various depths of the Live Coral Zone (no measurements were made deeper than 27 m). Calculated (not measured) vertical and lateral (one side only) growth rates are presented in Table 9.22. It may be seen that estimated growth varies with depth and that the growth rate at 45 m is only 41.0% of the growth rate at 20 m. Growth at greater depths is undoubtedly reduced by the prevailing lower temperatures and diminished light. Growth on a given side is only 75.9% of growth in the vertical direction, which may be due to reduced light.

Table 9.17 Biomass Summary and Caloric Conversions for the Algal Sponge Zone (below 45 m)†

Advective Import

Group	Biomass (dry wt.) (kg/m^2/24-hr.)	Conversion Factor (kcal/g-dry wt.)	Biomass Equivalent (kcal x 10^6)
x_1 Phytoplankton	4.512	4.477	0.021
x_2 Zooplankton	0.233	4.813	0.001

Reef-Associated Groups

-Producers

Group	Biomass (dry wt.) (kg/m^2/hr)	Conversion Factor (kcal/g-dry wt.)	Biomass Equivalent (kcal x 10^6)
x_3 Soft algae			
- Winter	28,818 - 42,500	4.000	115.272 - 170.000
- Spring	111,618 - 164,616	4.000	446.472 - 658.464
- Summer	46,625 - 65,765	4.000	186.500 - 263.060
- Fall	29,800 - 43,958	4.000	119.200 - 175.832
x_4 Coralline and endolithic algae	1,038,000 - 2,077,000	4.000	4,152.000 - 8,308.000

Producer Standing Crop ($x_3 + x_4$)	Winter	4,267.272 - 8,478.000
	Spring	4,598.472 - 8,966.464
	Summer	4,338.500 - 8,571.060
	Fall	4,271.200 - 8,483.832

†No population estimates are available for consumer groups in this zone.

Table 9.17 (Continued)

Reef-Associated Groups (Continued)

-Consumers

Group

x_7 Plankton feeders

- Fishes

  Yellowtail reeffish, *Chromis enchrysurus*

- Invertebrates

  Sponges

  Atlantic thorny oyster, *Spondylus americanus*

x_{10} Herbivores

- Invertebrates

  Snails, *Cerithium* spp.

x_{12} Omnivores

-Fishes

  Reef butterflyfish, *Chaetodon sedentarius*

- Invertebrates

  Sea urchins, *Astropyga magnifica* and *Pseudobolita maculata*

x_{14} Resident predators

- Fishes

  Red snapper, *Lutjanus campechanus*

  Groupers, *Mycteroperca* spp.

Table 9.18 Gross Primary Production Calculations for the Live Coral Zone†

Month	Visible Radiation at Surface (kcal/m^2/day)	Visible Radiation at Log Mean Depth (kcal/m^2/day)	Gross Primary Production/Unit Area at Log Mean Depth (kcal/m^2/day)	Surface Area of Live Coral Zone (km^2)	Total Daily Primary Production Rate (kcal x 10^6/day)	Total Monthly Primary Production Rate (kcal x 10^9/mo)
January	1100	594	34.5	2.55	88	2.728
February	1310	707	41.0	2.55	105	2.940
March	1615	872	50.6	2.55	129	3.999
April	1955	1056	61.2	2.55	156	4.680
May	2325	1256	72.8	2.55	186	5.766
June	2505	1353	78.5	2.55	200	6.000
July	2500	1350	78.3	2.55	200	6.200
August	2170	1172	68.0	2.55	173	5.363
September	1855	1002	58.1	2.55	148	4.440
October	1675	905	52.5	2.55	134	4.154
November	1335	721	41.8	2.55	107	3.210
December	1025	554	32.1	2.55	82	2.542
		Total Annual Gross Primary Production of Live Coral Zone (kcal x 10^9/yr)				52.022

†Visible radiation is assumed to represent one-half of the total radiation. An efficiency of 5.8% is assumed for gross production (Odum and Odum, 1955).

Table 9.19 Gross Primary Production Calculations for the Algal-Sponge Zone†

Month	Visible Radiation at Surface (kcal/m^2/day)	Visible Radiation at Log Mean Depth (kcal/m^2/day)	Gross Primary Production/Unit Area at Log Mean Depth (kcal/m^2/day)	Surface Area of Algal-Sponge Zone (km^2)	Total Daily Primary Production Rate (kcal x 10^6/day)	Total Monthly Primary Production Rate (kcal x 10^9/mo)
January	1100	317	18.4	18.30	336	10.416
February	1310	377	21.9	18.30	401	11.228
March	1615	465	27.0	18.30	494	15.314
April	1955	563	32.7	18.30	598	17.940
May	2325	670	38.9	18.30	708	21.948
June	2505	721	41.8	18.30	765	22.950
July	2500	720	41.7	18.30	763	23.653
August	2170	625	36.3	18.30	664	20.584
September	1855	534	31.0	18.30	567	17.010
October	1675	484	28.0	18.30	512	15.872
November	1335	384	22.3	18.30	408	12.240
December	1025	295	17.1	18.30	313	9.703
Total Annual Gross Primary Production of Algal-Sponge Zone (kcal x 10^9/yr)						198.86

†Assumptions are as in Table 9.18

Table 9.20 Standing Crop and Production Estimates for the Live Coral Zone†

Measure and Group	Biomass (dry wt.) (kg x 10^3)			Caloric Equivalent (kcal x 10^6)		
Standing Crop	(Min.)		(Max.)	(Min.)		(Max.)
Producers						
-Zooxanthellae	15.9	-	31.8	63.6	-	127.2
-Soft algae (avg.)	4.2	-	6.9	16.8	-	27.6
-Cor. & endo. algae	278.9	-	557.7	1115.4	-	2230.8
Total producers	299.0	-	596.4	1195.8	-	2385.6
Coral tissue	121.3	-	242.6	448.8	-	897.6
Other consumers	255.6+	-	255.6+	1104.3+	-	1104.3+
Total Standing Crop	675.9+	-	1094.6+	2748.9+	-	4387.5+

Production

Gross primary production	13,006 x 10^6 kg	52,022 x 10^6 kcal
Net production (58.3% of gross production)		30,329 x 10^6 kcal
Respiratory loss (41.7% of gross production)		21,693 x 10^6 kcal

Ratio of Gross Production to Standing Crop Biomass (caloric equivalent)

-Minimum standing crop estimate	52,022 : 2749 =	18.9 : 1
-Maximum standing crop estimate	52,022 : 4388 =	11.8 : 1

†The relationship of net production and respiration to gross production is based upon data from Odum and Odum (1955) for the live coral reef at Eniwetok Atoll.

Table 9.21 Standing Crop and Production Estimates for the Algal-Sponge Zone†

Measure and Group	Biomass (dry wt.) (kg x 10^3)			Caloric Equivalent (kcal x 10^6)		
Standing Crop	(Min.)		(Max.)	(Min.)		(Max.)
Producers						
-Soft algae (avg.)	54.2	-	79.2	216.8	-	316.8
-Cor. & endo. algae	1038.0	-	2077.0	4152.0	-	8308.0
Total producers	1092.2	-	2156.2	4368.8	-	8624.8
Consumers	--		--	--		--
Total Standing Crop	--		--	--		--

Production

Gross primary production	49,740 x 10^6 kg	198,860 x 10^6 kcal
Net production (74.2% of gross production)		147,554 x 10^6 kcal
Respiratory loss (25.8% of gross production)		51,306 x 10^6 kcal

†The relationship of net production and respiration to gross production is based upon data from Smith and Marsh (1973) for an algal reef at Eniwetok Atoll.

Table 9.22 Estimated Mean Annual Accretion Rates of *Montastrea annularis* (on top and on side) for Representative Water Depths of the Live Coral Zone. Derived from data in Table 6.4

Water Depth (m)	Vertical Growth (mm/yr)	Lateral Growth (mm/yr)
20.0	8.3	6.3
25.0	7.3	5.6
30.0	6.4	4.8
35.0	5.4	4.0
40.0	4.4	3.3
45.0	3.4	2.6

However, accretion of the entire reef also involves the filling of spaces between heads by calcareous debris derived from the reef rock. Shinn et al. (1977) measured historical rates of accretion for shallow reefs in Florida, obtaining values from 0.65 to 4.85 m per 1000 years. According to the above data it would take a given coral head 120.5 years to grow one metre vertically. At these rates, assuming constant sea level and no tectonic movement of the seafloor, a reef at a depth of 20 m would take 4000 to 30,000 years to reach the surface of the water.

DATA NEEDS FOR FULL MODEL EVALUATION

The biological study of the East Flower Garden system was originally designed to provide a descriptive picture of the standing crop of some of the more important groups, particularly the corals and major fish species. As an afterthought it was decided to construct a model of the reef and to present the data in the context of the model, using the aid of existing literature to approach the evaluation of the model. Although the appropriateness of the borrowed data is in some cases open to question, the orders of magnitude appear to be reasonable, and valuable insights have been obtained which would not otherwise have been possible.

However, it is abundantly clear that the present data base as given in Tables 9.6 to 9.22 does not provide much of the information required by the equations shown in Tables 9.3 to 9.5. Hence, a brief summary of major data needs for full model evaluation is in order, and this is provided below:

- Cloud cover, surface radiation, and light penetration at various depths should be determined throughout the year.

- Nutrient levels, phytoplankton, zooplankton, and other suspended matter should be determined at various depths throughout the year.

- Seasonal variations in standing crops of the major producer and consumer groups should be evaluated.

- Seasonal studies on gross and net production and respiration by the reef ecosystem as well as the major producer groups should be accomplished.

- Food and feeding studies should be carried out on the major consumer species to assist in proper assignment to feeding groups and to provide data on food intake in relation to availability.

- Studies are needed on seasonal aspects of reproduction, recruitment, dispersal, and predation for the major consumer groups.

- Seasonal changes in respiration, growth, and fecal production should be carried out for the major consumer groups.

- Dynamics of the particulate organic detritus and calcareous debris pools should be investigated.

Detailed investigation of all these problems would be an extremely costly and time-consuming operation, but even a limited effort to evaluate the model should prove extremely rewarding. A two-year seasonal study of light penetration, nutrient and plankton levels, metabolic changes with depth, and biomass estimates would provide a much sharper focus on both biomass and overall metabolism of the two reef zones. It would permit evaluation of the transferability of borrowed data and establish the degree to which this reef system is unique among the studied reefs on the world. The major question which derives from the present analysis is the degree to which the East Flower Garden reef complex is autotropic and the degree to which it is plankton-dependent and how this trophic ratio changes with depth and with the seasons. Within this context the uniqueness of this reef system will likely be established.

SELECTED REFERENCES

Abbott, R.E., 1975. The Faunal Composition of the Algal-Sponge Zone of the Flower Garden Banks, Northwest Gulf of Mexico. M.S. thesis. Dept. of Oceanography, Texas A&M Univ., College Station, TX, 205 pp.

Abbott, R.E., 1979. Ecological Processes Affecting the Reef Coral Population at the East Flower Garden Bank, Northwest Gulf of Mexico. Ph.D. thesis. Dept. of Oceanography, Texas A&M Univ., College Station, TX, 154 pp.

Admiraal, W. and H. Peletier, 1979. Sulphide tolerance of benthic diatoms in relation to their distribution in an estuary. Br. Phycol. J., 14, 185-196.

Amery, G.B., 1978. Structure of continental slope, northern Gulf of Mexico. In Bouma, A.H., G.T. Moore, and J.M. Coleman, eds., Framework, Facies, and Oil Trapping Characteristics of the Upper Continental Margin, AAPG Stud. in Geol., 7, 141-153.

Angelovic, J.W., 1976. Environmental Studies of the South Texas Outer Continental Shelf, 1975. Vol. 2: Physical Oceanography. Final Report to the Bureau of Land Management, Contract 08550-IA5-19, U.S. National Marine Fisheries Service, Gulf Fisheries Center, Galveston, TX, NTIS Order No. PB-283-872/AS, 290 pp.

Ankar, S. and B.O. Jansson, 1973. Effects of an unusual natural temperature increase on a Baltic soft-bottom community. Mar. Biol., 18, 9-18.

Antoine, J.W., W. Bryant, and B. Jones, 1967. Structural features of continental shelf, slope, and scarp, northeastern Gulf of Mexico. AAPG Bull., 51, 257-262.

Avent, R.M., M.E. King and R.H. Gore, 1977. Topographic and faunal studies of shelf-edge prominences off the central eastern Florida coast. Int. Revue gesamten Hydrobiol., 62 (2), 185-208.

Ayala-Castanares, A., 1981. Foraminiferos Recientes de La Laguna de Tamiahua. An. Inst. Cienc. Del Mar y Limnol., Univ. Nal. Auton. Mexico, 8(1), 103-158.

Bahr, L.M. and W.P. Lanier, 1981. The Ecology of Intertidal Oyster Reefs of the South Atlantic Coast: A Community Profile. FWS/OBS-81/15.

Baines, P.G., 1973. The generation of internal tides by flat-bump topography, Deep-Sea Res., 20, 179-205.

Baines P.G., 1974. The generation of internal tides over steep continental slopes, Phil. Trans. Roy. Soc., 277(A), 27-58.

Bak, R.P.M., 1977. Coral reefs and their zonation in Netherlands Antilles. AAPG Stud. in Geol., 4, 3-16.

Baker, P.A. and J.N. Weber, 1975. Skeletal growth variations in the reef coral, Montastrea annularis, with depth. Geol. Soc. Am., Abs. with Prog., 7, 24.

Baldwin, O.D., and J.A.S. Adams, 1971. K^{40}/Ar^{40} ages of the alkali igneous rocks of the Balcones faulting trend of Texas. Tex. J. Sci., 22, 223-231.

Ballard, R. and J. Grassle, 1979. Return to oases of the deep. Natl. Geog. Mag., 156, 689-705.

Ballard, R.D. and E. Uchupi, 1970. Morphology and Quaternary history of the continental shelf of the Gulf Coast of the United States. Bull. Mar. Sci., 20(3), 547-559.

Bathurst, R.G.C., 1975. Carbonate Sediments and Their Diagenesis. 2nd ed. Elsevier, Amsterdam, 658 pp.

Behringer, D.W., R.L. Molinari, and J.F. Festa, 1977. The variability of anticyclonic current patterns in the Gulf of Mexico. J. Geophys. Res., 82, 5469-5476.

Berger, W. and H. Thierstein, 1979. On phanerozoic mass extinctions. Naturwissenschaften, 66, 46-47.

Bernard, B.B., J.M. Brooks, and W.M. Sackett, 1976. Natural gas seepage in the Gulf of Mexico. Earth and Plan. Sci. Lett., 31, 48-54.

Bernard, B.B., J.M. Brooks, and W.M. Sackett, 1977. A geochemical model for characterization of hydrocarbon gas sources in marine sediments. Proc. Ninth Annu. Offshore Technol. Conf., OTC 2934, Houston, TX, 435-438.

Berry, W. and P. Wilde, 1978. Progressive ventilation of the oceans: an explanation for the distribution of the lower Paleozoic black shales. Am. J. Sci., 278, 257-275.

Berryhill, H.L., Jr., 1981. Map Showing Paleogeography of the Continental Shelf During the Low Stand of Sea Level, Wisconsin Glaciation, Corpus Christi 1° x 2° Quadrangle, Texas. U.S. Geological Survey, 1:250,000, Map #I-1287-E.

Berryhill, H.L., Jr., and A. R. Trippet, 1980. Map Showing Water Circulation and Rates of Sedimentation in the Port Isabel 1° x 2° Quadrangle, Texas. U.S. Geological Survey, 1:250,000, Map #I-1254-A.

Berryhill, H.L., Jr., and A.R. Trippet, 1981a. Map Showing Water Circulation and Rates of Sedimentation in the Beeville 1° x 2° Quadrangle, Texas. U.S. Geological Survey, 1:250,000, Map #I-1288-A.

Berryhill, H.L., Jr., and A.R. Trippet, 1981b. Map Showing Water Circulation and Rates of Sedimentation in the Corpus Christi 1° x 2° Quadrangle, Texas. U.S. Geological Survey, 1:250,000, Map #I-1287-A.

Berryhill, H.L., Jr., G.L. Shideler, C.W. Holmes, S.S. Barnes, G.W. Hill, E.A. Martin, and C.A. Pyle, 1976. Environmental Studies, South Texas Outer Continental Shelf, 1976. Final Report to the Bureau of Land Management, Contract AA550-MU6-24, NTIS Order No. PB-277-337/AS, 626 pp.

Berryhill, H.L., Jr., ed., 1975. Environmental Studies, South Texas Outer Continental Shelf, 1975: An Atlas and Integrated Summary. Final Report to the Bureau of Land Management, Contract 08550-MU5-20, NTIS Order No. PB80-217763, 303 pp.

Blaha, J.P. and W. Sturges, 1981. Evidence for wind-forced circulation in the Gulf of Mexico. J. Mar. Res., 39(4), 711-733.

Blumberg, A.F. and G.L. Mellor, 1981. A numerical calculation of the circulation in the Gulf of Mexico. Prepared for Division of Solar Technology, U.S. Dept. of Energy, Contract #DE-AC02-78ET 20612, by Dynalysis of Princeton, Princeton, N.J. [pages not numbered].

Boaden, P.J.S., 1975. Anaerobiosis, meiofauna and early metazoan evolution. Zool. Scr., 4, 21-24.

Boaden, P.J.S., 1977. Thiobiotic facts and fancies (aspects of the distribution and evolution of anaerobic meiofauna). Acad. Wiss. Lit. Mainz Mikrofauna Meeresbodens, 61, 45-63.

Boaden, P.J.S., 1980. Meiofaunal thiobios and "the Arenicola negation": case not proven. Mar. Biol. (Berl.), 58, 25-29.

Boaden, P.J.S., and H.M. Platt, 1971. Daily migration patterns in an intertidal meiobenthic community. Thalassia Jugosl., 7, 1-12.

Bobb, W., R. Boland, F. Hermann, J. O'Meara, W. Savage, W. Rinne, and C. Gransee, 1971. Model Studies of Outfall Systems for Desalination Plants (Part II - Estuary models). Office of Saline Water Research and Development Progress Report #736, 183 pp.

Borowitzka, L.J., 1981. The microflora--adaptations to life in extremely saline lakes. Hydrobiologia, 81, 33-46.

Bosellini, A. and R.N. Ginsburg, 1971. Form and internal structure of recent algal nodules (rhodolites) from Bermuda. J. Geol., 79, 669-682.

Braunstein, J., and C.E. McMichael, 1976. Door Point: a buried volcano in southeast Louisiana. Gulf Coast Assoc. Geol. Soc., Trans., 26, 79-80.

Briggs, J.C., 1974. Marine Zoogeography. McGraw-Hill, New York, 475 pp.

Bright, T.J., 1977. Coral reefs, nepheloid layers, gas seeps and brine flows on hard-banks in the northwestern Gulf of Mexico. Proc. Third Int. Coral Reef Symp., Univ. Miami, Rosenstiel School of Marine and Atmospheric Science, 1, 39-46.

Bright, T.J. and L.H. Pequegnat, eds., 1974. Biota of the West Flower Garden Bank. Gulf Publishing Co., Houston, TX, 435 pp.

Bright, T.J. and R. Rezak, 1976. A Biological and Geological Reconnaissance of Selected Topographical Features on the Texas Continental Shelf. Final Report to U.S. Dept. of the Interior, Bureau of Land Management, Contract #08550-CT5-4, NTIS Order No. PB80-166036, 377 pp.

Bright, T.J. and R. Rezak, 1977. Reconnaissance of reefs and fishing banks of the Texas Continental Shelf. In Geyer, R.A., ed., Submersibles and Their Use in Oceanography, Elsevier, New York, 113-150.

Bright, T.J. and R. Rezak, 1978a. South Texas Topographic Features Study. Final Report to U.S. Dept. of the Interior, Bureau of Land Management, Contract #AA550-CT6-18, NTIS Order No. PB-294-768/AS, 772 pp.

Bright, T.J. and R. Rezak, 1978b. Northwestern Gulf of Mexico Topographic Features Study. Final Report to U.S. Dept. of the Interior, Bureau of Land Management, Contract #AA550-CT7-15, NTIS Order No. PB-294-769/AS, 667 pp.

Bright, T.J., J.W. Tunnell, L.H. Pequegnat, T.E. Burke, C.W. Cashman, D.A. Cropper, J.P. Ray, R.C. Tresslar, J. Teerling, and J.B. Wills, 1974. Biotic zonation on the West Flower Garden Bank. In Bright, T. and L. Pequegnat, eds., Biota of the West Flower Garden Bank, Gulf Publishing Co., Houston, TX, 4-54.

Bright, T.J., P.A. LaRock, R.D. Lauer, and J.M. Brooks, 1980a. A brine seep at the East Flower Garden Bank, northwestern Gulf of Mexico. Int. Rev. gesamten Hydrobiol., 65, 535-549.

Bright, T.J., E. Powell, and R. Rezak, 1980b. Environmental effects of a natural brine seep at the East Flower Garden Bank, northwestern Gulf of Mexico. In Geyer, R.A., ed., Marine Environmental Pollution, Elsevier Oceanography Series, 27A, Elsevier, New York, 291-316.

Bright, T.J., S. Viada, C. Combs, G. Dennis, E. Powell, and G. Denoux, 1981. East Flower Garden monitoring study. In Northern Gulf of Mexico Topographic Features Study, Final Report to U.S. Dept. of the Interior, Bureau of Land Management, Contract #AA551-CT8-35, Vol. 3, Part C, NTIS Order No. PB81-248676.

Bright, T.J., C. Combs, G. Kraemer, and G. Minnery, 1982. Biological monitoring at the Flower Garden Banks. In Environmental Studies at the Flower Gardens and Selected Banks, Final Report to U.S. Dept. of the Interior, Minerals Management Service, Contract #AA851-CT0-25, Chapter III, NTIS Order No. PB83-101303, pp. 39-102.

Broecker, W., 1961. Radiocarbon dating of late Quaternary deposits, South Lousiana: A discussion. Geol. Soc. Am. Bull., 72, 159-162.

Brooks, D.A. and M.C. Eble, 1982. Moored Array Observations in the Western Gulf of Mexico: Current Meter Data Report for the July 1980 to February 1981 Mooring Period. Dept. of Oceanography, Texas A&M Univ., Tech. Rep. #82-12-T, 259 pp.

Brooks, H.K., 1973. Geological oceanography. Section E. In Jones, J.I., R.E. Ring, M.O. Rinkel, and R.E. Smith, eds., A Summary of the Knowledge of the Eastern Gulf of Mexico, State Univ. Syst. of Fla., Inst. of Oceanography, St. Petersburg, FL, IIE, 1-49.

Brooks, J.M., T.J. Bright, B.B. Bernard, and C.R. Schwab, 1979. Chemical aspects of a brine pool at the East Flower Garden Bank, northwestern Gulf of Mexico. Limnol. Ocean., 24(4), 735-745.

Bryant, M.P., L.L. Campbell, C.A. Reddy, and M.R. Crabill, 1977. Growth of Desulfovibrio in lactate or ethanol media low in sulfate in association with H_2-utilizing methanogenic bacteria. Appl. Environ. Microbiol., 33, 1162-1169.

Bryant, W.R., A.A. Meyerhoff, N.K. Brown, Jr., M. Furrer, T.E. Pyle, and J.W. Antoine, 1969. Escarpments, reef trends and diapiric structures, Eastern Gulf of Mexico. AAPG Bull., 53(12), 2506-2542.

Cairns, S.D., 1977. Stony Corals. I. Carophylliina and Dendrophylliina (Anthozoa:Scleractinia). In Memoirs of the Hourglass Cruises, Marine Research Laboratory, Florida Dept. of Natural Resources, St. Petersburg, FL, Vol. 3, Part IV, 27 pp.

Capurro, L.R.A. and J.L. Reid, 1970. Contributions on the Physical Oceanography of the Gulf of Mexico. Vol. 2, Gulf Publishing Co., Houston, TX, 288 pp.

Carpelan, L.H., 1967. Invertebrates in relation to hypersaline habitats. Contrib. Mar. Sci., 12, 219-229.

Carsey, J.B., 1950. Geology of Gulf coastal area and continental shelf. AAPG Bull., 34, 361-385.

Cartwright, D. and A.J. Woods, 1963. Measurements of upper and lower tidal currents at Banc de la Chapelle. Deutsche Hydrograph. Zeit., 16, 64-76.

Cavanaugh, C.M., S.L. Gardiner, M.L. Jones, H.W. Jannasch, and J.B. Waterbury, 1981. Prokaryotic cells in the hydrothermal vent tube worm Riftia pachyptila Jones: possible chemoautotrophic symbionts. Science (Wash., D.C.), 213, 340-342.

Cervignon, F., 1966. Los Peces Marinos De Venezuela. Monographs No. 11 and 12, 2 vols., Fundacion La Salle de Ciencias Naturales, Fondo De Cultura Cientifica, Caracas, Venezuela, 1387 pp.

Chamberlain, C.K., 1966. Some Octocorallia of Isla de Lobos, Veracruz, Mexico. Brigham Young Univ. Geol. Stud., 13, 47-54.

Chavez, E.A., 1973. Observaciones generales sobre las comunidades del arrecife de Lobos, Veracruz. An. Esc. Nac Cienc. Biol. Mex., 20, 13-21.

Chavez, E.A., E.Y. Sevilla, and M.L. Hidalgo, 1970. Datos acerca de las comunidades bentonicas del arrecife de Lobos, Veracruz. Revista de la Sociedad Mexicana de Historia Natural, Tomo XXXI.

Chittenden, M.E., Jr., and J.D. McEachran, 1976. Composition, Ecology and Dynamics of Demersal Fish Communities on the Northwestern Gulf of Mexico Continental Shelf, with a similar synopsis for the Entire Gulf. Dept. of Oceangraphy, Texas A&M Univ., Tech. Rep. TAMU-SG-76-208.

Chittenden, M.E. and D. Moore, 1977. Composition of the ichthyofauna inhabiting the 110-meter bathymetric contour of the Gulf of Mexico, Mississippi River to the Rio Grande. Northeast Gulf Sci., 1, 106-114.

Claypool, G.E. and I.R. Kaplan, 1974. The origin and distribution of methane in marine sediments. In Kaplan, I.R., ed., Natural Gases in Marine Sediments, Plenum, New York, 99-139.

Cline, J.D. and F.A. Richards, 1967. Oxygenation of hydrogen sulfide in seawater at constant salinity, temperature, and pH. Environ. Sci. Technol., 3, 838-843.

Cloud, P.E., Jr., 1968. Atmospheric and hydrospheric evolution on the primitive Earth. Science (Wash., D.C.), 160, 729-736.

Cochrane, J.D. and F.J. Kelly, Jr., 1982. Proposed annual progression in the mean Texas-Louisiana shelf circulation. Trans. Am. Geophys. Union., 63(45), 1012.

Cohen, Y., W. Krumbein, M. Goldberg, M. Shilo, 1977a. Solar Lake (Sinai) 1. Physical and chemical limnology. Limnol. Ocean., 22, 597-608.

Cohen, Y., W. Krumbein, and M. Shilo, 1977b. Solar Lake (Sinai) 3. Bacterial distribution and production. Limnol. Ocean., 22, 621-634.

Collard, S.B. and C.N. D'Asaro, 1973. The Biological Environment: Benthic Invertebrates of the Eastern Gulf of Mexico. A summary of the Eastern Gulf of Mexico. State Univ. Syst. of Fla., Inst. of Oceanography, St. Petersburg, FL, 1-27.

Continental Shelf Associates, Inc., 1980. Video and Photographic Reconnaissance of Phleger and Sweet Banks, Northwest Gulf of Mexico. Prepared for Bureau of Land Management, Washington, D.C., Contract No. AA551-CT9-36, 20 pp.

Continental Shelf Associates, Inc., 1982. Environmental Monitoring Program for Platform "A," Lease OCS-G 3061, Block A-85, Mustang Island Area, East Addition, Near Baker Bank. Final Report to Conoco, Inc., 171 pp.

Copeland, B.J., 1967. Environmental characteristics of hypersaline lagoons. Contrib. Mar. Sci., 12, 207-218.

Copeland, B.J. and S. Nixon, 1974. Hypersaline lagoons. In Odum, H., B. Copeland, and E. McMahan, eds., Coastal Ecological Systems of the United States, The Conservation Foundation, Washington, D.C., 1, 312-330.

Copeland, B.J., H.T. Odum, and F.N. Moseley, 1974. Migrating subsystems. In Odum, H., B. Copeland, and E. McMahon, eds., Coastal Ecological Systems of the United States, The Conservation Foundation, Washington, D.C., Vol. 3, 422-453.

Corliss, J., J. Dymond, L. Gordon, J. Edmond, R. Von Herzen, R. Ballard, K. Green, D. Williams, A. Bainbridge, K. Crane, and T. van Andel, 1979. Submarine thermal springs in the Galapagos rift. Science (Wash., D.C.), 203, 1073-1083.

Craig, H., 1969. Geochemistry and origin of the Red Sea brines. In Degens, E.T. and D.A. Ross, eds., Hot Brines and Recent Heavy Metal Deposits in the Red Sea. Springer-Verlag, New York, 208-242.

Crezee, M., 1976. Solenofilomorphidae (Acoela), major component of a new turbellarian association in the sulfide system. Int. Rev. gesamten Hydrobiol., 61, 105-129.

Crout, R.L. and R.D. Hamiter, 1981. Response of bottom waters on the west Louisiana shelf to transient wind events and resulting sediment transport. Trans. Gulf Coast Assoc. Geol. Soc., 31, 273-278.

Culver, D.A. and G.J. Brunskill, 1969. Fayetteville Green Lake, New York. V. Studies of primary production and zooplankton in a meromictic marl lake. Limnol. Ocean., 14, 862-873.

Cummins, K.W. and J.C. Wuycheck, 1971. Caloric equivalents for investigations in ecological energetics. Mitt. Internat. Verein. Limnol., 18, 1-151.

Curray, J.R., 1965. Late Quaternary history, continental shelves of the United States. In Wright, H.E., Jr. and D.G. Frey, eds., the Quaternary of the United States, Princeton Univ. Press, Princeton, NJ, 728-736.

Davies, D.K. and W.R. Moore, 1970. Dispersal of Mississippi sediment in the Gulf of Mexico. J. Sediment. Petrol., 40(1), 339-353.

Davis, G.E., 1982. A century of natural change in coral distribution at the Dry Tortugas: A comparison of reef maps from 1881 and 1976. Bull. Mar. Sci., 32(2), 608-623.

Defenbaugh, R.E., 1976. A Study of the Benthic Macroinvertebrates of the Continental Shelf of the Northern Gulf of Mexico. Ph.D. thesis. Dept. of Oceanography, Texas A&M Univ., College Station, TX, 410 pp.

Degens, E. and D. Ross, eds., 1969. Hot Brines and Recent Heavy Metal Deposits in the Red Sea. Springer-Verlag, New York, 593 pp.

Demaison, G.J. and G.T. Moore, 1980. Anoxic environments and oil source bed genesis. AAPG Bull., 64, 1179-1209.

Dennis, G.D., III, 1982. The Origin and Zoogeographical Affinities of the Continental Shelf Ichthyofauna of the Northern Gulf of Mexico. Unpublished technical report prepared for Dr. R.M. Darnell, Texas A&M Univ. College Station, TX, 31 pp.

Dennis, R.E. and E.E. Long, 1971. A User's Guide to a Computer Program for Harmonic Analysis of Data at Tidal Frequencies. NOAA Tech. Rep. NOS 41, Office of Marine Surveys and Maps, Oceanographic Division, Rockville, MD, 31 pp.

Dodge, R.E., A. Logan, and A. Antonius, 1982. Quantitative reef assessment studies in Bermuda: A comparison of methods and preliminary results. Bull. Mar. Sci., 32(3), 745-760.

Downey, M.E., 1973. Starfishes from the Caribbean and the Gulf of Mexico. Smithson. Contrib. Zool. No. 126, 158 pp.

Dustan, P., 1975. Growth and form in the reef-building coral Montastrea annularis. Mar. Biol., 33, 101-107.

Dustan, P., 1979. Distribution of zooxanthellae and photosynthetic chloroplast pigments of the reef-building coral Montastrea annularis Ellis and Solander in relation to depth on a west Indian coral reef. Bull. Mar. Sci., 29 (1), 79-95.

Earle, S.A., 1969. Phaeophyta of the Eastern Gulf of Mexico. Phycologia, 7(2), 71-254.

Earle, S.A., 1972. Benthic algae and seagrasses. In Atlas Folio No. 22, Chemistry Primary, Productivity, and Benthic Algae of the Gulf of Mexico, American Geographical Society, New York, 15-18, 25-29, and plate 6.

Edwards, G.S., 1971. Geology of the West Flower Garden Bank. Texas A&M Sea Grant Publ., TAMU-SG-71-215, 199 pp.

Edwards, P., 1976. Illustrated Guide to the Seaweeds and Seagrasses in the Vicinity of Port Aransas, Texas. Univ. of Texas Press, Austin, TX, 126 pp.

Ehlers, U., 1973. Zur Populationsstruktur interstitieller Typhloplanoida und Dalyellioida (Turbellaria, Neorhabdocoela) Untersuchungen an einem mittellotischen Sandstrand der Nordseeinsel Sylt. Akad. Wiss. Lit. Mainz Mikrofauna Meeresbodens, 19, 1-105.

Ehrlich, R. and B. Weinberg, 1970. An exact method for characterization of grain shape. J. Sediment. Petrol., 40, 205-212.

Elliott, B.A., 1979. Anticyclonic Rings and the Energetics of the Circulation of the Gulf of Mexico. Ph.D. thesis. Dept. of Oceanography, Texas A&M Univ., College Station, TX, 188 pp.

Elliott, B.A., 1982. Anticyclonic rings in the Gulf of Mexico. J. Phys. Ocean., 12, 1292-1309.

El-Sayed, S.Z. and J.T. Turner, 1977. Productivity of the Antarctic and tropical/subtropical regions: A comparative study. In Proceedings of SCOR/SCAR Polar Oceans Conference, Antarctic Institute of North America, Montreal, Canada, 463-503.

Etter, P.C. and J.D. Cochrane, 1975. Water temperature on the Texas-Louisiana Shelf. Marine Advisory Bulletin, Commerce. Texas A&M Sea Grant Publ., TAMU-SG-75-604, 22 pp.

Everett, D.K., 1971. Hydrologic and Quality Characteristics of the Lower Mississippi River. Louisiana Dept. Public Works, 48 pp.

Fandino, V.S., unpublished. Algunos Estudies Sobre las Madreporas del Arecife "La Blanquilla," Veracruz, Mexico. Universidad Autonoma Metropolitana, 103 pp. Aptado postal 55-535, Mexico D F, Dpto. Zootecnia.

Farris, R.A., 1976. Systematics and Ecology of Gnathostomulida from North Carolina and Bermuda. Ph.D. thesis. University of North Carolina at Chapel Hill, 197 pp.

Felbeck, H., 1981. Chemoautotrophic potential of the hydrothermal vent tube worm, Riftia pachyptila Jones (Vestimentifera). Science (Wash., D.C.), 213, 336-338.

Felbeck, H., J.J. Childress, and G.N. Somero, 1981. Calvin-Benson cycle and sulphide oxidation enzymes in animals from sulphide rich habitats. Nature (Lond.), 293, 291-293.

Felder, D.L. and A.C. Chaney, 1979. Decapod crustacean fauna of Seven and One-Half Fathom Reef, Texas: species composition, abundance, and species diversity. Contrib. Mar. Sci., 22, 1-29.

Fenchel, T. and R. Riedl, 1970. The sulfide system: A new biotic community underneath the oxidized layer of marine sand bottoms. Mar. Biol. (Berl.), 7, 255-268.

Fenchel, T. and A. Thane, 1977. Anaerobiosis and symbiosis with bacteria in free-living ciliates. J. Protozool., 24, 154-163.

Flint, R.W. and C.W. Griffin, eds., 1979. Environmental Studies, South Texas Outer Continental Shelf, Biology and Chemistry. Final Report to U.S. Dept. of the Interior, Bureau of Land Mangement, Contract AA550-CT7-11, Executive Summary, NTIS Order No. PB81-106692, 75 pp.

Folk, R.L., 1974. Petrology of Sedimentary Rocks. 2nd ed. Hemphill Publication Co., Austin, TX, 182 pp.

Fontugne, M.R. and J.C. Duplessy, 1981. Organic carbon isotopic fractionation by marine plankton in the temperature range -1 to 31°C. Oceanologica Acta, 4, 85-90.

Forristall, G.Z., R.C. Hamilton, and V.J. Cardone, 1977. Continental shelf currents in Tropical Storm Delia: Observations and Theory. J. Phys. Ocean., 7, 532-546.

Fotheringham, N., 1980. Beachcomber's Guide to Gulf Coast Marine Life. Gulf Publishing Co., Houston, TX, 124 pp.

Frankenberg, D. and K.L. Smith, 1967. Coprophagy in marine animals. Limnol. Ocean., 12, 443-450.

Fredericks, A.D. and W.M. Sackett, 1970. Organic carbon in the Gulf of Mexico. J. Geophys. Res., 75, 2199-2206.

Frohlich, C., 1982. Seismicity in the Central Gulf of Mexico. Geology, 10, 103-106.

Fry, B. and P.C. Parker, 1979. Animal diet in Texas seagrass meadows: Delta C-13 evidence for the importance of benthic plants. Est. Coast. Mar. Sci., 8, 499-509.

Gallardo, V.A., 1977. Large benthic microbial communities in sulphide biota under Peru-Chile subsurface countercurrent. Nature (Lond.), 268, 331-332.

Gallaway, B.J. and G.S. Lewbel, 1982. The Ecology of Petroleum Platforms in the Northwestern Gulf of Mexico: A Community Profile. FWS/OBS-82/27, 91 pp.

George, R.Y. and P.J. Thomas, 1979. Aspects of Fouling on Offshore Oil Platforms in Louisiana Shelf in Relation to Environmental Impact. Final report, Offshore Ecological Investigations, Gulf Universities Research Consortium, 54 pp.

Ginsburg, R.N. and M. Stanley, 1970. Seminar on organism-sediment interrelationships. Reports of Research, 1969, Bermuda Biological Station for Research, Spec. Publ. No. 6, St. George's West, Bermuda, 111 pp.

Gittings, S.R., 1983. Hard-Bottom Macrofauna of the East Flower Garden Brine Seep: Impact of a Long Term, Point-Source Brine Discharge. M.S. thesis. Dept. of Oceanography, Texas A&M Univ., College Station, TX, 72 pp.

Goedicke, T.R., 1955. Origin of the pinnacles on the continental shelf and slope of the Gulf of Mexico. Tex. J. Sci., 7, 149-159.

Goldhaber, M.B. and I.R. Kaplan, 1974. The sulfur cycle. In Goldberg, E., ed., The Sea, Vol. 5, Marine Chemistry, Wiley, New York, 569-655.

Goreau, T.F., 1959. The ecology of Jamaican coral reefs: I. Species composition and zonation. Ecology, 40, 67-90.

Goreau, T.F. and J.W. Wells, 1967. The shallow-water scleractinia of Jamaica: Revised list of species and their vertical distribution range. Bull. Mar. Sci., 17(2), 442-453.

Gould, H.R. and R.H. Stewart, 1955. Continental terrace sediments in the northeast Gulf of Mexico. In Finding Ancient Shorelines, Soc. Econ. Paleontol. Mineral., Spec. Pub. 3, Tulsa, OK, 3-20.

Gould, W.J. and W.D. McKee, 1973. Vertical structure of semi-diurnal tidal currents in the Bay of Biscay. Nature, 244, 88-91.

Grimm, D.E. and T.S. Hopkins, 1977. Preliminary characterization of the octocorallian and scleractinian diversity at the Florida Middle Ground. Proc. Third Int. Coral Reef Symp., Univ. Miami, Rosenstiel School of Marine and Atmospheric Science, 1, 135-141.

Haines, E.B. and C.L. Montague, 1979. Food sources of estuarine invertebrates analyzed using $^{13}C/^{12}C$ ratios. Ecology, 60, 48-56.

Hammen, C.S., 1980. Total energy metabolism of marine mollusks in anaerobic and aerobic states. Comp. Biochem. Physiol. A. Comp. Physiol., 67, 617-621.

Harding, J.L., and W.D. Nowlin, Jr., 1966. Gulf of Mexico. In Fairbridge, Rhodes W., ed., Encyclopedia of Oceanography, Reinhold, New York, 324-331.

Harrington, D.L., 1966. Oceanographic Observations on the Northwest Continental Shelf of the Gulf of Mexico, 1963-1965. Contribution No. 329, National Marine Fisheries Service Biological Laboratory, Galveston, TX, 25 pp.

Hawkins, J.W., 1983. Sources of relict sand on the northeast Texas Continental Shelf. M.S. thesis. Dept. of Oceanography, Texas A&M Univ., College Station, TX, 63 pp.

Hayes, S.P. and D. Halpern, 1976. Variability of semidiurnal internal tide during coastal upwelling. Memoires Societe Royale des Sciences de Liege, 10, 175-186.

Hedgpeth, J.W., 1953. An introduction to zoogeography of the northwestern Gulf of Mexico with reference to the invertebrate fauna. Publ. Inst. Mar. Sci., Univ. Tex., 3, 107-224.

Hedgpeth, J.W., 1954. Bottom communities of the Gulf of Mexico. Fishery Bulletin 89, Fish. Bull. Fish and Wildlife Service, 55, 203-214.

Heilprin, A., 1890. The corals and coral reefs of the western waters of the Gulf of Mexico. Proc. Acad. Nat. Sci. Phil., 42, 301-316.

Hildebrand, H.H., 1954. A Study of the Fauna of the Brown Shrimp (Penaeus aztecus Ives) Grounds in the Western Gulf of Mexico. Publ. Inst. Mar. Sci., Univ. Texas, 3(2), 233-366.

Hildebrand, H.H., 1955. A Study of the Fauna of the Pink Shrimp (Penaeus duorarum Burkenroad) Grounds in the Gulf of Campeche. Publ. Inst. Mar. Sci., 4(1), 169-232.

Hildebrand, H.H., 1957. Estudios Biologicos Preliminares Sobre La Laguna Madre De Tamaulipas. Ciencia, 17(7-9), 151-173.

Hoese, H.D. and R.H. Moore, 1977. Fishes of the Gulf of Mexico, Texas, Louisiana, and Adjacent Waters. Texas A&M Univ. Press, College Station, TX, 327 pp.

Hogg, N.G., 1980. Effects of bottom topography on ocean currents. In Hide, R. and P.W. White, eds., Orographic Effects in Planetary Flows, GARP Publications Series No. 23, WMO-ICSU Joint Scientific Committee, 167-205.

Holmes, C.W., 1982. Geochemical indices of fine sediment transport, northwest Gulf of Mexico. J. Sediment. Petrol., 52(1), 307-321.

Holser, W., 1977. Catastrophic chemical events in the history of the ocean. Nature, 267, 403-408.

Hopkins, T.S. and W. Schroeder, 1981. Physical and chemical oceanography. In Northern Gulf of Mexico Topographic Features Study, Final Report to U.S. Dept. of the Interior, Bureau of Land Management, Contract #AA551-CT8-35, Dept. of Oceanography, Texas A&M Univ., Tech. Rep. #81-2-T, Vol. 5, 21-47.

Hopkins, T.S., D.R. Blizzard, and D.K. Gilbert, 1977. The molluscan fauna of the Florida Middle Ground with comments on its zoogeographical affinities. Northeast Gulf Sci., 1(1), 39-47.

Horne, W. and J. Meincke, 1976. Note on the tidal current field in the continental slope area off northwest Africa. Memoires Societe Royal des Sciences de Liege, 10, 31-42.

Hudson, J.H., 1981. Growth rates in Montastrea annularis: A record of environmental change in Key Largo Coral Reef Marine Sanctuary, Florida. Bull. Mar. Sci., 31, 444-459.

Hudson, J.H. and D.M. Robbin, 1980. Effects of drilling mud on the growth rate of the reef building coral, Montastrea annularis. In Geyer, R.A., ed., Marine Environmental Pollution, Elsevier Oceanography Series, 27A, Elsevier, New York, 455-470.

Hudson, J.H., E.A. Shinn, R.B. Halley, and B. Lidz, 1976. Sclerochronology: A tool for interpreting past environments. Geology, 4, 361-364.

Hulings, N.C. and J.S. Gray, 1976. Physical factors controlling abundance of meiofauna on tidal and atidal beaches. Mar. Biol. (Berl.), 34, 77-83.

Humm, H.J., 1973. The Biological Environment; Salt Marshes, Benthic Algae of the East Gulf of Mexico, Seagrasses, Mangrove. A summary of the Eastern Gulf of Mexico. State Univ. Syst. of Fla., Inst. of Oceanography, St. Petersburg, FL, 1-6.

Humm, H.J. and H.H. Hildebrand, 1962. Marine algae from the Gulf Coast of Texas and Mexico. Publ. Inst. Mar. Sci., Univ. Texas, 8, 227-268.

Huntsman, G.R. and I.G. MacIntyre, 1971. Tropical coral patches in Onslow Bay. Underwater Nat. Bull. Am. Littoral Soc., 7(2), 32-34.

Land, L.S., J.C. Lang, and B.N. Smith, 1975. Preliminary observations on the carbon isotopic composition of some reef coral tissues and symbiotic zooxanthellae. Limnol. Ocean., 20, 283-287.

Lang, J.C., 1973. Interspecific aggression by scleractinian corals. 2. Why the race is not only to the swift. Bull. Mar. Sci., 23(2), 260-279.

LaRock, P.A., R.D. Lauer, J.R. Schwarz, K.K. Watanabe, and D.A. Wiesenburg, 1979. Microbial biomass and activity distribution in an anoxic, hypersaline basin. Appl. Environ. Microbiol., 37, 466-470.

Lauer, R.D., 1979. Sulfur Deposition in the East Flower Gardens, Gulf of Mexico. M.S. thesis. Florida State University, 33 pp.

Leadbetter, E.R., 1974. Beggiatoaceae Migula. In Buchanan, R.E. and N.E. Gibbons, eds., Bergey's Manual of Determinative Bacteriology, 8th ed., Williams and Wilkins, Baltimore, 112-115.

LeBlanc, R.J., 1972. Geometry of sandstone reservoir bodies. In Cook, T.D., ed., Underground Waste Management and Environmental Implications, AAPG Mem. 18, 133-190.

LeBlond, P.H. and L. Mysak, 1978. Waves in the Ocean. Elsevier, New York, 602 pp.

Levert, C.F. and H.C. Ferguson, Jr., 1969. Geology of the Flower Garden Banks, northwest Gulf of Mexico. Trans. Gulf Coast Assoc. Geol. Soc., 19, 89-100.

List, R.J., 1966. Smithsonian Meteorological Tables. Smithsonian Institution, Washington, D.C., Section X, Radiation and Visibility Tables, 411-478.

Logan, B.W., 1969. Carbonate Sediments and Reefs, Yucatan Shelf, Mexico: Part 2, Coral Reefs and Banks, Yucatan Shelf, Mexico (Yucatan Reef Unit). AAPG Mem., 11, 129-198.

Logan, B.W., J.L. Harding, W.M. Ahr, J.D. Williams, and R.G. Snead, 1969. Carbonate Sediments and Reefs, Yucatan Shelf, Mexico: Part 1, Late Quaternary carbonate sediments of Yucatan Shelf, Mexico. AAPG Mem., 11, 5-128.

Loya, Y., 1976. Effects of water turbidity and sedimentation on the community structure of Puerto Rican corals. Bull. Mar. Sci., 26, 450-466.

Loya, Y., 1978. Plotless and transect methods. In Stoddart, D.R. and R.E. Johannes, eds., Coral Reefs: Research Methods, UNESCO, Paris, 197-217.

Lyons, W.G. and S.B. Collard, 1974. Benthic Invertebrate Communities of the Eastern Gulf of Mexico. Proceedings of Marine Environmental Implications of Offshore Drilling Eastern Gulf of Mexico: 1974. Contributions No.233, FDNR/MRL, 157-167.

Macdonald, K. 1982. Introductory Overview: Southwest Florida Shelf Ecosystems Study. Proceedings Third Annual Gulf of Mexico Information Transfer Meeting, Minerals Management Service, New Orleans, LA, 31-35.

MacIntyre, I.G., 1972. Submerged reefs of the Eastern Caribbean. AAPG Bull., 56, 720-738.

Marmorino, G.O., 1982. Summertime Coastal Currents in the Northeastern Gulf of Mexico. Unpublished manuscript, Dept. of Oceanography, Florida State Univ., Tallahassee, FL, 30 pp.

Martin, R.G., 1978. Northern and eastern Gulf of Mexico continental margin: Stratigraphic and structural framework. In Bouma, A.H., G.T. Moore, and J.M. Coleman, eds., Framework, Facies, and Oil-Trapping Characteristics of the Upper Continental Margin, AAPG, Tulsa, OK, 21-42.

Martin, R.G. and A.H. Bouma, 1978. Physiography of Gulf of Mexico. In Bouma, A.H., G.T. Moore, and J.M. Coleman, eds., Framework, Facies, and Oil-Trapping Characteristics of the Upper Continental Margin, AAPG, Tulsa, OK, 3-19.

Mathis, B. and T. Dorris, 1968. Community structure of benthic macroinvertebrates in an intermittent stream receiving oil field brines. Am. Midl. Nat., 80, 428-439.

Matsuyama, M., 1979. On the purple sulfur bacterium Chromatium sp., densely populating the mid-depth of Lake Kaiike, Kamikoshiki Island, Kagoshima Prefecture. Jpn. J. Limnol., 40, 20-28.

Matsuyama, M. and E. Shirouzu, 1978. Importance of photosynthetic sulfur bacteria, Chromatium sp., as an organic matter producer in Lake Kaiike. Jpn. J. Limnol., 39, 103-111.

Mayor, A.G., 1915. The lower temperature at which reef corals lose their ability to capture food. Yearbook, Carnegie Inst. Pub. 183, 6, 1-24.

McConnaughey, T. and C. McRoy, 1979. Food-Web structure and the fractionation of carbon isotopes in the Bering Sea. Mar. Biol. (Berl.), 53, 257-262.

McFarlan, E., Jr., 1961. Radiocarbon dating of late Quaternary deposits, South Louisiana. Geol. Soc. Am. Bull., 72, 129-158.

McGrail, D.W., 1977. Shelf edge currents and sediment transport in the northwestern Gulf of Mexico. (Abs.) Trans. Amer. Geophys. Union, 58, 1160.

McGrail, D.W., 1978. Boundary layer processes, mixed bottom layers, and turbid layers on continental shelves. (Abs.) Trans. Amer. Geophys. Union, 59, 1110.

McGrail, D.W., 1979. The role of air-sea interaction in sediment dynamics. (Abs.) Abstracts of Papers at the 145th National Meeting, American Assoc. for the Advancement of Science, 45.

McGrail, D.W., 1982. Anomalous flow on the Outer Continental Shelf in the Gulf of Mexico and its effect on sediment transport. (Abs.) Trans. Am. Geophys. Union, 63 (3), 65.

McGrail, D.W. and M.R. Carnes, 1983. Shelfedge dynamics and the nepheloid layer. In Stanley, D.J. and G.T. Moore, eds., ShelfBreak: Critical Interface on Continental Margins, Soc. Econ. Paleontol. and Mineral., Special Pub. No. 33, 251-264.

McGrail, D.W. and D. Horne, 1979. Currents, thermal structure and suspended sediment distribution induced by internal tides on the Texas Continental Shelf. Paper presented at the spring meeting of the American Geophysical Union SANDS Symposium.

McGrail, D.W. and D. Horne, 1981. Water and sediment dynamics [Flower Garden Banks]. In Northern Gulf of Mexico Topographic Features Study, Final Report to U.S. Dept. of the Interior, Bureau of Land Management, Contract #AA551-CT8-35, Vol. 3, NTIS Order No. PB81-248676, Part B, 9-45.

McGrail, D.W. and D.W. Huff, 1978. Shelf sediment and local flow phenomena: in situ observations. (Abs.) Program, AAPG-SEPM Annual Convention, 93.

McGrail, D.W. and R. Rezak, 1977. Internal waves and the nepheloid layer on continental shelf in the Gulf of Mexico. Trans. Gulf Coast Assoc. Geol. Soc., 27, 123-124.

McGrail, D.W., D.W. Huff, and S. Jenkins, 1978. Current measurements and dye diffusion studies. In Bright, T. and R. Rezak, eds., Northwestern Gulf of Mexico Topographic Features Study, Final Report to U.S. Dept. of the Interior, Bureau of Land Management, Contract #AA550-CT7-15, NTIS Order No. PB-294-769/AS, pp. III-3 to III-72.

McGrail, D.W., M. Carnes, D. Horne, T. Cecil, J. Hawkins, and F. Halper, 1982a. Water and sediment dynamics at the Flower Garden Banks. In Environmental Studies at the Flower Gardens and Selected Banks, Final Report to Minerals Management Service, Contract #AA851-CT0-25, NTIS Order No. PB83-101303, pp. 103-226.

McGrail, D.W., M. Carnes, D. Horne, and J. Hawkins, 1982b. Hydrographic Data Report. Northern Gulf of Mexico Topographic Features Study. U.S. Dept. of the Interior, Bureau of Land Management, Contract #AA851-CT0-25. Dept. of Oceanography, Texas A&M Univ., Tech. Rep. #82-4-T, 516 pp.

McGrail, D.W., F. Halper, D. Horne, T. Cecil, M. Carnes, 1982c. Time Series Data Report. Northern Gulf of Mexico Topographic Features Study. U.S. Dept. of the Interior, Bureau of Land Management, Contract #AA851-CT0-25. Dept. of Oceanography, Texas A&M Univ., Tech. Rep. #82-5-T, 155 pp.

McGrail, D.W., R. Rezak, and T.J. Bright, 1982d. Environmental Studies at the Flower Gardens and Selected Banks: Northwestern Gulf of Mexico, 1979-1981. Final Report to Minerals Management Service, Contract #AA851-CT0-25, NTIS Order No. PB83-101303, 314 pp.

McGrail, D.W., T.M. Cecil, and F.B. Halper, 1982e. Stacking of nepheloid and boundary layers at the shelf edge in the Gulf of Mexico. (Abs.) Trans. Am. Geophys. Union, 63, 988.

McNulty, J.K., R.C. Work, and H.B. Moore, 1962. Some relationships between the infauna of the level bottom and the sediment in south Florida. Bull. Mar. Sci. Gulf. Caribb., 12, 322-332.

Merrell, W.J. and J.M. Morrison, 1981. On the circulation of the Western Gulf of Mexico with observations from April 1978. J. Geophys. Res., 86 (C5), 4181-4185.

Moore, D.R., 1958. Notes on Blanquilla Reef, the most northerly coral formation in the western Gulf of Mexico. Publ. Inst. Mar. Sci., Univ. Tex., 5, 151-155.

Moore, D.R. and H.R. Bullis, Jr., 1960. A deep water coral reef in the Gulf of Mexico. Bull. Mar. Sci. Gulf and Caribb., 10, 125-128.

Moseley, F.N. and B.J. Copeland, 1974. Brine pollution system. In Odum, H.T., B.J. Copeland, and E.A. McMahon, eds., Coastal Ecological Systems of the United States, The Conservation Foundation, Washington, D.C., 342-352.

Muller, U. and P. Ax, 1971. Gnathostomulida von der Nordeseeinsel Sylt mit Beobachtungen zur Lebensweise und Entwicklung von Gnathostomula paradoxa Ax. Acad. Wiss. Lit. Mainz Microfauna Meeresbodens, 9, 1-41.

Murray, G.E., 1961. Geology of the Atlantic and Gulf Coastal Province of North America. Harper, New York, 692 pp.

Nakai, N., 1960. Carbon isotope fractionation of natural gas in Japan. J. Earth Sci., 8, 174-180.

Nichols, J.A., 1976. The effect of stable dissolved-oxygen stress on marine benthic invertebrate community diversity. Int. Rev. gesamten Hydrobiol., 61, 747-760.

Niiler, P.P., 1976. Observations of low-frequency currents on the West Florida continental shelf. Mem. R. Soc. Sci. Liege, ser. 6, 10, 331-358.

Nissenbaum, A., B.J. Presley, and I.R. Kaplan, 1972. Early chemical diagenesis in a reducing fjord, Saanich Inlet, British Columbia. 1. Chemical and isotopic changes in major components of interstitial waters. Geochim. Cosmochim. Acta, 36, 1007-1027.

Nowlin, W.D., Jr., 1972. Winter circulation patterns and property distributions. In Capurro, L.R.A. and J.L. Reid, eds., Texas A&M University Oceanographic Studies, Vol. 2, Gulf Publishing Co., Houston, TX, 3-53.

Nowlin, W.D., Jr. and H.J. McLellan, 1967. A characterization of the Gulf of Mexico waters in winter. J. Mar. Res., 25(1), 29-59.

Nowlin, W.D., Jr., and C.A. Parker, 1974. Effects of a cold-air outbreak on shelf waters of the Gulf of Mexico. J. Phys. Ocean., 4(3), 467-486.

O'Brien, D.J. and F.B. Birkner, 1977. Kinetics of oxygenation of reduced sulfur species in aqueous solution. Environ. Sci. Technol., 11, 1114-1120.

Odum, H.T., 1972. An energy circuit language for ecological and social systems: Its physical basis. In Patten, B.C., ed., Systems Analysis and Simulation in Ecology, Chapter 4, Vol. 2, Academic Press, 139-211.

Odum, H.T. and E.P. Odum, 1955. Trophic structure and productivity of a windward coral reef community on Eniwetok Atoll. Ecol. Monogr., 25, 291-320.

Oppenheimer, C.H. and K.G. Gordon, 1972. Texas Coastal Zone Biotopes: An Ecography. Interim Report for the Bay and Estuary Management Program (CRMP). Univ. of Texas Marine Science Institute, Port Aransas, TX [pages unnumbered].

Oremland, R.S. and B.F. Taylor, 1978. Sulfate reduction and methanogenesis in marine sediments. Geochim. Cosmochim. Acta, 42, 209-214.

Oseid, D.M. and L.L. Smith, Jr., 1974a. Factors influencing acute toxicity estimates of hydrogen sulfide to freshwater invertebrates. Water Res., 8, 739-746.

Oseid, D.M. and L.L. Smith, Jr., 1974b. Chronic toxicity of hydrogen sulfide to Gammarus pseudolimnaeus. Trans. Am. Fish. Soc., 103, 819-822.

Ostle, B. and R.W. Mensing, 1975. Statistics in Research. 3rd ed. Iowa State Univ. Press, Ames, IA, 596 pp.

Ott, J.A., 1972. Determination of fauna boundaries of nematodes in an intertidal sand flat. Int. Rev. gesamten Hydrobiol., 57, 645-663.

Ott, J.A., B. Fuchs, R. Fuchs, and A. Malasek, 1976. Observations on the biology of Callianassa stebbingi Borrodaille and Upogebia litoralis Risso and their effect upon the sediment. Senckenberg Maritima, 8, 61-79.

Parker, P.L., E.W. Behrens, J.A. Calder, and D. Schultz, 1972. Stable carbon isotope ratio variations in the organic carbon from Gulf of Mexico sediments. Contrib. Mar. Sci., 16, 139-147.

Parker, P.L., R.S. Scalan, J.K. Winters, and D. Boatwright, 1981. High molecular weight hydrocarbons, Delta C-13, and total organic carbon in sediment. In Northern Gulf of Mexico Topographic Features Study, Final Report to U.S. Dept. of the Interior, Bureau of Land Management, Contract #AA551-CT8-35, Vol. 2, NTIS Order No. PB81-248650, Chapter IXC, 100-114.

Parker, R.P., J.M. Morrison, and W.D. Nowlin, Jr., 1979. Surface Drifter Data from the Caribbean Sea and Gulf of Mexico, 1975-1978. ONR #N00014-75-C-0537, Dept. of Oceanography, Texas A&M Univ., Tech Rep. #79-8-T. 157 pp.

Pequegnat, W.E., 1970. Deep-water brachyuran crabs. In Pequegnat, W.E. and F.A. Chace, Jr., eds., Contributions on the Biology of the Gulf of Mexico, Vol. 1, Texas A&M Univ., College Station, TX, 171-204.

Pfennig, N., 1975. The phototrophic bacteria and their role in the sulfur cycle. Plant and Soil, 43, 1-16.

Pielou, E.C., 1966. The measurement of diversity in different types of biological collections. J. Theor. Biol., 13, 131-144.

Pionetti, J. and A. Toulmond, 1980. Tide-related changes of volatile fatty acids in the blood of the lugworm Arenicola marina (L.). Can. J. Zool., 58, 1723-1727.

Poag, C.W., 1973. Late Quaternary sea levels in the Gulf of Mexico. Trans. Gulf Coast Assoc. Geol. Soc., 23, 394-400.

Pollock, L.W., 1971. Ecology of intertidal meiobenthos. Smithson. Contrib. Zool., 76, 141-148.

Poole, R.W., 1974. An Introduction to Quantitative Ecology. McGraw-Hill, New York, 532 pp.

Porter, J.W., 1972. Ecology and species diversity of coral reefs on opposite sides of the Isthmus of Panama. In Jones, M.L., ed., The Panama Biota: A Symposium Prior to the Sea Level Canal, Bull. Biol. Soc. Wash., 2, 89-116.

Powell, E.N., 1977. Particle size selection and sediment reworking in a funnel feeder, Leptosynapta tenuis (Holothuroidea, Synaptidae). Int. Rev. gesamten Hydrobiol., 62, 385-408.

Powell, E.N. and T.J. Bright, 1981. A thiobios does exist--Gnathostomulid domination of the canyon community at the East Flower Garden brine seep. Int. Rev. gesamten Hydrobiol., 66(5), 675-683.

Powell, E.N., M.A. Crenshaw, and R.M. Rieger, 1979. Adaptations to sulfide in the meiofauna of the sulfide system. 1. ^{35}S-sulfide accumulation and the presence of a sulfide detoxification system. J. Exp. Mar. Biol. Ecol., 37, 57-76.

Powell, E.N., M.A. Crenshaw, and R.M. Rieger, 1980. Adaptations to sulfide in sulfide system meiofauna: End products of sulfide detoxification in three turbellarians and a gastrotrich. Mar. Ecol. Progr. Ser., 2, 169-177.

Powell, E.N., T.J. Bright, A. Woods, and S. Gittings, 1983. Meiofauna and the thiobios in the East Flower Garden brine seep. Mar. Biol., 73, 269-283.

Prinsenberg, S.J. and M. Rattray, Jr., 1975. Effects of continental slope and variable Brunt-Vaisala frequency on the coastal generation of internal tides. Deep-Sea Res., 22, 251-263.

Prinsenberg, S.J., W. Wilmot, and M. Rattray, Jr., 1974. Generation and dissipation of coastal internal tides. Deep-Sea Res., 16, 179-195.

Pulley, T.E., 1952. A zoogeographic study based on the bivalves of the Gulf of Mexico. Ph.D. thesis. Harvard University, 215 pp.

Pulley, T.E., 1963. Texas to the tropics. Houston Geol. Soc. Bull., 6, 13-19.

Pyle, C.A., 1977. Late Quaternary Geologic History of the South Texas Continental Shelf. M.S. thesis. Dept. of Oceanography, Texas A&M, Univ., College Station, TX, 72 pp.

Randall, J., 1965. Grazing effects on sea grasses by herbivorous reef fishes of the West Indies. Ecology, 46, 255-260.

Rannefeld, J.W., 1972. The Stony Corals of Enmedio Reef Off Veracruz, Mexico. M.S. thesis. Dept. of Oceanography, Texas A&M Univ., College Station, TX, 104 pp.

Rattray, M., Jr., 1960. On the coastal generation of internal tides. Tellus, 12, 54-62.

Rattray, M., Jr., J.G. Dworski, and P.E. Kovala, 1969. Generation of long internal waves at the continental slope. Deep-Sea Res., 16, 179-195.

Rau, G.H., 1981. Hydrothermal vent clam and tube worm $^{13}C/^{12}C$: Further evidence of nonphotosynthetic food sources. Science (Wash., D.C.), 213, 338-339.

Rau, G.H. and J.I. Hedges, 1979. Carbon-13 depletion in a hydrothermal vent mussel: Suggestion of a chemosynthetic food source. Science (Wash., D.C.), 203, 648-649.

Reed, J.H., 1977. Barium and Vanadium Determination by Neutron Activation Analysis--A Study of Procedures. Report to U.S. Dept. of the Interior, Bureau of Land Management, Contract #AA550-CT7-38, 84 pp.

Reed, J.K., 1980. Distribution and structure of deep-water Oculina varicosa coral reefs off central eastern Florida. Bull. Mar. Sci., 30(3), 667-677.

Reid, R.O. and R. Whitaker, in press. Numerical Model for Astronomical Tides in the Gulf of Mexico. U.S. Army Engineer Waterways Experiment Station, Vicksburg, MS.

Reimers, T., 1977. Anoxische Lebensraume: Struktur und Entwicklung der Mikrobiozonose an der Granzflache Meer/Meeresboden. Ph.D. thesis. Christian-Albrechts - Universitat, Kiel, 134 pp.

Reise, K., 1981a. Gnathostomulida abundant alongside polychaete burrows. Mar. Ecol. Progr. Ser., 6, 329-333.

Reise, K., 1981b. High abundance of small zoobenthos around biogenic structures in tidal sediments of the Wadden Sea. Helgol. Meeres., 34, 413-425.

Reise, K. and P. Ax, 1979. A meiofaunal "thiobios" limited to the anaerobic sulfide system of marine sand does not exist. Mar. Biol. (Berl.), 54, 225-237.

Reise, K. and P. Ax, 1980. Statement on the thiobios-hypothesis. Mar. Biol. (Berl.), 58, 31-32.

Revsbech, N.P., B.B. Jorgensen, and T.H. Blackburn, 1980a. Oxygen in the sea bottom measured with a microelectrode. Science (Wash., D.C.), 207, 1355-1356.

Revsbech, N.P., B.B. Jorgensen, T.H. Blackburn, and J. Lomholf, 1980b. Distribution of oxygen in marine sediments measured with micro-electrodes. Limnol. Ocean., 25, 403-411.

Rezak, R., 1977. West Flower Garden Bank, Gulf of Mexico. Stud. Geol., 4, 27-35.

Rezak, R., 1981. Geology. In Northern Gulf of Mexico Topographic Features Study, Final Report to U.S. Dept. of the Interior, Bureau of Land Management, Contract #AA551-CT8-35, Vol. 1, NTIS Order No. PB81-248650, pp. 23-59.

Rezak, R., 1982a. Geology of the Flower Garden Banks. In Environmental Studies at the Flower Gardens and Selected Banks, Final Report to Minerals Management Service, Contract #AA851-CT0-25, Chapter II, NTIS Order No. PB83-101303, pp. 19-37.

Rezak, R., 1982b. Geology of selected banks. In Environmental Studies at the Flower Gardens and Selected Banks, Final Report to Minerals Management Service, Contract #AA851-CT0-25, Chapter VI, NTIS Order No. PB83-101303, pp. 253-300.

Rezak, R., ed., 1981. Proceedings: Second Annual Gulf of Mexico Information Transfer Meeting. Held April 30-May 1, 1981, New Orleans, LA. Texas A&M Univ., Dept. of Oceanography, Tech. Rep. #81-5-T, 115 pp.

Rezak, R. and T.J. Bright, 1981a. Northern Gulf of Mexico Topographic Features Study. Final Report to U.S. Dept. of the Interior, Bureau of Land Management, Contract #AA551-CT8-35. 5 vols., 995 pp. NTIS Order Nos. : Vol I, PB81-248650; Vol. II, PB81-248668; Vol. III, PB81-248676; Vol. IV, PB81-248684; Vol. V, PB81-248692.

Rezak, R. and T.J. Bright, 1981b. Seafloor instability at East Flower Garden Bank, northwest Gulf of Mexico. Geo-Marine Letters, 1(2), 97-103.

Rezak, R. and W.R. Bryant, 1973. West Flower Garden Bank. Trans. Gulf Coast Assoc. of Geol. Soc. 23rd Annual Conv. (Oct. 24-26), 377-382.

Rezak, R. and G.S. Edwards, 1972. Carbonate sediments of the Gulf of Mexico. Texas A&M Univ. Ocean. Stud., 3, 263-280.

Rezak, R. and T.T. Tieh, 1980. Basalt on Louisiana Outer Continental Shelf. EOS, Trans. Am. Geophys. Union, 61(46), 989.

Rhoads, D.C., 1974. Organism-sediment relations on the muddy sea floor. Ocean. Mar. Biol. Ann. Rev., 12, 263-300.

Rhoads, D.C. and J.W. Morse, 1971. Evolutionary and ecologic significance of oxygen-deficient marine basins. Lethaia, 4, 413-428.

Riedl, R.J.M., 1970a. On Labidognathia longicollis, nov. gen., nov. spec., from the west Atlantic coast (Gnathostomulida). Int. Rev. gesamten Hydrobiol., 55, 227-244.

Riedl, R.J.M., 1970b. Semaeognathia, a new genus of Gnathostomulida from the North American coast. Int. Rev. gesamten Hydrobiol., 55, 359-370.

Rigby, J.K. and W.G. McIntyre, 1966. The Isla de Lobos and associated reefs, Veracruz, Mexico. Brigham Young Univ. Geol. Studies. 13, 1-46.

Roberts, H.H., L.J. Rause, Jr., N.D. Walker, and J.H. Hudson, 1982. Cold water stress in Florida Bay and northern Bahamas: A product of winter air outbreaks. J. Sediment. Petrol., 52(1), 145-155.

Roos, P.J., 1964. The distribution of reef corals in Curacao. Stud. Fauna Curacao, 20, 1-51.

Roos, P.J., 1971. The shallow water stony corals of the Netherlands Antilles. Vitgaven "Natuurwetenschappelijke Studiekring voor Suriname en de Nederlandse Antillen," 37(64), 1-108.

Rosenberg, R., 1977. Benthic macrofaunal dynamics, production, and dispersion in an oxygen-deficient estuary of west Sweden. J. Exp. Mar. Biol. Ecol., 26, 107-133.

Round, F.E., 1979. A diatom assemblage living below the surface of intertidal sand flats. Mar. Biol. (Berl.), 54, 219-223.

Sackett, W.M., W.R. Eckelmann, M.C. Bender, and A.W.H. Be, 1965. Temperature dependence of carbon isotope composition in marine plankton and sediments. Science (Wash., D.C.), 148, 235-237.

Sahl, L.E., W.J. Merrell, and D.W. McGrail, 1982. Currents and property distribution on the Texas shelf and slope in March 1981 and 1982. (Abs.) Trans. Am. Geophys. Union, 63, 1012.

Salvador, A., 1980. Late Triassic-Jurassic paleogeography and the Gulf of Mexico. In Pilger, R.H., Jr., ed., Proceedings of a Symposium, the origin of the Gulf of Mexico and the early opening of the Central North Atlantic Ocean, School of Geoscience, Louisiana State University, Baton Rouge, 101 pp.

Sanchez-Gil, P., A. Yanez-Arancibia, and F.A. Linares, 1981. Diversidad, Distribucion y Abundancia de las Especies y Poblaciones de peces Demersales de la Sonda De Campeche. An. Inst. Cienc. Del Mar y Limnol., 8(1), 209-240.

Schott, F., 1977. On the energetics of baroclinic tides in the North Atlantic, Ann. Geophys., 33, 41-62.

Schroeder, W.W. and D.W. McGrail, 1982. Shelf current observations during tropical storms. (Abs.) Trans. Am. Geophys. Union, 63 (3), 66.

Shepard, F.P., 1937. Salt domes related to Mississippi submarine trough. Geol. Soc. Am. Bull., 48, 1349-1361.

Shepard, F.P., 1960. Rise of sea level along northwest Gulf of Mexico. In Shepard, F.P., F.B. Phleger, and T.H. Van Andel, Recent Sediments, Northwest Gulf of Mexico, AAPG, Tulsa, OK, 338-344.

Shepard, F.P., 1963. Submarine Geology. 2nd ed. Harper and Row, New York, 557 pp.

Shideler, G.L., 1977. Late Holocene sedimentary provinces, South Texas Outer Continental Shelf. AAPG Bull., 61(5), 708-722.

Shideler, G.L., 1978. A sediment-dispersal model for the South Texas continental shelf, northwest Gulf of Mexico. Mar. Geol., 26, 289-313.

Shideler, G.L., 1981. Development of the benthic nepheloid layer on the South Texas continental shelf, western Gulf of Mexico. Mar. Geol., 41, 37-61.

Shinn, E.A., 1974. Oil structures as artificial reefs. In Colunga, L. and R. Stone, eds., Proceedings of an International Conference on Artificial Reefs, Center for Marine Resources, Texas A&M Univ., College Station, TX, 91-96.

Shinn, E.A., 1975. Coral reef recovery in Florida and in the Persian Gulf. Shell Oil Environmental Conservation Dept., Environ. Geol., 1, 241-254.

Shinn, E.A., J.H. Hudson, R.V. Halley, and B. Lidy, 1977. Topographic control and accretion rate of some coral reefs: South Florida and Dry Tortugas. In Proc. Third Int. Coral Reef Symp., Univ. of Miami, Miami, FL, 1-7.

Shipp, R.L. and T.S Hopkins, 1978. Physical and biological observations of the northern rim of the DeSoto Canyon made from a research submersible. Northeast Gulf Sci., 2 (2), 113-121.

Shokes, R.F., P. Trabant, B. Presley, and D. Reid, 1977. Anoxic, hypersaline basin in the northern Gulf of Mexico. Science (Wash., D.C.), 196, 1443-1446.

Smith, F.G.W., 1971. Atlantic Reef Corals: A Handbook of the Common Reef and Shallow-water Corals of Bermuda, Florida, the West Indies, and Brazil. Rev. ed. Univ. Miami Press, Coral Gables, FL, 164 pp.

Smith, G.B., 1976. Ecology and distribution of eastern Gulf of Mexico reeffishes. Fla. Mar. Res. Publ., 19, 78 pp.

Smith, N.P., 1980b. Temporal and spatial variability in longshore motion along the Texas Gulf coast. J. Geophys. Res., 85(C3), 1531-1536.

Smith, S.V. and J.A. Marsh, Jr., 1973. Organic carbon production on the Windward Reef flat of Eniwetok Atoll. Limnol. Ocean., 18(6), 953-961.

Sorenson, L.O., 1979. A Guide to the Seaweeds of South Padre Island, Texas. Gorsuch Scarisbrick Publishing Co., Dubuque, IA, 123 pp.

Stafford, J.M., 1982. An Evaluation of the Carbonate Cements and Their Diagenesis on Selected Banks, Outer Continental Shelf, Northern Gulf of Mexico. M.S. thesis. Dept. of Oceanography, Texas A&M Univ., College Station, TX, 78 pp.

Stearn, C.W. and C. Colassin, 1979. A simple underwater pneumatic hand drill. J. Paleontol., 53(5), 1257-1259.

Steel, R.G.D. and J.H. Torrie, 1960. Principles and Procedures of Statistics. McGraw-Hill, New York, 481 pp.

Sterrer, W. and R. Rieger, 1974. Retronectidae: A new cosmopolitan marine family of Catenulida (Turbellaria). In Riser, N. and M. Morse, eds., The Biology of the Turbellaria, McGraw-Hill, New York, 63-92.

Stetson, H.C., 1953. The sediments of the western Gulf of Mexico, part I--The continental terraces of the western Gulf of Mexico: Its surface sediments, origin, and development. Papers in Physical Oceanography and Meteorology, M.I.T./W.H.O.I., 12(4), 1-45.

Steward, R.G., 1981. Light Attenuance Measurements of Suspended Particulate Matter: Northeastern Gulf of Mexico. M.S. thesis. Dept. of Marine Science, Univ. of South Florida, St. Petersburg, FL, 140 pp.

Stoddart, D.R., 1969. Ecology and morphology of recent coral reefs. Biol. Rev. Camb. Philos. Soc., 44, 433-498.

Sundeen, D.A., and P.L. Cook, 1977. K-Ar dates from Upper Cretaceous. Geol Soc. Am. Bull., 88, 1144-1146.

Sverdrup, H.U., M.W. Johnson, and R. Fleming, 1942. The Oceans, Their Physics, Chemistry and General Biology. Prentice-Hall, New Jersey, 1087 pp.

Takahashi, M. and S. Ichimura, 1970. Photosynthetic properties and growth of photosynthetic sulfur bacteria in lakes. Limnol. Ocean., 15, 929-944.

Taylor, J.L., L. Feignenbaum, and M. L. Stursa, 1973. Utilization of Marine and Coastal Resources. A summary of the Eastern Gulf of Mexico. State Univ. Syst. of Fla., Inst. of Oceanography, St. Petersburg, FL, 1-63.

Temple, R.F., D.S. Harrington, and J.A. Martin, 1977. Monthly Temperature and Salinity Measurements of Continental Shelf Waters of the Northwestern Gulf of Mexico, 1963-1965. U.S. Dept. of Commerce, National Oceanic and Atmospheric Administration and National Marine Fisheries Service, Tech. Rep. #SSRF-707, 26 pp.

Theede, H., A. Ponat, K. Hiroki, and C. Schlieper, 1969. Studies on the resistance of marine bottom invertebrates to oxygen deficiency and hydrogen sulfide. Mar. Biol. (Berl.), 2, 325-337.

Thierstein, H. and W. Berger, 1978. Injection events in ocean history. Nature, 276, 461-466.

Thistle, D. and F. Lewis, III, 1979. Literature Search on the Soft-bottom Benthos of the open waters of the Gulf of Mexico. Ocean Chemistry Laboratory Atlantic Oceanographic and Meteorological Lab. NOAA 20 Sept. 1979.

Torgrimson, G.M. and B.M. Hickey, 1979. Barotropic and baroclinic tides of the continental slope and shelf off Oregon. J. Phys. Ocean., 9, 945-961.

Tresslar, R.C., 1974. Corals. In Bright, T.J. and L.H. Pequegnat, eds., Biota of the West Flower Garden Bank, Gulf Publishing Co., Houston, TX, 116-139.

Trippett, A.R. and Berryhill, H., 1982. Geology of the continental shelf edge and upper continental slope off southwest Louisiana. U.S. Dept. of the Interior, Minerals Management Service. Open File Report #82-02, Sheet VI.

Trowbridge, A.C., 1930. Building of Mississippi Delta. AAPG Bull., 14, 867-901.

Tunnell, J.W., Jr., 1973. Molluscan population of a submerged reef off Padre Island, Texas. Bulletin of the American Malacological Union, Inc., 25-26.

Tunnell, J.W. and A.H. Chaney, 1970. A checklist of the mollusks of Seven and One Half Fathom Reef, Northwestern Gulf of Mexico. Contrib. Mar. Sci., 15, 194-203.

Uchupi, E., and K.O. Emery, 1968. Structure of continental margin off Gulf Coast of United States. AAPG Bull., 52, 1162-1193.

U.S. Naval Weather Service Command, 1975. Summary of Synoptic Meteorological Observations. Vol 4, May 1975, Area 28, Galveston, TX.

Van Andel, T.H., 1960. Sources and dispersion of Holocene sediments, northern Gulf of Mexico. In Shepard, F.P., F.B. Phleger, and T.H. Van Andel, eds., Recent Sediments, Northwest Gulf of Mexico, AAPG Bull., Tulsa, OK, 34-55.

Van Andel, T.H. and J.R. Curray, 1960. Regional aspects of modern sedimentation in northern Gulf of Mexico and similar basins, and paleogeographic significance. In Shepard, F.P., F.B. Phleger, and T.H. Van Andel, eds., Recent Sediments, Northwest Gulf of Mexico, AAPG Bull., Tulsa, OK, 345-364.

Van Andel, T.H. and D.M. Poole, 1960. Sources of recent sediments in the northern Gulf of Mexico. J. Sediment. Petrol., 30(1), 91-122.

Vaughan, T.W., 1916. On recent Madreporaria of Florida, the Bahamas, and the West Indies and on collections from Murray Island, Australia. Carnegie Inst. Wash. Year Book, 220-231.

Viada, S.T., 1980. Species Composition and Population Levels of Scleractinian Corals Within the Diploria-Montastrea-Porites Zone of the East Flower Garden Bank, Northwest Gulf of Mexico. M.S. thesis. Dept. of Oceanography, Texas A&M Univ., College Station, TX, 96 pp.

Villalobos, A. 1971. Estudios Ecologicos en un Arrecife Coralino en Veracruz, Mexico. Symposium on Investigations and Resources of the Caribbean Sea and Adjacent Regions, UNESCO and FAO, 531-545.

von Brand, T., 1944. Occurrence of anaerobiosis among invertebrates. Biodynamica, 4, 1-328.

Warren, L.M. and R.P. Dales, 1980. Glucose degradation in the polychaete annelid Owenia fusiformis Delle Chiaje under anaerobic conditions. Comp. Biochem. Physiol. B. Comp. Biochem., 65, 443-445.

Watkins, J.S., J.W. Ladd, R.T. Buffler, F.J. Shaub, M.H. Houston, and J.L. Warzel, 1978. Occurrence and evaluation of salt in deep Gulf of Mexico. In Bouma, A.H., G.T. Moore, and J.M. Coleman, eds., Framework, Facies, and Oil-Trapping Characteristics of the Upper Continental Margin, AAPG, Tulsa, OK, 43-65.

Weatherly, G.L., 1972. A study of the bottom boundary layer of the Florida current. J. Phys. Ocean., 2, 54-72.

Weatherly, G.L., 1975. A numerical study of time-dependent turbulent Ekman layers over horizontal and sloping bottoms. J. Phys. Ocean., 5, 288-299.

Weatherly, G.L., S.L. Blumsack, and A.A. Bird, 1980. On the effect of diurnal tidal currents in determining the thickness of the turbulent Ekman bottom boundary layer. J. Phys. Ocean., 10, 297-300.

Weigand, J.G., H. Farmer, S. Prinsenberg, and M. Rattray, Jr., 1969. Effects of friction and surface tide angle of incidence on the coastal generation of internal tides. J. Mar. Res., 27, 241-259.

Wells, J.W., 1957. Coral reefs. In Hedgpeth, J.W., ed. Treatise on Marine Ecology and Paleoecology. Geol. Soc. Amer. Mem. 67, 1, 609-631.

Wells, J.W., 1973. New and old Scleractinian corals from Jamaica. Bull. Mar. Sci., 23(1), 16-58.

Wentworth, C.K., 1922. A scale of grade and class terms for clastic sediments. J. Geol., 30, 377-392.

Wieser, W., J. Ott, F. Schiemer, and E. Gnaiger, 1974. An ecophysiological study of some meiofauna species inhabiting a sandy beach at Bermuda. Mar. Biol. (Berl.), 26, 235-248.

Wilson, O., 1969. Three coral reefs of Bermuda's North Lagoon: Physiography and distribution of corals and calcareous algae. In Ginsburg, R.N. and P. Garrett, eds., Seminar on Organism-Sediment Interrelationships, Reports of Research, Bermuda Biological Station for Research, Spec. Publ. No. 2, St. George's West, Bermuda, 51, 64.

Wilson, R.F., 1963. Organic carbon in some aquatic ecosystems. Publ. Inst. Mar. Sci., Univ. Tex., 9, 64-67.

Winker, C.D., 1982. Cenozoic shelf margins, northwest Gulf of Mexico. Trans. Gulf Coast Assoc. of Geol. Soc., 32, 427-448.

Wiseman, W.J., Jr., D.W. McGrail, and L.J. Rouse, Jr., 1982. Shelf break exchange driven by cold fronts. (Abs.) Trans. Am. Geophys. Union, 63, 1012.

Withjack, M.O. and C. Scheiner, 1982. Fault patterns associated with domes: An experimental and analytical study. AAPG Bull., 66, 302-316.

Wong, W., W.M. Sackett, and C.R. Benedict, 1975. Isotope fractionation in photosynthetic bacteria during carbon dioxide assimilation. Plant Physiol., 55, 475-479.

Yanez-Arancibia, A., F.A. Linares, and J.W. Day, Jr., 1980. Fish Community Structure and Function in Terminos Lagoon, A Tropical Estuary in the Southern Gulf of Mexico. Estuarine Perspectives, Academic Press, New York, 465-482.

Zartman, R.E., M.R. Brock, A.V. Heyl, and H.H. Thomas, 1967. K-Ar and Rb-Sr ages of some alkali intrusive rocks from central and eastern United States. Am. J. Sci., 265, 848-870.

APPENDIX

GEOLOGIC TIME SCALE

Era	Period	Age (10^6 yr)	Gulf of Mexico
CENOZOIC	QUATERNARY		Beginning of Recent time ~ 20,000 yrs. BP
	2 ± 1	0	Beginning of Pleistocene
	TERTIARY		Great influx of terrigenous sediment
	65 ± 2		Rapid deepening of Gulf
MESOZOIC	CRETACEOUS	100	Shallow-water carbonate deposition
	135 ± 5		
	JURASSIC		Salt deposition
	190 ± 5		Terrigenous sedimentation Block faulting
	TRIASSIC	200	
	225 ± 5		
	PERMIAN		
	270 ± 5		
PALEOZOIC	CARBONIFEROUS	300	
	340 ± 10		
	DEVONIAN		
	400 ± 10	400	
	SILURIAN		
	430 ± 10		
	ORDOVICIAN		
	500 (?)	500	
	CAMBRIAN		
	600 (?)	600	
PRECAMBRIAN	OLDEST ROCKS IN SOLAR SYSTEM	5000	

Time scale is not proportionally accurate in this diagram.

The Department of the Interior Mission

As the Nation's principal conservation agency, the Department of the Interior has responsibility for most of our nationally owned public lands and natural resources. This includes fostering sound use of our land and water resources; protecting our fish, wildlife, and biological diversity; preserving the environmental and cultural values of our national parks and historical places; and providing for the enjoyment of life through outdoor recreation. The Department assesses our energy and mineral resources and works to ensure that their development is in the best interests of all our people by encouraging stewardship and citizen participation in their care. The Department also has a major responsibility for American Indian reservation communities and for people who live in island territories under U.S. administration.

The Minerals Management Service Mission

As a bureau of the Department of the Interior, the Minerals Management Service's (MMS) primary responsibilities are to manage the mineral resources located on the Nation's Outer Continental Shelf (OCS), collect revenue from the Federal OCS and onshore Federal and Indian lands, and distribute those revenues.

Moreover, in working to meet its responsibilities, the **Offshore Minerals Management Program** administers the OCS competitive leasing program and oversees the safe and environmentally sound exploration and production of our Nation's offshore natural gas, oil and other mineral resources. The MMS **Minerals Revenue Management** meets its responsibilities by ensuring the efficient, timely and accurate collection and disbursement of revenue from mineral leasing and production due to Indian tribes and allottees, States and the U.S. Treasury.

The MMS strives to fulfill its responsibilities through the general guiding principles of: (1) being responsive to the public's concerns and interests by maintaining a dialogue with all potentially affected parties and (2) carrying out its programs with an emphasis on working to enhance the quality of life for all Americans by lending MMS assistance and expertise to economic development and environmental protection.